18

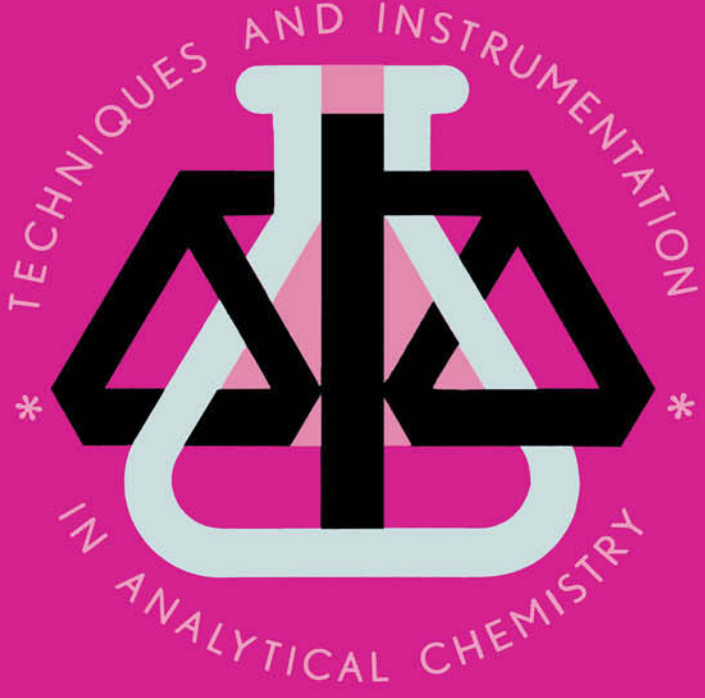

INSTRUMENTAL METHODS IN FOOD ANALYSIS

edited by
J.R.J. Paré and J.M.R. Bélanger

ELSEVIER

TECHNIQUES AND INSTRUMENTATION IN ANALYTICAL CHEMISTRY — VOLUME 18

INSTRUMENTAL METHODS IN FOOD ANALYSIS

TECHNIQUES AND INSTRUMENTATION IN ANALYTICAL CHEMISTRY

Volume 1 **Evaluation and Optimization of Laboratory Methods and Analytical Procedures. A Survey of Statistical and Mathemathical Techniques**
by D.L. Massart, A. Dijkstra and L. Kaufman

Volume 2 **Handbook of Laboratory Distillation**
by E. Krell

Volume 3 **Pyrolysis Mass Spectrometry of Recent and Fossil Biomaterials. Compendium and Atlas**
by H.L.C. Meuzelaar, J. Haverkamp and F.D. Hileman

Volume 4 **Evaluation of Analytical Methods in Biological Systems**
Part A. Analysis of Biogenic Amines
edited by G.B. Baker and R.T. Coutts
Part B. Hazardous Metals in Human Toxicology
edited by A. Vercruysse
Part C. Determination of Beta-Blockers in Biological Material
edited by V. Marko

Volume 5 **Atomic Absorption Spectrometry**
edited by J.E. Cantle

Volume 6 **Analysis of Neuropeptides by Liquid Chromatography and Mass Spectrometry**
by D.M. Desiderio

Volume 7 **Electroanalysis. Theory and Applications in Aqueous and Non-Aqueous Media and in Automated Chemical Control**
by E.A.M.F. Dahmen

Volume 8 **Nuclear Analytical Techniques in Medicine**
edited by R. Cesareo

Volume 9 **Automatic Methods of Analysis**
by M. Valcárcel and M.D. Luque de Castro

Volume10 **Flow Injection Analysis – A Practical Guide**
by B. Karlberg and G.E. Pacey

Volume11 **Biosensors**
by F. Scheller and F. Schubert

Volume12 **Hazardous Metals in the Environment**
edited by M. Stoeppler

Volume13 **Environmental Analysis. Techniques, Applications and Quality Assurance**
edited by D. Barceló

Volume14 **Analytical Applications of Circular Dichroism**
edited by N. Purdie and H.G. Brittain

Volume15 **Trace Element Analysis in Biological Specimens**
edited by R.F.M. Herber and M. Stoeppler

Volume16 **Flow–through (Bio)Chemical Sensors**
by M. Valcárcel and M.D. Luque de Castro

Volume 17 **Quality Assurance for Environmental Analysis**
Method Evaluation within the Measurements and Testing Programme (BCR)
edited by Ph. Quevauviller, E.A. Maier and B. Griepink

Volume 18 **Instrumental Methods in Food Analysis**
edited by J.R.J. Paré and J.M.R. Bélanger

TECHNIQUES AND INSTRUMENTATION IN ANALYTICAL CHEMISTRY — VOLUME 18

INSTRUMENTAL METHODS IN FOOD ANALYSIS

Edited by

J.R.J. Paré
J.M.R. Bélanger
Environment Canada, Environmental Technology Centre,
Ottawa, Ontario, Canada K1A OH3

1997
ELSEVIER
Amsterdam — Lausanne — New York — Oxford — Shannon — Tokyo

ELSEVIER SCIENCE B.V.
Sara Burgerhartstraat 25
P.O. Box 211, 1000 AE Amsterdam, The Netherlands

ISBN: 0-444-81868-5

This book is printed on acid-free paper.

Printed in The Netherlands

Contents

Preface

Writing a book on "instrumental methods in food analysis" presented a major philosophical dilemma. We live in the era of the information highway and, upon first impression, there are already (too) many monographs dealing with the various analytical instrumental techniques filling already overcrowded bookshelves. Hence, why another handbook on the topic?

From our experience, despite the dramatic developments in tools to access information, there are still serious deficiencies in terms of communication between the various fields. This is partly the result of a certain resistance to delve in areas related to "other" fields and to the drawback of this same accrued access to information, namely so much information that it is virtually impossible to access it all! Furthermore, depleted financial resources associated with science and technology activities over the last few years have put serious budget constraints on libraries and their priorities.

Hence, our challenge was to produce a tool that would be useful while being able to overcome the hurdles mentioned above. To address the problem we elected to edit a book that would involve both instrumental analysis experts and food scientists. To achieve this we solicited contributions from recognised workers in each area. All chapters are written by instrumental analysis workers who have experience in food science, or by food scientists with extensive expertise in instrumental methods. Wherever we had problems in identifying a single author meeting the two criteria we took on the role of "marriage councillors" and arranged for chapters to be written by two (or three) authors combining the desired qualifications. We also elected to allow as much freedom as possible to the authors, minimising as much as possible the editing of the writing style of their contributions. The rationale here being that there are numerous flavours to instrumental methods, hence why not avoid the often monotonous style found in the conventional monograph/textbook. Our goal was to free the authors from editorial constraints while concentrating on relatively short - though very representative - chapter that encompasses all the basics required to proceed with work in-house that the reader might need to do.

The second line of thought behind this book was that we wanted a monograph that can be used by graduate students and industry-based technical and operations staff alike. To achieve this goal we chose the following general layout: Brief theoretical considerations, mode of operations, specific

example(s), and a tabular survey of food analysis applications. Naturally, there was flexibility in the format but overall it was adhered to quite well.

Another major decision was the selection of "instrumental methods" to be included. We opted to pursue the methods that were widely used in food analysis, or those that offered ample room for furthering their use in the food analytical laboratory. Chromatographic techniques in general were of interest (Chapter 1), recognising however the relative importance of high-pressure liquid chromatography (Chapter 2) and gas chromatography (Chapter 3). Spectroscopic methods were also prime candidates and our choice centred around Fourier transform infrared, nuclear magnetic resonance, and mass spectrometry (Chapters 4, 6, and 7, respectively). Inorganic analysis has been covered in Chapter 5 on atomic spectroscopy and a special emphasis has been put on electrochemical methods (Chapter 8) which too often are forgotten in conventional "instrumental analysis" books. Electrophoresis is still emerging as a powerful tool and offers excellent potential in food analysis and as such warranted a chapter of its own (Chapter 9).

Finally, no analysis can be made without appropriate sample preparation. In today's economic climate, the need - and search - for new ways to prepare samples is becoming increasingly important. This is especially true as several "analytical" techniques are now limited, in general terms, by the ability to produce acceptable samples. Our choice rested with two, relatively new, techniques, the microwave-assisted processes (MAP™[1], Chapter 10) and supercritical fluid extraction (Chapter 11).

The choice of these two techniques was guided by the current trend of developing ever more environmentally-friendly technologies. For example, both techniques offer significant promises to meet the so-called "sustainable development" guidelines adopted by several countries and, accordingly, that are reflected in new regulations dealing with wastes and waste management. For example, it is estimated that 100,000,000 litres of solvent are used yearly solely for performing laboratory analyses on a world-wide, inter-disciplinary basis. Clearly, techniques such as MAP and SFE could contribute significantly to a reduced consumption of such chemicals and, by the same token, enhance our overall quality of life.

The result of all these reflections - and of course of numerous hours of dedicated writing and work from all our contributors - is now open in front of you and we invite you to be the judge as to whether we succeeded in meeting our goals.

---

[1] MAP is a Trade-Mark of Her Majesty the Queen in Right of Canada as represented by the Minister of the Environment.

We hope that you will find this monograph useful and that it will act as a mentor to all those graduate students in food science that have an inclination toward the analytical side of their field. On the same vein, we hope that technical personnel within the various food institutions, research and production alike, will find herein a useful tool if and when a need arises to remedy an analytical problem.

We would like to close this (lengthy!) preface by expressing our sincere thanks to the editorial staff at Elsevier Science, the Publisher, for their patience with us during the preparation of this book. Finally, a special acknowledgement is made to Dr. D. E. Thornton, Director, Environmental Technology Centre, for allowing us to pursue this venture as he, like us, is committed to supporting a healthier environment by offering "green" technologies to all sectors of the industry.

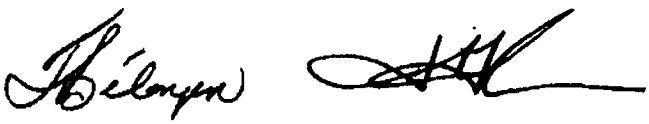

Ottawa, ON, Canada
December 18, 1996

This Page Intentionally Left Blank

J.R.J. Paré and J.M.R. Bélanger (Editors)
Instrumental Methods in Food Analysis

Chapter 1

Chromatography: Principles and Applications

Jacqueline M. R. Bélanger, Martine C. Bissonnette and J. R. Jocelyn Paré

Environment Canada, Environmental Technology Centre, Ottawa, ON, Canada, K1A 0H3

1.1 INTRODUCTION - HISTORICAL BACKGROUND

Separation of analytes is an important and crucial part of the analysis of an unknown mixture. Chromatography meets this challenge. In 1906, Mikhail Semenovich (Michael) Tswett (a Russian botanist), also referred to as the Father of Chromatography, was the first to describe the technique. In one of his experiments, he reported the separation of coloured leaf pigments (chlorophyll) by passing a petroleum ether solution through a column packed with adsorbent chalk particles. Tswett observed that, as the pigments travelled down the column, distinct yellow and green coloured bands appeared and were eluting or coming off the column at different rates. The separation technique called chromatography, of Greek origin "chroma" (colour) and "graphein" (to write), was born. At the time, Tswett assumed that the technique should also work well with colourless substances. He performed various studies such as the separation of isomeric chlorophyll and carotenoids but at the time, the general interest of chemists was isolation and purification of large quantities of materials. Tswett's work, performed with very small amounts of materials, was not appreciated in his lifetime.

The technique was almost forgotten until it was resurrected in 1930 by Kuhn, Winterstein and Lederer. They separated the components of egg yolk by passing them through a glass column packed with calcium carbonate and identified two components: lutein and zeaxanthin.

During another experiment two isomers of a biologically important substance present in carrots, alpha- and beta-carotene, were characterised following a preliminary separation of carrot extracts on alumina. Chromatography was resuscitated!

In 1941 the term "partition column chromatography" appeared, thanks to the work of Nobel recipients Martin and Synge. They separated the acetyl derivatives of amino acids by introducing them into a column containing water adsorbed on silica gel and using an non-miscible solvent, chloroform, as the mobile phase. Next, Martin, in collaboration with Consden and Gordon, used a flat filter paper wetted by water as the stationary phase and n-butanol as the mobile phase, and were able to perform the separation of amino acids. As stated by Synge, partition chromatography made possible the merging of chemistry with biology [1].

It is only in 1958, when Stahl standardised the procedure and showed its wide applications, that thin layer chromatography (a derivative of paper chromatography) became a technique that is now used extensively and has become a "classic"! Gas chromatography (GC) was first described in 1952 by Martin and James and, by the 1960's, became the most sophisticated and used analytical technique for mixtures of gases and for volatile liquids and solids. This naturally led to its counterpart: liquid chromatography or high-performance Liquid Chromatography (HPLC); preferred technique for separation of non-volatile or thermally unstable species.

This chapter will discuss planar chromatography and column chromatography in general. The more advanced techniques such as gas chromatography (GC) and high performance liquid chromatography (HPLC) will be discussed extensively in subsequent chapters.

1.2 CHROMATOGRAPHY: A SEPARATION TECHNIQUE

As mentioned previously, the objective of chromatography is to separate the various substances that make up a mixture. The applications range from a simple verification of the purity of a given compound to the quantitative determination of the components of a mixture. The chromatographic system consists of a fixed phase (stationary phase) and a moving phase (mobile phase). The mixture to be analysed or solute is introduced into the system *via* the mobile phase, and it is the affinity of the solute for one phase over the other which will govern its separation from the other components. Each component is retained to a different degree in the system and retention is based on various attraction forces. This gives rise to different modes of separation which will be presented in this chapter.

1.3 THEORY

Chromatography is the name given to methods by which two or more components of a mixture are physically separated. The chromatography system consist of a stationary phase which can be a solid or a liquid supported on a solid; and a mobile phase which flows continuously around the stationary phase. The mobile phase can be gaseous or liquid. Depending on the nature of the mobile and stationary phases, the following types of chromatography can be achieved: Gas-Solid (GS), Gas-Liquid (GL), Liquid-Liquid (LL) and Liquid-Solid (LS) chromatography.

A mixture of analytes is introduced as a solution onto the stationary phase and the mobile phase sweeps the components through it. Each analyte equilibrates or partitions between the phases in a different manner, primarily because they exhibit a different affinity for the stationary phase. Thus, each analyte has a specific equilibrium constant, and will have a different migration rate. This causes the analytes to be retained for different periods of time on the stationary phase, and to elute at different rates from the column. Each component of a mixture will be associated with a specific retention time. This type of chromatography is termed elution chromatography.

The interactions between the sample components and the mobile and stationary phases can be classified as either adsorption or absorption (also called partition chromatography). In adsorption chromatography the sample is attracted to the surface of the phase, usually to the surface of a solid stationary phase. In absorption chromatography the sample diffuses into the interior of the stationary phase. Most chromatographic separations are a combination of both adsorption and absorption phenomena.

1.3.1 Basic Chromatography Concepts

At this point, a number of definitions and concepts are required to simplify the description of the techniques reported in this chapter.

1.3.1.1 Chromatogram

A chromatogram is a graphical representation of the compounds eluting from a chromatographic system. In cases where the analytes elute off the stationary phase it is represented by a detection system response as a function of the elution time (t), or the volume of the mobile phase (V). Both time and volume can be used interchangeably on the abscissa because the flow rate (F) of the mobile phase is generally constant and $V = t\ F$. Each compound produces a peak which has a Gaussian shape. Figure 1 shows an example of a three-component chromatogram. Note that the chromatogram is quite different for planar chromatography and that it will be described in

more details in section 1.7 of this chapter. However, most of the principles discussed in this section are applicable to all types of chromatography.

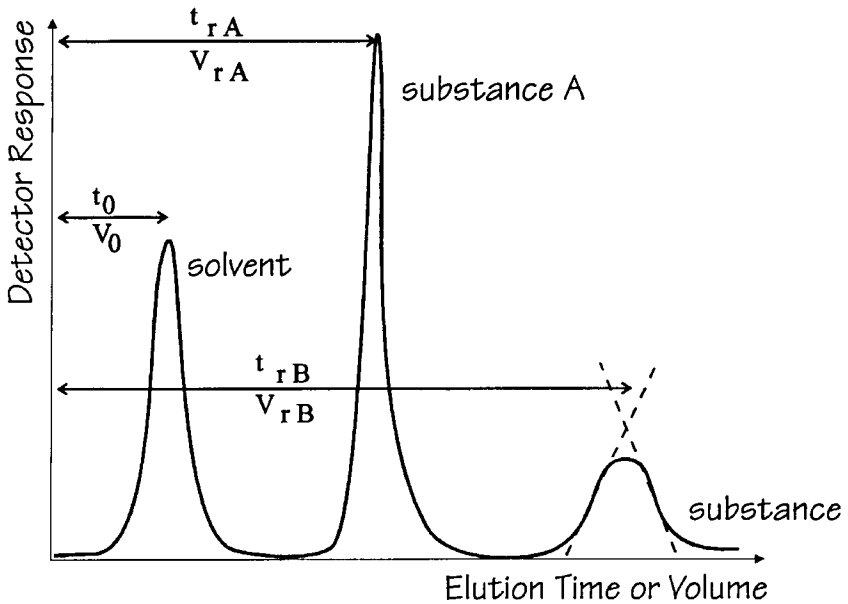

Figure 1: Chromatogram of a two-component mixture in solvent.
t_0 = time for solvent to travel through the column;
t_{rA} = retention time of substance A;
t_{rB} = retention time of substance B;
Units can also be expressed in terms of volume.

1.3.1.2 Distribution Coefficient

The distribution coefficient K (also called partition coefficient) corresponds to the distribution of the analyte (X) between the stationary (s) and mobile (m) phases, as it elutes through the column. In equation form, K corresponds to the ratio of the concentration of the analyte [X] in the stationary phase over the concentration of the analyte in the mobile phase.

$$K_X = [X]_S/[X]_m \quad (1)$$

1.3.1.3 Retention volume

The total volume of the mobile phase (V_r) required to elute an analyte is the sum of the volume of the mobile phase (V_m) and the volume of the mobile phase which flows while the analyte is held immobile ($V_S K_X$), or the tendency of an analyte to sorb on a defined amount of stationary phase.

$V_r = V_m + V_S K_X$ **(2)**

In a more practical manner, the value of V_r can be obtained from the chromatogram since

$V_r = Ft_r$ **(3)**

where F is the flow rate of the mobile phase (volume/time) and the retention time (t_r) is the time required for an analyte to elute completely through the column (from injector to detector). Similarly, V_m, also called the dead volume or interstitial volume, can be obtained from the chromatogram to give $V_m = Ft_0$ where t_0 is the time required for a solvent or non-retained molecule to traverse the column.

1.3.1.4 Capacity factor

A more practical quantity for the distribution of the analyte between the two phases is the capacity factor, k_X, which is defined by the total number of moles of x in the stationary phase over the total number of moles of x in the mobile phase

$k_X = V_S[X]_S/V_m[X]_m = V_S K_X/V_m$ **(4)**

where V_S is the volume of the stationary phase within the column and V_m is the volume of the mobile phase.

By substituting for V_r and V_m in equation (1), a simpler expression for the capacity factor is obtained:

$k_X = t_r\text{-}t_0/t_0 = t'_r/t_0$ **(5)**

1.3.1.5 Gaussian profile

All molecules of a given component do not move at an identical velocity. The centre of the elution band represents the average retention time of the analyte. Some molecules travel slower, some faster. This variation in velocity is a result of the number of sorption and desorption of the analytes and is what gives the detected signal its Gaussian profile.

1.3.1.6 Theoretical plates

The number of theoretical plates (N) is a quantitative measure of the efficiency of a column and can be obtained directly from the chromatogram:

$N = 16(t_r/t_w)^2$ **(6)**

In equation (6) t_w is the width at the base of the peak, measured in the same units as t_r. The theoretical plate model assumes the column to be made of a series of plates. The distribution of the analyte between the mobile and stationary phase occurs at each plate. Therefore, the higher the number of plates, the better the separation since more sorption-desorption cycles occur. Column efficiency can also be expressed in terms of Height Equivalent to a Theoretical Plate value (HETP or H-value):

$$H = L/N \quad \textbf{(7)}$$

This equation has the units of length since L corresponds to the column length. Thus, a column with a low H value is preferred to a high value.

1.3.1.7 Selectivity

The selectivity or separation factor (S) refer to a system's ability to distinguish between two components, and is governed by the distribution of the analyte between the mobile and stationary phases. It is also called relative retention and as S decreases towards a value of 1, the separation becomes more difficult. The only way to modify this parameter is to change one or both phases. A and B correspond to two different analytes.

$$S = t_{rB}\text{-}t_0/t_{rA}\text{-}t_0 = k_B/k_A \quad \textbf{(8)}$$

1.3.1.8 Resolution

The resolution (R) is the degree of separation between two components. In chromatography, a value of R=1 is considered the minimum value to achieve a quantitative separation and corresponds to a 2% overlap of the peak area. At R=1.5, cross-contamination is less than one percent (1%) and the peaks are considered to be at baseline separation. This kind of separation is essential in preparative chromatography where pure compounds are required.

$$R = 2\, t_{rB} - t_{rA}/t_{WA} + t_{WB} \quad \textbf{(9)}$$

By replacing equations (5), (6) and (8) in equation (9), another form of expression for the resolution is obtained.

$$R = 1/4\, N^{-1/2}\, (S - 1/S)\, (k'/1 + k') \quad \textbf{(10)}$$

This expression shows that resolution is a function of three factors which can be adjusted independently: the column efficiency (N), the selectivity (S) and the capacity (k').

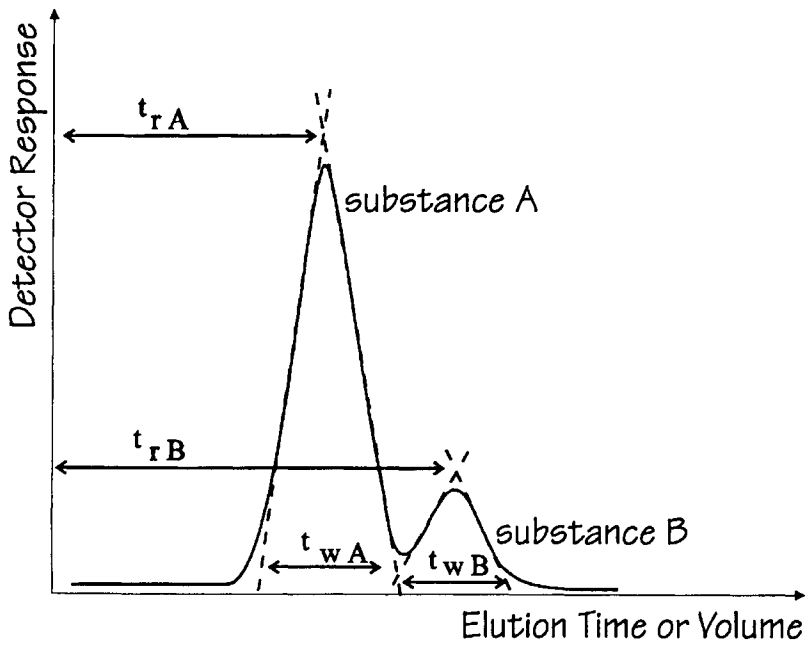

Figure 2: Chromatogram illustrating baseline separation or R = 1.5 for two substances A and B. t_r = retention time of substance; t_w = peak width at baseline for each substance.

1.3.1.9 The chromatographic compromise

Three elements interact in chromatography: resolution, analysis speed and capacity. Any one component can be improved at the expense of the others. In analytical chromatography, sample capacity is not a priority; resolution and speed are required. However, when performing preparative chromatography, sample capacity and resolution are important to obtain large amounts of pure compounds, therefore speed must be sacrificed.

1.3.1.10 Kinetic processes

Chromatography is a dynamic process. As the analyte passes through the column, concentration gradients exist and result in diffusion of the analyte. This is called the kinetic process. Another process involved during elution is mass transfer. These topics are discussed briefly in terms of the rate theory. The Van Deemter theory describes the factors contributing to band spreading in gas chromatography and how they interact. This band broadening is expressed in terms of H and is a function of the average linear mobile phase velocity μ.

$$H = A + B/\mu + C\mu \quad (11)$$

The A term corresponds to the eddy diffusion which describes the irregular flow through the packed particles in a column causing different pathways and different exit times for the solute molecules. The B term is the longitudinal molecular diffusion or random diffusion along the column. The last term C, corresponds to the mass transfer in the stationary phase. This mass transfer occurs between the mobile and stationary phase of the chromatographic system and is dependant on several factors such as particle size, column diameter and diffusion coefficient.

To apply this equation to different situations and not exclusively to gas chromatography, it needs to be modified. The rate theory was developed and showed that term A was negligible and that term C corresponds to the sum of mass transfer in the stationary phase and in the mobile phase.

$$H = B/\mu + (C_S + C_M)\mu \quad (12)$$

This equation tells us that in order to obtain a high H-value, the thickness and the particle size of the stationary phase must be small to favour mass transfer and that D_L (diffusion coefficient in the liquid phase) must be large.

1.4 PHYSICAL FORCES AND INTERACTIONS

As mentioned earlier, most chromatographic separations are a result of the interaction between adsorption and absorption phenomena. Both involve physical forces between the analyte and the phases of the chromatographic system. There is also a phenomenon called chemisorption which consists of a chemical reaction between the analyte and the stationary phase. The next few paragraphs describe the types of forces present in chromatography.

1.4.1 Ionic Interactions

Ions are present in aqueous solution and are important mainly in liquid chromatography. According to Coulomb's law, ions of the same charge are repulsed whereas ions of opposite charge are attracted. These forces are long-range and relatively strong. Ionic interactions can also take place between ions and the polar end of a dipolar molecule, and are referred to as ion-dipole forces.

1.4.2 Van der Waals Forces

Van der Waals forces are weaker than ionic interactions and include three types of interactions: dipole-dipole, dipole-induced dipole and induced dipole-induced dipole. Dipolar forces can be compared to magnetic forces where a

polar end of a molecule will attract the opposite-charge polar end of another molecule. The dipole-induced dipole phenomenon can be compared to a magnet attracting nonmagnetic iron and is dependant on the polarisability of a molecule. Larger molecules generally have greater polarisability. The last type of interaction, induced dipole-induced dipole, consist of weak forces that exist even in mono-atomic gases that are symmetrical and non-polar. At any instant, this symmetry can be distorted by the motion of the electrons of a given atom and produces a momentary polarity which can attract or will be attracted by a second polar atom in the vicinity. This will produce a net attraction. Dispersion or induced dipole-induced dipole forces can occur in all molecules and are a function of polarisability of the molecule or atom. Note that dispersion is the only force between non-polar hydrocarbons such as alkanes.

1.4.3 Hydrogen Bonding

A hydrogen bond can be formed between molecules containing a hydrogen atom bonded to an electronegative atom like oxygen or nitrogen. Some can receive and donate a hydrogen atom. This is the case for alcohols, amines and water. Other molecules such as ethers, aldehydes, ketones and esters can only accept hydrogen atoms from the previous molecules. Hydrogen bonds are relatively strong forces (5 kcal/mol) but are considered weak bonds because, as opposed to the other types of forces which are randomly oriented in space, the hydrogen bonds are directional. These forces or weak bonds are extremely important in chromatography since the surface of many stationary phase materials contain hydroxyl groups.

1.4.4 Charge Transfer

When two molecules or ions combine by transferring an electron from one to the other, the process is called charge-transfer. This process occurs mostly in gas chromatography.

1.5 MODES OF SEPARATION

1.5.1 Adsorption Chromatography

Adsorption chromatography is based on interactions between the solute and fixed active sites on the stationary phase. It is also referred to as liquid-solid chromatography (LSC). The adsorbent is generally an active, porous solid with a large surface area, such as silica gel, alumina or charcoal and can be packed in a column, spread on a plate, or impregnated into a porous paper. The active sites of the stationary phase interact with the functional groups of the compounds to be separated, thus, adsorption chromatography is well suited for separating classes of compounds. For example, silica gel (silanol groups) will interact with the polar functional groups and have little effect on

the non-polar groups. Therefore, separation of alcohols from hydrocarbons is feasible.

1.5.2 Partition chromatography

When solute molecules distribute themselves between two non-miscible liquid phases (mobile and stationary) according to their relative solubility, the process is referred to as liquid-liquid (LLC) or partition chromatography. The liquid stationary phase is uniformly spread on an inert support and the mobile phase chosen differs greatly in polarity from the stationary phase to avoid mixing. In general, the stationary liquid is polar and the mobile phase is non-polar causing greater retention of polar compounds. When the polarities of the stationary and mobile phases are reversed, the polar components elute faster and the technique is referred to as reverse-phase LLC. Because of the subtle effects of solubility differences, LLC is well suited for separating homologues and isomers. However, LLC requires a lot of care because the mobile phase must be pre-saturated with stationary phase and the system temperature must be carefully controlled to avoid stationary phase removal. Bonded phase chromatography (BPC) solved that problem by chemically reacting the stationary phase with the support and producing a very stable and efficient separation medium.

1.5.3 Ion-Exchange Chromatography

The ion-exchange chromatography (IEC) process allows the separation of ions and polar molecules. It is based on the affinity of ions in solution for opposite charged ions on the stationary phase. The stationary phase is usually a resin onto which ionic groups are bonded. Because ion formation is favoured in aqueous solutions, the mobile phase is usually a buffered aqueous solution containing a counter ion whose charge is opposite and in equilibrium with the total charge of the stationary phase. The retention of the analyte in the system is governed by the competition between the solute and the counter ion for the ionic sites on the stationary phase. This method has found application in inorganic chemistry for separating metallic ions and in the separation of water-soluble proteins, nucleotides and amino acids.

1.5.4 Size-Exclusion Chromatography

Size-exclusion chromatography (SEC) differs from the other methods in that the separation is based on physical sieving processes and not on chemical phenomena. The stationary phase is chemically inert and there is selective diffusion of solute molecules into and out of the mobile phase-filled pores in a three-dimensional network which may be a gel or a porous inorganic solid. The degree of retention is dependant on the size of the solvated solute molecule relative to the size of the pore. Smaller molecules will permeate the smaller pores, intermediate-sized molecules will permeate some pores and

large molecules will be completely excluded therefore, larger molecules will elute faster. SEC is widely used in the separation of high-molecular-weight organic compounds (polymers) and bio-polymers from smaller molecules.

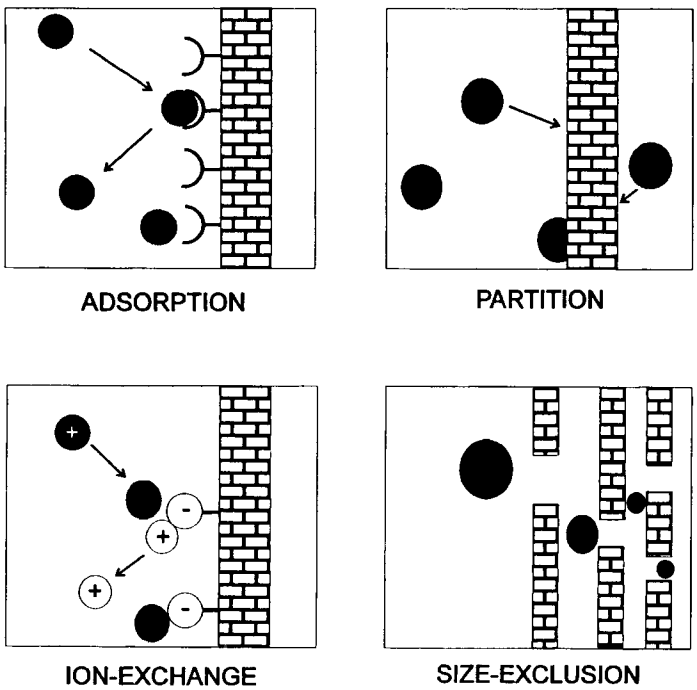

Figure 3: Visual representation of the four modes of chromatographic separation.

1.6 STATIONARY PHASES VERSUS MOBILE PHASES

As mentioned earlier, the stationary phase can be a liquid or a solid. When liquid, it can be coated directly on the inside walls of a capillary tube, or it can be coated on a inert solid support and be handled like a solid. In effect, there are three stationary phase configurations: a solid packed into a column (as in SEC), a solid coating the surface of a flat, plane material (as in thin layer chromatography - TLC) and a liquid coated on the inside wall of an open tube (LLC). The mobile phase can be a liquid (as in LC) or a gas (as in GC). Often, when the mobile phase is a liquid, a combination of liquids is used to achieve the appropriate elution characteristics. In TLC, a mixture is used throughout the elution whereas in LC, the concentration of the various liquids forming the mobile phase is gradually changed (gradient). The characteristics of a gaseous mobile phase are modified by varying the temperature of the chromatographic system.

1.7 PLANAR CHROMATOGRAPHY

1.7.1 Paper Chromatography

Paper chromatography (PC) appeared in 1943, and is the result of the work by Consden, Gordon and Martin. It is the simplest type of chromatography, and has been used quite extensively in the past. Today, paper chromatography has been replaced by thin layer chromatography for most applications. Nevertheless, it will be covered here, not only for historical reasons, but also because paper chromatography can still be very useful in certain circumstances.

1.7.1.1 Theory

Paper chromatography is actually a liquid-liquid partitioning technique. Although paper consists of cellulose, the stationary phase consists of water saturated cellulose from the water in the atmosphere. Cellulose is formed of units of anhydride glucose linked in chain by oxygen atoms. It has been suggested that the stationary phase be considered as a solution of concentrated polysaccharide. To maintain the water saturation, most solvents used in paper chromatography contain some water. Therefore, the components that are highly water-soluble or have the greatest hydrogen-bonding capacity move slower.

The degree of retention of a component is called the retardation factor (R_f) and corresponds to the distance migrated by an analyte over the distance migrated by the solvent (also called solvent front). The expression of the movement of a substance in comparison to another is the retention ratio R_r and corresponds to the distance migrated by analyte A over the distance migrated by analyte B. The R_f -value is the most commonly used term and a reasonable value for good resolution is about 0.4 to 0.8.

1.7.1.2 Technique

Paper chromatography is performed on a sheet or strips of paper (most often Whatman No. 1 or Whatman No. 3 filter paper for analytical work, and Whatman No. 3 or Whatman 3MM for preparative work). Low-porosity paper will produce a slow rate of movement of the developing solvent and thick papers have increased sample capacity. The sample is dissolved in a volatile solvent and spotted with a capillary glass tube or micro-pipet on the paper. An optimum spot diameter of 2 mm is preferable and, to achieve good separation, the maximum quantity of sample should not exceed 500 μg. The mobile phase depends on the nature of the substances to be separated. A single organic solvent saturated with water may work, but some polar compounds may require the addition of an acid, a base, or a complexing agent

to allow separation; this is called a binary system. In some cases, a ternary solvent (three components) may be required.

Separation takes place in a closed chamber using ascending or descending mobile flow. In ascending paper chromatography, the bottom of the paper is placed into the mobile phase, which flows upwards through the fibres by capillary action. In descending chromatography, the solvent is placed in a trough at the top of the developing chamber, and the paper is suspended in that trough. Some of the solvent is also poured into the bottom of the tank in order to saturate the chamber with solvent vapours. In this system, the spotted end of the paper is at the top of the tank and elution takes place towards the bottom of the tank by both capillary and gravity. It should be noted that the spots of substance to be developed should not be touching the solvent, since the analytes might dissolve in the mobile phase before elution takes place. Similar results are obtained whether the analyst used descending or ascending modes of elution, it is mainly a choice of personal preference.

1.7.1.3 Detection

Typically, development of a paper chromatogram takes anywhere from 2 to 4 hours. Once elution is finished, the paper is removed from the tank, and the solvent front is marked where the solvent has stopped using a pencil line or by tearing the paper on each side where the solvent has stopped. The paper is then dried in a fume hood and location of the substances can be observed. When the substances are coloured, a visual detection is simple, but when they are invisible, they may be detected using physical or chemical methods. If a compound fluoresces, it can be detected under an ultraviolet lamp; if it is labelled (radioactive), it can be detected by an appropriate counter or scanner. The chemical methods consist of reacting the compound with a reagent to produce a coloured product, e.g., hydrogen sulphide will convert metallic ions into coloured sulphides, amino acids can be revealed using ninhydrin dissolved in acetone, and silver nitrate solution will react with reducing substances such as sugars. All these reagents can be applied to the chromatogram either by dipping the paper in the solution or by spraying it. Heat may be required to complete the reaction. A hair dryer or hot plate can be used as a source of heat.

It is possible to obtain reproducible and accurate quantitative results in PC using standardised conditions. The following measurement techniques can be used: visual comparison of the spots, physical measurements of coloured spots using transmission reflectance or fluorescence, radioactivity and spot-area measurement. Spot removal which consists of cutting or scraping the spot from the paper, and extracting the compound is followed by analysis using other techniques such as spectroscopy.

In cases where separation is difficult, two dimensional chromatography can be performed. It consists of developing a square sheet of paper subsequently in two directions, perpendicular to each other using different mobile phases.

Paper chromatography is usually used for highly polar compounds such as sugars, amino acids and natural pigments. Some advantages of paper chromatography are: a small amount of sample is required, a high level of resolution, ease of detection and simplicity of the apparatus.

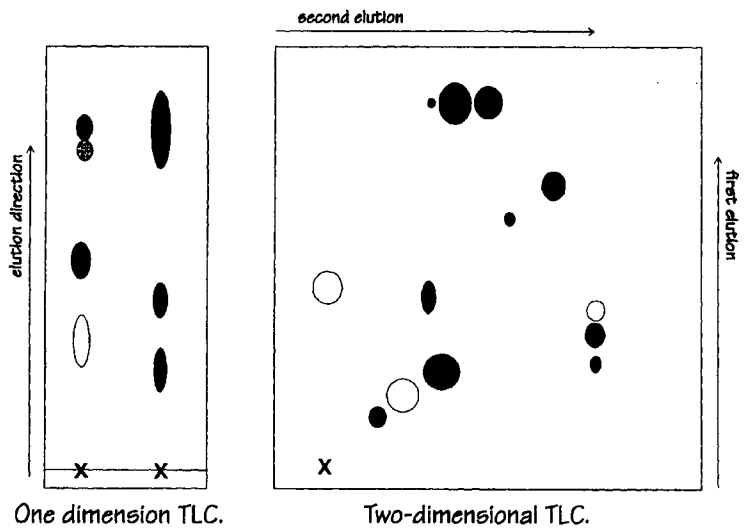

Figure 4: Schematic representation of one and two dimensional thin layer chromatography (TLC). Dotted lines represent solvent front; X is where the sample was spotted.

1.7.2 Thin Layer Chromatography

Complementary to paper chromatography, but used more frequently because of the wide availability of stationary phases, is thin layer chromatography (TLC). It is simple, fast, reproducible and can achieve high resolution. It is usually performed on a square plate or on strips. A variation of this type of planar chromatography is carried out on a rotating circular plate using an instrument called a Chromatotron.

1.7.2.1 Theory

TLC is considered a solid-liquid partitioning technique. Most plates consist of a glass, aluminium or polyethylene plates which can be coated with a variety

of materials such as silica gel, alumina, cellulose, polyamides and reversed bonded-phase coatings. The plates can be easily prepared by spreading a slurry made of powder and solvent on a plate and air dried. For analytical work, the thickness of the layer is 0.2-0.3 mm whereas for preparative work which involves large amounts of analytes and solvents, it varies from 2 to 10 mm. The commercially available plates are more expensive, but the quality of the coating is more consistent. As in PC, the development solvent used depends on the materials to be separated, thus the determination of the appropriate solvent or mixture of solvents is made by trial and error. The retardation factor and retention ratios described in the paper chromatography section also apply to TLC. The technique only became popular around 1956 when E. Stahl devised a convenient spreader for TLC plates [2].

The ideal way to optimise thin layer chromatography (plate and eluent) when there is no previously performed experiment described in the literature is by evaluation of the properties of the analyte and comparison with available materials. Then, a series of systems has to be tried out. As an example, nine types of plates and eight eluents and their various mixtures, were studied to optimise the separation of coloured pigments of paprika (*Capsicum annuum*). Both adsorption and reversed phase TLC were studied. The best separations were achieved by using acetone as organic modifier on impregnated diatomaceous earth support. Hydrophilic fractions were separated using acetone-water (85-15) whereas hydrophobic fractions required acetone-water in a different proportion (95-5). The presence of tetrahydrofuran (THF-acetone-water, 15:75:10) in the eluent mixture also lead to good separation efficiency [3].

1.7.2.2 Technique

Common plates used are 20*20 cm in size. For screening purposes, microscope slide plates are also used. The mixture or sample is applied using a glass capillary or a micro-pipet. The diameter of the spot ranges from 2 to 5 mm. The ascending technique, where the solvent migrates in a vertical fashion along the plate through capillary action is the most common. The inner wall of the tank is often covered with chromatography paper in order to saturate the tank with solvent. Saturation of the tank should be carried out one hour before running the plate in order to ensure the solvent has reached an equilibrium. In choosing a solvent, the elutropic series is generally recommended as the starting point. It is comprised of hexane, carbon tetrachloride, benzene or toluene, chloroform, diethylether and ethanol.

Development of a chromatographic plate takes between 20-30 minutes for a 10 cm distance as compared to approximately 2 hours for paper. Like PC, the solvent front is marked and the plate is allowed to dry.

1.7.2.3 Detection

If the compounds are colourless, visualisation has to be made using physical of chemical detection methods similar to the ones used for PC. A variation of UV revelation consists of adding a fluorescent indicator (such as a mixture of zinc and cadmium sulphide) to the adsorbent as the plates are coated; the whole plate fluoresces and the compounds present quench this fluorescence and produce dark spots on the plate. The most common chemical reagent is iodine. The vapour from its crystals reacts with all organic compounds (except saturated hydrocarbons and alkyl halides) to form brown or yellow complexes. The spots have to be marked immediately as the iodine sublimes off the plate and the colour fades. Another method previously discussed is the use of UV light to reveal spots. Several other chemical methods are available, to name a few: dilute solution of silver nitrate forms silver halides with alkyl halides, concentrated sulphuric acid chars most organic functional groups, 2,4-dinitrophenylhydrazine reacts to form yellow and orange spots with aldehydes and ketones, ferric chloride reveals phenols, and bromocresol green reacts with carboxylic acids. The list is endless. Some of the more recent detection methods involve electrochemical detectors and, is obviously, applicable for electrochemically active compounds. The technique is based on the voltammetric detection of the solute at a platinum micro-wire electrode during TLC plate development. The resulting current is measured and compared against a calibration curve. The method is rapid, selective and relatively inexpensive [4].

A review of the applications of thin layer chromatography for the analysis of foodstuff was written by Sherma [5]. A book entitled "TLC, Reagents and Detection Methods" is an extensive review of the available physical and chemical TLC revealing agents [6].

As in PC, two dimensional TLC is often performed to resolve complex mixtures. Again, quantitation is relatively difficult because of the various parameters involved: nature of the adsorbent, nature of the mobile phase, temperature of the system, amount of sample used, vapour-pressure equilibrium between the plate and the development chamber atmosphere. A brief review of instrumentation which can be used to standardise these parameters and recent advances in thin layer chromatography was published by Touchstone [7]. Some chromatography tips can help to resolve TLC contamination problems, these include: yellow band or streak at or near the solvent front, unexpected sample component tailing and drastic reduction in fluorescence intensity with fluorescent plates were briefly discussed in the May 1992 issue of American Laboratory [8]. The advent of computer-controlled scanning densitometers allowed reliable qualitative and quantitative determination of analytes. Aflatoxins in sunflower oil seed crops were analysed and the results were satisfying enough for routine work, allowing any harmful concentration of aflatoxins to be detected [9].

Preparative TLC is still very much in use as a preliminary separation technique when there is interference of peaks in mixtures to be analysed by GC or HPLC. An example of this is the characterisation of the double-bond configurations of fatty acid methyl esters derived from hydrogenated soybean oil and margarine which required preparative TLC using silver nitrate/silica gel coated plates to separate the mixture prior to GC analysis [10].

A variation of preparative thin layer chromatography is centrifugal chromatography and one of the first commercial instruments produced is the "Chromatotron". A round glass disk of approximately 30 cm in diameter is coated with a chosen adsorbent and mounted on a rotor. As the plate turns, solutions of samples and solvent are delivered to the system. A solvent gradient is recommended and upon elution, it forms concentric bands of separated substances which leave the edge of the plate. Each fraction is collected and UV sensitive compounds are detected as separation occurs. This type of instrument is designed for preparative separations on silica gel and alumina and is not recommended for cellulose or reversed phase sorbents [11]. The major advantages of the Chromatotron is that it does not require as much solvent as column chromatography, the set up is easy and the analysis time is reduced. Today, the technique is referred to as rotation planar chromatography (RPC) and includes variations to the Chromatotron method which are described in a brief review by Nyiredy and co-workers [12].

Thin layer chromatography is not a thing of the past as commented by Sherma [13]. A possible reason why planar chromatography is not as widely used as liquid chromatography is the lack of education of young scientists as they are only familiarised with some of the paper/TLC techniques using iodine or UV as detection methods. One of the greatest advances in TLC is high performance TLC or HPTLC. In a typical HPTLC experiment, sample and standard solutions are applied to a 10 x 10 cm high performance silica gel plate of 200 μm thickness using mechanical or automated spot or band applicator. The mobile phase is optimised and chromatograms are produced by horizontal, multiple, or over-pressure development. The separated zones are detected and quantified using an automated densitometric scanning device to observe natural visible absorbance, UV absorbance or fluorescence.

Multiple development was traditionally performed manually. It consists of repeated developments of a plate in the same direction with the same solvent over the same distance. The result is narrower bands and improved resolution and detection sensitivity. The R_f values become very precise and are adequate enough for identification. A variation of this method is automated multiple development (AMD) and shows promising future. The HPTLC/AMD method was used to monitor phenylureas, carbamates and triazines in drinking water. HPTLC can also be performed using polar modified stationary phases to separate pesticides in various foodstuffs such as triazines in corn, asparagus, tomatoes, grapes and potatoes [14].

For the reader interested in staying up to date with TLC, the Journal of Planar Chromatography, first published in 1988, is a good source of information. Two books are also suggested for the reader who wishes to study planar chromatography in greater depth. The first one discusses planar chromatography, from the basics to instrumentation and computer-aided methods [15]. The second book concentrates on TLC and describes sample preparation, sample application, phases selection, visualisation, quantitation, special techniques and combined methods such as TLC-GC, TLC-IR and TLC-MS. It also contains a useful list of suppliers for TLC instrumentation and equipment [16].

1.8 COLUMN CHROMATOGRAPHY

Column liquid chromatography is actually the parent of all the other types of chromatography. As stated previously, this is the type of set-up used by Tswett as he pioneered into the field of chromatography. The technique he used is now called classical open-column liquid chromatography or simply LC.

The physical apparatus required to do LC is fairly simple. A glass tube referred to as the chromatographic column is packed with a filling consisting of the adsorbent. The liquid which is passed through the column is called the chromatographic solvent or elution solvent. If a coloured substance is placed into the column and left to migrate down the column under the influence of the solvent, coloured zones will appear. This series of zones is termed the chromatogram. In situations where the eluted substance is not coloured, the chromatogram can not be observed and has to be monitored using a physical or chemical revealing technique or by screening the aliquots eluting from the column using TLC. By carefully adjusting a few parameters, almost any mixture of analytes can be separated. Some important parameters include the adsorbent chosen, the polarity of solvent(s), size of column (length and diameter) and rate of elution. The choice of adsorbent and solvent is governed by rules similar to those for TLC. A polar adsorbent will have better retention capabilities for a polar analyte whereas the polar analyte will elute more quickly when the adsorbent is non-polar. It is necessary to optimise the different polarities of the adsorbent/solvent combination in order to allow for maximum separation of the analytes. A system comprising of a polar stationary phase and a non-polar mobile phase is considered a normal-phase LC system and the opposite situation is called reverse-phase LC or RPLC. A more complete list of available packing materials can be found in commercial catalogues.

The column size and amount of adsorbent must be selected as a function of the amount of material to be chromatographed. As a general rule, the amount of adsorbent is 25-30 times, by weight, the amount of material to be analysed and the column has a height-to-diameter ratio of about 8:1. For example, a 1g sample will require 30g of adsorbent in a 130mm long column

with a 16-mm diameter. The degree of difficulty of separation is also an important factor in choosing the column. The above conditions might be modified to increase resolution and analysis speed. Finally the flow rate of the solvent is significant in the effectiveness of the separation: the mixture to be separated has to remain on the column long enough to allow an equilibrium between the stationary and the mobile phases. Because they may be overloaded and eluted extensively, the classical columns are the most suited for preparative work [17]. HPLC - the subject of chapter 2 - is a modification of classical LC and uses shorter column characterised by a smaller diameter packed material of smaller diameter.

Performing classical LC is a simple process. Porous metal frit or glass wool is placed at the bottom of the column and the column is filled with sorbent until it is full. The slurry method involves slowly pouring a mixture of sorbent and solvent into a column half filled with solvent. Gently tapping the sides of the column ensures an even packing free of air bubbles and will produce better chromatography. One should never let the column dry during packing. Another technique called the dry packing method can also be used and involves packing the sorbent while it is dry and moistening the column afterwards. It is not recommended for use with silica gel or alumina since they produce a lot of heat during solvation and will result in uneven packing, air bubbles and cracking. In general, gravity is sufficient to force the liquid through the column but, with column packing of less than 100 μm diameter, a small pump can be used to accelerate the process.

Before use, the column should be conditioned by washing it with a series of solvents. The sample is then solubilised in a small amount of solvent (usually the first elution solvent) before injection on the column. In the event that compounds of different polarities are to be eluted, more than one solvent might be required in the elutropic order, less polar solvents first followed by more polar ones. When the same solvent is used to elute the mixture, the process is isocratic whereas when an increase or decrease in solvent polarity is required, it is called solvent gradient elution. Aliquots are then collected as they exit the column. If the mixture contains coloured compounds, the various bands can be monitored visually and collected individually. Different methods can be used to monitor colourless compounds. The first procedure consists of collecting fractions or aliquots of constant volume in pre-weighed flasks, evaporating the solvent and re-weighing flask plus any residue. A graph of weight versus fraction number can be plotted to determine the amount and the number of components present in the mixture. Another method is to mix an inorganic phosphor into the column adsorbent and when illuminated by UV light, the column fluoresces. However, many solutes have the ability to quench the fluorescence and a dark band will appear allowing the separation to be followed visually. Finally, TLC can be used to monitor the eluted solvent at regular intervals.

The rest of this section describes techniques arising from modification of the classical LC principle.

1.8.1 Liquid-Solid Chromatography (LSC)

LSC is mainly an adsorption process but a complicated one because the molecules of the mobile phase compete with analyte molecules for the active sites on the solid surface and silica is energetically heterogeneous. The stationary phase will become polar since any water present in the system will adsorb in multiple layers. Therefore, covering the surface with a monolayer of water can improve the efficiency of the system. Apart from these difficulties, the technique is still popular for preparative work. The mobile phase has to be of proper polarity, low viscosity, compatible with the detector and volatile enough if the analytes are to be recovered by evaporation of the mobile phase. The solvent(s) can be used in isocratic and gradient elution modes. The latter has the advantage of performing better separation of the components in a mixture but requires a lot of solvent and time to re-equilibrate the column to its original polarity. Open-column chromatography using activated MgO and diatomaceous earth (1:1 ratio) is used to conduct the determination of carotenes and xanthophylls in dried plant materials (grass, yellow corn, amaranth) and mixed feed. This packing, using hexane-acetone (90:10) or hexane-acetone-methanol (80:10:10) mixtures as eluents, was found to be better than silica gel as the adsorbent because it prevents degradation or irreversible adsorption of the analytes [18].

1.8.2 Liquid-Liquid Chromatography (LLC)

Separation in LLC arises from the partitioning of analytes between two immiscible liquids, one being held immobile on a stationary solid support and the other one being the mobile phase. This process is also called partition chromatography. To achieve this, one phase has to be polar (often the stationary) and the other has to be non-polar. LLC requires that the mobile phase be pre-saturated with the stationary phase to avoid stripping the latter. The technique operates with a fairly limited number of solvent combination and is limited to compounds with comparatively low partition coefficient as the stationary phase must be a good solvent for the sample but a poor solvent for the mobile phase. Obviously, in LLC, solvent programming or elution gradient is ruled out. However, LLC is a very useful technique since it can resolve minute differences in the solubility of the solutes. Since the activity coefficients (thus partition coefficient) of members of a homologous series vary with molecular size, selecting solvents with very different polarities will magnify these small differences and separation will be achieved. This is one of the main advantages of LLC over LSC since the latter cannot discriminate compounds which are so similar in polarity.

A few variations of LLC can be performed. One of them is rotation locular counter-current chromatography or RLCC. It consists of a series of columns (*e.g.* 16 in the case of the Eyela model RLCC-A) [19] interconnected in series by Teflon™ tubing. The columns (in vertical position) are filled with the stationary phase, then, the mobile phase displaces half of the stationary phase (system in horizontal position). The sample is introduced in the system *via* a sample loop and the mobile phase is pumped through the system at a typical flow rate of 1-2 mL/min. An optimum angle for the system is about 30°. The column assembly rotates along the length of the column axis at speeds between 20 and 100 rpm. Chromatography can be performed in ascending mode where the stationary phase is lighter than the mobile phase or in descending mode where the stationary phase is the heavier component. RLCC is a complement to the DCCC (droplet counter current chromatography) technique. Although the number of theoretical plates is less in RLCC than is DCCC, it can accommodate larger amounts of material and can be operated with a larger number of solvents, meaning relatively non-polar compounds can be separated. Furthermore, it is possible to perform gradient elution in RLCC.

The DCCC process is based on the partitioning of solutes between a steady stream of droplets of mobile phase and a column of surrounding stationary phase. Each drop represents more or less one theoretical plate. The system consists basically of 200 to 600 vertical columns of narrow bore glass (20 to 60 cm by 1.5 to 2 mm id) interconnected in series by Teflon tubes. A flow rate of 10 mL/hr (much slower than RLCC, producing more theoretical plates) is used for the mobile phase. The sample and the mobile phase are introduced at the bottom of the first tube (ascending mode when mobile phase is lighter than the stationary phase). At the end of the first capillary tube, the droplet is transferred to the next tube *via* the Teflon connection and new droplets are generated.

DCCC is indicated for preparative scale of polar compounds as it is fast and uses a small amount of solvent. A paper by Hostettmann reviews the application of DCCC in natural products isolation. Some of the compounds separated included saponins, diterpenoids, xanthones, sugars, alkaloids, lipids and peptides. DCCC is efficient and reproducible. The main difficulty resides in choosing the appropriate solvent system to allow for good droplet formation [20]. The technique is also useful for unstable compounds because the polar phase is often acidified. For example [21], anthocyanins from black currents and raspberries were successfully separated using DCCC in both analytical and preparative chromatographic modes. It was found that a BAW mixture consisting of n-butanol-acetic acid-water (4:1:5) was the most efficient. The separation of less polar anthocyanins is obtained in descending mode whereas the ascending mode favours the more polar compounds.

1.8.3 Bonded-Phase Chromatography (BPC)

The difficulties encountered in LLC can be overcome by the use of chemically bonded stationary phases or bonded-phases. Most bonded phases consist of organochlorosilanes or organoalkoxysilanes reacted with micro-particulate silica gel to form a stable siloxane bond. The conditions can be controlled to yield monomeric phases or polymeric phases. The former provides better efficiency because of rapid mass transfer of solute, whereas the polymeric phases provides higher sample capacity. BPC can be used in solvent gradient mode since the stationary phase is bonded and will not strip. Both normal-phase BPC (polar stationary, non-polar mobile) and reversed-phase BPC (non-polar stationary, polar mobile) can be performed. The latter is ideal for substances which are insoluble or sparingly soluble in water, but soluble in alcohols. Since many compounds exhibit this behaviour, reversed phase BPC accounts for about 60% of published applications. The main disadvantage of silica bonded phases is that the *p*H must be kept between 2 to 7.5. However, bonded phases with polymer bases (polystyrene-divinylbenzene) can be used in the *p*H range of 0 to 14.

One application is the analysis of bio-polymers which is conducted under mild conditions to avoid denaturation of the component. In this case, water is used as the mobile phase. However, many non-polar bonded phases are too hydrophobic to be used with water alone, therefore, supports prepared by bonding C_{18}, C_8, C_5 or phenyl ligates to Sepharose or polyamide coated silica have been developed. This type of chromatography is called hydrophobic interaction chromatography (HIC). The hydrophobic interaction between bio-analytes and the stationary phase is increased at high ionic strengths, thus, by decreasing ionic strength gradient, gradient elutions can be achieved.

Normal-phase BPC is found to be the preferred technique in many applications. The separation of PAHs according to the number of condensed rings (up to four rings) using a diamino column and a heptane mobile phase was achieved with normal phase BPC. Separation of alkanes from lipids and of saccharides from steroids, and fat-soluble vitamins is done efficiently by BPC. Reversed-phase (RP) BPC is performed using a hydrophobic stationary phase and a polar mobile phase (water mixed with methanol or acetonitrile). It is an extremely popular technique because non-ionic, ionic and ionisable compounds can often be separated using a single column and mobile phase, the column is relatively stable, the solvents inexpensive and readily available. In RP-BPC, the elution order is often predictable as retention time increases with the hydrophobic character of the solute. Finally, columns equilibrate rapidly, meaning faster sample turnaround.

1.8.4 Ion-Exchange Chromatography (IEC)

IEC is applicable to ionic compounds, ionisable compounds such as organic acids or bases, and to compounds that can interact with ionic groups (chelates or ligands). It is very useful to separate any charged particle such as proteins, nucleotides and amino acids. The stationary phase has charge-bearing functional groups and the mobile phase contains a counter-ion, opposite in charge to the surface ionic group in equilibrium with the resin in the form of an ion pair. When a solute ion of the same ionic charge is present, the following equilibrium takes place:

Cation exchange: $X^+ + R^-Y^+ \Leftrightarrow Y^+ + R^-X^+$
Anion exchange: $X^- + R^+Y^- \Leftrightarrow Y^- + R^+X^-$

where X is the sample ion, Y the mobile phase ion (counter-ion) and R is the ionic site (fixed ion) on the column. Desorption is then brought about by increasing the salt content or by altering the *p*H of the mobile phase. Common ion-exchangers contain diethylaminoethyl (DEAE) or carboxymethyl (CM) groups.

When performing classical IEC, a number of items are important and need to be considered such as the selectivity of the resin, the nature of the counter-ion and its concentration and the *p*H of the mobile phase. The most commonly used stationary phase or resin is the cross-linked styrene/ divinylbenzene copolymer where appropriate acidic or basic functional groups (strong and weak) are placed on the phenyl rings. The counter-ion is important when selecting a resin because if it is too strongly retained on that resin, no other ion will be able to displace it. For cation resins, monovalent ions are less retained than divalent cations. Li is less retained than H, Na, NH_4, K, Rb, Cs, Ag, Tl. Those ions being monovalent, are also less retained than UO_2, Mg, Zn, Co, Cu, Cd, Ni, Ca, Sr, Pb, Ba in increasing order of strength. For anions, the least retained ion is F^-, followed by OH^-, acetate, formate, Cl^- SCN^-, Br^-, chromate, nitrate, I^-, oxalate, sulphate, and citrate. Commonly used resins are in the chloride form for anion and hydrogen form for cation. The counter-ion in the mobile phase will also affect the partition ratios; thus, gradient elution by modifying the *p*H can be used to increase the analysis speed. Classical IEC in open column was found useful in the separation of amino acids which, upon exit of the column, were reacted with coloured ninhydrin and detected in a flow-through colorimetric detector. However, it is a slow process and the resolution is not very good.

Modern IC uses high efficiency ion-exchange materials and continuous flow through detection after removing the ions that cause the mobile phase to a have a high conductivity at the detector. It consists of a fast, highly efficient resin which has about one-tenth to one-thousandth the sample capacity of the old polystyrene resin. The new method, simply called ion chromatography

(IC) uses a low-capacity column combined with a conductivity detector. Its most frequent application is the determination of trace anions in aqueous solution. Here is how, in suppressed mode IC, the separation of two simple anions is accomplished. Basic mobile-phase buffers are first used to separate the anions in the separator column. The mobile phase then flows through a high-capacity cation-exchange column called the suppressor column, which contains a hydrogen form resin. The mobile phase is then converted into a low-conducting weak acid and the sample ions to highly conducting, fully ionised acids. Its main advantage is the reduction of the total ionic content of the mobile phase which allows the measurement of sample anions in a weakly conducting buffer. The main inconvenience is that, eventually, the resin becomes exhausted and needs to be regenerated. Peak broadening is also observed with the presence of a second column. IC can also be performed in non-suppressed mode by having the mobile phase going directly to the conductivity cell. Although simple to perform and the absence of band broadening, the method makes it difficult to measure small amounts of sample ions in such a highly conducting medium. Other detectors such as UV can be used and eliminate the necessity for a suppressor column. A salt gradient can be used to improve the resolution and decrease analysis time. Common buffers include tris-phosphate and acetate compounds.

Phytate or inositol hexaphosphate is a potential source of phosphorus present in many grains and seeds. The phytic acid is determined by treating the sample with EDTA and separation and quantitation using anion-exchange column (resin AG 1-X8 and eluent 0.8M NaCl) followed by reaction with a solution of ferric sulfosalicylate. The coloured complex can be observed in the UV range at 300 nm [22].

1.8.5 Ion-Pair Chromatography (IPC)

The most common type of IPC is the reverse phase mode. It is used for separating ionic or ionisable compounds through the formation of neutral ion pairs in solution. Its main advantage over IEC is that it facilitates the analysis of samples that contain both ion and molecular species. In IPC, ionic species are not retained much and *p*H is used to control the partition ratios by modifying the degree of ionisation. Two mechanisms have been proposed to explain the results of IPC. The first one assumes that the ion pairs are formed in the mobile phase and behave as non-ionic fragments similar to other polar molecules. The other claims that counter-ions selectively sorb in the stationary phase and attract and retard the analyte ions by an ion exchange mechanism. As IPC is practised, a bonded reverse phase separation is usually the first system tried. If required, an ion pair reagent (the charge on the reagent being in opposite charge to the analytes) which will increase analyte partition ratios can be added. The use of ion pair reagent can also improve a chromatogram by increasing the retention times and improving the peak shapes. The main disadvantages of IPC are that

ionic solutions are often corrosive and reduce column life, they often absorb in the UV and the silica based supports are limited to *p*H values below 7.5.

Another form of ion chromatography is ligand exchange chromatography where a cation exchange resin is used to separate analytes that can form coordination complexes with the metal attached to the resin.

Ion-exchange chromatography involves more variables than other forms of chromatography. Distribution coefficients and selectivities are functions of *p*H, solute charge and radius, resin porosity, ionic strength and type of buffer, type of solvent and temperature. The number of experimental variables makes IEC a very versatile technique but a difficult one because of the effort needed to optimise a separation.

One recent application in IEC consists of solid phase extraction disks which are used to eliminate matrix interference prior to analysis. The disk contains a membrane composed of resin beads enmeshed in a PTFE membrane, housed in a polypropylene housing. The resin is treated to remove specific ions such as H^+ to remove hydroxide, Ag^+ for excess halides and Ba^{2+} to remove sulphate. Other disks such as hydroxide for acid removal and neutral styrene-divinylbenzene to eliminate hydrophobic components which can damage resin based IC columns are being developed [23].

A summary of the applications of ion chromatography in the analysis of foods can be found in one of the Journal of Chromatography Library [24]. The same volume also describes in great detail the principles of ion chromatography.

1.8.6 Size-Exclusion Chromatography (SEC)

Gel filtration, gel-permeation chromatography and molecular sieve chromatography are part of a more general technique called size-exclusion chromatography. Originally, gel filtration applied to a technique using dextran gels to separate biochemical polymers using aqueous mobile phases. The name gel permeation chromatography appeared when separation of synthetic organic polymers on polystyrene gels using non-aqueous mobile phases took place. The term size-exclusion is the preferred term and the older terms should be discarded. This technique is mostly used for separating and characterising substances of high molecular weight. The molecules are separated according to their size, the principle being a physical sieving process, not one of chemical attractions and interactions.

The stationary phase consists of materials with different pore sizes and the molecules permeate the phase as they elute. The mobile phase solely serves as a carrier for the analyte as it does not induce any chemical interaction. In SEC, small molecules penetrate the porous structure more easily than large

ones, thus, large molecules elute first. The separation occurs in decreasing order of size. Although the molecular weight is usually relative to the size of the molecule, configuration of the molecule is also important. The technique is primarily used for large molecules such as proteins, peptides, nucleic acids and carbohydrates.

Looking at equation (2):

$$V_r = V_m + V_s K_x \qquad \textbf{(2)}$$

the partition coefficient takes a slightly different meaning when applied to size exclusion. V_m is referred to as the void volume and V_s as the total pore volume. In a true permeation process, if all pores were accessible to a small solute molecule, the distribution of the analyte in the stationary phase X_s would equal the distribution in the mobile phase X_m and the partition coefficient K_x would be equal to 1. If all analyte molecules are excluded from the pores, $X_s=0$ and $K_x=0$. Intermediate-sized molecules have access to various portions of the pore volume, therefore, $0<K_x<1$. This is the process which usually takes place in SEC. The components are identified using a prepared molecular weight versus retention time calibration curve.

A popular material for gel chromatography is Sephadex (cross-linked polymeric carbohydrate) which is used for separating large molecules such as proteins, nucleic acids, enzymes and carbohydrates. The more cross-linking, the smaller the "hole" size in the stationary phase. The mobile phase consists of water or an aqueous solution. The hydroxyl groups on the polymer can also adsorb water and cause the material to swell. In some instances, some of the hydroxyl groups have been alkylated and the material can swell under both aqueous and non-aqueous conditions. Other types of gel consist of polyacrylamide polymers (Bio-Gel P and Poly-Sep AA) or cross-linked polystyrene and polyvinylacetate. Those are considered semi-rigid gels and will swell to 1 to 2 times their dry volume. The more rigid materials, such as porous glass or porous silica beads, do not swell at all, but salt gels (polydextran-Sephadex or agarose) swell many times their dry volume. A drawback of these soft gels is their limited compressibility to low column-inlet pressures. Rigid hydrophilic gels and controlled-pore-size glasses can withstand higher pressures. The rigid silica-based packing of 5-10 μm average particle size are now in current use in many laboratories. Typical mobile phase buffers consist of ammonium formate, ammonium carbonate, pyridinium formate, ammonium acetate, pyridinium acetate to which a salt is added to avoid non-specific adsorption.

Since the columns are defined in terms of their molecular-weight exclusion limits, it might be necessary to connect as many as eight columns in series to perform a separation. With non-aqueous mobile phases, polystyrenes with

known narrow molecular-weight ranges are used whereas with aqueous mobile phases, soluble dextrans or polyethyleneoxides are employed.

Aside from separating high molecular weight molecules ranging between *e.g.*, 2 000 and 2 000 000 daltons, such as proteins, nucleic acids and polysaccharides, SEC can be used to determine the average molecular weight and the molecular-weight distribution of polymers. Polymers usually consist of units comprised in a distribution range of molecular weights.

High performance SEC coupled with detection by refractive index and viscosity was used to characterise citrus pectins having varying degrees of methylesterification (DM). In water, high methoxy pectins undergo a sequential size expansion with decreasing concentration. Citrus pectins are broad molecular weight distributions of pectic substances that contain a mixture of thermodynamically stable and metastable aggregates [25].

1.9 DETECTORS

The number of detectors used in LC is quite limited. The three most popular being: ultraviolet absorption (UV), refractive index (RI) and molecular fluorescence emission. Other detectors used in LC are thoroughly discussed in an earlier review [26].

UV is the most popular detector but has limited usage and is not universal as not all compounds absorb in that range. Current instruments can be set at specific wavelengths but care must be exercised in the choice of solvent to be used since some solvents are not transparent to UV. The new photo-diode array instruments are very useful because they can acquire a full spectrum and data manipulation can be performed to aid in the detection of unresolved peaks at one specific wavelength.

Refractive index is a universal technique but its sensitivity is weaker than UV by about three orders of magnitude. In deflection RI, a beam is shone on the reference and sample cells and the difference in RI is measured. When an analyte is present in the sample cell, the beam is deflected and the difference in RI is no longer zero. The Fresnel type RI is based on the principle that the fraction of light reflected at a glass-liquid interface is proportional to the angle of incidence and the relative refractive indices of the substances. The detector then responds to the varying intensity of the light striking it. The main disadvantages of the RI detector are its relative lack of sensitivity and that it cannot be used when solvent gradients are used as eluents. However, its universality makes it ideal for SEC.

Fluorescence detectors are generally about 100 times more sensitive and more selective than UV detectors. The most interesting designs use a laser as

the excitation source. The latter can be focused on a very small area and a sample volume as small as 1 nL is sufficient to produce a good signal.

Other less popular and still developing detectors include the electrochemical detector. The acronym used is LCEC. It is an amperometric method and when it operates at high current efficiency it is called coulometric. The term polarographic is used when the electrode is mercury. Electrochemical applications are discussed in more detail in Chapter 8.

1.10 PREPARATIVE LIQUID CHROMATOGRAPHY (PREP LC)

Today, LC is often used as a preparative separation tool. It is used to remove unwanted matrix interference from samples, to isolate a synthesised compound from its reaction mixture or to separate one specific chemical form of a chiral natural product using a large column which allows the separation of large amounts of material. Preparative LC is usually used for samples ranging in size from a few hundred milligrams up to several grams. The operation can be performed in low and high pressure modes. Operation under gravity flow up to several hundred kPa of pressure is considered low pressure. A review of the various packings and stationary phases available for prep LC was compiled by K.K. Unger and R. Janzen [27]. In summary, the quality of the stationary phase can be affected by the bed stability and flow resistance, chemical resistance and purity, solute accessibility, mass and biological recovery, fouling, regeneration and cost. Adsorption type packings offer a high selectivity combined with adequate laudability whereas ion exchangers and affinity media are best suited for bio-polymers because of their high selectivity and high sample capacity.

Sample clean-up can be done rapidly using a short LC column operated under gravity flow or under vacuum, centrifuge or syringe pressure. The most popular phases include silica and bonded phases. Disposable and inexpensive columns are available and can be found under the following trade names: Sample Enrichment and Purification, PreSep Extraction, Bond-Elute, and solid-phase extraction. For example, purification of sulfamethazine in milk by SPE followed by quantitative analysis by TLC has been described earlier [28] and a study comparing Fluorisil and silica Sep-Paks as a means of separating chlorinated hydrocarbon pesticides from soybean oil has shown that Fluorisil gave the best recovery [29].

Low pressure LC is very similar to the experiment performed by Tswett. A variety of stationary phases can be used and relatively large particle sizes are needed to keep the pressure drop low and facilitate packing. The ideal mobile phase should be inexpensive and volatile to facilitate sample recovery. The eluent is collected in separate tubes using an automated fraction collector. Since the samples often contain a lot of impurities, the column is very likely to be contaminated. Cleaning can be achieved by rinsing with solvents or

discarding the packing material. The second alternative is probably less expensive considering the cost of solvents and waste disposal. The technique can be called Medium Pressure LC when a pump is used to pressurise the solvent reservoir and force the analytes out of the column.

A variation of low pressure LC is performed using a column of dry packing. The column consists of a Nylon tube containing the stationary phase and with a hole at the bottom. The sample and mobile phase are introduced as a mixture and the flow is stopped before the eluent can exit the column. The column is then sliced and each section is screened for analytes using a revelation technique and extracted when required. This method has the advantage of allowing the handling of larger samples.

Flash chromatography is a quick preparation technique that is, in effect, a hybrid between medium pressure and short column chromatography. It uses a short, fat column (*e.g.*, 1-5 cm i.d. x 45 cm) packed with silica gel and filled with solvent. Compressed air is used to compress and remove the air from the solvent which then elutes quickly. The sample is then added and the column filled again. Pressure is adjusted to achieve a separation in 5-10 minutes. It is a fast and inexpensive method for the preparative separation of mixtures requiring only moderate resolution. Use of 40-63 μm silica gel and a pressure driven flow rate of 2.0 in/min are essential for successful separation [30].

High Performance Prep LC is another variation of prep LC and is discussed in more detail in Chapter 2.

1.11 SPECIAL TOPICS

Pseudo-Phase or **Micellar LC** is obtained by using an aqueous micellar solution which contains a surfactant as the mobile phase. The stationary phase is bonded and non-polar, hence reverse-phase separation occurs. The mobile phase is conferred special properties and allows unique selectivity. The technique is inexpensive and produces low amounts of toxics since small volumes of organic solvents are required. The amounts of solvent are small enough that micellar chromatography can be coupled with Inductively Coupled Plasma-Mass Spectrometry (ICP-MS) for the detection of organotin compounds [31]. Further information is available in an earlier review on this specific topic [32].

Affinity Chromatography is performed on a unique stationary phase which has a specific bio-active ligand bonded onto a solid support. It is mostly used with bio-molecules and only the active component of a sample is attracted to the stationary phase (*e.g.*, wheat germ lectin for polysaccharides and soybean trypsin inhibitor for proteases). The remaining chemicals are washed off and

the analyte is eluted with the appropriate solvent. A more thorough discussion of this technique can be found in available books [33, 34].

A synthesised stationary phase called internal surface reverse phase (ISRP) or Pinkerton column appeared in 1985 [35]. The packing material operates with two mechanisms, size exclusion and reverse phase bonded sorption. The outside walls of the bead are non adsorptive whereas the small inner channels consist of the ISRP. The size exclusion part cleans up the sample to remove large proteins which tend to clog the reverse phase column and the ISRP allows small analyte molecules to penetrate and be separated.

High Performance Liquid Chromatography (HPLC), Gas Chromatography (GC) and Supercritical Fluid Chromatography (SFC), and Electrophoresis, are topics covered in details in Chapters 2, 3, and 9, respectively. Consequently, they are not discussed further in this chapter.

1.12 FUTURE TRENDS

Interesting advances have been made in TLC such as: an automated development chamber which improves reproducibility, a cutting technology which can be used with pre-coated plates, a densitometer for quantitative evaluation of plates, as well as new computerised application databases [36]. TLC plates are getting smaller in size (surface) which leads to an increase in elution speed and to a decrease in solvent consumption.

Sample preparation using SPE is important for removing interference and concentrating the analytes. Automated systems to perform that procedure are being developed and increase reproducibility. New cartridges are being developed: such as exchange resins for isolation of DNA, RNA and high capacity silica particles for large samples. New stable bonded phases are being developed and increase sample loading, resolution and analysis time.

The continued concern over various residues and additives lead to more efficient and rapid testing methods. Conventional chromatographic testing will be replaced by a 2-tiered approach involving rapid on the spot screening (bio-sensor, immunoassay or portable GC) followed by confirmation by conventional methods. More selective detectors such as mass spectrometry (MS), tandem MS-MS and Fourier Transform infra-red will be used and sample preparation will be improved by using SPE, new extraction technologies, and laboratory robotics [36].

1.13 SUMMARY

This chapter has shown that there are basically two types of chromatography: development, which consists of paper and thin layer, and elution, which

utilises columns. Table 1 emphasises the main differences between paper, thin layer and column chromatography.

TABLE 1
Main Features of Paper, Thin Layer, and Column Chromatography

Paper	Inexpensive, easy to quantitate, difficult to reproduce because of variation in fibres, susceptible to chemical attack
Thin Layer	Economical for routine use, detection instrumentation allows better quantitation, automation allows good reproducibility, variety of solvents available
Column	Good preparation tool, can be quantitative and qualitative, selective, non-destructive and efficient with very small samples, wide applications range

TABLE 2
Examples of Compounds Analysed by Various Types of Chromatography

Matrix	Analyte	Chromatography	Method of Detection	Refs
Animal tissues (liver or muscle)	Sulfonamide	TLC - silica gel	Fluorescence	[37]
Corn, Peanuts &, products, Coconut Cocoa beans, Eggs	Aflatoxins- B_1, B_2, G_1, G_2, M_1	TLC - silica gel	Fluorescence and/or Rf comparisons or UV	[38-47]
Food	Colour additives	Column (cellulose) SolkaFloc BW 40) OR C-18	Spectrophotometric	[48, 49]
Non-alcoholic beverages	Non nutritive sweeteners	TLC - silica gel H	UV (254 nm) OR spay (chromogenic agent)	[50]
Bread	Volatile acids	Paper	Spray (chromogenic reagent	[51]
Vanilla extract	Vanilla resins	Paper	UV	[52]
Soybean and	Crude Lecithin lipids and phospholipids	Chromatotron	Spray (1% $Ce(SO_4)_2$) (w/v) in 10% aq. H_2SO_4	[53]

1.14 APPLICATIONS TO FOOD ANALYSIS

As demonstrated throughout this chapter, chromatography can be used for qualitative and quantitative determination of various food constituents. Following appropriate extraction procedures for the matrix under consideration, the analytes can be separated and then be analysed by various chromatographic modes using different media. The literature is full of good examples in this regard. Table 2 lists some of these applications. Different types of chromatography are reported for a whole diversity of food matrices. This table is by no means exhaustive. It is used here as an indication of the multitude of possibilities offered by the chromatographic field for food analysis. For detailed procedures and other applications, the reader is referred to the "Official Methods of Analysis, Association of Official Analytical Chemists, Agricultural Chemical; Contaminants; Drugs, Kenneth Helrich (Ed.) Vols. 1 and 2, 15th Edition (1990) [37].

1.15 GENERAL BIBLIOGRAPHY

1. J. M. Miller, Chromatography, Concepts & Contrasts, John Wiley & Sons, USA, 1988.

2. G. D. Christian and J. E. O'Reilly, Instrumental Analysis, Allyn & Bacon, USA, 1986.

3. Pavia *et al.*, Introduction to Organic Laboratory Techniques, 2nd edition, Saunders College Publishing, USA, 1982.

4. Abbott and Andrews, An Introduction to Chromatography, Houghton Mifflin Company, Boston, 1965.

1.16 REFERENCES CITED

1. L. S. Ettre, *Amer. Lab.* January 1992, pp 48C-48J and references therein.

2. E. Stahl, *Pharmazie* 11 633 (1956).

3. T. Cserhati, E. Forgacs, and J. Hollo, *J. Planar Chrom.* **6**, Nov/Dec 472 (1913).

4. I. Smalera and I. F. Cheng, *Microchemical Journal* **47,** 182 (1993).

5. J. Sherma in "Food Analysis - Principles and Techniques, Vol. 4, Separation Techniques", D. W. Greenwedel and J. R. Whitaker (eds), Marcel Dekker Inc., Chap. 5, pp. 297-363 (1984-87).

6. H. Jork, W. Funk, W. Fischer, and H. Wilmer, Thin Layer Chromatography, Reagents and Detection Methods, VCH, New York, 1990.

7. J. C. Touchstone, *J. Chromato. Sci.* **26**, 645 (1988).

8. K. Palmer and F. Rabel, Planar Chromatography Background Contaminants: Some Causes and Cures, *Amer. Lab.* May 1992, p. 28BB-28DD.

9. I. Drusany *et al., J. Planar Chomato.* 4,490 (1991).

10. M. M. Mossoba *et al.*, J. Agri. Food Chem. **39**, 695 (1991).

11. Harrison Research, Instruction Manual, Chromatotron Model 8924, Palo Alto, CA, 1990.

12. S. Nyiredy *et al., J. Planar Chromato.* **2**, 53 (1989).

13. J. Sherma, *J. Assoc. Off. Anal. Chem. Int.* **75 (1)**,15 (1992).

14. H. E. Hauck, M. Mack, S. Reuke, and H. Herbert, *J. Planar Chromato.* **2**, 268 (1989).

15. R. E. Kaiser, Chromatographic Methods: Planar Chromatography, **Vol. 1,** Heuthig Verlag, Germany, (1986).

16. J. C. Touchstone, Practice in Thin Layer Chromatography, 3rd Edition, J. Wiley & Sons, U.S.A., (1992).

17. J. E. Conaway, *J. Assoc. Off. Anal. Chem.* **74 (5)**, 715 (1991).

18. B. H. Chen and S. H. Yang, Food Chemistry (Analytical Methods Section), Elsevier Science Publishers, UK 61 (1992).

19. R. P. Instrumentation Inc., RLCC-A Instruction Manual, Montréal, QC, Canada, (1986).

20. K. Hostettmann, *Planta Medica* **39 (1)**, 1 (1980).

21. G. W. Francis and O. M. Anderson, *J. Chromatog.* **283**,445 (1984).

22. K. D. Bos, C. Verbeek, C. H. Peter van Eeden, P. Slump, and M. G. E. Wolters, *J. Agric. Food Chem.* **39**, 1770 (1991).

23. R. Saari-Nordhaus, L. M. Nair, and J. M. Anderson Jr., Elimination of Matrix Interferences in Ion Chromatography using Solid Phase Extraction Disks, PittCon '93, Atlanta, GA, U.S.A.

24. P. R. Haddad and P. E. Jackson, Ion Chromatography: Principles and Applications, Elsevier, The Netherlands, 593 (1990).

25. M. L. Fishmen, D. T. Gillespie, S. M. Sondey, and R. A. Barford, *J. Agric. Food Chem.* **37**, 584 (1989).

26. H. G. Barth, W. E. Barber, C. H. Lochmuller, R. E. Majors, and F. E. Regnier, *Anal. Chem.* **58**, 211R (1986).

27. K. K. Unger and R. Janzen, *J. of Chromatogr.* **373**, 227 (1986).

28. J. Unruh, E. Piotrowski, D. P. Schwartz, and R. Barford, *J. Chomatogr.* **519**, 179 (1990).

29. R. E. Sapp, *J. Agric. Food Chem.* **37**, 1313 (1989).

30. W. C. Still, M. Kahn, and A. Mitra, *J. Org. Chem.* **43 (14)** 2923 (1978).

31. H. Suyani, D. Heitkemper, J. Creed, and J. A. Caruso, *Appl. Spectros.* **43**, 962 (1989).

32. M. F. Borgerding and W. L. Hinze, *Anal. Chem.* **57**, 2183 (1985).

33. H. Schott, Affinity Chromatography: Template Chromatography of Nucleic Acids and Proteins, Academic Press, New York, (1984).

34. P. Mohr and K. Pommerening, Affinity Chromatography, Marcel Dekker, New York, (1985).

35. I. H. Hagestam and T. C. Pinkerton, *Anal. Chem.* **57**, 1757 (1985).

36. R. Stevenson, *Amer. Lab.*, May, 28C (1992).

37. "Official Methods of Analysis", Association of Official Analytical Chemists, Agricultural Chemical; Contaminants; Drugs, Kenneth Helrich (Ed.) Vols. 1 and 2, 15th Edition (1990).

38. G. M. Shannon and O. L. Shotwell, *J. Assoc. Off. Anal. Chem.* **62**, 1070 (1979).

39. O. L. Shotwell and C. E. Holaday, *J. Assoc. Off. Anal. Chem.* **64**, 674-677 (1981).

40. R. M. Eppley, L. Stoloff and A. D. Campbell, *J. Assoc. Off. Anal. Chem.* **51**, 67 (1968).

41. A. E. Waltking, *J. Assoc. Off. Anal. Chem.* **53**, 104 (1970).

42. M. E. Stack, *J. Assoc. Off. Anal. Chem.* **57**, 871 (1974).

43. Peter M. Scott, *J. Assoc. Off. Anal. Chem.* **71**, 70-76 (1988).

44. P. M. Scott, *J. Assoc. Off. Anal. Chem.* **52**, 72 (1969).

45. P. M. Scott and W. Przybylski, *J. Assoc. Off. Anal. Chem.* **54**, 540 (1971).

46. F. J. Bauer and J. C. Amstrong, *J. Assoc. Off. Anal. Chem.* **54**, 874 (1971).

47. M. W. Trucksees, L. Stoloff, W. A. Pons Jr., A. F. Cucullu, L. S. Lee and A. O. Franz Jr., *J. Assoc. Off. Anal. Chem.* **60**, 795 (1977).

48. *USDA Bull.*, 1390, Suppl. 1 (1930).

49. Mary L. Young, *J.Assoc. Off. Anal. Chem.* **71 (3),** 458-461 (1988).

50. T. Korbelak, *J. Assoc. Off. Anal. Chem.* **52**, 487 (1969).

51. J. A. Young, G. Schwartzman and A. L. Melton, *J. Assoc. Off. Anal. Chem.* **48**, 622 (1965).

52. J. Fitelson, *J. Assoc. Off. Anal. Chem.* **43**, 600 (1960); **45**, 250 (1962).

53. S. Bergheim, K. E. Malterud and T. Anthonsen, *J. Lipid Res.* **32**, 877 (1991).

This Page Intentionally Left Blank

J.R.J. Paré and J.M.R. Bélanger (Editors)
Instrumental Methods in Food Analysis

Chapter 2

High Performance Liquid Chromatography (HPLC): Principles and Applications

Jacqueline M. R. Bélanger (1), J. R. Jocelyn Paré (1), and Michel Sigouin (2)

1) Environment Canada, Environmental Technology Centre, Ottawa, ON, Canada K1A 0H3, and 2) Agriculture and Agri-Food Canada, Laboratory Services Division, Ottawa, ON, Canada, K1A 0C6

2.1 INTRODUCTION

High Performance Liquid Chromatography (HPLC) was developed in the early 1960's. Today it has grown into an essential tool for the modern analytical laboratory and it has replaced gas chromatography (GC) for a variety of analyses. HPLC is a technique that is usually covered in undergraduate courses devoted to instrumental analytical methods. In its applications to food analysis, the technique has gained increased acceptance mainly because it met two basic factors, namely: i) the need for a wide range of rapid analyses for nutrients; and ii) the need for methods that can be easily automated. In spite of those notable advantages, the integration of HPLC in the food laboratory has been slow compared to other areas like pharmaceutical chemistry and forensic toxicology. This might be due to factors such as the complexity of the matrices found in most food systems and the very low levels at which many of the components of interest are found in foodstuffs. However, today a multitude of analyses performed by HPLC exist and are recognised by the Association of Official Analytical Chemists. The technique certainly holds a promising future for food analysis.

2.2 RANGE OF APPLICATIONS

A noteworthy feature of HPLC is that it is often suitable for organic compounds that are too unstable or insufficiently volatile to be amenable to gas chromatography analysis without prior derivatisation. It is suited for the separation of a wide range of chemicals, including pharmaceuticals, foods, heavy industrials and biochemicals. The number of published HPLC analytical methods these days is so large that a literature search is likely to provide a set of chromatographic conditions for almost any type of compounds. Alteration of these conditions to suit the matrix involved might be the only required step for the food scientist to perform a HPLC analysis of a new compound.

In food science, HPLC has been applied to several categories of substances: carbohydrates, lipids, vitamins, additives, synthetic colourings, natural pigments, contaminants (degradation products, pesticides, or naturally occurring substances), as well as amino acids and others [1]. Due to space limitations in this text, all of these classes will not be covered, but a limited number of specific examples will be presented. Other applications can be found in recently published books and journals.

2.3 THEORY OF LIQUID CHROMATOGRAPHY

This section will describe briefly the parameters that can be adjusted in the laboratory in order to optimise the technique. For a more elaborate description of the separation theory of chromatography, the reader is referred to the appropriate chapter in this book; the following references are also suggested [2-4].

To a certain extent, HPLC remains an empirical science. Therefore, the ability and experience of the operator are quite certainly the most useful guidelines to decide on the chromatographic conditions to be used, as will be exemplified further.

2.3.1 Basic Principles

HPLC is a form of liquid chromatography, where separation (or partition) occurs between a mobile phase (the solvent) and a stationary phase (the column packing). It is the ability with which the sample constituents will distribute themselves between the two phases that will effect the separation. Depending on the nature of the stationary phase, the separation process can be of four different modes:

i) adsorption chromatography, where the separation is based upon repeated adsorption-desorption steps;

ii) partition chromatography where the separation is based on partition between the mobile and the stationary phase;

iii) ion-exchange chromatography where the stationary phase is made up of an ionic surface of opposite charge to that of the sample; and

iv) size exclusion chromatography where the sample is separated according to its molecular size through a column filled with a material having precisely controlled pore size.

Adsorption chromatography is the most widely used and, in practice, we refer to two modes of action, depending on the polarity of the two phases:

Normal phase chromatography, where the stationary phase is polar in nature (*e.g.*, silica or alumina) and the mobile phase is non polar (*e.g.*, hexane). In this mode, polar samples are retained more strongly by the column therefore allowing elution of non polar compounds first.

Reversed-phase chromatography, where the stationary phase is non-polar in nature (*e.g.*, hydrocarbon) and the elution solvent (or mobile phase) is polar (*e.g.*, water or methanol). This being the exact reverse of normal phase chromatography, non-polar compounds will be retained longer on the column [5].

To change the polarity of the mobile phase, a mixture of solvents can be used to elute the compounds. When composition of such a solvent mixture remains constant throughout the elution step, it is referred to as an **isocratic** elution. On the other hand, when the composition of the solvent mixture is varied during the course of the elution step, we are using a so-called **gradient** elution.

Diffusion of molecules in a solvent will depend on the nature of the molecules and on the nature of the solvent. Two important factors are the size of the molecules and the viscosity of the solvent. The analyst has no control on the size of the molecules, but should always choose the solvent that has the lower viscosity. For example when facing the choice between methanol (viscosity = 0.54 cP at 25°C) and ethanol (viscosity = 1.08 cP at 25°C), methanol should be chosen.

Table 1 is a summary of the modes of liquid chromatography and the basis on which retention takes place. Also indicated in the table are the various types of column packing and the functional groups which are the active sites.

In an ideal separation, all the peaks are separated as shown in Figure 1 and the resolution is defined by equation (1):

TABLE 1
Various Types of Chromatography

Mode	Type of Retention	Functional Groups	Column Packing
Adsorption	Polarity	-Si(OH)-O-Si(OH)-	Silica gel
Partition (solubility)	Polar interaction	NH_2; CN	Bonded phase - normal
	Non-polar hydrophobic interactions		Bonded phase - reverse
		Dimethylsilane	RP-2
		Octylsilane	RP-8, C-8
		Octadecylsilane	RP-18, ODS
Ion-Exchange	Charge	Sulfonic acid	Strong cation exchanger
		Quaternary amine	Strong anion exchanger
		$-NH_2$	Weak anion exchanger
Size-exclusion	Molecular size	Sulfonated divinyl benzene	Aqueous gel
		Divinylbenzene	Organic gel
		Silica gel	Controlled pore silica
		Porous gel	Controlled pore glass
Chiral	Optical activity		
Affinity	Biological activity		

$$R_s = 2(t_{R2} - t_{R1})/(w_{b1} + w_{b2}) \quad (1)$$

where:

R_s = resolution of the sample
t_R = retention time
w_b = peak width at the base of each peak equivalent to 4 σ, σ being the standard deviation in a normal distribution curve *i.e.*, obtained by drawing tangents to the inflection points as shown in Figure 1.

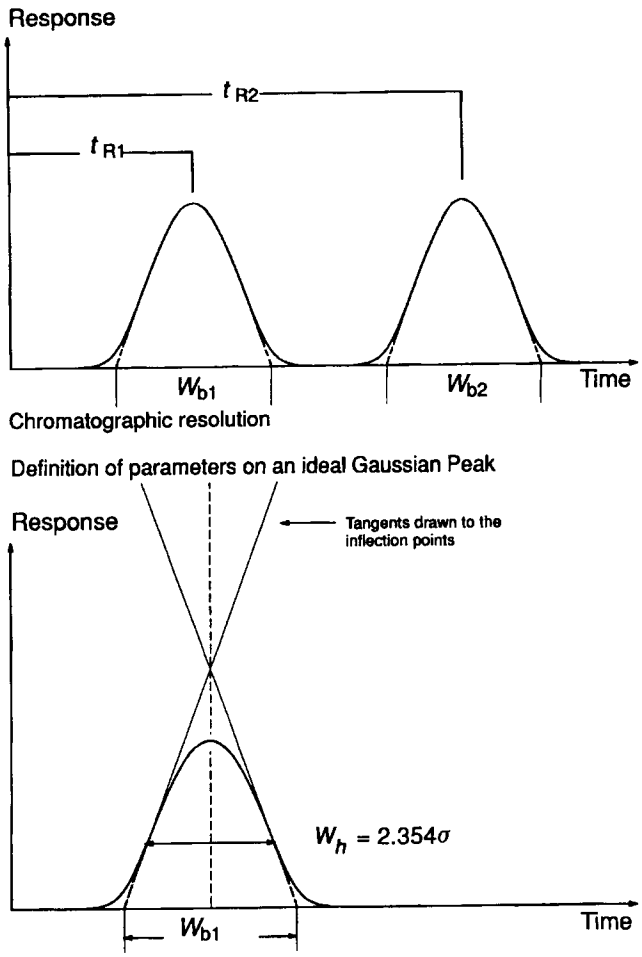

Figure 1: Definition of **top trace)** chromatographic resolution and **bottom trace** of parameters for an ideal Gaussian peak.

The narrower the peaks will be, (*i.e.*, the smaller w_b) the better the separation. The ability to achieve narrow peaks is what has made HPLC such a powerful technique. The peak width (the standard deviation) is an indication of peak sharpness and of the number of theoretical plates. Sharpness of peak reflects how good a column is. The sharper the peaks, the more sample components can be separated in a given time.

The separation is influenced by thermodynamic and kinetic factors. The retention times are dependent on a thermodynamic control while the reduction in the peak widths are dependent on kinetic factors.

The dynamic equilibrium of the constituents in the two phases (liquid and solid) is governed by the distribution factor **K**, defined in equation (2):

$K = C_s/C_m$ **(2)**
where:

K = distribution coefficient
C_s = concentration of sample in the stationary phase
C_m = concentration of sample in the mobile phase

The equilibrium can also be characterised by the capacity factor (also called capacity ratio) **k**, as in equation (3):

$k = a_s/a_m$ **(3)**

where:

k = capacity factor
a_s = amount of sample in the stationary phase
a_m = amount of sample in the mobile phase

In practice we should try to get k greater or equal to 3 for the first peak of interest in the chromatogram. This is to make sure that it is separated from the solvent and impurities; and obtain a k value not higher than k = 10-15 for the other peaks because if higher, then the analysis would take too much time.

Expressing the amounts of sample (a) in terms of the concentrations and volumes leads to equation (4):

$k = C_sV_s/C_mV_m$ **(4)**

The capacity factor, K (equation (2)), can be related to the equilibrium distribution constant by the ratio V_s/V_m, known as the phase ratio (ϑ) (equation (5)):

$k = K \,.\, V_s/V_m = K\,\vartheta$ **(5)**
Expressing this factor in terms of the mean residence times ($\bar{t}$) of the sample molecules in the stationary and mobile phases leads to equation (6):

$k = \bar{t}_s/\bar{t}_m$ **(6)**

The larger the value of k, the longer the time the molecules spend in the stationary phase. The mean proportion of time spent by the sample molecules in the mobile phase (R) then becomes, equation (7):

$R = \bar{t}_m/\bar{t}_m + \bar{t}_s = 1/1 + k$ **(7)**

By analogy, if we relate this to the relative migration rate of the sample band down a chromatography column (see chapter on chromatography), this expression then becomes:

$R = u_{\text{sample band}}/u_{\text{mobile phase}} = 1/1+k$ **(8)**

where:

$u_{\text{sample band}}$ = velocity of sample band
$u_{\text{mobile phase}}$ = velocity of mobile phase

The velocities, u, are inversely related to the elution times of the sample band, t, and an imaginary band with zero retention, t_o, therefore leading to equation (9);

$t/t_o = u_{\text{mobile phase}}/u_{\text{sample band}}$ **(9)**

Combination of equations 8 and 9 gives equation (10);

$k = (t - t_o)/t_o$ **(10)**

where:

t = retention time of the sample
t_o = the mobile phase hold up time

Hence, here we use the retention time (t) instead of the retention volume; and instead of the interstitial volume, we use the mobile phase hold up time t_o to represent the time needed for the mobile phase molecules to travel from the front to the end of the column at a given flow rate (sometimes called "solvent front", as in thin layer chromatography).

Retention times are directly affected by the temperature of the column. Therefore it is essential to maintain a constant column temperature during the whole analysis, in order to achieve reproducibility. A minor variation in the retention time might not affect the qualitative analysis of a sample but will most likely provide a false answer for a quantification analysis due to band broadening.

An ideal HPLC curve is a linear isotherm leading to symmetrical Gaussian peaks as depicted in Figure 1. Quite often, tailing peaks are encountered in a chromatogram; they are due to the difference in active chromatographic sites on the column. Fronting peaks are also encountered but to a much lesser

extent. Variations in sample loading on the column (and hence concentration increase) will result in non-linear isotherm curves.

Column performance or column efficiency is measured in terms of the number of theoretical plates (N) for a particular column. This is an important factor to consider when comparing columns. Hence, equation (11):

$N = (t_R/\sigma)^2$ **(11)**

where N = plate number

Rewritten in terms of baseline peak widths (see Figure 2) equation (11) converts to equation (12);

$N = 16(t_R/4\sigma)^2 = 16\ (t_R/w_b)^2$ **(12)**

Assuming an ideal Gaussian distribution, this can now be rewritten as:

$N = 5.545\ (t_R/w_h)^2$ **(13)**

where w_h is the width at half height

When comparing columns, the plate height (H) is simply defined as the column height per plate (known also as the height equivalent to a theoretical plate (HETP)):

$H = L/N$ **(14)**

where L = column length.

2.4 THE MOBILE PHASE - The solvent

The choice of the solvent will depend on the nature of the operation mode, *i.e.*, isocratic or gradient elution (and, of course, on the solubility of the sample in the chosen elution medium). The polarity for such an elution medium can, therefore, vary from buffered aqueous solutions to hydrocarbons. The chosen medium (including water) needs to always be very pure. HPLC grade solvents are commercially available and should always be used. The choice of a gradient eluent is always done by trial and error, usually starting with a single solvent and increasing the concentration of the second mobile phase component by usually using an initial mixing rate of 2% per minute to achieve the desired conditions in the mobile phase. In some circumstances, up to 3 different solvents can be used. However, this is not generally the case since getting the right gradient solvent is not easy due to parameters such as viscosity, and changing the detector's response when it is a ultraviolet or

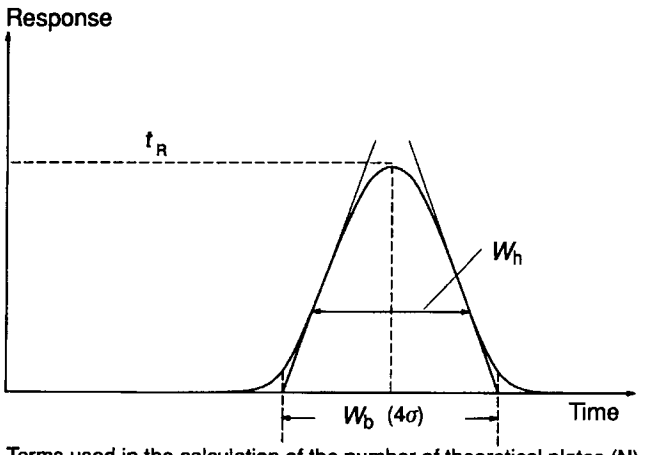

Figure 2: Definition of terms used in the calculation of the number of theoretical plates.

refractive index (see the theory section). Nevertheless, in an automated system, a third solvent is used at times to flush "clean" the column after the analysis has been performed and when the column is to be stored away for a period of time exceeding a few hours.

In choosing the mobile phase the following points must be kept in mind; the proper eluting strength and polarity, a low viscosity, a compatibility with the detector, and finally, whether the solvent needs to be removed from the analyte after the analysis has been performed. If it does, then this solvent should be easily removable by evaporation without significant analyte loss.

It is a good practice to always degas the solvent before using it. This can be achieved in a variety of ways: by applying heat, vacuum or ultrasound, or by purging with an inert gas such as helium. The latter is preferred, since continuous degassing can be performed throughout the experiment. Amongst the problems encountered when solvents are not degassed we note: air bubble formation in the pumps, eventually leading to the loss of solvent flow; bubbles formation at the column outlet, where high pressure is released, and thus leading to severe disruption of the chromatogram; or baseline drift because of dissolved air (as with a refractive index detector for example).

2.5 INSTRUMENTATION

Figure 3 shows the major components of a HPLC system. These are the reservoir(s) for the mobile phase(s), the pump(s), a solvent gradient and

solvent flow programmer, a sample inlet fitted with an appropriate filter and a loop, a column, sometimes a column oven, a detector, a recorder, and almost invariably, an integrator. Automatic injectors, sample carousels and collectors are also commonly used. A brief description of each of these components is given in this section.

2.5.1 The Injector

A few methods are used to inject the sample onto the column, the simplest one being a direct injection with a micro-syringe. But most systems will use sampling devices. The most common way of injecting the sample on the column is an injection valve in which the sample is injected into a holding loop. Loops are designed to inject a specific volume onto the column, usually of the order of 10 to 20 μL for an analytical column.

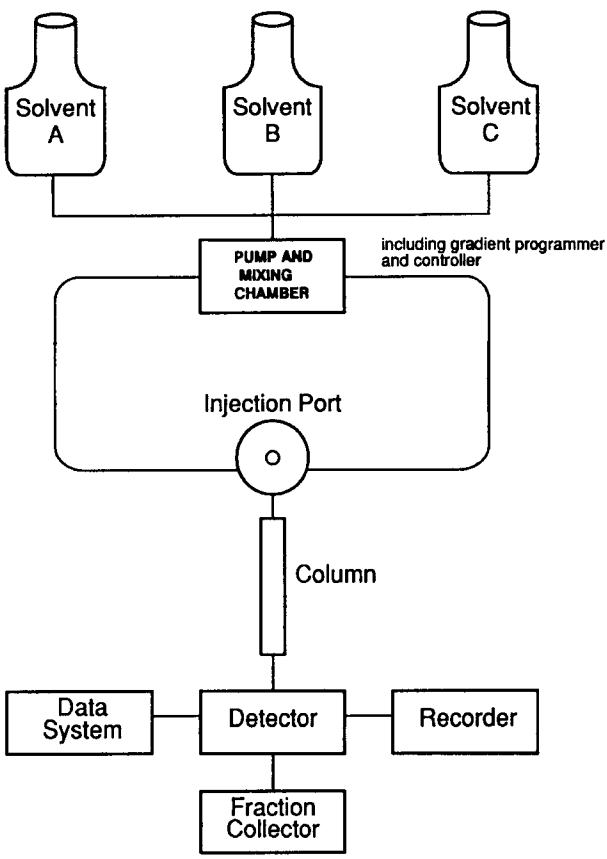

Figure 3: Schematic depicting the main components of an HPLC system.

2.5.2 The Stationary Phase - The column

Two of the most important steps in the development of an analytical method are the selection of the separation mode and the appropriate column packing. The columns most commonly encountered have an internal diameter (i.d.) of 4.5 to 5 mm and are 10 to 25 cm in length; they are packed with stationary phases having 5 to 10 Tm in diameter. Usually made of stainless steel, the compressing end fittings of the columns are of various designs. Column packing is very important for chromatography resolution. Nevertheless, particle size cannot be reduced to less than 3 μm. Even then, only short columns can be used, otherwise resistance to solvent flow increases and pressure rises too high. There is also a limit to the number of theoretical plates (N) one can achieve. Another difficulty is that it is more difficult to pack a long column efficiently. Joining columns together does not appear to produce an additive effect in terms of plate numbers. This is due to problems associated with thermal gradients which develop across the column diameter as a result of the increased pressure required (and diffusion problems occurring between the columns, no matter how small the inter-column volume is).

The chemical composition of the stationary phase encountered in columns are of the following types: silica, styrene-divinylbenzene, polysaccharides and other polymers, as well as diatomaceous earths. The C_{18}, NH_2, SugarPak™ and silica column of packing of 5 μm and 20-25 cm in length are the ones most commonly used in food laboratories, performing about 95% of the work.

The choice of the column type will naturally vary with the application. The various types of separation will depend on the column packing and the type of interactions required, as indicated in Table 1.

In choosing a type of separation over another for a given sample, we must consider the following parameters: its molecular weight, its solubility, its polarity, and its ionic character (or lack thereof). We must also look at methods that were previously reported in the literature for this type of compound. These characteristics can be found for most compounds in a reference book such as the Merck Index [6].

Most HPLC separations are carried out at room temperature. In special circumstances column temperature needs to be changed. This can be done by water jackets, column ovens or heated metal blocks.

If handled properly, columns can have a long lifetime and quite often can be regenerated by passing a series of solvents of increasing eluting strength through them, followed by a similar elution but in the reverse order. For a normal phase column the following sequence can be used: hexane, methylene

chloride, methanol, methylene chloride, hexane. For a reverse phase column acetonitrile is routinely used. About 20 column volumes of each solvents are used at very high flow rate.

The most important steps one can take in protecting an HPLC column are filtration of solvents, filtration of sample solutions, the use of an additional pre-column filter and/or a guard column, replacing end frits and part of the packing, gentle handling, keeping connecting fittings clean, not over tightened, and storing them well capped in an appropriate solvent. It is also a matter of selecting appropriate fittings and tubing. "Zero dead volume" fittings and tubing are most desirable; they will affect separation quality resulting in peak broadening and to possible diffusion in "large" volumes. Even an excellent column, with high plate counts, cannot be any better than the other components!

2.5.3 The Pump

The pumps are electronically controlled to regulate pressure and flow rates within narrow limits. A programmer is normally used to regulate the delivery of a solvent mixture of fixed (isocratic) or changing composition (gradient). It is important to maintain the pumping system so that the solvent flow is constant during the analysis. A change in solvent flow will influence the retention times as noted earlier, and therefore induce errors in the identification of the sample. Reproducibility in chromatograms of standards and samples is essential.

Modern analytical HPLC pumps are capable of pumping flow rates as low as 1 or 10 μL/min up to 5 or 10 mL/min. Since the efficiency in separation increases as the flow decreases, flow rates are generally maintained low.

2.5.4 The Detector

The detector can be considered as the "soul" of a HPLC system. Connected to the outlet end of the column, its role is to monitor the column effluent in real time. Detectors can be the most sophisticated and expensive component of the system. Classification of detectors is of two sorts, selective detectors which give different responses depending on the molecular structure of the sample under analysis, or universal detectors, for whom the response is similar for most compounds. Absorbance and fluorescence detectors are termed selective detectors, while the refractive index (RI) is a "universal detector". The Ultraviolet-Visible (UV-Vis) detector is more selective and sensitive, being able to detect amounts as low as 10^{-10}g/mL, while the RI detector's sensitivity is in the range of 10^{-7}g/mL. Therefore selective detectors can be used to minimise interference from unwanted components. As for fluorescence detectors, their sensitivity is in the range of 10^{-13}g/mL for

selected compounds. The sensitivity of a detector is defined as the ratio of detector response to the sample concentration.

HPLC detectors can absorb in three different optical absorption regions:

Ultraviolet (UV): 190-400 nm
Visible (Vis): 400-700 nm
Infrared (IR): 2-25 Tm

There are three main classes of optical absorbance detectors:

i) fixed wavelength UV absorption detectors, (normally the detection is fixed at 254 or 280 nm, or both);

ii) variable wavelength or UV-Vis absorbance detectors; and

iii) IR absorption detectors

Of these, IR detectors are not frequently used because they have limited sensitivity and suffer from significant solvent interference. Their major use has been in exclusion chromatography.

Another important characteristic when selecting a detector is whether it is destructive or not. The commonly used optical detectors are non-destructive, thus allowing for the recovery of the compound under analysis, and its use in subsequent characterisation steps.

Gradient elution requires a detector that will be insensitive to the change in the solvent composition. The UV-Vis and fluorescence detector meet this requirement but the RI does so only in rare cases.

2.5.4.1 Types and applications

As with other chromatographic techniques, there is no universal detector for HPLC. Based on their response, detection systems are classified as follows:

Solute-specific detectors; these are based upon the characteristic nature of the solute. For example the ability a solute might have to absorb light at a given frequency whereas the solvent system does not. Among detectors of this type we note: Ultraviolet-Visible (UV-Vis), fluorescence, electrochemical (EC) and conductivity detectors.

Bulk property detectors; they make use of the variations in the characteristic properties of the bulk solution (the solvent or solvent mixture). Hence variations are the direct result of the elution of the solute. The most widely spread of these detectors is the refractive index (RI) detector.

In some cases there is a need to modify the eluate in order for detection to occur. In those instances, we refer to the following type of detection systems:

Desolvation detectors: these detectors imply that the elution solvent must be evaporated before the solute can be detected. These include FID and mass detectors (see HPLC-MS section).

Derivatisation: the detectability of certain compounds can be improved by chemical derivatisation prior to the HPLC analysis, or after the separation but prior to the detection (post-column derivatisation); the latter can be easily automated and is shared commercially by several manufacturers.

In routine analysis of food constituents, 90% of the work is done with either the UV-Vis or RI detectors. The fluorescence detector is used for 8-9% of the work and the amperometric conductivity one for about 1-2%. In view of their extensive use, a brief description of the UV-Vis, fluorescence and RI detectors follow.

2.5.4.2 Ultraviolet-Visible Detectors

The ultraviolet-visible, UV-Vis, detector is considered the "workhorse" of detectors for HPLC systems. Since UV principles are well-described in several undergraduate textbooks, only a limited description of the principles involved in UV-absorbance will be given in here.

As the sample enters the flow cell, the sample concentration is related to the fraction of light transmitted through the cell by Beer's law (equation (15)):

$\text{Log } I_o/I = \varepsilon bc$ (Beer's Law) **(15)**

$I_o/I = 1/T$ (definition of transmittance) **(16)**

$A = \text{Log } I_o/I = \varepsilon bc$ (definition of absorbance) **(17)**

where:

I = transmitted light intensity
I_o = incident light intensity
T = transmittance
ε = molar absorptivity (or molar extinction coefficient of the sample)
b = cell path length (expressed in cm)
c = sample concentration (moles/L)
A = absorbance

In commercial fixed wavelength UV detectors, λ_{max} is often set at 254 nm. This specific wavelength will provide a wide range of applications, giving strong absorption bands for biologically important compounds such as amino acids, proteins, enzymes and nucleic acid constituents.

On the other hand, the more sophisticated variable wavelength UV-Vis detector will allow the detection of carbohydrates in the low wavelength (190-225 nm) region. Carbohydrates such as fructose, glucose, sucrose, *etc.* which are transparent at 254 or 280 nm, required either RI detection or post column derivatisation before the advent of the variable wavelength detector.

The basic components of a UV-Visible detector are a radiation source, normally consisting of a deuterium lamp for the UV region and a tungsten lamp for the visible region (mainly used for specialised applications such as chlorophylls), a lens, a filter or a monochromator to isolate the narrow wavelength band desired, a slit, a flow cell and a light detector.

Good sensitivity detectors are available to cover the entire UV and visible regions (200-400 nm and 400-800 nm, respectively). Most organic compounds in solution can therefore be detected. However, in some cases, like the detection of sugars for example, the sample will absorb in the same region as the HPLC grade solvent (195-200 nm) (see Table 2). Also, the wavelength at which maximum absorption (λ_{max}) occur might not be the optimum wavelength to use, this is true in cases where other compounds absorb in the same region as the sample. Moving away from λ_{max} might reduce the sensitivity but improve the selectivity of detection. It must be remembered that the detector being concentration-responsive, in order to achieve valid comparisons between standards and samples, all factors that may affect the concentration in the cell must be maintained constant. Consequently, as seen in equation (15), it is also impossible to correlate quantitation curves between two different substances since they might have largely different ε. Hence, the need to make extensive use of standards.

Because of its high sensitivity for some compounds, its good selectivity, its ease of operation, the fact that it is non destructive, and that gradient elution is possible, UV-Vis detectors are nearly universal at low wavelength (200 nm). All these factors, taken together, account for the fact that the UV-Visible detector is the one most often used in the food analysis laboratory.

2.5.4.3 Fluorescence Detectors

Fluorescence detectors are used in the detection of *e.g.,* aflatoxins, polynuclear aromatics, certain vitamins and derivatised amino acids. Fluorescence (molecules that absorb and subsequently re-emit radiation) is a more selective mode of detection than absorbance. It is often a phenomenon

of higher intensity, hence it offers more sensitivity, and allows for the analysis of trace levels. The basic components of fluorometers are similar to the ones of UV-Vis detectors, with variations in their geometric configuration.

The source lamp provides light that passes through an optical system. This system focus the beam and select the wavelength for excitation of the sample. The sample cell is of quartz and the light beam is focused on it. When the fluorescing molecule is present in the cell, the light of a wavelength different from that used to excite the molecule is emitted in all directions. The emission optical system collects and filters the light, which is then focused onto the detector. There are two different classes of fluorescence detectors: those that use monochromators for selection of the excitation and/or emission wavelength (these detectors are the more expensive ones), and those that replace the monochromators with filters.

TABLE 2
UV Characteristics of Some HPLC Solvents

Solvent	UV cut off λ (nm)*
n-pentane, cyclohexane, 2-propanol, ethanol	210
hexane	200
carbon disulphide	380
toluene	285
benzene	280
diethyl ether, dioxane	220
chloroform	245
methylene chloride	235
acetone	330
ethyl acetate	260
acetonitrile	190
methanol	205

**The UV cut off is the wavelength at which the transmission falls to 10% for good commercial HPLC grade solvents.*

2.5.4.4 Refractive Index Detectors

Refractive index detectors are mostly used for sugar and lipid analyses. The presence of dissolved solutes in the mobile phase will cause a change in the refractive index. However, it is important to realise that the intrinsic characteristic makes up for the fact that gradient elution is usually not employed with a refractive index detector, as a change in the mobile phase implies a change in the refractive index which can barely be differentiated from that resulting from the presence of dissolved solute(s).

Two types of RI detectors are available. The first one uses a flow cell that is made up of two compartments that are separated by a glass membrane. To zero the detector, both compartments are filled with the eluting solvent; a light beam is shined through the whole cell, and is reflected back again. When used in a real analytical situation, the passage of the solute in one compartment causes a deflection from the initial zero conditions, therefore providing a detector response. Another commonly used type of detector uses a Fresnel prism. In the latter, it is the amount of light that is reflected internally from the glass-liquid interface that is compared to the one reflected by the reference side, *i.e.*, the one made up of the pure mobile phase. Some of the most severe limitations of the RI detector is its poor minimum detection limit and its incompatibility with gradient elution.

2.5.4.5. HPLC-Mass Spectrometry

The use of a mass spectrometer (MS) as a detector for HPLC is not a standard technique yet, but developments are rapid and the technique is receiving wider and broader acceptance. Needless to say that linked to a MS, liquid chromatography becomes an even more powerful technique, allowing for separation and providing structural information on the compound under investigation (see chapter on mass spectrometry). Furthermore, a lot of facts, principles and phenomena that were presented for gas chromatography-mass spectrometry (see chapter on GC) still applies for HPLC-MS. A variety of interfaces have been developed to date that are amenable to EI, CI and FAB ionisation modes, the most popular ones being direct liquid interface (DLI), moving belt transport, electrospray and thermospray. The major drawback of LC/MS was the limited amount, or complete lack thereof, of structural information provided by the mass spectra of the compound analysed. Although molecular ions and pseudo-molecular ions are frequently observed, quite often very little fragmentation occurs. The recently introduced ion spray is poised for great success and provides information that was not available from LC-MS before. It will alleviate, in part, this structure pitfall. The cost of such systems are relatively high therefore forbidding, for the time being, a more generalisation of the technique in a number of laboratories.

2.6 SOME ADVANTAGES OF HPLC OVER OTHER TECHNIQUES

One of the major advantage of HPLC is its ability to handle compounds of limited thermal stability or volatility, therefore avoiding derivatisation procedures. The separation times are usually short, varying between 5 to 10 minutes for each run. Usually sample preparation is minimal. The technique is precise, normally quantitative, can be very sensitive and is usually non-destructive. HPLC columns can be used many times without regeneration, and the resolution achieved on such columns far exceeds that of the older

methods. Because also of its ease of operation and the basic systems being more affordable, HPLC is still gaining importance in the analytical laboratory. That the technique lends itself to automation and quantitation is also very appealing. Preparative and semi-preparative HPLC is also possible. A remaining ghost that haunts the technique might be that there is no sensitive universal detector for HPLC.

2.7 APPLICATIONS OF HPLC TO FOOD ANALYSIS

A number of very good reviews on food analysis can be found in the literature [7-12]. Table 3 presents a very limited representation of the kind of work involved in a food laboratory. All basic constituents of foodstuffs - proteins, lipids, carbohydrates and vitamins - are amenable to liquid chromatography. Various types of columns and detectors used for those analysis demonstrate the versatility of the technique. Almost any type of food matrix can be extracted in order to identify and quantitate trace amounts of analytes.

In order to familiarise the reader with the type of sample preparation required and the type of information provided by high performance liquid chromatography, an example depicting the analysis of organic acids in fruit juices follows.

2.7.1 ORGANIC ACIDS IN APPLE JUICE

Problematic:
Very often, fruit juices are brought to the food laboratory for analysis in order to investigate if the product was tampered with and/or if it is the result of some form of adulteration. When the sample is brought to the laboratory, the analyst commissioned to perform the analysis surveys the list of authorised HPLC methods and determine whether there is one suitable for the type of compound submitted. Once a method has been identified, it can be either used as such or slightly modified, depending on the substrate at hand. In this particular case, a method already exists in the registry, hence it can be applied directly to the sample under analysis. The method involved is one where organic acids such as ascorbic, malic and succinic acids can be analysed in fruit juices. The mode of liquid chromatography separation involved in this method is hydrophobic ion suppression. An acidic buffer is used in the mobile phase that lowers the *p*H and therefore suppresses the ionisation or organic acids. This also facilitates column retention of the acids. The sample components are eluted through and separated in a reverse-phase column (C18 packing) and detected with a UV detector set at 220 nm. The sample acids are compared to an external standard (in this case both fumaric and malic acids were used) to confirm peak identity and quantitation. The mobile phase is a 2% aqueous potassium dihydrogen phosphate (KH_2PO_4) adjusted to a *p*H of 3.2 with phosphoric acid. The elution rate is 0.5 mL/min.

Chromatogram A

The sample that yielded chromatogram A is the sample of apple juice under scrutiny. The peak at retention time 4.9 min is malic acid and the one at 7.2 min is fumaric acid. The malic acid peak should always be present in a given quantity. The concentration in fumaric acid should not be more than 2 ppm, if otherwise, it is indicative of a juice sample that was submitted to some kind of non-approved treatment or that was adulterated.

Chromatogram B

Chromatogram B is the result of the analysis performed on an authentic apple juice.

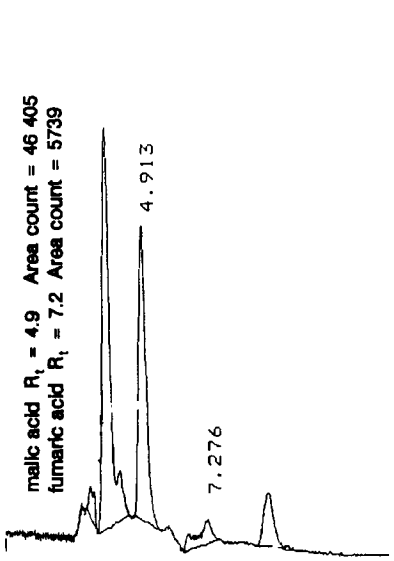

Chromatogram A

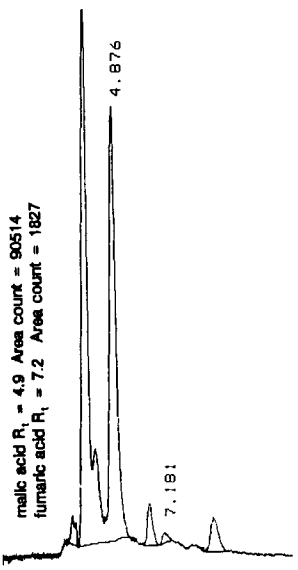

Chromatogram B

Chromatogram C

Chromatogram C is again the same apple juice as in chromatogram B but this time it was spiked with 0.5 ppm of fumaric acid. This has the advantage to identify without any doubt the presence of fumaric acid at retention time 7.2 and also by comparing the area count of fumaric acid in chromatogram C and B it gives the amount of fumaric acid present in chromatogram B.

Chromatogram D

Chromatogram D is 100 ppm of a standard of malic acid. Note that the standard also contains some fumaric acid as a contaminant in it. It is important to note the amount of fumaric acid present in the standard

sample, so that when an apple juice sample is spiked with a standard like malic acid, then adjustment can be made for the amount of fumaric present in the original sample.

Chromatogram E

Chromatogram E is the sample of apple juice under scrutiny, spiked with 100 ppm of malic acid. The increased concentration of both malic and fumaric acids is due to the presence of these organic acids in the original sample, plus the addition of malic acid contaminated with fumaric acid. The verification of the purity of the standard is very important as contamination will give an erroneous result. Spiking is essential in that it: 1) contributes to identify the peak of interest through comparison of retention times, 2) enables the analyst to perform a recovery experiment since the original concentration of the standard is known. From these data, it can be concluded that the sample under scrutiny meet the standards of the authentic apple juice sample.

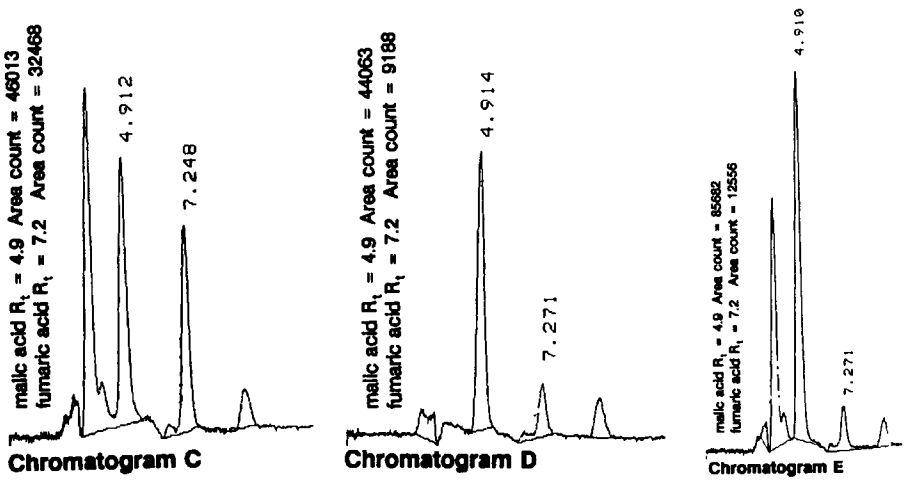

2.8 FUTURE TRENDS

In the biological field new columns are necessary to identify biologically active compounds. Chiral and affinity columns are currently on the market, but many others with various properties are being developed.

The interface of high performance liquid chromatography to inductively coupled plasma-mass spectrometry (HPLC-ICP-MS) will provide a very useful and powerful tool in analysing metal bearing compounds. It is still relatively new, extremely expensive, and requires a high level of expertise to achieve good reliable results.

Another trend is the advent of capillary HPLC. This technique provides extremely high separating power. When well developed, it will be a quantum leap forward for the separation of complex matrices.

TABLE 3
Example of Compounds Analysed by HPLC

Analyte	Matrix	Column and detector	Ref.
Ascorbic Acid	Soft drinks, baby food, milk powder, potato granules and peelings	Silica column bonded (amino-nitrile group - Partisil PAC); Isocratic elution: mobile phase - CH_3COOH:CH_3OH (75:25); UV detector @ 248 nm.	[13]
Caffeine and theobromine	Cocoa, chocolate liquor, chocolate & chocolate coatings	Partisil 10 ODS column; Isocratic elution; mobile phase - methanol: water:acetic acid (20:79:1); UV detector @ 272 nm.	[14, 15]
Saccharin and acesulfame-K	Orange drink & diabetic chocolate	Partisil 10 mm ODS 3 column; mobile phase - Potassium dihydrogen ortho-phosphate, tetra-butyl ammonium hydrogen sulphate, CH_3OH, HCl, & H_2O, final *p*H = 4; UV detector @ 227 nm for acesulfame-K and @ 212 nm for saccharin.	[16]
Benzoic acid, sorbic acid, methyl-, ethyl- & propyl-*p*-hydroxybenzoate	Yoghurt, buttermilk, cheese, soft drinks, cream products & wine	Spherisorb S5C8 column (Hichrom); Mobile phase - CH_3OH:0.01M ammonium acetate (40:50), *p*H = 4.5; UV detector @ 240 nm.	[17]
Styrene	All foods	ODS column; Mobile phase CH_3OH: H_2O (7:3); UV detector @ 254 nm.	[18]
Sugars	Meats, cereals, syrups, fruits, fruit juices	Dionex ion chromatograph; Column HPIC AS6 or AS6A, pulsed amperometric detector with Au electrode; mobile phase - for sucrose to maltose: 150 mM NaOH + 0.30mM zinc acetate for sucrose to maltoheptaose & 150 mM NaOH + 150mM sodium acetate. **OR** (2nd Method): SugarPak Column at90°C; RI detector, H_2O mobile phase.	[19]

Table 3 Continued

Free tocopherols & tocotrienols	Animal and vegetable oils and fats	Partisil 5 (5 mm) column; mobile phase - heptane: wet heptane (sat. with water): propan-2-ol (49.55:49.55:0.9); Fluorescence detector (excitation @ 290 nm & emission @ 330 nm).	[20]
Vitamin A palmitate	Fortified & skimmed milk powders, & baby foods	Partisil 5 column (efficiency of at least 20, 000 plates); isocratic elution; mobile phase - hexane:wet hexane:diethyl ether (49: 49:2); UV detector @ 325 nm.	[21]
	Riboflavin breakfast, milk, meat & pharmaceutical products	Cereals & fortified Partisil ODS-3 column; mobile phase - 0.1 M trisodium citrate; 0.1M citric acid:water:methanol; Fluorescence detector (excitation @ 449 nm & emission @ 520 nm.	[22]

2.9 REFERENCES

1. R. Macrae (ed.), "HPLC in Food Analysis", Food Science and Technology; a Series of Monographs. 2nd edition, Academic Press, London, (1988).

2. L. R. Snyder and J. J. Kirkland, "Introduction to Modern Liquid Chromatography", 2nd edition, John Wiley and Sons, New York, (1979).

3. C. F. Poole and S. A. Schuette, "Contemporary Practice of Chromatography, Elsevier, Amsterdam, (1984).

4. J. M. Miller, "Chromatography: Concepts and Contrasts", J. Wiley & Sons, (1988).

5. P. Jandera and J. Churacek, "Gradient Elution in Column Liquid Chromatography", Elsevier, New York, (1985).

6. The Merck Index, Merck & Cie Inc., Rahway, N.J. USA (published annually).

7. M. J. Saxby, "Developments in Food Analysis Techniques", Vol. 1 (R.D. King, ed.) Applied Science Publishers, London, P. 125, (1978).

8. T. N. Tweeten and C. B. Euston, *Food Technol.*, pp. 29, Dec. (1980).

9. R. Macrae, *J. Food. Technol.* **15**, 93 (1980).

10. R. Macrae, *J. Food. Technol.* **16**, 1 (1981).

11. R. Macrae (ed.), "HPLC in Food Analysis", Academic Press, London, (1982).

12. J. F. Lawrence, "Food Constituents and Food Residues, Their Chromatographic Determination", Marcel Dekker, New York, (1984).

13. J. Carnevale, *Food Technol. Aust.* **32** (6), 302, (1980).

14. W. R. Kreiser and R. A. Martin, *J. Assoc. Off. Anal. Chem.* **61**, 1424 (1978); *ibid*, **63**, 591 (1980).

15. B. L. Zoumas, W. R. Kreiser, and R. A. Martin, *J. Food Sci.* **45**, 314 (1980).

16. P. T. Sack and D. C. Porter, "Analytical Method for the Determination of Acesulfame-K in Food Stuffs", Leatherhead Food Res. Assoc., Research Report No. 506 (1985).

17. V. Gieger, *Lebensmittelchem. u. gerichtl. Chem.* **36**, 109 (1982).

18. M. J. Saxby, D. E. Hyams, and P.E. Dawson, Leatherhead Food Research Association, Technical Circular No. 711 (1980).

19. P. T. Slcak, and E. Coombes, "Assessment of the Dionex 2000i series ion chromatograph as a means of determining reducing and non-reducing sugars in foodstuffs", Leatherhead Food Research Association, Technical Note No. 15 (1984).

20. J. B. Rossell, B. King, and M. J. Downes, "Detection of Adulteration in Edible Vegetable Oils", Leatherhead Food Research Association, Technical Circualr No. 790 (1982).

21. J. N. Thompson, G. Hatina, and W. B. Maxwell, *J. Ass. Off. Anal. Chem.* **63** (4), 894 (1980).

22. British Pharmacopoeia, **Vol. 1**, HMSO, London (1980).

This Page Intentionally Left Blank

J.R.J. Paré and J.M.R. Bélanger (Editors)
Instrumental Methods in Food Analysis

Chapter 3

Gas Chromatography (GC): Principles and Applications

Zhendi Wang and J. R. Jocelyn Paré

Environment Canada, Environmental Technology Centre,
Ottawa, ON, Canada K1A 0H3

3.1 INTRODUCTION

In 1906, a Russian botanist, Mikhail Tswett [1], reported the separation of different coloured constituents of leaves by passing the petroleum ether extract of leaves through a column packed with calcium carbonate. He used the term "chromatography", derived from the Greek words "chromatus" and "graphein" meaning "colour" and "to write", to describe the separation process. Tswett's original work is of significance and is generally considered as the beginning of chromatography. However, his paper remained virtually unnoticed in the literature for a few decades.

The development of column chromatography did not progress until the publication of a most valuable paper by Martin and Synge [2] in 1941, for which they were later awarded the Nobel Prize. In that paper they introduced liquid-liquid chromatography plate theory, a first model that could describe column efficiency. Also in the same paper, they first suggested the possibility of using gas as the mobile phase in a chromatographic system. Ten years later, James and Martin [3] introduced the first gas chromatography apparatus. This first gas chromatography was suitable only for the detection and determination of acids and bases. The first commercial instrument was delivered by Griffin and George (London) in late 1954.

In 1955 Glueckauf [4] derived the first comprehensive equation describing the relationship between height equivalent to a theoretical plate (HETP) and

particle size, particle diffusion and film diffusion ion exchange. At about the same time, the Dutch scientists van Deemter, Zuiderweg and Klinkenberg [5] developed the rate theory, an alternate to the plate theory, describing the chromatographic process in terms of kinetics and mass transfer. The equation derived by van Deemter et al. was later called the van Deemter equation, and the plot obtained from the van Deemter equation was called the van Deemter plot. Since then, gas chromatography was developed and matured rapidly. By the early 1980s, fused-silica capillary columns, selective and sensitive detectors, fully automated systems, and sophisticated techniques such as gas chromatography-mass spectrometer (GC-MS) and gas chromatography-infrared spectrometer (GC-IR) were part of our tools; gas chromatography by this time was a well-established, well-known analytical technique.

Today gas chromatography is likely the most widely used instrumental technique in the world, and its annual growth is above the average growth of the analytical instrument industry. One survey reports that the worldwide sales of GC instruments and accessories in 1990 were U.S. $700 millions [6]. An estimated 23,300 GC systems were sold in 1990 [6]. This number is higher than any other analytical instruments sold in the same year.

Gas chromatography has been widely used in foods, petroleum products, pesticide and pesticide residues, pharmaceutical products, environmental monitoring, clinical chemistry and a number of other fields. The major advantages of modern GC reside in the high resolution, the speed, the sensitivity, and the precision and the accuracy that characterises it. An overview of each factor is given below.

High resolution: A 50 meter capillary column can easily generate 100,000 theoretical plates and thereby separate complex mixtures better than with any other separation techniques available today. As an example, Figure 1 depicts the chromatogram of milfoil oil obtained in our laboratory using a HP benchtop GC-MS system and a 30 meters DB-5 capillary column [7]. Over 100 peaks were separated in 30 minutes, and 28 peaks have been identified.

Speed: Most chromatograms are complete in a matter of minutes. For some simple samples, analysis times of seconds are even possible.

Sensitivity: With a flame ionisation detector, the measurement of parts-per-million (ppm) level of almost all volatile organic compounds can be easily achieved. When using selective detectors such as electron-capture and nitrogen-phosphorus detectors, levels as low as parts-per-billion (ppb) have been routinely measured.

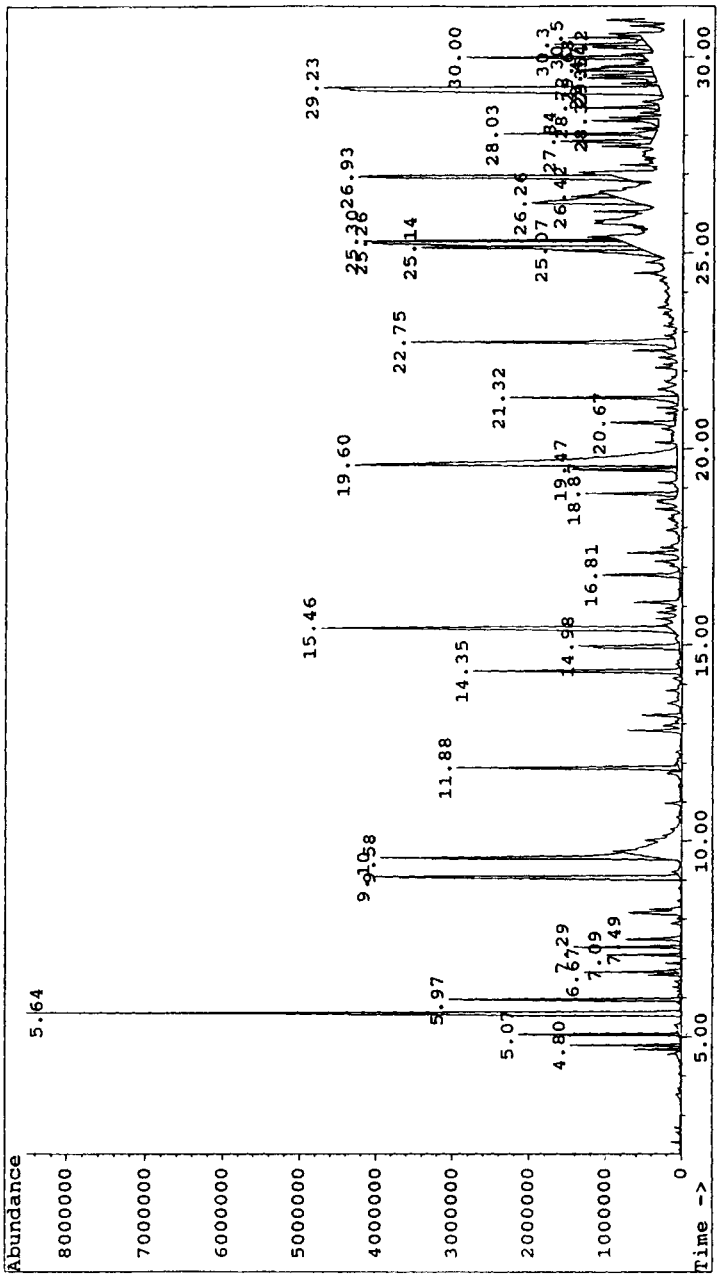

Figure 1: Typical capillary gas chromatogram of milfoil oil.

Precision and accuracy: Gas chromatography enables analysts to perform quantitative analysis accurately under a variety of conditions. Automation and computer control of all critical chromatographic parameters has produced levels of precision and accuracy not thought possible a decade ago. There are many excellent publications detailing the theory and practice of gas chromatography [8-14]. This chapter is trying to highlight some of more important principles of GC and to discuss some applications to food separation and analysis.

3.2 PRINCIPLES

The basis for gas chromatographic separation is the distribution of an analyte between two phases. One of these phases is a stationary phase, and the other is a mobile gas phase which is essentially inert, moving through a GC column and passing over the stationary phase. If the stationary phase is a solid, it is termed gas-solid chromatography (GSC); if the stationary phase is a liquid (generally a non-volatile liquid supported on an inert solid), we speak of gas-liquid chromatography (GLC). There are wide range of liquid phases available with usable temperature up to 400°C, making GLC the most versatile and selective form of gas chromatography; hence most of our discussion will be focused on the gas-liquid chromatography.

In GC, a sample (usually a mixture of analytes) is introduced into the mobile phase through an injection system. Since the analytes have to be introduced into the gas phase, the temperature of the inlet system of the GC can be controlled from lower than 0°C to avoid the loss of the very volatile components of samples to over 300°C to volatilise the components that have very low volatility.

Once the sample enters into contact with the mobile phase in the column, the components of the sample interact to varying extent with the stationary phase and partition between the stationary and the mobile phase, resulting in differential migration rates through the column. At any given time, a particular analyte is either in the mobile phase, moving along with the moving gas, or in the stationary phase and diffusing in it. Such sorption-desorption process occurs repeatedly until each analyte forms a separate band and leaves the column.

As the analyte emerges from the end of the GC column, it enters into a detector and produces some form of signal, the strength and duration of which is, in the best cases, related to the amount of, or to the nature of the analyte. Generally, the signal is amplified and passed to an electronic integrator, a computer, a strip chart recorder or an other means by which the chromatogram is obtained and the quantitation of the analyte is then made.

3.3 DEFINITIONS

The definitions, terms and symbols used in gas chromatography vary throughout the literature. Those used in this chapter are a combination of those used widely and routinely and those recommended by the International Union of Pure and Applied Chemistry (IUPAC).

3.3.1 Terms Referring to the Retention of Analytes

1. The average flow velocity of gas ($\bar{u}$): The ratio of the column length, L, to the non-retained carrier gas hold-up time in the column, t_M is the average flow velocity of gas:

$$\bar{u} = L \cdot t_M^{-1} \quad \textbf{(1)}$$

2. The retention volume (V_R): The retention volume is defined as follows:

$$V_R = t_R \cdot F_c = V_M + KV_S \quad \textbf{(2)}$$

where F_c is the carrier gas flow rate at the column outlet and at the column temperature. In most cases, GC is operated with a constant flow. The retention time, t_R, is the time from injection of the sample to the recording of the peak maximum of the component peak. V_S is the stationary phase volume, K is the partition coefficient and V_M is the mobile phase volume.

3. The mobile phase volume or dead volume (V_M): The mobile phase volume (often called dead volume) is defined in the same way as V_R:

$$V_M = t_M \cdot F_c \quad \textbf{(3)}$$

4. The adjusted retention volume (V'_R): This is the retention volume of an analyte minus the retention volume for the non-retained peak, expressed as:

$$V'_R = V_R - V_M = t_R F_c - t_M F_c = (t_R - t_M) F_c = t'_R \cdot F_c = KV_S \quad \textbf{(4)}$$

where t'_R is the adjusted time of the analyte.

5. The column capacity factor (k'): k' is defined directly from the retention times:

$$k' = (t_R - t_M) t_M^{-1} = t'_R \cdot t_M^{-1} \quad \textbf{(5)}$$

k' is a measure of the ability of the column to retain a sample component.

6. The distribution constant (K): K is also called partition coefficient. But IUPAC recommends distribution constant rather than partition coefficient

(because of overlap with the liquid-liquid extraction parameter of the same name). It is defined as the ratio of the concentration of a sample component in the stationary phase to its concentration in the mobile phase.

$K = C_S \, . \, C_M^{-1}$ **(6)**

7. The retention ratio (R):

$R = t_M \, . \, t^{-1}_R$ **(7)**

This is the ratio of the hold-up time of the mobile phase to the retention time of a given sample component. Combining equations (5) and (7) gives equations (8) and (9):

$k' = (1 - R) \, R^{-1}$ **(8)**
$R = (1 + k')^{-1}$ **(9)**

The theory of chromatography defines k' as the ratio of the mass of a sample component present in the stationary phase and mobile phase. Thus, k' is proportional to the apparent thermodynamic equilibrium constant.

3.3.2 Terms Referring to Column Efficiency

1. Normal distribution: Generally, the peak profiles in the chromatograms are assumed to be symmetrical, and are treated by the well-known normal or Gaussian distribution equation:

$y = y_M \exp[-(t - t_R)^2 \, (2F^2)^{-1}]$ **(10)**

where signal y is dependent on retention time, t. The signal is equal to its maximum value when $t = t_R$. The standard deviation of the Gaussian curve is depicted by F, and its square, F^2, is the variance of the Gaussian curve. These two parameters are used to describe the chromatographic peak broadening. For a normal distribution, the width at the base line, W, has a value of 4F, the width at 60.7% of the peak height is 2F, and the width at half of the peak height is 2.354 F, which is often expressed as $W_{1/2}$.

2. Peak asymmetry: There are many factors that can produce peak asymmetry. In a number of cases, the peaks recorded with a gas chromatograph are not Gaussian. Several measures have been used to characterise peak asymmetry and to study the influence of experimental conditions on peak asymmetry. The most simple and widely-used measure is the asymmetric ratio, A_S, defined as follows:

$A_S = BC \, . \, AB^{-1}$ **(11)**

where AB and BC are the two segments measured at 10% of the peak height, as depicted in Figure 2. For a symmetrical peak, the value of A_S is 1. For tailed and fronted peaks, the values of A_S are greater and smaller than 1, respectively.

3. Plate number: The plate number, or the number of theoretical plates is widely used to described the efficiency of a column, it can be expressed as:

$$N = (t_R . F^{-1})^2 \quad \textbf{(12)}$$

As discussed above, for Gaussian peaks, the standard deviation can be expressed in terms of the peak width (W = 4F), thus we have:

$$N = (4t_R . W^{-1})^2 = 16 (t_R . W^{-1})^2 \quad \textbf{(13)}$$

Similarly, from $W_{1/2} = 2.354$ F, we can also write :

$$N = 5.54 (t_R . W^{-1}{}_{1/2})^2 \quad \textbf{(14)}$$

From equations (12), (13), and (14), it can be seen that the plate number is a measure of the relative peak broadening that has occurred while the sample component passed through the column in time t_R. As retention time increases, the value of W increases, that means the peak broadens. If the adjusted retention time, t_R, is used, the peak number is called the effective plate number and written as:

$$N_{eff} = 16 (t'_R . W^{-1})^2 \quad \textbf{(15)}$$

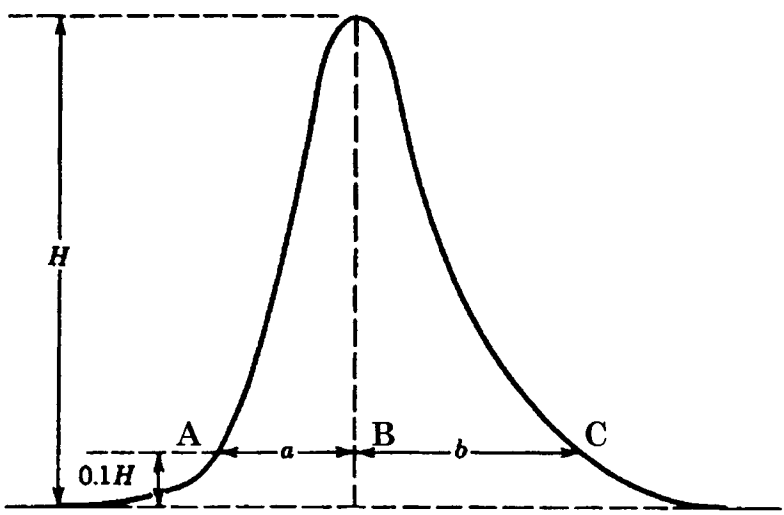

Figure 2: Definition of peak asymmetric ratio, A_S.

Combining equations (5), (13) and (15), the effective plate number can be related to the plate number by the following equation:

$$N_{eff} = N[k' (k' + 1)^{-1}]^2 \quad \textbf{(16)}$$

The effective plate number increases with increase of k', and approaches to N at high k' values. In general, the effective plate number is a better parameter to describe the performance of a column. It is especially true when we compare the efficiency of the capillary column with the packed column.

*4. **Plate height:*** The plate height, height equivalent of a theoretical plate (HETP), is calculated by dividing the column length by the theoretical plate number:

$$H = L \,.\, N^{-1} \quad \textbf{(17)}$$

Obviously, H is the measure of the column efficiency that is independent of the total column length. The HETP is usually expressed in the unit of length such as millimetre. The smaller HETP means higher efficiency of column.

3.3.3 Terms referring to sample component separation

*1. **Relative retention:*** The relative retention, or the column selectivity, is defined as the ratio of the adjusted retention times or volumes of two components under identical conditions:

$$\alpha = t_{R,2} \,.\, t_{R,1}^{-1} = V'_{R,2} \,.\, V'^{-1}_{R,1} = k'_2 \,.\, k'^{-1}_1 \quad \textbf{(18)}$$

As defined by equation (18), the value of α is usually larger than 1, which means that compound 2 is retained longer on the column than compound 1. The value of α is affected by the nature of the stationary phase and the temperature. For a given column, it is a function of the temperature.

*2. **Resolution:*** The resolution is the degree of separation between two peaks and is defined as follows:

$$R_{1,2} = 2 (t_{R,2} - t_{R,1}) (W_1 + W_2)^{-1} = 2d (W_1 + W_2)^{-1} \quad \textbf{(19)}$$

where d is the distance between the maxima of two peaks, and W is the width of each peak at its base as described before. The large value of $R_{1,2}$ indicates the better separation of two peaks For complete separation, a value of the resolution larger than 1.5 is necessary. When the resolution decreases below 1.0, the interference between two peaks becomes stronger and stronger, and the valley between two peaks even disappears at R=0.5.

*3. **Separation number:*** The separation number (SN), or Trennzahl (TZ) in German, is the possible number of peaks between two consecutive peaks of n-paraffin:

$$SN = (t_{R,x+1} - t_{R,x}) \, (W_{1/2,x+1} + W_{1/2,x})^{-1} - 1 = TZ \qquad \textbf{(20)}$$

SN is a measure of the separation power of a column in a particular range of retention. It is usually considered as the maximum number of peaks with equal height that could be placed between those two peaks of the successive paraffins or two successive homologs with carbon number x and x+1. for example, SN 7 means that 7 components eluting adjacent to each other with the same peak height can be resolved between two successive paraffins in that region of the chromatogram. It should be noted that the separation number also depends strongly on the column temperature, increasing with decrease of the temperature.

*4. **Retention index:*** There are two types of retention index, namely the isothermal retention and the linear temperature programming index. Both indices express the retention characteristics of a chemical compound analysed by GC to the retention of the homologous series of normal aliphatic hydrocarbons analysed under identical conditions. Under both retention index systems, a chemical compound is bracketed by two aliphatic hydrocarbons that are assigned a retention index value corresponding to the number of carbon atoms in the hydrocarbon molecule multiplied by 100. The isothermal retention index, RI_i, is defined as a logarithmic interpolation between two successive aliphatic hydrocarbons eluted just prior to and just after the compound A under the isothermal GC conditions, and is calculated for compound A as follows:

$$RI_i = 100 \, (\log V'_A - \log V'_Z) \, (\log V'_{Z+1} - \log V'_Z)^{-1} + 100Z \qquad \textbf{(21)}$$

where:

V'_A is the adjusted retention volume of compound A;
V'_Z is the adjusted retention volume of hydrocarbon Z eluted just before compound A;
V'_{Z+1} is the adjusted retention volume of hydrocarbon Z+1 eluted just after compound A;
and Z is the number of carbon atoms in hydrocarbon Z.

Experimentally, RI_i is determined by the following equation:

$$RI_i = 100[\log(t_A - t_{CH4}) - \log(t_Z - t_{CH4})][\log(t_{Z+1} - t_{CH4}) - \log(t_Z - t_{CH4})]^{-1} + 100Z \qquad \textbf{(22)}$$

where t_A, t_Z, and t_{Z+1} are the retention times of compound A, hydrocarbons Z and Z+1, respectively.

The retention time of the non-retained hydrocarbon methane is represented as t_{CH4}. Similarly, the temperature programming index, RI_p is experimentally determined by equation (23):

$$RI_p = 100\ (t_A - t_Z)\ (t_{Z+1} - t_Z)^{-1} + 100Z \qquad \textbf{(23)}$$

The retention index value represents the retention characteristics of that compound as being equivalent to the retention characteristics of a hypothetical normal alkane containing the "retention index divided by 100" equivalent carbon atoms. For example, $C_{12}H_{26}$ would have values of 1,200 and $C_{13}H_{28}$ would have a value 1,300. A compound that eluted under identical conditions between $C_{12}H_{26}$ and $C_{13}H_{28}$ would be represented by a numerical value between 1,200 and 1,300 index units, say 1,254, meaning that this compound has a retention analogous to the normal hydrocarbon having a chain length 12.54 carbon atoms. One of the advantage of the retention index system is that retention indices of compounds are quite reproducible between laboratories using the same GC column and conditions. In addition, for a given chemical compound, we always can find a pair of n-alkanes that are eluted just before and just after that compound.

There are many books and other sources that discuss the retention index from theoretical and practical aspects. One comprehensive book is "The Sadtler Standard Gas Chromatography Retention Index Library" [15]. This series of book (from Volume 1 to Volume 4) provides detailed data on the retention indices for more than 2,000 compounds under varying isothermal and temperature programming GC conditions for the purpose of the general identification of unknown compounds.

3.4 THEORY OF GAS CHROMATOGRAPHY

As mentioned earlier, the plate theory has played a role in the development of chromatography. The concept of "plate" was originally proposed as a measurement of the performance of distillation processes. It is based upon the assumption that the column is divided into a number of zones called theoretical plates, that are treated as if there exists a perfect equilibrium between the gas and the liquid phases within each plate. This assumption implies that the distribution coefficient remains the same from one plate to another plate, and is not affected by other sample components, and that the distribution isotherm is linear. However, experimental evidences show that this is not true. Plate theory disregards that chromatography is a dynamic process of mass transfer, and it reveals little about the factors affecting the values of the theoretical plate number. In principle, once a sample has been introduced, it enters the GC column as a narrow-width "band" or "zone" of its composite molecules. On the column, the band is further broadened by interaction of components with the stationary phase which retains some components more than others. Increasing

the mobile phase velocity will increase the non-equilibrium effect, providing for a faster exchange of analyte molecules between the mobile and stationary phases and thus decreasing the non-equilibrium effect. van Deemter et al. studied the broadening of chromatographic bands, and proposed the famous "rate theory", expressed by the following van Deemter equation:

$$H = A + B \cdot u^{-1} + Cu \quad \textbf{(24)}$$

The van Deemter rate theory identified three major factors that cause band or zone broadening during the chromatographic process: the eddy diffusion or the multi-path effect (A-term), longitudinal diffusion or molecular diffusion of the analyte molecules (B-term), and resistance to mass transfer in the stationary phase (C-term). The broadening of a zone was expressed in terms of the plate height, H, and was described as a function of the average linear velocity of the mobile phase, u.

The A-term is a measure of the band broadening resulting from the variety of pathways that the analyte molecule can take to pass through the column packing. The magnitude of A is dependent upon the level of uniformity of the packing particles. When a sample migrates down the column, some molecules take longer paths than others as a result of the distribution in particle sizes. In addition to the occurrence of different pathways, there exist variations in the velocities of the mobile phase within these pathways. The combined effect of these factors is an overall broadening of the sample band. In general, reduction in the particle size bring about a decrease in the contribution of the A term to the value of the plate height (H).

The B-term is a measure of the longitudinal diffusion of the analyte molecules in the carrier gas, due to concentration gradients within the column. This type of diffusion occurs at the molecular level -- the analyte molecules migrate from the higher concentration region to the lower concentration region. For a given analysis, the molecular diffusion is a function of both the sample and the carrier gas and it is inversely proportional to the carrier gas flow rate, u. A low flow rate increases the diffusion time, while a high flow rate increases the mixing of the analyte molecules in the carrier gas. Either of these two factors increases the B-term and, consequently, contributes to an increase in the value of H. Hence, in packed columns, there is an optimum flow rate that is between these two extremes, at which the contribution of the B-term to H is a minimal. Furthermore, molecular diffusion is also affected by the nature of the carrier gas. Dense gases such as nitrogen or carbon dioxide have less effect on longitudinal band broadening than lighter ones such as helium or hydrogen.

The C-term is a measure of the resistance to mass transfer in the liquid phase. Because there is a continuous flow in the column, the concentration of the analyte (*i.e.* mass transfer of analyte molecules) in the liquid phase keeps changing from one zone to the next one. The whole process is a dynamic non-

equilibrium process. The C-term is directly proportional to the carrier gas flow rate and to the thickness of the liquid phase, and inversely proportional to the partition coefficient of the analyte in the liquid phase, therefore, to the relative solubility of the analyte in the liquid phase. Hence, the Cu term can be notably reduced by using a moderate flow rate (which allows more time for equilibrium) and using a thin liquid phase film (which minimises diffusion within the liquid phase).

Taking into consideration all of the effects discussed above, the van Deemter equation can be formulated in a more detailed form as follows:

$$H = 2\lambda d_P + 2\lambda D_g + 8k' d_f^2 u \pi^{-2} D_l^{-1} (1 + k')^{-2} = A + B \,.\, u^{-1} + Cu \qquad \textbf{(25)}$$

Where:
λ is a "dimensionless" constant characteristic of the packing;
d_p is the particle diameter;
D_g is the diffusion coefficient of the analyte in the carrier gas;
k' is the capacity factor;
d_f is the effective film thickness of the liquid phase;
D_l is the diffusion coefficient of the analyte in the liquid phase; and
u is the apparent linear carrier gas flow rate.

This equation indicates that in order to obtain the best column performance, we must minimise the contribution of each term to H. Figure 3 shows the plot of H as a function of the velocity of the carrier gas.

Various modifications to the original van Deemter plate height equation have been proposed in the literature in order to improve the unicity of this equation for different situations [7, 16-22]. If we further consider the fact that resistance to mass transfer can occur in the stationary phase as well as in the mobile phase, then Equation 25 may be rewritten in the more general form:

$$H = A + B \,.\, u^{-1} + C_l u + C_g u \qquad \textbf{(26)}$$

Where the C-term is split into two parts -- one for the resistance in the liquid phase ($C_l u$) and the another one for the resistance to mass transfer in the gas phase ($C_g u$). Hawkes [22] suggested that the C_g term was an indefinite combination of several factors, including particle size, column diameter and the diffusion coefficient of the analyte in the carrier gas. The most important parameter in Hawkes equation is the column diameter, d_c. For both packed and open tubular columns, the analyte zone broadening is a function of the square of the diameter. For further details, please consult the paper by Hawkes.

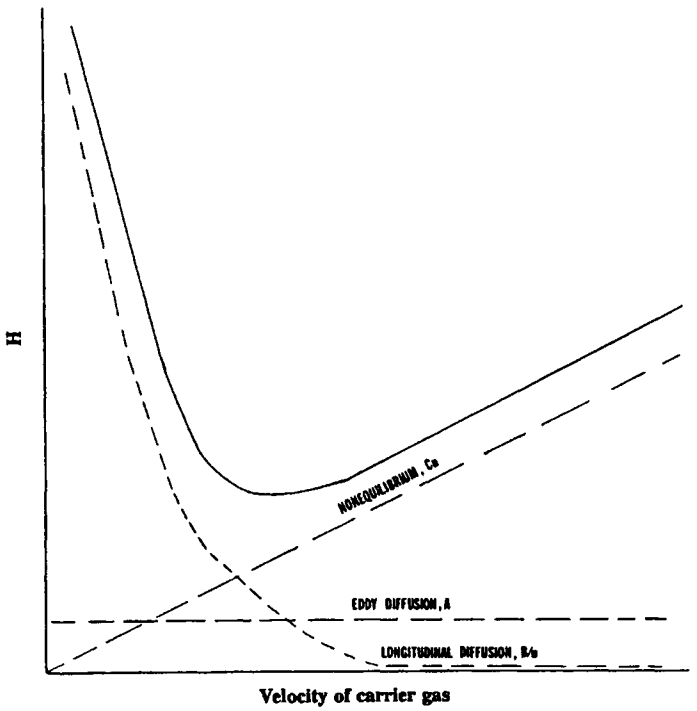

Figure 3: van Deemter plot of H as a function of the velocity of the carrier gas.

The plate height, by the classical definition as shown in equation 17, is determined by dividing the column length, L, by the theoretical plate number, N. This definition is somewhat artificial, because actually there is no fixed value of N on the column. The rate theory redefines the plate height (H or HETP) as follows:

$$H = F^2 . L_Z^{-1} \quad \textbf{(27)}$$

Where F^2 is the variance of analyte molecules about their mean in the analyte broadening zone which have a concentration profile in the Gaussian distribution shape, and the L_z is the distance the zone has moved (please note that L_z does not necessarily refer to column length here). Obviously, this is a more meaningful and useful concept, which views the HETP as the length of column necessary to achieve equilibrium between the liquid and mobile phase. In addition, equation 27 can be related to the random diffusion process (actually, the movement of analyte molecules between the two phases is like the molecule motion in a random diffusion process) defined by the Einstein diffusion equation:

$$F^2 = 2Dt \quad \textbf{(28)}$$

Where D is the diffusion coefficient and t represents the time molecules spend in the mobile phase from the start of the random diffusion process. For the chromatographic process, the term t can also be expressed in terms of L_Z and the velocity of the mobile phase u:

$$t = L_Z \cdot u^{-1} \quad \textbf{(29)}$$

and Equation 28 becomes:

$$F^2 = 2DL_Z \cdot u^{-1} \quad \textbf{(30)}$$

Combining Equations 12 and 17 gives:

$$H = L_Z F^2 \cdot t_R^{-2} \quad \textbf{(31)}$$

As emphasised above, L_Z is defined as the distance the analyte zone has moved in the column. If L_Z is assumed to be equal to t_R, then L_Z represents the retention time and equation 30 can be rearranged as:

$$F = (Ht_R)^{1/2} \quad \textbf{(32)}$$

The significance of Equation 32 is that it indicates that peak broadening is proportional to the square root of the retention time. As observed from chromatograms, the longer the retention time, the wider the peak is.

3.5 THE APPLICATION OF THE RATE THEORY

The value of the van Deemter equation is in its indication of the requirement for the minimisation of zone broadening and, therefore for the maximisation of resolution. It tells that the analyte zone broadening with packed columns can be reduced by using uniform packing with small particle diameter (small d_P), thin film on the solid support (small d_f), narrow internal diameter columns (small d_c). The eddy diffusion can be minimised by avoidance of packing irregularity and by the application of small particles, as well as by using a column with reduced internal diameter. The longitudinal diffusion also can be reduced by using small particle diameter and uniform packing. As well, the longitudinal diffusion term recommends a high flow rate to minimise H. The C term demands a low flow rate, and suggests to use a thin stationary phase to reduce the resistance due to the migration of analyte molecules in the stationary phase.

From the above discussion, it seems that the van Deemter equation contains some contradictory requirements. A small particle size is demanded by each term, but too small particles will obviously obstruct the mobile phase flow rate. The molecular diffusion term demands a high flow rate, while the mass transfer term requires a low flow rate. In practice, some compromise must be made to

obtain the optimum HETP. The particles are usually as small as are consistent with a reasonable flow rate. Once the column is chosen, HETP can be varied by changing the flow rate.

In open tubular columns, because the thin liquid film is deposited directly on the wall of the column rather than the solid supports, the A term is zero, therefore eliminating one of the major contributor to zone broadening. Comparing to packed columns, the resistance to mass transfer is also reduced in both the liquid phase due to the application of very thin film of the stationary phase, and in the mobile phase due to the application of very narrow internal diameter columns. The typical open tubular columns have an internal diameter of 0.25 mm and a film thickness of 0.25 μm. A combination of all these factors makes for the fact that capillary GC columns have much lower plate height value and substantially more theoretical plates. The effect of carrier gas and linear velocity on capillary column efficiency is illustrated in Figure 4, which shows a family of van Deemter plots for common carrier gases.

van Deemter plots in Figure 4 show that the optimum velocity is around 30-40 cm/sec for hydrogen, approximately 30 cm/sec for helium, and around 12-14 cm/sec for nitrogen. These plots demonstrate the advantages of using either helium or hydrogen as carrier gas because of the following facts:

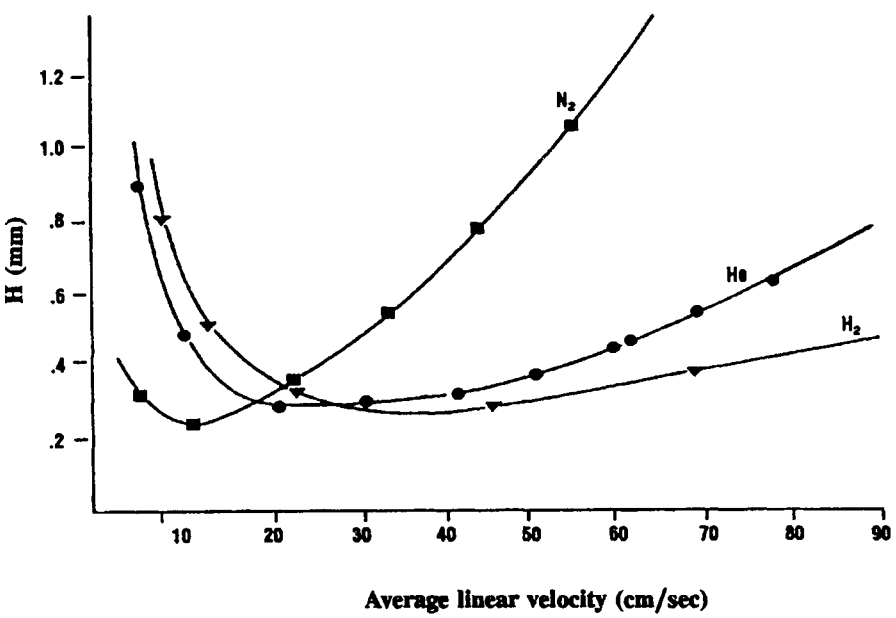

Figure 4: van Deemter plots for different carrier gases in open tubular column.

(1) Minima for H_e or H_2 occur at much higher linear velocities than N_2, permitting to use higher velocities than N_2 with only very small loss in efficiency. Fast analysis can be obtained using H_e or H_2.

(2) H_e or H_2 exhibit relatively flat minima, so changes in linear velocities will be not significant to column efficiency during temperature-programmed analysis.

(3) for any given compound, the minimum in the N_2 plot is quite pronounced, consequently, there is only small linear velocity range over which column efficiency is maximized. In addition, another benefit is using H_2 has the lowest column head pressure due to the lowest viscosity.

3.6 INSTRUMENTATION

A gas chromatographic system is composed of four major components: carrier gas source, sample introduction system, column and detector. The major suppliers of gas chromatography apparatus in today's world market include Hewlett-Packard (which is considered by most as the industry standard), Varian, Perkin-Elmer, Shimadzu, and Carlo-Erba.

3.6.1 Carrier gas source

A high pressure cylinder containing the carrier gas is used as the carrier gas source. Theoretically, any gas which can transport the sample through the column can be used as carrier gas. However, a number of restriction must be placed on the selection of a carrier gas. First, the carrier gas must be inert, not reacting with analytes and with any components of the GC system. Second, the carrier gas must be suitable with the detectors. Finally, the carrier gas must be of high-purity grade and not hazardous. High-purity helium is widely used for capillary GC-FID applications. Usually, to ensure high quality GC analysis, a drying tube and/or sorbent trap is connected between the gas cylinder and the GC injection part to remove trace level of water vapour, hydrocarbons, oxygen and other impurities.

A two stage regulator is used at the outlet of the carrier gas cylinder to set an appropriate cylinder outlet pressure to the GC system and to monitor the residual pressure in the cylinder. Most GC instruments are equipped with a flow controller and flow meter. The flow controller is used to ensure obtaining a constant flow despite changes in pressure and pressure drops through the GC column. The flow meter is used to set a carrier gas flow rate to a desirable level and to monitor the stability of the carrier gas flow.

3.6.2 Sample introduction (inlet) system

Gas chromatographic samples are generally introduced onto GC column through an injection port, in which there is a self-sealing septum to ensure no

leaking will occur. Gaseous samples are best handled by on-column introduction, which eliminates band broadening due to the dead volume of the injection port. Liquid samples are usually introduced with a syringe. Sample injection sizes depend on the concentrations of the sample components being analysed, the capacity of the column, and the sensitivity of the detector. Typical liquid sample size may range from 0.1 to 10 μL for packed columns, and from 0.001 to 0.5 μL for capillary columns. For capillary GC, the smaller volumes are obtained with a sample splitter, which separate the carrier sample mixture into two streams, the larger part is vented while the smaller part is directed to the column (a so-called split injection). The injection temperature of the port (usually higher than the column temperature) must be hot enough to allow instantaneous vaporisation of the sample without thermally decomposing the sample components.

Proper injection technique is required for reproducible, quantitative data. An injection technique called the solvent-flush method, is recommended for the introduction of liquid samples. This technique involves the following steps: (1) rinsing the syringe with solvent, completely filling and expelling the syringe several times; (2) wiping excess solvent from the syringe needle; (3) drawing about 1:L of solvent into the syringe, followed by about 1μL of air, then followed by drawing in excess sample; (4) positioning the syringe plunger for the required injection volume, and wipe excess sample from the needle; (5) drawing in air until the sample is entirely within the syringe barrel; and (6) inserting the syringe into the injection port, rapidly depressing the plunger, and after a delay of about 1 second quickly and smoothly withdrawing the syringe. This injection technique ensures the complete transfer of the sample into the GC column, and the solvent following the sample helps to wash sample components from the syringe and needle bore.

3.6.3 Columns

There are two general classifications of gas chromatographic columns, packed and capillary or open tubular columns.

3.6.3.1 Packed columns

Packed columns are tubes of copper, stainless steel, glass or other materials formed in any shape that will fit the GC oven (common forms are U-shape, W-shape, and coiled tubes). They are generally 1 to 4 m in length, 2-4 mm I.D and 1/8 or 1/4. in O.D. Packed columns are prepared by filling them with finely divided stationary-phase-coated support (the support particle size range from 40 to 60 mesh for coarse particles, and from 100 to 160 mesh for fine particles). The two ends are fitted with glass wool plugs, to retain packing materials.

Most packed column supports are prepared from diatomaceous earth, which is composed of skeletons of diatoms. The diatomite is basically an amorphous

hydrous silica. The diatomite supports can be further divided into three main types: Firebrick-derived supports, Filter-aid-type supports, and Chromosorb G supports. These various diatomite supports may be used directly after acid washing to remove impurities and to reduce surface adsorption, or after silylation (treating supports with dimethyl dichlorosilane, or hexamethyl disilazane and then neutralising with methanol), which masks the surface hydroxyl groups and therefore minimises adsorption of analytes by support.

Liquid stationary phase selection is extremely important for the satisfactory chromatographic separation. The stationary phase should be chosen for good chemical and thermal stability in addition to suitable selectivity.

One of the most important parameters to characterise the stationary phase is the McReynolds constant which was first proposed by Rohrschneider [24-26] and then further developed by McReynolds [27], as shown in equation (33):

$$\Delta RI = ax' + by' + cz' + du' + es' \qquad \textbf{(33)}$$

Where RI is retention index (see equation 22), ΔRI represents retention index difference (for example, the retention index for benzene was 649 on a non-polar 20% squalane column, and 1169 on a highly polar SP-2340 stationary phase column under identical GC conditions, then ΔRI=520).

From a large number of experiments (226 stationary phases were studied, and 68 compounds on 25 columns were analysed), McReynolds selected 10 most valuable compounds (the most valuable five are benzene, n-butanol, 2-pentanone, nitropropane, and pyridine) as "probes" to characterise columns. The polarity of the column as measured with benzene is termed X' and is equal to ΔRI/100 for benzene. Similarly, y, z, u and s are the I/100 terms for the other four probe compounds. The coefficient a, b, c, d and e for x, y, z, u and s terms are constants, which are defined for these five probe compounds. For benzene, a=100 and b, c, d and e=0. For n-butanol, b=100, and a, c,d and e=0, and so on for the other three probe compounds. Many GC manufacturers present the values of McReynolds constants for various stationary phases in their catalogues. Table 1 list McReynolds constants for some commonly used stationary phases.

One of the most valuable usage for the McReynolds system is to identify stationary phases. For example, SE-30 and DC-200 or OV-101 are very similar stationary phases (with different names but practically similar retention patterns). This system also allow for a rapid selection of phases with different retention properties, to separate compounds that have different functional groups, such as alcohol from ketones, aromatic from aliphatics, or saturates from unsaturates. It should be noted that the McReynolds system is not only applied to packed columns, but also to the selection of capillary column stationary phases.

TABLE 1
McReynolds Constants for Commonly Used Stationary Phases

Phases	x'	y'	z'	u'	s'
Squalane	0	0	0	0	0
Apiezon L	32	22	15	32	42
Methyl Silicones					
SE30	15	53	44	64	41
OV-1	16	55	44	64	42
DC 410	18	58	47	66	46
DC 200	16	57	45	66	43
OV-101	17	57	45	67	43
Dexil 300	47	80	103	148	96
Dexil 400	72	108	118	166	123
Methylphenyl Silicone					
DC 550	74	116	117	178	135
DC 710	107	149	153	228	190
OV-17	119	158	162	243	202
Trifluoropropyl Silicone					
QF-1	144	233	355	463	305
OV-210	146	238	358	468	310
Polyphenyl Ethers					
OS-138	182	233	228	313	293
Carbowax 20M	322	536	368	572	510
Carbowax 1540	371	639	453	666	641
Diethylene Glycol Succinate	496	746	590	837	835
Cyanopropyl Silicone					
SP-2340	520	757	659	942	800
N,N-Bis-(2-Cyanoethyl)-Formamide	690	991	853	1110	1000

3.6.3.2 Capillary column

According to the type and form of the coating, capillary column may be subdivided into wall-coated open tubular (WCOT) type, porous-layer open tubular (PLOT) type, and support coated open tubular type. The most

important and the most widely used type is wall-coated open tubular column. If it is not specified, the capillary column is generally of the WCOT type. The internal surface of the capillary column is coated directly with a thin film of liquid (typically from 0.1 to 3.0 μm). Capillary columns vary in length from 25 to 100 m and in internal diameter from 0.05 to 0.53 mm (called microbore and megabore, respectively).

Capillary columns started to be used in research laboratories since the early 1960s, but they were not accepted as practical, reliable and quantitative tools until the 1980s. The introduction of thin-walled fused silica capillary columns in 1979 [28] dramatically changed the gas chromatography and the latter technique rapidly dominated the world gas chromatography market. Two primary advantages of fused-silica capillary columns are flexibility and inertness. It can be handled almost like rubber tubing. Preparation, installation and exchange of fused-silica capillary column became much simpler than glass ones. Inertness results from the application of high purity fused silica, which contains typically less than 1 ppm of the common metal iron.

Capillary columns are typically coated by a dynamic or a static method. In the dynamic method a dilute coating solution is passed slowly through the column at a controlled rate, followed by nitrogen drying. In the static method the column is filled with the coating solution, which is then evaporated in a laminar fashion using a special oven, leaving a thin film deposition of the coating on the internal wall of the column.

One of the major problems of capillary column is the long-term stability of the stationary phase film. In order to solve this problem, technology called cross-linking and surface-bonding has been developed. The stationary phase is cross-linked, and bonded to the wall surface of the capillary column. This stabilising process gives the stationary phase polymer increased chemical stability, that means, the stationary phase is not adversely affected by large solvent injections or solvent rinsing for removing soluble contaminants, in addition to better thermal stability and low bleed levels.

Another interesting development in capillary GC columns is the introduction of new high temperatures metal capillary column. At the 43rd Pittsburgh Conference & Exposition on Analytical Chemistry and Applied Spectroscopy, 1992, a metal capillary column for triglyceride separations at temperature up to 370^{0}C was introduced. Diameters of this type of columns are 0.25 or 0.5 mm. The same firm also introduced a similar column for simulated distillation of hydrocarbons starting at n-pentane.

3.6.4 DETECTORS

The GC detector sense the emergence of an analyte as it exits from the GC columns, producing an electrical signal that is proportional in intensity to the

concentration or the mass of the eluted analyte. Since the introductions of gas chromatography, over 40 detectors have been developed. Some are designed to respond to most compounds in general, while others are designed to be selective for particular types of substances.

There are 4 major parameters which should be considered when evaluating the performance of a detector. They are:

Sensitivity: It is the response to the amount of the corresponding compound introduced. The minimum detectable amount is defined as the minimum detectable level (MDL). There are many factors which could affect MDL, including the GC inlet and column, the way the signal is integrated, and the random noise from the GC system's electrical circuits;

Signal to noise ratio (S/N): The signal is generally measured from the base of the peak to its maximum in any convenient units. Noise is defined as the average distance between the highest excursion of the baseline to the lowest excursion in a section of baseline (several peak widths long) in the same units as signal. For detectable peaks, the S/N should be larger than 2;

Selectivity: The selectivity of the detector is expressed as the relative sensitivity for two compounds or possibly for two classes of compounds. Universal detectors respond to just about everything eluted from the column. Thermal conductivity detectors and Mass spectrometers operated in the total ion mode can be considered universal detectors. Selective detectors may be element selective, structure/ functional group selective, or selective to other properties of analytes. The flame ionisation detector, for example, is selective for compounds that can be ionised in an air/hydrogen flame, whereas the electron capture detector is selective for halogenated compounds, organometallic substances or other materials that readily emit electron when submitted to beta-particle irradiation. Specific detectors are those that are so selective that they can distinguish particular structure or elements with high degree of certainty. The flame photometric detector, for example, is specific for phosphorus or sulphur-containing compounds. A mass spectrometer detector operated in selective ion monitoring mode offers very high specificity for the selected fragment ions of compounds of interest; and

Dynamic range: The dynamic linear range represents the range of sample quantity for which the signal detector is a linear function of the sample quantity.

The most widely used detectors include the flame-ionisation(FID), the thermal conductivity (TCD) and electron capture detectors (ECD).

3.6.4.1 Flame Ionisation Detector (FID)

The flame ionisation detector has become the most popular detector for GC over the last 40 years, and nothing suggests that this position will ever be challenged. The reasons for that come from its simplicity, reliability, relatively high sensitivity for wide variety of organic compounds, and excellent linearity (as high as 10^8)

The FID utilises a flame produced by the combustion of hydrogen and air. Very little ions are formed because of the combustion of the hydrogen and air. Large increase in ions will occur when organic compounds are introduced into the flame through the FID jet. The ions will be attracted by the FID collector on which a polarising voltage is applied, and produce a current, which is proportional to the quantity of analyte in the flame. For optimal FID operation, the carrier, hydrogen and air flow must be properly set and adjusted.

3.6.4.2 Thermal Conductivity Detector (TCD)

The principle of the TCD is based upon the variations of the thermal conductivity of a mixture with its composition. If the resistor of a TCD is heated by a current and cooled by a gas stream passing by, the equilibrium temperature will vary depending on the composition of the gas. In turn, the resistance of the resistor will also vary, depending on its temperature. During operation, a pure carrier gas is passed over one filament, and the effluent gas containing the sample components is passed over another. These filaments are in opposite arms of a Wheatstone bridge circuit that measures the difference in their resistance. As long as no sample is in the effluent, the resistance of both wires are of equal value. But whenever a sample component is eluted with the carrier gas, it brings about a small change in resistance in the effluent arm. The change in resistance is proportional to the concentration of the sample component in the carrier gas, and is recorded by an appropriate data handling system.

TCDs, were originally made with a Wheatstone Bridge circuitry. Since 1979 some advances on TCD structure have been made. The recently designed TCDs use only a single filament to examine alternatively relative thermal conductivity of the reference versus column effluent gas flow. This single filament design eliminates the need to "match" the resistance or temperature coefficient of the filaments, resulting in the reduction in the noise and in the thermal drift.

3.6.4.3 Electron Capture Detector (ECD)

The electron capture detector principle is based on the phenomenon that electronegative specifies (CX) can react with thermal electrons to form

electronegatively charged ions. The loss of such electrons is related to the quantity of analyte in the samples.

$$CX + e^- \rightarrow CX^- + \text{energy} \quad \textbf{(34)}$$

In order to produce low-energy thermal electrons, the carrier gas is ionised by high energy beta particles from a radioactive source (^{63}Ni) placed in a small cell. The electron flow produces a small current (background current) which is collected and measured. When the sample molecules, which have significant electron affinity, are eluted, they react with the electrons and capture them, giving rise to the formation of negative ions. These negative ions drift much more slowly in the electrical field and react much more rapidly with positive ions than electrons. Thus, the current observed decreases by the amount corresponding to the number of electrons captured.

In the early stages, ECD used a constant and relatively low (10 - 20 V) voltage applied to the detector cell and the variations of the current during the analyte elution were recorded. A recent design applies pulse frequency (which is constantly adjusted) to maintain the cell current at a constant value. This method avoid reactions of analyte molecules with high energy electrons, and offer a much wider dynamic linear range than the constant frequency ECD.

Relatively few compounds show significant electronegativity, and so ECD is a quite selective detector, allowing the determination of trace constituents in the presence of non capturing substances. High-electron-affinity atoms or groups include halogens, carbonyls, nitro-groups and some polycyclic aromatics. ECD have very low sensitivity for hydrocarbons other than aromatics.

3.6.4.4 Mass Selective Detector (MSD)

The mass spectrometer has long been recognised as the most powerful detector for a gas chromatograph for its high sensitivity and high specificity. Mass spectral data provide the qualitative information for identification and characterisation of sample components, that is lacking in other GC detector. In the last decade, the requirement for GC to measure and identify trace amount of environmentally toxic chemicals and pesticides has dramatically driven the development of so-called benchtop GC/MSD. Now the moderate price GC/MSD has become the routine analysis technique in many labs, and this trend is likely to be maintained in the next decade. The typical benchtop GC/MSD provides two operation modes-- scanning mode and selective ion monitoring (SIM) mode. It has a resolution of 0.5 ± 0.05 dalton. By comparison, some of the more sophisticated mass spectrometers have resolution 0.001 dalton (see Chapter 7 on mass spectrometry). The mass range, in scan mode, is between 10-650 daltons. In SIM mode, the MSD can monitor several individually selected masses at one time and numerous groups of masses can be selected for each run.

TABLE 2
Characteristics of Some Other Detectors

Detectors	Operation Principle	Detection Limit	Dynamic Range	Selectivity
Nitrogen Phosphorus (NPD)	Alkali ions are usedt o enhance ionization of N- & P-compounds	0.1-10 pg	10^4	P, N
Flame Photometric (FPD)	Flame excitation produces chemiluminescent species of S- and P-hydrocarbons	1-20 pg	10^3 for S 10^4 for P	High selective for S, P
Helium Ionization (HID)	He atoms excited by radioactive source and ionize compounds with low ionization potential	1 ng	10^4	Respond to all gases and vapours except to Ne
Photo-ionization (PID)	Samples are ionized by excitation by photons from a UV lamp	1-10 pg	10^7	More sensitive to aromatics than to aliphatics
Electrolytic Conductivity (ELCD)	Mixing effluent with reaction gas, then with deionized solvent, measuring conductivity	0.1-5 pg	10^6 for Cl 10^4 for S 10^4 for N	Chlorinated S- and N-compounds
Microwave Plasma (MPD)	High temperature microwave plasma excitation produces emission	0.1-20 pg	10^3-10^4	Halogenated compounds

One important aspect which should be pointed out is that there is a basic incompatibility between GC and MSD, the mass spectrometer operate at pressures of 10^{-5} torr or less, whereas the gas chromatograph effluent operates at about 760 torr. An interface device is necessary to handle the pressure differences. The simplest and most efficient interface in GC/MSD is a direct capillary column interface. The low flow rate of the narrow bore column and the high pumping rate of an oil diffusion pump backed by a suitable direct drive mechanical pump assure pressures less than 10^{-4} torr and allow for the direct insertion of the column end into the mass spectrometer. Interfacing megabore

or packed column is more complicated and is accomplished using a splitter or a jet separator. In these cases, a separate piece of capillary column is usually installed as the transfer line.

Table 2 presents the basic characteristics of some other detectors commonly used for the detection of gas chromatographic effluent.

3.7 INSTRUMENTATION SUMMARY

Although gas chromatography has become a well-established and powerful analytical technique, there are some limitations to gas chromatography. First, GC requires an auxiliary spectroscopic system, usually MS or FTIR, to confirm the identity of peaks. Another major limitation is that GC is applicable only to thermally-stable volatile compounds. This means that most high molecular weight components and biological compounds can only be analysed with difficulty at best if at all possible.

Despite the continued improvements of GC in the past four decades, there are still some areas of GC that require attention. Theses include automated sample preparation, improved sample introduction devices, automated and optimised flow control for both column and detector gases, and improved stability of selective detectors. The combination of all these improvements will result in the next generation of gas chromatography, heralding the 21st century.

3.8 APPLICATIONS OF GC TO FOOD ANALYSIS

Several reviews on food analysis can be found in the open literature [29-32] and the chapters dealing with chromatography and gas chromatography have introduced several references directly related to this topic. Consequently, for the purpose of this particular chapter, we shall discuss only four specific applications of gas chromatography to food analysis. These examples were chosen solely to demonstrate the broad range of applications that gas chromatography can cover and the mere fact that they were selected here should not be interpreted as a judgement of their value over other related references.

3.8.1 Headspace of volatile compounds

Much interest is devoted to the analysis of volatiles released from food materials be it fresh or during a processing function such as cooking for example. The introduction of a gaseous material onto a gas chromatographic column is a most simple step to achieve and, as the name implies, is a most suitable way to achieve a separation of the components of the same gas. There are situations, however, where the separation of the volatiles is difficult as a result of the wide range of compounds that can be produced in the headspace or by simple virtue of their relatively low concentration. Hence it can be necessary

to design a way to "trap" the volatiles prior to their introduction onto the gas chromatograph so as to pre-separate them or to concentrate them.

In a representative paper dealing with such work, Macku and Shibamoto [33] have exemplified an application of GC whereby they were able to monitor the formation of volatiles resulting from the addition of a glycine moiety to lipids during heating. The experimental set-up was quite simple, they passed a stream of purified air over the headspace of the heated materials under investigation (corn oil with and without glycine were used in that particular experience), drawing along the volatiles into a second container. The volatiles were in turn extracted simultaneously with dichloromethane. The resulting extract was fractionated by distillation and the various fractions were subjected to GC analysis. This simple approach allowed the workers to detect over 120 compounds in the headspace of their particular corn oil! Among the 70+ substances that were successfully identified one could find aldehydes, ketones, alcohols, hydrocarbons, heterocyclic compounds, esters and some other miscellaneous compounds. The Kovats indices were used as the samples had been spiked internally with non-interfering substances.

Our laboratory has also introduced a related application for the detection of food volatiles by applying the Microwave-Assisted Process (MAP™) to fresh citrus fruits [34-40]. These examples demonstrate well the capacity GC has to monitor a wide range of chemical functionalities with a single analytical protocol.

3.8.2 Characterisation of cheeses

Cheeses (as are wines and sausages) are still the source of much pride in a number of regions around the world. The globalisation of markets has seen novel economic unions that brought along with them a requirement, although not necessarily a desire, to standardise the various foods found everywhere. Consequently, specialty foods such as cheeses were prime targets for the development of analytical methods that would provide an efficient way to categorise them. We all know that there is virtually a countless number of cheese varieties. Their composition is as diversified, hence the task at hand is not trivial. Actually, if we take into account the fact that the mechanisms of aromas production in cheeses during ripening and maturing are not well understood and agreed upon, then the challenge is phenomenal. Nevertheless, a Spanish team presented an ingenious GC analytical protocol that can be used as a base for future work [41].

Their approach is deceptively simple. They make use of micro simultaneous distillation-extraction apparatus to generate the solutions that they can in turn inject directly onto the column head of the gas chromatograph! Their results can be used to demonstrate the versatility that characterises GC so well. Not only did the chromatograms so produced differed enough to allow them to

characterise a number of cheese varieties but the nature of the substances detected opens the door to further understanding of the various proteolytic processes taking place during cheese maturation. Again this example is used to demonstrate that a simple GC analytical procedure, aimed at routine work, can be used as effectively in some state-of-the-art research activities. These attributes are at the base of the great popularity enjoyed by gas chromatography in so many other disciplines besides food analysis.

3.8.3 Chirospecific analysis of natural flavours

All what has been introduced in this chapter on gas chromatography can be developed into an "exponential" application. The chapter on chromatography has introduced the concept of multi-dimensional chromatography, from that precept it is possible to design and conceive separation protocols that make use of the same chromatographic technique in two dimensions or more, as it is possible to combine two or more chromatographic techniques. Gas chromatography is no exception as it can be seen from a paper dealing with the application of multi-dimensional gas chromatographic analysis of natural flavours and essential oils that is chirospecific [42].

Many flavour compounds are stereo-isomeric and the separation of their chiral components can not be achieved easily with the use of a single column. Although more and more stereospecific columns are being developed and introduced to the market, very few offer the degree of analytical performance sought for in adulteration work for example. The paper chosen here as an example [41] reports on a judicious combination of one polar, non-chiral column for the preliminary direct introduction of the complex mixture (as would be done in one-dimension gas chromatographic analysis) to a chiral column to which the separated effluents of the first column are directed onto, hence effecting the separation on the basis of their relative stereochemistry. Many consumer food products must be tested for fraudulent adulteration. The natural components are in most cases of a given conformation and high resolution nuclear magnetic resonance (NMR) spectroscopy was quite often the only tool available to the analyst (see the appropriate chapter in this book on NMR). The capital and operational costs associated with that technique however made it difficult to access at best. Multi-column GC, or more appropriately termed multi-dimensional GC, is an effective, yet cost sensitive, solution to some of these analyses.

3.8.4 The human nose as a GC detector!

Finally, much has been said about the human nose and its fantastic ability at detecting even trace amounts of various chemicals...when properly trained that is! See reference 43 for an overview of the scope of olfaction (and taste!). Not surprisingly, the human nose has also been put to work as a gas chromatograph

detector. The technique, often referred to GC sniffing is more appropriately termed GC-olfactometry.

Marin and co-workers [44] presented an interesting paper in 1992 on the application of GC-olfactometry to the assessment of the effects of plastic polymers on the aroma character of orange juices. They used data generated from GC-FID, GC-MS and GC-Olfactometry to demonstrate the influence of limonene contents onto the overall aroma of orange juice. The problems at hand with GC-olfactometry are mainly centred around the fact that the human nose does not have a linear response. Hence calibration is somewhat more tedious as the specific sensitivities to all components are non-related to each other.

A "good nose" can be trained in a matter of six months and usually will demonstrate a certain bias toward certain odours. Nevertheless, once the nose "well trained", the data it generates from GC-olfactometry can be extremely useful, especially when plotted as another dimension to a regular GC-FID, or GC-MS traces.

Needless to say that this detector is somewhat more sensitive to operating conditions prevailing at the time where the GC analysis is performed. Some noses have even been reported as outright useless when inoculated with common cold symptoms...whereas others have been documented to be attracted toward specialty products such as wines, fine liqueurs, and...

3.9 REFERENCES

1. M. Tswett, *Ber. Deut. Bot. Ges.* **24**, 384 (1906).

2. A. J. P. Martin and R. L. M. Synge, *Biochem. J.* **35**, 1358 (1941).

3. A. T. James and A. J. P. Martin, *Biochem. J.* **50**, 679 (1952).

4. E. Glueckauf, *Trans. Farad. Soc.* **51**, 34 (1955).

5. J. J. van Deemter, F. . Zuiderweg and A. Klinkenberg, *Chem. Eng. Sci.* **5**, 271 (1956).

6. H. M. McNair, *LC-GC* **10**, 238 (1992).

7. J. C. Giddings, Dynamics of Chromatography, Part I, Principles and Theory, Marcel Dekker, New York, 1965.

8. B. L. Karger, L. R. Snyder and C. Horvath, An Introduction to Separation Science, John Wiley & Sons, New York, 1973.

9. J. M. Miller, Separation Methods in Chemical Analysis, John Wiley & Sons, New York, 1975.

10. J. M. Miller, Chromatography: Concepts and Contrasts, John Wiley & Sons, New York, 1987.

11. W. Jennings, Gas Chromatography with Glass Capillary Columns, 2nd Ed., Academic Press, New York, 1980.

12. R. L. Grob (ed.), Chromatographic Analysis of the Environment, Marcel Dekker, New York, 1983.

13. R. L. Grob (ed.), Modern Practice of Gas Chromatography, Marcel Dekker, New York, 1985.

14. G. Guiochon and C. L. Guillemin, Quantitative Gas Chromatography: For Laboratory Analysis and On-line Process Control, Elsevier, New York, 1988.

15. The Sadtler Standards Gas Chromatography Retention Index Library, Sadtler and Sanyo, 1985.

16. E. Glueckauf, M. J. E. Golay and J. H. Purnell, Ann. N. Y. Acad. Sci. **72**, 612 (1956).

17. M. J. E. Golay, in Gas Chromatography, V. J. Coates, H. J. Noebels, and I. S. Fagerson (eds.) Academic Press, New York, 1958.

18. R. J. Loyd, B. O. Ayers and F. W. Karasek, *Anal. Chem.* **32**, 689 (1960).

19. W. L. Jones, *Anal. Chem.* **33**, 829 (1961).

20. R. Kieselbach, *Anal. Chem.* **33**, 806 (1961).

21. J.H. Beynon, S. Clough, D. A. Crooks and G. R. Lester, *Trans. Farad. Soc.* **54**, 705 (1958).

22. S. J. Hawkes, *J. Chem. Educ.* **60**, 393 (1983).

23. S. J. Hawkes, *Anal Chem.* **58**, 1886 (1986).

24. L. Rohrschneider, *J. Chromatogr.* **22**, 6 (1966).

25. L. Rohrschneider, Advances in Chromatography, Vol. IV, J. C. Giddings and R. A. Keller (eds.), Marcel Dekker, New York, 1967, p333.

26. L. Rohrschneider, *J. Gas Chromatogr.* **6**, 5 (1968).

27. O. McReynolds, *J. Chromatogr. Sci.* **8**, 685 (1970).

28. R. Dandeneau and E. H Zerenner, *J. High Resol. Chromatogr. Chromatogr. Commun.* **2**, 351 (1979).

29. M. J. Saxby, "Developments in Food Analysis", Vol. 1, R. D. King (ed.), Applied Science Publishers, London (1978).

30. R. Macrae, *J. Food Technol.* **15**, 93 (1980).

31. R. Macrae, *J. Food Technol.* **16**, 1 (1981).

32. J. F. Lawrence, "Food Constituents and Food Residues; Their Chromatographic Determination", Marcel Dekker, New York (1984).

33. C. Macku and T. Shibamoto, *J. Agr. Food Chem.* **39**, 1265-1269 (1991).

34. J. R. J. Paré, M. Sigouin, and J. Lapointe, *US Patent* **5,002,784**, March 1991, and several international counterparts.

35. J. R. J. Paré, *US Patent* **5,338,557**, August 1994, and several international counterparts.

36. J. R. J. Paré, *US Patent* **5,458,897**, October 1995; and several international counterparts.

37. J. R. J. Paré, *US Patent* **5,377,426**, January 1995, and several international counterparts.

38. J. R. J. Paré, *US Patent* **5,519,947**, May 1996; and several international counterparts.

39. J. R. J. Paré, J. M. R. Bélanger, A. Bélanger, and N. Ramarathnam, in Food Science and Human Nutrition, G. Charalambous (ed.), Elsevier Science Publishers, Amsterdam (1992), pp. 141-144..

40. MAP is a trademark of Her Majesty the Queen in Right of Canada as Represented by the Minister of Environment.

41. M. de Frutos, J. Sanz, and I. Martinez-Castro, *J. Agr. Food Chem.* **39**, 524-530 (1991).

42. A. Mosandl, K. Fischer, U. Hener, P. Kreis, K. Rettinger, V. Schubert, and H.-G. Schmarr, *J. Agric. Food Chem.* **39**, 1131-1134 (1991).

43. S. D. Roper and J. Atema (eds), "Olfaction and Taste IX", *Ann. NY Acad. Sci.* 510, 1987.

44. A. B. Marin, T. E. Acree, J. H. Hotchkiss, and S. Nagy, *J. Agr. Food Chem.* **40**, 650-654 (1992).

This Page Intentionally Left Blank

J.R.J. Paré and J.M.R. Bélanger (Editors)
Instrumental Methods in Food Analysis

Chapter 4

Fourier Transform Infrared Spectroscopy: Principles and Applications

Ashraf A. Ismail, Frederick R. van de Voort, and Jacqueline Sedman

Department of Food Science and Agricultural Chemistry, Macdonald Campus, McGill University, Ste-Anne de Bellevue, QC, Canada H9X 3V9.

4.1 INTRODUCTION

Mid-infrared (IR) spectroscopy is a well-established technique for the identification and structural analysis of chemical compounds. The peaks in the IR spectrum of a sample represent the excitation of vibrational modes of the molecules in the sample and thus are associated with the various chemical bonds and functional groups present in the molecules. Thus, the IR spectrum of a compound is one of its most characteristic physical properties and can be regarded as its "fingerprint." Infrared spectroscopy is also a powerful tool for quantitative analysis as the amount of infrared energy absorbed by a compound is proportional to its concentration. However, until recently, IR spectroscopy has seen fairly limited application in both the qualitative and the quantitative analysis of food systems, largely owing to experimental limitations.

The development of Fourier transform infrared (FTIR) spectroscopy during the past two decades has revitalised the field of IR spectroscopy. This is due not only to the superior performance of FTIR spectrometers by comparison to that of the dispersive IR spectrometers that they have virtually replaced, but also to a number of other factors. First, the development of FTIR

spectrometers has been paralleled by advances in sample handling techniques. Second, the dedicated computer that is an integral component of all FTIR systems has been extensively exploited in the development of sophisticated data handling and data analysis routines. As a result of these developments, FTIR spectroscopy has the potential to become an important tool for the quantitative analysis of foods.

This chapter will focus on the application of FTIR spectroscopy in the quantitative analysis of foods. Following a brief discussion of the fundamental principles of IR spectroscopy, we will describe the instrumentation, data handling techniques, and quantitative analysis methods employed in FTIR spectroscopy. We will then consider the IR sampling techniques that are most useful in FTIR analysis of foods. Finally, a survey of FTIR applications to the quantitative analysis of food will be presented. Although important, the so-called hyphenated techniques, such as GC-FTIR, will not be covered in this chapter. Similarly, near-IR (NIR) spectroscopy, which has found extensive use in food analysis, is beyond the scope of this chapter.

4.2 PRINCIPLES OF INFRARED SPECTROSCOPY

Molecular absorption of electromagnetic radiation in the infrared region of the spectrum (see Figure 1) promotes transitions between the rotational and vibrational energy levels of the ground (lowest) electronic energy state. This is in contrast to absorption of the energetically more powerful visible and ultraviolet radiation, which induces transitions between vibrational and rotational energy levels of different electronic levels. Infrared spectroscopy is concerned primarily with molecular vibrations, as transitions between individual rotational states can be measured only in the infrared spectra of small molecules in the gas phase.

A non-linear molecule made up of N atoms is said to possess 3N degrees of freedom because if the position of each atom were to be described by three coordinates (*e.g.*, x, y, and z in a Cartesian coordinate system), the position, shape, and orientation of the molecule in three-dimensional space would be completely defined. As a total of three coordinates are required to describe the translation of the molecule (for instance, along the x, y, and z axes), the molecule has three translational degrees of freedom. Another three degrees of freedom represent the rotation of the molecule about the three axes. The remaining 3N-6 degrees of freedom correspond to vibrational motions, and the molecule is said to have 3N-6 normal vibrational modes. These vibrational modes can be described in terms of bond stretching and various types of bending vibrations (see Figure 2). In the case of a linear molecule, there are only two rotational degrees of freedom since rotation about the bond axis is not possible. Therefore, a linear molecule has 3N-5 normal vibrational modes.

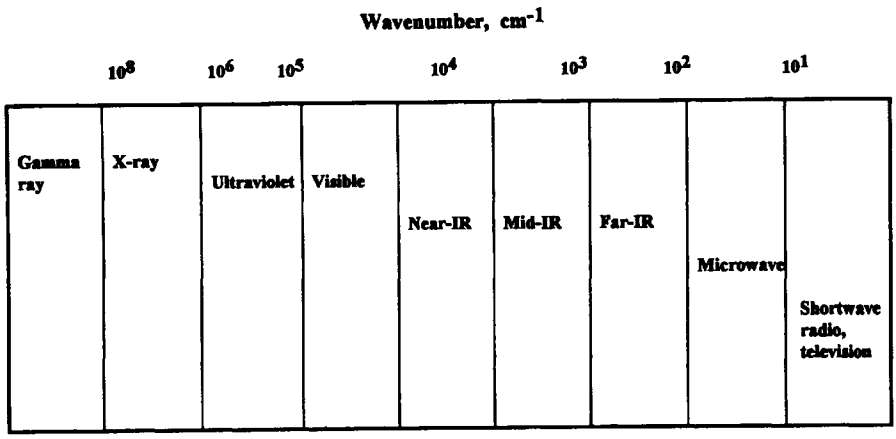

Figure 1: The regions of the electromagnetic spectrum.

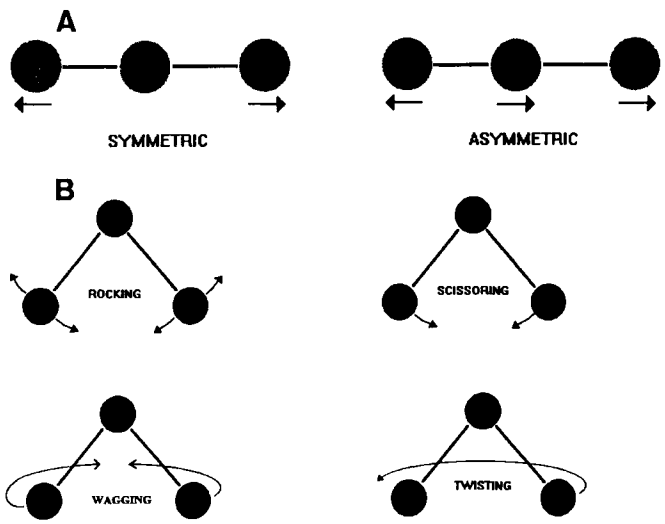

Figure 2: Types of molecular vibrations: a) Stretching vibrations; and b) bending vibrations.

Thus, a simple diatomic molecule A-B has (3 x 2) - 5 = 1 vibrational mode, which corresponds to stretching along the A-B bond. This stretching vibration resembles the oscillations of two objects connected by a spring. Thus, to a first approximation, the model of a harmonic oscillator can be used to describe this vibration, and the restoring force (F) on the bond is then given by Hooke's law:

$$F = -kx \qquad (1)$$

where k is the force constant of the bond, and x is the displacement. Under this approximation, the vibrational frequency ν is given by:

$$\nu = (1/2\pi)(k/\mu)^{1/2} \quad \textbf{(2)}$$

with μ the reduced mass of the system, as defined by the following equation:

$$\mu = m_A \cdot m_B / (m_A + m_B) \quad \textbf{(3)}$$

where m_A and m_B are the individual atomic masses of A and B.

The unit of frequency (ν) is reciprocal seconds (sec^{-1}). However, by convention, band positions in infrared spectra are given in wavenumbers ($\bar{\nu}$), expressed in units of reciprocal centimeters (cm^{-1}), and are often termed "band frequencies." In older literature, band positions are often reported in units of wavelength (λ), *i.e.*, microns (μ). The relation between these units is given by equations (4) and (5):

$$\bar{\nu} = 1/\lambda \quad \textbf{(4)}$$
$$\nu = c/\lambda \quad \textbf{(5)}$$

where c = velocity of light, hence 10 μ = 1000 cm^{-1} and 2.5 μ = 4000 cm^{-1}.

For a many-atom molecule, the situation is more complicated than equation (2) may suggest because the measured vibrational frequencies do not, in general, correspond to pure vibrations but rather to mixtures of different vibrations. Furthermore, electrical effects, steric effects, the nature, size and electronegativity of neighbouring atoms, phase changes and hydrogen bonding may all cause shifts in frequency [1]. On the other hand, the above treatment is the basis for the concept of group frequencies. According to this concept, various functional groups would be expected to exhibit characteristic absorption frequencies that would allow their presence in a compound to be established from its IR spectrum. The general validity of this concept is illustrated by the tabulation of selected group frequencies in Table 1. It may be noted that the stretching vibrations of bonds to hydrogen occur at high frequencies and are shifted to lower frequencies upon H-D exchange, as indicated by equation (3). The effect of the force constant, k in equation (2), which is related to bond strength, may be observed by comparing, *e.g.*, the stretching frequencies of carbon-carbon triple and double bonds. Because of their lower frequencies, carbon-carbon single-bond stretching vibrations and the majority of bending vibrations are extensively mixed, and specific absorption bands cannot usually be assigned to these vibrations. Rather, these vibrations give rise to a multitude of bands in the "fingerprint" region of the spectrum (1200-700 cm^{-1}) which prove very useful in confirming the identity of a compound. In fact, the IR spectrum of a compound may be

considered its most characteristic physical property, and two substances that have identical IR spectra may, with very few exceptions, be considered to be identical [1].

TABLE 1
Selected Functional Group Absorptions

Functional group	Frequency (cm^{-1})	Remarks
-OH	3600-3200	O-H (H-bonded) stretching vibration
-NH and NH_2 (H-bonded)	3300-3000	-N-H stretching vibration
$-CH_3$	2962 (±10), 2872 (±10)	C-H stretching doublet
$-CH_2-$	2926 (±10), 2853 (±10)	asymmetric and symmetric vibration
=C-H	3082-3000	
-C≡N	2260-2200	stretching
-C≡C	2250-2040	stretching
-C=O		
Acids	1770-1750	monomeric stretching, C=O
Acid salts	1610-1550	asymmetric stretching of CO_2^- group (strong)
Esters	1745-1725	C=O stretching
Aldehydes	1735-1715	C=O stretching
Ketones	1720-1710	C=O stretching
Amides	1700-1600	C=O stretching (Amide I band)
-C=N	1670-1618	C=N stretching
-C=C- (*trans*)	1678-1665	C=C stretching
-C=C- (*cis*)	1662-1648	C=C stretching
-N-H	1590-1500	-N-H bending
-N-D	1490-1400	-N-D bending
-C-N	1280-1030	C-N stretching

The quantum-mechanical treatment of molecular vibrations leads to modifications of the harmonic oscillator model. While the Hooke's law treatment presented above would indicate a continuum of vibrational states, the molecular vibrational energy levels are quantised:

$$E = (v + 1/2)h\nu \qquad \textbf{(6)}$$

where h is Planck's constant, v is the vibrational quantum number, and ν is the fundamental vibrational frequency. Accordingly, a molecule will absorb infrared radiation of a particular frequency only when this frequency matches the frequency of one of the molecule's fundamental vibrational modes. As can be seen from equation (6), in the harmonic oscillator approximation, the

quantum-mechanical treatment predicts equally spaced vibrational energy levels. It also predicts that, at room temperature, only transitions from the ground-state vibrational level (v = 0) to the first excited vibrational level (v = 1) will occur. However, experimentally, overtone bands, corresponding to transitions to higher vibrational levels, are observed, and their frequencies fall somewhat short of being integral multiples of the fundamental vibrational frequency. These effects are attributed to the anharmonic nature of molecular vibrations. Anharmonicity also gives rise to combination bands, which represent the simultaneous excitation of two fundamental vibrational modes. Overtone and combination bands, being "forbidden" bands, are approximately an order of magnitude weaker than fundamental modes. Near-IR (NIR) spectroscopy is concerned with the study of bands of this type in the near-infrared region of the spectrum (12,800-4000 cm^{-1}).

Finally, it is important to note that all molecular vibrations do not give rise to infrared absorption bands. A fundamental vibrational mode will only be "IR active" when excitation of this vibration results in a change in the dipole moment of the molecule. Accordingly, N_2, O_2, and other homonuclear diatomics do not give rise to any IR absorption bands. Similarly, the symmetric stretching of a linear X-Z-X molecule (see Figure 2), such as CO_2, will not be an IR-active vibration. Furthermore, the symmetry of a molecule has an effect on the number of absorption bands that it will exhibit in its IR spectrum. For example, two vibrations will give rise to a single IR absorption band when they are identical in energy (degenerate vibrations) as a result of molecular symmetry. The prediction of the number of bands that will be observed in the IR spectrum of a molecule on the basis of its molecular structure, and hence symmetry, is the domain of group theory [2].

4.3 INSTRUMENTATION

An infrared spectrometer essentially consists of a source of continuous infrared radiation, a means for resolving the infrared radiation into its component wavelengths, and a detector. The procedure that is involved in recording the IR spectrum of a sample can be represented mathematically by the following equation:

$$T(\bar{\nu}) = I(\bar{\nu})/I_0(\bar{\nu}) \qquad (7)$$

where T is defined as the transmittance, I is the intensity of the infrared radiation reaching the detector when the sample is placed between the source and the detector, I_0 is the intensity reaching the detector with no sample in the beam, and $\bar{\nu}$ is the wavenumber of the infrared radiation. Conceptually speaking, the spectrum is obtained by measuring the transmittance at equally spaced wavenumber intervals, $\Delta\bar{\nu}$, where $\Delta\bar{\nu}$ is termed the

resolution. Usually, the y axis of the spectrum is converted from units of percent transmittance (%T = 100 x T) to absorbance units, the relationship between absorbance (A) and transmittance being given by equation (8):

$$A = -\log T \quad (8)$$

The first commercial scanning infrared spectrometers, in the 1940s, employed a prism to resolve the infrared radiation into its component wavelengths. The prism was replaced by a diffraction grating in the 1960s, allowing an improvement in resolution. The principle of operation of a double-beam, optical-null grating spectrometer is illustrated schematically in Figure 3. Radiation from the infrared source is divided into a sample beam and a reference beam and passes through the sample and a reference, placed in the respective beams. The sample beam and the reference beam are then alternately passed by the chopper onto the entrance slit of the monochromator, where they are dispersed by a diffraction grating, and impinge onto a detector. When the energy of both the sample and the reference beam in the frequency interval exiting the monochromator are equal, no signal is produced by the detector. However, when there is a difference in energy, such as will result from absorption of energy by the sample, the detector will produce a pulsating electrical signal, which is then amplified. This signal drives an attenuating comb into the reference beam, restoring the energy balance between the sample and reference beams. The amount of reference beam compensation required is a direct measure of the absorption by the sample. By coupling the motion of a recorder pen to that of the attenuator, the IR spectrum of the sample is plotted on a chart recorder.

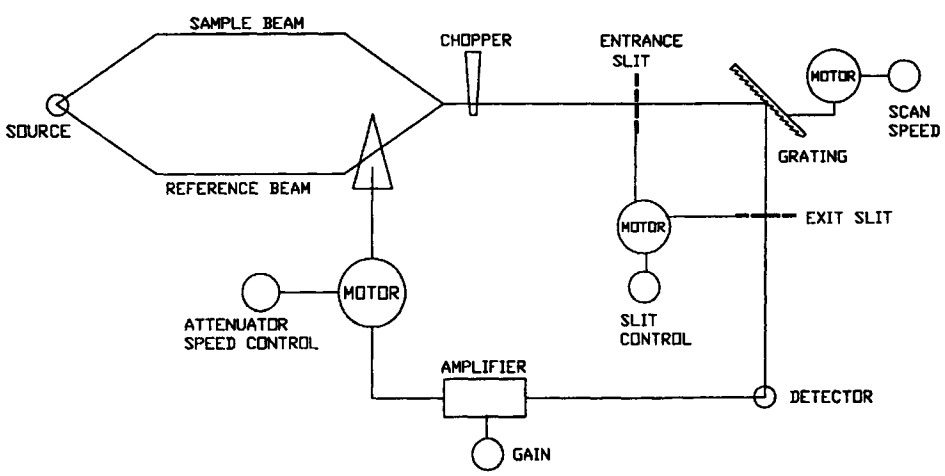

Figure 3: Schematic diagram of a double-beam dispersive IR spectrometer.

The major historical developments in infrared instrumentation described above all represented refinements on the original design of a dispersive infrared spectrometer. Beginning in the 1970s, infrared instrumentation was revolutionised by the development of Fourier transform infrared (FTIR) spectroscopy The principles of FTIR spectroscopy have been described in detail by Griffiths and de Haseth [3], and their book is recommended as a general reference for FTIR theory and techniques. FTIR spectroscopy is based on interferometry and thus differs fundamentally from traditional dispersive infrared spectroscopy. The optical principle of the Michelson interferometer, which is employed in most FTIR spectrometers, is illustrated schematically in Figure 4. The Michelson interferometer uses a beamsplitter to divide the beam of radiation from the infrared source into two parts, one part being reflected to a stationary mirror and the other part being transmitted to a moving mirror. When the beams are reflected back, they recombine at the beamsplitter, producing a constructive/destructive interference pattern due to the varying path difference travelled by the two components of the beam. After the infrared energy has been selectively absorbed by the sample, fluctuations in the intensity of the energy reaching the detector are digitised in real time, yielding an interferogram (Figure 5). The interferogram contains all the information that is required to produce the infrared spectrum of the sample, but this information is in the time domain. In order to obtain interpretable information, the interferogram must be converted to the frequency domain by Fourier transformation. In FTIR spectroscopy, the interferogram is usually a plot of intensity as a function of the path difference between the stationary and the moving mirror, known as the retardation δ, which is proportional to time t because the moving mirror travels at constant velocity v, *i.e.*, $\delta = 2vt$ centimeters.

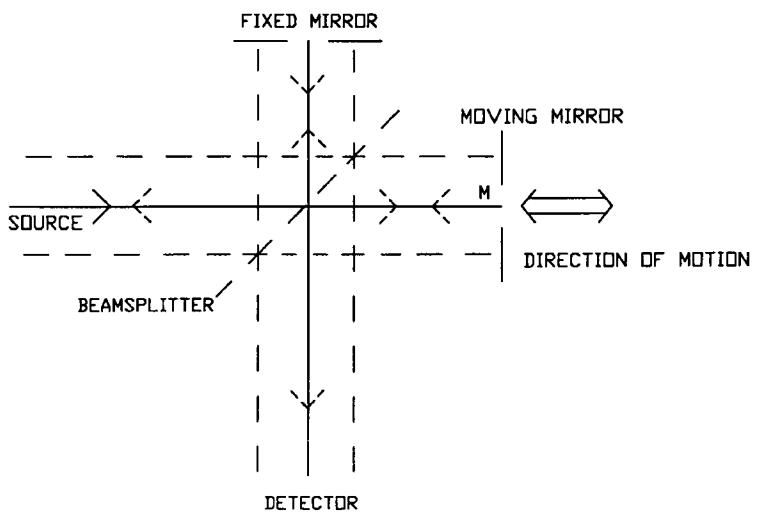

Figure 4: Schematic diagram of a Michelson interferometer.

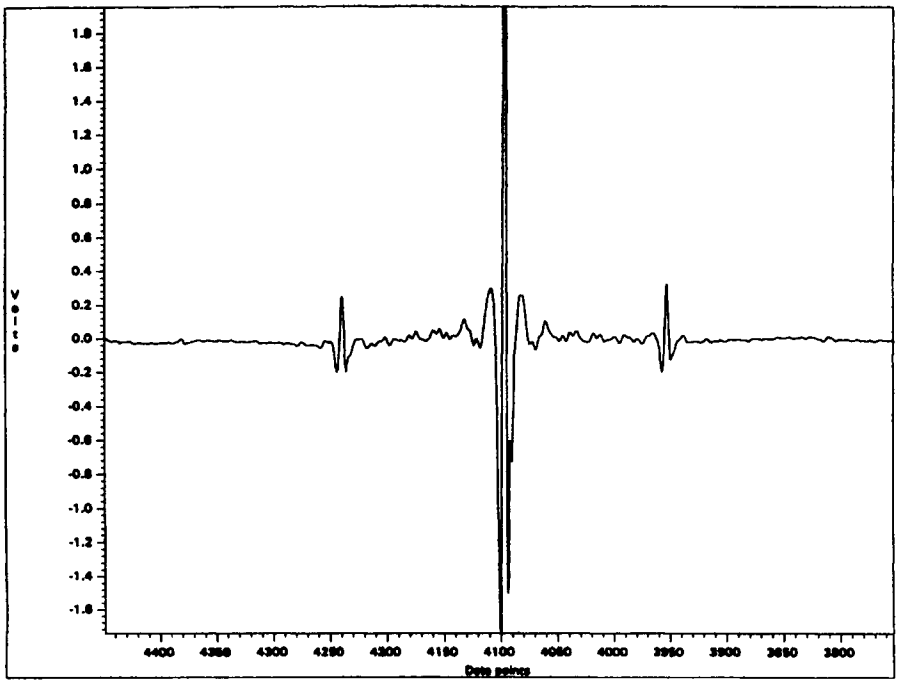

Figure 5: An interferogram produced by an FTIR spectrometer.

Fourier transformation of the interferogram I(δ) then yields a spectrum with the x axis in units of wavenumbers (cm^{-1}), $I(\bar{\nu})$, in accordance with the following relationship (equation (9)):

$$I(\delta) = 0.5H(\bar{\nu})I(\bar{\nu}) \cos 2\pi\bar{\nu}\delta \qquad \textbf{(9)}$$

where $H(\bar{\nu})$ is a single wavenumber-dependent correction factor that accounts for instrumental characteristics. A computer that can carry out this operation using the Cooley-Tukey fast Fourier transform (FFT) algorithm is an integral component of all FTIR instruments. In fact, while Michelson had already designed his interferometer in 1891, it was only with the development of the FFT algorithm and, beginning in the 1970s, with the availability of minicomputers in the laboratory that FTIR spectroscopy became practicable. Since that time, FTIR spectroscopy has undergone very rapid development, such that FTIR spectrometers have now virtually completely replaced dispersive instruments.

The major reasons for the present dominance of FTIR instrumentation are the significant advantages that interferometers have over dispersive instruments. These include a dramatic improvement in signal-to-noise ratio,

a significant reduction in scan time (an FTIR spectrometer can record the entire spectrum of a sample in a one-second scan), higher energy throughput, and superior resolution. Another important advantage for data manipulation and quantitative applications is that wavelength accuracy is maintained by using an internal reference laser, and thus wavelength drifts over time are eliminated as a possible source of error.

The substantial computing power of FTIR systems has also been an important factor in the success of FTIR spectroscopy. FTIR software packages provide a wide variety of data handling routines that facilitate spectral acquisition and interpretation and enhance the utility of IR spectroscopy as both a qualitative and a quantitative analysis tool. In the following section, we will discuss some data handling techniques. FTIR software for multi-component analysis will be covered in the subsequent section on quantitative analysis methods.

4.4 DATA HANDLING TECHNIQUES

4.4.1. Spectral Ratioing

Most FTIR spectrometers are single-beam instruments, and, accordingly, in terms of equation (9), they yield $I(\bar{\nu})$, termed a single-beam spectrum. In order to obtain an absorbance spectrum, the operations represented by equations (7) and (8) must be performed. That is, the single-beam spectrum of a sample consists of the emittance profile of the IR source on which are superimposed the absorption bands of the sample as well as the air background spectrum (*i.e.*, absorption bands of carbon dioxide and water vapour present in the optical path). In order to eliminate the contributions of the source and the air background, the single-beam spectrum of the sample is digitally ratioed against a single-beam spectrum recorded with no sample in the beam $[I_0(\bar{\nu})]$, and the absorbance spectrum is then computed. Alternatively, the single-beam spectrum of the sample $[I(\bar{\nu})^S]$ may be ratioed against the single-beam spectrum of a reference sample $[I(\bar{\nu})^R]$, thereby eliminating the spectral features common to the sample and the reference in addition to the contributions from the source and air background. This operation is equivalent to a 1:1 subtraction of the reference spectrum ratioed against an open-beam spectrum from the sample spectrum ratioed against the same open-beam spectrum ($A^S - A^R$) but requires only a single mathematical manipulation, *i.e.*, equation (10):

$$A^S - A^R = -\log [I(\bar{\nu})^S/I_0)(\bar{\nu})] - \{-\log [I(\bar{\nu})^R/I_0(\bar{\nu})]\} = -\log [I(\bar{\nu})^S/I(\bar{\nu})^R] \quad \textbf{(10)}$$

It should be noted that the contributions of the air background spectrum will only be completely removed by the spectral ratioing procedure if they are constant. Changes in the relative humidity and CO_2 levels in the air in the

optical path between the measurements of I and I_0 will be reflected in the absorbance spectrum and may interfere in the analysis of this spectrum. For this reason, FTIR spectrometers are usually continually purged with dry, CO_2-free air or dry nitrogen, although some are sealed and desiccated units. Figure 6 illustrates the effects of purging by comparing the open-beam spectra of an unpurged and a well-purged FTIR spectrometer. It should be noted that opening the sample compartment to insert a sample will change the relative humidity and CO_2 levels sufficiently to produce spectral artefacts, so that some amount of time (usually on the order of a few minutes) is required to re-establish the purge before the spectrum is recorded. The presence of water vapour can be readily detected in the spectrum by the appearance of a series of spikes between 3900 and 3600 cm^{-1}, and 1800 and 1500 cm^{-1}, while CO_2 gives rise to a doublet with maxima at 2362 and 2340 cm^{-1}.

4.4.2 Co-Adding

The signal-to-noise ratio (S/N) of a spectrum is increased by repetitive scanning as the contributions of random noise are averaged out by co-addition of scans (equation (11):

$$S/N \sim (\text{Number of scans})^{1/2} \quad \textbf{(11)}$$

In FTIR spectroscopy, signal averaging to improve S/N can be performed in either the time domain (*i.e.*, by co-addition of interferograms) or in the frequency domain (*i.e.*, by co-addition of spectra). The former alternative is clearly more efficient as only a single Fourier transform needs to be computed. It should be pointed out that FTIR spectroscopy is more amenable to signal averaging than conventional dispersive IR spectroscopy. In FTIR spectroscopy all frequencies are measured simultaneously in a single one-second scan, and thus the time required to collect multiple scans is greatly reduced. This is one of the fundamental advantages of FTIR spectroscopy, known as Fellgett's advantage.

4.4.3 Baseline Correction

A number of interactive baseline correction algorithms are available with standard FTIR software. The algorithms allow the user to generate a straight line correction (or an exponential function) between different points along the spectrum (Figure 7). Thus, these routines can be used to compensate for a continuously sloping or elevated baseline or to establish reference points for the measurement of peak height/area. Caution is required, however, in employing baseline correction routines so as not to introduce spectral artefacts or obliterate weak features in the spectrum. As a standard practice, it is advisable to keep baseline correction to a minimum and to set baseline limits away from bands employed for analysis.

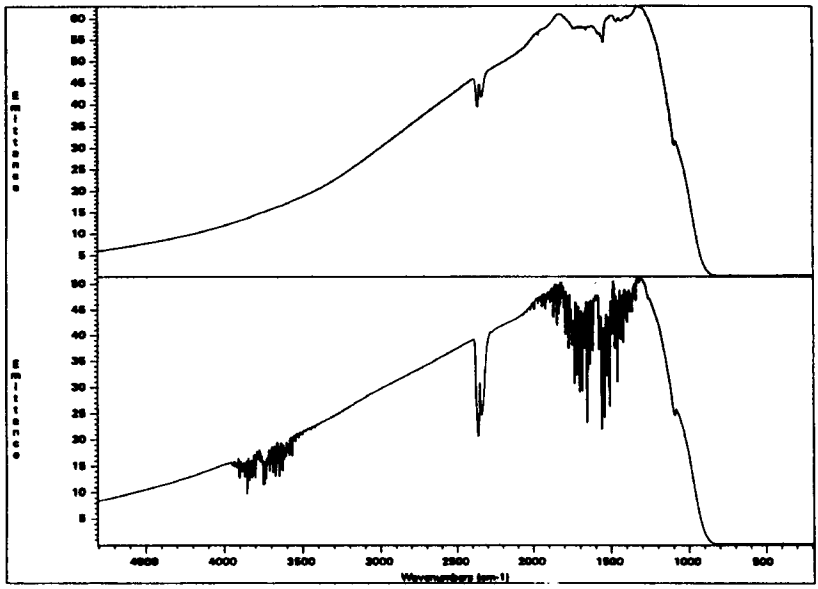

Figure 6: Open-beam spectra recorded with an unpurged (bottom) and a well-purged (top) FTIR spectrometer.

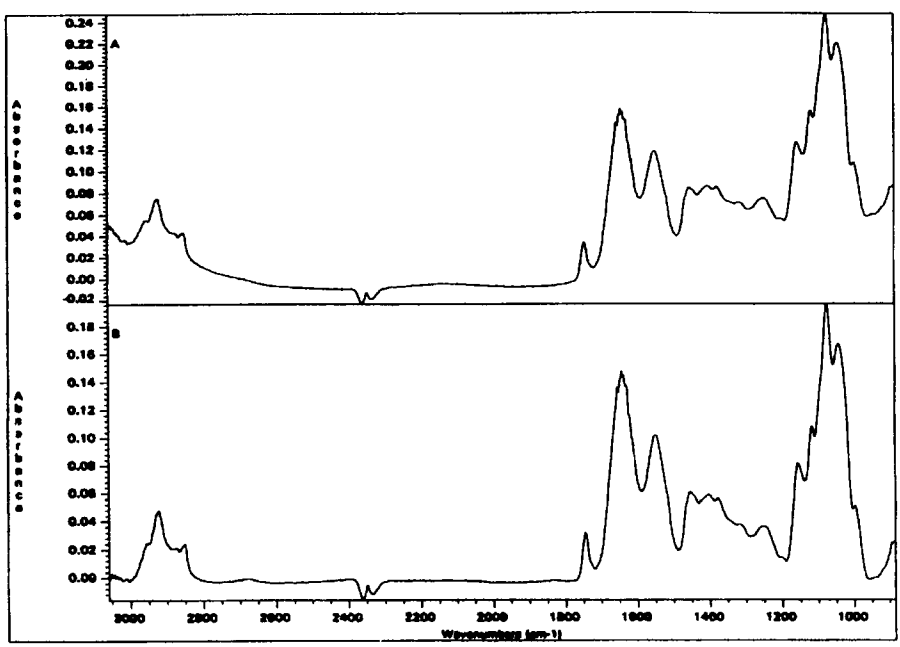

Figure 7: FTIR spectrum of milk before a) and after b) baseline correction. The spectrum was recorded with the use of an ATR sampling accessory and has been ratioed against a single-beam spectrum of water.

4.4.4 Peak Measurements

The measurement of band intensity and peak location represents one of the most basic forms of spectral data processing. With the digitisation of the spectral information, many algorithms have been written to measure peak height and peak location. The user usually defines some minimum-intensity threshold below which no peak will be identified. This approach, however, has limitations in measuring overlapping bands. In such cases, resolution enhancement techniques (see Section 4.4.5) may be employed. In carrying out quantitative analyses based on Beer's law (see Section 4.5.1), measurement of peak area in place of peak height can result in improved precision of the analysis. With digitised spectra, the areas of well-resolved bands can be easily calculated by integrating over the band.

4.4.5 Measurement of Overlapping Bands

Two mathematical methods, derivative spectroscopy and Fourier self-deconvolution (FSD), have been found to be extremely useful in identifying the location of overlapping bands. The mathematical principles of these "resolution enhancement" techniques are described in references [3] and [4].

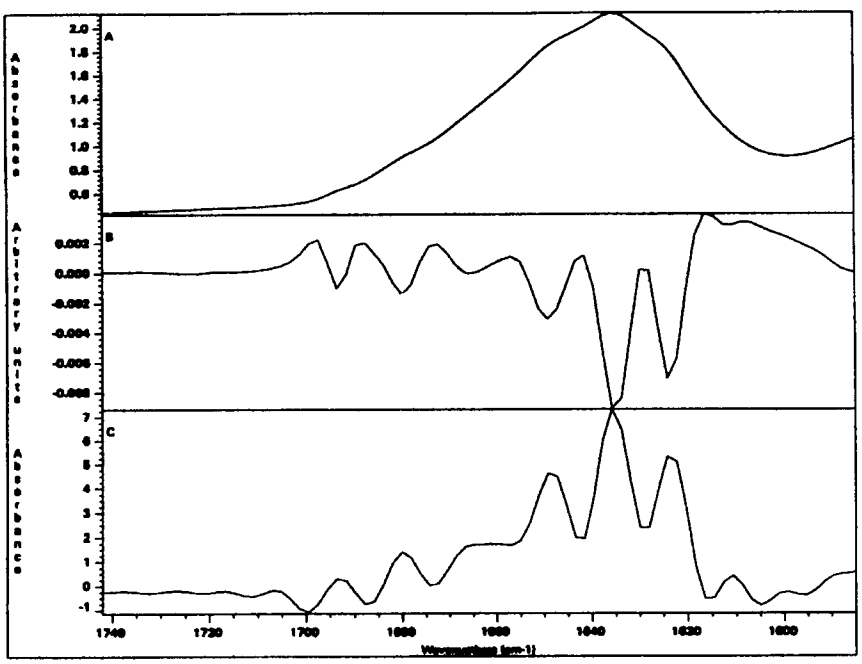

Figure 8: A) The amide I' band profile in the FTIR spectrum of β-lactoglobulin in D_2O; B) the second derivative of the spectrum in A); C) the spectrum in A) after Fourier self-deconvolution with a bandwidth of 13 and k = 2.

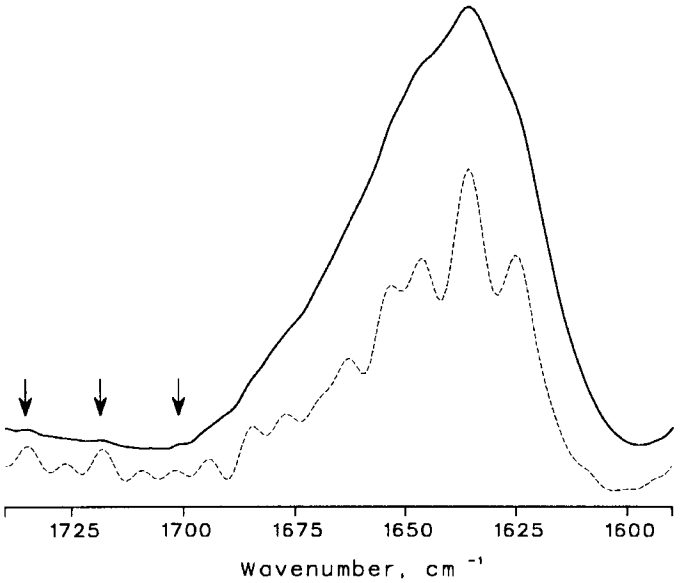

Figure 9: The effect of the presence of water vapour on Fourier self-deconvolution. The solid trace is the spectrum of the same sample as in Figure 8A recorded without adequate purging of the spectrometer. Comparison of the spectrum obtained after Fourier self-deconvolution (dashed line) with that in Figure 8C reveals the appearance of additional bands due to water vapour.

Figures 8B and 8C illustrate the use of second-derivative spectroscopy and FSD, respectively, to resolve the overlapping component bands of the amide I' band profile in the FTIR spectrum of β-lactoglobulin (Figure 8A). Both of these techniques should only be applied to spectra that exhibit a high signal-to-noise ratio (>1000:1), or otherwise artefacts may be introduced by resolution enhancement. The presence of water vapour in the region of the spectrum of interest will also produce features in the processed spectrum that may be misinterpreted as absorption bands of the sample (Figure 9).

4.4.6 Smoothing and Interpolation

Spectral smoothing increases the signal-to-noise ratio of the spectrum at the expense of resolution. Thus, while smoothing produces smoother looking bands, some information content may be lost. Furthermore, it may cause changes in the measured peak position and band shape. Interpolation represents the inverse of smoothing. That is, the resolution is artificially enhanced to provide a better definition of band shape. This may be achieved by polynomial fitting of the spectral data points.

4.4.7 Spectral Subtraction

Spectral subtraction is an extremely useful method to remove solvent absorption features from the spectrum of a solution, thereby revealing more detail about the spectral features of the solute(s). Spectral subtraction has proved very effective in other applications, including successive spectral stripping of pure components from a complex mixture and monitoring starting material depletion and product formation (Figure 10). Spectral subtraction is performed on absorbance spectra as the absorbance scale is linear. The difference spectrum is calculated by equation (12):

$$A\bar{\nu}\,(\text{Difference spectrum}) = A\bar{\nu}\,(\text{Sample}) - (\text{SF})^{*}A\bar{\nu}\,(\text{Reference}) \qquad \textbf{(12)}$$

where SF is a scaling factor. The value of the subtraction scaling factor can be interactively adjusted to compensate for pathlength changes or dilution effects. It should be noted that if solute-solvent interaction takes place, solvent bands may undergo broadening. This results in an inability to completely subtract the solvent bands, resulting in residual solvent bands

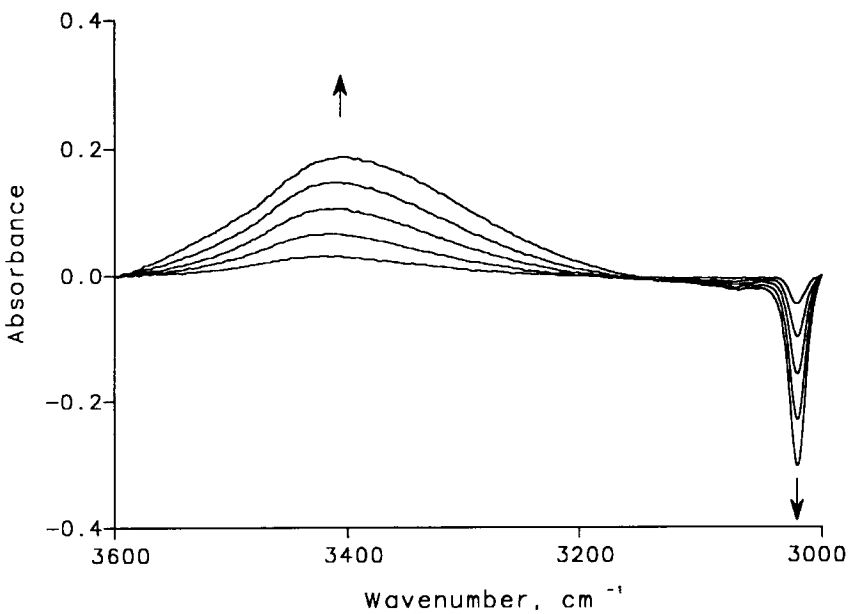

Figure 10: Example of reaction monitoring by FTIR spectroscopy through the use of spectral subtraction. The oxidation of trilinolenin at 40°C as a function of time can be followed by monitoring the increase in the hydroperoxide absorption band (3444 cm^{-1}) and the decrease in the *cis* (H-C=C) absorption band (3011 cm^{-1}). These changes are clearly observed by subtracting the spectrum of the unoxidised oil from subsequent spectra recorded as a function of time.

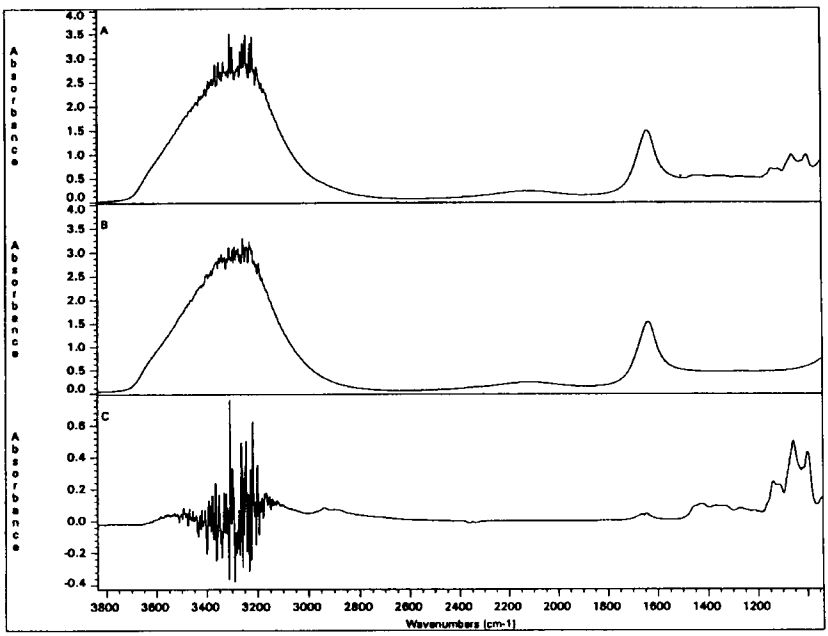

Figure 11: FTIR spectra of a 10% solution of sucrose in water A) and of water B) and the difference spectrum obtained by spectral subtraction (A-B). The features in the difference spectrum are the absorption bands of sucrose. The region between 3500 and 3150 cm^{-1} is obscured by digitisation noise due to the intense water absorption band in this region.

with a derivative-like shape. In addition, in regions of intense absorption by the solvent, insufficient energy may reach the detector for proper digitisation of the signal, resulting in loss of spectral information owing to digitisation noise (Figure 11).

4.5 QUANTITATIVE ANALYSIS

As IR spectroscopy is a secondary method of analysis, the development of quantitative analysis methods requires calibration with a set of standards of known composition, prepared gravimetrically or analysed by a primary chemical method, to establish the relationship between IR band intensities and the compositional variable(s) of interest. Once a calibration has been developed, it can then be used for the prediction of unknowns, provided two general conditions are met: i) the spectra of the unknowns are recorded under the same conditions as employed in the calibration step (*i.e.*, same instrumental parameters, identical means of sample handling, *etc.*) and ii) the composition of the calibration standards is representative of that of the unknowns.

In this section, various approaches that are employed for calibration will be described, in order of increasing mathematical sophistication. These range from a simple Beer's law plot, which is an adequate basis for calibration in the case of a simple system, such as a single component dissolved in a non-interacting solvent, to the sophisticated multivariate analysis techniques that are required for more complex systems. The data handling capabilities of FTIR systems have allowed these latter techniques to be implemented in the instrument software and applied directly to spectral data, bringing a resurgence to quantitative IR spectroscopy during the past decade.

4.5.1 Beer's Law

As with other types of absorption spectroscopy (*e.g.*, UV-visible spectroscopy), the basis of quantitative analysis in infrared spectroscopy is the Bouguer-Beer-Lambert law or Beer's law (equation (13)):

$$A_{\bar{\nu}} = \varepsilon_{\bar{\nu}} bc \qquad \textbf{(13)}$$

Here, $A_{\bar{\nu}}$ is the absorbance (defined in equation (8)) measured at frequency $\bar{\nu}$, $\varepsilon_{\bar{\nu}}$ is the molar absorption coefficient of the absorbing species at this frequency, b is the pathlength of the IR cell, and c is the concentration of the absorbing species. Application of Beer's law for the determination of the amount of a compound present in a solution requires that $\varepsilon_{\bar{\nu}}$ be determined by measuring the absorbance of a solution of known concentration. Of course, in order to attain better accuracy, it is preferable to prepare a series of solutions of different concentrations, spanning the concentration range of interest, and obtain $\varepsilon_{\bar{\nu}} b$ from a plot of absorbance *versus* concentration by linear least-squares regression. This procedure averages out the errors due to instrumental noise, measurement errors, and other sources of random variation. In addition, it allows deviations from Beer's law in the concentration range of interest to be detected, such as may arise from hydrogen bonding, dimerisation, and other intermolecular interactions. Such interactions may then be modelled by the introduction of higher order terms into the equation relating absorbance to concentration.

When more than one component is present in the solution, the above approach will generally not be satisfactory as it cannot account for any contributions of additional components to $A_{\bar{\nu}}$, nor can it model interactions between components. Therefore, more complicated mathematical approaches are required for multi-component systems. We will describe here the three techniques that are most commonly used in multi-component analysis.

4.5.2 Classical Least Squares (K-Matrix)

The classical least squares (CLS) approach is based on the representation of Beer's law in matrix form [5]. Consider the simplest case of a two-component system. Owing to the additive nature of Beer's law, the following equations can be written as follows (equations (14) and (15)):

$$A\bar{\nu}\,1 = \bar{\nu}\,1_x bc_x + \bar{\nu}\,1_y bc_y \quad \textbf{(14)}$$

$$A\bar{\nu}\,2 = \bar{\nu}\,2_x bc_x + \bar{\nu}\,2_y bc_y \quad \textbf{(15)}$$

These equations can be rewritten in matrix form (equation (16) as:

$$\begin{vmatrix} A\bar{\nu}1 \\ A\bar{\nu}2 \end{vmatrix} = \begin{vmatrix} \varepsilon\bar{\nu}1_x b & \varepsilon\bar{\nu}1_y b \\ \varepsilon\bar{\nu}2_x b & \varepsilon\bar{\nu}2_y b \end{vmatrix} \begin{vmatrix} c_x \\ c_y \end{vmatrix} \quad \textbf{(16)}$$

or as equation (17):

$$A = KC \quad \textbf{(17)}$$

The calibration step in the CLS approach then involves the determination of the elements of the K matrix using the spectral data for a series of calibration standards. For an n-component analysis, this involves the solution of a matrix equation of the form given in equation (18):

$$\begin{vmatrix} A_{11} & A_{12} & \dots & A_{1m} \\ A_{21} & A_{22} & \dots & A_{2m} \\ \dots & \dots & \dots & \dots \\ A_{l1} & A_{l2} & \dots & A_{lm} \end{vmatrix} = \begin{vmatrix} k_{11} & k_{12} & \dots & k_{1n} \\ k_{21} & k_{22} & \dots & k_{2n} \\ \dots & \dots & \dots & \dots \\ k_{l1} & k_{l2} & \dots & k_{ln} \end{vmatrix} \begin{vmatrix} c_{11} & c_{12} & \dots & c_{1m} \\ c_{21} & c_{22} & \dots & c_{2m} \\ \dots & \dots & \dots & \dots \\ c_{n1} & c_{n2} & \dots & c_{nm} \end{vmatrix} \quad \textbf{(18)}$$

where l is the number of frequencies at which absorbance measurements are made ($l \geq n$), and m is the number of calibration standards ($m \geq n$). If $l > n$ or $m > n$, the problem is said to be over-determined; that is, more data are used than are necessary for solution of the equation. Over-determination reduces the effects of errors in preparation of the standards, spectral noise, and other random errors and is generally required to obtain a good calibration.

The major limitation of the CLS technique becomes apparent if we consider the form of equations (14) and (15). In this two-component case, the absorbance measured at frequency $\bar{\nu}_1$ (or $\bar{\nu}_2$) is written as a sum of the contributions of the two components to this absorbance. If a third component is present, but not explicitly taken into account, any absorbance due to this component at frequency $\bar{\nu}_1$ will be attributed to components x and y. An alternative approach that does not suffer from this drawback is the inverse least squares method, which will be described in the following section.

4.5.3 Inverse Least Squares (P Matrix)

In the inverse least squares (ILS) approach [6], the matrix equation expressing Beer's law is rearranged into equation (19):

$$C = PA \quad \textbf{(19)}$$

That is, concentration is expressed as a function of absorbances at a set of frequencies. Thus, in the calibration step, only the concentrations of the component(s) of interest need be known. However, all components that may be present in the samples to be analysed must be included in the calibration standards. In other words, as in classical least squares, it is essential that the set of calibration standards be representative of the samples to be analysed; however, unlike the classical least squares case, it is not necessary to know the concentrations of interfering component(s) in the calibration standards.

There are several mathematical limitations inherent in the inverse least squares method. The number of frequencies employed cannot exceed the number of calibration standards in the training set. The selection of frequencies is further limited by the problem of collinearity: that is, the solution of the matrix equation tends to become unstable as more frequencies that correspond to absorptions of a particular component x are included because the absorbances measured at these frequencies will change in a collinear manner with changes in the concentration of x. Thus, the possibilities for averaging out errors through the use of over-determination are greatly reduced by comparison with the classical least squares method, in which there are no limitations on the number of frequencies employed.

4.5.4 Partial Least Squares (PLS)

Partial least squares (PLS) regression is a sophisticated multivariate analysis technique that is finding increasing use in quantitative infrared spectroscopy [7, 8]. PLS is a form of factor analysis; a detailed description of the mathematical basis of PLS is available elsewhere [8] and is beyond the scope of this chapter. For the purposes of our discussion here, the key difference between PLS and the methods discussed above is that a PLS calibration does not entail establishing direct relationships between concentration and absorbance measurements at specified frequencies (*i.e.*, peak heights or peak areas). Instead, a PLS calibration model is developed by compressing the spectral data for the training set into a series of mathematical "spectra", known as loading spectra or factors. Then, PLS decomposes the spectrum of each calibration standard in the training set into a weighted sum of the loading spectra, and the weights given to each loading spectrum, known as "scores", are regressed against the concentration data for the standards. When the spectrum of an unknown is analysed, PLS attempts to reconstruct

the spectrum from the loading spectra, and the amounts of each loading spectrum employed in reconstructing the spectrum, *i.e.*, the "scores", are then used to predict the concentration of the unknown.

PLS is a powerful technique that shares the advantages of both the CLS and ILS methods but does not suffer from the limitations of either these methods. A PLS calibration can, in principle, be based on the whole spectrum, although in practice the analysis is restricted to regions of the spectrum that exhibit variations with changes in the concentrations of the components of interest. As such, the use of PLS can provide significant improvements in precision relative to methods that use only a limited number of frequencies [9]. In addition, like the inverse least squares method, PLS treats concentration rather than spectral intensity as the independent variable. Thus, PLS is able to compensate for unidentified sources of spectral interference, although all such interferences that may be present in the samples to be analysed must also be present in the calibration standards. The utility of PLS will be demonstrated by several examples of food analysis applications presented in Section 4.7.

Overfitting of the spectral data is always possible in developing a PLS calibration model, as the fit between the actual and the predicted values for the calibration standards will necessarily be improved by increasing the number of loading spectra included in the model. However, these additional loading spectra may just represent the noise in the spectra of the calibration standards, and their inclusion in the PLS calibration model will then deteriorate its performance in the prediction of unknowns. Thus, validation of a PLS calibration model is required in order to select the optimum number of loading spectra. This may be achieved by testing its performance with standards not included in the calibration set. Alternatively, the "leave-one-out" cross-validation technique may be employed, whereby the calibration is performed n times with n - 1 standards and the nth standard is predicted as an unknown. The predicted residual error sum of squares (PRESS) is then computed from the errors in the predictions obtained for the n standards by cross-validation and plotted as a function of the number of factors employed in the calibration, allowing the number of factors which gives the best predictive accuracy to be identified.

4.6 SAMPLING METHODS

Infrared spectroscopy can be used to examine a wide range of samples, including gases, liquids and solids. The traditional sampling methods generally involve measurements in the transmission mode; that is, the sample is placed in the optical path of the infrared beam, allowing the beam to pass through the sample. These methods impose fairly severe limitations on sample thickness (except for samples in the gas phase) because the amount of infrared energy absorbed by the sample is proportional to its

thickness and, beyond a certain thickness, the sample will not transmit any infrared radiation in the regions of the spectrum where it is strongly absorbing, so that no signal will reach the detector. Thus, for example, to obtain the IR spectrum of a pure liquid, a sample thickness of <0.015-0.025 mm is generally required. In the case of solutions, depending on their concentration, a sample thickness of 0.1 to 1.0 mm may be required to obtain the spectrum of the solute; however, the portions of the spectrum where the solvent absorbs will be effectively "blanked out." For solids and emulsions, these limitations on sample thickness are compounded by restrictions on particle size. Good quality spectra will not be obtained from samples containing particles whose dimensions are comparable to or exceed the wavelength of the radiation passing through the sample, owing to light scattering effects. In order to overcome these problems, a number of other sampling techniques have been developed. These include various techniques that involve measurements in the reflection mode, known as specular, diffuse, and internal reflection. Another alternative is a technique called photoacoustic spectroscopy, which is based on the measurement of the photoacoustic signal produced by the thermal expansion of a gas enclosed in a chamber with the sample owing to the heat generated by the sample upon absorption of infrared energy. With one or another of these sampling techniques, it is possible to obtain the infrared spectrum of samples in virtually any form, including solid chunks, powders, polymer films and coatings, fibers, gels, pastes, viscous liquids, and samples containing particulates, with minimal or no sample preparation. However, each of these techniques has its own limitations, particularly in relation to quantitative analysis applications.

Numerous books cover the topic of sampling methods in infrared spectroscopy (see, *e.g.*, references [10-12]), and a detailed description of all the various alternatives is beyond the scope of this chapter. Instead, we will focus on the two sampling methods that are most commonly employed in food analysis applications, namely, the use of transmission cells for recording the spectra of solutions and the total internal reflection technique, also known as attenuated total reflectance (ATR). Readers who wish to learn about the techniques not covered here may consult the references cited above.

4.6.1 Transmission Cells

The IR spectra of liquids and solutions are recorded in the transmission mode by placing the sample between two windows made of IR-transmitting material in a transmission cell. A schematic representation of a transmission cell is presented in Figure 12. The spacer placed between the two windows determines the sample thickness or cell pathlength (b in equation (13)). Transmission cells may be either demountable or sealed. In the case of demountable cells, the sample is loaded into the cell by disassembling the cell, applying the sample onto the face of one of the windows, and

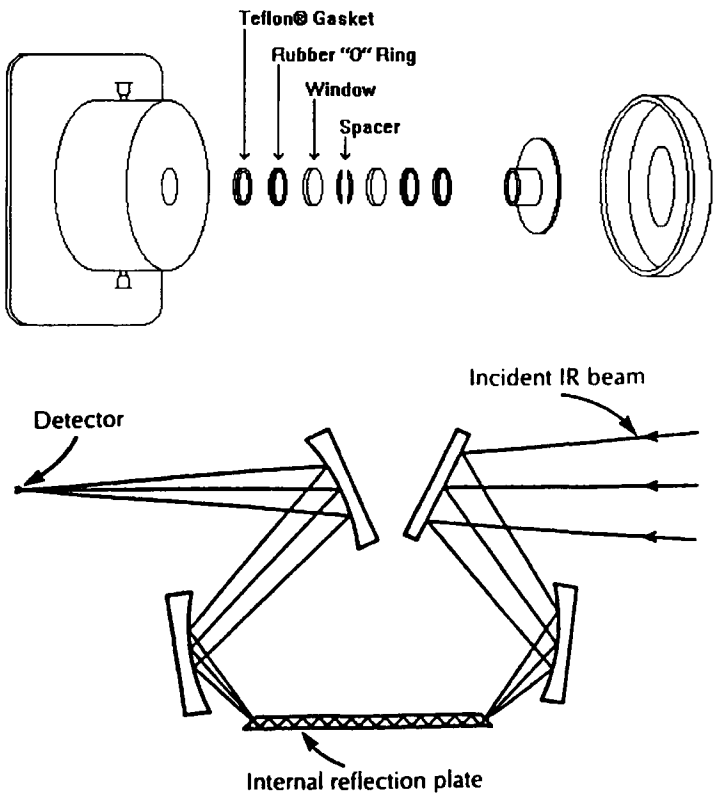

Figure 12: Schematic representation of an infrared transmission cell (top) and of an attenuated total reflectance (ATR) accessory (bottom).

reassembling the cell. Sealed cells have two injection ports on the top metal plate of the cell, allowing introduction of the sample with a syringe. Some types of these cells are permanently sealed with mercury amalgam, while others can be disassembled to clean the windows or change the pathlength. For quantitative analysis work, sealed cells are to be preferred as the pathlength is fixed, whereas the pathlength of a demountable cell may vary from sample to sample, depending on the pressure applied on the screws when the cell is assembled. However, it may be necessary to use a demountable cell for samples that are too viscous to inject; in such cases, the samples should all contain an internal standard with a distinct absorption band that can be used to measure variations in pathlength.

Most IR windows are highly polished salt crystals of various types (Table 2). The most common and least expensive window materials are NaCl and KBr. As can be seen in Table 2, both of these materials have good transmission characteristics across most of the mid-IR spectral range, with NaCl having a somewhat earlier cut-off at the low-frequency end. Unfortunately, as both

these materials are highly water soluble, they will fog in contact with samples containing moisture and will be destroyed by aqueous samples. The water-insoluble window materials are considerably more expensive than NaCl and KBr; CaF_2 and BaF_2 are commonly employed with aqueous samples but do not transmit below approximately 1000 and 800 cm^{-1}, respectively. Silver bromide (AgBr) has good transmission characteristics, but it is a soft, and thus easily scratched, fairly reactive, and photosensitive material. Finally, ZnS and ZnSe windows are often the best choices for aqueous samples, as they transmit down to approximately 715 and 515 cm^{-1}, respectively, are resistant to chemical attack, and are relatively hard. Their high refractive index is a disadvantage of these materials, for reasons that will be made apparent in the discussion of pathlength determination below.

The selection of the pathlength of a transmission cell depends on the nature of the samples that are to be examined. As mentioned above, for pure liquids a pathlength of 0.015-0.025 mm will usually be appropriate. The optimal pathlength for solutions will depend on both the concentration range of the component of interest and the infrared absorption characteristics of the solvent. Thus, the most suitable solvents for IR work are those whose absorptions do not "blank out" large regions of the IR spectrum, even when cells of relatively long pathlength (*i.e.*, up to 1 mm) are required in order to detect the absorptions of low concentrations of solutes. The solvents that meet this criterion are aprotic solvents whose molecules are small and symmetrical, such as carbon disulphide and carbon tetrachloride. On the other hand, water is a poor solvent from an IR perspective, because of its two intense and extremely broad (owing to hydrogen bonding) absorptions, centered at 3300 and 1650 cm^{-1} (Figure 13). Thus, fairly narrow pathlengths (<0.040 mm) are required for aqueous samples.

TABLE 2
Properties of Infrared Window Materials

Material	Transmission range (cm^{-1})	Solubility in water	Refractive index
Sodium Chloride (NaCl)	40,000-625	soluble	1.49
Potassium Chloride (KCl)	40,000-500	soluble	1.46
Potassium Bromide (KBr)	40,000-400	soluble	1.52
Calcium Fluoride (CaF2)	66,666-1,110	very slightly	1.39
Barium Fluoride (BaF2)	50,000-870	slightly	1.42
Infrared Quartz (SiO2)	50,000-2,500	insoluble	1.74
Cesium Iodide (CsI)	10,000-200	very soluble	1.74
Thallium Bromide-Iodide (KRS-5)	15,385-250	very slightly	1.74
Silver Chloride (AgCl)	25,000-435	very slightly	1.98
Silver Bromide (AgBr)	20 000-285	very slightly	2.2
Irtran-2 (ZnS)	10,000-715	insoluble	2.2
Zinc Selenide (ZnSe)	10,000-555	insoluble	2.4
Germanium (Ge)	5,000-850	insoluble	4.0

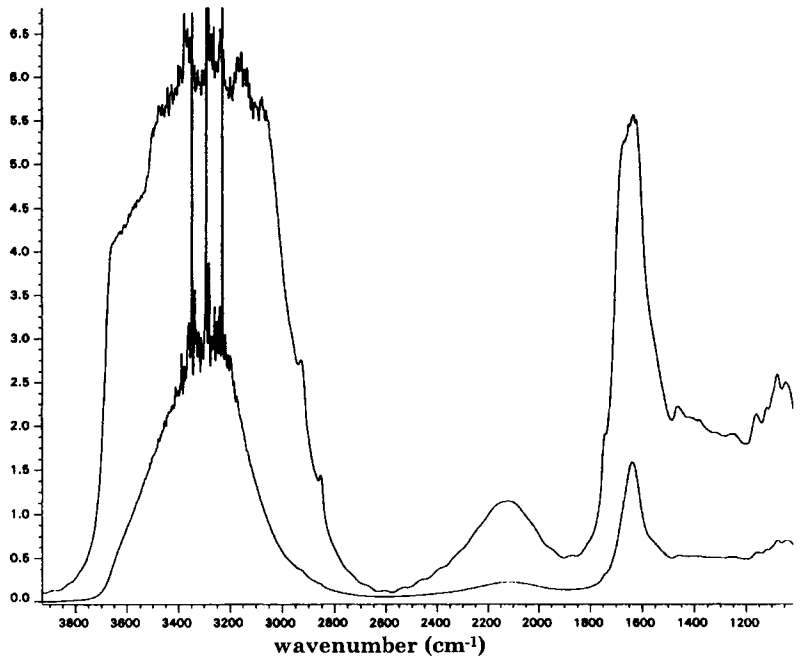

Figure 13: FTIR spectrum of milk recorded in a transmission cell (top) and by ATR (bottom).

As the absorbance of a component in solution depends not only on its concentration but also on the cell pathlength (equation (13)), for quantitative work it is necessary to measure the pathlength accurately; otherwise, the quantitative methods developed will be specific to the cell used for the calibration. The pathlength of a transmission cell can be determined by using the interference fringes that appear in the spectrum of the empty cell (Figure 14), caused by the difference between the refractive index of the IR windows and that of the air space between them. The pathlength can be calculated using equation (20):

$$b = n / 2 (\bar{\nu}_1 - \bar{\nu}_2) \quad \textbf{(20)}$$

where b is pathlength, and n is the number of fringes between $\bar{\nu}_1$ and $\bar{\nu}_2$. Interference fringes can also be observed in the spectrum of a sample when there is a large difference between the refractive index of the sample and that of the window material, and they may be sufficiently prominent to obscure weak features in the spectrum of the sample. These fringes may also affect quantitative accuracy as their positions will shift with slight changes in the temperature (and hence the refractive index) of the sample or the windows. These effects are generally only significant with window materials of high refractive index such as ZnS and ZnSe.

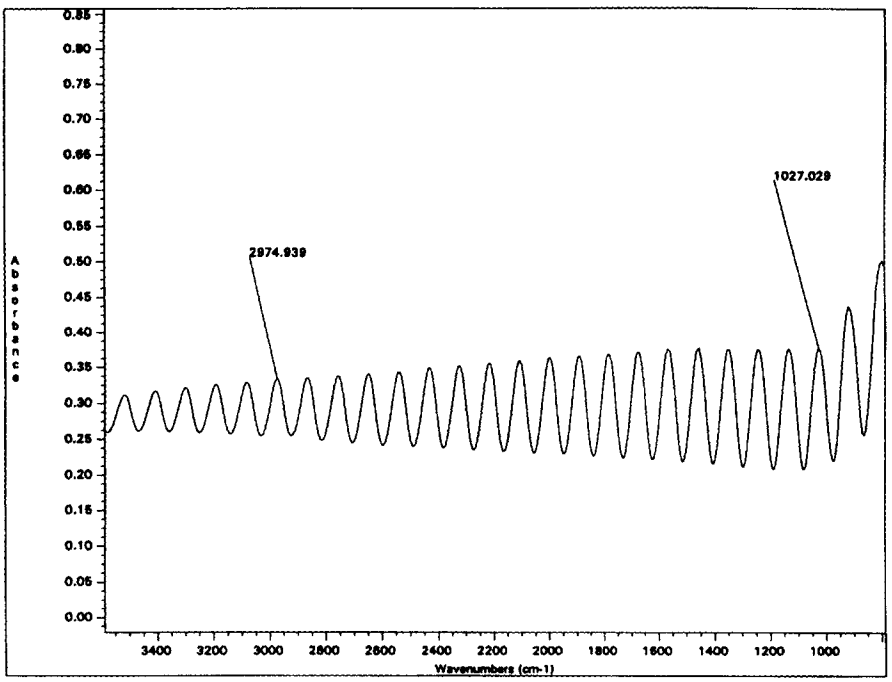

Figure 14: FTIR spectrum of an empty transmission cell with ZnS windows. The pathlength of the cell can be calculated from equation (20) to be 0.046 mm.

4.6.2 Total Internal Reflection (Attenuated Total Reflectance)

The attenuated total reflectance (ATR) sampling technique, which was developed in the 1960s, is based on the effect of the angle of incidence of a light beam on its reflection from a surface (Figure 12B). When the angle of incidence is small, partial reflection and partial refraction occur. However, above a critical angle of incidence, total internal reflection occurs at the surface. In the ATR technique, the sample is placed in contact with a crystal of a high-refractive index material, known as an internal reflection element (IRE). Light from the infrared source is launched into the IRE at an angle such that it undergoes multiple internal reflection as it travels down the crystal, giving rise to an evanescent wave at the surface of the IRE which decays exponentially as it propagates away from the surface of the IRE through the sample. The distance from the surface at which the intensity of the evanescent wave decays to 1/e of its value at the surface is defined as the depth of penetration, d_p. The evanescent wave is attenuated by the absorption of radiation by species on or near the surface of the IRE, and measurement of this attenuation as a function of wavelength yields the infrared spectrum of these species. The effective pathlength in an ATR

measurement is given by the product of the number of internal reflections and the depth of penetration, d_p, given by:

$$d_p = \lambda/\{2\pi n_1[\sin^2(\theta) - (n_2/n_1)]^{1/2}\}$$

where λ is the wavelength of the radiation in the IRE, n_1 is the refractive index of the IRE material, n_2 is the refractive index of the medium surrounding the IRE, and θ is the angle at which the incident light strikes the interface. The effective pathlength can thus be altered by varying the angle of incidence as well as by the choice of the IRE material. It should be noted that the depth of penetration, and hence the effective pathlength, decreases on going from the high-frequency end to the low-frequency end of the spectrum. Therefore, the relative intensities of the peaks in the ATR spectrum of a sample will not be the same as those in the spectrum recorded for the same sample in a transmission cell (see Figure 13).

Among the IR-transmitting materials listed in Table 2, ZnSe and Ge crystals are suitable materials for fabrication of IREs owing to their high refractive indices, Germanium providing a shorter depth of penetration than ZnSe. The effective pathlength of a Ge ATR accessory with 8 reflections and $\theta = 45^o$ can be calculated from the above equation to be approximately 0.0016 mm for λ = 3 μ (3333 cm^{-1}) and 0.003 mm for λ = 6 μ (1667 cm^{-1}) . By comparison the corresponding values for a ZnSe ATR accessory are 0.0024 mm for λ = 3 μ and 0.006 mm for λ = 6 μ. Because of their short effective pathlengths, ATR sampling accessories have proved particularly useful in work with aqueous solutions (Figure 13). The utility of the ATR sampling technique in the analysis of foods has been extensively discussed in the literature [13-17].

4.7 APPLICATIONS

4.7.1 Milk Analysis

The application of IR spectroscopy to the quantitative determination of fat, protein, and lactose in milk is an Official Method of the Association of Official Analytical Chemists (AOAC) [18]. Commercial IR milk analysers are extensively used as a basis for milk payment, dairy herd recording, and routine quality control in the dairy industry [19]. Although the methodology for IR milk analysis was originally developed with dispersive spectrometers [20], the milk analysers currently on the market (*i.e.*, Milkoscan, Multispec) are filter-based instruments. Quantitation of each component is based on measurements at two specific wavelengths, corresponding to a wavelength at which the component absorbs (sample wavelength) and a reference wavelength where no significant absorption occurs (see Table 3). Each measurement wavelength is selected by interposing a narrow-band interference filter in the IR beam. Thus, analytical speed is a function of the

number of components analysed. Automated versions of these instruments are capable of analysing one milk sample every 20 seconds [21]. IR milk analysers are calibrated with a set of calibration milks that have been analysed by suitable reference methods, for example, the Mojonnier method for fat content, Kjeldahl analysis for protein content, and polarimetry for lactose content. The AOAC specifications on the reproducibility and accuracy (relative to the reference methods) are stringent (Table 3) but are routinely met by commercial IR milk analysers.

The application of FTIR spectroscopy to the analysis of milk has been investigated, and its performance compared to that of conventional filter-based instrumentation [22]. Calibration of the FTIR spectrometer for the determination of fat, protein, lactose, and total solids was performed through the use of PLS. The FTIR method using modified Nicolet 510 research spectrometer was able to provide a four-component analysis of milk in ~12 seconds per sample and met the AOAC specifications for milk analysis [22]. The results of this study demonstrated that the use of FTIR spectroscopy would allow payment laboratories to analyse for more components and with appropriate sample handling gain sample throughput speed. A commercial version of an FTIR milk analyser is presently on the market in Europe. An FTIR method for the direct determination of water in milk has also been reported [23].

The casein content of milk is an important indicator of cheese yield, and cheese yield formulas are used to determine milk payment in some cheese plants. Milks of similar protein content but dissimilar casein/whey ratio do not produce the same cheese yield. The methods presently used for casein estimation are based on precipitation of casein from the milk and involve a series of steps including centrifugation, aspiration of fat, filtration, drying and weighing. Two methods for the determination of the casein content of milk with the use of a commercial IR milk analyser have been described [24,

TABLE 3
AOAC Specifications for IR Milk Analysis

Component	Frequency, cm^{-1}		Accuracy		Reproducibility	
	Sample	Reference	MD_a[d]	SDD_a[e]	MD_r[f]	SDD_r[g]
Fat	1744.6[a]	1792.1	≤ 0.05%	≤ 0.06%	≤ 0.02%	≤ 0.02%
Protein	1548.6[b]	1497.0	≤ 0.05%	≤ 0.06%	≤ 0.02%	≤ 0.02%
Lactose	1043.1[c]	1302.1	≤ 0.05%	≤ 0.06%	≤ 0.02%	≤ 0.02%

Notes: a) ν (CO) ester linkage; b) protein amide II band; c) C-OH; d) mean difference for accuracy; e) standard deviation of the differences for accuracy; f) mean difference for reproducibility; and g) standard deviation of the differences for reproducibility.

25], based on IR measurement of the protein content before and after removal of the casein from the milk by isoelectric precipitation [24] or by renneting [25], with the casein content determined from the difference between the two IR measurements.

A rapid FTIR method for the direct determination of the casein/whey ratio in milk has also been developed [26]. This method is unique because it does not require any physical separation of the casein and whey fractions, but rather makes use of the information contained in the whole spectrum to differentiate between these proteins. Proteins exhibit three characteristic absorption bands in the mid-infrared spectrum, designated as the amide I (1695-1600 cm^{-1}), amide II (1560-1520 cm^{-1}) and amide III (1300-1230 cm^{-1}) bands, and the positions of these bands are sensitive to protein secondary structure. From a structural viewpoint, caseins and whey proteins differ substantially, as the whey proteins are globular proteins whereas the caseins have little secondary structure. These structural differences make it possible to differentiate these proteins by FTIR spectroscopy. In addition to their different conformations, other differences between caseins and whey proteins, such as their differences in amino acid compositions and the presence of phosphate ester linkages in caseins but not whey proteins, are also reflected in their FTIR spectra. These spectroscopic differences are illustrated in Figure 15, which shows the so-called fingerprint region in the FTIR spectra of sodium caseinate and whey protein concentrate. Thus, FTIR spectroscopy can provide a means for quantitative determination of casein and whey proteins in the presence of each other.

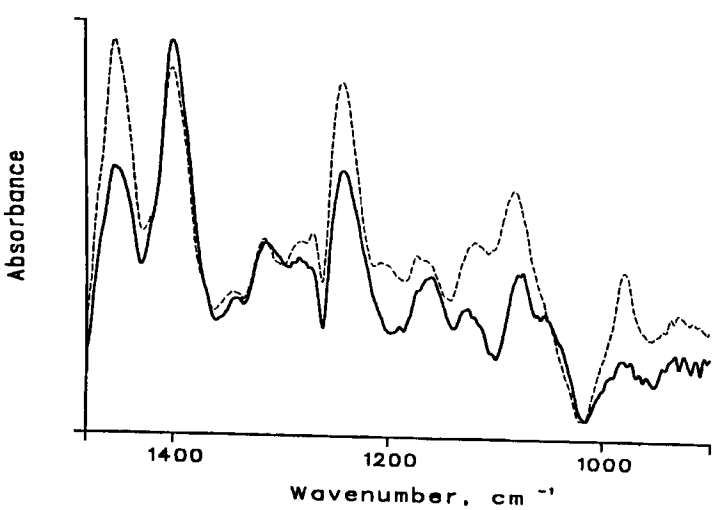

Figure 15: FTIR spectra of sodium caseinate (---) and whey protein concentrate (___) in water. The spectral features of water have been removed from the spectra by rationing against the spectrum of water.

The feasibility of this approach was demonstrated by Mendenhall and Brown [27], who developed an FTIR method for the detection of adulteration of nonfat dry milk (NDM) with whey protein concentrate. Validation of the method using 135 reconstituted NDM samples adulterated with whey protein concentrate yielded an excellent correlation ($r > 0.99$) between the actual concentrations and the values predicted by the FTIR method. Because the low concentrations of whey proteins in milk [14-24% of the total protein content] make their accurate determination by FTIR spectroscopy difficult, the analytical method developed for determination of the casein/whey ratio in milk involved the FTIR determination of total protein content and casein content, with the whey content being obtained by difference. The total protein determination was based on the previously developed PLS calibration model for FTIR analysis of milk [22]. A set of 12 standards were prepared for the calibration of the FTIR spectrometer for the determination of casein content by mixing varying amounts of sodium caseinate, whey protein concentrate, butterfat, lactose and water. PLS regression was employed to establish correlations between the FTIR spectra of these standards and their casein contents. Using the 1800-950 cm^{-1} region of the spectrum, the PLS calibration model predicted the casein content of the standards to within 0.08% of the actual values. The FTIR method was validated with 36 milk samples spiked with known amounts of sodium caseinate and whey protein concentrate. The predictions of the spiked amounts in these samples were within 0.09% for casein and within 0.12% for whey.

4.7.2 Meat Analysis

Following the successful development in the mid-1960s of IR milk analysers, described above, attempts were made to extend their use to the analysis of meat [28-30] as well as fish [31]. Although the results of this work demonstrated the viability of IR analysis of these types of samples, the application of the methods developed was limited because the commercially available equipment was specifically designed for milk analysis applications.

A major difficulty encountered in IR analysis of meat has been sample preparation. For analysis in the transmission mode, samples must be converted to a milk-like emulsion in which the globule sizes are smaller than the analytical wavelengths (2-8 μ), in order to avoid light scattering effects. A homogeneous emulsion can be prepared by adding warm dilute base to the meat and blending with a Polytron mixer for ~1 minute. The resulting suspension can then be homogenised and pumped through a transmission cell. However, the ball check-valve homogenises built into IR milk analysers cannot handle the insoluble particles present in meat suspensions [32], and thus a filtration step is required. The need for filtration reduces the quantitative accuracy of the IR method.

Recently, these sampling problems have been addressed in the development of an FTIR method for the determination of fat and protein in raw meat [32]. The use of a custom-designed high-pressure valve homogenise was found to eliminate the requirement for filtration of meat suspensions prior to IR analysis. The homogenates obtained were injected directly into a heated (65°C) flow-through transmission cell, with a 0.037-mm pathlength. The accuracy and reproducibility of the FTIR method were reported to be superior to those of the reference chemical methods

(Soxhlet for fat and micro-Kjeldahl for protein). The preparation of freeze-dried meat mixtures to serve as calibration standards was also described in this work [32]. The availability of such pre-analysed, reconstitutable, shelf-stable calibration standards would facilitate the implementation of FTIR methods in the meat processing industry, in a similar manner as has been reported for milk analysis [33,34].

4.7.3 Fats and Oils

Edible oils are ideal candidates for FTIR spectroscopic analysis, as they can be applied directly in their neat form onto an ATR crystal or pumped through a transmission flow cell, to produce high-quality spectra. Solid fats can be handled in an analogous manner if the ATR crystal or flow cell is heated and thermostated to a temperature above the melting point of the fat. Both fats and oils, being relatively simple molecular systems composed primarily of triglycerides, give rise to fairly uncomplicated spectra, and most of the important absorption bands lie over the range of ~3500 cm^{-1} to 800 cm^{-1} (Figure 16), a region where most of the more rugged transmission windows and ATR materials transmit. From a practical standpoint, the development of FTIR oil analysis methods is of interest because they can potentially meet the need for rapid quality control methods in the fats and oils industry. At present, there is a strong driving force in the industry to replace chemical methods of analysis by automated instrumental methods, in order to improve efficiency and to address increasing environmental concerns about the use of large volumes of solvents and reagents in quality control laboratories [35]. Owing to the wealth of detail in the IR spectra of fats and oils, IR spectroscopy can be used both to determine bulk properties, such as the iodine value (a measure of total unsaturation) and saponification number (a measure of weight-average molecular weight), and to monitor chemical changes taking place, for example, as an oil is hydrogenated or undergoes oxidation. Thus, a large number of the chemical methods that are routinely used in fats and oils analysis can potentially be replaced by FTIR methods.

Despite the potential advantages of employing IR spectroscopy in fats and oils analysis, the only recognised application of IR spectroscopy in this area is the determination of isolated *trans* isomers in fats and oils by dispersive IR spectroscopy, which is an official method of the American Oil Chemists'

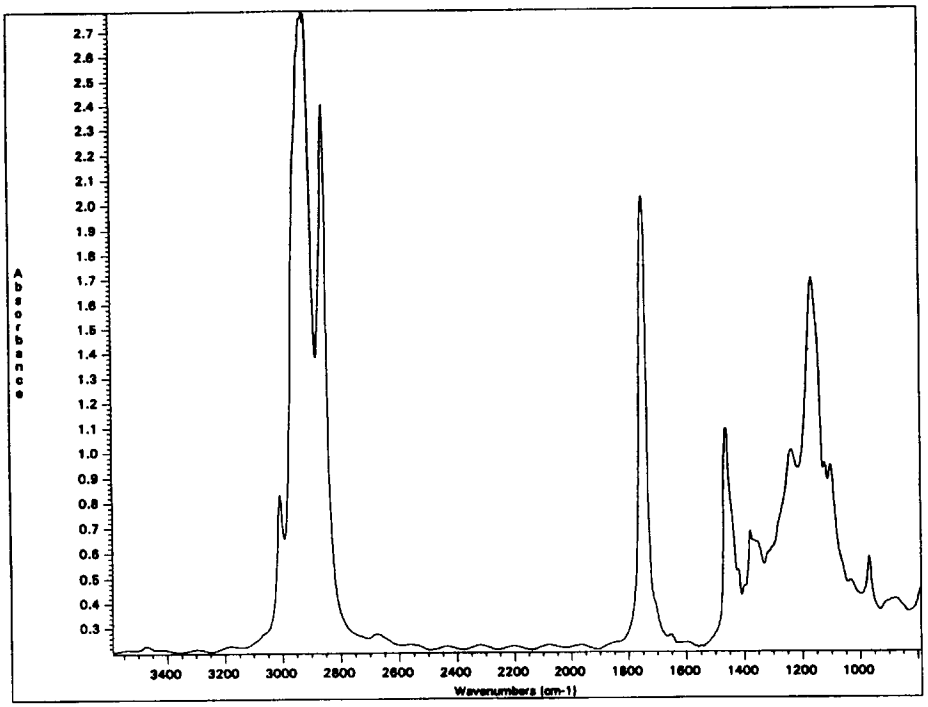

Figure 16: FTIR spectrum of Soya oil recorded by ATR.

Society (AOCS) [36]. Most unsaturated bonds in naturally occurring fats and oils are in the *cis* configuration, but *trans* double bonds may be present in processed fats and oils as a result of isomerisation during processing or as the consequence of oxidation. Furthermore, when oils are hardened by hydrogenation for their use in formulating margarines and shortenings or partially hydrogenated to stabilise them to oxidation, there is the concurrent conversion of *cis* to *trans* double bonds. The AOCS method for determining *trans* content is based on the measurement of the characteristic absorption of isolated *trans* bonds at 10.3 μ (967 cm^{-1}), which is due to their C=C-H bending vibration. The sample is dissolved in carbon disulphide, and its spectrum is recorded in a fixed-pathlength (0.2 to 2.0 mm) transmission cell with NaCl or KBr windows. The peak height at 10.3 μ is then measured relative to a baseline drawn between 10.05 μ (995 cm^{-1}) and 10.65 μ (937 cm^{-1}). Calibration of the system involves recording the spectrum of trielaidin (a C18:1t triglyceride) under the same conditions. The *trans* content of the sample is then expressed as % *trans* relative to a value of 100% for trielaidin, using equation (21):

$$\% \textit{ trans} = (a_{sample} / a_{trielaidin}) \times 100 \qquad (21)$$

where a = A/bc, and A is absorbance (peak height), b is the cell pathlength in centimeters, and c is the concentration of the CS_2 solution used in the measurement, expressed in grams per liter. A modified procedure is required for samples containing low levels of *trans* isomers as their *trans* values are overestimated by the method because the contribution that a weakly overlapping triglyceride absorption makes to the measured peak height at 10.3 μ becomes significant. The AOCS method requires that samples containing less than 15% isolated *trans* isomers be saponified and methylated prior to analysis. For such cases, calibration is performed with methyl elaidate in place of trielaidin.

While the AOCS method employs a dispersive IR spectrometer, a number of researchers have described adaptations of this method for use with an FTIR spectrometer. Lanser and Emken (37) developed an FTIR method based on measurement of the area of the *trans* peak and obtained good agreement with the results from gas-chromatographic analysis. Sleeter and Matlock [38] developed an FTIR procedure for measuring the *trans* content of oils in their neat form using a 0.1-mm KBr transmission cell. Their procedure considerably simplified the *trans* analysis, especially from the standpoint of sample handling, since the need for dissolution of the sample in CS_2 was eliminated. Furthermore, this FTIR method was shown to provide higher accuracy and a significant reduction in total analysis time (2.5 min/sample) in comparison with the traditional AOCS method, as well as having the advantage of being amenable to automation [38].

IR spectroscopy can be used, in principle, to measure not only *trans* content but also total unsaturation. The chemical measure of total saturation is the iodine value (IV), defined as the number of centigrams of iodine absorbed per gram of sample. The iodine value is an important parameter in the fats and oils processing industry, but the traditional method for its determination [36] is tedious. The idea of using IR spectroscopy as a means of rapidly determining IV has been around for some time [39,40]; although the results from this early work with dispersive instruments and transmission sampling methods demonstrated the potential utility of this approach, its application was limited. More recently, a somewhat more versatile FTIR/ATR method based on peak height measurements was described [41]. Another FTIR/ATR approach that has being investigated [42] uses the whole spectrum, in conjunction with PLS, for the simultaneous determination of both iodine value and saponification number (SN), another important parameter, related to the weight-average molecular weight of fats and oils. Calibration of the instrument was based on the use of pure triglyceride standards rather than pre-analysed oils, allowing for the development of a calibration independent of a chemical method, as the exact IV and SN of the calibration standards were known from their molecular structure. Spectral libraries developed for the standards were supplemented by generating additional spectra of mixtures of these primary standards using spectral co-addition,

and a PLS calibration model was developed. The calibration obtained was used to analyse commercially available fats and oils with a wide range of IV and SN values. The samples were analysed in their neat form on a heated (65°C) ATR crystal, with the time taken for analysis and prediction of both IV and SN being on the order of 2 minutes per sample, and the results were in good agreement with the chemically determined values for these samples (see Figure 17). Subsequently, a similar method was developed for use with a flow-through transmission cell, and the system was recalibrated using PLS to provide results in terms of both % *cis* and % *trans* as well as IV and SN [43]. The calibration developed to predict % *trans* was shown to provide accurate results down to *trans* levels of 1%. Thus, unlike the AOCS method for the determination of *trans* isomers, as well as similar FTIR methods based on measurement of the peak height of the *trans* band, described above, the PLS-based FTIR method can account for the contribution of overlapping triglyceride absorptions to the intensity of the *trans* band. Consequently, this method has the advantage that no methylation step is required for oils with low *trans* contents.

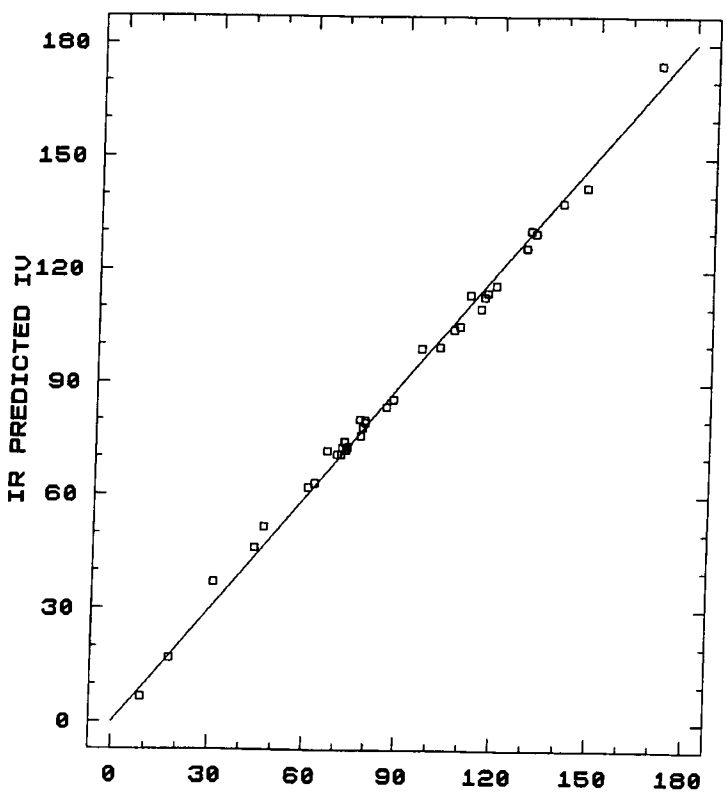

Figure 17: A plot of infrared (IR) predicted *versus* chemically determined iodine value for 37 oils.

TABLE 4
Peak Positions of the Functional Group[a] Absorptions of Reference Compounds Representative of Products Formed in Oxidised Oils

Compound	Vibration	Frequency (cm^{-1}) at peak maximum
Water	ν **OH**	3650 & 3550
	δ **HOH**	1625
Hexanol	ν R**OH**	3569
t-Butyl hydroperoxide	ν RO**OH**	3447
Hexanal	ν RH**C**=O	2810 & 2712
	ν RH**C=O**	1727
Hexenal[b]	ν RH**C**=O	2805 & 2725
	ν RH**C=O**	1697
	ν R**C**=**C**H-HC=O	1640
	δ R**C**=**C**H-HC=O	974
2,4-Decadienal[b]	ν RH**C**=O	2805 & 2734
	ν RH**C=O**	1689
	ν R**C**=**C**H-HC=O	1642
	δ R**C**=**C**H-HC=O	987
4-Hexen-3-one[b]	ν R**C(=O)**HC=CHR	1703 & 1679
	ν RC(=O)H**C**=**C**HR	1635
	δ RC(=O)H**C**=**C**HR	972
Oleic acid	ν RCO**OH**	3310
	ν R**C(=O)**OH	1711

Note: a) bold face indicate functional groups involved; b) All double bonds in the *trans* form.

Another potential area of application of FTIR spectroscopy is in the determination of the oxidative status or stability of an oil. Autoxidation is a major deteriorative reaction affecting edible fats and oils, and it is of major concern to processors and consumers from the standpoint of oil quality, as the oxidative breakdown products cause marked off flavours in an oil. A wide range of end products are associated with the autoxidative deterioration of fats and oils, the most important being hydroperoxides, alcohols, and aldehydes. Moisture, hydrocarbons, free fatty acids and esters, ketones, lactones, furans, and other minor products may also be produced, with the free fatty acids becoming more important in thermally stressed oils. In addition, there is significant *cis* to *trans* isomerisation and conjugation of double bonds in the hydroperoxides formed as an oil oxidises.

In order to investigate the feasibility of employing FTIR spectroscopy to assess the oxidative status or forecast the oxidative stability of an oil, van de Voort *et al.* [44] constructed a spectral library by recording the FTIR spectra of oils spiked with various compounds representative of common oil oxidation

products. *t*-Butyl hydroperoxide was selected to represent hydroperoxides, the primary oxidation products of fats and oils. Alcohols, saturated aldehydes, and α,β-unsaturated aldehydes, which have all been reported as major secondary oxidation products [44], were all represented in the spectral library by C_6 homologues, with α,β,γ,δ-unsaturated aldehydes represented by *trans, trans*-2,4-decadienal, a major decomposition product from heated, oxidised polyunsaturated fats and oils. Although ketones are minor products in oxidised oils, a C_6 allylic ketone was included in the spectral library to investigate the extent of overlap between the aldehyde and ketone absorptions. Water and oleic acid were also included in view of their possible presence in oils, particularly under hydrolysis conditions. The functional group frequencies of these reference compounds are tabulated in Table 4.

Examination of Table 4 shows that each of the various types of oxidation products gives rise to discernible and characteristic absorptions in the FTIR spectrum. Similar absorption bands were detected in the spectra of oils oxidised under accelerated conditions and monitored in real time by FTIR spectroscopy [44].

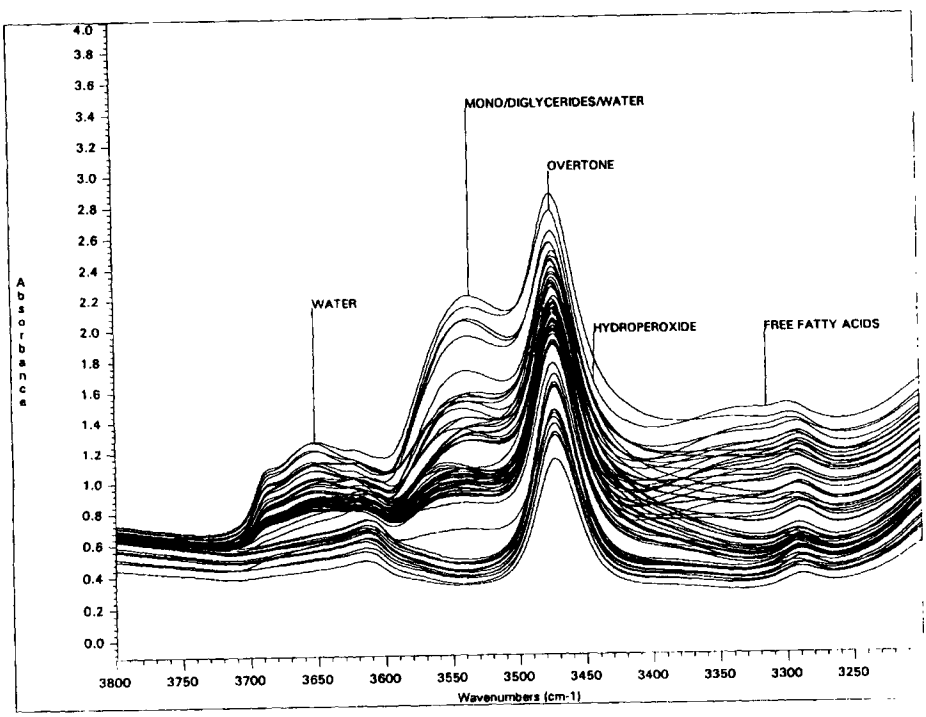

Figure 18: FTIR spectrum of a mixture of varying amounts of OH-containing components, such as moisture, monoglycerides, and free fatty acids, which may potentially interfere with the determination of hydroperoxide content (PV) in oxidised oils.

On the basis of the results of this study, van de Voort *et al.* [44] proposed a quantitative approach whereby the oxidative state of an oil could be determined through calibrations developed with oils spiked with appropriate compounds representative of the functional groups associated with typical oxidative end products. These concepts were subsequently put into practice with the development of a calibration for the determination of peroxide value (PV), the chemical measure of hydroperoxides, which are the primary products of oil oxidation. Calibration standards were prepared by the addition of *t*-butyl hydroperoxide to a variety of base oils [45]. Varying amounts of other OH-containing components, such as moisture, mono-glycerides, and free fatty acids, were added to the calibration standards as the O-H stretching absorptions of these components may potentially interfere with the PV determination (Figure 18). Through the use of PLS, the variable spectral contributions of these components were built into the calibration model, such that they do not affect the PV determination.

Other applications of FTIR spectroscopy related to the assessment of the oxidative state of fats and oils are expected to be forthcoming shortly. The evaluation of total carbonyl content is an obvious candidate, and it may also prove possible, through the use of PLS, to establish correlations between

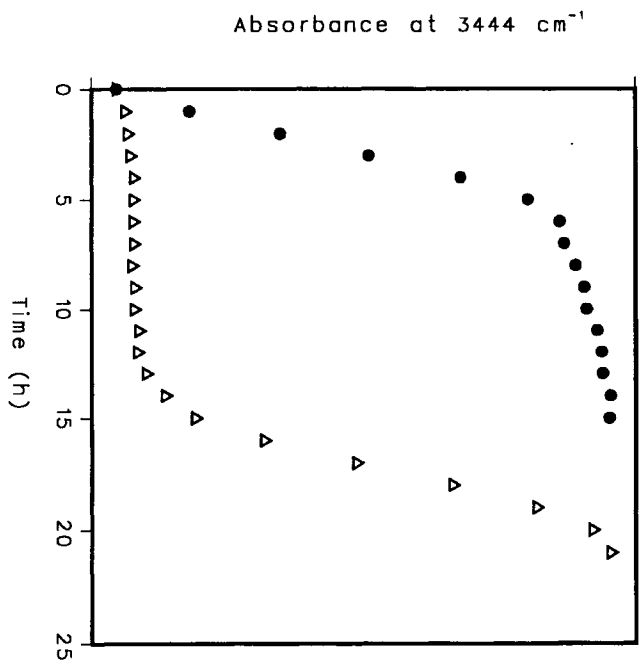

Figure 19: A plot of the increase in peak height of the ν(COO-H) band (at 3444 cm^{-1}) as a function of time due to the formation of hydroperoxides in trilinolenin heated at 40°C in the presence (Δ) and absence of (•) of vitamin E (1%).

FTIR spectral data and the anisidine value, which is primarily a measure of conjugated aldehydes. The potential utility of FTIR spectroscopy in the evaluation of the oxidative stability of oils has also been discussed [44]. The growth of the hydroperoxide peak over time in the FTIR spectrum is evident when an oil is heated on an ATR crystal (Figure 10); this implies that the susceptibility of an oil to oxidation can be monitored by heating the oil under controlled conditions on an ATR crystal, in a procedure somewhat analogous to the active oxygen method [36], but carried out more rapidly and dynamically. The utility of FTIR oil monitoring experiments of this type in the evaluation of antioxidant performance has been demonstrated (Figure 19) [46].

Other examples of FTIR analysis of fats and oils include the determination of free fatty acids in crude [47] and processed oils [48] and the authentication of oils [49] (see Section 4.7.6). As exemplified by the IV/SN/*cis*/*trans* method described above [43], FTIR spectroscopy can be used to simultaneously perform a number of common fat and oil analyses on the basis of a single spectral measurement. Thus, FTIR oil analysis can provide substantial savings in terms of time and labour for quality control laboratories in the fats and oils industry. In order to facilitate practical implementation of FTIR oil analysis methodologies in the industry, a number of issues must be addressed, specifically in the areas of sample handling and automation. In this regard, a prototype FTIR oil analysis unit has recently been assembled (Figure 20). The system is equipped with a specially designed sample handling accessory (Figure 21), which includes a heated flow-through transmission cell with heated input and output lines, and is designed for operation at 80°C, a temperature suitable for handling both fats and oils. Samples are pre-warmed in a microwave oven and are loaded into the cell by aspiration. The unit is pre-calibrated and programmed for the determination of IV, SN, *cis* content, and *trans* content and incorporates a dynamic calibration adjustment that eliminates the need for recalibration over time. With the development of systems of this type for quality control or "at-line" applications, FTIR spectroscopy may be anticipated to play a major role in fats and oils analysis in the near future.

4.7.4 Analysis of High-Fat Food Products

The rapid analysis of food products is crucial in food processing in order to allow manufacturing processes to be adjusted while production is underway and to ensure that product quality and regulatory specifications are adhered to. Traditional chemical methods [50], such as the Mojonnier method, which can be used to analyse for fat and moisture, the Soxhlet method for analysis of fat, or the vacuum-oven method for moisture determination, all present constraints in terms of time, manpower, and/or the need for substantial amounts of solvents. If timely analytical results are not available, batches in production may need to be reworked if out of specification, involving additional time and expense. For these very practical reasons, there is a need

in the food industry for simple, rapid methodologies capable of monitoring an ongoing manufacturing process. FTIR spectroscopy can rapidly provide compositional information in terms of the fat, protein, carbohydrate, and moisture content in foods, and, as such, it can be considered a potentially cost-effective tool for quality control applications in the food industry.

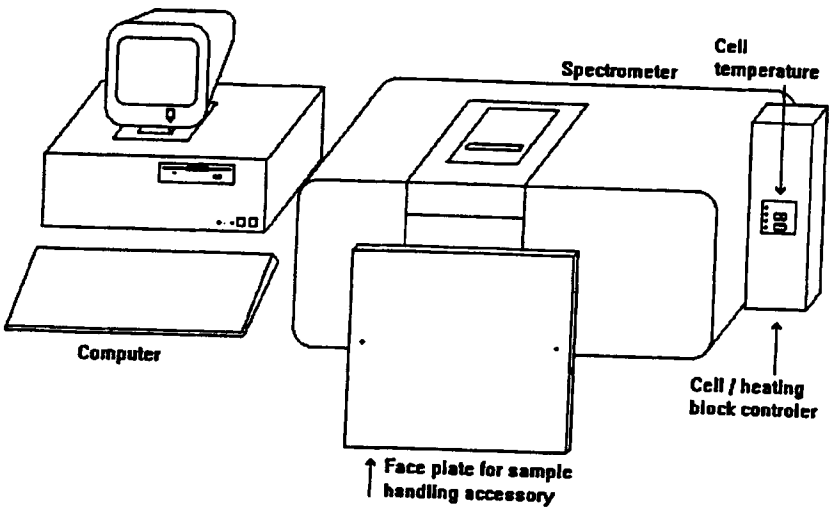

Figure 20: A prototype FTIR oil analysis unit.

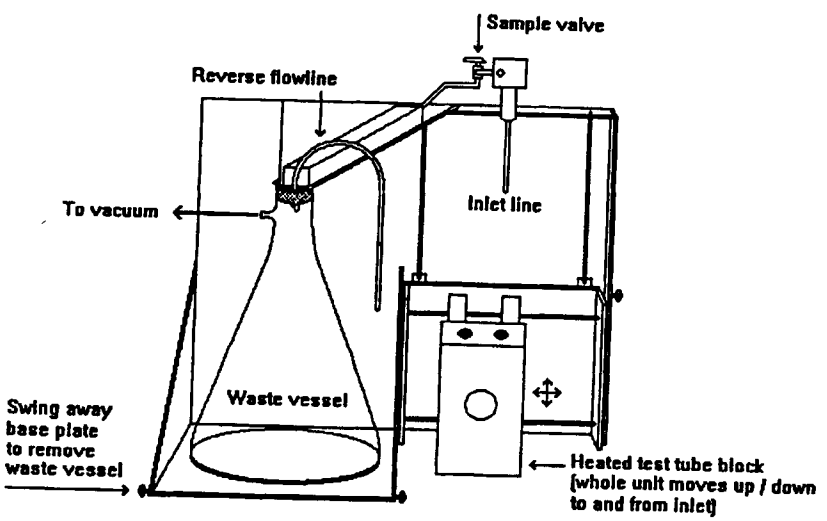

Figure 21: A schematic of sample handling accessory designed for the analysis of fats and oils by FTIR spectroscopy.

FTIR methodology for the analysis of high-fat food products has been developed and applied to the determination of fat in butter (51), peanut butter, and mayonnaise [52]. The method is based on the extraction of the fat in the sample, as well as any moisture, into 1-propanol, warmed to 40°C; under these conditions, both fat and moisture are soluble. This method was initially applied to the determination of fat and moisture in butter, with solids determined by difference [51]. Mixtures of anhydrous butter oil and water in propanol were employed as calibration standards. The standards were warmed to 40°C, and their spectra were recorded by placing ~1 mL on a ZnSe ATR crystal maintained at 40°C. Calibration was performed by using multiple linear regression to relate the intensities of the carbonyl signal of the ester linkage of fat (1748 cm^{-1}) and the HOH bending absorption of water (~1650 cm^{-1}) to the fat and moisture content, respectively. For the analysis of butter, a 2-g sample was taken, to which 18 g of 45°C propanol were added. The sample was shaken and placed on the heated ATR crystal, and the fat and moisture content were calculated from the calibration developed. Butter samples supplied and pre-analysed by a processor were analysed by the FTIR method, and the results were within ±0.5% of the values reported by the processor for each component [51].

Because of the simplicity of preparing the calibration standards, this approach was subsequently extended to peanut butter and mayonnaise [52]. The method was, however, modified by using a flow-through transmission cell, having a pathlength of 0.1 mm, instead of an ATR sampling accessory. The transmission technique was found to be simpler, more reproducible, and more efficient in terms of sample handling. In addition, the use of the ATR technique for samples containing fat has the disadvantage that fat tends to adhere to the surface of the ATR crystal and is difficult to remove even with thorough cleaning. Furthermore, any residual fat on the crystal surface make a major contribution to the IR spectrum recorded by the ATR technique because only molecules at or near the surface are sampled in an ATR measurement (see Section 4.6.2). For the analysis of the fat content in peanut butter, the calibration standards were solutions of peanut oil in propanol (6-9 g per 75 g), while the calibration standards for the analysis of fat and water in mayonnaise were prepared by adding varying amounts of the oil used in the mayonnaise formulation and water to propanol. The FTIR predictions obtained for peanut butter samples from the peanut oil calibration were adjusted by a bias correction factor to compensate for the effects of extraction efficiency and insoluble solids. For commercial peanut butters and mayonnaises, the FTIR method provided predictions within ±0.30% of the values determined by the Mojonnier method, with a sample turnaround time of 5-7 min. As such, the method would be suitable for quality control applications and is rapid enough to monitor an ongoing manufacturing process.

4.7.5 Sugar Analyses

Quantitative analysis of sugars by IR spectroscopy is generally based on the bands in the 1250-800 cm^{-1} region of their spectra (Figure 22). The major bands in this region correspond to C-O-H bending vibrations. Although individual mono- and disaccharides each have a characteristic set of absorption bands in this region, in the spectra of mixtures of these sugars these bands are extensively overlapped (Figure 22). Individual sugars in aqueous solution can be readily quantitated by FTIR spectroscopy with the use of the ATR sampling technique [53]. Kemsley *et al.* [54] employed this technique to record the spectra of sugar mixtures (sucrose, glucose, and fructose) in water and used the **K**-matrix and **P**-matrix approaches to obtain calibrations for the individual sugars. While the results from the **K**-matrix approach did not prove satisfactory, the **P**-matrix calibrations yielded predictions for soft drink samples that were in reasonable agreement with high-pressure liquid-chromatographic (HPLC) data. The potential utility of FTIR spectroscopy as a means for the determination of the sucrose content in sugar cane juice, which is often used as a basis for cane sugar payment in the sugar cane industry, has also been demonstrated [55]. The calibration standards employed were reconstituted sugar cane juices, prepared by adding sucrose, glucose, and fructose to water at the levels found in natural juices. Correlations between the FTIR spectral data for these samples, obtained using the ATR sampling technique, and their sucrose content were established by principal component regression (PCR), a multivariate analysis technique related to PLS.

An important quality control application that has been investigated is the determination of dextrose equivalent (DE) and dry substance (DS) measures, employed in corn syrup production, by FTIR spectroscopy [56]. DE is a particularly important measure of the sweetening power which develops as corn starch is converted to syrup, but the standard copper sulphate titration method for determination of DE is tedious and time consuming. PLS calibrations have been obtained for both DE and DS, and, with the use of a flow-through ATR accessory, the FTIR technique could provide a means of continuous on-line process measurement. In another study [57], PLS regression was applied in the analysis of the three main components (glucose, maltose, and fructose) of the dry substance in glucose syrups. The samples were diluted in distilled water (1 g/2 mL), owing to the high level of dry matter in these syrups (~70% w/v), and their spectra were recorded using a horizontal ATR sampling accessory. The FTIR predicted concentrations for glucose, maltose, and fructose were within 3-5% of the HPLC data for these samples, with the higher end of this error range corresponding to samples containing high levels of unquantified oligosaccharides.

On a more fundamental level, the utility of FTIR spectroscopy as a technique for the quantitative measurement of the open-chain form of sugars has been

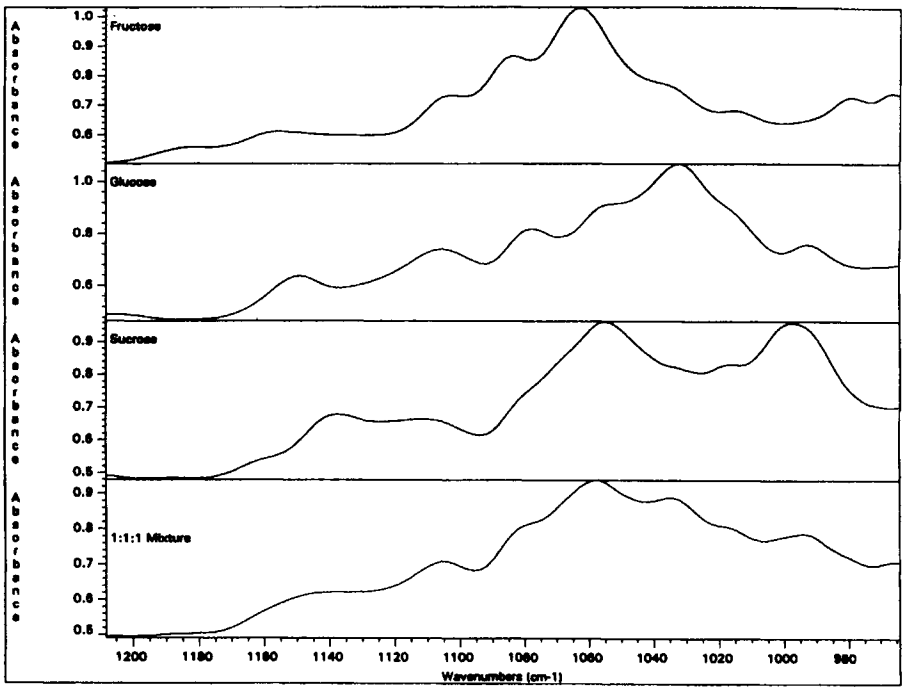

Figure 22: FTIR spectra of various sugars in solution (10% w/v) recorded by ATR.

demonstrated [58, 59]. An absorption band in the spectrum of D-fructose in D_2O solution at 1728 cm^{-1} has been assigned to the open form [58], and this assignment was confirmed by isotopic substitution [59]. FTIR spectroscopy thus allows the quantitation of the open-chain tautomers of keto/aldehydo reducing sugars, which is important in determining their relative reactivities in the formation of Maillard reaction intermediates, and the monitoring of the concentration of the open-chain form as a function of temperature and pH (Figure 23). Basic quantitative investigations of this nature have important ramifications in terms of predicting colour and flavour formation in products undergoing heating, especially for microwave applications [60].

4.7.6 Detection of Adulteration

Adulteration of food products is an important problem from a regulatory and economic perspective. The possible use of FTIR spectroscopy as a rapid means of authenticating food products and detecting their adulteration is under investigation. The development of this methodology is still in an early stage, and basic research is in progress to determine whether FTIR spectroscopy can be applied in a routine manner for detection of adulteration. The potential utility of FTIR spectroscopy in this regard derives both from

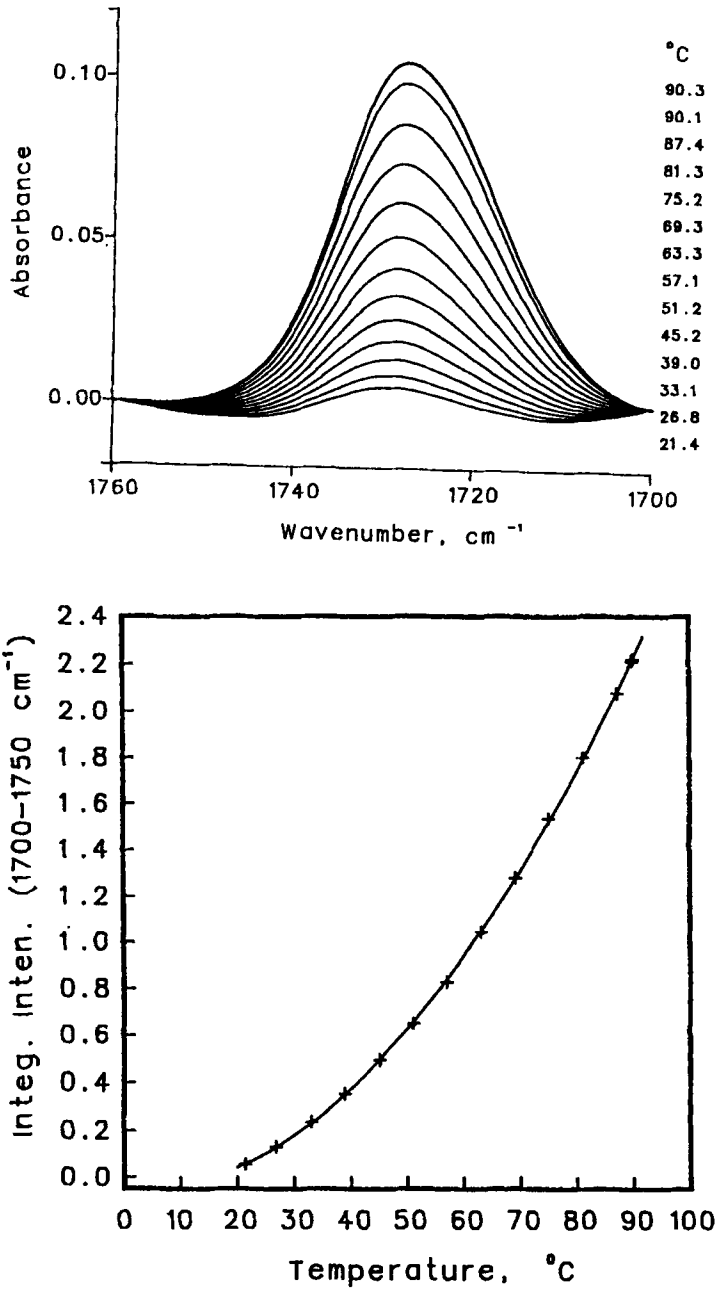

Figure 23: Top - the increase in carbonyl absorption band of the open-chain of D-fructose (in D_2O) as a function of temperature between 21 and 90°C; and **bottom** - The plot of % open-chain form of D-fructose as a function of temperature at *p*H 9.

the wealth of information that the IR spectrum of a sample provides about its composition and from the powerful data handling capabilities of FTIR systems, which make it possible to exploit this information effectively. In effect, the IR spectrum of a substance can be considered its "fingerprint," and even subtle differences in composition between two samples will be reflected in their IR spectra. However, in order to employ FTIR spectroscopy for authentication of a particular food product, a data base composed of the spectra of a large number of samples of the product must be generated in order to encompass all sources of spectral variability (*e.g.*, due to regional or processing variations) that may be encountered in an authentic product. A variety of data reduction techniques, such as principal component analysis, spectral searching routines, pattern recognition, and neural networks, can then potentially be employed to compare the spectra of samples with the spectra of authenticated products in the data base.

The potential utility of FTIR spectroscopy for the authentication of vegetable oils has been examined in recent work by Lai *et al.* [49], employing multivariate statistical methods, specifically, principal component analysis and discriminant analysis. These authors demonstrated that the spectral data for oils of different plant origin could be clustered by application of principal component analysis. However, they found that the differences between the spectra of some samples of different oil types were comparable in magnitude to the variations between replicate spectra of individual samples. It was therefore concluded that the development of a reliable method for classification of oils on the basis of their plant origin would require a larger data base of oil spectra, including replicate spectra of individual samples recorded over a period of time. These authors also demonstrated the ability of FTIR spectroscopy, in conjunction with discriminant analysis, to differentiate between extra virgin and refined olive oils, despite the strong similarities between the spectra of these two types of oil. They concluded that FTIR spectroscopy can potentially serve as a rapid and simple method for the detection, and possibly quantification, of adulteration of oils.

In a similar vein, Wilson *et al.* [61] recorded the FTIR spectra of fruit jams of different types using a diffuse reflectance (DRIFT) sampling accessory. Despite distortions in the spectra, associated with the use of the DRIFT technique, the different jams were found to exhibit characteristic and reproducible patterns, indicating that jams of different fruit content can be differentiated on the basis of their FTIR spectra. The authors suggested the potential utility of this technique for the detection of adulteration of jams, for instance, by the substitution of fruit content by cheaper vegetable material.

4.8 CONCLUSIONS

The examples discussed above are but a few of the potential applications of FTIR spectroscopy which could assist food companies in their day-to-day quality control operations or development work. The acceptance and implementation of any FTIR analysis method by the food industry requires that the method be pre-programmed and made user friendly (*e.g.*, menu-driven) so that the operator does not require any special skills or training. This is easily achieved with the FTIR instrumentation and software currently on the market. Clearly, a large number of useful time-saving methodologies can be envisaged where expensive, time-consuming, traditional chemical methods can be replaced by a simple, rapid and accurate FTIR method. Although FTIR analytical methodology has seen very limited use in the food industry, over the next few years the implementation of existing and yet to be developed FTIR-based quality control methods may be anticipated.

4.9 REFERENCES

1. A. D. Cross, *Introduction to Practical Infrared Spectroscopy*, Butterworths, London (1960).

2. F. A. Cotton, *Chemical Applications of Group Theory*, John Wiley & Sons, New York (1971).

3. P. R. Griffiths and J. A. de Haseth, *Fourier Transform Infrared Spectrometry*, John Wiley & Sons, New York (1986).

4. D. G. Cameron and D. J. Moffatt, *J. Testing Eval.* **12**, 78 (1984).

5. C. W. Brown, P. F. Lynch, R. J. Obremski, and D. S. Lavery, *Anal. Chem.* **54**, 1472 (1982).

6. R. A. Crocombe, M. L. Olson, and S. L. Hill, in *Computerized Quantitative Infrared Analysis*, ASTM STP 934, G.L. McClure (ed.), American Society for Testing and Materials, Philadelphia, pp. 95-130 (1987).

7. M. P. Fuller, G. L. Ritter, and C. S. Draper, *Appl. Spectrosc.* **42**, 217 (1988).

8. D. M. Haaland and E. V. Thomas, *Anal. Chem.* **60**, 1193 (1988).

9. D. M. Haaland and R.G. Easterling, *Appl. Spectrosc.* **34**, 539 (1980).

10. R. G. J. Miller and C. Stace (eds.), *Laboratory Methods in Infrared Spectroscopy*, Heyden and Sons, London (1979).

11. J. R. Ferraro and K. Krishnan (eds.), *Practical FT-IR Spectroscopy: Industrial and Laboratory Chemical Analysis*, Academic Press, New York (1990).

12. P. B. Coleman (ed.), *Practical Sampling Techniques for Infrared Analysis*, CRC Press, Boca Raton, Florida (1993).

13. A. G. Cameron, *J. Food Technol.* **2**, 223 (1967).

14. J. M. Wilson, I. Ben-Gera, and A. Kramer, *J. Food Sci.* **36**, 162 (1971).

15. P. S. Belton, A. M. Saffa, and R. H. Wilson, *Analyst* **112**, 1117 (1987).

16. R. H. Wilson, *Trends Anal. Chem.* **9**, 127 (1990).

17. F. R. van de Voort and A. A. Ismail, *Trends Food Sci. Technol.* **2**, 13 (1991).

18. Official Methods of Analysis, 14th ed., AOAC, Arlington, Virginia (1980).

19. F. R. van de Voort, S. Kermasha, B. L. Mills, and K. F. Ng-Kwai-Hang, *J. Dairy Sci.* **71**, 290 (1987).

20. J. D. S. Goulden, J. Shields, and R. Haswell, *J. Soc. Dairy Technol.* **17**, 28 (1964).

21. D. A. Biggs, *J. Assoc. Off. Anal. Chem.* **62**, 1202 (1979).

22. F. R. van de Voort, J. Sedman, G. Emo, and A. A. Ismail, *J. Assoc. Off. Anal. Chem.* **75**, 780 (1992).

23. E. Hop, H.-J. Luinge, and H. van Hemert, *Appl. Spectrosc.* **47**, 1180 (1993).

24. D. M. Barbano and M. E. Dellavalle, *J. Dairy Sci.* **70**, 1524 (1987).

25. A. H. Karman, M. A. J. S. van Boekel, and A. P. Arentsen-Stasse, *Neth. Milk Dairy J.* **41**, 175 (1987).

26. M. Gupta, A. Reza Rejaei, A. A. Ismail and F. R. van de Voort, *submitted for publication.*

27. I. V. Mendenhall and R. J. Brown, *J. Dairy Sci.* **74**, 2896 (1991).

28. O. C. Bjarno, *J. Assoc. Off. Anal. Chem.* **65**, 696 (1982).

29. B. L. Mills, F. R. van de Voort, and Y. Kakuda, *J. Meat Sci.* **11**, 1 (1984).

30. B. L. Mills, F. R.van de Voort, and W. R. Usborne, *J. Assoc. Off. Anal. Chem.* **66**, 1048 (1983).

31. G. S. Darwish, F. R. van de Voort, and J. P. Smith, *Can J. Fish Aquatic Sci.* **46**, 644 (1988).

32. B. Dion, M. Ruzbie, F. R. van de Voort, A. A. Ismail, and J. S. Blais, *Analyst* **119**, 1765 (1994).

33. F. R. van de Voort, A. A. Elkashef, and B. L. Mills, *J. Assoc. Off. Anal. Chem.* **73**, 688 (1990).

34. F. R. van de Voort, A. A. Elkashef, and J.-S. Blais, *J. Assoc. Off. Anal. Chem.* **74**, 772 (1991).

35. J. Steiner, *Inform.* **4**, 955 (1993).

36. Official Methods and Recommended Practices of the American Oil Chemists' Society, 4th ed., American Oil Chemists' Society, Chicago, Illinois (1989).

37. A. C. Lanser and E. A. Emken, *J. Am. Oil Chem. Soc.* **65**, 1483 (1988).

38. R. T. Sleeter and M. G. Matlock, *J. Am. Oil Chem. Soc.* **66**, 121 (1989).

39. R. G. Arnold and T. E. Hartung, *J. Food Sci.* **36**, 166 (1971).

40. J. L. Bernard. and L. G. Sims, *Ind. Res. Dev.* (August) 81 (1980)

41. A. Afran and J. E. Newbery, *Spectroscopy* **6**, 31-34 (1991).

42. F. R. van de Voort, J. Sedman, G. Emo, and A. A. Ismail, *J. Am. Oil Chem. Soc.* **69**, 1118 (1992).

43. F. R. van de Voort, A. A. Ismail, and J. Sedman, *J. Am. Oil Chem. Soc.* **72**, 873 (1995).

44. F. R. van de Voort, A. A. Ismail, J. Sedman, and G. Emo, *J. Am. Oil Chem. Soc.* **71**, 243 (1994).

45. F. R. van de Voort, A. A. Ismail, J. Sedman, J. Dubois, and T. Nicodemo, *J. Am. Oil Chem. Soc.* **71**, 921 (1994).

46. A. A. Ismail, F. R. van de Voort, J. Sedman, and T. Nicodemo, Paper presented at the 85th Annual Meeting of the American Oil Chemists' Society, Atlanta, Georgia, May 8-12, 1994.

47. A. C. Lanser, G. R. List, R. K. Holloway, and T. L. Mounts, *J. Am. Oil Chem. Soc.* **68**, 448 (1991).

48. A. A. Ismail, F. R. van de Voort, G. Emo, and J. Sedman, *J. Am. Oil Chem. Soc.* **70**, 335 (1993).

49. Y. W. Lai, E. K. Kemsley, and R. H. Wilson, *J. Agric. Food Chem.* **42**, 1154 (1194).

50. Y. Pomeranz and C. E. Meloan, *Food Analysis: Theory and Practice*, Avi Publishing Co., Westport, Connecticut (1982).

51. F. R. van de Voort, J. Sedman, G. Emo, and A. A. Ismail, *Food Res. Int.* **25**, 193 (1992).

52. F. R. van de Voort, J. Sedman, and A. A. Ismail, *Food Chem.* **48**, 213 (1993).

53. J. Hopkins and J. Newberry, *FT-IR Spectral Lines* **7**, 2 (1986).

54. E. K. Kemsley, Li Zhuo, M. K. Hammouri, and R. H. Wilson, *Food Chem.* **44**, 299 (1992).

55. F. Cadet, D. Bertrand, P. Robert, J. Maillot, J. Dieudonné, and C. Rouch, *Appl. Spectrosc.* **45**, 166 (1991).

56. M. P. Fuller, M. C. Garry, and Z. Stanek, *Am. Lab.* **22**, 58 (1990).

57. F. de Lène Mirouze, J. C. Boulou, N. Dupuy, M. Meurens, J. P. Huvenne, and P. Legrand, *Appl. Spectrosc.* **47**, 1187 (1993).

58. V. A. Yaylayan and A. A. Ismail, *J. Carbohyd. Chem.* **11**, 149 (1992).

59. V. A. Yaylayan, A. A. Ismail, and S. Mandeville, *Carbohyd. Res.*, **248**, 355 (1993).

60. V. Yaylayan, A. A. Ismail, and A. Huyghues-Despointes, in *Maillard Reaction: Relevance to Food, Health and Disease,* T. Labuza and G. Reineccius (eds.), Birkhauser Verlag, Basel (**in press**).

61. R. H. Wilson, P. T. Slack, G. P. Appleton, Li Sun, and P. S. Belton, *Food Chem.* **47**, 303 (1993).

This Page Intentionally Left Blank

J.R.J. Paré and J.M.R. Bélanger (Editors)
Instrumental Methods in Food Analysis

Chapter 5

Atomic Absorption, Emission and Fluorescence Spectrometry: Principles and Applications

William D. Marshall

Department of Food Science and Agricultural Chemistry, Macdonald Campus, McGill University, Ste-Anne de Bellevue, QC, Canada H9X 3V9

5.1 A BRIEF HISTORICAL PERSPECTIVE OF ATOMIC SPECTROSCOPY

The history of atomic spectroscopy is closely related to the study of sunlight. In 1802, the German scientist Wollaston reported the presence of black regions (lines) in the spectrum of sunlight. These regions have come to be known as Fraunhofer lines in honour of the scientist who spent much of his illustrious career studying them. It was suggested, as early as 1820, that these Fraunhofer lines resulted from absorption processes which occurred within the sun's atmosphere. Using an experimental apparatus similar to Figure 1, Kirchoff and Bunsen demonstrated that the typical yellow light emitted by sodium compounds, when placed in a flame, was identical to the black "D" line in sun's spectrum. A series of studies using this very early spectrometer lead Kirchoff (1859) to suggest that any material which can emit light at a given wavelength can also absorb light at that same wavelength. He was the first scientist to recognise that there is a close relationship between the absorption spectrum and the emission spectrum of the same element. Visual observations must have played an essential part in the technical innovations of evolving metallurgical technologies.

Characteristic colours of fumes (flames), as described by Agricola in 1550, were used to "control" the process of smelting of ores. Talbot (1826) and Wheatstone (1835) reported that the colours of flame and spark induced

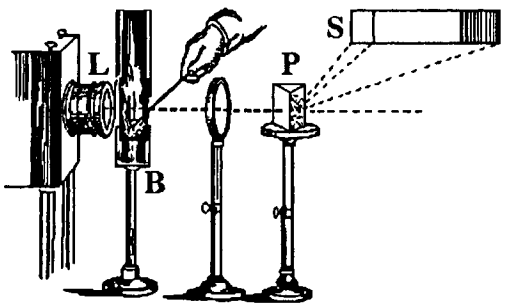

Figure 1: The Kirchoff experimental apparatus as illustrated in a book by Tyndall. The absorption spectrum of sodium atoms appears on the screen S when a sodium salt is introduced into a flame B. The sodium D line is superimposed on the Fraunhofer spectrum of sunlight, which passes through lens L, and is dispersed by a prism P.

emissions were characteristic of specific substances. The quantitative aspects of atomic spectroscopy were developed only within the last 60-70 years. The substitution of photoelectric devices for visual detection and the development and commercialisation of instruments date back to the late 1930s. The development of these instruments was made possible not only because of continued progress in our understanding of the fundamental composition and behaviour of atoms but was also supported by the increasing realisation that the presence of minor and trace amounts (low mg/kg) of certain elements could influence industrial processes appreciably. Thus, instruments were developed in response to a technological requirements.

Modern atomic spectroscopy can be divided conveniently into three related techniques on the basis of the processes used to generate, then to detect and measure the free atoms of analyte. Whereas atomic absorption spectrometry (AAS) measures the quantity of light absorbed by atoms of analyte, atomic emission and atomic fluorescence measure the quantity of radiation emitted by analyte atoms (albeit under different conditions) which have been promoted to higher energy levels (excited states). Atomic emission (AE) and atomic fluorescence (AF) differ fundamentally in the processes by which analyte atoms acquire the extra energy of their excited states; either *via* collisional events (AE) or by the absorption of radiant energy (AF). Each of these three spectroscopic approaches can be classified as a trace technique (implying both a high sensitivity and a high selectivity), is applicable to many elements, and yet relative to the other two, each offers certain advantages and disadvantages.

Since the introduction of commercial atomic absorption spectrometry instruments in the early 1960s, this technique has rapidly gained wide

acceptance to the point where surveys of instruments available in scientific laboratories have suggested, consistently, that an AAS instrument is the fourth or fifth most popular instrument (exceeded only by a balance, a *p*H meter, an ultra violet - visible spectrophotometer and possibly an HPLC). Whereas certain atomic emission techniques were described in the twenties and thirties, and used in the intervening years, this technique has undergone a renaissance with the development of "continuous" plasma techniques for atomising the sample and presenting it to the instrument. Of the three atomic spectroscopic approaches, the pioneering developmental studies which demonstrated the possibilities associated with atomic florescence are the most recent and for the most part few instruments for AFS have been commercialised.

5.2 INTRODUCTION TO ATOMIC ABSORPTION SPECTROSCOPY (AAS)

AAS involves the study of the absorption of radiant energy (usually in the ultra violet or in the visible region of the electromagnetic spectrum) by isolated atoms in the gaseous phase. Since, in AAS, the analyte is presented to the optical beam of the instrument as free atoms, all the possible rotational and vibrational energy levels are degenerate (of the same energy). In contrast to the absorption spectra of polyatomic chemical species (ions or molecules) where there is a multiplicity of possible transitions corresponding to different rotational and vibrational energy levels superimposed on different electronic energy levels, the spectra of free atoms are characterised by only a relatively few sharp absorbances (line spectra) which can be correlated with changes in electronic energy levels. The vast number of possible different energy levels available to polyatomic species result in almost a continuum of possible transitions. The result is that spectra of ions (molecules) are composed of rather broad bands which result from the partial resolution of many individual transitions. Thus, one feature of atomic spectra is their simplicity relative to the spectra of polyatomic species.

As an example, consider the energy level diagram (a partial Grotrian diagram) for sodium (Figure 2). The vertical axis provides a measure of the energy differences between the individual energy levels (which are depicted as horizontal lines). As the principal quantum number "n" is increased, the energy difference between successive levels decreases until the orbital electron is free from the influence of the nucleus (ionisation). The different "stacks" of these energy levels represent differences in the orbital angular momentum quantum number "l". Finally, for $l > 1$, the two stacks which appear for each value of l (p, d, f) represent slightly different total orbital angular momenta (combination of electron orbital angular momentum and electron spin angular momentum) and are referred to as multiplets. The electronic configuration or an isolated Na atom (at its lowest or ground state energy level) can be symbolised as $1s^2 2s^2 2p^6 3s^1$ indicating that the eleventh

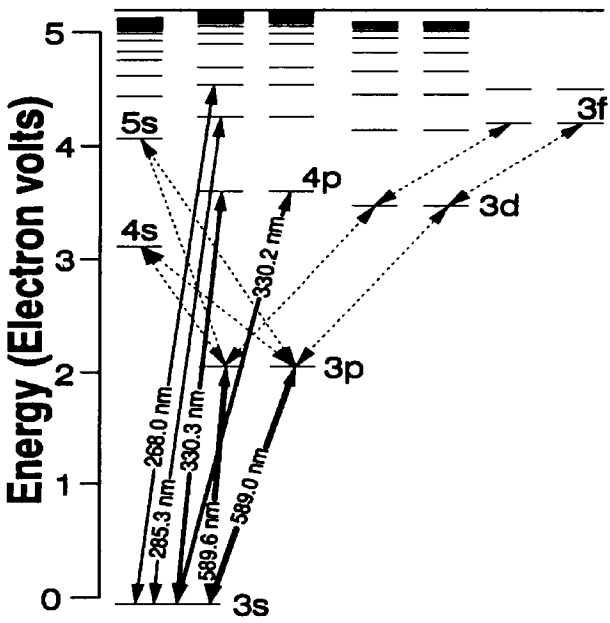

Figure 2: A partial Grotrian diagram for the element sodium illustrating the observed atomic absorptions as solid arrows.

orbital electron of this atom resides at a 3s energy level above a filled inner shell of 10 electrons. By absorbing energy, a Na atom can be promoted from its lowest (ground state) energy level to a higher energy level (excited state). Depending on the quantity of energy absorbed, transitions between different energy levels are possible (as suggested by Figure 2). However, not all of the possible transitions are actually observed. For example, there are no arrows (which represent observed transitions) connecting levels of the same l quantum number nor are there any transitions between states corresponding to a change in the l-value of 2. The spectra of isolated atoms obey the "selection rule" $\Delta l = \pm 1$.

Since the relationship between energy and wavelength is an inverse one,

$\Delta E = hc/\lambda$

where: ΔE is the difference in energies between the two states; h is a constant of proportionality (Planck's constant); c is the speed of light in a vacuum; and λ is the wavelength in reciprocal cm

the smaller the difference in energy between the electronic levels, the longer the wavelength of the electromagnetic radiation required to cause the

transition from the lower to the higher energy level. The probability that an absorption will occur is greatest if precisely the correct energy is supplied to the ground state atom. It is the outermost electron(s) which are the least tightly held by the nucleus and are the easiest to promote to higher energy levels. Much more energetic radiation (X-ray region of the electromagnetic spectrum) are required to cause the promotion of inner electrons to higher energy levels. Since atoms of different elements have different electronic configurations, the outermost electron(s) will be at appreciably different energy levels and their promotion to higher energy levels will require the absorption of radiation of appreciably different energies. In practice, the AAS technique is characterised by almost no spectral interference. Early researchers in the field of AAS have systematically examined the spectra of all the elements which can be directly studied with this technique and have identified the most "sensitive" absorption lines. For sodium, the relative "responses" at different wavelengths are suggested by the relative thickness of the arrows in Figure 2.

Not all elements can be measured directly with commercial AA spectrometers. Those elements which possess metallic character are characterised by outermost electrons which are easily lost (low ionisation energies). These same "valence" electrons can be promoted to higher energy levels (but not lost) by the absorption of radiation in the visible or ultra violet regions. With increasing non metallic character, it becomes increasingly more difficult to promote the valence electrons to higher energy levels (the wavelength of the required electromagnetic radiation becomes shorter). Since the components of air appreciably absorb the radiation which is much below 200 nm, it is not conventionally feasible to work at wavelengths lower than 190 nm unless provision is made to rigorously exclude this interference. In practice, commercial AA spectrometers can be used to measure some 76 elements directly.

In order to measure the light absorbed, the sample must be presented to the optical beam of the spectrometer as isolated atoms. The sample, dissolved in a suitable solvent, is converted to free atoms prior to entering the optical beam by passing the sample through a flame. The Boltzmann relationship predicts that, for most elements, the fraction of total atoms which are at higher energy states range from 10^{-10}-10^{-4} at 3,000K. Thus, there is insufficient thermal energy in the flame to promote an appreciable portion of the free atoms from their ground state to higher energy levels; they are virtually all available to absorb energy from the light source.

In practice, not all elements are detected with equal ease (some elements are detected more efficiently than others). The probability of light absorption of a particular wavelength (λ) per unit volume is a function of the total number of free atoms in that volume and a constant which is characteristic of a particular transition. This constant (termed the oscillator strength)

represents the average number of electrons per atom which can be excited by the incident radiation (of wavelength λ). It is a physical property of an analyte atom which does not vary under normal operating conditions. Thus, to a first approximation, the absorption phenomenon is predicted to be independent of temperature and wavelength (in contrast to atomic emission which suffers from severe losses in intensity at shorter wavelengths). Not surprisingly then, the appreciably different values for the oscillator strength for different elements will cause the AAS technique to produce lower limits of detection for certain analyte elements than for others.

The natural line width of an atomic absorption line is extremely narrow; an estimate of this width can be obtained from the uncertainty principle:

$$\Delta E \Delta \tau = h/2\pi$$

where: ΔE is the range of energies over which the excited state atom emits and τ is an upper limit of the lifetime of the excited state (10^{-8} sec).

The natural line width (as measured by the range of energies emitted when the excited state atom returns to the ground state) is predicted to be *ca.* 10^{-5} nm. In practice, this range of energies is broadened (up to 100-fold) by several effects including Doppler and Lorenz broadening to result in "half widths" between 0.005 and 0.0005 nm. The range of energies emitted by atoms as they return from the same excited state to the ground state follows a roughly Gaussian distribution. By convention, the range of energies associated with an emission (or the reverse process) is expressed as the width of this curve at half height (half width). This very narrow absorption band presents a major problem.

5.3 HOW ARE ATOMIC ABSORBANCES MEASURED ?

The Problem: If a conventional continuum source is used to provide the incident radiation to the analyte, the intensity of the required radiation is too weak and worse there is no moderately priced monochromator available with sufficient resolving power to isolate the required radiation from the rest of the output from the source. One of the fundamental requirements for quantitative absorption is that the width of the radiation which is incident on the analyte must be smaller than the width of the absorption line.

The Solution: As proposed initially by Sir Allen Walsh, one innovative solution is to use a source of incident radiation which emits the spectrum of the element to be determined. Thus, rather than using a continuum source of incident radiation, a lamp which emits the spectrum of the analyte is used. The required resonant line then only has to be isolated from the other spectral lines by means of a monochromator. As suggested in Figure 3, the

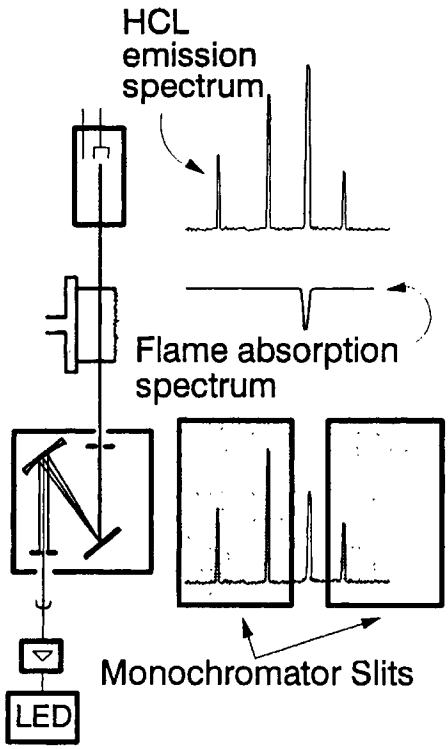

Figure 3: A schematic representation of the role of the monochromator in transmitting only one emission from the hollow cathode lamp to the detector.

emission of a hollow cathode lamp consists of several sharp emissions. The absorption band of the analyte is broadened relative to the most intense emission line from the lamp. A monochromator is then required only to isolate the radiation transmitted by the sample from the other spectral emissions of the lamp. One consequence of this approach is that the technique requires a separate radiation source for each element to be measured. The radiation transmitted by the monochromator is quantified with a detector (a measuring device, called a transducer, which converts the light energy into an electrical signal).

5.4 COMPONENTS OF AN AA SPECTROMETER

5.4.1 An Overview

The general construction of an atomic absorption spectrometer is surprisingly simple (Figure 4) and not unlike the more familiar spectrophotometer used

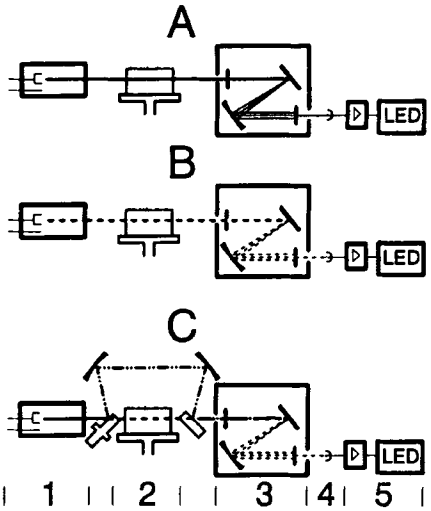

Figure 4: AAS instrumental configurations in which a continuous signal (A), or a modulated signal (B, C) which is generated by the hollow cathode lamp (1), passes through the flame (2), to the monochromator (3), and the transducer (4). The resulting electrical signal is amplified and displayed (5). In configuration (C), the continuous signal is split into reference and sample beams by a mechanical chopper.

for liquid phase studies. It consists of: a light source, "1", which emits the spectrum of the element to be determined; "2", an "atom reservoir" (an absorption cell) in which free atoms of the analyte are formed - usually a flame; a monochromator, "3" (a device to resolve the transmitted light into its component wavelengths) with an adjustable exit slit to select the wavelength corresponding to the resonant line; and, "4", a detector with ancillary electronics to measure the radiation intensity and to amplify the resulting signal. As described, this instrument is a flame photometer which, for our purposes, has one crucial disadvantage - the flame is a luminous source of radiation. The instrument must recognise the contribution from the flame and disregard it. The power of the beam transmitted to the detector (P) will be equal to the power of the beam incident on the sample (P_O) minus the power of the beam absorbed (P_A) by the sample plus a contribution from the luminosity of the flame itself (P_F).

$$P = P_O - P_A + P_F$$

Virtually all AA spectrometers operate with a radiation source which is modulated (chopped mechanically or electrically at a fixed frequency). The net effect is that the detector receives a modulated signal from the emission source and a constant signal from the flame. The constant signal from the

luminous flame is then subtracted electronically (filtered out by the instrument) from the modulated signal which originated from the lamp. The modulated radiation from the lamp is symbolised in Figure 4B as a dotted line (in contrast to the solid line for the lamp radiation in Figure 4A).

A natural question arises here. If the mean lifetime of the excited state is so very short (10^{-8} sec as an upper limit), and the excited state atom can return to the lower ground state energy by emitting light of the same energy why doesn't this emission cancel out the decrease in the power of the beam transmitted to the detector? Two effects limit the decrease in the signal due to analyte emission; (i) not all the excess energy is lost by light emission (a portion is lost in collisions with other species in the flame a process termed "non radiative transition") and (ii) the emitted light is omnidirectional (given off in all directions) so that only a very small fraction is emitted in exactly the same direction as the radiation from the hollow cathode lamp.

A further refinement to AA spectrometers consists of interposing a mechanical chopper (a circular disk with a highly reflecting surface and opposite quadrants removed) into the light path prior to the flame. Radiation from the lamp source will be passed alternately through the flame then diverted around the flame. The separated beams are then recombined after the flame compartment so that the two signals can be compared. In theory this approach can compensate for drift over time in the output from the lamp, changes in the flame and/or changes in the detector response. The ability to compensate for these effects is obtained at the expense of a decrease in the intensity of the radiation incident on the analyte (half the beam is diverted to form a "reference" beam). It is also imperative that the diverted beam be exactly realigned with the beam which has traversed the flame. The stability of the components of modern spectrometers is such that the use of a "double beam" unit is of less importance than it once was.

5.4.2 Light Sources

The most popular radiation sources for AAS are hollow cathode lamps (HCLs). These devices contain a hollow cathode cylinder which has been coated with the analyte of interest and a collector anode which is located near the constricted orifice of the cathode cylinder. The lamp typically has been filled with an inert gas (usually neon) under a partial vacuum. Under an applied voltage of 100-400 V, atoms of the filling gas are ionised and accelerated to the cathode surface where they dislodge analyte atoms. The analyte atoms which "sputter" from the cathode surface are excited to a higher energy level by collisions with other species and emit the emission spectrum of the analyte. Since most of these emissions occur within the cylinder, the emitted light which escapes through the orifice is reasonably focused. The more analyte atoms which are sputtered from the cathode surface and subsequently excited, the more intense the light source becomes.

However, "sputtering rates" vary appreciably from element to element so that lamps of elements with a high sputtering rate (Cu, Zn, and Ag) provide an adequate signal at low currents. By contrast lamps for W and Zr must be operated at higher currents to achieve similar sputtering rates. Interestingly, the "line broadening" which results from this configuration is appreciably less than the line broadening of the corresponding analyte absorption band in the flame.

Continued design improvements have largely overcome a problem of "self reversal" - a condition in which there is a development of a cloud of ground state free atoms of analyte at the cathode exit. The cloud can absorb an appreciable proportion of the centre of the broadened emissions which originate from within the cathode. The profile of the emissions which exit the lamp under these conditions has a high proportion of "non absorbable" radiation (aptly described as "broad wings") which contributes to non linear calibration curves. The use of short pulses of a correspondingly higher current to the lamp rather than an alternating or a direct current provides a higher lamp intensity without appreciably affecting the useful lifetime of the lamp. A rule of thumb regarding the applied current to a hollow cathode lamp is that a current corresponding to 50-70 % of the maximum provides maximum reproducibility whereas a current greater that 70 % of maximum will provide maximum sensitivity. Many AAS instrument have a lamp turret which can accommodate four to six lamps and maintain them at operating temperature so that stabilisation time is minimised. To change elements, the required lamp can be rotated into position and the operating parameters optimised with a minimum of time and effort.

One variation in lamp design which can be especially useful for certain elements (such as As, Se, Cd, Pb, Ni, Pd, and Bi) has been the incorporation of a boosted discharge from a second anode (isolated from the first) to increase the efficiency of excitation of the sputtered analyte atoms. The cathode is a hollow cylinder rather than a cup and the primary anode (a circular disk) is positioned below the cylinder. A potential between the two is applied using the instrument's electronics. Although the lamp intensity is typically less than a normal HCL under these conditions, a separate current applied to an electron emitter (positioned above the cathode cylinder) causes a discharge of electrons into the region of the sputtered ground state atoms. The added electron density increases the probability of collisional excitation with sputtered analyte atoms and the net result is a more intense radiation from the lamp. The boosted current affects primarily the excitation process and not the sputtering process so that the rate at which sputtered material irreversibly captures the fill gas is unaffected.

Electrodeless discharge lamps (EDLs) are also available commercially. As the name implies, these emission sources provide a glow discharge by virtue of the fact that a sealed bulb, containing a monatomic gas at low pressure, and

some volatile pure analyte metal or metal salt, is positioned within an intense microwave field. In general, EDLs provide a more intense emission but more susceptible to intensity drifts with time than are HCLs.

A number of "multi-element" lamps are also available commercially. Various metals, in powdered form, are mixed in predetermined ratios, pressed and sintered to produce the cathode material. However, only certain combinations are practicable. The obvious advantages of this format is that fewer lamps are required and the time required to switch from one element to another is minimised, however, the intensity of the emissions are generally lower than from the corresponding single element lamps.

5.4.3 Nebuliser/Atomiser Assemblies

To be detected by AAS, the analyte must be presented to the optical beam of the instrument as free atoms. The process of converting analyte ions/molecules, dissolved in a suitable solvent, to gaseous atoms is accomplished by the nebuliser flame assembly. The nebuliser (from the Latin nebula meaning cloud) creates an aerosol (a fine mist) of the liquid sample which is mixed with an oxidant gas and a fuel gas (to support the flame combustion). The mixture is ignited above the burner assembly. The liquid droplets are desolvated, the resulting microcrystals are melted and vaporised and finally the gaseous products are thermally dissociated to produce free atoms. The combustion speed of most flames is such that the conversion from liquid droplet to free atoms must be accomplished within a few milliseconds.

Additionally, the flame is a highly reactive environment which contains numerous combustion products (including CO_2, CO, C, H_2O, O, O_2, OH, NO, N_2) in addition to the analyte. Analyte atoms which are reactive in this environment can only be produced by temperature dependent equilibria. Competing side reactions can be extensive. Included among these side reactions is the possibility of ionisation. The spectral characteristics of the product ions are completely different from the parent free atoms. The net result is that the efficiency of production of analyte atoms is very much dependent on the operating characteristics of the flame.

5.4.4 Nebulisers

Virtually all modern flame AAS (FAAS) instruments make use of a pre-mix nebuliser in combination with a laminar burner design. A typical design is presented in Figure 5. The flows of gaseous fuel and oxidant gases into the nebuliser create a Venturi effect across the exit of a capillary tube. As a result, liquid sample is aspirated through the capillary (at rates of 2 to 6 mL/min) and exits into the nebuliser chamber as an aerosol (with a rather wide range of droplet sizes). An impact bead or a flow spoiler is typically used to further smash up the droplets and to increase turbulence of the flow

respectively. The larger droplets preferentially impact on the surfaces of the flow spoiler or on the walls and condense. Whereas condensed liquid flows to a drain and is discarded, smaller droplets are swept by the turbulent flow up into the burner assembly. Although somewhat improved with recent design modifications, some 90-95 % of the sample entering the nebuliser is recondensed and lost to the drain. The flow rate of the liquid sample into the instrument and the sizes of the droplets produced are also influenced appreciably by the viscosity, density and the surface tension of the liquid sample. The subsequent processes leading to atomisation can also be relatively inefficient. Despite these gloomy efficiencies and the fact that the sample material is enormously diluted (by several liters per minute of fuel and oxidant gases) in the process of atomisation by a flame, low to sub mg/kg sensitivities are achieved routinely for a wide number of analytes.

5.4.5 Flames

Three flames are used routinely in FAAS, the most popular of which is a combination of air with acetylene (C_2H_2). With a typical operating range between 2,125 and 2,400°C, this combination offers sufficient thermal energy to extensive atomisation of many elements. The resulting flame is virtually transparent over a wide range of wavelengths (becoming noticeable below 230 nm and increasing to 65% at the 193.7 nm resonant line for arsenic).

Moreover, the ratio of fuel to oxidant can be varied appreciably without extinguishing the flame although the flame is normally operated under stoichiometric or slightly oxidising conditions (slight excess of oxidant). A high luminosity is indicative of an excess of fuel gas which results in a higher background emission due to non-oxidised carbon. With this flame ionisation of analyte atoms is not appreciable (except for alkali and alkaline earth metals). Oxygen is not normally used as an oxidant in premix nebuliser - FAAS because of the increased combustion speed of the resulting flames (10- to 15- fold relative to air as the oxidant gas) and the increased danger of a flashback.

A burner head, typically with a single slot (10 x 0.2 cm), is aligned along the axis of the optical beam from the radiation source. The nebuliser/burner assembly is mounted on a platform which provides for positional adjustment in both the vertical and horizontal planes. The optimal height of the optical beam above the burner slot varies with each analyte element (and somewhat with the sample composition) is established experimentally for each standard solution. An impressive graphic presentation of the spatial distribution of analyte atoms of sodium, calcium, or molybdenum in an air/C_2H_2 flame (under identical operating conditions) has been presented by Rann and Hambly (*Anal. Chem.* **37**, 880, 1965).

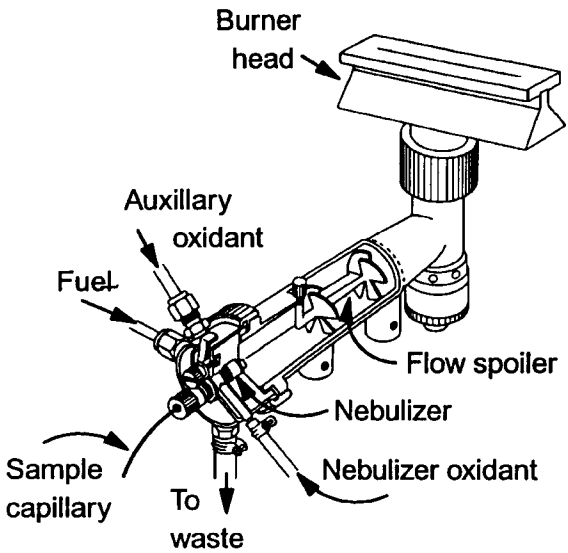

Figure 5: A cut away representation of a typical AAS pneumatic nebuliser-atomiser assembly showing the position of a flow spoiler within the nebuliser chamber.

A combination of nitrous oxide (N_2O) with air provides an increased operating temperature (2,650-2,900°C,) without a large an increase in the burning velocity (285 *versus* 160 cm/sec). The higher operating temperature can be exploited to atomise certain elements more efficiently; by contrast, other elements (*e.g.*, Al, La, Ti, or the rare earth elements) are more extensively ionised under these conditions. This combination of gases has the disadvantage that several strong emissions from CN, CH, C_2, and NH species can interfere with the detection process (Christian, G.D., *Anal. Chem.* **41,** 24A, 1969). One other gas combination, which has found limited application in AAS, is a combination of air with H_2 with or without an inert gas.

5.4.6 Optics

The spectral range of interest for AAS spans from the near infrared (852.1 nm for Cs) to the vacuum ultra violet (193.6 nm for As). A monochromator is a device which separates, isolates, and controls the intensity of a narrow region of the radiant energy which is transmitted to the detector (characterised by its spectral slit width). It consists of an entrance slit, a dispersing unit (a diffraction grating) and an exit slit. The greater the intensity of the radiation transmitted to the detector the lower the signal amplification required (which contributes to electronic noise). However, the entrance and exit slits must be of similar mechanical widths (aperture size) so that, in practice, a compromise must be chosen (slit width *versus* narrow

spectral band pass). Spectral slit width and mechanical slit width are related by the "linear reciprocal dispersion" (nm/mm). The "linear dispersion" is a measure of the performance of the monochromator (for a linear dispersion of 2 nm/mm, a 0.1 mm mechanical slit width will result in a 0.2 nm spectral bandpass. A spectral bandpass corresponding to 0.2 nm is generally adequate for most elements. In principal, there is no advantage to working with narrower slits. An example of the possible influence of "slit width" on calibration curves for silicon is illustrative (Figure 6). There are six emission lines for Si between 250 and 253 nm (Figure 6A). With a sufficiently narrow slit width, each resonance line can be isolated form the other emissions and plots of absorbance *versus* concentration are linear for each line (Figure 6B). Not surprisingly, as the spectral slit width is increased, the calibration plots become increasingly curvilinear (Figure 6C). However, a maximum slope for a calibration curve, although desirable, is not the only consideration in optimising operating conditions. An increased slope implies an increased ability to discriminate between samples containing similar concentrations of analyte (there is a greater change in absorbance per unit change in concentration). However, an increasingly narrow slit passes less energy to the sample so that "noise" (random fluctuations in the signal) is increased proportionally. A second parameter of importance is the signal to noise (S/N) ratio which must be maximised. In this case, the signal to noise ratio is optimal at 0.2 nm and decreases for both narrower and wider slits (Figure 6D).

5.4.7 Detector(s)

A device capable of converting radiant intensity (in the absence or presence of sample) into an electronic signal will provide a measure of the transmittance of the sample (P/P_o). Photons which are incident on the detector (a photomultiplier tube) bombard a photoemissive surface. The flux of electrons which are dislodged is proportional to the intensity of the incident radiation and, under the influence of an applied voltage, they are accelerated toward a collector anode. Additional photoemissive plates (called dynodes) are interposed between the cathode source and the anode collector to cause a multiplier effect. Each electron dislodged from one plate will be accelerated to a second plate where it will dislodge several electrons so that a high flux of electrons will be collected by the anode. The magnitude of the multiplier effect is operator controlled in that the difference in potential between successive plates influences the acceleration of an electron dislodged from the first plate and, in consequence, the number of electrons which will be dislodged by its impact with the second surface. These potential differences are adjusted by the operator-controlled "gain" settings (of which a broad range is available). However, thermally induced emissions from the cathode and/or intervening dynodes in the absence of incident radiation will generate a "dark current", the magnitude of which will increase in proportion to the gain. The detector and ancillary electronics of modern instruments are capable of recognising and displaying the smallest differences in absorbance

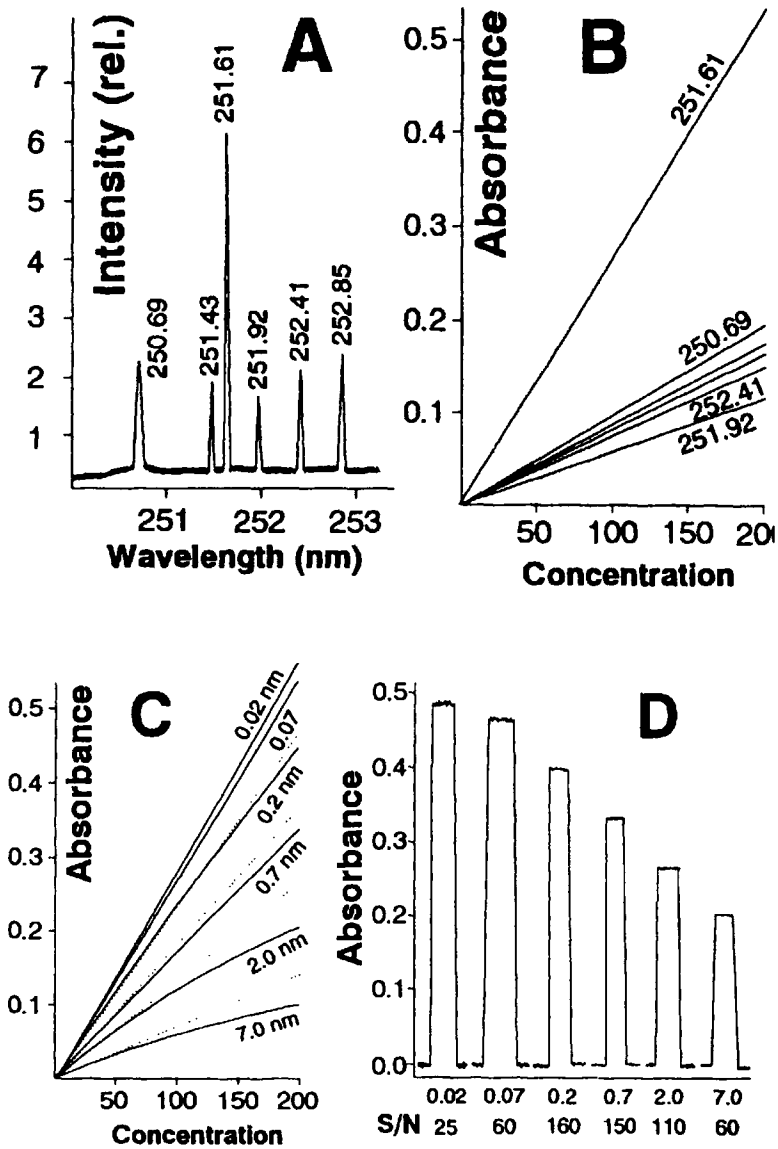

Figure 6: The influence of spectral slit width on AAS calibration curves for silicon using each of the six spectral emission lines between 250 and 253 nm (A). Provided that a sufficiently narrow spectral slit width is used, linear calibration plots are obtained at each λ (B), however at 251.61 nm, as the slit width is increased, calibration plots become increasingly curvilinear (C). An optimum signal/noise ratio is obtained with a spectral slit width of 0.7 nm (D).

(0.0001 A units can be of interest) to obtain good precision and a low limit of detection. Since the detector actually measures the radiant flux density (intensity) in the presence or absence of analyte, the direct readout would be in transmittance (P/P_o) or in percent transmission (% T = $100P/P_O$) or in some early models % absorption (100 - %T). Since linear relationships are easier to handle than logarithmic relationships, %T is converted into absorbance units automatically by the instrument:

$A = \varepsilon bc = -\log (P/P_0) = 2 - \log \%T$

5.4.8 Support Gases

A number of precautions are necessary when working with compressed gases. Acetylene is customarily purchased in 9,000-litre cylinders (type K) which will provide some 30 hours of instrument operation (air/C_2H_2 flames consume approximately 5 L/min and N_2O/C_2H_2 flames consume some 15 L/min). Since it is difficult to compress this gas to greater than 30 psi without special precautions to prevent explosive decomposition, the commercial product comes dissolved in acetone. Since C_2H_2 is in liquid solution, the pressure drop (as measured by pressure regulator) will not be linear with the gas removal (a pressure of 75 psi indicates a nearly empty tank). Recommended practice is to switch tanks when the head pressure falls to between 100 and 75 psi. The ratio of C_2H_2 to acetone will decrease as the tank becomes depleted so that the response for certain elements will also decrease. Finally, C_2H_2 should not be permitted to come in contact with copper, silver, or mercury which can form metal-acetylides (which can decompose violently).

Nitrous oxide is purchased in cylinders containing 15,000 litres which provides some 12 hours of operation of an N_2O/C_2H_2 flame. When removed from the tank at 15-20 L/min expansion of the gas in the pressure regulator can freeze the diaphragm rendering it inoperative. Heated regulators for N_2O are recommended for AAS applications. As with C_2H_2, a portion of the N_2O in the cylinder is liquefied so that the drop in head pressure with consumption will not be linear. The areas where this gas is stored or used should be well ventilated as this gas is an asphyxiant and a potential hazard in a confined space.

Many laboratories prefer to obtain their air from a compressor rather than purchasing cylinders. A compressor capable of delivering at least 30 L/min at a pressure of 40 psi is recommended. A water and oil trap between the compressor and the instrument is a necessity. A cylinder containing 6,200 L will last some 5 hours and the O_2 content is somewhat variable from cylinder to cylinder.

5.4.9 AAS Measurements

An AAS measurement involves a series of sequential steps. Initially, the instrument operating parameters must be set up for the analyte element. Detailed operating procedures and recommended parameters for each analyte element are tabulated in the "analytical methods" manual which came with the instrument. Having installed the required hollow cathode lamp (HCL) and permitted it to equilibrate at the correct operating current, the alignment of the lamp and the chosen monochromator wavelength are then optimised using the lamp/energy display of the instrument. The flame is ignited and water is aspirated while the flame stabilises over several minutes. Once equilibrated, the aspiration rate of the nebuliser assembly is optimised by maximising the absorbance of a standard. Similarly, the fuel oxidant gas ratio and the position of the burner head are adjusted to maximise the analyte response. The absorbance of the sample blank is then established by aspirating sample solvent. Finally, each of the samples is determined sequentially. Typically, for a measurement, sample is aspirated until the absorbance has stabilised (approximately 20 s). If the absorbance is recorded continuously, each sample will result in a vertical displacement above the mean background reading. Blank is aspirated between samples to establish that there is no sample carry over from one sample to the next.

5.5 AAS, A RELATIVE TECHNIQUE

A number of approaches have been used to compare the relative AAS response to different analyte elements. At one time, it was conventional to compare the responses in terms of the concentration (mg/mL) or the amount of analyte that would result in a signal corresponding to 0.0044 A (*i.e.*, a 1% absorption). For a given calibration curve (A = f[C]) "sensitivity" was equated with the slope:

"sensitivity" = $\Delta A/\Delta[C]$

Since the Beer-Lambert relationship predicts a linear relationship, the "sensitivity" (identical to the slope) is independent of the concentration (at least over the linear range of the calibration curve). In the intervening years, an alternate approach has also been used. Since AAS involves a differential measurement {peak height (or area) - background signal} the detection limit is represented by the smallest concentration (or amount) which can be differentiated reliably from the background signal. At the 95 % level of confidence, this corresponds to twice the standard deviation associated with the background signal and three standard deviations increase the confidence level above 99 %. The limit of detection is influenced by two parameters, the slope of the calibration curve and variations in the background signal (noise). Any modification to the operating conditions which increases both parameters equally does not improve (lower) the detection limit.

Improvements in the detection limit can only be achieved if the S/N ratio is improved. Unfortunately, different methods have been used to quantify the variations in a background signal. One approach is simply to measure the average difference between the maximum and minimum (referred to as peak to peak, p-p) whereas a second approach approximates the variations in the noise by a sine wave. If the sine wave approximation is valid, the average is the root mean square of the signal (abbreviated as rms). The difference between these approaches result in estimates which vary by a factor of approximately 3 [*i.e.*, S/N(rms) = 2.8 S/N(p-p)]. Fortunately, most authors specify their method for estimating the noise. It is also important to recognise that the limit of detection is an extrapolated value and is calculated based on the best possible conditions with virtually no interference. In practice, the lowest amount (or concentration) which can be reliably detected is some three to five times this estimate.

Within the last decade there has been a concerted effort to harmonise the approaches to reporting the limits of detection (LOD) for different analytical techniques. The concentration at the limit of detection is given by

$$LOD = 3S_b/g$$

where:

- S_b is the standard deviation associated with the blank signal; and
- g is the slope of the linear calibration curve.

5.5.1 Possible Approaches to Improving the S/N Ratio

Here the possibilities are somewhat limited. For the most part, it is not possible to decrease the background noise appreciably (mainly a function of the instrumental design). Alternatively, increasing the intensity of the incident radiation (higher lamp current) also increases the level of noise (the noise generated by the lamp is also increased). The parameter which can be influenced appreciably is the signal.

5.6 INTERFERENCES

Since AAS is a relative rather than an absolute technique, quantitation is performed by comparison with a standard. Any difference in behaviour of the analyte atoms in the sample and in the standard implies an interference. Interferences are classified conveniently into four categories; chemical, physical, background, and spectral. Whereas background and spectral interferences result from the influence of "non specific" signals, chemical and physical interferences can have a positive or negative influence on the number of ground state analyte atoms present in a unit volume of the flame.

5.6.1 Chemical Interferences

When comparing different samples using the same atomisation technique, a chemical interference causes a change in the total number of free atoms being released within the atom reservoir. Changes in the atomisation efficiency are caused by the formation of chemical compounds (which can be atomised more or less efficiently relative to a reference standard). Analyte free atoms can react with other species formed within the reactive environment of the atomiser to form products which are more difficult to melt/vaporise or to dissociate. The net effect is to change (usually to lower) the mean lifetime of the analyte atoms in the optical beam of the instrument. The principal causes are the formation of oxides (or oxide radicals), hydroxides (hydroxide radicals), or carbides and nitrides. Thus, this type of interference is strongly dependent on the flame type. Since the flame combustion products are present in vast excess (relative to the analyte) this influence is often independent of analyte concentration. The net result is that the instrumental response to some 30 elements (*e.g.*, Al, Si, B, or the lanthanides) is appreciably better with an N_2O/C_2H_2 flame than with an air/C_2H_2 flame. The higher operating temperature of the N_2O/C_2H_2 combination as well as a decrease in oxy and hydroxy ions/radicals favour a more efficient release of free atoms. At the same time the higher operating temperature promotes ionisation of the analyte atoms. It is also sometimes possible to reduce the influence of hydroxide and/or oxide formation by lowering the viewing height above the burner slot (raising the burner head platform) so that a cooler region of the flame is monitored. This approach, however, also reduces the time available for the desolvation - vaporisation - atomisation process.

In addition to flame effects, chemical interferences which result from the sample matrix are also known. The consequence of this type of interference is that if it is not detected (and compensated for) it can result in appreciable error. Well studied interferences in the determination of Ca, are the influences of Al and of PO_4^{3-}. Aqueous solutions of calcium as $CaCl_2$ are atomised more efficiently than are solutions of $Ca(NO_3)_2$ principally because the formation of $CaO/Ca(OH)_2$ is more extensive in the latter case (CaO has a melting point of 2577°C). Thus, the acid used to prepare aqueous Ca standards influences the instrumental response appreciably. The atomisation efficiency can be further suppressed by the formation of $Ca_3(PO_4)_2$ or $CaAl_2O_4$.

If raising the operating temperature or changing the chemical environment are not practical, chemical interferences can sometimes be eliminated or compensated for chemically. Three approaches can be considered:

- addition of the interfering ion to the standards;
- binding up the interfering ion by adding an excess of a second cation; and
- shielding the cation to be measured by complex formation.

An example of the first approach (matrix assimilation) would be to match the acid content in the standards with the acid content in the samples. Matrix assimilation is only effective provided that the interference is not severe and the sample matrix is relatively simple. For more marked interferences, a second cation can act as a release agent. As an example, lanthanum [as $La(NO_3)_3$] can be added to solutions in which Ca is to be determined in the presence of PO_4^{3-}, silicate or aluminate in an air/C_2H_2 flame. An example of the third approach would be to add a strong complexing agent (such as EDTA) to both samples and standards. Many metals have an appreciable tendency to hydrolyse in aqueous media; moreover the hydroxides can be sparingly soluble yet precipitates can be difficult to detect visually in dilute solutions. To limit this process, samples are customarily prepared in acidic media.

5.6.2 Physical Interferences

The sources of this type of interference are differences in the bulk properties (viscosity, specific gravity and/or surface tension) of the sample and standard solutions. These physical interferences principally affect the nebulisation process. As the viscosity of the solution is increased, less sample will be aspirated per unit time and the resulting droplets will be larger in size (so that more sample will be recondensed in the nebulisation chamber and exit to drain). This type of interference gradually becomes increasingly apparent above 1 % dissolved solids - and organic molecules (biopolymers, proteins and sugars) have a proportionately greater effect than inorganic salts. If the physical properties of the standards cannot be matched to the sample solutions, an alternate approach is to use a pump to deliver the solutions, at a constant rate, to the nebuliser.

Whereas increasing viscosity of sample solutions (relative to standards) attenuate the response, the use of organic solvents to prepare samples can have the opposite effect (increased signal relative to aqueous standard). Not only does the decreased viscosity results in a faster feed rate, a finer nebulisation and a more efficient desolvation but also the combustion of organic solvents are highly exothermic (CCl_4 is an exception) resulting in a hotter flame. By contrast, the dissociation of H_2O is endothermic and cools the flame appreciably. As a rule of thumb the signal enhancement varies as the log of the product of the viscosity and the boiling point. Again, samples and standards should be dissolved in the same solvent - it might be necessary to readjust the fuel flow rate to return the flame to stoichiometric conditions. Analytes can often be concentrated advantageously *via* a process of solvent extraction in which the cationic analyte is solubilised in a non polar organic solvent and removed from an aqueous sample by reaction with a suitable complexing agent. However, since even small quantities of water can alter the combustion characteristics of an organic solvent appreciably, standards

should be prepared in identical fashion so that the organic phase is saturated with water.

5.6.3 Ionisation Interferences

Several elements are partially ionised by the thermal energy of the atom reservoir. Since ionised atoms have an altered electronic configuration, energy levels are changed appreciably resulting in completely different absorption and emission spectra. Ionised atoms will not be detected at the same wavelength as ground state atoms. The extent of ionisation for a given set of operating conditions is concentration dependent:

$M ====== M^+ + 1e^-$

$K_{EQ} = [M^+][e^-] / [M]$

This effect is analogous to the situation in solution chemistry in which the degree of ionisation $\{[A^-]/([A^-] + [HA])\}$ of a weak acid (HA) in an unbuffered solution increases as the solution is diluted. As a consequence, in AAS, calibration curves of absorbance *versus* analyte concentration when ionisation of the analyte atoms is appreciable, will be curvilinear (towards the absorbance axis). Possible remedies include using a different flame (or flame conditions) to reduce the thermal energy of the flame. An air/H_2 flame virtually eliminates the ionisation of alkali metals. However, for other elements, the reduced thermal energy considerably reduces the efficiency of atomisation (lanthanides) or increases chemical interferences appreciably (Ba). A second remedy involves the addition of a large excess of an easily ionised element to both standards and samples. Both K and Cs are easily ionised and can be used to generate a high concentration of free electrons within the flame (shifting the analyte equilibrium in favour of the free atom). The influence of adding 0.2 % (w/v) of KCl on the calibration curve for Barium is provided in Figure 7. Weltz has suggested that for elements which are easily ionised (ionisation energy (I.E.) $\leq$ 5.5 eV), some 10g/L of a second more easily ionised element can be used to eliminate this interference. For analytes with 5.5 < I.E. < 6.5 1, 2 g/L of additive, and for analyte elements with I.E. $\geq$ 6.5 eV, 0.2 g/L of additive are suggested.

5.6.4 Background Interferences

The two fundamental sources of background interferences include (i) light scattering by solid (smoke particles, micro crystals of sample) or liquid droplets and (ii) true absorption of the incident radiation by ions, molecules and/or radicals which originate within the sample solution. The background interferences result in overestimates of the analyte concentration Since the detector can only measure a change (decrease) in the intensity of the transmitted signal it cannot differentiate light lost by scattering or molecular

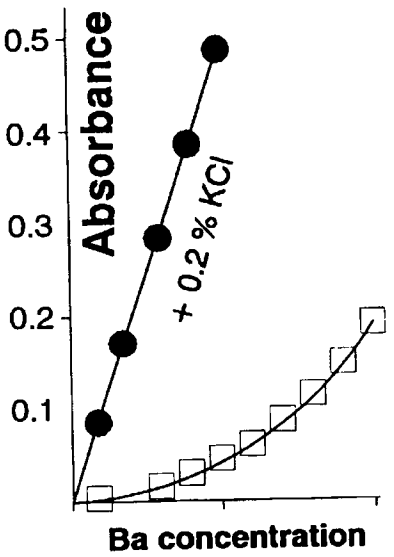

Figure 7: The influence, on the calibration curve for barium, of adding 0.2% (w/v) KCl to each standard.

absorption from light lost by atomic absorption. Light scattering is highly dependent on the instrumental operating conditions. According to Raleigh's stray light law, the scattering coefficient (τ) is given by:

$$\tau = P/P_0 = 24\pi^3 Nv^2/\lambda^4$$

In other words the magnitude of the effect is predicted to be directly proportional to:

- the number of particles (N) per unit volume;
- the square of the particle volume (v) (doubling the radius of the particle causes τ to increase 64-fold); and
- the inverse of the (wavelength, λ)^4 (τ increases 265-fold in going from 800 to 200 nm).

Scatter will be greater for "total consumption" burners which produce larger sample droplets, for solutions of higher dissolved matter, and for light below 250 nm.

As an example of the second type of background interference, there is a CaOH "molecular absorption" band which corresponds almost exactly to the atomic 553.6 nm line for Ba. A 1 % solution (10,000 mg/g) of Ca has been

reported to result in an absorbance of 0.30 when measured with the 553.6 nm line of a Ba hollow cathode lamp.

Attempts to compensate for background interferences exploit the fact that the phenomenon is rather broad band relative to the line width of atomic absorptions. Raleigh's law suggests that τ can vary by as much as 20 % over 10 nm (in the region of 200 nm) and the variation in polyatomic (molecular/ionic) absorbances can be even greater. Thus, to be as accurate as possible, the magnitude of the interference should be measured as close to the atomic resonance line as possible. The most popular approach to background correction employs a dual channel system in which light from a hollow cathode lamp and from a continuum source are passed in rapid succession through the atom reservoir. As suggested in Figure 8, a mechanical chopper can be used to direct light from either source through the flame of a single beam instrument. In Figure 8A the emission spectrum from the two sources are presented. If the influence of the exit slit ($\cong$2 nm slit width, Figure 8B) of the monochromator on each of these two spectra is considered, Figure 8C is the portion of the light source emissions transmitted to the detector (in the absence of analyte atoms in the flame). When analyte is present in the flame (Figure 8D), the intensity of the emission from the HCL (P_o) will be reduced (say $P/P_o = 0.8$ corresponding to A = 0.097). By contrast, since the absorption line width is only $\cong$ 0.002 nm, the absorption of the same amount of light from the continuum source (spectral width 2 nm) will have a negligible effect on the light transmitted to the detector ($P/Po \cong 1.0$). By contrast, if a background interference is present the light from both sources will be affected equally (Figure 8E). Finally, when both analyte and background interference influence the signal (Figure 8F), the intensity of the light from the HCL is attenuated by both but the light from the continuum is attenuated only by the interference. The difference in transmittance (P/P_O) between these two signals must result from the analyte.

5.6.5 Spectral Interferences

In practice, AAS is virtually free of spectral interference. The majority of reported interference have been observed for less sensitive analyte lines rather than the major resonance line which is conventionally used for analysis. The only major exception is the overlapping of the 213.895 nm line for Fe (a "minor" emission line) by the resonance line for Zn at 213.856 nm. In practice this interference would only be evident if traces of Zn were being determined in samples of Fe.

5.7 CALIBRATION TECHNIQUES

Given the less than quantitative nebulisation/atomisation process and the myriad competing reactions which can modify the lifetime of analyte free

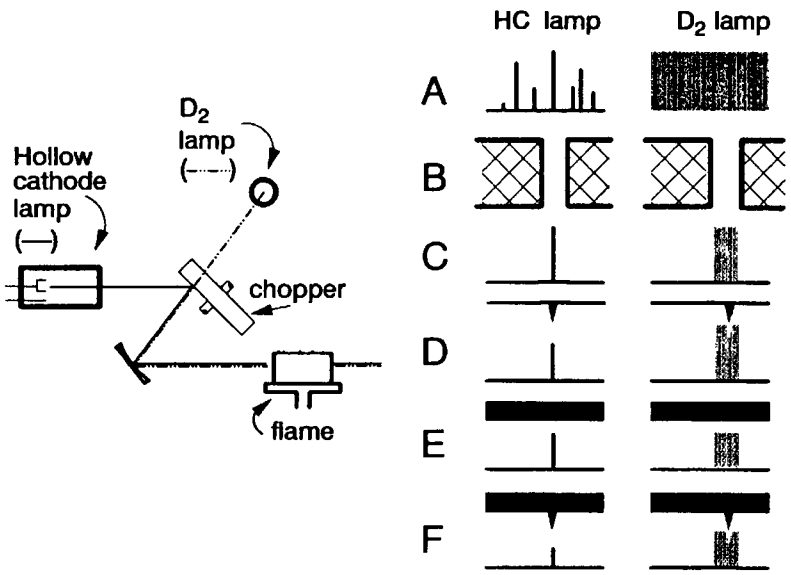

Figure 8: A schematic representation illustrating the effect of analyte and of background on the emissions from both a hollow cathode lamp and a deuterium lamp. Whereas the background attenuates both signals equally, the analyte attenuates the HCL signal only and the difference in attenuation must result from the analyte.

atoms within the atom reservoir, it is not surprising that the changes in the intensity of the detector signal, in the absence or presence of analyte, cannot be directly related to analyte concentration in the sample. AAS is a relative technique in the sense that the instrument response to a sample must be compared with the response to an analytical standard. Two approaches have been popular.

5.7.1 Method of External Standards

Standard solutions of known concentration of analyte to provide absorbances between 0.2 and 0.8 are prepared by serial dilutions of a stock solution of an authentic standard. Each standard solution is aspirated into the flame and the observed absorbance is recorded. A calibration curve is then prepared by plotting absorbance *versus* concentration of analyte. As predicted by the Beer - Lambert relationship, the resulting plot will be linear or have a slight curvature (towards the concentration axis) at higher concentrations. The absorbance of an unknown, measured under identical operating conditions, is then related to analyte concentration in the unknown using the calibration curve (*i.e.*, a process of linear interpolation is used). A prerequisite to successfully using the method of external standards is that the sample and standard solutions behave identically in the flame; no measurable

interferences can be present in one solution but not in the other. Minor chemical and especially physical interferences in the sample solution(s) can be compensated for by matching the matrix of the sample(s) and standards. This approach is suitable if a large number of similar samples are to be determined and the sample matrix is reasonably well characterised.

The major cause of curvilinear calibration plots is considered to be the presence of unabsorbable light (stray light) within the radiation incident upon the analyte atoms. With increasing concentrations of analyte free atoms in the flame, the proportion of incident radiation transmitted to the detector decreases until, in the limit, only stray light is transmitted. The resulting calibration plot will become increasingly curvilinear as this limit is approached. The "standard conditions" section of the "analytical methods" manual, which was delivered with your AAS instrument, will provide a guide to optimal operating conditions as well as the range of analyte concentrations over which the instrumental response can be anticipated to be linear.

5.7.2 Method of Standard Additions

In this approach, small volumes (v or 2v or 3v *etc.*) of a concentrated standard are added to separate aliquots of the sample of volume V. After thorough mixing, the difference in absorbance between the amended sample and the unamended sample must have resulted from the added standard. Moreover, those interferences which modify the instrument response to the analyte in the sample will influence the added standard in identical fashion (see below). If the absorbance of sample itself and of each of the amended solutions are plotted *versus* the amount of added standard, a calibration curve is obtained which does not pass though the origin but rather cuts the absorbance axis at some positive value (absorbance of the sample without added standard). Extrapolation of the calibration curve back to the concentration axis provides a measure of the analyte originally present in the sample. However, the absorbance of each amended solution must be volume corrected (*i.e.,* after one addition of standard, the observed absorbance A_1 is multiplied by (V + 1v)/V, after two additions the observed absorbance A_2 is multiplied by (V + 2v)/V *etc.*). The use of multiple additions demonstrates that, within the concentration range of interest, absorbance varies linearly with analyte concentration.

This approach is easier than it sounds provided that the instrument can display "concentration" (with a ± sign) and has provision to automatically zero the readout (standard features of modern instruments). The sample (V mLs plus v mL of distilled water) is aspirated and the concentration mode readout is set to zero. A separate aliquot (V mL) of sample (plus v mL of added standard) is then aspirated and the concentration mode readout is set to the amount of standard added. Distilled water is then aspirated and the "concentration" mode readout will provide the amount of analyte present

(preceded by a - sign). To use the simplified procedure it must be assumed that the absorbances of sample and spiked sample are within the linear range of the analyte response.

The method of standard additions will correct for physical and minor chemical interferences which are independent of concentration (*i.e.*, interferences which influence the slope of the calibration plot only). Concentration dependent chemical interferences and ionisation interferences cannot be eliminated since both influences result in curved calibration plots (which are difficult to extrapolate back to zero concentration). Additionally, this calibration technique cannot correct for background interferences since the two components of the net signal (true analyte absorbance and interference) cannot be separated. A deuterium background correction system can be used in combination with this technique to correct for background interferences.

5.8 MINIMIZING UNCERTAINTIES

Since AAS is typically a trace technique, it might happen that the analyte content of certain samples are above the linear range of the response. The initial temptation to simply dilute the offending samples should be resisted in favour of a more efficient procedure. By simply rotating the burner head somewhat a portion of the flame is removed from the optical beam. The net effect is that the pathlength of the sample within the optical beam is shortened. Standards are simply rerun under the modified conditions and a new calibration plot is established. Since all manipulations of the sample(s) and/or standards increase uncertainty, it is to be anticipated that the linear range of the analyte response will be increased appreciably but that the anticipated precision should not be adversely affected. By contrast, having to dilute samples will probably decrease the precision as well.

5.9 NON-FLAME ATOMIZATION TECHNIQUES

A number of flameless atomisation techniques have been developed to (i) increase the efficiency of production of analyte atoms within the optical beam of the instrument and/or (ii) exploit the volatility of analyte transformation products.

5.9.1 Electrothermal Atomisation (Graphite Furnace) AAS

This technique is probably the most sensitive atomic spectrometric technique which is routinely available to the analyst. A small quantity (typically 20 μL) of sample is deposited into the interior of a hollow graphite tube which is mounted horizontally within the optical beam of the instrument (Figure 9A). In successive stages, the tube is heated (electrical resistance) to cause:

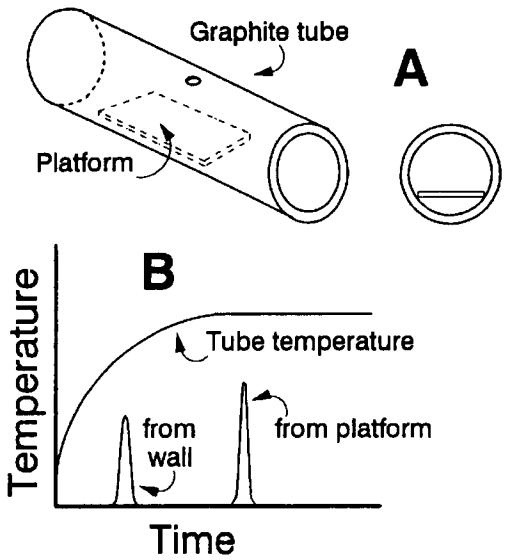

Figure 9: A graphite tube fitted with a platform insert, (A). In operation, (B), the temperature of the platform lags behind the temperature of the wall, which causes the analyte to be volatilised into a hotter environment and results in an increased AAS signal.

- solvent evaporation (drying stage);
- matrix decomposition (charring stage);
- analyte atomisation (atomisation stage); and
- furnace cool-down (and vapour clean out prior to introduction of the next sample).

The direct introduction of sample (through a small hole in the upper surface of the tube) into the graphite tube makes differences in the physical properties (viscosity, solvent composition *etc.*) between sample and standard virtually insignificant. A second advantage of this design is that volatilisation of the analyte atoms occurs into a confined space so that the atom residence time within the optical beam is appreciably longer than with flame or plasma techniques. Despite the small sample volumes, the limits of detection are at least an order of magnitude (often two or three orders) lower than with either flame AAS or plasma-AES.

The more efficient are the first two steps of the furnace heating program, the less severe will be the interference in the final stage. The sample, which usually contains less than 1 ng of analyte, will form a thin film of microcrystals as the solvent is evaporated assuring a good contact with the tube surface. To aid in dispersing potential interferents, the tube is sheathed, both inside and outside, with a flowing stream of inert gas during

the first two stages (often referred to as cycles). Typically the flow of "purge gas" to the interior is halted during the atomisation cycle. Generally, the analyte is volatilised purely by vaporisation, which can occur at temperatures well below the boiling point of the analyte compound. Because of the small amount of analyte and the low partial pressure of analyte within the tube atmosphere, volatilisation is very efficient. It is desirable to have as much of the analyte atomised at the same time as possible to result in a high density of analyte atoms within the light path. Typically, the atomisation process occurs over 0.1 s and heating rates during the atomisation can be up to 2,000°/s. In consequence, an instrument is required that will respond rapidly to changes in absorbance. Provision must also be made to integrate the absorbance signal over time since a "steady state" condition is never achieved; moreover, many physical parameters influence the peak shape (temperature, heating rate, sample matrix, sample positioning and spreading *etc.*). Most operators have concluded that an automatic sampling device (a robot arm) which reproducibly positions a fixed volume of analyte solution into the graphite tube is more a necessity than a luxury.

There have been two major improvements in tube design. A roughly rectangular shaped platform can be inserted within the tube (Figure 9A). The temperature of the platform surface, which is heated radiatively, lags behind the tube wall temperature during the atomisation cycle. When atomisation does eventually occur (Figure 9B), the products are released into hotter surround gases and better sensitivity is obtained. A second improvement is the use of pyrolytic carbon coated tubes which provide an impervious barrier between the liquid sample and the carbon of the tube. This barrier virtually eliminates the penetration into the tube by the sample and the attendant decrease in volatilisation/atomisation. The platform is composed only of pyrolytic carbon. At the same time the formation of less volatile analyte carbides is also reduced.

When attempting to take advantage of the lower limits of detection provided GF-AAS, one must not lose site of the fact that there has been a 100 - 1,000 fold increase in the matrix, causing background interferences to become appreciably more severe than for flame-AAS. The continuum (deuterium) background correction system which is the correction technique of choice for FAAS, is less suitable for GF-AAS. Two competing techniques have been developed and incorporated into instruments by different AAS manufacturers. Both systems measure the background contribution at the exact wavelength being used to monitor the analyte and accomplish this by alternately measuring the sum (background plus analyte signal) then background signal alone many times over the course of the atomisation sequence. One of these techniques is referred to as Zeeman background correction and the second is the Smith-Hieftje correction system. Both techniques appear to be analyte concentration limited.

More recently, much research has been directed to identifying suitable "matrix modifiers" (for many analytes, the technique does not work well without them). These additives can be used to increase the volatility of the matrix (reducing interferences) or to decrease the volatility of the analyte (acting as an analyte keeper). Palladium or Pd-Mg mixtures seems to be emerging as an effective modifier for many analytes (the maximum charring temperature is typically increased 100-300°C). The major limitations associated with the graphite furnace techniques has been considered to be the many physical and chemical interferences which have been extensively reported in the literature. These interferences are now largely controllable with a combination of platform techniques, newer high-quality graphite materials, accurate background correction techniques and the use of matrix modifiers.

5.9.2 Hydride Generation (Chemical Vaporisation)

A second approach to flameless atomisation has been very successful for the eight "hydride forming" elements (As, Se, Pb, Sn, Sb, Ge, Bi, and Te). The analytical approach in this case is to convert the analyte to its corresponding hydride (AsH_3, SeH_2, *etc.*) and to sweep the volatile product from the reaction mixture into a quartz T-tube positioned within the optical beam of the AAS instrument. The thermally labile analyte is swept from the sample with a flow of inert purge gas and is decomposed (atomised) within the upper part to the electrically heated T-tube. Hydride formation is induced by the reaction of sodium borohydride with the analyte in an acidic solution. The byproduct, H_2, helps to efficiently sweep the product up into the T-tube. As with GF-AAS a steady-state condition is not achieved so that quantitation is performed by peak height or peak area measurements of the signal displacement with time. It should be noted that not all compounds containing a "hydride forming" element are readily reduced with BH_4^-/H^+. By contrast, mercury can be analysed using a related "cold vapour" technique. The appreciable vapour pressure of this element at room temperature can by exploited to purge it from a liquid sample.

5.10 ATOMIC EMISSION SPECTROMETRY (AES)

Of the three approaches to atomic spectrometry, AES is the oldest and yet relatively recent developments have rekindled a broad interest in this technique. Atomic emission is inherently a multi-element technique; modern instrumental designs exploit this advantage by either (i) incorporating several detectors mounted along the focal plane of the monochromator (true simultaneous operation) or (ii) employing a monochromator capable of rapidly scanning (switching) between analyte emission lines so as to determine several analytes sequentially. A major advantage of either approach is the ability to rapidly obtain a more complete picture of the sample composition. An apt analogy is the information supplied by a chromatogram as compared

to the information conveyed by any one peak. A modern highly automated instrument can determine some 40 - 50 elements per minute (under ideal conditions). A further advantage of AES relative to AAS is that non metallic elements can be routinely detected with this technique including the halogens, phosphorous and sulphur.

It can be deduced from theoretical principles that for AES to achieve detection limits which are comparable to AAS over the full spectral range the temperature of the of the excitation source must exceed 6,000 K. The atom reservoir in virtually all modern AES instruments consists of a plasma (a hot partially ionised gas) which can be produced by chemical, electrical, or even by the interaction of an electromagnetic field with a noble gas such as argon. The production of a plasma in the absence of combustion processes requires some means of ionising the gaseous medium. Electrically produced plasmas accelerate electrons to sufficient velocities so that their collision with gas atoms or molecules results in ionisation. Alternately, plasmas can be sustained by inductive coupling with the magnetic field generated by a radio frequency (RF) source. In this case, the ionisation process is initiated by providing "seed" electrons from a Tesla coil or a spark. Although several kinds of plasmas have been used successfully in AES [microwave induced plasma (MIP), direct current plasma (DCP)], an inductively coupled plasma (ICP) has become the most popular by far.

A typical ICP torch construction is presented in Figure 10. An oscillating magnetic field is generated by the two or three turn, water cooled, copper coil which surrounds the outer quartz tube of a three concentric tube assembly. These magnetic fields are created by high frequency currents from a RF generator which flow through the induction coil. The induced magnetic field, generated by the induction coil, accelerates electrons within the flowing gas to sufficient velocities to cause ionisation when they collide with Ar atoms. The electrons released in the ionisation process are themselves accelerated to cause further collisions/ionisation. Under the influence of the induced field, charged species flow in closed annular paths. The net result is a self sustaining white hot fireball which can approach temperatures of 10,000 K. Under optimal operating conditions the fireball takes on a torroidal shape. Sample aerosols, generated with a conventional pneumatic nebuliser, are swept by a separate flow of Ar through the central (injection) tube and into the plasma and enter the "hole" of the doughnut shaped plasma. The plasma is supported with some 10 L/min of argon, introduced tangentially between the middle and outer tubes. This flow also centers the fireball and protects the outer silica containment tube. Lower flow rates of Ar can be added to the plasma *via* the channel between the inner and middle tube. Several design modifications permit a stable plasma to be maintained with lower flow-rates of Ar and an accompanying reduction in the required operating power.

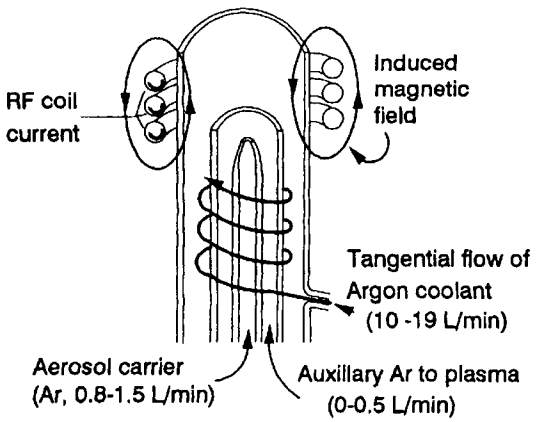

Figure 10: A cut away representation of the three concentric tube design of an argon inductively coupled plasma torch. The pneumatically generated sample aerosol is entrained up through the central quartz tube and enters the hole of the toroidally shaped plasma.

Like flame-AAS, ICP-AES is typically a steady-state technique - sample is aspirated, *via* the nebuliser, into the plasma at a constant rate. Since the same devices are used for sample introduction as in FAAS, nebulisation efficiencies are rather similar with most of the sample being discarded to drain. Aspiration of water into the system can cool the plasma appreciably. One feature of current ICP nebulisers which has been beneficial has been to pass the sample aerosol through a condenser which causes larger droplets to coalesce more efficiently. The net result is a sample aerosol which has been more completely desolvated. Typically, a 1 μg/mL analyte liquid solution results in roughly 10^{10} atoms/cm^3 of the plasma (an enormous dilution). The preferred optical viewing window, which is used for analysis, occurs 5-15 mm above the RF coils (just above the primary plasma cone) and below the flame-like luminous afterglow. While passing through the plasma, the stream of sample aerosol experiences a temperature of approximately 7,000 K during a residence time of a few ms.

Advantages of AES, relative to flame-AAS, include the lack of a requirement for a radiation source. Collisions within the plasma serve to promote analyte atoms to excited state levels. Additionally, this technique is characterised by linearities of response which span three to four orders of magnitude. Limits of detection for ICP-AES are similar to those obtained with flame-AAS (typically within a factor of 3 to 5 - some elements are slightly less responsive in flame-AAS others slightly more responsive). ICP-AES does require a fairly high resolution monochromator/detection system to scan carefully across analyte emission lines and to be able to resolve them from the other emissions and from the high luminosity of the torch. There are many spectral

emission lines for each element, in addition to sharp emissions resulting from the argon support gas as well as molecular bands from atmospheric contaminants such as OH, NH and N_2 all superimposed on a relatively intense background continuum. The relatively high background emission of this technique is the major impediment to lower detection limits. Thus, the spectral emissions in AES are rather numerous, complicated and spectral overlaps are frequent requiring the capabilities of a dedicated microcomputer for spectral processing and data reduction. Recent design improvements have (i) greatly simplified the operation of these spectrometers with more powerful and user-friendly software and (ii) lowered the manufacturing costs of simultaneous ICPs by incorporating a novel detector which is similar, in concept, to a diode array. The latter improvement obviates the requirement for multiple detectors.

5.10.1 ICP - mass spectrometry

A 10- to 100-fold improvement in the limits of detection of ICP-OES can be achieved by interfacing an ICP emission source with mass spectrometry. The higher operating temperatures of the torch are capable of producing analyte ions efficiently so that the predominant form of most analytes is a singly charged ion. It has been claimed that the formation probability is over 90 % for most elements. A quadrupole instrument is a simple, compact form of mass spectrometer which separates ions on the basis of their mass-to-charge (m/e) ratio. The entire mass range can be scanned in a fraction of a second. The unit generates a time dependent electrical field which is capable of focusing ions on the pulse-counting detector. Successive scans are stored in memory and built up to form the final spectrum. Typically, the total data acquisition times are of the order of a few minutes. In operation, sample is aspirated into a pneumatic nebulisation chamber and the resulting aerosol is partially desolvated in a condenser. It then enters the argon plasma where desolvation is completed, followed by analyte melting, vaporisation, atomisation and finally ionisation. The central stream of the plasma is sampled *via* an orifice in a water-cooled, nickel plated cone and passes through a series of skimmers which strip away most of the argon from the sample stream while reducing the pressure to 10^{-5} torr. Finally the analyte ion enriched sample flow is mass analysed in the quadrupole spectrometer. Since each element (except indium) has at least one isotope of unique mass, the mass spectra from this technique are much simpler than the corresponding optical emission spectra. Additionally, the vast majority of elements have more than one isotope; the identity of a trace element can be corroborated by the presence of isotope ions in ratios corresponding to their natural abundance.

There are, however, several ions which are produced by the torch. Poly-atomic ions containing elements from the solvent and/or the analyte and/or Ar are common. Given the resolving power of quadrupole mass analysers

(≅0.5 atomic mass unit) spectral interferences can become important. As examples, argon dimer (^{40}Ar-^{40}Ar) interferes with the most abundant isotope for selenium, $^{80}Se^{+}$, and ^{40}Ar-^{35}Cl interferes with the only isotope for arsenic, $^{75}As^{+}$. Additionally, the ICP torch can tolerate only low levels of organic solvents in the aqueous sample stream and remains sensitive to the levels of total dissolved solids (< 2 % maximum). Matrix effects can either suppress or enhance the analyte signal and, because of mass discrimination of the lighter elements, corrections may have to be applied to measurements of isotopic ratios.

Despite these difficulties, this multi-element technique provides superior sensitivities and can be anticipated to become the technique of choice for the ultra-trace determinations of nutrients/metallic contaminants in foods.

5.11 FLAME, FURNACE OR PLASMA - WHICH TO CHOOSE ?

Flame AAS is a well established technique which suffers from relatively few interferences and these are well characterised. The instrument is relatively inexpensive, easy to operate and, of the three techniques, requires the least operator experience. For most elements the LODs achieved with FAAS or with ICP-OES are comparable - within a factor of two or three of each other. The ICP approach is advantageous (i) for elements that form refractory oxides and (ii) for elements which are characterised by low ionisation energies. Included in the former are B, V, Ti and W which are only partially dissociated in the flame. Typical of the latter group are elements Mg, Ca, Be, Zr and the rare earth elements whose most sensitive emission lines are from ions rather than atoms. By contrast, the more volatile heavy elements such as Cd and Zn have slightly lower limits of detection by FAAS.

For the analysis of major elements (rather than trace determinations), AAS has been demonstrated to provide coefficients of variation (CVs) of approximately 0.2 % which is not appreciably different from ICP-OES. Both techniques can be automated to a high degree. For example, a highly automated AAS can determine six elements in 50 samples within 35 min. Other examples in which a larger number of elements are to be determined in a fewer number of samples would favour ICP-OEs in terms of speed of analysis. In both cases the actual analysis time is small relative to the time required for sample preparation.

The principal advantage of the furnace technique is one of sensitivity which is improved 10- to 100-fold relative to either flame or plasma. The principal disadvantage is probably the time required for each analysis which can be up to several minutes coupled with a somewhat limited linear dynamic range. In practice, the furnace is limited to ultra-trace determinations.

5.12 ATOMIC FLUORESCENCE SPECTROMETRY (AFS)

Atomic fluorescence involves the absorption of incident radiation (radiational activation of analyte ground state atoms) and measuring the radiation emitted from the excited state as this atom dissipates its excess energy. Since emitted light is omnidirectional, the detector can be placed at any angle relative to the axis of the incident radiation (typically at 90°). Thus unabsorbed incident radiation from the source which is highly directional does not interfere with the detection process. If the photon emitted returns the atom directly to its ground state, the technique is referred to as resonance fluorescence. By contrast, non resonance fluorescence implies either of two events. The excess energy can be dissipated by the emission of a photon of energy corresponding to a transition directly from the excited state to some lower excited state followed by a radiationless transition (collisional event) back to the ground state with the excess energy of the lower excited state usually being dissipated to the surroundings as heat. In "stepwise" non resonance fluorescence, the fluorescence occurs after a radiationless event. In non resonance fluorescence, regardless of the actual process, the wavelength of the emitted photon (λ_{EM}) is longer than the wavelength used for excitation (λ_{EX}). As is the case with the more familiar technique of solution fluorescence, this offers the opportunity for greater selectivity in discriminating fluorescence emissions from scattered light (of λ_{EX}). The scattered light can be rejected with an appropriate filter.

Since, in AFS (in contrast to AAS) it is not necessary to be able to discriminate between P and Po, an intense incident radiation can be used to provide λ_{EX} and, moreover, the spectral band width of the incident radiation is not important. At extremely high levels of incident radiation, it is possible to approach a saturation condition in which the two energy levels (the lower and upper) become equally populated. A process of "stimulated emission" can occur which enhances the rate of return back to the ground state. If a photon of incident radiation encounters an excited state atom, it has a high probability of inducing a downward transition causing the excited state atom to emit a photon of energy identical to the incident photon. This phenomenon is analogous to the process used to generate emissions from a laser. At low intensities of incident radiation, stimulated emission is a relatively rare event because of the low concentration of excited state atoms. As the intensity is increased, the excited state is increased proportionately and in the limit the proportion of excited state atoms undergoing stimulated emission far exceeds the number undergoing either resonance fluorescence or collisional deactivation. Under these conditions, the relative populations in the ground state and excited state become almost independent of the environmental conditions in the atom reservoir (the relative populations depend only on the atoms intrinsic properties). Also, a slight variation in the intensity of the exciting source doesn't affect the populations in the two states. Tunable

lasers represent a radiation source which is capable of these intensities. The technique is known as LEAF (laser-excited atomic fluorescence). Not surprisingly, a number of other sources of incident radiation can also be used for AFS studies including narrow, broad, and even continuum sources (*e.g.*, pulsed hollow cathode lamps, or even an ICP torch). An optimum would be a combination of a source with a high spectral radiance coupled with an atomisation device which emits a low background. A variety of atom reservoirs (to provide the ground state analyte atoms) including various flames and plasmas can also be used.

5.13 TRACE METAL DETERMINATIONS IN BIOLOGICAL SAMPLES

As analysts, we often forget and/or fail to communicate to our customers that the numbers which are actually generated from an analysis are used to predict the concentration(s) of analyte(s) which is (are) present in the bulk material. As such they are estimates only and are subject to uncertainties. These uncertainties can be appreciable. For a trace element analysis to be of any value whatever, two conditions must be rigidly met. The analytical sample, which is actually presented to the instrument (typically less than 1 mL) must be (i) homogeneous and (ii) a miniature replica of the bulk material which has been sampled.

From a review of the repeatability of a broad range of analyses performed by the U.S. Food and Drug Administration (FDA) Horrwitz observed a correlation between the CV (coefficient of variation for replicate determinations) and the analyte concentration which was independent of: (i) the analyte identity, (ii) the analytical method and (iii) the sample type. Roughly, a CV of "10% was to be anticipated if the analyte was present at the low mg/kg level, but " 30-60% if the analyte was present at low µg/kg concentrations (Horwitz, W., and Albert, R., *Anal. Proc. (London),* **24**, 49, (1987)) Much of this variation is considered to result from the problem of sampling. Biological materials are heterogeneous with respect to both particle size and to analyte concentrations, as well as varying appreciably from one food to another in terms of bulk composition (muscle *versus* fat *versus* bone *versus* grain *versus* packaging material). For biological materials in general, the problem of obtaining a sample which is a true miniature replica of the bulk material is especially severe and can be anticipated to contribute appreciably to the overall uncertainty associated with the final result.

The analysis of foods, and biological materials in general, for trace elements poses special analytical problems which are not encountered with other sample types. Certain elements of interest are typically present at levels ranging from low to sub µg/kg at one extreme whereas other analyte elements are present at more than 100 mg/kg. Since an analyte trace element can be

present in many different chemical forms (different oxidation states, combined with different anions or bound to proteins or to other organic ligands), the organic portion of the sample can result in appreciable matrix interferences during the detection process. Typically, to minimise these interferences the laboratory sample is pre-treated to convert these different forms of the analyte to a common cationic form while destroying the organic components of the sample (which are oxidised to CO_2 and H_2O). For the most part, these oxidation (digestion) procedures are cumbersome, time consuming, error prone, and limited by the size of sample which can be treated. The pre-analysis digestion serves to solubilise the analyte(s) to increase homogeneity, and to reduce potential interferences.

Two generalised digestion procedures are popular; (i) samples can be "dry ashed" in a furnace at 500 to 600°C and the ash solubilised in an acid solution or (2) the sample can be "wet" digested with a combination of heat, strong acids, and/or oxidising agents. Often, a triacid mixture consisting of concentrated nitric acid, with lesser amounts of 57% (v/v) perchloric and sulphuric acids (40:4:1) is used to digest plant material, however, the proportions of reagents, the sample size (2 g or less) and the volume of the final digest must be rigidly controlled to avoid analyte loss *via* precipitation (*e.g.*, $CaSO_4$ and/or $PbSO_4$). These digestion reagents are highly corrosive. Moreover, the concentration, by evaporation, of perchloric acid digests can volatile perchlorate salts from the mixture. These salts can accumulate on the walls of the fume hood venting system with explosive results. More recently, efforts have been directed to automating the digestion process and to shortening the time required for sample pre-treatment by optimising procedures using microwave digesters. However, digestion procedures which are effective for one food matrix may not be effective with a different food. In general, a source book of recommended digestion procedures should be consulted prior to an analysis of a food matrix.

A further major source of error is contamination; trace elements are ubiquitous and unless special precautions are taken, the sample will inevitably be contaminated. It would seem that an attention to detail and efforts to avoid contamination which boarder on the fanatical is the only way to minimise contamination. As a rule of thumb, the total analytical reagent blank for a given trace element should be reproducible and should result in values which are at least a factor of ten lower than the lowest level being measured in a sample.

5.13.1 Validating Results

Recognising that all analytical results represent estimates of the concentration of an analyte within a food/biological matrix, the most important characteristic of any result is a statement of its uncertainty interval. Typically, the repeatability of an analysis performed on a particular

sample, is used to estimate this uncertainty interval as expressed in terms of an estimate "s" of the relative standard deviation "σ" (equal to the coefficient of variation, CV). To decide whether an analyte is actually present is readily solved conceptually but, in practice, it remains somewhat controversial. It is universally accepted that an analyte should be reported when its calculated concentration is three or more standard deviations above the mean method blank. The decision as to whether an analyte is absent is more difficult. The American Chemical Society (ACS) guidelines suggest that the user of the data is, most often, in the best position to make this decision and, further, that it is his/her responsibility to make this decision (Keith, L.H., *Chemtech*, 486, (1991)).

In addition to measuring precision, efforts must be made to assess the accuracy of methods which have not been validated. Two approaches are possible. The accuracy of a procedure can be assessed by comparing analytical results generated using two independent methods which are based on totally different detection principles. Biases of one method, relative to a second method, can sometimes be detected by comparing the results for several analyte concentrations generated by both methods. In practice, two independent methods might not be available or the spectroscopic technique associated with a second independent procedure might not be readily available to the analyst. A second approach to method validation involves the analysis of a certified reference material (CRM) which is as close as possible to the samples in terms of both bulk composition and analyte concentration. These reference materials will have a certified concentration of the analyte as well as a specified shelf life when stored under appropriate conditions. Unfortunately, the number of biological CRMs which are available remains very limited.

5.14 REFERENCES

Having persisted through this introduction to atomic spectroscopy, you might want to consult the following references for a more detailed discussion of the appropriate topic.

AAS (Flame and Furnace)

1. H. Falk, *CRC Crit. Rev. Anal. Chem.* **19**, 29 (1988).

2. W. Slavin, "Graphite Furnace AAS - a Source Book", Perkin-Elmer Corporation, Ridgefield, CN (1984).

3. W. Slavin, "Atomic absorption spectrometry", in *Metallobiochemistry*, Part A, J. F. Roirdian and B. T. Vallee (eds.), Methods in Enzymology, **Vol. 158**, Academic Press Inc., New York, NY, p. 145 (1988).

4. W. Slavin and G. R. Carnick, *CRC Crit. Rev. Anal. Chem.* **19**, 95 (1988).

5. B. Weltz, "Atomic absorption spectrometry", VCH Publishers, Weinheim, Germany (1985).

Inductively Coupled Plasma AES

6. P. W. J. M. Boumans (ed.), "Inductively Coupled Plasma Emission Spectroscopy, Vol. 1: Methodology, Instrumentation and Performance", John Wiley & Sons, Inc., New York, NY (1980).

7. K. A. Wolnik, "Inductively Coupled Plasma Emission Spectrometry", in *Metallobiochemistry, Part A*, J. F. Roirdian and B. T. Vallee (eds.), Methods in Enzymology, **Vol. 158**, Academic Press Inc., New York, NY, p. 191 (1988).

Atomic Fluorescence Spectroscopy

9. R. G. Michel, "Atomic Fluorescence Spectrometry", in *Metallobiochemistry, Part A*, J. F. Roirdian and B. T. Vallee (eds.), Methods in Enzymology, **Vol. 158**, Academic Press Inc., New York, NY, p. 222 (1988).

ICP - Mass Spectrometry

10. G. M. Hieftje and G. H. Vickers, *Anal. Chim. Acta* **216**, 1 (1989).

11. K. E. Jarvis, A. L. Gray, and R. S. Houk, "Handbook of Inductively Coupled Plasma Mass Spectrometry", Blackie, Glasgow, UK (1992).

Digestion Procedures / Reference Materials

12. S. G. Capar, "*Metals and other elements at trace levels in foods*", Official Methods of Analysis of the Association of Official Analytical Chemists, Vol. 1 Agricultural Chemicals; Contaminants; Drugs, 15TH Edition, AOAC Inc., Arlington, VA, Chapter 9, p. 237 (1990).

13. C. Veillon, "Standards for metal analysis", in *Metallobiochemistry, Part A*, J. F. Roirdan, and B. T. Vallee (eds.), Methods in Enzymology, **Vol 158**, Academic Press Inc., New York, NY, p. 56 (1988)..

J.R.J. Paré and J.M.R. Bélanger (Editors)
Instrumental Methods in Food Analysis

Chapter 6

Nuclear Magnetic Resonance Spectroscopy (NMR): Principles and Applications

Calin Deleanu (1) and J. R. Jocelyn Paré (2)

1) "Costin D. Nenitescu" Institute of Organic Chemistry, NMR Department, Spl. Independentei 202 B, P. O. Box 15-258, Bucharest, Romania and 2) Environment Canada, Environmental Technology Centre Ottawa, ON, Canada K1A 0H3

6.1 INTRODUCTION

The Nuclear Magnetic Resonance (NMR) technique is now half a century old [1,2]. One might consider this as a long time, or at least as a time sufficiently long to justify the fact that NMR is by now a technique present in both advanced research and basic undergraduate courses in so many fields like chemistry, physics, biology, food sciences, medicine, material sciences, and so on. But if we consider the formidable progress that took place in these years, with NMR opening several stand-alone research fields (to mention only liquid-, solid-, localized-, low resolution-NMR, NMR Imaging and Microscopy) and the explosion of new techniques and instrumentation, then 50 years is a rather short time. By now, high resolution NMR is the most powerful technique for structure elucidation of chemical compounds in solution. It is also one of the most expensive techniques in terms of equipment, but meanwhile, very significantly, a technique which is already part of almost all research and teaching establishments. While the manufacturers are continuously pushing the limits of the instrumentation, trying to cope with every day developments in theoretical knowledge, the research, teaching and health establishments keep buying equipment costing roughly a million US

dollars each, knowing exactly that the last generation of equipment they just bought will be obsolete in less than 5 years, requiring thus continuous costly upgrading, and probably a new purchase in ten or fifteen years. Moreover, high resolution NMR spectrometers are some of the instruments with the highest running costs. Clearly, there is something very interesting going on around NMR, and those who will not be able to cope with these developments will face a disadvantage in many research fields. But this is only one of the medal's face, namely that of the advanced research. On the other side there are already established NMR analytical techniques for which low cost routine spectrometers have been developed, and where NMR proved in many cases to be the most competitive method in terms of costs, man-power, time, accuracy and in some cases the only acceptable method. The readers of this book should be familiar with the need of solving problems like determining the solid phase content in fats, water content of pulped sugar, total fat content, oil content of seeds, or the geographic origin of wines, for which NMR is a very competitive method and often the best method available to date.

The following part of the present chapter will present an introduction to the NMR field, trying to avoid deep mathematical and physical explanations, but rather presenting the conclusions of these treatments. For those interested in a deeper presentation of various topics which follow, references to more extensive books are made.

6.2 NOTES ON LITERATURE

Clearly, trying to cover a domain so vast as NMR in all its aspects ranging from theory, *via* fundamental research, to established routine analyses is a difficult task even for a dedicated book. We will therefore go through some aspects of the NMR phenomenon and we will recommend some books (among very many NMR books one could find in a library's index guide) dealing with various aspects of the field.

For NMR spectroscopists there is a quasi general consensus in quoting the Bible of the field, with its Old (published in 1959 by Pople, Schneider and Bernstein) [3] and New Testament (by Ernst, Bodenhausen and Wokaun) [4]. Other books, dealing more with the theory of the phenomenon than with its applications, could be recommended [5-9].

Very good introductory books, [10-12] with a pragmatic approach, focusing on structure elucidation, are quoted here rather as a subjective option of the authors, than an attempt to list all the good NMR books. An easy to read book with a very special flavor, which stimulates those who actually want to themselves play with the spectrometer is Derome's book [13]. Books dealing with specialized aspects and applications of NMR to chemistry, biology, biochemistry and medicine are also available. Surprisingly, one would have difficulties in quoting books devoted to NMR in food sciences. We are aware

of only one book devoted exclusively to NMR applied to food sciences [14]. One reason for this might be a wide spread general feeling that NMR is a too expensive technique in comparison with the benefits it generates. A very wrong idea, both in terms of unicity of some of the information provided (one only needs to have a look to the major food science journals publishing NMR papers) and of the existence of specially designed low cost analytical instruments.

Another aspect we would like to underline is the general fact that because of the continuously increasing amount of publications, it becomes more and more difficult to handle the information. Thus, some specialized databases and abstracting publications tend to become the principal guiding source through the literature in some particular fields. The advantages of carrying out an electronic search are obvious, and there is no need to emphasize here this aspect. The drawback however, particularly for NMR, is that these abstracting publications cover almost exclusively journals in fields like chemical, medical, biological, or food sciences, with little cross references. Thus, there is some risk of rediscovering the wheel in terms of NMR applications. If one carries NMR searches for a particular topic in a particular science domain, we strongly advise carrying searches for the same topic in the other mentioned domains.

Thus, looking to the NMR keyword in *Food Sciences and Technology Abstracts*, on CD-ROM, until June 1996, we could find only one book exclusively dedicated to the NMR field [14]. The same search revealed several books specialized in a particular food stuff or covering general analytical techniques, having a chapter in NMR. The present chapter is by no means trying to cover this gap, but only to draw attention to various aspects of NMR in food sciences, literature data being one of these aspects.

6.3 THE ELECTROMAGNETIC SPECTRUM

Similarly to other forms of molecular spectroscopy, the NMR phenomenon is associated with absorption and emission of energy. Before going into the details of NMR it is useful to compare the energy associated with it with the energy required to produce other types of spectroscopy in the context of the continuous electromagnetic spectrum (Figure 1).

An absorption spectrum (Figure 2) is a line, or a collection of lines of various intensities situated at different frequency (or wavelength) positions. These lines in the spectrum correspond to transitions between various energy levels in the studied molecule (Figure 3). The transitions are stimulated by the electromagnetic radiation having exactly the same energy ($E_0 = h\nu_0$) as the energy gap (ΔE) between the affected energy levels.

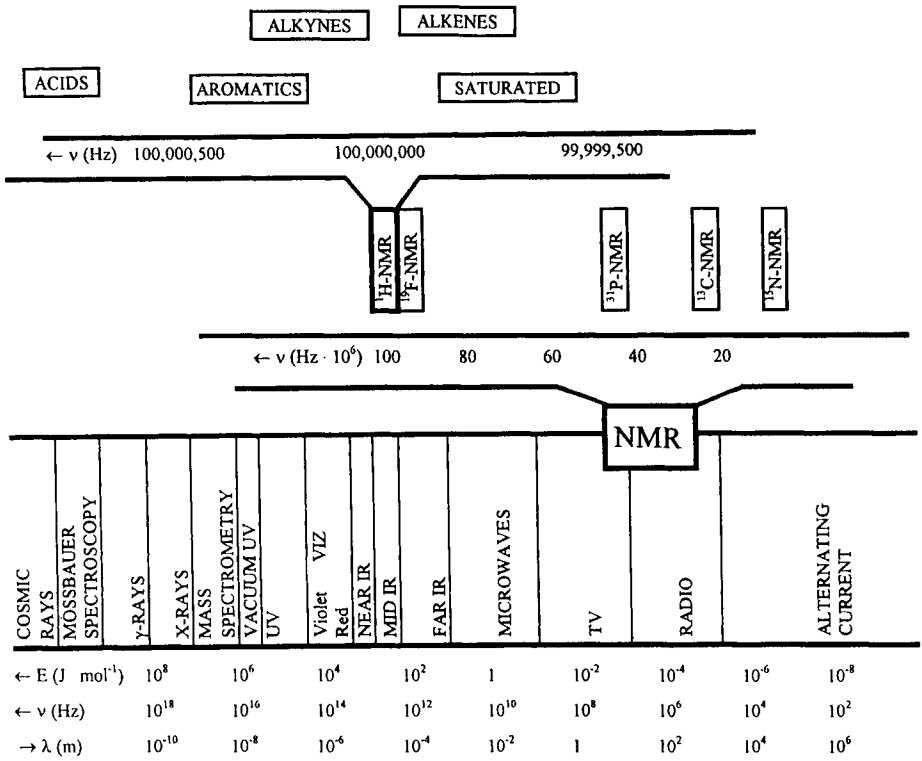

Figure 1: The electromagnetic spectrum.

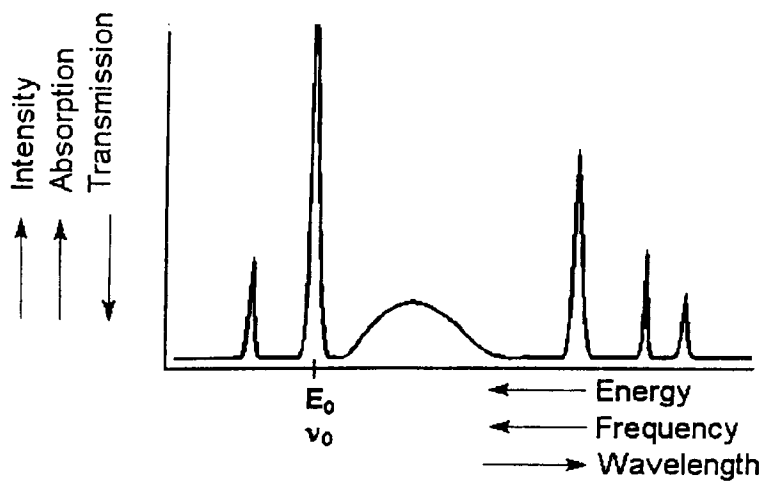

Figure 2: An absorption spectrum and the associated parameters.

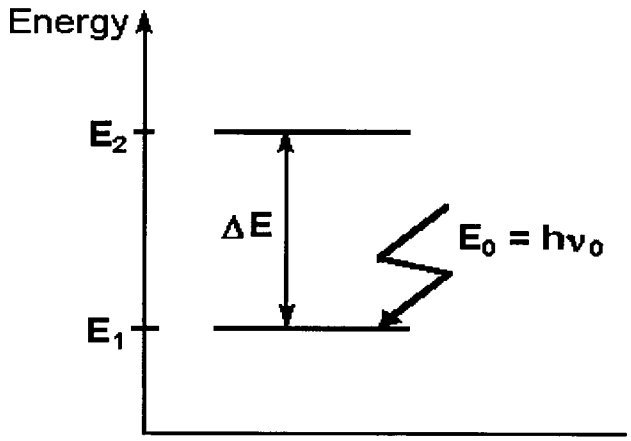

Figure 3: Energy levels in atoms and stimulation of transitions by external energy.

Going back to the electromagnetic spectrum, one can easily note that the energy associated with the NMR phenomenon is very weak in comparison with the other common types of spectroscopy. The radiation generating the NMR transitions is situated in the radiofrequency domain.

The difference between NMR and other forms of spectroscopy is that the absorption of energy takes place only in the presence of a magnetic filed.

6.4 THE NMR PHENOMENON

6.4.1. Nuclei active in NMR

Some atomic nuclei behave like microscopic bar magnets. The general condition for a nucleus to behave in this way is to have an odd number of protons and/or neutrons (*i.e.,* to have the spin quantum number, *I* different from zero). Most common nuclei in NMR (^{1}H, ^{13}C, ^{31}P, ^{19}F) have the spin number (*I*) equal 1/2 and are named *spin 1/2 nuclei.* The following discussion will be particularized for the spin 1/2 nuclei, but the general rules and conclusions are valid for all cases.

Fortunately, although not all the nuclei in the periodic table are active in NMR, almost every element has one or more than one isotope active in NMR. Some difficulties arise when the natural abundance of the active isotopes is very low. But with present instrumentation, spectra of practically any active nucleus can be recorded.

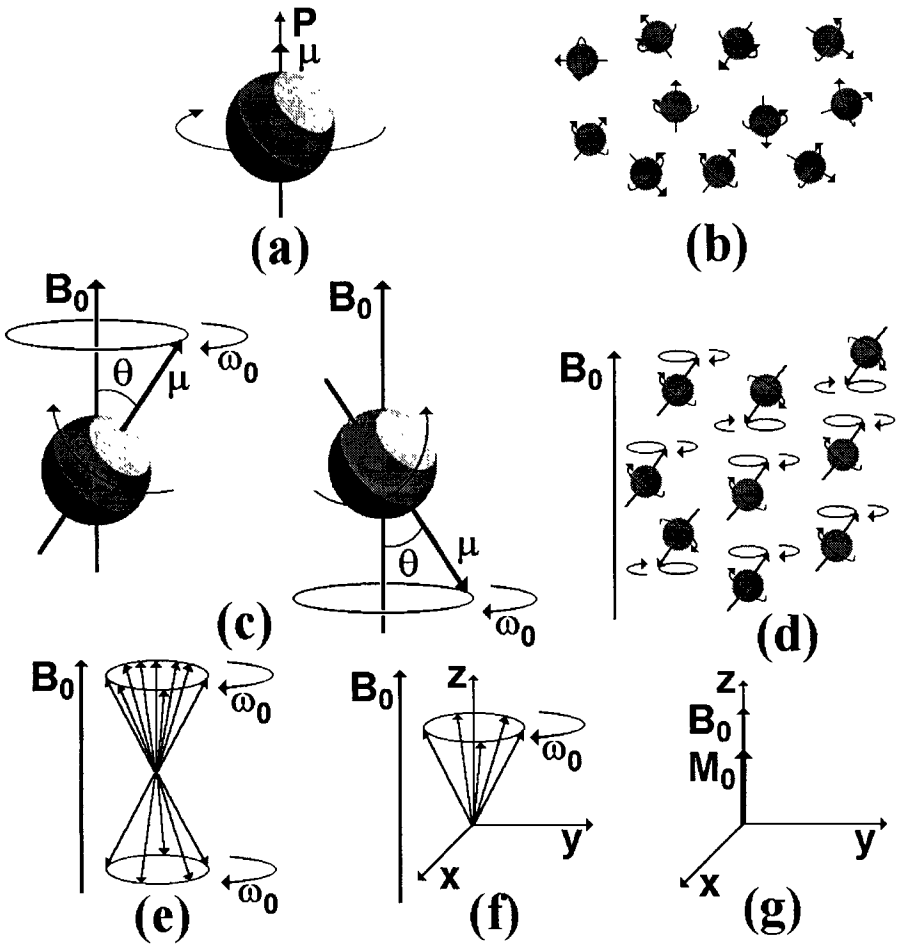

Figure 4: Magnetic properties of nuclei with spin quantum number ½; a) an electrically charged nucleus under the spinning motion generates an angular momentum P and a magnetic moment μ; b) in the absence of an external magnetic field the individual magnetic moments are randomly oriented; c) in the presence of an external magnetic field B_0 the spin ½ nuclei may adopt only one of the two allowed orientations; d) under the influence of an external magnetic field all nuclei in the sample adopt one of the allowed orientations; e) the number of nuclei oriented parallel to the external magnetic field is slightly greater than the number of nuclei oriented antiparallel. Only the individual magnetic moments are shown; f) the uncancelled magnetic moments; g) the macroscopic result of the excess magnetic moments is a global magnetization M_o pointing the same direction as the external magnetic field.

6.4.2. Nuclei in an external magnetic field. The equilibrium

An electrically charged body when rotating generates a magnetic field. Obeying to this universal law, the nucleus of an atom being electrically charged, and spinning generates a magnetic field (Figure 4a). Doing this, it behaves like a bar magnet, and is able to interact with other magnetic fields. The generated *magnetic moment* (μ) is proportional to the *angular momentum* (P). The proportionality factor γ is named *gyromagnetic ratio* and is a constant for each nucleus type.

$$\mu = \gamma P$$

In the absence of other magnetic fields, the magnetic moments (μ) for a collection of many atoms are randomly oriented and in continuous reorientation due to thermal motion (Figure 4b). The result is that the macroscopic sample has no magnetization, because of the averaging to zero of the elementary magnetic moments.

If an *external magnetic field* (B_0) is applied to the sample, the magnetic moments are allowed to adopt only some quantized orientations (*e.g.*, θ = 54°44' for ^1H nuclei) in relation with this field (Figure 4c). In this situation a supplementary movement takes place. The magnetic moment (μ) precesses around the direction of the external magnetic field (B_0) with an angular speed ω_0 (*e.g.*, for ^1H nuclei in a field B_0 of 2.35 T, ω_0 is 100 MHz, *i.e.*, 100,000,000 rotations per second). The rotation frequency ω_0 is named the *Larmor frequency* and is in fact the *absorption frequency* of that particular type of nucleus in a certain external magnetic field (B_0). This rotation can be clockwise or counterclockwise, depending on the sign of the gyromagnetic ratio (γ).

$$\omega_0 = - \gamma B_0$$

Thus, in the presence of the external magnetic field B_0 all the individual magnetic moments adopt one of the allowed orientations (Figure 4d). For nuclei spin 1/2, only two orientations are allowed: *"parallel"* (by convention designed as $\uparrow$) and *"antiparallel"* ($\downarrow$) to the external magnetic field. The two allowed orientations have different energies, thus the number of nuclei adopting each orientation is not equal (Figure 4e). The lower energy state (parallel to the B_0 field for the positive γ nuclei) is the most populated one. The macroscopic result of this status is that the individual magnetic moments, do not cancel to zero anymore, but produce a net magnetization (M_0) on the direction of the external magnetic field (z axis) pointing in the same direction as the individual magnetic moments in the more populated orientation (Figure 4f,g). In the equilibrium situation the precessing

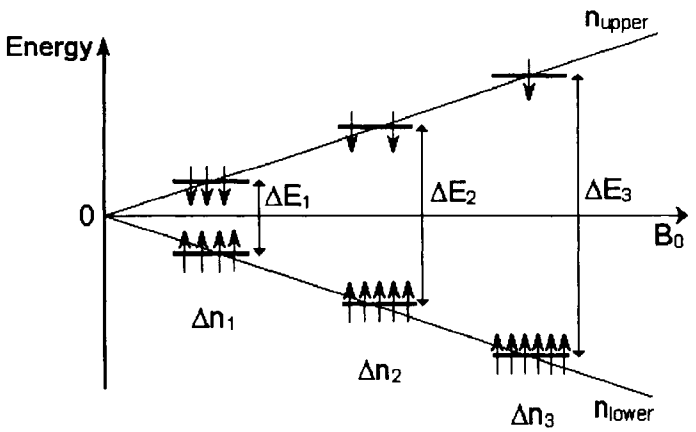

Figure 5: The dependence of the energy gap (ΔE) between parallel and antiparallel orientations of atomic nuclei on the strength of the external magnetic field (B_o) The difference in populations (Δn) also increases as the magnetic field strength increases.

magnetic moments are randomly distributed on the surface of a cone around the z axis, thus their projections in the x-y plane canceling to zero (Figure 4f). The macroscopic result is that there is no net magnetization in the x-y plane, but only along the z axis (Figure 4g).

The energy gap (ΔE) between spatially quantized (allowed) orientations of the magnetic moments (Figure 5) depends on the gyromagnetic ratio (γ, which is a constant for each type of nucleus) and on the external magnetic field applied to the sample (B_0, which is dependent on the strength of the magnet, thus being dependent on the constructive characteristics of the spectrometer).

$$\Delta E = \gamma h B_0 / 2\pi$$

where, h is the Planck's constant.

6.4.3 The Resonance condition

In order to induce the NMR phenomenon, irradiation of the sample with a frequency (ν_0) corresponding to the energy gap between the two energetic levels (parallel and antiparallel in the previous example) should be performed. The energy required ($E_0 = h\nu_0$) is in the radiofrequency range, the associated frequency having values between 10 MHz (or even less) and 800 MHz (the present instrumental limit), depending on the type of instrument and nucleus. It is very common to refer to a particular spectrometer in terms of absorption frequency for the ^1H nuclei rather than in terms magnetic field strength.

TABLE 1
Gyromagnetic Ratios and Resonance Frequencies for Some Common Nuclei at Different Magnetic Flux Densities (B_0)

Isotope	^{1}H	^{13}C	^{31}P	^{19}F	^{15}N
Giromagnetic Ratio, γ (10^7 rad T^{-1} s^{-1})	26.7519	6.7283	10.8394	25.1815	-2.7126
Natural abundance (%)	99.98	1.11	100	100	0.37
Absolute sensitivity*	1.00	$1.8\ 10^{-4}$	$6.6\ 10^{-2}$	0.83	$3.9\ 10^{-6}$
Magnetic Field (T)	Resonance frequency (MHz)				
0.23	10	2.5	4.1	9.4	1.0
0.47	20	5.0	8.1	18.8	2.0
1.41	60	15.1	24.3	56.5	6.1
1.88	80	20.1	32.4	75.3	8.1
2.11	90	22.6	36.5	84.7	9.1
2.35	100	25.1	40.5	94.1	10.1
4.70	200	50.3	81.0	188.2	20.3
5.87	250	62.9	101.2	235.2	25.3
7.05	300	75.4	121.4	282.2	30.4
9.40	400	100.6	161.9	376.3	40.5
11.74	500	125.7	202.4	470.4	50.7
14.09	600	150.9	242.9	564.5	60.8
17.62	750	188.6	303.6	705.6	76.0

*This is the sensitivity at constant field, taking into account the natural abundance.

The absorption of energy stimulating transitions between the two levels of energy in a magnetic field is called *magnetic resonance*. Thus, the *resonance condition* obtained by equaling E_0 to ΔE can be expressed either as:

$$\nu_0 = \gamma B_0 / 2\pi$$

or (using the angular frequency $\omega_0 = 2\pi\nu_0$), as:

$$\omega_0 = \gamma B_0$$

Table 1 presents gyromagnetic ratios and resonance frequencies for some common nuclei at different magnetic flux densities (B_0).

6.4.4. Inducing a population inversion

One can imagine two ways to invert the populations of the two energetic states (n_{lower} and n_{upper}). One way would be to invert the direction of the B_0

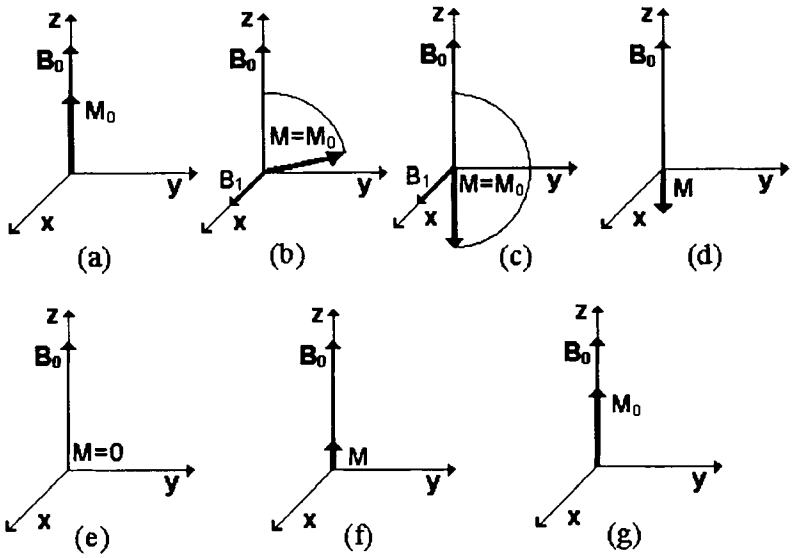

Figure 6: A simplified description of the evolution of the magnetization during an NMR experiment. In reality this evolution is characteristic for the projection of the magnetization vector M on the z axis M_z. a) the equilibrium; b) and c) the effect of a perpendicularly magnetic field B_1; d) to g) relaxation.

field for a while, than to suddenly come back to the initial orientation. The other way could be to apply another magnetic field (B_1) pointing along the x axis for a while. This second possibility is in fact the experimental solution.

The effect of a perpendicularly oriented field (B_1) is to rotate the magnetization around it in the y-z plane (Figure 6b,c). Depending on how this secondary magnetic field is applied, there are two fundamentally different types of spectrometers, namely: *Continuous Wave* (CW) and *Pulse Fourier Transform* (PFT) spectrometers. In the CW case the magnetic field B_1 (with its associated frequency ν_1) is continuously increased from the beginning of the experiment until its end. In this way, when the resonance condition is reached for a particular type of nuclei, (thus ν_1 becoming equal with ν_0), the energy is absorbed, transitions take place and the magnetization M_0 deviates (as in Figure 6b). As the B_1 field further increases, the energy is no longer absorbed, and the populations return to the initial states, the magnetization (M_0) returning also to its initial position (Figure 6a). As the continuously increasing B_1 field matches the resonance condition for another type of nuclei in the sample (ν_{02}), energy is again absorbed, magnetization flips and a new signal is recorded by the spectrometer. It is important to note that signals for a sample are acquired one by one as the monochromatic CW

frequency associated with the field B_1 exactly matches the resonance frequency for each particular type of nuclei. The sweeping of the whole range of frequencies usually takes a few minutes. As this type of spectrometers are less and less used because of many inconveniences, the description of the CW technique has only a theoretical and historical importance. All the remaining of the discussion will refer exclusively to the PFT technique. The same effect of flipping the magnetization (M_0) around the x axis is achieved in PFT NMR spectroscopy, by applying for a very short time (in the range of microseconds) an intense pulse of polychromatic frequencies, thus the B_1 field matching the resonance conditions for a much broader range of nuclei. Usually all the nuclei of a particular element in the sample (regardless of their environment in the molecule) are turned around the *x* axis (Figure 6b) during the radiofrequency (r.f.) pulse. It takes only a few microseconds to accomplish the resonance condition for a whole range of nuclei, and then (*i.e.,* after the magnetization M_0 has been inverted), the r.f. pulse is turned off.

6.4.5. Returning to the equilibrium. Relaxation

Once the temporary magnetic field B_1 (which, for reasons not developed in our simplified treatment, is an oscillating field) is turned off, the system which was perturbed returns to normal. The process of returning to the equilibrium status is called *relaxation.* We recall that the macroscopic magnetization is in fact the vectorial resultant of the individual magnetic moments precessing around the B_0 field (*i.e.,* z axis). Thus, as the population returns to normal, less and less nuclei are in the upper energy state, until they reach the initial difference Δn for the equilibrium state. This process should have as effect an evolution of the macroscopic magnetization as in Figure 6d-g. In reality this is what is happening with the projection of the magnetization (M) on the *z* axis (M_z). As it regards the global magnetization vector, this vector once flipped away from the z axis (Figure 6b) is subjected to the same tendency as the individual magnetic moments μ (Figure 4c-f), thus rotating around the z axis (*i.e.,* B_0 field) (Figure 7a). The magnetization M_0 is subjected to two tendencies. One tendency is to rotate (precess) around the B_0 field (Figure 7a), the other tendency is to flip back to the position parallel with the z axis, pointing the same direction as the B_0 field (positive z axis) (Figure 4.4b). The result of these two tendencies simultaneously acting on the magnetization is a recovery trajectory as in Figure 7c. During the relaxation process, one can imagine the arrow of the magnetization vector always touching the internal surface of a sphere.

6.4.6. The NMR signal. Free Induction Decay

The trajectory of the magnetization after the r.f. pulse is shown in Figure 7c. As the magnetization turns around the z axis the projection on the y axis evolves between a maximum positive and a minimum negative value (Figure 7d). The reason why the maxima and minims have not always the same

magnitude, is that each time the magnetization crosses the y-z plane it does it under a different flip angle (α), *i.e.*, the arrow of the magnetization vector touches another x-y plane of the sphere it describes. The evolution of the projection of the magnetization on the z axis as a function of time is easier to understand. Thus, as the flip angle goes smaller, the projection returns toward the initial M_0 value, and doing this it passes through the zero value (Figure 7e). The free evolution of the magnetization after an r.f. pulse is called *Free Induction Decay* (FID). The recorded FID (detected as a projection of the magnetization on the y axis) is in fact the raw result of an NMR experiment. Usually the NMR experiment ends up with a so called detection pulse which turns the magnetization M_0 by a *flip angle* (α) of 90° or smaller. Thus the evolution of the magnetization in time during the detection of the FID reassembles the Figures 4.4f-h, the most common pattern for the FID being that in Figure 7g.

Although the NMR experiment is considered finished once the signal (FID) was recorded and the detector was switched off, the resulted signal is of limited help for the analyst because of its complexity. In order to obtain the NMR spectrum one should transform the time domain data into a frequency domain data. Figure 8 shows the forms of the two functions we just mentioned, namely f_2 which represents the amplitude of the signal as a function of time (Figure 8a), actually the FID, and f_1 which represents the amplitude of the signal as a function of frequency (Figure 8b), actually the NMR spectrum. The mathematical transformation linking these two functions is called *Fourier transform* (FT):

$$f_1(\omega) = \int_{-\infty}^{+\infty} f_2(t)\, e^{-\omega t}\, dt$$

For a real signal resulting from a sample containing more than one kind of nuclei, thus presenting more than one line in the NMR spectrum, the actual FID is much more complex than that shown in Figure 8a In fact the complexity of the FID was the principal factor delaying the introduction of FT-NMR spectrometers and pulse techniques until the 1970s. Nowadays we do not have to bother anymore with the transformation itself, as this is automatically performed by the spectrometer's computer. However there are other treatments of the FID signal previous to its Fourier transformation of which the spectroscopist should be aware. On the way the signal is processed depend very important characteristics of the NMR spectrum, like the resolution or sensitivity. Last but not least, we should mention that FT is by far the most popular way of transforming the FID into the frequency spectrum, but it is not the only way.

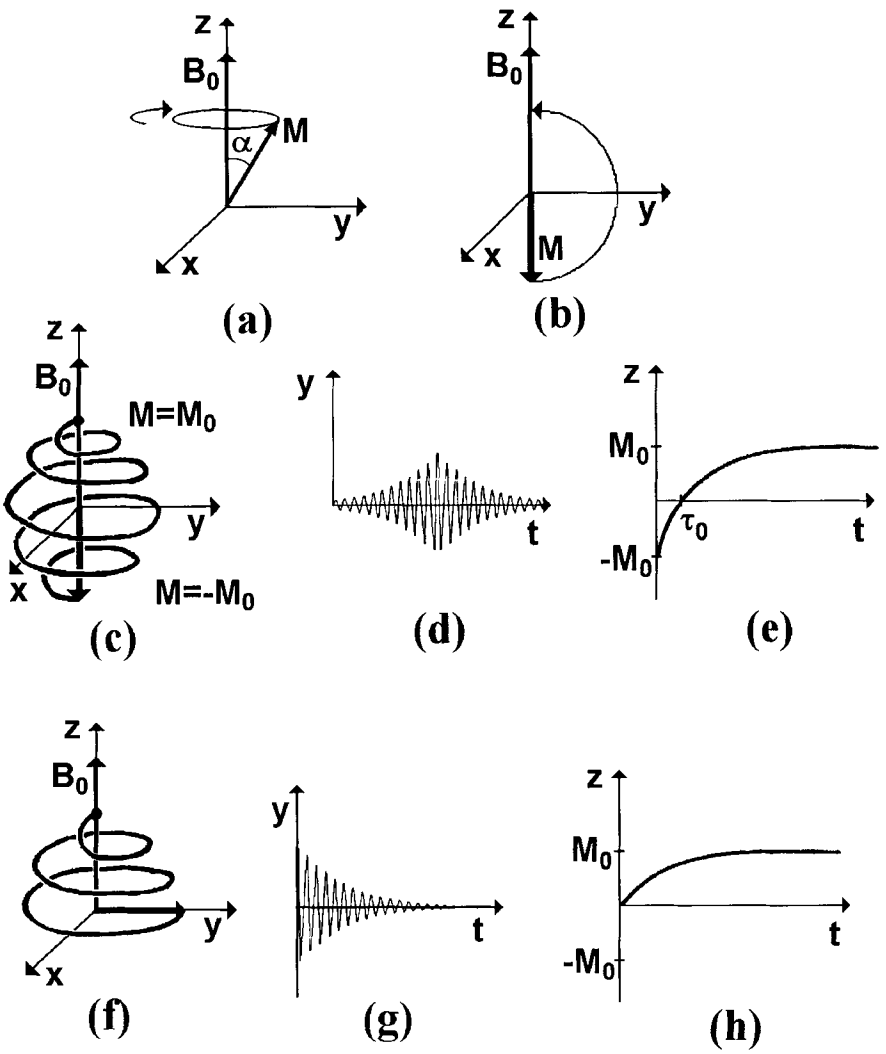

Figure 7: A more accurate description of the relaxation process: a) one of the tendencies of a tipped magnetization is to precess around the external magnetic field; b) another tendency is to realign parallel with the external magnetic field; c) the actual trajectory of the magnetization under the combination of the two tendencies after a 180° pulse; d) projection of the magnetization on the y axis after a 180° pulse; e) projection of the evolution of the magnetization on the z axis after a 180° pulse; f) the trajectory of the magnetization during relaxation after a 90° pulse; g) projection of the magnetization on the y axis after a 90° pulse; h) projection of the evolution of the magnetization on the z axis after a 90° pulse.

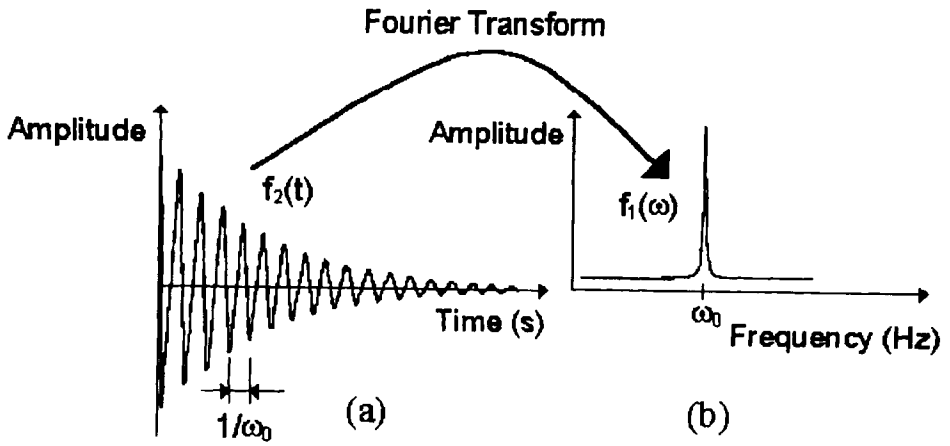

Figure 8: The two forms of the NMR data; a) the FID representing the signal as a function of time and b) the spectrum representing the signal as a function of frequency.

6.5. TYPES OF INFORMATION PROVIDED BY THE NMR SPECTRA

6.5.1 Chemical Shifts

The nucleus of a particular element which is part of a molecule experiences an effective magnetic field (B_{ef}) which is smaller than the external magnetic field B_0. The reason for this phenomenon is the shielding of the nucleus by electrons. The electrons shielding the nucleus could be those belonging to the same atom, those involving the atom in chemical bonds or those of the neighbor atoms. Each atom (of the same element) in a different position in a molecule will have a different electronic surrounding, thus experiencing a different effective magnetic field. The difference between the resonance frequency of a free nucleus and the same nucleus in a chemical environment is named *chemical shift*. The chemical shift is measured by the dimensionless parameter δ as the difference between the resonance frequency of the studied nucleus (ν) and the resonance frequency of the nucleus of the same element in a reference compound (ν_{ref}). In order to make this parameter independent of the field strength (and thus independent of the constructive characteristics of the spectrometer) the difference frequency is also divided to the resonance frequency of the standard. As the difference in frequency is very small, the resulting expression is further multiplied with 10^6, thus the chemical shift δ being expressed as parts per million (ppm):

$$\delta = [(\nu - \nu_{ref})/\nu_{ref}]\ 10^6$$

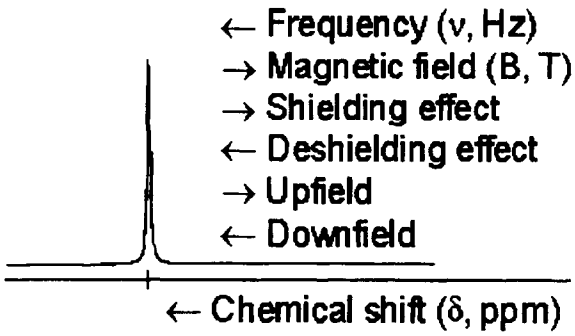

Figure 9: Parameters and nomenclature associated with the NMR spectrum.

The most usual reference standard is the tetramethylsilane (TMS) which is used for both ^{1}H- and ^{13}C-nuclei in organic solvents. For aqueous solutions other standards like sodium 3-trimethylsilylpropionate or dioxane are used. When referring to an NMR spectrum the conventions as in Figure 9. are used. Note that the scale under the spectrum should always be marked in δ values.

6.5.2. Intensity of the signals

The area under a NMR signal is proportional to the number of nuclei giving rise to that signal. Thus the ratios of the integrals of various signals in the NMR spectrum represent the relative numbers of atoms for those signals. This property is very valuable in structure elucidation problems. If one refers the integrals of signals in a sample, to the integral of a signal belonging to a compound which was added in a known concentration to the sample, then the concentrations of compounds in complex mixtures can be determined. The accuracy of the integration of NMR signals depends dramatically on the experimental conditions. Each type of nucleus has different characteristics in terms of relaxation properties. In order to obtain fully relaxed signals, one should employ appropriate waiting (relaxation) delays.

Another aspect of the problem is the sensitivity of the spectrum. This is commonly expressed as the signal-to-noise ratio. There are many aspects influencing the sensitivity, among them the gyromagnetic ratio and the natural abundance are the most important ones.

The external magnetic field (B_0) also influences the sensitivity. The dependence of the energy gap (ΔE) on the strength of the external magnetic field (B_0) was presented in Figure 5. It is important to note that as the B_0 field increases it is not only the energy gap that increases, but as a

consequence of this, the population difference Δn between the lower and upper energy levels that also increases.

$\Delta n = n_{lower} - n_{upper}$

The immediate result of this observation is that, for instance when a transition of the type ΔE_3 is induced, in comparison with a ΔE_2 transition (Figure 5), the intensity of the corresponding line in the spectrum would be higher. Thus, one of the advantages of recording NMR spectra at the highest available magnetic field is the increase in sensitivity.

There are other ways to increase the intensity of the signal, but on compromising on the accuracy of the quantitation (see section 6.5.6).

6.5.3 Coupling Constants. Spin-spin coupling

As each individual nucleus active in NMR behaves as a small magnet it is not surprising that these local magnetic fields interact for neighboring nuclei in a molecule. There are several ways in which the magnetic nuclei interact. We will focus now on the interactions of nuclei through chemical bonds. Although we will not try to provide a detailed explanation for this, it is essential to remember that this sort of interaction is mediated by the bonding electrons. Thus, the most intense effect is to be expected for nuclei directly bonded, and the effect is expected to diminish as the number of bonds between two nuclei increases. As we find it logical to expect an interaction between connected magnetic nuclei, we should see now which is the effect of this interaction in the NMR spectrum. The observable effect is the splitting of the signal of a particular nucleus in direct relationship with the number and type of neighboring nuclei. As the vast majority of organic compounds contain hydrogen atoms, and as the natural abundance of the magnetic active isotope ^1H is very high (Table 1), it is to be expected that most of the compounds we are encountering will have spectra with patterns complicated by these splittings. In fact the coupling patterns provide very valuable information for structure assignments. In some cases however (*e.g.*, when observing ^{13}C-nuclei) it is useful to remove this interaction (using the decoupling technique) and obtain single peaks for each type of nucleus. Even in these cases the coupling constants are of tremendous importance. There are a huge number of possibilities for exploiting the coupling effects in both one and multidimensional NMR spectra. Recording most of the spectra mentioned in *section* 6.5.9 is possible only by playing with the through-bond coupling effects. Figure 10 provides an explanation for the coupling patterns.

As it was shown previously (Figure 9) the strength of the magnetic field is increasing in a NMR spectrum from left to right. If we consider two magnetically active nuclei (*e.g.*, protons) belonging to the same molecule, but situated at a distance sufficiently big so that the effect of their local magnetic

fields is not transmitted through bonds, than the signals of these nuclei (H^A and H^B) are singlets positioned in the spectrum according only to the influence of the chemical shift (Figure 10a). We recall that the effective magnetic field experienced by a particular nucleus (*e.g.*, H^A) depends on the strength of the shielding effect of the surrounding electrons. In the same way (if the through-bond distance is short), another local magnetic field (*e.g.*, generated by H^B) could alter the effective magnetic field experienced by the observed nucleus (H^A). The difference in this case is that the local magnetic field could have two directions (for nuclei with spin quantum number higher than 1/2, more than two directions are allowed). Thus, half (almost half, with a very good approximation) of the population of the neighbor nuclei (H^B) are producing a local field at the position of the observed nuclei (H^A) which is parallel ($\uparrow$) with the external field (B_0), and the other half of nuclei H^B are producing a local field of the same magnitude but opposing the external field ($\downarrow$) (Figure 10b). The effect of these two additional magnetic fields is that for half of the population of the observed nuclei (H^A) the effective magnetic field is increased ($\uparrow$) and for the other half the effective magnetic field is diminished ($\downarrow$). Thus, in one case ($\uparrow$) the required external magnetic field for the resonance of H^A is smaller because it is "helped" by the added magnetic field produced by H^B, whereas for the other case ($\downarrow$) the external magnetic field required to produce the resonance of the same nuclei H^A is bigger because it has to overcome the "opposition" of the additional magnetic field produced by H^B. The result in the spectrum is that instead of one line corresponding to the resonance position of the H^A nuclei, there are two equally intense lines, *i.e.*, a doublet pattern (Figure 10b). The same effect has the proton H^A on the signal of the proton H^B. Thus the difference between the two lines of the H^A doublet (denoted J_{AB}) is equal with the distance between the lines of the H^B doublet (J_{BA}).

Figure 10c presents the splitting pattern of the observed proton (H^A) in the presence of two identical neighboring protons (H^B). A similar judgment allows us to draw all possible combinations for the two additional magnetic fields produced by two protons H^B at the position of the proton H^A. Thus, when both H^B protons are producing a field which adds to the external magnetic field ($\uparrow\uparrow$), the signal in the spectrum appears deshielded, on the contrary, when the field generated by the both H^B protons opposes the external magnetic field, the signal in the spectrum is shielded. There is also the possibility that one of the H^B protons generates a parallel and the other an antiparallel local field ($\uparrow\downarrow$). In this case the two fields cancel each other and the external magnetic field is not affected. The signal in the spectrum appears at the position dictated only by the chemical shift of the H^A proton. There is also still another possible combination, namely when the first considered H^B proton generates an antiparallel field and the second one a parallel oriented magnetic field ($\downarrow\uparrow$). Of course, one cannot distinguish between the last two combinations ($\uparrow\downarrow$ and $\downarrow\uparrow$), the lines in the spectrum

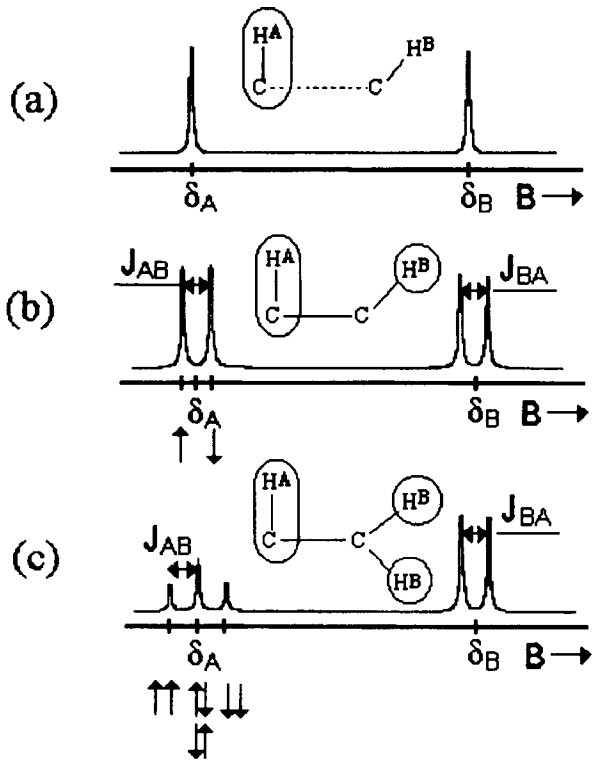

Figure 10: The effect of spin-spin coupling on the NMR spectrum of two hydrogen atoms H^A and H^B ; a) if the number of chemical bonds separating the two atoms is sufficiently great, there is no observable coupling effect; b) two atoms separated by a small number of bonds show characteristic doublet coupling patterns; c) an atom (H^A) having two equivalent neighbor atoms (H^B) shows a characteristic triplet coupling pattern.

appearing in the same place. However, as the two degenerate combinations arise from a population of H^B nuclei which is double than in the first two cases, the inner line of the triplet has a double intensity in comparison with either of the outer lines. In the same way it can be predicted the pattern of a signal under the influence of regardless how many neighboring magnetic nuclei. If the neighboring nuclei are not identical, then the pattern is more complicated.

In all cases the chemical shift of the H^A nuclei is unaltered, thus is situated in the middle of the doublet in the first case or on the position of the central line of the triplet in the second case. The distance between the two lines is called *coupling constant* (J) and it is always expressed in Hz, as it is not affected by

the strength of the external magnetic field (it is independent of the type of spectrometer). We recall that the chemical shift is never expressed in Hz (because in this way it would be field dependent), but in the dimensionless parameter δ as ppm (which is field independent).

It is easy to accept now that the strength of the coupling constant depends on the strength of the local magnetic field produced by the neighboring nuclei. Thus, the coupling constant J will be higher (the distance J_{AB} will be larger) when the neighboring nuclei are closer (less chemical bonds separating them). Also, for the same number and type of bonds the coupling constant J will have different values depending on the geometry of the compound, *i.e.*, the molecular angles. A typical dependence of the coupling constant on the dihedral angle for bonds of the type H-C-C-H is presented in Figure 11.

The equation matching the curve of the coupling constant (J) as a function of the dihedral angle H-C-C-H (φ) is known as the Karplus equation [15]. The original equation predicts very well the coupling constants in saturated compounds. In order to increase the prediction power, several alternatives have been introduced for specific classes of compounds.

The coupling mechanism we discussed in this section is known under the following alternative names: *Spin-spin coupling, Scalar coupling, J-coupling, or Indirect coupling.*

6.5.4. Linewidth of the NMR signal

In order to fully characterize a signal in a NMR spectrum one should list its position (chemical shift), multiplicity (splitting pattern), coupling constant (J) and its linewidth at half-height ($\Delta\nu_{1/2}$).

Figure 12a shows how the half-height linewidth is measured. For small molecules in solution, typical half-height linewidths are about 0.1 Hz. However, the linewidth depends of several factors which we only mention here. Some of them will be discussed later (sections 6.5.8 and 6.6.2). Thus, the linewidth could be influenced by factors like: relaxation time (short relaxation times like in solids give rise to broad lines whereas, long relaxation times like in liquids give rise to narrow lines, see Figure 12b,c.), the relaxation mechanism (*e.g.*, nuclei with quantum number greater than 1/2 give rise to rather broad lines), chemical exchange, intramolecular rotations, temperature, presence of paramagnetic impurities, the homogeneity of the sample, the homogeneity of the spectrometer's magnetic field, interactions with neighboring nuclei (especially those with spin greater than 1, *e.g.*, ^{14}N), mathematical manipulations of the data prior to the Fourier transformation of the FID (*e.g.*, sensitivity *versus* resolution enhancement), acquisition time, or the number of collected data points. We will not address these problems in this chapter. The interested reader is advised to refer to other books [3-13].

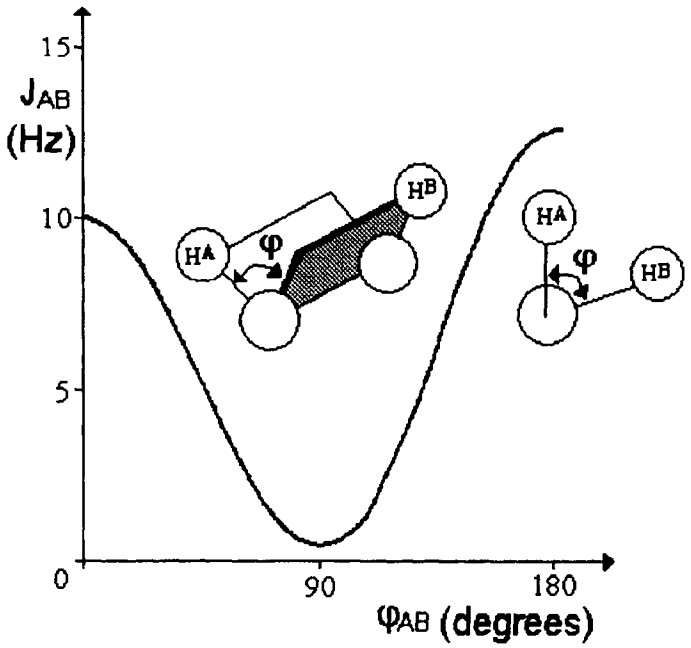

Figure 11: Typical dependence of the three bonds coupling constant J_{AB} on the dihedral angle φ_{AB}.

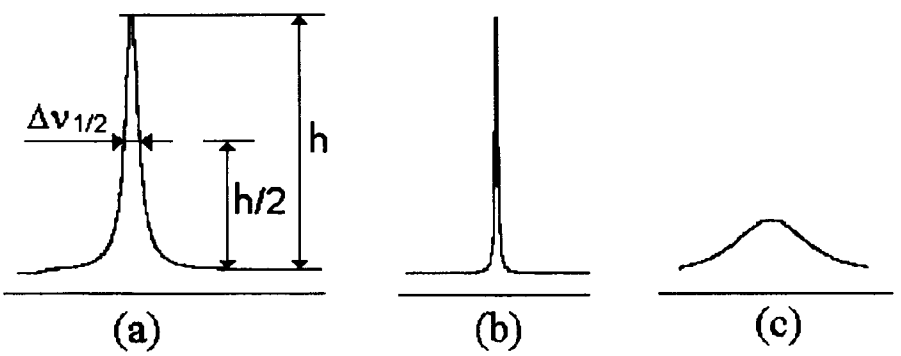

Figure 12: a) Measurement of the half-height linewidth parameter ($\Delta\upsilon_{1/2}$). Small linewidths b) are characteristic for long T_2 relaxation times as in liquids, whereas large linewidths c) are typical for short relaxation times as in solids.

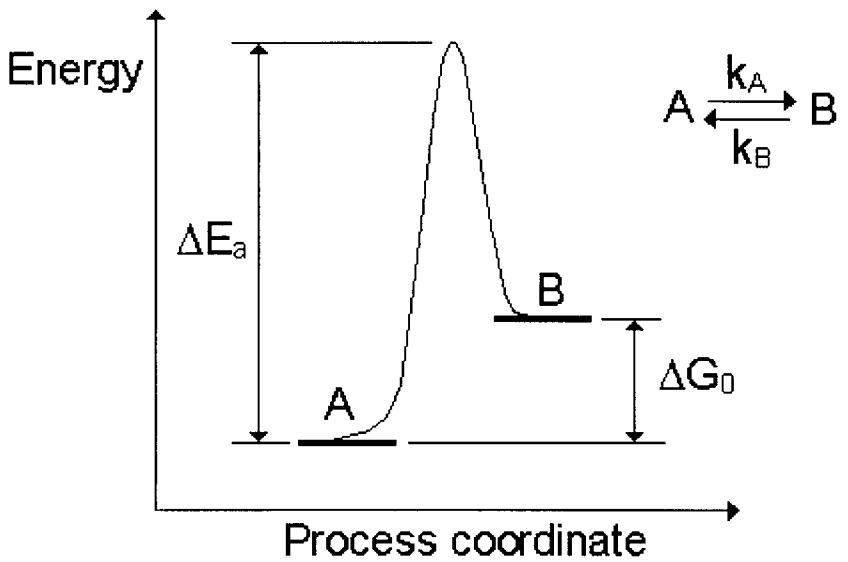

Figure 13: An equilibrium reaction and the associated parameters.

6.5.5 Activation Energies - Chemical Exchange - Dynamic Phenomena

In cases when dynamic equilibria are present NMR can also provide valuable information. An equilibrium of two conformations (A and B) and the associated parameters is presented in Figure 13.

In order to obtain relevant information on the dynamic process, spectra at variable temperature should be recorded. This means that one should record a series of spectra for the same sample at various temperatures ranging from a temperature below the point where the equilibrium is frozen and up to a point where the equilibrium is sufficiently fast that in the NMR spectrum there is no more possible to distinguish the individual signals for the two conformations A and B, but only an average signal. The analysis of this series of spectra takes into account the concentrations of the two species A and B, the temperature where the signals for a particular atom in the two conformations averages (the coalescence temperature), the difference in chemical shifts between the signals of the same atom in the two conformations at low temperature, the half-height linewidths at low temperature, and the signal's multiplicity (splitting pattern). For complex signals it is common to make use of specialized computer programs for lineshape analysis. The information which can be obtained includes: the rate constants (k), the activation energy (E_a), the pre-exponential factor in the Arrhenius function (A) and the difference between free enthalpies of the two conformers (ΔG_0). When more than one mechanism for rearrangements or

other chemical exchange processes are suspected, the variable temperature experiments could also provide valuable information for assigning the pathway of the rearrangement. The same sort of information can be obtained for chemical reactions (*e.g.,* protonation - deprotonation processes). For more details on dynamic NMR we recommend some specialized books [16-18].

6.5.6. Intramolecular Distances. Nuclear Overhauser Effect. Dipolar coupling

Another important property of the magnetic active nuclei is their interaction through space. These interactions take place through different mechanisms than those mediated by the bonding electrons (see section 6.5.3). As in the case of the through bonds spin-spin coupling (responsible for the splitting patterns) the through-space dipolar coupling is also an effect of the local magnetic field generated by the neighboring magnetic nuclei at the position of the observed nucleus.

There is a fundamental difference between the two types of coupling mechanisms. For the spin-spin coupling, the effect of the neighboring nuclei is independent on the orientation of the molecule in the sample (thus, isotropic with respect to the direction of the external magnetic field). For the dipolar interactions (Figure 14) the intensity and direction of the additional field experienced by the observed nucleus (*e.g.,* A) depend on the position of the neighboring nuclei (*e.g.,* B), thus on the relative orientation of the molecule with respect to the external magnetic field (B_0). For instance, in Figure 14a the local field opposes the external field, whereas in the situation described by Figure14b, it adds to it. Note that r is the through-space distance between the two atoms which do not need to be directly bonded. There are two extreme cases, namely the rapid tumbling of small molecules in non viscous solutions, when the effect of dipolar coupling averages to zero, and the solids for which characteristic broad coupling patterns can be seen (see section 6.5.8). In solution, although the splitting pattern of the dipolar coupling cannot be seen, there is another phenomenon which can be observed, namely the *Nuclear Overhauser Effect* (NOE). This effect represents the enhancement (or generally the change in intensity) of the line corresponding to the observed nucleus (A) when a neighboring (in space) nucleus (B) is irradiated.

The normal process for energy dissipation is by interaction with neighboring magnetic nuclei which could absorb the energy of the excited nuclei. These nuclei could be either nuclei belonging to the same molecule or to other molecules (*e.g.,* the solvent). Without trying to explain the mechanism we will only state that the two nuclei (A and B) have a dipolar interaction. Through this dipolar interaction the magnetization of the saturated (irradiated) nucleus B is transferred to the observed nucleus A. In this situation apart from the normal relaxation pathway of the nuclei A (see

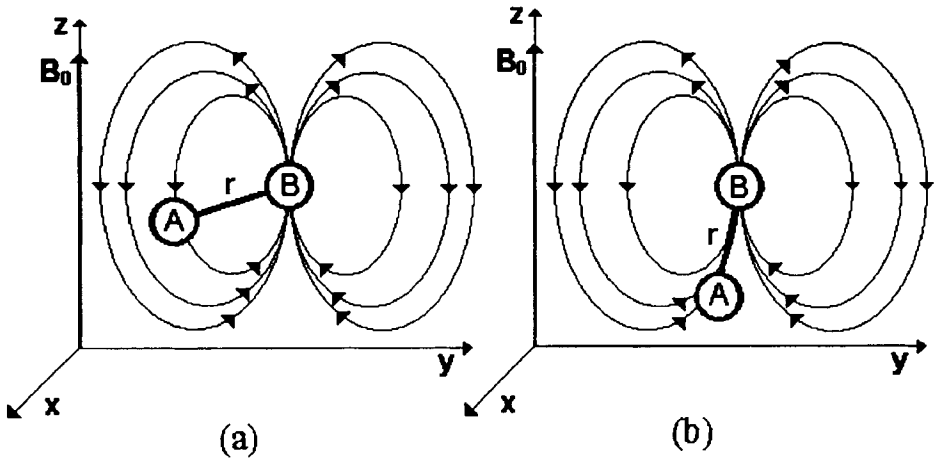

Figure 14: Dipolar coupling. The local magnetic field generated by a neighbor magnetic nucleus (H^B) has different values and orientations at the position of the observed nucleus (H^A) depending on the orientation of the molecule. Thus, in some cases the local field opposes (a) the external magnetic field B_o, whereas in other cases it adds to it (b).

section 6.6.1), another pathway named cross relaxation is available for them (only if the neighboring nucleus B is irradiated). This pathway is made possible by the tumbling motion of the molecule combined with the dipolar interaction, combination leading to a correlated fluctuating local field experienced by both A and B nuclei, the final result being that the two neighboring nuclei can undergo simultaneous reorientation of their spins (spin-flip). The theory is however much more complicated, and we recommend specialized books [19] for those interested.

It is important to underline that the intensity of the lines in the NMR spectrum can be altered by irradiating the neighboring nuclei (Figure 15) and that this through-space effect has very useful applications in assigning the three dimensional structure of molecules. There are several types of spectra which make use of this remarkable phenomenon. For proteins for instance, the assignment of three-dimensional structure in solution is always based on the study of the NOE effects using various types of 2D-, 3D- or 4D-NMR spectra. The change in signal intensity by NOE can be expressed in a quantitative form in terms of efficiency (η_{NOE}), taking into account the original (i_0) and the NOE affected (i) intensities of the observed signal:

$$\eta_{NOE} = (i - i_0) / i_0$$

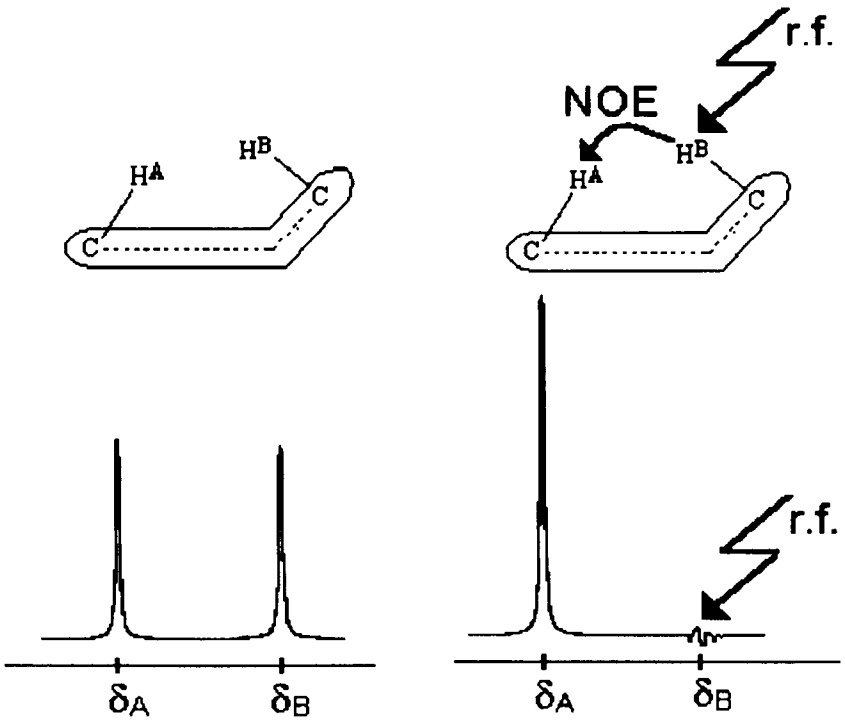

Figure 15: The NOE effect for two neighbor protons; a) in the normal ^{1}H-NMR spectrum the two signals are equally intense; b) When the neighbor H^B proton is irradiated, the intensity of the signal corresponding to the H^A proton is enhanced by the NOE effect.

Finally we should mention that in some cases the NOE effects are unwanted, for instance when exact quantitation is required. In such cases, special experimental measures should be taken, on one hand to minimize the induced NOE and on the other hand to allow sufficient time for any residual NOE to vanish before collecting a new set of data.

6.5.7. Molecular motions

Apart from molecular tumbling (when molecules as a whole undergo translations, rotations and collisions with other molecules under the thermal motion), there are also rotations of atoms and groups of atoms which are intramolecular processes characterizing the structural and energetic states of the studied compound. The NMR techniques could provide valuable information on these processes as well. When the energy associated with these geometrical changes is sufficiently high, energy barriers can be deduced from dynamic NMR spectroscopy as it was mentioned above (section 6.5.5).

Another type of information is provided by the relaxation time associated with each signal in the spectrum. As it was mentioned above (section 6.4.5), the global relaxation time is the time required by a particular atom to return to the equilibrium status (population distribution) after it was excited by an r.f. field. The relaxation time depends (among other factors) on the existence in the neighborhood of the excited nuclei of other magnetic nuclei which could "help" the excited ones to relax faster. Assuming there are some neighboring magnetic nuclei, (*e.g.,* when observing a ^{13}C nucleus which has attached ^{1}H nuclei), there is still another factor affecting the relaxation process, namely the mobility of that part of the molecule. In order to quantify the mobility, the parameter named *correlation time* (τ_C) is commonly used. Correlation time represents the time that a particular site (atom) in the molecule remains in the same position. When a particular atom stays a longer time in a favorable position, the relaxation process is faster. Thus, for small molecules in non-viscous solutions, the relaxation time is shorter for sites with long correlation times. This information is of vital importance for understanding the mobility of various compounds or parts of compounds, *e.g.,* protein chains in various environments or attached to various binding sites.

A good example is a fatty alcohol like decanol [20-22] (Figure 16). In this case owing to the hydrogen bondings which link the OH group to other molecules, the mobility of that side of the molecule is restricted in comparison with the rest of the chain. Thus, the shortest relaxation time (0.65 s) is that of the carbon atom directly linked to the OH group, and the relaxation time increases toward the "free" end of the chain with the CH_3 group having the longest relaxation time (3.10 s). The deduced correlation times from this experimental data show that the shortest correlation time, thus the highest mobility in the chain is experienced by the CH_3 group. If one compares different molecules, it is easy to understand that the small molecules move faster than the large molecules, and also that less viscous solutions allow a faster movement for comparable size molecules. In this way valuable information related to the size of the studied molecule as well as on the medium can be deduced from the correlation time obtained by NMR techniques. Further examples can be found in other books [19, 20]. It is also common to measure relaxation times for broad (unresolved) signals arising from a group of atoms in macromolecules and to deduce mobility information for parts of the molecule on the basis of these "group" relaxation times. Moreover, relaxation times for the whole sample (as in low-resolution NMR), provide very useful information on the physical structure of the sample (Figure 17).

In order to obtain accurate relaxation times, and thus correlation times, special experimental conditions (not so critical for other types of NMR information) have to be ensured. Thus, apart from particular NMR techniques (pulse sequences) one should ensure special sample preparations (*e.g.,* to use appropriate solvents, eliminate any paramagnetic impurity, degas

τ_C (ps/rad)	5	11	15	21	28	28	28	30	30	36
T_1 (s)	3.10	2.20	1.60	1.10	0.84	0.84	0.84	0.77	0.77	0.65

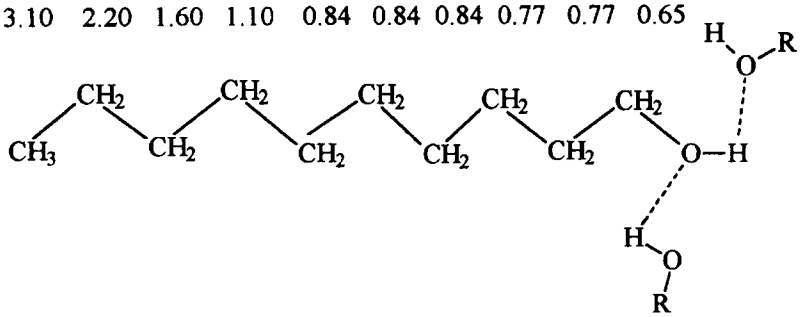

Figure 16: Correlation times (τ_c) and relaxation times (T_1) for carbon atoms in decanol.

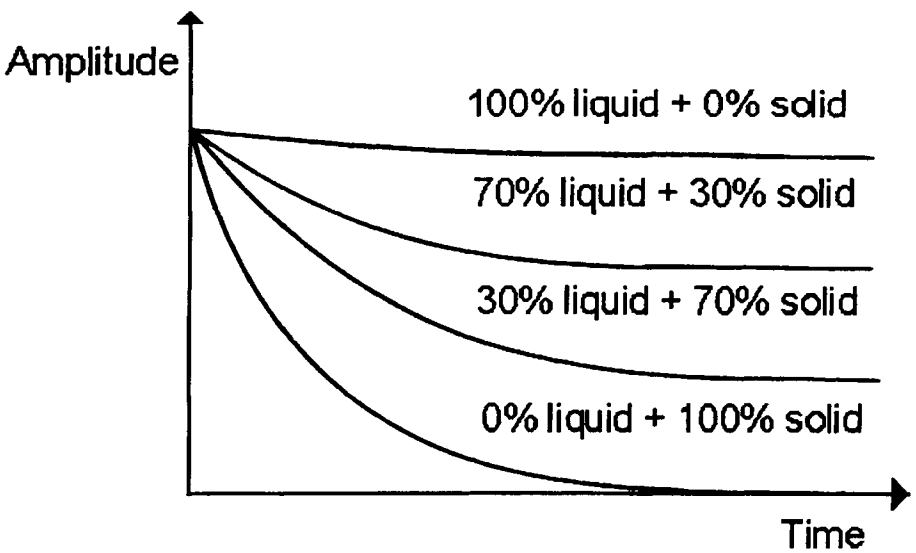

Figure 17: Bulk signal amplitude for samples containing various liquid to solid ratios. The signal decays exponentially with a T_2 relaxation time constant.

the sample). On the other hand, depending on the correlation times for a particular class of compounds, for solving other sorts of problems, and for collecting other types of NMR information as discussed in previous sections, the experimental conditions for recording NMR spectra have to be adjusted accordingly (*e.g.*, to employ appropriate relaxation delays, adjust the viscosity of the solvent, intentionally add paramagnetic compounds to the sample).

6.5.8 Characteristic features of high resolution NMR spectra in solids

In spite of the fact that the principles of the technique are the same, there are several factors causing significant differences between spectra of solids and liquids. In order to obtain high-resolution spectra in solids, specially designed spectrometers (or parts of the spectrometer) have to be used. Although it is possible to use the same spectrometer for both solution and solid state studies (and nowadays the manufacturers are developing systems which can easily be modulated for any technique like solution state NMR, solid state NMR, NMR Imaging, NMR Microscopy, or Localized NMR spectroscopy), usually each customer configures a particular spectrometer for only one experimental technique. The fact that in practice the spectrometers are dedicated either to solution or to solid state, contributes to the relative separation of these two fields in terms of dedicated teams. In general the solution state NMR is more often used than the solid state, and so are the number of available instruments. The same trend can be found in terms of books. We indicate some titles in solid-state NMR for the interested reader [23-25].

There are two factors we discussed previously and which affect in a very different way the spectra of solids. These are the relaxation time and the dipolar (through space) coupling.

The relaxation time associated with the signal decay is very short in solids. This is so because, on one hand the molecules are "packed" close one to another and are not separated by solvent molecules. In this way the magnetic nuclei are close to each other. On the other hand, the correlation time is very long, as there is almost no change in the position of various groups and atoms in solids. These two situations lead to a very fast relaxation process. As it was shown in Figure 12c, a short relaxation time gives rise to very broad lines in the NMR spectrum. In order to have a simple physical explanation for the broadening of the line, we can look to this phenomenon from the viewpoint of the lifetime in a particular state. Thus, once excited by the r.f. pulse, the nucleus is in another energy state. The relaxation time determines the lifetime of the excited nucleus. According to Heisenberg's uncertainty principle as the lifetime of a certain particle is shorter, the uncertainty of its energy is greater. In our case this means that a shorter lifetime induces a higher uncertainty in the energy gap ($\Delta E'$) between the two states of the nucleus and thus a greater uncertainty in the resonance frequency ($\Delta\nu'$) in the spectrum, this resulting in a broader line (Figure 18).

The other factor mentioned previously is the through space dipolar coupling between magnetic nuclei. As it was shown (Figure 14) this interaction depends on the relative position of the atoms with respect to the external (B_0)

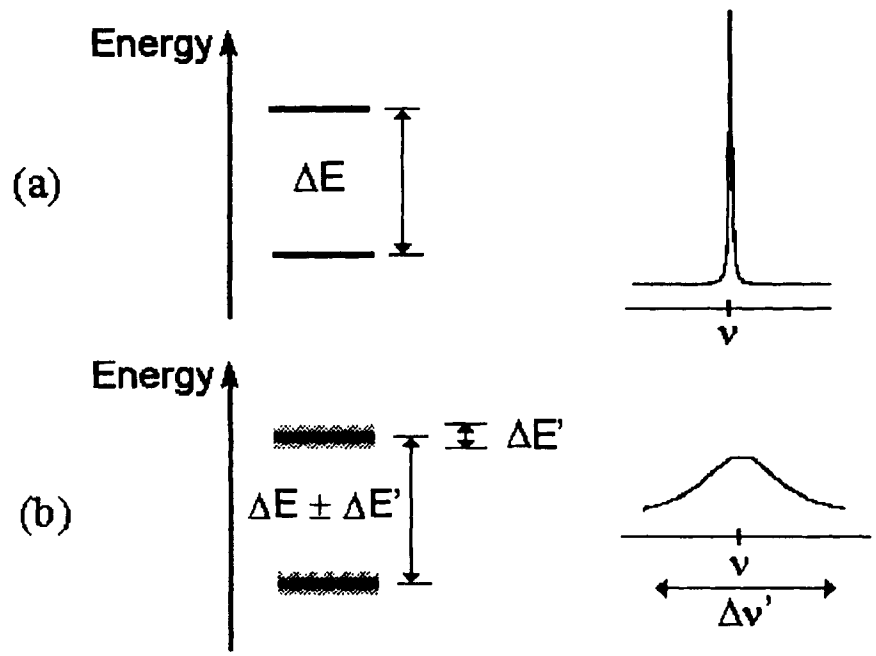

Figure 18: The influence of the lifetime of the nucleus on a particular energy level and the linewidth of the signal. a) if the lifetime and the associated relaxation time (T_2) is sufficiently long, the energy gap can be accurately measured and the position of the line in the spectrum can be well determined; b) if the time spent by the nucleus on a certain energy level is too short, the energy cannot be precisely measured and the line in the spectrum is broad.

magnetic field. In solids the molecules are not tumbling but rather occupy a fixed position in relation to the external field. This leads to the situation that the through-space coupling is no longer averaged to zero, so the spectrum will contain characteristic splitting patterns. However, the situation is still more complicated, as not all the molecules have the same orientation, but they are randomly oriented. As the coupling constant depends on the orientation of the molecules, a characteristic broad coupling pattern, named powder pattern, is present in solids (Figure 19). A coupling constant (K_{AB}), can be measured in this case. Moreover, if in the case of spin-spin (through bonds) couplings, chemically equivalent nuclei (*e.g.*, those in a CH_3 group) do not couple to each other, in the case of dipolar coupling, there are additional splittings generated by equivalent nuclei.

Another problem related to relaxation in solids is the following. Thus, one thing is the disappearance of the magnetization (M) in the x-y plane (the

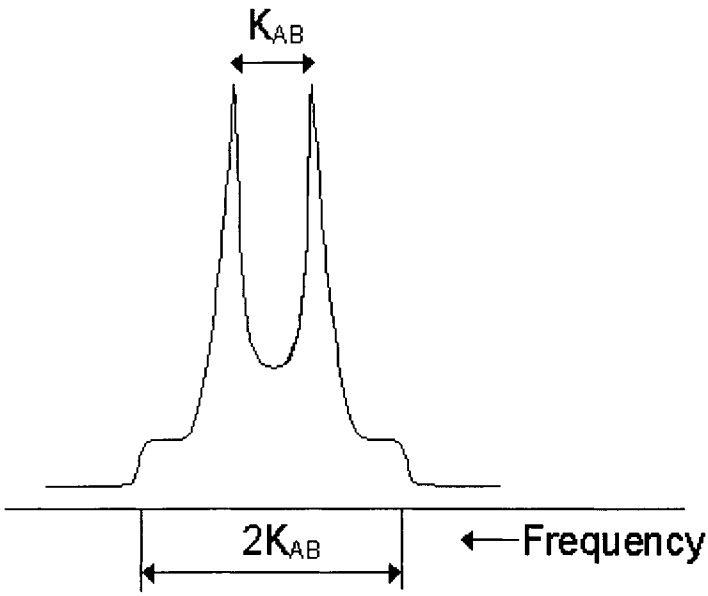

Figure 19: The characteristic powder pattern of the NMR signals in solids. The coupling pattern and the line broadening are due to the through space dipolar couplings.

signal detection plane), this being the short relaxation process discussed above, and a different process is the further relaxation of the magnetization along the z axis until its original magnitude (Figure 7 and section 6. 6). In solids this second process is very long in comparison with liquids. Although this process has no direct influence on the shape of the signal, it makes the experimental time very long because of the required relaxation delay.

There is still another factor contributing to the line broadening in solids which is worth being mentioned, namely the chemical shift anisotropy. Thus, the chemical shift of a particular nucleus depends on electron shielding. As the electron shielding also depends on orientation, and as all possible orientations are present in solids, this is an additional source of line broadening.

In order to overcome the problems arising from the factors described above and to obtain high resolution solid-state NMR spectra, special techniques and special spectrometer designs are employed. These differences will be mentioned in section 6.7.10 referring to spectrometer design.

6.5.9. Some common types of high resolution NMR spectra

We are presenting a series of one dimensional (1D) and two dimensional (2D) NMR spectra to exemplify the power of the technique. It is beyond the purpose of the present chapter to cover all types of NMR spectroscopy. Sometimes the same technique is known under several alternative acronyms, and in other cases different techniques provide the same information. We mention some of the most popular techniques listing alternative acronyms, but without detailing the full names or technical aspects. The interested reader should refer to already quoted books for more information [10,11,13]. A good compendium on basic 1D and 2D types of NMR spectra is Nakanishi's book [26] whereas some 2D-, 3D- and 4D-spectra are well explained in Evans' book [27]. However, as the techniques advance very fast, following more recent reviews and original publications is essential.

The Decoupling NMR experiment. Irradiation with a monochromatic r.f. having the same frequency as the resonance frequency of the nuclei in a particular group, produces the decoupling of the signals of the nuclei belonging to directly bonded groups. This technique simplifies the spectrum and facilitate the assignment of signals. Both homo- (same type of isotope being both irradiate and observed) and hetero-decoupling are usual.

The NOE spectra. The irradiation with monochromatic r.f. of the same frequency as the resonance frequency of one of the groups (but of lower power than that required for the decoupling experiment), produces an increasing intensity for the signals of the through-space neighboring groups.

2DNOE (NOESY). This type of spectrum produces the same information as a NOE spectrum, but showing all the connections in one spectrum. Another advantage is that one can see neighborhoods even for signals which are overcrowded or too close to be selectively irradiated. The spectrum appears as a square with spots located on the main diagonal which are projections of the signals of the normal ^{1}H-NMR spectrum (shown on the axes). These spots are named **diagonal peaks**. The off-diagonal spots, named **cross peaks** represent the NOE connections. Thus a NOE correlation is present if there is a cross peak connecting two diagonal peaks.

DEPT (APT) spectra. It is usual to record the ^{13}C-NMR spectra with broad-band hydrogen decoupling, thus removing the coupling patterns and showing only a singlet peak for each carbon atom in the molecule. The DEPT and APT spectra appear as "manipulated" ^{13}C NMR spectra, showing both positive and negative peaks, which enable one to assign various types of carbon atoms according to the number of hydrogen atoms being attached to them.

H,H-COSY spectra are looking similar to the **2DNOE** spectra, the diagonal peaks representing again the projections of all signals in the ^{1}H-NMR

spectrum (which is plotted on two edges of the COSY spectrum). The cross peaks in this case show only the correlations through bonds. Thus a COSY spectrum provides the information of a series of all possible homodecoupling experiments.

H,C-COSY (HETCOR, HMQC). This type of spectra provides a direct correlation between the signals of the carbon atoms and the signals of the hydrogen atoms directly attached to them (C-H). The normal ^{1}H-NMR spectrum is plotted along one of the edges and the ^{13}C-NMR spectrum is plotted along the other edge of the 2D spectrum. In this case the spectrum is no longer symmetrical and there are no diagonal peaks. The cross peaks provide the correlation information. The quaternary carbon atoms show no correlation peaks as they have no hydrogen atoms linked to them.

Long Range H,C-COSY (Long Range HETCOR, COLOC, HMBC). These spectra resemble the H,C-COSY one, the difference being that the cross peaks are no longer representing correlations between directly linked carbon and hydrogen atoms, but correlations over two or three bonds (C-C-H or C-C=C-H). Thus, some of the carbon atoms in the spectrum show correlation peaks with two different hydrogen atoms, as they have more than one different neighbor. Also the quaternary carbons show correlation peaks as they usually have neighbor hydrogen.

C,C-COSY (INADEQUATE, CCC2D). In this type of spectrum pairs of neighbor carbon atoms are linked by 2D peaks situated on the same parallel line. This is one of the most powerful 2D experiments enabling the entire carbon skeleton of a molecule to be mapped.

J-Resolved Spectroscopy. These spectra (either homo- or hetero-nuclear) are 2D spectra which allow the identification of coupling patterns and coupling constants. Each atom signal in the 1D spectrum plotted on one of the edges of the spectrum shows in the 2D spectrum a number of spots equaling the multiplicity of the 1D signal. Coupling patterns for otherwise overcrowded 1D spectra can be identified.

nD-NMR spectra.

We mentioned above only a very small part of the available 1D and 2D NMR techniques. Many other techniques are known not only as 1D and 2D but also employing more dimensions. We could for instance consider a 3D experiment H,H-COSY - H,C-COSY in which the peaks are spread inside a cube. Cutting the cube on a slice corresponding to the signal of one carbon atom would produce a COSY spectrum in which would be present only the H-H correlations of the hydrogen atom linked to the carbon atom for which the slice was selected. It is obvious that as we increase in dimensionality the

data are more and more spread thus interpretation of very crowded 1D spectra becoming easier.

6.5.10. Low resolution *versus* high resolution NMR

The parameters and phenomena discussed in the previous sections are common to all types of NMR spectroscopy (low- and high-resolution spectroscopy, solid- and liquid-state, localized or not, one- and multi-dimensional, imaging).

In principle, there is no clear cut border separating low resolution and high resolution spectroscopy. Resolution can be defined as the minimum distance between two lines in a spectrum at which they can be still distinguished. Starting from this definition and considering the dependence of the energy gap for the same nuclear transition on the magnetic field strength (Figure 5), we can see that the resolution increases continuously, as the external magnetic field increases. Thus, the number of distinct lines in a spectrum will increase for a particular compound and observed nucleus from one to the maximum possible number for that compound, as the spectrometer's magnetic field increases. In this respect one cannot define the minimum field for obtaining the maximum resolution otherwise than on a case by case basis. Moreover, as we mentioned in previous sections there are also other factors, like the homogeneity of the sample, viscosity of the solution and aggregation state which are dramatically affecting the resolution obtained for the same compound.

In common practice, in low resolution NMR our concern is with the analysis of the NMR signal in the time domain (FID) and the characterization of the physical structure of the bulk sample. The global relaxation behavior can provide extremely useful information on various aspects like the moisture determination or solid fat content. This global characterization of the sample in terms of molecular dynamics was the key to successful use of low field NMR in food sciences. Adding to this valuable information, the low cost of the low resolution instruments, the easy use of the instrument (not requiring special training), the specialized software (providing direct results to particular problems), one can hardly imagine a food chemistry department without making use of low resolution NMR spectrometers. It is thus easy to quote several analytical methods in food chemistry standardized on low resolution NMR spectroscopy.

The success of the high resolution NMR techniques was ensured originally by its extreme power in solving the structure of pure compounds. It is very often that the ultimate argument in determining the structure of an unknown compound is the NMR. Thus, the main applications of high resolution NMR are based on studying individual signals in the frequency domain (the common NMR spectrum). Relaxation measurements for individual signals

(thus combining the study of the time and frequency domains) provide valuable information both in terms of structural assignments and of mobility of various parts of the molecule. Interactions between different molecules (*e.g.,* identifying binding sites in biopolymers) are also common examples showing the power of the high resolution NMR. The main application of high resolution NMR in food sciences is in researches requiring structure assignment of newly isolated compounds. Adding to this restricted area the high costs of the instruments and also the high running costs, we can see the reason why the high resolution NMR instruments are not so widely used in food sciences as the low resolution ones. However in the early 1990s an increased interest was shown in studying complex mixtures (usually in solution) by high resolution NMR. This had a considerable impact in fields like food sciences and medicine.

6.6 MORE ON RELAXATION

As we have seen above, relaxation is a crucial process in the NMR technique. It is difficult to cover all aspects of the topic, but it is worth having a closer look to it.

Thus it is important to note that there are several mechanisms helping the excited nuclei to relax to the equilibrium state. The equilibrium state is the original distribution of atomic nuclei between the allowed energy levels (corresponding to allowed orientations) in the external and static magnetic field (B_0). There are at least two time constants characterizing the relaxation process. Thus the global time constant is called *the spin-lattice relaxation time* or *longitudinal relaxation time* (T_1) and represents the time required for the spin system to return exactly to the equilibrium state (Figure 6d-g and 4.4.e,h). The other relaxation constant refers to the return of the global magnetization (M) parallel to the z axis (*i.e.,* disappearance of the projection of magnetization in the x-y plane) as in Figure 7d,g. The time constant associated to this process is called *spin-spin relaxation time* or *transverse relaxation time* (T_2). As it is shown in Figure 20 the T_2 relaxation time can be either smaller then or equal to T_1.

6.6.1. Spin-lattice relaxation time (T_1)

The evolution of the projection of the magnetization (M) on the z axis (M_z) is described by the differential equation:

$$dM_z / dt = - (M_z - M_0) / T_1$$

After a pulse, the variation in time of the population difference (Δn) between the two states for a collection of spin 1/2 nuclei (Figure 5) can be considered an exponential growing according to the equation:

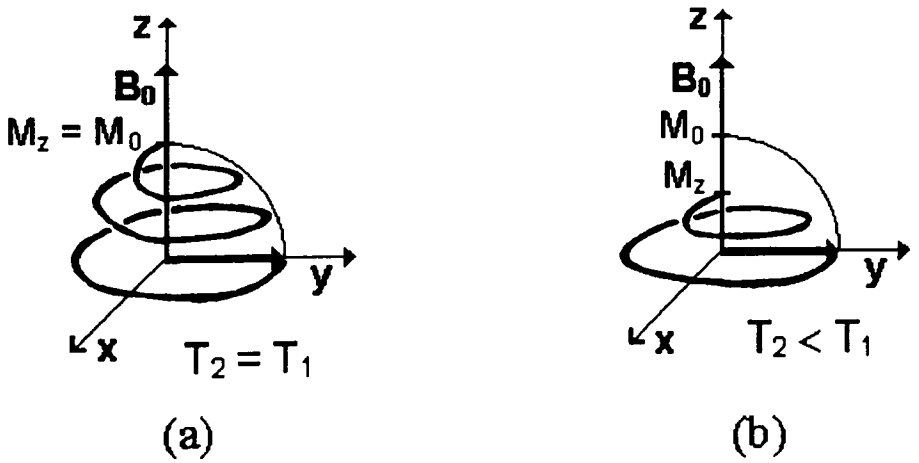

Figure 20: The relaxation process and magnetization trajectory for the case a) when spin-spin relaxation time T_2 equals the spin-lattice relaxation time T_1, and b) when spin-spin relaxation time is smaller than the spin-lattice relaxation time.

$$\Delta n(t) = \Delta n_{equilibrium}(1\text{-}e^{-t/T1})$$

The spin-lattice relaxation process is associated with the transfer of energy (which was previously absorbed from the external r.f. pulse), to the lattice (*i.e.*, the surrounding medium). The emission of energy is not spontaneous. Thus, the main mechanism leading to the dissipation of energy is the interaction of the excited spins with neighboring spins (dipolar coupling) in molecular motion. As the molecules undergo tumbling consisting of rotations, translations, vibrations and collisions with a wide range of velocities, and as the through-space dipolar coupling between magnetic nuclei depends on distance and position, the nuclei experience oscillating local magnetic fields (Figure 14). The oscillation of theses fields is modulated by the random tumbling motion. As there are a wide range of frequencies associated with these molecular motions, some of the motions have the right frequency to generate an oscillating magnetic field at the frequency of the NMR spectrometer (ν_0). It is this time dependent magnetic field that is responsible for the transition of the nuclei back to the fundamental state. Further, it is straightforward that the correlation time plays an important role in the probability to find the component of the molecular movement having the resonance frequency. Thus, a dependence of the relaxation time on the correlation time is expected to have a minimum for the optimum value of the correlation time (Figure 21).

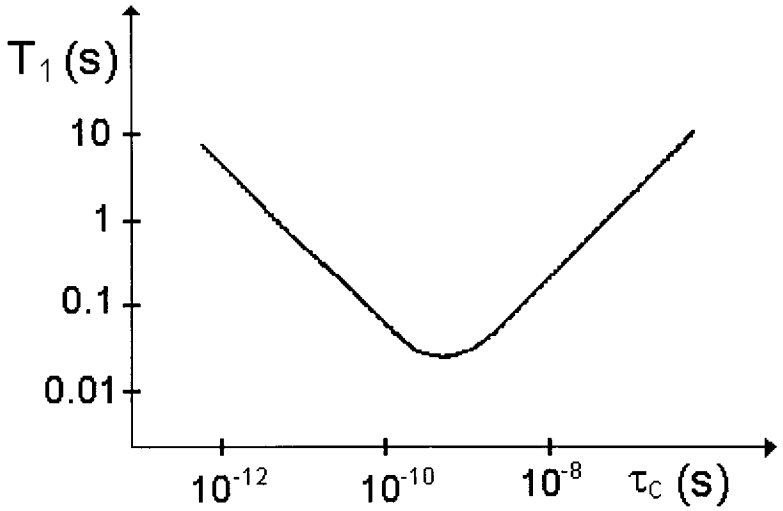

Figure 21: Dependence of the relaxation time (T_1) on the correlation time (τ_c). Left side of the plot is characteristic for small molecules in non-viscous solutions and the right side is characteristic for large molecules and viscous solutions.

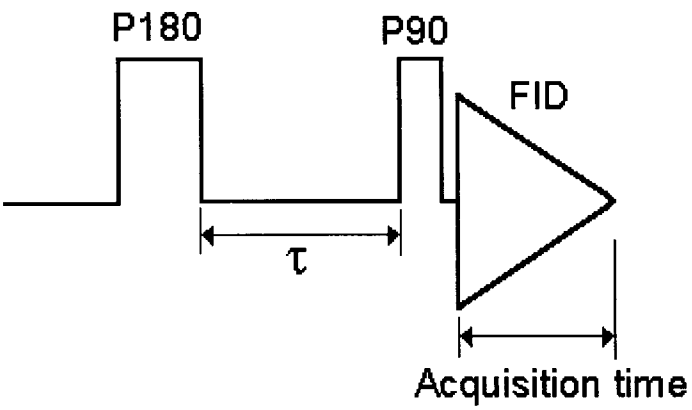

Figure 22: The inversion-recovery pulse sequence used for determination of the T_1 relaxation time.

The probability to find the right component of the frequency of the molecular motion for correlation times higher or smaller than the optimum value are

smaller, thus leading to longer relaxation times. For most small organic molecules in non-viscous solutions the situation is represented by the left side of the curve in Figure 21. Thus the molecular tumbling is fast (correlation time small) and conditions which slow down the motion are shortening the relaxation time. For large molecules (*e.g.*, long proteins) the molecular tumbling is rather slow and the normal situation is found on the right side of the plot in Figure 21. Thus, for such compounds, slowing further the motion is increasing the relaxation time. A reasonable short T_1 is desirable because it cuts down the experimental time and increases the sensitivity, but below a certain value, a too short T_1 broadens the lines, thus destroying the resolution. Estimation of T_1 values is essential for quantitation purposes. Thus one should employ a relaxation delay of at least 5 times the longest T_1 in the molecule in order to obtain accurate integrals for signals.

There are several methods for experimentally determining the T_1 relaxation time. We will briefly mention here the **inversion-recovery** technique (Figure 22). In this technique two pulses have to be employed. A first pulse (P180) having the appropriate length turns the magnetization by 180° (Figure 6c) and after a variable delay τ, another pulse (P90) having the appropriate length turns again the magnetization by 90°. After the first pulse (P180), during the τ delay, the magnetization freely evolves toward the equilibrium position (Figure 6d-f). The projection on the z axis of the magnetization during this relaxation process decreases along the -z axis, reaches the zero position and then increases along the +z axis until it reaches the initial value M_0 (Figure 6g). A series of experiments is repeated with stepwise increasing values of the τ delay. After each τ interval a P90 pulse is employed and the signal generated by the magnetization immediately collected by a detector situated on the y axis. For the situations when after the τ delay the magnetization on the z axis did not reach the zero value (Figure 6d), a new pulse (P90) in the same direction as the previous one (along x axis) further turns the magnetization (clockwise) toward the negative y axis. Thus the detected signal produces a negative line in the spectrum. The negative signal stepwise decreases in intensity as the τ delay increases and the magnetization (M_Z) before the second pulse approaches the zero value. For a certain value for τ, when the magnetization has exactly zero value (Figure 6e), no signal is detected on the y axis. Further increasing the τ interval leads to a progressively increasing positive signal detected on y axis, as the P90 pulse turns the magnetization on the positive y axis (Figure 6f). After a certain value for τ, when the magnetization reached the M_0 initial value, further increasing this delay produces the same positive intensity for the line in the spectrum (Figure 6g). The plot of the intensity of the signal as a function of τ matches a curve similar to that shown in Figure 7e, with the exception that the experimental curve shows an arbitrary scale for the z axis, representing the intensity of the signal in the spectrum, and not the actual value for the magnetization. It can be shown that the relationship between

the value of the τ delay for the point when the intensity of the detected signal is zero (τ_0) and the T_1 relaxation time is:

$$\tau_0 = T_1 \ln 2$$

6.6.2. Spin-spin relaxation time (T_2)

This relaxation process refers only to the period required for the projection of the magnetization (M) into the x-y plane (M_{xy}) to vanish. In other words T_2 is the time required for the magnetization M to realign along the z axis (Figure 7c,d). As the signal detector is placed along the y axis, it is thus the T_2 which determines for how long the NMR signal (FID) lasts (Figure 7d,g). As we have seen previously, the relaxation time T_2 has a major influence on the linewidth. In other words, we cannot measure very precisely the frequency of a signal which lasts for a too short period, thus a short T_2 give rise to broad peaks:

$$\Delta\nu_{1/2} = 1 / \pi T_2$$

If the effect of T_2 on the NMR spectrum is not so difficult to understand, the mechanism for the vanishing of the M_{xy} projection of the global magnetization M is rather complex, and there are several factors affecting this process. It is essential to note that T_2 cannot be longer than T_1 (Figure 20).

As T_2 is usually shorter than T_1 there must be some additional factors contributing to the relaxation process associated with T_2. The mechanism by which T_2 is decreasing in the x-y plane, without affecting the z projection, is a fanning (or dephasing) of the global magnetization vector. Once the vector M was tipped under a certain angle α by an r.f. pulse (Figure 23a), the projections of the M vector are M_z and M_y, the component on the x axis (M_x) being zero. The projection in the xy plane (M_{xy}), in this case equals the M_y projection. Once the r.f. pulse turned off, the magnetization begins to relax. In this moment one of the natural tendencies for the global magnetization (M) is to rotate (precess) around the z axis (which is the direction of the external magnetic field B_0). If we ignore the other tendency (namely to align the vector M along the z axis), the result is a precession around the z axis under the same tip angle α (Figure 23b). In this situation the M vector remains constant, and also constant remain the two projections M_z and M_{xy}. The other projections M_x and M_y are not constant, but they oscillate between a maximum positive and a minimum negative value equal to M_{xy}. Figure 23c shows the same situation as in Figure 23b, but viewed as a projection in the xy plane. In order to explain a decreasing of the M_{xy} component of the magnetization M while leaving the M_z component constant, we have to consider a spreading of the M vector into several components pointing in different directions on the same circle (Figure 23d). In this case the

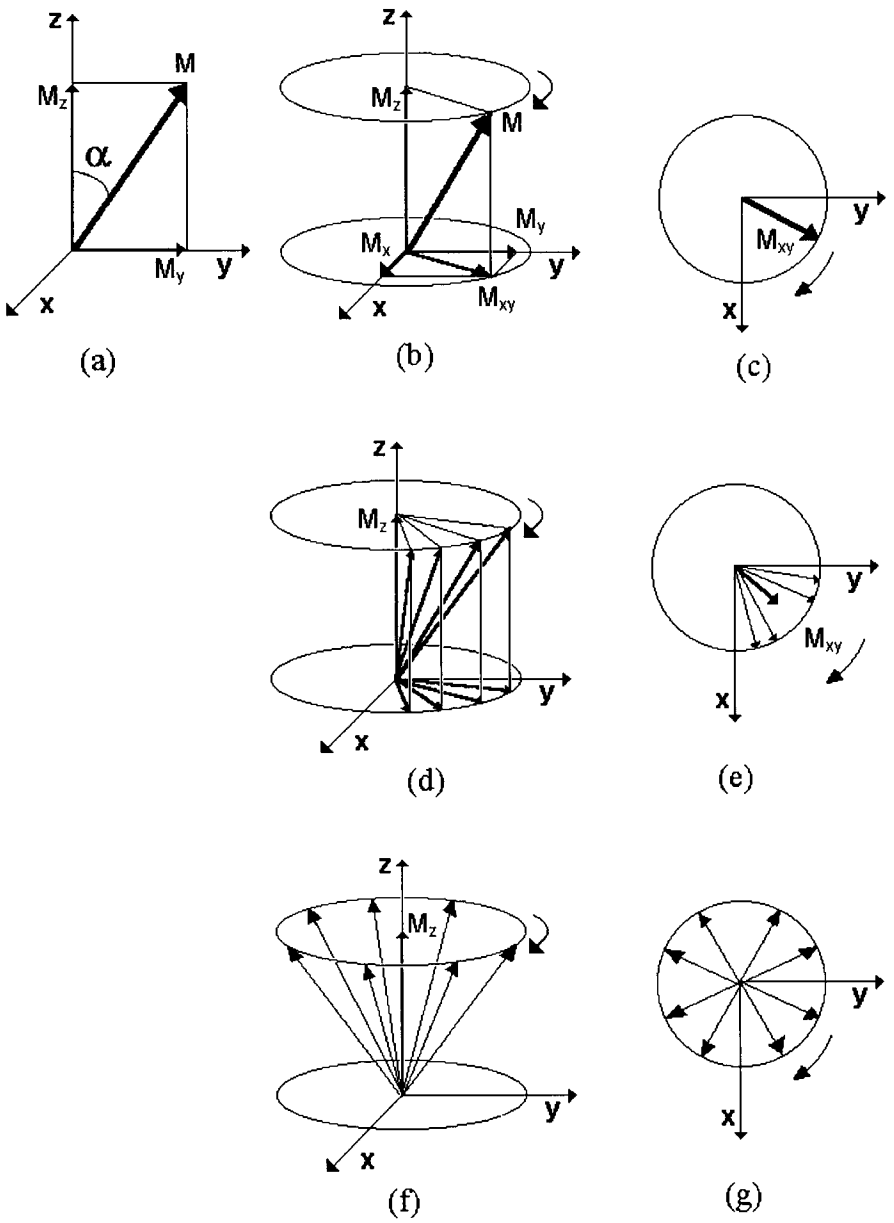

Figure 23: The relaxation process associated with the T_2 time constant. The external magnetic field B_o, which is not explicitly shown, has the same direction as the z axis. a) an r.f. pulse flips the magnetization vector *M* by an angle α away from the equilibrium position; b) once the pulse turned off the magnetization freely precess around the z axis. c) the same situation as in the previous figure but viewed as a projection in the x-y plane; d) not

Figure 23 cont:

all the molecules in the sample experience the same external magnetic field, thus there are several components of the magnetization precessing with different speeds. This situation leads to a fanning of the magnetization vector which is increasing in time. e) the same situation as in the previous figure, but viewed as a projection in the x-y plane; f) after a sufficiently long time the fanning process reached the situation when the magnetization vector is uniformly spread on the rotation cone around the z axis. The projection on the z axis was not affected, but the projection in the x-y plane vanished; g) the same situation as in the previous figure viewed as a projection in the x-y plane. Individual components of the magnetization are canceling in this plane.

projection on the z axis M_z is unaltered, as the individual components have a common projection on the z axis. If we consider however the components in the x-y plane (Figure 23e), it is clear that the sum of the individual projections which is the global M_{xy} component, is smaller in this case by comparison with the previous situation. If the process of fanning out continues, eventually it is reached the situation when the M vector is equally spread on the surface of the rotation cone around the z axis (Figure 23f). Again, this situation does not affect the M_z component, but the sum (M_{xy}) of the individual projections in the xy plane is zero (Figure 23g). In fact we reached the situation when the magnetization is fully relaxed in the xy plane. There are several factors affecting the dephasing process, and (contrary to the T_1 relaxation mechanism), dephasing not necessary requires dissipation of energy, thus the T_2 process can be faster than T_1.

One of the factors affecting the dephasing and thus, contributing to the T_2 relaxation time is the spin-spin interaction. Chemical exchange phenomena (when present) contribute very significant to the shortening of T_2. Scalar coupling (J-coupling) is another source for T_2 shortening.

This relaxation time is very important as it is associated to the "natural linewidth". However the time constant T_2 cannot be directly quantified, because there are other factors which also contribute to the dephasing process. These factors are experimental factors and are related to the inhomogeneity of the B_0 field in the sample. As different molecules in the sample experience slightly different B_0 fields, their precession frequency (and resonance frequency, ν_0) is slightly different, thus the dephasing is faster, T_2 becomes shorter, and the actual line in the spectrum is artificially broadened.

As a result of the superposition of internal (sample's characteristics) and external (experimental) factors affecting the T_2 process, by measuring the half-height linewidth we can deduce only a global T_2 time denoted as T_2^*:

$$\Delta\nu_{1/2} = 1 / \pi\, T_2^*$$

The same is true if we consider the time required for the FID signal to vanish (Figure 7d,g) when we would again obtain the T_2^* rather than the T_2 time constant.

In order to obtain the natural T_2 constant (which is a function only of the molecular characteristics of the studied compound) we should subtract the artificial contribution of the experimental factors (field inhomogeneity) from T_2^*.

An experimental method for measuring the T_2 constant is the **spin-echo method**. Briefly, the idea is to do "something" (at some stage in the development of the experiment), to invert for a while the effect of the inhomogeneity of the external field. The result would be that the dephasing effect, inverted but with the same magnitude, would produce a refocusing of the magnetization. Figure 24 presents the evolution of the magnetization during a spin-echo experiment. The pulse sequence includes a train of one 90° pulse (P90) and two 180° pulses (P180) separated by appropriate delays (τ) and the acquisition time (Figure 24a). The experiment begins with a 90° pulse (P90) which turns the magnetization along the y axis (Figure 24b,c). At this moment the magnetization in the x-y plane (M_{xy}) equals the initial magnetization vector (M_0) as magnitude. The magnetization begins to dephase, some components rotating faster, others slower (Figure 24d). After the time τ the first 180° pulse (P180) is employed. In this way the fanned magnetization is turned around the x axis (Figure 24e). The fanned magnetization continue to evolve with different speeds as a result of the experimental inhomogeneities. However, as they have been rotated with 180°, the last components of the magnetization have the fastest movement, and the first ones the slowest movement. Thus after exactly the same time interval τ, the magnetization refocuses (Figure 24f). The only difference is that the M_{xy} magnetization is shorter than the original M_0 vector. This shortening is due to the "true" T_2 relaxation process generated by the intramolecular factors. At this point the magnetization M_{xy} continues to evolve and the field inhomogeneities which refocused the vectors, are now further defocusing them, as the individual components continue to rotate (Figure 24g). After another τ time interval, a second 180° pulse is applied (Figure 24h), the M_{xy} magnetization refocuses again (Figure 24i), this time even shorter in magnitude, and the process continues (Figure 24j) while the signal is detected. In fact large numbers of 180° pulses are employed. The experiment is repeated, beginning with only one 180° pulse and each new

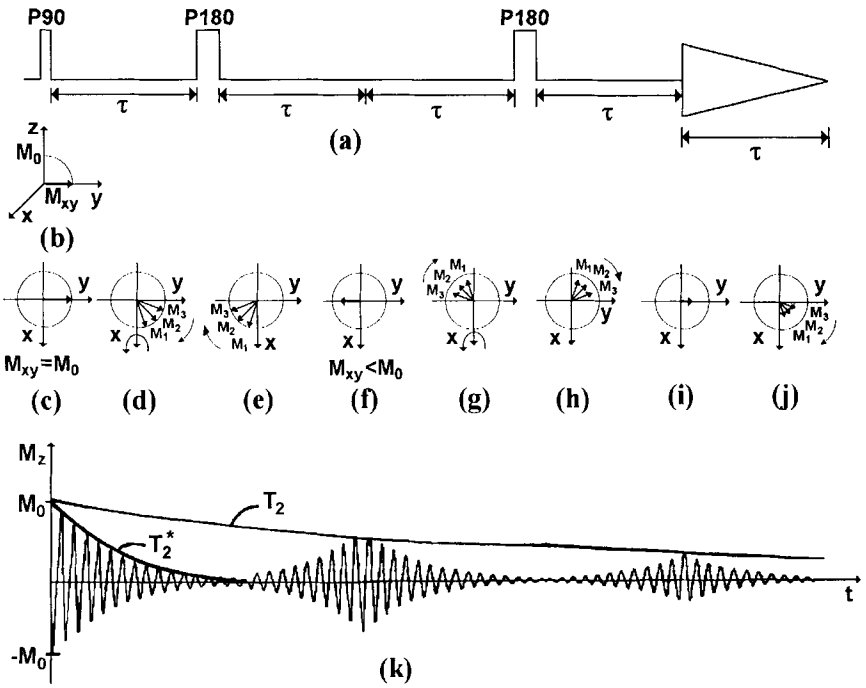

Figure 24: a) The spin-echo pulse sequence; b) and c) the first 90° pulse turns the initial magnetization M_o along the y axis; d) during the first τ interval the magnetization defocuses e) the first 180° pulse turns the magnetization around the x axis, thus inverting the ordering of the individual components; f) after another τ interval the magnetization refocuses; g) the further free evolution defocuses again the magnetization; h) after the second 180° pulse the magnetization is again inverted; i) the magnetization refocuses one more time; j) the defocusing takes place while the FID is recorded; k) the evolution of the magnetization in time during the spin-echo experiment and the two time constants T_2 and T_2* associated with this process.

experiment contains a new 180° pulse. In this way, each FID collects a further and further echo. Plotting the amplitude of the signal generated by each echo as a function of time allows the determination of the T_2 relaxation time, not affected by experimental imperfect conditions (Figure 24k). The much faster relaxation time for individual echoes is the T_2* relaxation time (Figure 24k).

6.7. INSTRUMENTAL AND EXPERIMENTAL CONSIDERATIONS

A schematic diagram of a NMR spectrometer is presented in Figure 25. Depending on the type of spectrometer some elements may be missing or additional ones may be present.

6.7.1. The spectrometer

One way to characterize the spectrometers is in relation with their type of magnet. Thus, there are permanent, resistive (electromagnets) and superconducting magnets. Another way is to specify the way of excitation of the sample. In this respect there are Continuous Wave (CW) and Pulse systems (PFT). Two different constructive types of CW spectrometers are also possible: with Magnetic Field Sweep (at fixed frequency) and with Frequency Sweep (at fixed magnetic field). Another way to characterize the NMR spectrometers is based on the mathematical treatment of data. Thus, there are spectrometers either with or without mathematical treatments. Nowadays Fourier Transform (FT) is a standard feature of spectrometers and some advanced systems have additional non-FT processing methods (Linear Prediction, Maximum Entropy Method, Hilbert Method, Bayesian Analysis). Still another way to characterize an NMR spectrometer is according to the field strength. Thus, there are Low Resolution and High Resolution spectrometers. The High Resolution are usually referred as low-, medium-, high- and ultra high-field spectrometers. NMR imaging and microscopy are already considered separated topics, and usually (because of the vastness of the field) treated separately in most discussions. There is still another NMR technique, namely localized NMR spectroscopy, which is sometimes treated as a branch of NMR spectroscopy, other times as a branch of NMR imaging. As we are not covering imaging in this chapter, we can again distinguish between two types of NMR spectroscopy (and spectrometers), namely localized- and non-localized- NMR spectroscopy.

6.7.2. The magnet

All types of magnets (permanent, resistive and superconducting) are presently used. For low resolution both permanent and resistive magnets are used. For high resolution low field (usually, up to 80 MHz, although theoretically up to 100 MHz), the tendency is to use electromagnets. Some permanent magnets are still in use in rather isolated cases. For fields higher than 100 MHz, only superconducting magnets can be used.

Permanent magnets generate a very stable magnetic field, but they should be well thermally insulated, and they are very heavy. They have been the most commonly used instruments until mid 1970s. Electromagnets, are lighter,

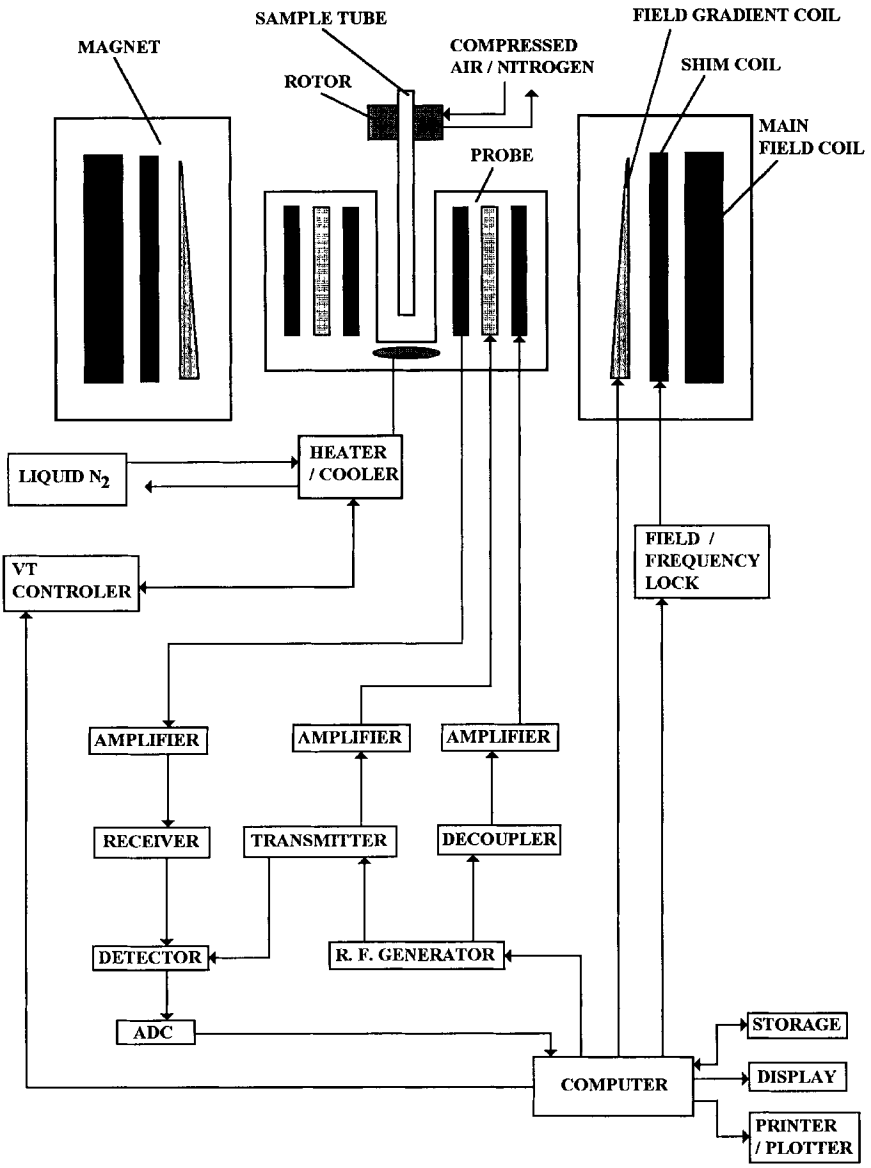

Figure 25: Block diagram of a high resolution NMR spectrometer.

but require an additional power source and a water-based cooling system. In order to ensure the required stability of the field an additional system of locking the field on the NMR signal of a nucleus in the sample which is not recorded is used in most of the cases. Commonly the field is locked on the deuterium signal of the solvent. Superconducting magnets are the only

available choice for fields higher than 100 MHz, because iron saturates at 2.35 T. Commercially available field strengths goes up to 800 MHz. Major advantages lie in the wide spread of signals, extremely high field stability (using the same locking system as the electromagnets), high resolution and sensitivity. The magnets are very light. Once energized, the superconducting magnets do not require an additional power source anymore. A major constraint introduced with the use of superconducting magnets comes from the need to cool the niobium-titanium coil with liquid helium. They also require liquid nitrogen for slowing down the evaporation rate of the liquid helium. Therefore an important characteristic of a superconducting magnet is the time interval between helium refills. The usual refill interval for liquid nitrogen is two weeks, whereas for liquid helium varies between two months and one year, depending on the type of magnet. However one can regard the superconducting magnets as more nature-friendly than the electromagnets because they do not waste water.

Apart from the coils generating the main magnetic field, the magnet has additional coils named shim coils, which generate additional weaker magnetic fields intended to compensate the inhomogeneity of the main magnetic field and the inhomogeneities introduced by the other components (probe, sample tube, sample, *etc.*).

Depending on the type of spectrometer and experiments desired, additional coils named field gradient coils can be also used. These coils are very common in (and have been first designed for) NMR imaging, but are essential for localized spectroscopy as well. Using such coils the homogeneity of the main magnetic field can be deliberately destroyed (making the field to continuously increase from one side of the sample to the other by a certain gradient) so that the resonance condition can be selected for only localized regions of the sample. Thus NMR spectra can be recorded for regions of the sample rather than for the average sample how is usually the case. This is of tremendous importance for nonhomogeneous samples as some food samples are.

6.7.3. The probe

The probe's various coils both transmit and detect the r.f. signals, and regulate the temperature. The number of coils depend on the purposes for which the probe is designed. It is also common that one coil has more than one function, *e.g.* both transmission of the pulses and detection of the signal for a particular nucleus. A wide range of options is available in terms of NMR probes, according to the type of experiment required (*e.g.*, type of nucleus, number of channels and thus the maximum number of dimensions in a spectrum that can be recorded, amount of sample, type of detection, temperature and pressure ranges, coupling with other analytical instruments, solid or solution state, *etc.*).

Once the spectrometer purchased, the probe is the most important part which could improve the spectrometer's performance. Upgrading the probe with latest generations can dramatically increase spectrometer's performance and this is the main way of coping with the progress of the technique.

6.7.4. The computer

As in any high technology, computers are one of the most important leading forces in the advancement of scientific equipment. Advancement in computers made possible the development of commercial pulse FT-NMR spectrometers in early 1970s, although the pulse methods have been known since late 1940s. In 1987 processing one of the first 3D-NMR spectra took seven hours and in 1990 a 4D-NMR spectrum was reported to require sixty two hours of computing. Nowadays these experiments can be performed routinely with latest generations of commercial NMR spectrometers, mainly because of advancement in computers and software. Until late 1980s the NMR computers were dedicated system computers. Since early 1990s all modern high resolution spectrometers are using standard workstations, and networking several such workstations and the NMR magnet is a common practice. Latest generations of low-resolution NMR spectrometers have usually a dedicated computer, but they have an interface allowing direct linking with common Personal Computers. Upgrading the computer is probably the second action after upgrading the probe, which must concern somebody wanting to extend the lifetime of an instrument. The third important action in the same direction is upgrading some electronic parts. Last action on the list is replacing the magnet.

6.7.5. The analog-to-digital converter

The NMR signal (FID) is detected by the Receiver as an electrical signal. This signal is transformed by the analog-to-digital converter (ADC) into numbers which can be further stored and manipulated by the computer. The ADC determines both the maximum spectral width which can be recorded by the spectrometer (a typical value is 150 KHz), and the dynamic range of the spectrum. The dynamic range is the difference in intensity between the highest and the smallest signals in the spectrum for which the smallest signal can still be recorded. Signals which are smaller than this minimum intensity are not collected as signals by the spectrometer regardless how many scans are accumulated.

6.7.6. The software

The software is continuously developed by the spectrometer manufacturers as part of their NMR system development. This software allows better and better control of the hardware and design of NMR experiments. Also, the same software development allows better and easier treatment of data (FID)

once the NMR experiment finished. For this second part of post processing, there are also third software companies developing their independent NMR processing programs. Common features of such post processing software include baseline correction, peak fitting, lineshape analysis, slice selections and peak projections, resolution or sensitivity enhancement, library searches and spectral matching, conversion of data between various types of instruments, simulation of NMR spectra and comparison with experimental ones, calculation of chemical composition of the sample or some physical properties, *etc.*

6.7.7. The Sample

For high resolution spectra sample handling is very important. As the homogeneity of the sample is critical, ensuring very well mixing with the solvent is very important. Filtration of the sample has to be employed quite often. For very dilute samples, contamination problems should be considered (*e.g.*, acetone from the washing process, or sweat from the fingertips). Degassing the sample is critical in some experiments. Avoiding the presence or on the contrary, deliberately adding paramagnetic species to the sample are also options which have to be taken in relation to the type of experiment performed.

Sample volume is also important. Each probe has a specific detection coil that receives signals from only a finite volume in the core of the magnet. There is an optimum volume, greater than this detection coil volume which minimizes field distortions caused by the solution/air interface. When enough sample is available, this optimum volume should be used. For samples in small quantities, other strategies can be used (*e.g.*, capillary tubes, vortex suppressers, microprobes, *etc.*).

When enough sample is available, the concentration is chosen depending on the information desired. Thus, high concentrations are desired for good signal-to-noise ratios (*e.g.*, nuclei with low natural abundance), for short recording times and for some two dimensional experiments (*e.g.*, H,C-COSY, COLOC, INADEQUATE). On the other hand, dilute solutions are preferred for higher resolution spectra, NOE experiments and other two dimensional experiments (*e.g.*, H,H-COSY).

6.7.8. The solvent

The routine high resolution NMR spectrometers lock the magnetic field on the deuterium frequency of the solvent. Although other techniques exist, the use of deuterated solvents is the best choice (when possible), as it gives better quality spectra.

Apart from the solubility of the sample, other factors should be considered when choosing a solvent. The price plays an important role as it varies greatly from one solvent to another. The viscosity of the solvent has an important effect on the resolution of the spectrum. Viscous solvents usually produce lower resolution spectra than non-viscous ones. The usual non-viscous solvents are: acetone-d_6, acetonitrile-d_3, chloroform-d, dichloromethane-d_2, and methanol-d_4. Usual viscous solvents are: benzene-d_6, dimethylsulfoxide-d_6, dimethylformamide-d_6, pyridine-d_5, toluene-d_8, water-d_2. In some experiments the number of deuterated atoms per molecule of solvent has to be considered. For instance a higher strength of the deuterium signal (*e.g.*, acetone-d_6 *versus* chloroform-d) is better for NOE experiments and for cases when the deuterated solvent is added in a small quantity to another undeuterated solvent. The boiling and melting points have to be considered when variable temperature experiments are planned. The position of the residual undeuterated solvent signal as well as the deuterium content have to be considered for samples in very small quantities. The presence or absence of water traces in the solvent may be relevant in some cases (*e.g.*, use of shift reagents, sensitive samples).

6.7.9 The sample tubes

The quality of the tube (*e.g.*, concentricity, wall thickness) is very important when very good resolution is required. Also, each type of probe has a lowest recommended quality sample tube and the use of lower quality tubes can lead to the damage of the probe. Each manufacturer specifies the quality parameters in terms of inner and outer diameters, wall thickness and concentricity. Each product has a specified tolerance for these parameters. Apart form the catalogue quality, the history of the tube is also very important (*e.g.*, how it was cleaned, dried, stored, even what samples have been previously analyzed in it, as these operations might lower its quality).

6.7.10 Special characteristics of high resolution solid-state spectrometers

As it was shown previously (section 6.5.8), some characteristics of the solid state make the NMR spectra look different for solids than for liquids. In order to obtain high-resolution spectra the following technical features are used.

Dipolar interactions (leading to coupling patterns between nuclei which are not directly bonded) can be minimized by using high-power decoupling fields. If the decoupling power usually employed for liquids is about 5 W, typically 50 -100 W are required for solids.

Broadening due to chemical shift anisotropy can be reduced using the magic-angle-spinning (MAS) technique. MAS involves very fast spinning of the

sample under an angle of 54.7° to the applied magnetic field. Normal spinning rate for liquid samples is 10 - 20 Hz, whereas for solids it is in the range 10 - 20 kHz, which means a supersonic speed.

Relaxation times can be reduced by a technique named cross-polarization (CP), which results in polarization transfer between highly polarizable ^{1}H-nuclei and the observed nuclei (usually ^{13}C).

Nowadays, ^{13}C-CPMAS NMR spectra are routinely recorded and most of spin 1/2 nuclei are accessible. Although not yet a routine practice ^{1}H and ^{19}F as well as two-dimensional spectra can be also recorded.

For solid state NMR, small ceramic rotors are used instead of classical sample tubes.

6.8 FUTURE TRENDS

It is difficult to make predictions on how the NMR field will develop. The variety of techniques, applications and instrumentation available today was hard to imagine only a few years ago. We will briefly mention some tendencies which could also be relevant for food sciences. But certainly the future will show much more than that.

The current state of the instrumentation could be summarized as follows. Samples can be investigated in all states: gaseous, liquid, dispersions in liquid, gels, solids. NMR spectra of practically all isotopes magnetically active have been recorded. The highest magnetic field commercially available is 800 MHz. The temperature that can be reached in specially designed NMR probes exceeds 2,000°C using laser-heating systems. High pressure NMR experiments can be carried at 10,000 atmospheres. The dynamic range has been pushed well above 10,000 : 1. The NOE enhancements of less than 1% are easily detectable. 3D experiments are routine and 4D experiments are often performed.

There is every reason to believe that both instrumental and theoretical aspects of NMR will continue to progress. New pulse sequences will be invented, computer power will continue to grow and field strength and homogeneity will increase. Already there is a project for building a 1,000 MHz spectrometer. Special design of the building, parking and even roads around that site are carefully considered in order to prevent the interference with the magnetic field. Probably, this will remain a unique project for a while, but it is likely that 800 MHz instruments will become popular in the next few years.

Although many efforts are directed toward increasing the magnetic field strength, it is worth mentioning an interesting aspect. Apparently increasing

the magnetic field does not necessarily increase the resolution. This statement might look somehow strange. There are some reports that running NMR spectra on large molecules (proteins) at 750 MHz, do produced a slightly worse resolution than at 600 MHz. The explanation seems to be the fact that chemical shift anisotropy may become the dominant mechanism for spin-lattice relaxation above a certain level of the magnetic field, thus the increase in line broadening becoming faster than the increase in chemical shift separation. This phenomenon might set (at least theoretically) an upper limit for some ^{1}H NMR studies (and other nuclei like ^{31}P). This would be true for large molecules and if a field strength limit would be reached this is likely to be set for biochemical studies rather than food fluids. For complex mixtures of small and medium size compounds, this anisotropy does not arise and we have every reason to state that NMR spectra of such mixtures should be run at the highest available magnetic field.

Further improvements in software are also to be expected. This will lead to both better hardware control and the post processing of data. There are already examples of controlling the spectrometer from a remote PC, but this is not yet a standard feature. Probably, in the future the workstations will cease to have the monopoly over instrument control and this will be possible without any compromise using PCs, with all the benefits these computers have in term of costs, popularity and software compatibility.

It is a general consensus that a new revolution in instrumentation is to be expected once the new materials with superconducting properties at the temperature of liquid nitrogen will be introduced.

A new application will probably become very popular quite soon. This is the magic-angle-spinning (MAS) spectra of non-solids. The benefit would be for all heterogeneous samples, polymers in suspension, gels, viscous liquids, *etc.*. Special probes for MAS of quasi-liquids have been already designed. Probably this is the signal for a new development stage in the NMR field which will make the combined solution- and solid-NMR spectrometers to become popular and often used by "solution state spectroscopists".

Localized spectroscopy will also steadily grow in popularity and be used in connection with solid or quasi-liquid techniques.

Coupling Liquid Chromatography with NMR is another field which is steadily growing. HPLC-NMR probes and accessories are already commercially available and it is a strong competition to develop this exciting new technique. Less then 150 ng can now be detected with such systems.

Non-FT FID processing will be more frequently used as the commercial spectrometers tend to include them as options in the standard configuration.

3D and 4D experiments will become very popular and the increase in dimensionality will continue.

Pulse Field Gradient techniques, as well as digital lock and digital filtering already became standard options for last generations of instruments.

Spectral width, dynamic range, resolution and sensitivity are expected to be pushed toward further and further limits.

Probably soon we will have to reconsider standard sentences as "the relatively low sensitivity of the method" or "the limited use of less sensitive nuclei". The nuclei to be recorded will be more and more often chosen on the exclusive basis of the information provided, and not on their "accessibility" as it is usually the case now.

Automation will continue to develop and the "black box" which is now the modern NMR spectrometer for most of the users might become even blacker as the computers and software become more and more user-friendly. More standardized analytical methods will be based on both low and high resolution NMR methods. Better shielded magnets will probably be developed and NMR will eventually be introduced in factories and more widely used for on-line quality controls.

Many of the "research" and high-resolution techniques will percolate to "routine" and low resolution. There are studies demonstrating that NMR can be successfully used to characterize complex mixtures, and when used with automatic sample changers and specialized software packages, the cost of the method can compete with other techniques. Adding to this cost-related aspect, some information which can hardly be obtained by other techniques (like the geographical origin of wines or the fatty acid distribution among the three possible sites of a triglyceride) and we should expect an increasing use of high resolution NMR techniques in food sciences in the years to come.

Another relatively new application is the so called Site Specific Nuclear Isotope Fractionation (SNIF) studied by NMR. This approach gained a wide recognition when it was proven to provide valuable information on the geographic origin of wines and on the synthetic *versus* natural origin of some food ingredients. The principle of the method is to measure the isotope ratio for a particular element (*e.g.*, ^{1}H to ^{2}H ratio). It is likely that SNIF-NMR techniques will be more and more extensively used for both product authentication and identification of origin. The extension of SNIF-NMR to ^{13}C as a more routinely technique will greatly improve the discrimination power of the technique.

Hybrids of NMR and other techniques (*e.g.*, atomic force microscopy) will probably lead to development of new and independent research fields.

6.9 APPLICATIONS OF NMR TO FOOD ANALYSIS

Relative to most other techniques discussed in this book, NMR has found a limited number of "niche" applications in food analysis. For example, the determination of oils is seeds (or fat in chocolate!), based upon low resolution, solid phase NMR is well used in quality control laboratories. Actually, most applications that found their way in food analysis are methods based upon the differences in relaxation times of various molecules (*e.g.* free water molecules *versus* bound water molecules). Consequently, for the purpose of this particular chapter, we shall discuss only two specific applications of NMR to food analysis. These examples were chosen solely to demonstrate the broad range of applications that NMR can cover and the reader is advised that the mere fact that they were selected here should not be interpreted as a judgement of their value over other related references.

6.9.1 Characterisation of ginsenosides by high resolution ^{1}H NMR

Panax spp., especially *Panax ginseng*, are purported to possess various health benefit qualities. In oriental countries it has been used as a traditional panacea for numerous health disorders for several centuries. Saponins are generally recognised as the main effective components of ginseng. Because of their close similarities in terms of structure they offer a real challenge to the analytical chemist in terms of separation. Furthermore, the relative complexity of their structures makes them perfect candidates for in-depth structural characterisation work by NMR.

A few years ago, while affiliated to a food research facilities, we carried out extensive work on the suitability of food irradiation for various foodstuffs. As part of an agreement with the International Atomic Energy Agency (IAEA) in Vienna, aiming at training foreign food scientists in the area of food irradiation, we undertook extensive studies related to the treatment of ginseng (*Panax ginseng*) by ^{60}Co (γ-rays) for the purpose of extending its shelf-life [28, 29]. During the course of these investigations we extracted and isolated several types of components including various known, and unknown ginsenosides.

The aglycones moiety of ginsenosides are of the dammarane triterpenes family (Figure 26). The actual ginsenosides are divided with respect to the level of substitution of the aglycone. We reported earlier NMR-based structural elucidation work [30] where we presented original proton-NMR data on various ginsenosides. Full assignment of the structure was possible only after combining a variety of spectra such as standard 1D ^{1}H and ^{13}C spectra, DEPT (using either a 135° or a 90° reading pulse [31]), COSY (or long-range COSY) [32], double-quantum filtered COSY [33, 34] with or without phase-sensitive detection using TPPI [35, 36], COSY with one, two, and three relay coherence transfer steps [37, 38], double-quantum spectroscopy [39], NOE difference

spectroscopy, 2D ROESY [40, 41], 2D heteronuclear ^{13}C-^{1}H correlation (HETCORR) [42], and carbon-hydrogen correlations from one-dimensional polarisation transfer spectra by least-square analysis (CHORTLE) [43]. To appreciate the complexity of the problem at hand, one must look at the structure of such compounds, or more simply, to look at their IUPAC name. For example, the nomenclature for the so-called ginsenoside Rb_1 is as follows: (3)-[β-D-glucopyranosyl(1→2)-β-D-gluco-pyranosyl]-(20)-[β-D-glucopyranosyl(1→6)-β-D-glucopyranosyl]-20S-protopanax-diol.

Figure 27 provides an example of one two-dimensional NMR spectrum. It depicts a phase-sensitive two-dimensional ROESY spectrum where only negative levels are shown. It was recorded for a pure sample of standard material ginsenoside Re This figure was drawn from reference [30] and the readers are strongly encouraged to review the discussion relating to the interpretation of that spectrum as 2-D spectra are, at best, difficult to interpret despite their "nice pictures" appearance.

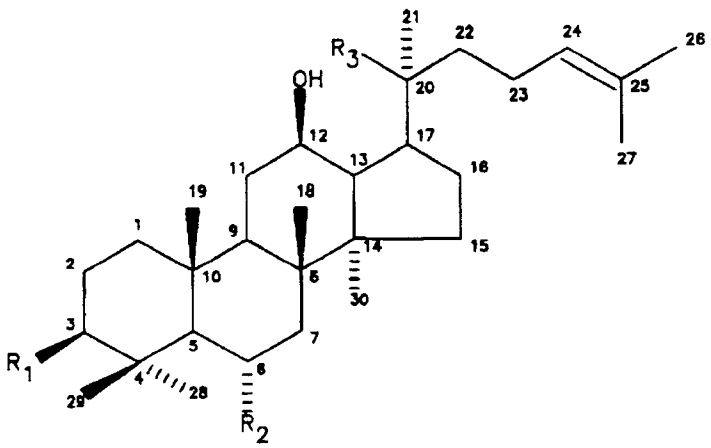

Compound	R1	R2	R3
20S-protopanaxdiol	OH	H	OH
20S-protopanaxtriol	OH	OH	OH
Ginsenoside Rb_1	O-Glcp^{2}-^{1}Glcp	H	O-Glcp^{6}-^{1}Glcp
Ginsenoside Rb_2	O-Glcp^{2}-^{1}Glcp	H	O-Glcp^{6}-^{1}Arap
Ginsenoside Rc	O-Glcp^{2}-^{1}Glcp	H	O-Glcp^{6}-^{1}Araf
Ginsenoside Rd	O-Glcp^{2}-^{1}Glcp	H	O-Glcp
Ginsenoside Re	OH	O-Glcp^{2}-^{1}Rhap	O-Glcp
Ginsenoside Rg_1	OH	O-Glcp	O-Glcp

Figure 26. General structures of the ginsenosides. Glcp = β-D-glucopyranose, Rhap = α-L-rhanmopyranose; Arap = α-L-arabinopyranose; Araf = α-L-arabinofuranose.

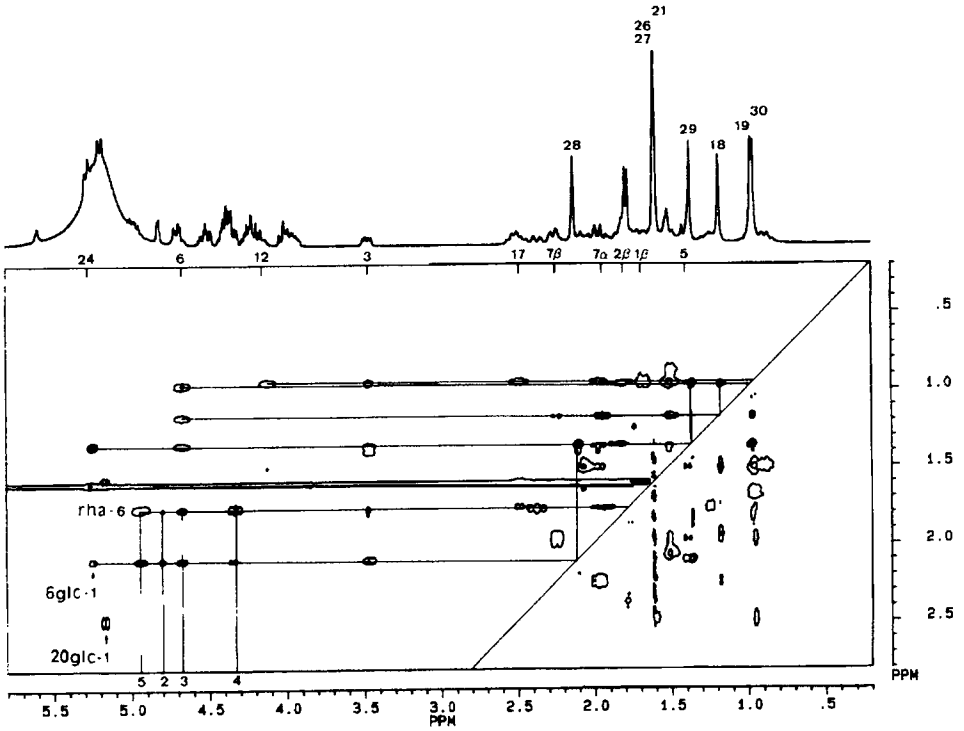

Figure 27. Typical phase-sensitive two-diemnsional ROESY spectrum of ginsenoside Re. Only negative levels are show. Reprinted from reference [30], with permission.

6.9.2 "SNIF-NMR"

Over the years, Site-Specific Natural Isotope Fractionation (SNIF) NMR has been used extensively in food analysis. Deuterium (^2H) is widely dispersed in the whole solar system and so it is as well on earth. Actually, the deuterium isotope ratio ($^2H/^1H$) in water, usually expressed in parts per million (ppm - just to confuse the matter a little more for NMR spectroscopists) ranges between 90 and 160 ppm according to the latitude where the measurement is made (the value increasing from the south pole to the equator). Water being the only source of hydrogen atoms involved in photosynthetic pathways, it follows that "fingerprint" deuterium contents are associated with such various pathways and with their origin. The latter being influenced by the climatic and geographical conditions prevailing at the time where the photosynthesis takes place.

A group or researcher at the Université de Nantes, led by G. J. Martin authored a technical brochure on behalf of Bruker, a NMR instrument manufacturer, that provides good background material on SNIF-NMR [44]. Although the brochure focuses on the "automation of wine NMR" (the term used by the

Table 2
NMR in the analysis of food sample*

Summary of work	NMR techniques reported	Ref.
^{13}C-NMR used to study composition & structure of plant material, including onions and tomatoes.	Pulse excitation; cross-polarisation excitation &magic angle spinning	[62]
Studies on the distribution of short-chain acyl groups between primary & secondary positions of triglycerides in fats, using high-resolution GLC and ^{1}H-NMR.	500-MHz ^{1}H NMR	[63]
The use of NMR to study the moisture content of various food products, including casein [64] butter bean,	^{17}O NMR transverse relaxation rates.	[64]
rigatoni pasta and snack food [65].	Non-invasive NMR imaging (MRI).	[65]
Development of a computerized method to visualize bruises in apples.	Magnetic Resonance Images	[66]
Detection of adulteration in fruit juices.	SNIF/NMR (deuterium) and SIRA/MS (stable isotope ratio analysis/mass spectrometry).	[67]
A validated and collaborative study for the detection of beet sugar in fruit juices.	SNIF-NMRREGISTERED Measurement of deuterium and carbon-13 levels.	[68]
Screening tool for determining the authenticity of orange juice.	^{1}H-NMR	[69]
Determination of oil in oilseeds [70].	Free induction decay (FID), echo signals in a spin-echo pulse sequence.	[70]
Determination of oil and water in oilseeds [71].	Pulsed NMR.	[71]
Studies on production, storage and quality control measures of dairy products including Cheddar, Brie, Danish Blue and Danish Harvarti cheeses, fromage frais and milk [72]	3 NMR imaging methods, *i. e.,*: 2-dimentional spin warp; 3-dimentional missing pulse steady-state free precession; and Dixon chemical shift resolved imaging sequences.	[72]
Monitoring of P-containing ingredients in cheese.	Cross-polarization magnetic angle spinning.	[73]

*A recent book on NMR in food science is also included in our reference list [74].

author to depict the automated analysis of wines (for enrichment or dilution) by NMR), several examples are used to demonstrate the power of NMR in identifying the origin of certain components in foodstuffs (here, for example, ethanol from various sources). A good number of basic references are provided dealing with the methodology used [45], the mechanisms involved [46-51], and applications to wines [52, 53], spirits [54, 55], beer [56], sugars [51, 57], and aromas and essential oils [58-61].

In summary, these applications allow for the positive identification of the origin of material, *e.g.*, wines, with respect to its geographical origin as well as the nature of the ingredients used to make it. This has significant impact on the marketing activities of these products, especially in the high-value added range or for the "appellation d'origine contrôllée". Obviously, the same techniques can be applied for quality control activities at the production site. Hence, it is safe to say that SNIF-NMR is a powerful technique with special value to the food scientists.

6.9.3 Survey of other applications

As per most chapters in this book, we include a short list (Table 2) of selected applications of NMR to food analysis. It will be obvious to those involved in daily use of NMR that these applications are by no means representative of the range of applicability of NMR to food science, rather they were selected for their practicality and their state of readiness of being implemented into daily food analysis activities.

6.10 REFERENCES

1. F. Bloch, W. W. Hansen and M. E. Packard, *Phys. Rev.* **69**, 127 (1946).

2. E. M. Purcell, H. C. Torrey and R. V. Pound, *Phys. Rev.* **69**, 37 (1946).

3. J. A. Pople, W. G. Schneider, and H. J. Bernstein, "High-Resolution Nuclear Magnetic Resonance", McGraw-Hill, New York, (1959).

4. R. R. Ernst, G. Bodenhausen and A. Wokaun, "Principles of Nuclear Magnetic Resonance in One and Two Dimensions", Clarendon Press, Oxford (1990).

5. C. P. Slichter, "Principles of Magnetic Resonance" (3rd edn), Springer-Verlag, Berlin (1990).

6. R. K. Harris, "Nuclear Magnetic Resonance Spectroscopy. A Physicochemical View", Longman, London (1986).

7. M. Goldman, "Quantum Description of High-Resolution NMR in Liquids", Clarendon Press, Oxford (1991).

8. A. Abragam, "The Principles of Nuclear Magnetism", Clarendon Press, Oxford (1986).

9. H. Günther, "NMR Spectroscopy", Wiley, Chichester (1980).

10. H. Friebolin, "Basic One- and Two-Dimensional NMR Spectroscopy", (2nd edn), VCH, Weinheim (1993).

11. J. K. M. Sanders and B. K. Hunter, "Modern NMR Spectroscopy. A Guide for Chemists." (2nd edn), Oxford University Press (1993).

12. R. J. Abraham, J. Fisher and P. Loftus, "Introduction to NMR Spectroscopy", John Wiley & Sons, Chichester (1988).

13. A. E. Derome, "Modern NMR Techniques for Chemistry Research", Pergamon Press, Oxford (1995).

14. P. S. Belton, I. Delgadillo, A. M. Gil and G. A. Webb (Eds.), "Magnetic Resonance in Food Science", Thomas Graham House, Royal Society of Chemistry, Cambridge (1995).

15. M. Karplus, *J. Chem. Phys.* **30**, 11 (1959).

16. L. M. Jackman and F. A. Cotton (Eds.), "Dynamic Nuclear Magnetic Resonance Spectroscopy", Academic Press, New York (1975).

17. J. Sandström, "Dynamic NMR Spectroscopy", Academic Press, New York (1982).

18. M. Oki (Ed.), "Applications of Dynamic NMR Spectroscopy to Organic Chemistry", VCH Publishers, Deerfield Beach (1985).

19. D. Neuhaus and M Williamson, "The Nuclear Overhauser Effect in Structural and Conformational Analysis", VCH Publishers, New York (1989).

20. E. Breitmaier and W. Voelter, "Carbon-13 NMR Spectroscopy. High-Resolution Methods and Applications in Organic Chemistry and Biochemistry", (3rd edn.), VCH, Weinheim (1990).

21. C. Chachaty, Z. Wolkowski, F. Piriou and G. Lukacs, *J. Chem. Soc. Chem. Commun.* 951 (1973).

22. D. Doddrell and A. Allerhand, *J. Amer. Chem. Soc.* **93**, 1558 (1971).

23. C. A. Fyfe, "Solid State NMR for Chemists", CFC Press, Guelph (1983).

24. M. Mehring, "High Resolution NMR in Solids", (2nd edn.), Springer Verlag, New York (1983).

25. B. C. Gerstein and C. R. Dybrowski, "Transient Techniques in NMR of Solids", Academic Press, Orlando (1985).

26. K. Nakanishi (Ed.), "One-dimensional and Two-dimensional NMR Spectra by Modern Pulse Techniques", Kodansha, Tokyo (1990).

27. J. N. S. Evans, "Biomolecular NMR Spectroscopy", Oxford University Press, Oxford (1995).

28. J.-H. Kwon, J. M. R. Bélanger, and J. R. J. Paré, *Radiat. Phys. Chem.* **34**, 953 (1989).

29. J.-H. Kwon, J. M. R. Bélanger, M. Sigouin, J. Lanthier, C. Willemot, and J. R. J. Paré, *J. Agric. Food Chem.* **38**, 830 (1990).

30. M.-R. Van Calsteren, J.-H. Kwon, J. M. R. Bélanger, and J. R. J. Paré, *Spectros. Int. J.* **11**, 117 (1993).

31. D. M. Doddrell, D. T. Pegg, and M. R. Bendall, *J. Magn. Reson.* **48,** 323 (1982).

32. A. Bax and R. Freeman, *J. Magn. Reson.* **44** 542 (1981).

33. U. Piantini, O. W. Sørensen, and R. R. Ernst, *J. Am. Chem. Soc.* **104,** 6800 (1982).

34. A. J. Shaka and R. Freeman, *J. Magn. Reson.* **51,** 169 (1983).

35. D. Marion and K. Wüthrich, *Biochem. Biophys. Res. Commun.* **113,** 967 (1983).

36. M. Rance, O. W. Sørensen, G. Bodenhausen, G. Wagner, R.R. Ernst, and K. Wüthrich, *Biochem. Biophys. Res. Commun.* **117,** 458 (1983).

37. G. Wagner, *J. Magn. Reson.* **55**, 151 (1983).

38. A. Bax and G. Drobny, *J. Magn. Reson.* **61**, 306 (1985).

39. T. H. Mareci and R. Freeman, *J. Magn. Reson.* **51**, 531 (1983).

40. A. A. Bothner-By, R. L. Stephens, J. Lee, D. C. Warren, and R. W. Jeanloz, *J. Am. Chem. Soc.* **106**, 811 (1984).

41. A. Bax and D. G. Davis, *J. Magn. Reson.* **63**, 207 (1985).

42. A. Bax and G. Morris, *J. Magn. Reson.* **42**, 501 (1981).

43. G. A. Pearson, *J. Magn. Reson.* **64**, 487 (1985).

44. G. J. Martin, Deuterium-NMR in the Investigation of Site-Specific Natural Isotope Fractionation (SNIF-NMR), Technical brochure by Bruker Analytische Messtechnik GMBH, No. NMR/A314/188 (1988).

45. G. J. Martin, X. Y. Sun, C. Guillou, and M. L. Martin, *Tetrahedron* 3285 (1985).

46. G. J. Martin, *Terahedron Lett.* **22**, 3525 (1981).

47. G. J. Martin and M. L. Martin, *C. R. Acad. Sci. Paris* **293**, 35 (1981).

48. G. J. Martin, M. L. Martin, F. Mabon, and M. J. Michon, *J. C. S. Chem. Comm.* 616 (1982).

49. G. J. Martin, B. L. Zhang, M. L. Martin, and P. Dupuy, *Biochem. Biphys. Res. Comm.* **111**, 890 (1983).

50. M. L. Martin, B. L. Zhang, and G. J. Martin. *FEBS Lett.* **158**, 131 (1983).

51. G. J. Martin, B. L. Zhang, N. Naulet, and M. L. Martin, *J. Amer. Chem. Soc.* **108**, 5116 (1986).

52. G. J. Martin and M. L. Martin, *J. Chim. Phys.* **80**, 293 (1983).

53. G. J. Martin, C. Guillou, N. Naulet, S. Brun, Y. Tep, J. C. Cabanis, M. T. Cabanis, and P. Sudraud, *Science des Aliments* **6**, 385 (1986).

54. G. J. Martin, M. L. Martin, F, Mabon, and M. J. Michon, *Anal. Chem.* **54**, 2380 (1982).

55. G. J. Martin, M. L. Martin, F, Mabon, and M. J. Michon, *J. Agric. Food Chem.* **31**, 311 (1983).

56. G. J. Martin, M. Benbernou, and F. Lantier, *J. Inst. Brew.* **91**, 242 (1985).

57. G. J. Martin, B. L. Zhang, L. Saulnier, and P. Colonna, *Carboh. Res.* **148**, 132 (1985).

58. G. J. Martin, M. L. Martin, F. Mabon, and J. Bricout, *J. Amer. Chem. Soc.* **104**, 2658 (1982).

59. G. J. Martin, M. L. Martin, F. Mabon, and J. Bricout, *Sci. Technol. Aliments* **3**, 147 (1983).

60. G. J. Martin, P. Janvier, and F. Mabon, *Analysis* **13**, 267 (1985).

61. G. J. Martin, P. Janvier, S. Akoka, F. Mabon, and J. Jurczak, *Tetrahedron Lett.* **27**, 2855 (1986).

62. T. J. Foster, S. Ablett, M. C. McCann, and M. J. Gidley, *Biopolymers* **39,** 51 (1996).

63. P. Kalo, A. Kemppinen, and I. Kilpelainen, *Lipids* **31**, 331 (1996).

64. A. Mora-Gutierrez, H. M. Farrell Jr., and T. F. Kumosinski, *J. Agric. Food Chem.* **44**, 796 (1996).

65. S. L. Duce and L. D. Hall, *J. Food Eng.* **26**, 251 (1995).

66. B. Zion, P. Chen, and M. J. McCarthy, *Comp. Electro. Agric.* **13**, 289 (1996).

67. G. G. Martin, V. Hanote, M. Lees, and Y. L. Martin, *J. AOAC Int.*, **79**, 62 (1996).

68. G. Martin, *Fruit Processing* **5**, 246 (1995).

69. J. T. W. E. Vogels, L. Terwel, A. C. Tas, F. van den Berg, F. Dukel, and J. van der Greef, *J. Agric. Food Chem.* **44**, 175 (1996).

70. P. N. Tiwari and P. N. Gambhir, *J. Amer. Oil Chem. Soc.* **72**, 1017 (1995).

71. G. Rubel, *J. Amer. Oil Chem. Soc.* **71**, 1057 (1994).

72. S. L. Duce, M. H. G. Amin, M. A. Horsfield, M. Tyszka, and L. D. Hall, *Int. Dairy J.* **5**, 311 (1995).

73. L. T. Kakalis, T. F. Kumosinski, and H. M. Farrell Jr., *J. Dairy Sci.* **77**, 667 (1994).

74. P. S. Belton, I. Delgadillo, A. M. Gill, and G. A. Webb (eds), *Magnetic Resonance in Food Science*, Thomas Graham House, Cambridge, UK, 294 pp. (1995).

This Page Intentionally Left Blank

J.R.J. Paré and J.M.R. Bélanger (Editors)
Instrumental Methods in Food Analysis

Chapter 7

Mass Spectrometry: Principles and Applications

J. R. Jocelyn Paré (1) and Varoujan Yaylayan (2)

1) Environment Canada, Environmental Technology Centre, Ottawa, ON, Canada K1A 0H3; and 2) Department of Food Science and Agricultural Chemistry, Macdonald Campus, McGill University, Ste-Anne de Bellevue, QC, Canada H9X 3V9.

7.1 INTRODUCTION

In 1898 Weiss first demonstrated that positive rays could be deflected by means of electronic and magnetic fields. However, the first mass spectra of simple low molecular weight substances are credited to J. J. Thompson in 1912. Mass spectrometry has since then come a long way. Mass spectrometry differs from most spectroscopic method in that it makes use of both, the physics and the chemistry of molecules (... and yes you are right, the word spectrometry is used instead of spectroscopy!). In its original form, mass spectrometry performs three main functions, namely the ionisation of molecules, the separation of these molecules according to their mass-to-charge-ratio, and the determination of the respective abundance of each ion so-produced.

In the early years, the petroleum industry acted as a catalyst for the development of this physical method. However, over the past twenty-five years, organic mass spectrometry has been the subject of a series of major developments. Some of them, such as the advent of commercially available interfaces for gas-liquid, high performance liquid, and supercritical fluid chromatographs, as well as novel ionisation techniques particularly well suited for high molecular weight, non-volatile macromolecules were welcome and well-accepted by the food analysts. Others, such as the introduction of relatively inexpensive quadrupole mass filters that proved to be reliable and

fast-scanning mass analysers, the extension of mass ranges and a significant increase in scan speeds through new developments in laminated magnet technology and ion optics, as well as the marketing of ever more powerful computer-based systems have entered the scene so spontaneously that the transition they brought about might well have gone unnoticed. Finally, more developments in ion physics and in gas-phase chemistry of ions led to applications that are still not well developed, nor well understood by the food analysts.

Together, all of these changes gave such a "new look" to mass spectrometry that it might well be hardly recognisable to someone who has not followed these trends as they occurred over the years. It is the intent of this chapter to deal with the fundamentals underlying the chemistry involved in mass spectrometry and to introduce more conventional aspects such as basic principles, instrumentation, ionisation processes and the like. However, it is also aimed at introducing some fundamental aspects of gas-phase ion chemistry that will, hopefully, demystify these processes and will help the analyst in designing novel analytical protocols that can be easily implemented and that will yield complementary and supplementary information. Novel applications making use of such new developments will also be presented.

7.2 THE PROCESS

Mass spectrometry is based upon the *in vacuum* separation of ions, in the gas phase, according to their mass-to-charge (m/z) ratio. In its original form, mass spectrometry made use of a technique called electron impact (EI) to ionise the substances to be analysed. This form of ionisation is still the most widely used today. The principle is simple: a high-energy electron (e^-) beam , of nominally 70 eV, produced by the passage of a current through a filament (usually made of tungsten) is directed toward the substance of interest, M. The electron beam is sufficiently energetic to cause the removal of an outer electron from M thus producing an ion-radical, $M^{+\cdot}$, often termed erroneously "the molecular ion" (care must be exercised to remember that the species is an ion-radical, and not an ion). Equation (1) exemplifies the ionisation process.

$$M + e^- \rightarrow M^{+\cdot} + 2e^- \quad \textbf{(1)}$$

This process imparts a relatively high level of energy to the resulting ion-radical. This energy is generally excessive and cause the ion-radical to further fragment, *via* unimolecular dissociation processes, so as to release this excess energy. The two main pathways are given in equations (2) and (3).

$$M^{+\cdot} \rightarrow A^+ + B\cdot \quad \textbf{(2)}$$

$$M^{+\cdot} \rightarrow C^{+\cdot} + D \quad \textbf{(3)}$$

The first pathway, equation (2), is a dissociative process that produces an ion, A^+, and a radical, $B\cdot$, while the second one, equation (3), results in the

production of another ion-radical, $C^{+\cdot}$, *via* the release of a neutral molecule, D. These species are then subjected to a series of changes in electrical potential. The latter, while being ineffective on the non-charged species (radicals and neutrals), will direct the charged ones into a mass analyser. The mass analyser can be of several type; they will be introduced later in this chapter. In general terms, suffice it to say that all the species that enter into the mass analyser are subjected to electromagnetic forces that effect a separation of the ions according to their mass-to-charge ratio (m/z).

These steps, ionisation and dissociations, must be carried out *in vacuum* so as to avoid collisions between the ions of interest and other substances (*e.g.* neutrals and radicals). Taken together, such a series of unimolecular dissociations are termed fragmentation patterns. They are characteristic of the structural features of the original molecular ion radical, hence the extensive applications of mass spectrometry to structure elucidation problems.

The process described above implies a chemical reaction between the substance of interest, M, and an electron, e^-, followed by further non-reversible dissociation reactions. The latter is true for all modes of ionisation, as shown in the following sections. Hence, it must be noted that mass spectrometry is a destructive method of analysis. Fortunately, the technique is very sensitive and only a minute amount of material is required to perform an analysis (often of the order of few picograms or less). Furthermore, as shown later in the section dealing with linked-scanning techniques, a single sample introduction step is often sufficient to allow for the performance of several experiments.

At this point, it is necessary to stress that the brief introduction given above used positive ions as examples. However, it must be remembered that the same holds true for negative ions. Hence, an ionisation reaction such as that presented in equation (4) takes place simultaneously to that of equation (1) in an electron impact ion source. On a technical standpoint, negative ions can be observed as easily as positive ones; a simple change in voltage potential within the source allows for directing these ions out of the source instead of their positive counterparts.

$$M + e^- \rightarrow M^{-\cdot} \quad \textbf{(4)}$$

The energy imparted in species such as $M^{-\cdot}$ however, is much larger than that imparted in its positive counterpart, $M^{+\cdot}$. The cascade of unimolecular dissociations that follows is so important that it produces mass spectra that usually are devoid of molecular ion information (*i.e.* no $M^{-\cdot}$ is observed) and gives rise to rather unorthodox reactions that can hardly be related to conventional chemistry principles (*e.g.* benzene, C_6H_6, under electron impact conditions and recorded in the negative ion mode, exhibits a large ion at m/z 72 that corresponds to C_6^-!). As a result of the limited structural information that

can be derived from them, electron impact derived negative ion mass spectra are seldom recorded or referred to.

A large amount of information can be obtained from a positive ion electron impact mass spectrum. In fact, in addition to information on the molecular weight, it is often possible to derive a fragmentation pattern from the various dissociation ions recorded which is characteristic of the substance under study. Unfortunately, as for the negative ion mode, there are several substances where the energy imparted to the molecular ion radical is so large that the latter dissociates entirely thus producing a complex mass spectrum that is devoid of molecular weight information.

To circumvent this phenomenon it is possible to lower the energy of the electron beam that is used (from 70 eV to, say, 20 eV). This procedure is often used in cases where we know the substrate in order to enhance the intensity of the molecular ion. In the case of unknowns, however, it is a less widely practised procedure. The reason for this lies in the fact that if we lower the ionisation energy, we will be in a situation where we will not know to which extent we are allowing other reactions to occur. Furthermore, for comparative purposes it would be very difficult to maintain an effective library of mass spectra if the conditions used to record them varied between each substrate. One of the first advantage that comes to mind about mass spectrometry is the existence of extensive libraries of spectra that were recorded under electron impact conditions over the years. These libraries are available to anyone and the fact that specific conditions were kept while recording the spectra allows for their use in comparative work.

7.3 OTHER IONIZATION TECHNIQUES

Another way to alleviate the problem of lack of molecular weight information resides in the use of so-called "soft ionisation techniques". These techniques have been developed to provide the mass spectrometrist with means to obtain mass spectra that almost invariably contained molecular weight information. In addition, in many instances, the limit of detection is enhanced as a result of the lesser number of ion species being produced for a same quantity of ionised material (less ion species for the same total ion count). However, these techniques suffer from reproducibility difficulties and, generally, offer less structural information. These factors might account for the fact that libraries for such mass spectra were never tabulated.

We will introduce only two soft ionisation techniques. Both techniques selected here, chemical ionisation and fast atom bombardment, make use of very different phenomena. Our choice is not intended to be exhaustive, nor to be representative of all processes involved, it is merely used to demonstrate two main variations brought forth to obtain novel, innovative ways of ionising various substances, and yet yield informative mass spectra.

7.3.1 Chemical ionisation (CI)

The key principle underlying the electron impact ionisation (EI) process is the fact that substances are ionised under relatively high vacuum conditions, the number of ion-molecule collisions is very small, hence fragmentation patterns are almost exclusively the result of unimolecular dissociation reactions. The chemistry of such reactions is relatively simple, as exemplified by equations (2) and (3).

When the energy imparted by the ionisation step is too large, excessive fragmentation occurs and the molecular ion radical is not observed. Chemical ionisation (CI) was the first so-called "soft ionisation" technique designed to alleviate this problem and to be used regularly in many laboratories. The technique is based upon the preferential ionisation of a gas, termed reactant gas, that is introduced along with the substance to be analysed. The reactant gas is allowed in the ionisation chamber in amounts that are large relative to the sample to be ionised. The ionisation source design differs with that of EI in that it allows the operating pressure to raise to about two orders of magnitude above that of EI. Under such conditions, the reactant gas is ionised preferentially to the substance of interest and because of the relatively high pressure found in the source, the molecular ion radical of the reactant gas undergoes several collisions with other ionised and non-ionised species.

The energy imparted by such ion-molecule collisions is much less than that derived from the electron impact taking place under EI conditions. Hence the so-produced ions do not fragment extensively and deceivingly simple spectra are observed. For example, if methane is used as the reactant gas, reactions (5) through (8) take place.

$$CH_4 + e^- \rightarrow CH_4^{+\cdot} + 2e^- \quad \textbf{(5)}$$

$$CH_4^{+\cdot} \rightarrow CH_3^+ + H\cdot \quad \textbf{(6)}$$

$$CH_4^{+\cdot} + CH_4 \rightarrow CH_5^+ + CH_3\cdot \quad \textbf{(7)}$$

$$CH_3^+ + CH_4 \rightarrow C_2H_5^+ + H_2 \quad \textbf{(8)}$$

The species CH_5^+ and $C_2H_5^+$ are strong Brönsted acids and can ionise other species *via* proton transfer mechanisms such as those exemplified in equations (9) and (10). These same species are highly reactive (CH_5^+ has never been isolated on earth, however it has been observed in the interstellar space) and they constitute up to 90% of the ionised species in the source. Consequently, they act as the primary ionising species and contribute the most to this form of chemical ionisation process.

$$CH_5^+ + M \rightarrow [M + H]^+ + CH_4 \quad \textbf{(9)}$$

$$C_2H_5^+ + M \rightarrow [M + H]^+ + C_2H_4 \quad \textbf{(10)}$$

Elimination reactions such as those found in equations (11) and (12) occur readily when the substrate is a good proton donor.

$CH_5^+ + M \rightarrow [M - H]^+ + CH_4 + H_2$ **(11)**
$C_2H_5^+ + M \rightarrow [M - H]^+ + C_2H_6$ **(12)**

Other reactant gases are commonly used for CI work. Isobutane, ammonia are amongst them. Equations (5) through (8) have their counterpart for other reactant gases and the nature of such a gas will determine the mass increments to be observed when recording the actual spectra (*e.g.* isobutane will yield cluster ions corresponding to $[M + C_2H_5]^+$ and $[M + C_3H_7]^+$). Equations (13) through (15) show the reaction sequence that defines such parameters in general terms for a reactant gas R.

$R + e^- \rightarrow R^{+\cdot} + 2e^-$ **(13)**
$R^{+\cdot} + R \rightarrow [R + H]^+ + R\cdot$ **(14)**
$[R + H]^+ + M \rightarrow [M + RH]^+$ **(15)**

Direct charge transfer mechanisms such as that of equation (16) are also possible. You will immediately note, however, that the ionised species so-produced is that of an ion-radical, hence the same problem of stability noted previously for EI conditions would apply.

$R^{+\cdot} + M \rightarrow M^{+\cdot} + R$ **(16)**

It is interesting to note that the very nature of CI, namely to produce low energy ions, renders negative chemical ionisation a very useful technique. Unlike EI, CI allows for the generation of stable negative ion species. The ionisation processes that take place are similar to those just described; actually they are their electronic counterpart as evidenced by equations (17) through (21).

electron capture: $M + e^- + B \rightarrow M^{-\cdot} + B$ **(17)**
ionisation of reactant gas: $R + e^- \rightarrow R^{-\cdot}$ **(18)**
hydrogen radical abstraction: $R^{-\cdot} + M \rightarrow [M - H]\cdot + RH^-$ **(19)**
proton abstraction: $R^{-\cdot} + M \rightarrow [M - H]^- + RH\cdot$ **(20)**
molecular hydrogen abstraction: $R^{-\cdot} + M \rightarrow [M - H_2]^{-\cdot} + RH_2$ **(21)**

The combination of both modes of operation, positive and negative offers complementary information. This is why most modern instruments offer the possibility of recording what is known as a PPINICI spectrum, the acronym being derived from pulsed positive ion/ negative ion chemical ionisation. This method allows for the automated quasi-simultaneous recording of positive ion and negative ion spectra.

Finally, it must be stressed again that the appearance of spectra recorded under CI conditions is highly dependent not only on the nature of the reactant gas but also on the pressure (hence the temperature) inside the ion source. The actual configuration of the source may also affect the spectra, although to a lesser degree. This lack of consistency in the operating conditions account for the fact that there is no extensive compilation of chemical ionisation-derived mass spectra.

7.3.2 Fast Atom Bombardment (FAB) and Secondary Ion (SIMS)

Fast atom bombardment mass spectrometry (FAB-MS) is a renewed old technique that is most often thought of in terms of a relatively novel mass spectral technique. In fact, as early as in 1966, Devienne and co-workers presented data on a technique that they called molecular beam for solid analysis (MBSA) [1]. The idea was further developed by the same group but was ignored by the rest of the scientific community until the announcement by Barber *et al.* [2] and by Surman and Vickerman [3] of the discovery of FAB stimulated efforts throughout the world as well as a number of international symposia and workshops devoted in whole, or in part to the understanding of FAB and its applications.

7.3.3 Principles and Instrumentation

The overall diagram of a fast atom bombardment ion source is fairly simple. It consists of three main elements; i) an atom gun, ii) a sample inlet, and iii) an ion extraction system. The atom gun is made up of an evacuated chamber that encloses a plate to which a high voltage potential (nominally 8 kV) is applied. The gas to be used for the "bombardment" is allowed into the chamber, through an appropriate inlet, where it is ionised by the high potential plate (see equation (22)). The ion beam so created is repelled by the same plate (at 8 kV) and, to a certain extent, regains its neutral character by electron-capture or by charge-resonance processes such as those exemplified by equations (23) and (24).

$$B + \text{high potential} \rightarrow B^{+}_{fast} \quad \textbf{(22)}$$

$$B^{+}_{fast} + e^{-} \rightarrow B_{fast} \quad \textbf{(23)}$$

$$B^{+}_{fast} + B \rightarrow B^{+} + B_{fast};\ E = 0 \quad \textbf{(24)}$$

Since the atoms do not suffer much loss in momentum they exit the atom gun and are aimed at the target where the sample is located. A high voltage plate, positioned at 90 degrees with respect to the atom beam, is used to deflect the remaining ions that have not been neutralised. Thus only the atom beam reaches the sample to be analysed.

In the past, workers in the field have used separate charge exchange chambers to carry out the neutralisation process described above. However, the source becomes extremely simple once it is realised that any high-pressure confined-discharge ion source will produce large quantities of fast neutral species. These arise by charge-resonance exchange between the ions produced in the discharge and the high-pressure non-ionised gas in the gun itself (equation (24)).

Saddle field-type ion sources are compact, simple and efficient. They have been widely adopted for this purpose. Their characteristics are well documented and they have been used since the early development of FAB.

The sample is loaded onto the tip of a probe along with a support-matrix (the following section deals in greater detail with the reasoning for the use of such a medium) which is inserted into the conventional ion source of the mass spectrometer at a location such that it intercepts the incoming beam of fast neutrals (from the atom gun). The angle of incidence of the beam is of importance and an angle of 70 degrees (*i.e.* 20 degrees with respect to the sample) is a good value. This gives rise to a sputtering phenomenon and the secondary ions so produced are then subjected to the effect of the ion extraction system that is already built into the mass spectrometer, *i.e.* an extraction plate (nominally at 6 kV) and a centring plate to focus the accelerated secondary ion beam into the molecular slit of the mass analyser.

The technique is very closely related to another condensed state ionisation method, secondary ion mass spectrometry (SIMS) but differs from this in that the accelerated inert gas ions used in SIMS are being charge-exchanged prior to the bombardment of the sample. On a theoretical basis it can be argued that the bombarding ions in SIMS effectively become bombarding atoms through a mechanism known as the Auger effect. Experimentally, the same ion gun is used in both methods. It has been demonstrated that the ion beam in SIMS contains many neutral atoms. This results from the fact that no means are deployed to prevent the spontaneous charge-exchange reactions from taking place.

On the other hand, turning off the deflector plates, used in FAB to clean the atom beam from residual ions that have not charge-exchanged, still produces a FAB-like spectrum. Devienne and Roustan, who have performed SIMS *versus* FAB studies on organics, did not report on the evidence, or lack thereof of a close similarity between the techniques and more recent SIMS studies indicate that it is possible to obtain SIMS results that are similar to those obtained by FAB.

It is not expected that the types of analyser and detector used in the mass spectrometer should be critical for the successful recording of FAB spectrum and thus far, the literature supports this statement. Single- and double-

focusing magnetic instruments as well as triple analysers have been used, as have single-quadrupole ones. By analogy to their use in SIMS experiments, time-of-flight instruments can also easily be converted to FAB. New ion sources can be purchased for older instruments, or a saddle field ion gun can be attached with relative ease and little modification and expense to existing FD, EI or CI sources. The most valuable aspect of FAB is its simplicity.

Other standard options available on modern mass spectrometers can also be carried out while using FAB as the ionisation mode. Metastable studies and linked-scan techniques to assign ion fragmentation pathways are possible as are collisional activation experiments to enhance fragmentation. Mass spectra obtained by FAB (including relative intensities) are reproducible when recorded on a given instrument as well as when recorded on widely different instruments. High resolution accurate mass measurements of FAB-generated ions was also shown to be possible but with some difficulty.

7.3.4 Sputtering

The sputtering phenomenon always held out the promise of being used as a general solid-state ionisation technique. It has been used for some time as a means of surface and bulk elemental analysis of solids in the ion microprobe. The phenomenon, which was first reported in 1852, is simply described. When a solid is bombarded by high-velocity particles, *e.g.* rare gas ions, of about 8 kV energy, then some of the solid material is taken into the gas phase. This is the result of momentum transfer from impinging particles to the target, setting up collision chains (some of which occur across the surface). The sputtered material can bear either positive or negative charge. Robb and Lehrle demonstrated the feasibility of such an ion source but credit is to be given to Benninghoven and co-workers along with Macfarlane for sharing the uniquely advantageous mass spectral results that can be obtained with organic compounds with such a source. In each of these studies, the quality of the results obtained was limited by the inherent performance of the mass spectrometers that were used, the technology of producing fast beams of rare gas atoms with controllable kinetic energy being well known.

7.3.5 Matrix Support

In early experiments, charged particles sputter sources were used, and the sample was deposited as a solution onto the probe and the solvent was evaporated to dryness before analysis. This method yielded mass spectra that were transient in nature with a relatively short lifetime (tens of seconds). Subsequently it was noted however that low vapour pressure liquids and oils gave spectra that lasted for hours. Examples were among a whole variety of pumping fluids such as Apiezon oils, Santovac 5, Convolex 10 and also some siloxanes frequently encountered as contaminants in organic samples. These early observations led to the search for low vapour pressure viscous solvents to

make a solution of the material under study so as to model the behaviour of fluids doped with solids.

One of the first successful solvents used was glycerol, it gave enhanced sensitivity (compared with solid sample preparations) and much longer sample lifetime (hours) provided that enough sample and glycerol was present to continue modelling the fluid conditions. A series of different solvents have also been used in FAB analysis: polyethylene glycol (PEG-200, 400 *etc.*), thioglycerol, ethanolamine, diethanolamine, macrocyclic ether (*e.g.* 18-crown-6), *etc.*. Glycerol, however is still, and by far, the most widely used solvent. These solvents exhibit their own characteristic spectra on top of that of the substance under study. This effect is often seen as a drawback as it can mask some of the peaks related to the solid sample and in most cases it complicates interpretation by adding unwanted peaks to the spectrum. For example, glycerol shows peaks of decreasing intensity at every [(n x 92) + 1] daltons corresponding to n glycerol molecule(s) solvating one proton. If a trace of a sodium salt is present, as it is often the case with samples obtained from some form of chromatographic separation technique, then another series of peaks at every [(n x 92) + 23] daltons arise in the spectrum.

On the other hand, the molecules under investigation might have the right surfactant properties and bulk solubility to give a mass spectrum in which the solvent background is totally suppressed. It has been claimed, after studying chlorophyll A, that for best results, the solid sample needed to be completely dissolved in the solvent rather than simply dispersed. In our laboratories, the latter has rarely been true [4, 5].

In principle, however, the objective is to submit the sample to the atom beam at a highly mobile surface concentration and for maximum sensitivity the sample should form a perfect monolayer at the surface of a substrate having low volatility. This is a characteristic of compounds that exhibit high surface activity in aqueous media, attributable to the presence of highly polar or ionic groups, giving hydrophilic properties to an otherwise hydrophobic molecule. Monolayer formation at the surface of a dilute solution implies a constant surface excess concentration. Following Gibbs, this arises when the surface tension depends linearly on the logarithmic bulk concentration ($\log_e C$) of the solution. In our example from above, the ratio of peaks due to glycerol to those due to the sample cation falls to zero as the monolayer becomes established. Under monolayer conditions, glycerol ions are absent from the spectrum, and the solute exhibits a maximum sputter ion yield that is independent of the bulk concentration. Additionally, since there is no increase in ion yield as we increase the solution concentration in this range, care must then be exercised for quantitative applications as we observe an "apparent" decrease in sensitivity measured relative to this concentration.

Since a monolayer of material is completely sputtered in a matter of seconds in a typical FAB ion source, it is essential that the sample surface be continuously regenerated during prolonged examination. This is done *in situ* by diffusion of the sample to the surface of the solution. It is therefore essential that the sample have some solubility in the low volatility solvent, or that it binds to the matrix, to provide the diffusion mechanism and also to act as a reservoir of material. Ionic groups that render compounds involatile, thus ruling out conventional methods of ionisation, are also those groups that frequently lead to solubility in polar solvents, and to the associated surfactant properties that facilitate good sample preparation for FAB ionisation. It follows that the detection of solvent substrate peaks in a FAB mass spectrum implies that optimal sample preparation has not been achieved. These conditions, however, are far from being atypical.

The sputtering of neutral species, which are not detected by the mass spectrometer, is probably the major process occurring at the surface. Similarly, the simple sputtering of ions that are naturally present in the sample, undoubtedly, must constitute an important source of ions in FAB mass spectra. Consequently, sample preparation methods such as spiking with various additives which lead to an increase in the concentration of ionic material in the sample, can lead to an enhanced sensitivity. Despite considerable speculation on the subject, the mechanism of ionisation in the sputtering of non-ionic compounds is still the subject of considerable controversies and eludes full understanding.

The complex solution and surface chemistry involved in a typical sample can lead to large apparent differential sensitivities between quite similar compounds. Nevertheless, the FAB ion source has proven to be a valuable method for the recording of mass spectra of compounds that were previously considered to be intractable by mass spectrometry because they were too ionic and too involatile. Without doubt the californium-252 source is the leader in terms of bombardment technique with respect to high molecular weight determination and this situation is likely to persist if we take into account the large amounts of energy available in this sputter process.

The exact role of the support matrix is ill-defined. In addition to the phenomenon just described, the matrix can influence stereochemical aspects by inducing, or forming, a given conformation of the sample and with such a high energy, it is also reasonable to assume that there might be some solvent-solute reactions taking place. It appears, therefore, that data on factors such as solubility, ionic character, charge localisation, stereochemistry, degree of interaction between solvent and solute, volatility, concentration, *etc.*, are necessary for the accurate prediction of the success, or otherwise, of an attempted FAB mass spectrum. The complexity of the process warrants further careful examination of the stereochemical aspects however, since some of the factors previously mentioned (solubility, ionic character, *etc.*) are readily

accessible and have been shown not to be of prime importance in the cases reported to date.

7.4 INSTRUMENTATION

The instruments commercially available to perform mass spectrometry are a reflection of the technique itself, very diversified. No matter what their degree of complexity is, they are all composed of similar basic components that can be described as follows: a sample introduction inlet, an ion source, a mass analyser, and a detector.

Each and every one of these components can be found under a variety of forms and shapes all presenting advantages, drawbacks, special applications, or the like. For the purpose of this chapter we will briefly overview each main component and we will end this section by the mass analyser. One type, namely double-focusing instruments, will be discussed in greater detail.

Mass spectrometry is able to analyse gases, liquids and solids. Consequently, the sample introduction inlet can take numerous shapes and forms. In its most simple form the inlet was designed for solids. It consists simply of an evacuation chamber that allows the operator to pump down the air surrounding the sample. The solid is then introduced directly into the ion source where it sublimes under the high vacuum conditions present there. The gaseous molecules are then subjected to ionisation as described earlier. The main factor to be remembered here is the fact that at the time where ionisation takes place, the sample be in the gaseous state.

Sample inlets can also be interfaces that allow the effluents of a variety of powerful separation techniques to enter the ion source at a rate that allows for vaporisation to take place. Hence, acronyms such as GC-MS, LC-MS, SFC-MS, *etc.*, relating to gas chromatography, liquid chromatography, supercritical fluid chromatography, *etc.* coupled to mass spectrometry are now well established in the jargon of the analytical community as these techniques have been widely accepted and they can be interfaced to any type of modern mass analyser.

The processes that take place in the ion source have already been described under the sections on the process and on the other ionisation techniques. The ion source itself consists in a chamber where the gaseous sample is subjected to one of the ionisation modes described earlier. The source is floated at a given potential and the resulting electrical field directs the ions out of the source. Various electrical lenses and slits are attached to this chamber, normally right at the exit, in order to focus the ions onto a single trajectory for their trip toward the mass analyser. The values of this potential and of the voltages applied to the lenses vary with the type of mass analyser used to subsequently separate the ions that exited the source. One example is provided below along with the description of a so-called double-focusing mass analyser.

The detector is simply a means of detecting ions. Electron multipliers were the preferred choice for a long time. They are now being replaced by longer lasting photomultipliers. The object of the detector is to detect reproducibly and in a recordable fashion a signal resulting from the interaction between the ions that left the mass analyser and that were focused onto the detector. That response must be proportional to the number of ions that reach the detector in order to allow for quantitation and structural information to be obtained. The next section will show that the relative abundance of fragment ions within a given mass spectrum is very informative of the structure of the original parent ion.

The mass analyser is the most important part of the mass spectrometer. Its main function is to separate ions that enter it according to their mass-to-charge ratio, m/z. You will recall from the theory of electromagnetism that it is possible to deflect the trajectory of charged species when the latter are submitted to a magnetic field or to an electrical field. Numerous electromagnetic devices are able to achieve this. Historically a magnetic field resulting from an electromagnet was used. These instruments were referred to as "single focusing" spectrometers. Although several "venerable" units are still in operation their commercial production has ceased. They have been replaced by smaller units based upon quadrupole technologies, or more recently, ion trap technologies. These instruments offer the advantage of being much easier to use and to maintain. Ironically, the theory behind these phenomena is much more complex (ions moving across a quadrupole-induced field adopt trajectories that can only be described by highly complex mathematical equations).

On the other hand, larger and more powerful spectrometers were developed whereby use was made of both electrical (E) and magnetic (B) fields in series, to accomplish an enhanced degree of ion separation. The term double-focusing spectrometers refers to these instruments. Historically, the electrostatic sector was placed right after the ion source, before the magnetic sector (see Figure 1), hence the term "conventional-geometry" was adopted. "Reversed-geometry" instruments, however, were more prominent as they offered more possibility to the operator in terms of linked-scans experiments (see next section). Double-focusing instrumentation will be described here in greater detail.

Figure 1 depicts, the main components of a double-focusing, normal geometry, mass spectrometer. Although one could scan any of the fields (the accelerating potential (V), the magnetic (B) or the electrical (E) fields), under normal operating conditions, V is set at a constant value (nominally 6-10 kV). The ions produced in the ion source are accelerated at V and exit (if of the proper charge) it *via* a molecular slit and transit through a region of the instrument that is not subjected to any field (the first field-free region). They subsequently enter the electrostatic sector where they are subjected to E that will have for effect to curve their trajectory. After exiting the electrostatic sector the ions go through a second field-free region, enter the magnetic sector (where B deflects them again) and finally reach the detector after exiting the magnetic sector.

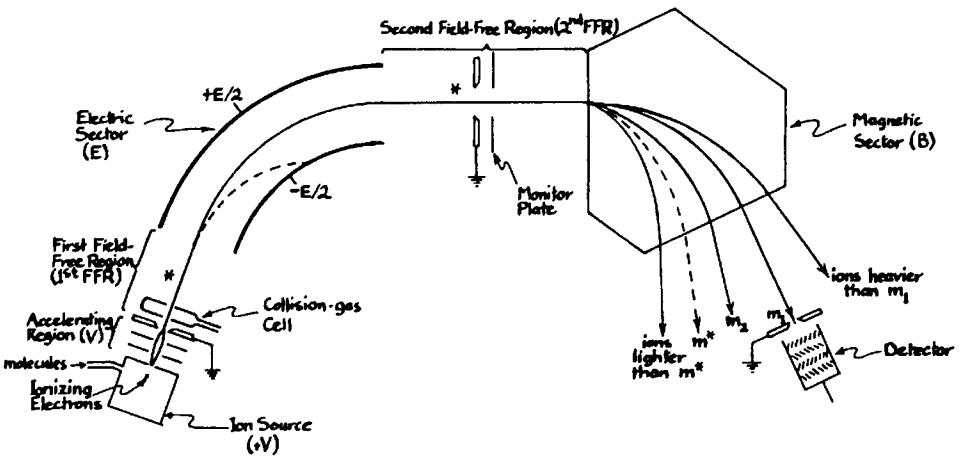

Figure 1: Schematic representation of a double-focusing mass spectrometer of normal geometry. The accelerating potential, V, is set at a constant value whereas the magnetic and electrical fields, B and E, are scanned so as to transmit stable ions m^+ (or $m^{+\cdot}$). Thus, fragment ions formed in the first and second field free regions are lost onto the walls of the magnetic and electrostatic sectors, respectively. Note that the magnetic field, is perpendicular to the plane of the page. Figure 1 is reproduced from reference 6 with permission of the copyright owner.

The degree of deflection that affects each charged species in each sector is dependent upon the mass and the charge of the species. In the next section, under linked-scanning techniques, you will find equations [25] through [29] that describe, mathematically, the effects that are inflicted upon the ions as they traverse the various sectors. These equations will be used later to demonstrate how to build a genealogical tree for a particular ion (ascending or descending).

They also imply that it is possible to discriminate between ions according to their velocity (the electrostatic sector) as well as to their mass (magnetic sector). It is this combined ability that allows for the performance of so-called high resolution mass measurements. Mass spectrometers could be thought of as very precise balances. So precise in fact that they can differentiate between the masses of CO^+, $N_{2+\cdot}$ and $C_2H_{4+\cdot}$ (respectively 27,9949, 28,0071, and 28,0313 daltons). The resolution required to differentiate these species is defined as the ratio of the mass to be measured to the incremental mass to be determined (*i.e.* M/ DM). In this particular case to differentiate between CO^+ and $N_{2+\cdot}$ requires a resolution of about 2 300 (from [28 / (28,0071 - 27,9949)]). The resolution is affected by several factors such as the rate at which the fields can be scanned, the difference between the masses to be determined, *etc.*

7.5 LINKED-SCANNING TECHNIQUES

This section is concerned with just one aspect of the relatively new development that has been termed in various ways such as mass separation/mass spectrometry or mass spectrometry/mass spectrometry (both offering the same acronyms MS/MS), two-dimensional mass spectrometry, tandem mass spectrometry, *etc.*. The acronym MS/MS is the most appropriate and is certainly the most widely used. The definitions and the nomenclature relevant to these techniques will be introduced as they will arise in our mathematical development of the scan laws.

As discussed in the introduction, a conventional mass spectrum is the result of several unimolecular dissociation processes. These can be represented by making an analogy to a genealogical tree such as that presented in Figure 2. In a standard mass spectrum all of the genealogical information is lost. However, it is possible to select one variable, namely one precursor ion, one daughter ion or one common neutral loss, and to perform some well-defined empirical procedures to regenerate the connectivity information. These relationships can be seen as two-dimensional mass spectra in which the ion current is now a function of two distinct variables, namely the mass-to-charge ratio of the precursor ion and that of the fragment ion. This can explain, in part, why the acronym MS/MS was adopted; it is a direct analogy to GC/MS where in both cases the ultimate characterisation is carried out by a mass spectral measurement, the difference lying in the initial separative process used (gas chromatography *versus* mass spectrometry).

MS/MS techniques can be performed on double-focusing sector instruments as well as on quadrupole or hybrid instruments. For the purpose of this discussion will concentrate on a condensed survey of double focusing sector instruments. References that provide substantial accounts on quadrupole and hybrid instruments used for MS/MS can be found in the bibliography at the end of this chapter.

It is not necessary to develop a full ion optics theory of ion trajectories in a double-focusing mass spectrometer to appreciate the fundamental principles involved in the development of linked-scan laws. For our purposes it is only necessary to use a one-dimensional model which considers only ions whose velocities are restricted to the main beam axis, usually denoted as the x-axis. In other words we ignore the other velocity components in the y-direction (*i.e.* the direction of the radial electric sector field) and in the z-direction (the so-called slit height direction). This approximation is acceptable if we consider the large difference in the kinetic energy ranges involved, nominally in the kilovolts for the x-axis versus a maximum of one volt for the y- and z-directions. The order of the two sectors does not affect the overall double-focusing action of the pair, the relatively small velocity dispersions for ions produced in the ion source can be fairly easily arranged to cancel exactly.

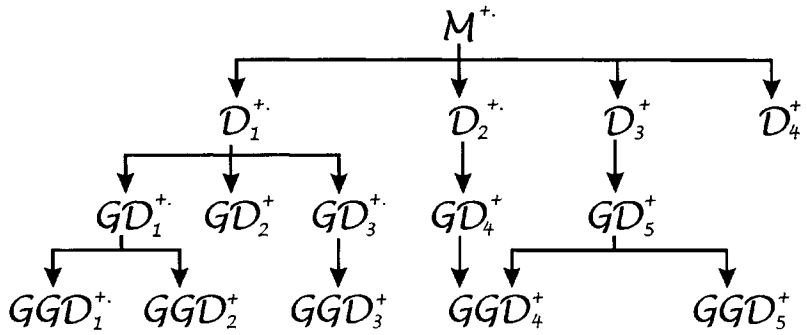

Figure 2: Hypothetical sequence of ion fragmentations occurring in a mass spectrometer; M stand for the parent, D daughter, GD grand daughter and GGD for grand grand daughter.

The magnetic sector creates a dispersion of ions according to their momentum-to-charge ratios, while the radial electric sector disperses them according to their ratios of kinetic energy-to-charge. In a one-dimensional model these results yield the following set of equations:

For the magnetic sector:

$B\,(zev) = mv^2/R$ **(25)**
$mv/ze = BR$ **(26)**
$m/ze = B^2R^2/2V$ **(27)**

where m = mass, ze = electric charge, v = velocity of ion (in x-direction), R = magnet radius, V = accelerating potential, B = magnetic field strength.

For the electric sector:

$mv^2/2 = ze\,V$ **(28)**
$E\,ze = mv^2/r$ **(29)**

where E = electric field strength, r = radius or circular trajectory in E.

Equation (25) represents the equivalence of the force created by the magnetic field over the beam of ions crossing the magnetic sector and the centrifugal force associated with the resulting trajectory. Equation (26) is simply a rearranged version of equation (25) whereas equation (27) is also a rearranged equation where the velocity was removed from the equation. This same equation is the basis for the use of the magnetic sector as a mass analyser. Equation (28) is a simple expression of the kinetic energy that the ions acquire when accelerated by the potential V and equation (29) is the expression of the

equivalence between the force exerted by the electric field on the moving electrons and the resulting centrifugal force.

The last information needed to understand the origins of the scan laws is the fact that the velocity of the fragments is the same as that of the precursor ion that fragmented to produce them (that is if we ignore any contribution to the kinetic energy of the fragments from the internal energy of the precursor ion). This result is derived briefly below for any system such as that described by equation (30) and the associated classical mechanics equations (31) through (33).

$M_1^{+\cdot} \rightarrow M_2^+ + M_3\cdot$ **(30)**

$m_1 = m_2 + m_3$ **(31)**

$m_1v_1 = m_2v_2 + m_3v_3$ **(32)**

$m_1v_{12} = m_2v_{22} + m_3v_{32}$ **(33)**

Equation (30): Dissociative process

Equation (31): Conservation of mass

Equation (32): Conservation of the linear momentum. Holds only if the dissociative process takes place in a field free region.

Equation (33): Conservation of kinetic energy. Holds only if the internal energies of the products equal that of the reactant prior to dissociation (*i.e.* a zero kinetic energy release process).

To be meaningful, m_1, m_2 and m_3 must have real positive values and in the centre-of-mass system, the kinetic energy balance of equation (33) becomes 0 (*i.e.* the left term of the equation is 0). Then the only way to satisfy equation (33) is for:

$v_1 = v_2 = v_3$ **(34)**

If there is kinetic energy release however, the peak shapes will be affected but the basic findings will remain the same and the mathematical treatment is not necessary for experimental work to be performed adequately. This report will not make any use of the changes in internal energy, T, occurring during some dissociative processes. Reviews on the subject are available.

The method used to derive scan laws is a systematic procedure that can generate a large number of possibilities. However, if we accept as feasible only the scan laws that meet the following two criteria:

i) scan laws in which at most two of the three fields (V, B, E) are varied simultaneously; and

ii) scan laws where the functional relationships between the fields is relatively simple so that it can be performed accurately and precisely enough to be useful;

then the number of scan laws is more reasonable.

A review by Boyd [6] described the mathematical derivation of most scan laws that meet these criteria. They are summarised in Table 1.

A few comments about Table 1 are necessary at this point. The list of linked-scan laws found in that table is complete (although not exhaustive) with respect to the two criteria selected. Where several linked-scan laws yield exactly the same information, only the one that offers the most advantages was included. For example a linked-scan law of B_2/V can be derived (for pre-selected mass m_1 and fragmentation occurring in the second field free region). But since the operation would require both, control of the magnetic field and ion source de-tuning and that none of these disadvantages applies to the widely used "MIKES" scan (mass analysed ion kinetic energy spectrum, *i.e.* scanning E only, Table 1) it follows that the scan law was omitted from the table.

TABLE 1[1]
Linked-Scan Laws for Double-Focusing Mass Spectrometer

Mass	Linked-Scan Law	v discrimination	Ref.
First Field-Free Region Fragmentations[2]			
m_1	$(V/E^2) = V_o/E_{o2}$; $B = B_1$	yes	7, 8
m_1	$(B/E) = B_1/E_o$; $V = V_o$	yes	9-11
m_2	scan V only; $E = E_o$; $B = B_2$	no	12
m_2	$(B^2/E) = (B_{22}/E_o)$; $V = V_o$	no	9
m_3	$(B/E) \times (1 - (E/E_o))^{1/2} = (B_3/E_o)$; $V = V_o$	yes	13-15
Second Field-Free Region Fragmentations[3]			
m_1	scan E only; $V = V_o$; $B = B_1$	no	16
m_2	$(B^2 \times E) = (B_{22} \times E_o)$; $V = V_o$	yes[4]	17
m_2	$(E/V^2) = E_o/V_{o2})$; $B = B_2$	yes[4]	17
m_3	$B^2 \times (1 - (E/E_o)) = B_{32}$; $V = V_o$	yes	17

Notes: 1. adapted from reference [6] (with permission of the copyright owner); 2. valid for instrument of either configuration; 3. valid only for instruments of reversed geometry; 4. very high velocity discrimination.

Furthermore, scan laws accounting for successive fragmentations (*e.g.*, first dissociative process in the first field free region and the subsequent one occurring in the second field free region) can also be derived. The latter, however, have not been included in Table 1.

It is interesting to note the greater versatility of the reversed geometry instruments over their conventional geometry counterparts. It lies principally in their ability to study dissociative processes taking place in the second field free region *via* linked-scan techniques (in conventional geometry these fragmentations can only be studied in a fashion identical to metastable ion studies in a single focusing instrument).

Finally it is important to stress (again) that if a particular scan law involves no velocity discrimination then the shapes of the peaks obtained by such a scan will reflect the full kinetic energy release distributions. This information can be of value but is obtained at the cost of resolving power (typically a few hundred). That information would not be directly useful for the goals that are to be set in this study and will not be discussed further here.

The two scan laws that were chosen for the purpose of this study are the B/E and the B^2/E. Reasons for this choice are numerous but the most important ones are their universality (applicable to instruments of either configuration) and their accessibility on commercial instruments without excessive extra costs.

7.5.1 The B/E scan

If the standard dissociative process of equation (30) occurs in the first field free region and V_1, B_1, and E_1 specify the conditions that allow the transmission of M_{1+}. then, from equation (28):

Energy of $M_2^+ = (m_2/m_1)V_1\,ze$ **(35)**

and from equation (26):

Momentum of $M_{2+} = (m_2/m_1)\,m_1v$ **(36)**

In order to collect the M_{2+} ions, and form equations (29) and (34), E must be adjusted to a value E_2 such that:

$E_1/E_2 = m_1/m_2$ **(37)**

Similarly, for the magnetic field B and from equations (26) and (34):

$B_1/B_2 = m_1/m_2$ **(38)**

From the last two equations (37) and (38):

$B_1/B_2 = E_1/E_2$ or B/E = constant **(39)**

The constant in equation (39) is determined by the pre-selected precursor ion $M_{1+\cdot}$. Hence a scan of B and E where the relation B/E is held constant yields all the daughter ions M_{2+} that arose from unimolecular dissociation of $M_{1+\cdot}$. This technique does not de-tune seriously the ion-source.

7.5.2 The B^2/E Scan

Considering the same dissociative process (equation (30)), it is possible to rewrite equations [35] and [36], respectively, as follows:

Energy of $M_{2+} = (m_2/m_1)\ V_1\ ez = m_2v_2/2$ **(40)**
Momentum of $M_{2+} = (m_2/m_1)\ .\ m_1v = m_2v$ **(41)**

Therefore, to collect the M_{2+} ions the following must be set:

Electric sector: $m_2v^2/r = E_2\ ze$ **(42)**
Magnetic sector: $m_2v = B_2R\ ze$ **(43)**

Combining equations (42) and (43) yields equation (44):

$B_2^2/E_2 = (m_2/ze)\ (r/R^2)$ = constant **(44)**

The constant in equation [44] is determined by the pre-selected daughter ion M_2^+. Hence a scan of B and E where the relation B^2/E is held constant yields all the precursor ions $M_1^{+\cdot}$ that unimolecularly dissociated to produce the daughter ion M_2^+.

7.6 APPLICATIONS OF MASS SPECTROMETRY IN FOOD SCIENCE - APPLICATIONS OF GC/MS

The main application of GC/MS in Food Science is in the area of flavour analysis. Food flavours are complex mixtures comprising a large number of functional groups in varying concentrations. Their numbers may range from 50 to 300 in fresh products such as fruits and vegetables to more than 700 in foods subjected to thermal processing such as roasting and baking. Today, more than 5000 flavour compounds have been identified in food products; the majority of them by GC/MS analysis.

Analysis of food flavours poses a special problem due to several factors. The flavour compounds represent less than 0.1 % of the weight of the food product, with components differing widely in their physical and chemical properties. Moreover, some flavour components such as terpenoids are thermally labile while others are very reactive, if special care is not exercised during their isolation, concentration and subsequent analysis some of the components could

be lost. A further complication may arise from the presence of trace components having low sensory detection thresholds, such compounds, even when present in ng/g levels can influence the overall flavour more than other volatiles present in much greater amounts.
It is clear from the preceding discussion that during sample preparation and analysis, extreme care should be taken so that the isolate retains the sensory properties of the food from which it was isolated.

7.6.1 Fractionation of the sample prior to GC/MS analysis

The complexity of flavour isolates and vast differences in the relative concentrations of individual compounds make it difficult to identify trace components in such mixtures even with the use of efficient capillary columns. A common approach to simplify the complexity of flavour isolates is to fractionate the sample into non-polar, moderately polar and strongly polar components by silica gel chromatography or separate the components into acidic, basic and neutral fractions by acid and base extractions.

7.6.1.1 Examples

The number of GC/MS studies of flavour volatiles is increasing every year. These studies include different food products such as fruits and vegetables, alcoholic beverages, cereals and grains, meat and fish products, essential oils and spices, prepared foods, *etc.*. GC/MS analysis was used to identify the volatiles of apple [18], beer [19], corn [20], cooked meats [21], cloves [22], Mayonnaise [23], *etc.*. Most of GC/MS analyses list a large number of components that contribute to the general background note of the particular food product. Only few examples are available that describe the identification of flavour impact compounds. Demole *et al.* [24] for example, identified the flavour impact compound of grapefruit juice, after careful multi-step chromatographic separation of the sample. 1-*p*-Menthene-8-thiol was found to have a threshold value of 2×10^{-5} ppb in water.

7.6.2 Applications of LC/MS

The advantage of high performance liquid chromatography over gas chromatography is that it can be used for the analysis of thermally labile or involatile organic compounds. Furthermore, minimal sample clean-up is required when using techniques such as pre-column concentration or column switching. However, liquid chromatography columns do not have the separatory power of GC columns (nominally 10,000 theoretical plates *versus* 250,000 plates for capillary GC columns - see appropriate chapters in this book). Unlike GC, current LC technology necessitates extensive method development for each class of compounds to be analysed. A number of applications of LC/MS have been developed for classes of compounds relevant to

Food Science such as lipids, carbohydrates, amino acids, nucleosides and vitamins.

The type of compound to be analysed by LC/MS and the ionisation source is usually determined by the type of interface used. Very volatile compounds are lost and heat sensitive compounds are decomposed using moving belt interface. Direct liquid introduction (DLI) interfaces are good for thermally labile compounds but they can be used only in conjunction with CI ionisation mode. Thermospray interfaces can ionise non-volatile organic compounds such as carboxylic acids, sugars and sulfonic acids, however, the resulting spectra are dependant on the solvent used. The advantage of particle beam interfaces is that they can produce classical EI spectra and they can be used for analysis of amino acids, alcohols, amides, ketones and esters.

7.6.2.1 Examples

LC/MS with direct liquid introduction (DLI) interface has been used for the analysis of glycerides. McFadden *et al.* [25] used methane gas for CI LC/MS analysis of coconut triglycerides. Ammonia has been widely used as a reagent gas for CI LC/MS analysis of di- and triglycerides. The latter yields abundant $[M + 1]^+$ and $[MH - RCO_2H]^+$ ions. Using this method various triglycerides have been characterised in corn oil and peanut oil [26, 27]. Underivatized mono- and di- saccharides have been analysed by DLI LC/MS [28] to obtain molecular weight information. Tsuge [29], using the same interface characterised underivatized amino acids.

7.6.3 Applications of FABMS

The group of compounds amenable to FABMS analysis is similar to that analysed by FD that is non-volatile polar solids, however, FAB is more suited to high molecular weight very polar solids and FD to compounds of lower polarity. The characteristic feature of FABMS spectra is the presence of intense $[M + H]^+$ ion in addition to considerable number of characteristic fragment ions that are useful for structure analysis.

In addition to molecular weight information, Fast Atom Bombardment Mass Spectrometry can also be used for sequencing polypeptides and oligonucleotides. One such example is the study of the amino acid sequence in the oligopeptide Antiamoebin I by Taylor *et al.* (30) by a combination of FAB and B/E-linked scans. This peptide contains 16 amino acids. The peak at m/z 1670 is the quasi-molecular ion $[M + H]^+$. A linked-scan experiment of the B/E type performed on this ion produced a peak at m/z 1422 which presented confirmatory evidence a loss of the terminal proline.phenylalaninol.H group. A similar B/E scan from the latter ion produces ions at m/z 1337 and m/z 1244 for the loss of aminobutyric acid and hydroxyproline.amino-isobutyric acid, respectively. This process can be repeated until all the amino acids are

sequenced. The presence of abundant fragmentation of polysaccharides has been exploited for glycosidic residue analysis by FABMS for sequence determination. Compounds with molecular weights up to 4000 amu have been analysed by FABMS.

7.6.4 Applications of MS/MS and linked-scan techniques

The main advantage of MS/MS is its ability to analyse specific target molecules directly from biological matrices without any sample preparation. One important application of MS/MS in food analysis can be the rapid screening of intact fruits or vegetables for the presence of mycotoxins or pesticides. For example intact lettuce leaves can be introduced directly into the ion source and analysed for the presence of the pesticide parathion. The CAD (methane gas) spectrum of this pesticide shows the parent ion at m/z 291 and two daughter ions at m/z 169 and m/z 154. If the peak at m/z 291 of the normal spectrum of the contaminated lettuce leaf is selected and its CAD spectrum is recorded and

TABLE 2
Further Examples of Applications of Mass Spectrometry in Food Science

Sample	Type of Analysis	Ref.
Amadori Products	EIMS	34
Grapefruit	MS/MS	35
Nutmeg	MS/MS	36
Mycotoxins	MS/MS and FAB	37, 38
Kiwi	GC/MS	39
Orange Juice	GC/MS	40
Pesticides in food	GC/MS	41
Tea	GC/MS	42
Red pepper	GC/MS	43
Fatty acids	GC/MS	44
Fresh fruits	GC/MS	45
Fermented foods	GC/MS	46
Food dyes	LC/MS	47
Vitamins	LC/MS	48
Carbohydrates	LC/MS	49
Nucleosides	LC/MS	50
Nucleotides	FAB	51
Phospholipids	FAB	52
Chlorogenic acids	FAB	53
Anthocyanins	FAB	54
Amino acids	FAB	55
Fruits Heterosides	FAB and MS/MS	56
Cholesterol	B/E	57
Various	general	58 - 62

compared to that of pure parathion, a positive identification can be made about the presence of the pesticide. To achieve the same results with GC/MS, a multi-step extraction and time consuming chromatographic separations will be required.

Similar results can be obtained by operating double-focusing magnetic sector instruments in the B/E - linked scan mode. In this mode, the ratio of B to E is kept constant as B is scanned. The resulting spectrum contains fragment ions from a selected precursor ion. Warburton *et al.* [31] used the B/E - linked scan mode to show that the peak at m/z 210 in the lemon juice corresponds to citric acid, and the m/z 369 peak in the egg yolk is due to cholesterol. In our laboratories we have used the same technique to elucidate the mechanism of ß-carboline formation in food from tryptophan Amadori product and the mechanism of pyrrole formation from lysine Amadori products [32, 33].

Table 2 summarises some typical references on the applications of mass spectrometry to Food science. The listed material was chosen for the range of products covered; it is not intended to be an exhaustive tabulation of applications. Some general references were also added at the end of the table.

7.7 REFERENCES

1. F. M. Devienne and G. Grandclement, *C. R. Acad. Sci.* **262**, 696 (1966)..

2. M. Barber, R. S. Bordoli, R. D. Sedgwick, and A. N. Tyler, *Chem. Comm.* 325. (1981).

3. D. J. Surman and J. C. Vickerman, *Chem. Comm.* 324 (1981).

4. J. R. J. Paré, *Ph. D. Thesis*, Carleton University, Ottawa, ON, Canada (1984).

5. J. R. J. Paré, K. Jankowski, and J. W. ApSimon, *Advances in Heterocyclic Chemistry* **42**, 335 (1987).
6. R. K. Boyd, *Spectros. Int. J.* **1**, 69 (1982).

7. S. Evans and R. Graham, *Adv. Mass Spectrom.* **6**, 429 (1974).

8. A. F. Weston, K. R. Jennings, S. Evans, and R. M. Elliott, *Int. J. Mass Spectrom. Ion Phys.* **20**, 317 (1976).

9. D. S. Millington and J. A. Smith, *Org. Mass Spectrom.* **12**, 264 (1977).

10. A. P. Bruins, K. R. Jennings, and S. A. Evans, *Int. J. Mass Spectrom. Ion Phys.* **26**, 395 (1978)

11. M. J. Lacey and C. G. Macdonald, *Org. Mass Spectrom.* **12**, 587 (1977).

12. M. Barber and R. M. Elliott, *12th Ann. Conf. Mass Spectrom. Allied Top.*, ASTM Committee E-14, MontrJal, Canada, paper 22 (1964).

13. M. J. Lacey and C. G. Macdonald, *Anal. Chem.* **53**, 691 (1979).
14. W. F. Haddon, *Org. Mass Spectrom.* **15**, 539 (1980).

15. B. Shushan and R. K. Boyd, *Anal. Chem.* **53**, 421 (1981).

16. J. H. Beynon, R. G. Cooks, J. W. Amy, W. E. Baitinger, and T. Y. Ridley, *Anal. Chem.* **45**, 1023A (1973).

17. R. K. Boyd, C. J. Porter, and J. H. Beynon, *Org. Mass Spectrom.* **16**, 490 (1981).

18. A. J. MacLeod, and N. M. Pieris, *J. Agric. Food Chem.* **29**, 49 (1981).

19. R. Tressl, L. Friese, F. Fendesak, and H. Koppler, *J. Agric. Food. Chem.* **26**, 1422 (1978).

20. R. G. Buttery, D. R. Black, W. F. Haddon, L. C. Ling, and R. Teranishi, *J. Agric. Food Chem.* **27**, 1 (1979).

21. T. Shibamoto, Y. Kamiya, and S. Mihara, *J. Agric. Food Chem.* **29**, 57 (1981).

22. W. D. Koller, *Z. Lebensm.-Unters.-Forsch.* **173**, 99 (1981).

23. S. P. Fore, M. G. Legendre, and G. S. Fisher, *J. Am. Oil Chem. Soc.* **55**, 482 (1978).

24. E. Demole, P. Enggist, and G. Ohloff, *Helv. Chim. Acta.* **65**, 1785 (1982).

25. W. H. McFadden, D. C. Bradford, D. E. Games, and J. L. Gower, A*m. Lab.* **9** (10), 55 (1977).

26. A. Kuksis, L. Marai, and J. J. Myher, *J. Chromatogr.* **273**, 43 (1983).

27. L. Marai, J. J. Myher, and A. Kuksis, *Can J. Biochem. Cell Biol.* **61,** 840 (1983).

28. P. J. Arpino, P. Krien, S. Vajta, and G. Devant, *J. Chromatogr.* **203**, 117 (1981).

29. S. Tsuge, New approaches to interfacing liquid chromatography and mass spectrometry. In "*Microcolumn Separations*" M. V. Novotny and D. Ishii

(eds.), Journal of Chromatography Library, **Vol 30**, Elsevier, Amsterdam, pp 217-241 (1985)

30. K. T. Taylor, D. Hazelby, and Wakefield, *Proc. of 9th Int. Sympos. Mass Spectrometry* (1982).
31. G. A. Warburton, J. R. Chapman, and K. T. Taylor, Direct mixture analysis using B/E linked scanning with MS80-DS55. *Kratos Data Sheet, No. 133* (1981).

32. V. Yaylayan, J. R. J. Paré, R. Laing, and P. Sporns, *Org. Mass Spectrom.* **25**, 141 (1990).

33. V. Yaylayan, J. R. J. Paré, R. Laing, and P. Sporns, Intramolecular nucleophilic substitution reactions of Lysine and tryptophan Amadori products. In "*The Maillard reaction in food processing, human nutrition and physiology*", P. A. Finot, H. U. Aeschbacher, R. F. Hurrell, and R. Liardon, (eds.), Birkhaüser-Verlag, Basel, pp. 115-120 (1990).

34. V. Yaylayan, and P. Sporns, *J. Agric. Food Chem.* **37**, 978 (1989).

35. J. N. Labows and B. Shushan, *Am. Lab.* **15** (3), 56 (1983).

36. D. V. Davis and R. G. Cooks, *J. Agric. Food Chem.* **30**, 495 (1982).

37. R. D. Plattner, Mass spectrometry/mass spectrometry as a tool for the identification and quantitation of mycotoxins. In *Mycotoxins and Phycotoxins*, P. S. Steyn and R. Vleggaar (Eds.), Elsevier, Amsterdam, pp. 195-204 (1986).

38. J. R. J. Paré, R. Greenhalgh, P. Lafontaine, and J. W. ApSimon, *Anal. Chem.* **57**, 1470 (1985).

39. W. Pfannhauser, R. Kellner, and G. Fischbock, GC/FTIR and GC/MS analysis of Kiwi flavors. In *Flavors and Off-Flavors*. G. Charalambous (Ed.). Elsevier, Amsterdam, pp. 357-373 (1990).

40. M. G. Moshonas and P. E. Shaw, Flavor evaluation of fresh and aseptically packaged orange juices. In *Frontiers of Flavors*. G. Charalambous (Ed.). Elsevier, Amsterdam, pp. 133-145 (1988).

41. H. J. Stan and P. Klaffenbach, *J. Anal. Chem.* **339** (3), 151 (1991).

42. Y. Musalam, A. Kobayashi, and T. Yamanishi, Aroma of Indonesian Jasmine tea. In *Flavors and Fragrances: A World Perspective*. B. M. Lawrence, B. D. Mookherjee and B. J. Willis (Eds.). Elsevier, Amsterdam, pp. 659-668 (1988).

43. L. F. Cesare, F. Tateo, A. Polesello, and E. Verderio, Recovery of flavouring fraction in powdered red pepper production. In *Flavors and Off-Flavors*. G. Charalambous (Ed.). Elsevier, Amsterdam, pp. 225-232 (1990).

44. M. Petrzika, W. Engst, and R. Macholz, *Nahrung* **35** (5), 491 (1991).

45. W. Liao, T. Joe, and W. G. Cusick, *J. Assoc. Off. Anal. Chem.* **74** (3), 554 (1991).

46. Y. Hasegawa, Y. Nakamura, Y. Tonogai, S. Terasawa, Y. Ito, and M. Uchiyama, *J. Food Prot.* **53**, 1058 (1990).

47. K. Harada, K. Masuda,M. Suzuki, and H. Oka, *Biol. Mass Spectrom.* **20**, 522 (1991).

48. J. van der Greef, A. C. Tas, M. C. Ten Noever de Brauw, M. Hohn, G. Meijerhoff, and U. Rapp, *J. Chromatogr.* **323**, 81 (1985).

49. C. N. Kenyon, A. Melera, and F. Erni, *J. Anal. Toxicol.* **5,** 216 (1981).

50. F. C. Alderweireldt, E. L. Esmans, and P. Geoes, *Nucleosides and Nucleotides* **4**, 135 (1985).

51. J. Eagles, C. Javanaud, and R. Self, *Biomed. Mass Spectrom.* **11**, 41 (1984).

52. G. R. Fenwick, J. Eagles, and R. Self, *Biomed. Mass Spectrom.* **10**, 382 (1983).

53. A. Sakushima, S. Hisada, S. Nishibe, and H. Brandenberger, P*hytochemistry* **24**, 325 (1985).

54. N. Satio, C. F. Timberlake, O. G. Tucknott, and I. A. S. Lewis, *Phytochemistry* **22**, 1007 (1983).

55. J. R. J. Paré and J. M. R. Bélanger, *Spectros. Int. J.* **7**, 337 (1989).

56. F. Fournier, L. Ma, J.-C. Tabet, C. Salles, J. C. Jallageas, and J. Crouzet, *Spectros. Int. J.* **8**, 273 (1990).

57. G. A. Warburton, A. G. Brenton, J. R. Chapman, and K. T. Taylor, Application of B/E linked scanning to structural differentiation using MS80-DS55. *Kratos Data Sheet, No. 134* (1981).

58. J. Gilbert, *Applications of Mass Spectrometry in Food Science,* Elsevier Applied Science, London. 440 pages (1987).

59. I. Horman, Mass Spectrometry. In "*Analysis of Foods and Beverages: Modern Techniques*". G. Charalambous (Ed.). Academic Press, pp. 142-203 (1984).

60. I. Horman, *Biomed. Mass Spectrom.* **8**, 384 (1981).

61. D. E. Games, N. J. Alcock, I. Horman, E. Lewis, M. A. McDowall, and A. V. Moncur, in *Anal. Chem. Symp. Ser.* **21**, pp. 263-80 (1984).

62. T. G. Hartman, C. T. Ho, J. D. Rosen, and R. T. Rosen, In *ACS Symp. Ser.* **409**, pp. 73-92 (1989).

J.R.J. Paré and J.M.R. Bélanger (Editors)
Instrumental Methods in Food Analysis

Chapter 8

Electroanalytical Techniques: Principles and Applications

James G. Dick

Methodologies Consultations Limited, 2760 Carousel Crescent, Suite 708, Gloucester, ON, Canada, K1T 2N4

8.1 GENERAL INTRODUCTION

Electrochemistry is the relationship between electrical properties and chemical substances in reactions. In its application to analytical chemistry, this generally involves the measurement of some electrical property under conditions which, directly or indirectly, allow an association between the magnitude of the property measured and the concentration of some particular chemical species. Such measurements are nearly always made in solution environments. The electrical properties that are most commonly measured are potential or voltage, current, resistance or conductance, or combinations of these. In some instances the electrical property may be a function of time, whereupon time may also be a variable to be measured. Capacitance is a property which, although not usually measured, has influence in polarographic or voltammetric analysis and requires consideration.

Electrochemical methods of analysis have grown greatly in application and importance over the last 40 years, and this has been largely due to the development and improvement of electronic systems permitting refinements in the measurement of the critical characteristics mentioned in the foregoing. In addition to this, the measurement systems and the advanced electronics now permit much of the work in electroanalytical chemistry to be automated and controlled by microprocessors or computers. Some electroanalytical techniques have become very widely accepted; others, such as polarography/voltammetry, less so. This has been due to early problems with equipment. Despite the fact

that such problems no longer exist, and that flexibility and very high sensitivity has rendered the method attractive, some industrial areas have been reluctant to recognise its value with respect to analytical control of their own operations.

The application of electrochemical methods to food analysis has been reasonably extensive. It has sometimes made rather slow progress, particularly where polarographic and voltammetric techniques are concerned. This has been due to the complexity of the matrices involved, and to the interferences arising out of this complexity. The faster rate of application in, for example, the field of pharmaceuticals can be explained by the fact that many of the products in this field involve one active ingredient, together with what are very frequently electrochemically-inert substances. There are, however, advantages to the application of electrochemical techniques to food analysis. These involve such factors as: 1. relatively inexpensive equipment; 2. small laboratory occupancy space; 3. ability to determine trace and ultratrace analyte levels using polarographic, voltammetric and amperometric techniques; 4. extended automation at minimal cost; 5. rapidity of analysis; 6. unaffected by turbidity, colour, or suspensions.

Electrochemistry and electroanalytical chemistry are usually covered in undergraduate courses in physical chemistry and in instrumental methods of chemical analysis. There are a number of different modes of electrochemical approach to chemical analysis. For this reason, the associated theory and the range of applications are best left to be discussed separately for the individual approach.

The order of presentation of the electroanalytical methods will be direct potentiometry with ion-selective electrodes, potentiometric titrations, voltammetry/polarography, polarisation titrations (amperometric and potentiometric), conductometry/coulometry and electrochemical detectors.

8.2 DIRECT POTENTIOMETRY - ION-SELECTIVE ELECTRODES

8.2.1 Introduction

Both direct potentiometry and the potentiometric titration method (see next Section) require the measurement of emf between an indicator electrode system and a reference electrode system, the two comprising a cell system. Despite the fact that potentials are usually referred to the standard hydrogen electrode (SHE) for tabulation purposes, they can be expressed relative to any acceptable reference system. In practice, the common reference electrodes are saturated KCl calomel (SCE), 3M KCl calomel or 3M KCl Ag/AgCl. In many present-day applications, the indicator and reference electrodes are combined in a single electrode system called a "combination electrode".

The measurement of potentials between indicator electrodes and reference electrodes is made under conditions of minimal flow of current, so that ohmic drop and electrode reactions are of no real significance, and the voltage measured is essentially identical to the cell potential capability. Such measurements are made on potentiometers with both *p*H and mV reading capabilities. Modern pH/mV instruments are electronic voltmeters with amplification circuitry of high input impedance. Although some current does flow during measurement, it is too low to affect the ion concentration in the solution under investigation. This situation also permits prolonged continuous measurement without significant change. The instrument is normally calibrated to read *p*H and mV, but may also be calibrated to read ion activity and concentration of a specific ion species. Many modern *p*H/mV potentiometers are microprocessor-controlled. This means that operator decisions, such as when the electrode system is sufficiently stable to start measurements and the setting of the ambient temperature are automatically determined. In addition, many potentiometers are equipped to warn the operator that he has in error used a calibrating buffer or solution different from the information entered to the unit.

Although the term "ion-selective electrode, (ISE)" came into use long after the application of, for example, the glass electrode system, the term is now usually applied to all potentiometric measuring electrodes that are capable of providing data concerning the concentration or activity of a particular chemical ion or species.

Table 1 shows the some of the various general types of ISE. The list is by no means complete, since many selective electrodes have been developed over recent years with the capability of being selective to a large variety of chemical substances.

8.2.2 General Theory

No ion-selective electrode is selective exclusively with respect to the ion specified. The presence of other ions can seriously impair electrode performance. Such interfering actions may take several forms, depending on the nature of the electrode and/or ion exchange material, and can be based on interfering ion and/or other chemical substance. Ion-selective electrode behaviour under interfering conditions can be represented by an expression first used by Nicolsky [1] for a glass electrode. In the situation involved, the glass electrode showed a mixed response to hydrogen and sodium ions. The expression is sometimes referred to as a simplified Eisenmann equation (2). Here concentrations have been used instead of activities.

$$E = \text{constant} \pm 0.059 \log(C_i + K_{ij}.C_j) \quad \textbf{(1)}$$

where:

E = electrode potential

TABLE 1
Potentiometric Electrode Types

Type	Some species sensed
Solid State	
Glass	H^+, Na^+, K^+
Crystal	Br^-, Cd^{2+}, Cl^-, CN^-, Cu^{2+}, F^-, I^-, Pb^{2+}, $S^=$, SCN^-,
Liquid Membrane	
Ion exchange	Ca^{2+}, Cl^-, K^+, NO_3^-
Neutral carriers	K^+ (valinomycin) Na^+ (monensin)
Impregnated polymer membrane	Cl^-, Br^-, I^-, $S^=$
Miscellaneous	
Gas	CO_2, NH_3 (NH_4), SO_2, O_2
Immobilised enzymes	Glucose oxidase, urease, amino acid oxidases, lysine oxidase, *etc.*

C_i = conc. of single-charge ion to which the electrode is primarily responsive (*e.g.*, H^+)
C_j = conc. of single-charge ion providing the interference (*e.g.*, Na^+)
K_{ij} = selectivity coefficient (includes ion mobilities across the glass membrane)

The ± sign will be + for cation-selective electrodes and – for those that are anion-selective. To be predominantly responsive to the concentration C_i, the factor K_{ij} must be small. Where liquid membrane ion-selective electrodes responsive primarily to double-charge ions are concerned, and for interference by single-charge ions, equation (1) modifies to:

$$E = \text{constant} \pm 0.059/z_i \log(C_i + K_{ij}.C_j^2) \quad \textbf{(2)}$$

where:

E = electrode potential
z_i = charge on ion to which electrode is primarily responsive (*e.g.*, Ca^{2+})
C_i = conc. of double-charge ion to which the electrode is primarily responsive (*e.g.*,Ca^{2+})
C_j = conc. of single-charge ion providing the interference (*e.g.*, Na^+)

K_{ij} = selectivity coefficient (includes ion mobilities across the liquid membrane)

The same remark relative to the " sign applies here as made before. For the Ca^{2+} ion-selective electrode, K_{ij} for Na^{+} interference is roughly 10^{-3}, indicating very approximately that the electrode is 1000 times more responsive to Ca^{2+} than to Na^{+}.

The interferences where solid electrodes are concerned are of different types, and will be discussed in conjunction with the details on these electrodes.

8.2.3 The Glass Electrode

8.2.3.1 Introduction

The *p*H glass electrode was discovered in the first decade of the century; Cremer [3] in 1906; Haber and Klemenslewicz [4] in 1909. Glass electrodes adequately selective to Na^{+} and K^{+} were not discovered until much later; Eisenmann [5] in 1957 and [6] in 1962.

8.2.3.2 Construction and Theory

Glass membrane electrodes have fixed reactive sites, so that they do not move towards the selective ion under investigation. The glass electrode for *p*H measurement consists of a silver/silver chloride electrode system immersed in a solution contained within a glass membrane sensitive to hydrogen ion activity (concentration). A glass tube contains a silver wire sealed through one end and protruding into the solution in the membrane, a thin-walled glass bulb made of special glass sensitive to hydrogen ions. The silver wire is coated with silver chloride and the bulb solution is usually 0.1 M HCl. A reference electrode can be used with such an electrode. A more common practice in the present day is to incorporate the reference electrode within the internal structure of the glass electrode. This called a "combination glass electrode".

A difference in potential is developed across the glass membrane on the basis of the difference between the hydrogen ion activities of the solution of immersion and the internal hydrochloric acid solution of the electrode. The potential for an electrode selective to an ion i is given by:

$$E = \text{constant} + 0.059/z_i \log \alpha_i \quad \textbf{(3)}$$

where:

Z_i = ion charge
α_I = ion activity

For univalent ions such as H^+, Na^+, and K^+,

$$E = \text{constant} + 0.059 \log \alpha_i \quad (4)$$

and for the hydrogen ion-selective glass electrode,

$$E = \text{constant} - 0.059\, p\text{H} \quad (5)$$

The ability of other ions (Na^+, *etc.*) to interfere increases with increasing solution *p*H, becoming more important at pH values in excess of 9. This effect, called "alkaline error", was investigated by Eisenmann [7]. In addition, the electrode suffers from what is known as "acid" error in solutions of about 0 pH and less. This situation was reported by Dole [8].

Glass electrodes selective to cations such as Na^+, K^+ or Li^+ depend largely upon the use of glass compositions with selective capabilities for these ions. Electrodes of favourable glass compositions yield, for example, response for Na^+ 3000 greater than that for K^+ and response for Ag^+ 1000 times that for Na^+. Most of such electrodes are also sensitive to the presence of hydrogen ion. In order to avoid significant interference by H^+, these electrodes are generally used at an analyte solution *p*H high enough ($\geq$ 9) to reduce the hydrogen ion activity to the point where response is primarily from the selective cation of interest.

8.2.3.3 Applications

Glass membrane electrodes selective to hydrogen ion can be used, after proper hydration and calibration, in the measurement of the *p*H of liquid foods of all types, solid foods taken into solution or into suspension, extracts of food substances, non-aqueous food solutions or extractions (activity rather than *p*H is measured here), *etc.* In such measurements, the value of the constant in equation 3 is assumed to be the same for the analyte solution and the calibrating buffer(s). This will be true only when the ionic strength and composition of the analyte solution and the buffer do not differ sufficiently to introduce significant differences in the junction potentials at the electrode and solution interfaces. Where there are apt to be important differences, the analyte solution and the buffer can be made relatively equal as to ionic strength by the introduction of a fixed volume of a neutral salt solution of specific strength. Where glass membrane electrodes sensitive to other cations are concerned, similar situations as to applicability exist.

While the presence of oils and fats do not necessarily render glass electrodes incapable of performing, the concentration of such substances is subject to some limitations, and the need for proper cleaning procedures after each reading essential when they are present.

8.2.4 Liquid Membrane Electrodes

8.2.4.1 Introduction

Liquid membrane electrodes were known for some years, but it is likely that the introduction of the calcium ion-selective liquid membrane electrode by Ross [9] in 1967 stimulated the intensive developmental research that resulted in the present commercial availability of liquid membrane electrodes for a significant number of cations and anions. In general the cations determinable are double-charge, while the anions are frequently single-charge.

8.2.4.2 Construction and Theory

Liquid-membrane electrodes have reactive sites capable of movement towards the selective ion under investigation. Liquid membrane ion-selective electrodes can be manufactured with or without an internal reference electrode. Those without an internal reference are sometimes made by simply coating a platinum wire with a liquid ion-exchanger dissolved in a water-immiscible polyvinylchloride polymer. When without the internal reference, an external reference such as a 3M Ag/AgCl electrode is used. The liquid membrane electrode is similar to the glass electrode, except that the membrane is a thin porous organic polymer layer saturated with a liquid ion exchanger dissolved in a water-immiscible organic solvent.

Figure 1 shows the essential construction of a liquid membrane ion- selective electrode with internal reference.

A general theory of the operation of liquid membrane electrodes has been given by Sandblom [10]. The potentiometric response to a given ion depends not only on the activity of the ion in the solution and in the membrane, but also on the equilibrium constant for the ion-exchange process, and on the mobility of the ion in the membrane. Since the internal aqueous solution does not suffer change, the potential developed must vary only with the composition of the analyte solution, affecting as it does only the outer interface with the membrane. The potential of the ion-selective membrane for the selective ion i in solution with a possible interference ion j of the same charge would be given, using concentrations, by:

$$E = \text{constant} \pm 0.059/z_i \log\{C_i + (u_j d_j/u_i d_i)C_j\} \quad \textbf{(6)}$$

where:

E = electrode potential
z_i = charge on the selective ion (*e.g.*, Ca^{2+})

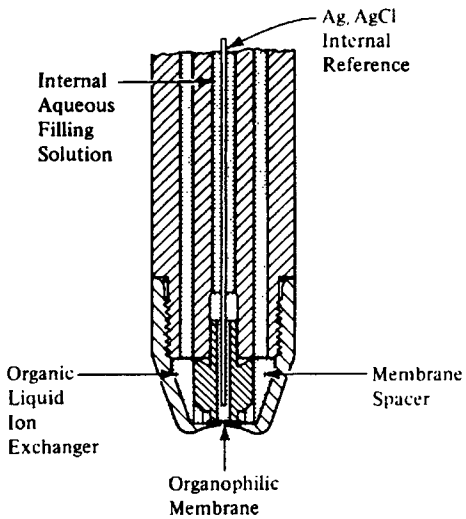

Figure 1: Liquid membrane ion-selective electrode with reference (courtesy of ATI Orion, Boston, MA).

C_i	=	conc. of double-charge ion to which the electrode is primarily responsive (*e.g.*, Ca^{2+})
U_i	=	mobility in the membrane of the ion to which the electrode is primarily responsive (*e.g.*, Ca^{2+})
C_j	=	conc. of the double-charge ion providing the interference (*e.g.*, Mg^{2+})
u_j	=	mobility in the membrane of the double-charge ion providing the interference
d_i	=	distribution ratio of ion i between the aqueous and membrane phases
d_j	=	distribution ratio of ion j between the two phases

For practical purposes, it is preferable to use equation (1) of the foregoing, allowing K_{ij} to represent the u and d ratios. Remember that, as indicated earlier, the ± sign must be + for cation-selective and – for anion-selective electrodes. Exchange sites and selectivity coefficients for various liquid membrane ion-selective electrodes can be found in Durst [11].

The general mechanism whereby liquid membrane ion-selective work can be explained, at least to an extent, by using the calcium ion-selective electrode as an example. A calcium long-chain organophosphorous compound is the ion-exchanger in the water-immiscible solvent reservoir and the soaked membrane. At the membrane interface with the analyte solution, the organic groups are oriented towards the organic liquid, with the polar -POOH ends towards the

aqueous analyte solution at the membrane interface. Preliminary soaking of the electrode to stability in a solution that is *ca.* 10^{-2}M to Ca^{2+} results in the conversion of the ion-exchanger at the interface to the calcium chelate. Subsequent immersion of the electrode in an aqueous analyte solution containing, for example low [Ca^{2+}], results in migration of Ca ions into the aqueous solution at the membrane interface. The larger organic phosphate radicals do not migrate due mainly to their large size and strong solubility in the water-immiscible organic solvent. The migratory action develops a positive charge at the membrane interface with the analyte solution. The magnitude of this charge, together with the charge of different magnitude at the membrane-internal solution interface, and relative to the reference system, provides a potential related to the concentration of the Ca^{2+} analyte in the solution under test.

It should be emphasised that, as with all electrodes used in direct potentiometry, activity is measured rather than concentration, although concentration is reported. Figure 2 gives an indication, for the calcium liquid membrane ISE, of the relationship between activity, concentration and response.

Since the concentration is related to the activity through the appropriate activity coefficient, and since this latter is dependent on the total ionic strength of the solution, calibration of the electrode with known [Ca^{2+}] solution(s) and its subsequent use in analyte solutions should be carried out under conditions of reasonable agreement of the ionic strengths. This is often accomplished, where required, by the addition of similar and exact volumes of a solution of ionic strength high enough to equalise the value in both calibration and unknown solutions. Ionic strength equalising solutions should not contain compounds interfering with the functioning of the liquid membrane. For example, phosphate-containing ionic strength equalisers can not be used with Ca-ISE liquid membrane electrodes for obvious reasons.

Liquid membrane electrodes are subject to interferences from ions other than that of prime selectivity. For example, the Ca-ISE is also responsive to Mg^{2+} and Ba^{2+}, the selectivity coefficients being approximately 0.01 for each ion. This indicates that the electrode is only 100 times more sensitive to Ca^{2+} than to these ions, and this is normally much more important with respect to Mg than to Ba where food analysis is concerned. There are techniques which can be used to minimise the interference of Mg^{2+}.

Liquid membrane electrodes tend to lose responsivity in time, and therefore the in-use daily checking of the response factor from the stabilising and/or calibration solution(s) should be closely followed to detect losses of responsivity. Most liquid membrane ISE electrodes today are supplied with replaceable membrane tips.

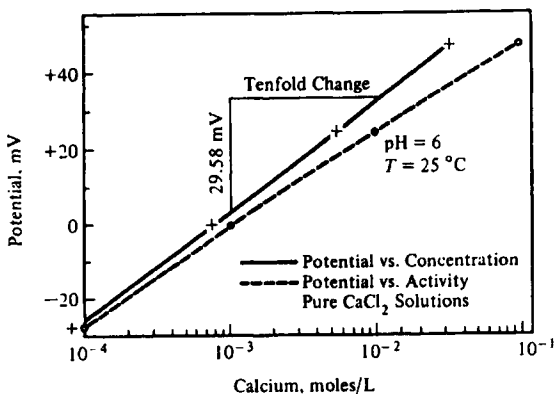

Figure 2: Calibration plots for activity and concentration *versus* potential (mV) for a Ca^{2+} ion-selective electrode (courtesy of ATI Orion Boston, MA).

8.2.4.3 Applications

Liquid membrane ISEs can be used, after the necessary calibration procedure, to measure the appropriate cation or anion in liquid foods, solid foods taken into solution or suspension properly, food extractions, *etc.*, providing always that the sample solutions do not contain significant concentrations of interfering ions or contaminating substances. It should be remembered that, in the majority of instances, application of liquid membrane ISEs in food analysis will be carried out in under quality control conditions, and will involve samples of generally well-known composition and analyte ranges.

There may be a need in certain instances to equalise ionic strengths in calibration and analysis situations. The basis for this was discussed earlier.

8.2.5 Solid State Electrodes Other Than Glass

8.2.5.1 Introduction

Solid state electrodes may be constructed as crystal membrane or precipitate-impregnated membrane type. The latter appeared on the scene first *ca.* 1950, but because of technical difficulties in their construction little advance in use was apparent until 1966. Around this time, both forms of solid state electrode started a climb to prominence as indicated by Buck [12] 1968, Eisenmann [13] 1969 and Ross [14] 1969.

Considerable literature has been written on the subject of liquid membrane ion-selective electrodes. Some of this is covered in the "Literature" list at the close of this Section.

8.2.6 Precipitate-Impregnated Membrane Electrodes

8.2.6.1 Construction and Theory

Precipitate-impregnated membrane electrodes for anion sensing have a slightly soluble inorganic salt of the anion of interest (usually sulphide and the halides chloride, bromide and iodide) suspended in an inert, slightly-flexible membrane. The support material for the membrane may be a substance such as silicone rubber, polyvinyl chloride, *etc.*, and the membrane-impregnating precipitate the silver salt of the ion of interest. The filling solution reflects the anion of interest, as does the internal reference, although an appropriate external reference system may be used. Figure 3 shows such an electrode for the determination of I^- ion. Note that the membrane is 50% by weight of AgI in silicone rubber, with an AgI reference system in a KI filling solution.

These electrodes have the silver ion as the mobile ion. Immersion in a solution of the selective ion results in a change in the silver ion activity, resulting in the development of a potential over the interfaces of the membrane. The theory will be discussed in detail for the crystal membrane solid-state electrode section to follow.

Precipitate-impregnated membrane electrodes have several disadvantages. They are usually slow in response and, in addition may be easily poisoned by many substances in the test solution under investigation. The sensitivity is as expected limited by the solubility of the precipitate substance. For example, with a molar solubility for AgI of about 10^{-8} the limit of detection for I^- is about 10^{-7} M; for a chloride ion selective electrode with an AgCl molar solubility of about 10^{-5}, the detection limit is *ca.* 10^{-4}M, about 1000 times poorer than for the I^- electrode. Finally, the selectivity of precipitate-membrane ISEs for other anions decreases with increasing solubility of the precipitate.

8.2.7 Crystal Membrane Electrodes

8.2.7.1 Construction and Theory

Crystal membrane solid-state ISEs respond to various anions (mostly single-charge) and to some cations (mostly double-charge). In commercial usage, they are not designed to respond analytically to more than a single selective ion. In common with glass membrane electrodes, crystal membrane electrodes have fixed reactive sites. They do not, therefore, travel to the analyte ion. In order to determine the activity (concentration) of a single-charge anion the membrane must incorporate a single-charge cation. Similarly, the determination of a double-charge cation requires the presence in the membrane of a double-charge anion.

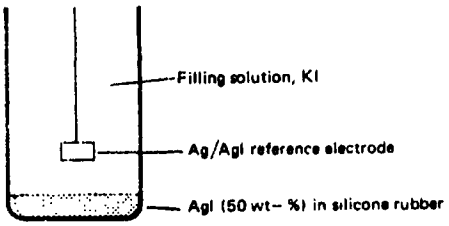

Figure 3: Precipitate-impregnated membrane ISE for iodide ion.

The membrane is a conducting solid. Both single crystal and pellet-pressed crystalline substance mixtures can be used in membrane construction. Table 2, accumulated from data available from several electrode manufacturers' data sheets, shows information relative to crystal membrane electrodes and their application capabilities. As can be seen, crystal membrane electrodes, with the exception of that selective to F^-, involve Ag_2S or crystal mixtures where one component is Ag_2S and the other the sulphide of the selective ion of interest. The membranes are generally produced by pressing the polycrystalline substance in a pellet press.

Electrodes of this type can be obtained with or without an internal reference system, although most of those in use commercially refer to external reference systems such as the double-compartmented 3M KCl Ag/AgCl electrode. The outer compartment, in contact with both the test solution and the reference system, can have a solution filling that is compatible with the system under measurement (*e.g.*, 3M KNO_3 filling for solutions containing Ag^+. Figure 4 shows typical crystal membrane ISEs. One has no internal reference and a only a simple conducting contact to the membrane inner surface. This electrode type would require the use of an external reference electrode. The other shows the use of an internal reference electrode.

In the case of the electrode having only Ag_2S in the membrane, the silver ions are the mobile species. Ag^+ activity is measured easily since the solubility of Ag_2S is very low (Ksp = *ca.* 10^{-49}). $S^=$ ions may also be measured since their activity in the test solution affects the activity of the Ag^+ ion on the basis of the solubility.

$$K_{sp} = (\alpha_{Ag+})^2.\alpha_{\alpha} \quad (7)$$

$$\alpha_{Ag+} = (K_{sp}/\alpha_{S=})^2 \quad (8)$$

TABLE 2
Crystal Membrane Electrodes

Ion	Membrane	Det. Limit (M)	Imp. Interferences
Br^-	$AgBr/Ag_2S$	$10^0 - 5x10^{-8}$	CN^-, $S^= \leq 10^{-7}$ M $I^- \leq 2x10^{-4}$ Br
Cl^-	$AgCl/Ag_2S$	$10^0 - 5x10^{-5}$	I^-, Br^-, CN^-, NH_3 $S^= \leq 10^{-7}$ M
CN^-	AgCN	$10^{-2} - 10^{-6}$	$S^= \leq 10^{-7}$ M $Cl^- \leq 10^6$ CN^- $Br^- \leq 5x10^3$ CN^- $I^- \leq 0.1$ CN^-
F^-	LaF_3	$10^0 - 10^{-6}$	$OH^- \leq 10^{-6}$ F^- F^- complexes
I^-	AgI/Ag_2S	$10^{-1} - 5x10^{-8}$	$S^= \leq 10^{-7}$ M
Ag^+ & S^-	Ag_2S, Ag^- S^-	$10^0 - 10^{-7}$ $10^0 - 10^{-8}$	$Hg^{2+} \leq 10^{-7}$ M effect of *p*H on $S^=$ activity
SCN^-	$AgSCN/Ag_2S$	$10^0 - 10^{-8}$	$OH^- \leq SCN^-$ $Br^- \leq 0.003$ SCN^- $I^- \leq 2x10^{-4}$ SCN^-
Cd^{2+}	CdS/Ag_2S	$10^{-1} - 10^{-7}$	Ag^+, Hg^{2+}, Cu^{2+} must be each $\leq 10^{-7}$ M High Fe^{3+} and Pb^{+2} may also interfere
Cu^{2+}	CuS/Ag_2S	$10^{-1} - 10^{-8}$	$S^=$, Ag^+, Hg^{2+} must be each $\leq 10^{-7}$ M High Cl^-, Br^-, Fe^{3+}, Cr^{3+} and Cd^{2+} may interfere
Pb^{2+}	PbS/Ag_2S	$10^{-1} - 10^{-6}$	Ag^+, Hg^{2+}, Cu^{2+} must be each $\leq 10^{-7}$ M Cd^{2+} and Fe^{3+} must not exceed Pb^{2+} sample level

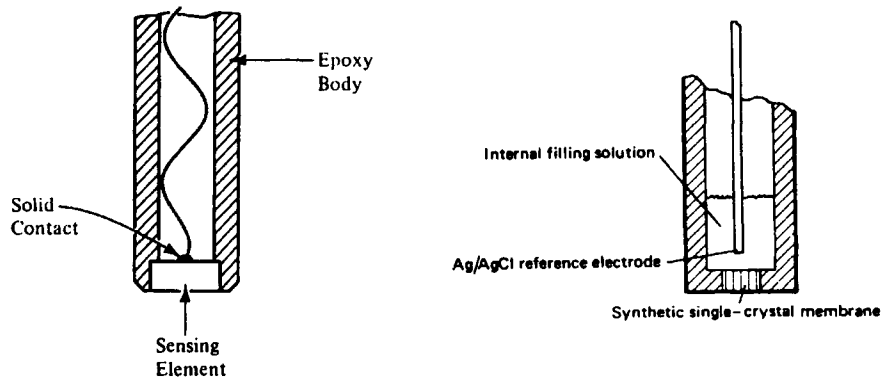

Figure 4: Crystal membrane ion-selective electrodes (courtesy of ATI Orion, Boston, MA).

Although it was indicated in Table 2 that the detection limit of Ag^+ and $S^=$ were 10^{-7}M and 10^{-8}M respectively, the activity of free Ag^+ can be measured to a limit of *ca.* 10^{-20}M when the test solution has complexes for silver present. In the same way, when H_2S is present in the test solution, $S^=$ can be measured to about the same limit.

Where the crystal membrane contains both Ag_2S and a silver halide, the electrode is then selective to the halide involved. The silver halide will have higher solubility than the silver sulphide. It will, however, have an equilibrium solubility such that the halide activity in the membrane will be significantly less than its activity in the test solution. The extent of the difference in activities on either side of the interface generates a potential difference resulting in the movement of the conducting silver ions. The extent of the difference in potential relates through this movement to the activity (concentration) of the halide in the test solution.

With metal sulphide/silver sulphide crystal membranes, the silver ions are again the mobile species. The cadmium ion-selective crystal membrane electrode (CdS/Ag_2S membrane) can be used as an example of the mechanism involved. CdS will be more soluble than Ag_2S. The activity of the sulphide ion will be controlled at the interface by that of the cadmium ion:

$$K_{sp,CdS} = \alpha_{Cd2+}.\alpha_{S=} \quad \textbf{(9)}$$

$$\alpha_{S=} = K_{sp,CdS}/\alpha_{Cd2+} \quad \textbf{(10)}$$

The activity of Ag^+ in the membrane is determined by that of $S^=$, so that we have:

$$K_{sp,Ag2\,S} = (\alpha_{Ag+})^2.\alpha_{S=} \quad \textbf{(11)}$$

$$\alpha_{Ag+} = (K_{sp,Ag2\,S}/\alpha_{S=})^{1/2} \quad \textbf{(12)}$$

A combination of equations 10 and 12, and insertion into the Nernst equation covering the conducting Ag^+ system yields an expression giving the electrode potential as a function of the activity (concentration) of the Cd^{2+} ion in the test solution.

$$E = \text{constant} + 0.059/2 \log \alpha_{Cd2+} \quad \textbf{(13)}$$

The crystalline substance LaF_3 used to form the membrane of the fluoride selective-ion electrode is a single crystal. The fluoride ion in the crystal lattice is smaller and has a lower charge than the lanthanum ion. It moves with relative ease through the lattice and is the conducting ion. The crystal lattice has defects, or points of vacancy, so that the fluoride ion can move into the vacancy.

Because of the size and charge requirements of the vacancy, as well as that of shape, ions such as chloride, bromide, and iodide can not enter the vacancies. Only hydroxyl ion, with a size and charge similar to that of the fluoride ion, can interfere by taking up lattice vacancies. Thus OH^- is the only interfering anion. There is a limitation as to the *p*H of the test solution. pH values less than *ca.* 4 result in the formation of HF, and this compound does not register as F^-at the electrode interface.

Because of the possibility of coatings appearing on the solid membrane surface in time, it is necessary to polish the surface occasionally with a recommended polishing powder.

8.2.8 Gas-Selective Electrodes

8.2.8.1 Construction, Theory and Applications

Gas-selective electrodes are used to a limited extent in food analysis although, in certain areas of food production their use is quite common. The oxygen-selective electrode is often used on the production lines for fruit and vegetable juices, where a vacuum has been applied to remove air before packaging, this in order to check the residual oxygen content. SO_2-selective electrodes are used to determine the SO_2 content of wines and other SO_2-treated liquids either directly or after the acid conversion of a component such as $NaHSO_3$ to SO_2. Other electrodes are available for similar measurements, such as nitrogen oxide (for nitrite contents) and carbon dioxide (for either CO_2 directly or CO_2 from acid-converted carbonate or bicarbonate salts). There are perhaps other more accurate ways of determining such analytes, but the gas-selective electrode is

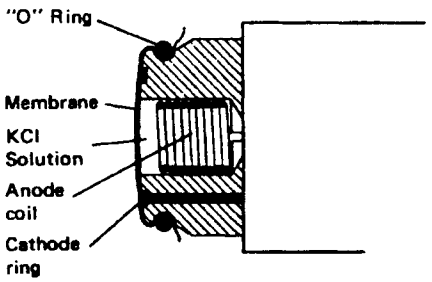

Figure 5: Oxygen-sensitive or -sensing electrode (courtesy of Arthur H. Thomas Company).

perhaps the best from the point of view of its ability to be applied as an on-line sensor. Figure 5 shows the structure of a typical gas-sensing electrode.

This electrode, as shown, is actually an amperometric rather than a potentiometric electrode. Since amperometry, to be covered in a later section, will deal largely with amperometric titrations, the oxygen electrode is discussed briefly here. The general construction involves a plastic film of a durable type at the electrode tip, stretched over a ring cathode of gold or platinum and a KCl reservoir with an anodic reference electrode coil. The film allows gases to diffuse, but excludes ions. Oxygen from the test medium diffuses through the film and is reduced by an appropriate potential applied at the cathode. This results in a diffusion-based or amperometric current between the cathode and the reference electrode. Interference can be anticipated from other gases diffusing, if these are present, such as the halogens and SO_2. The presence of H_2S results in electrode contamination. Calibration of the electrode is against air, with an assumed oxygen content of 20.9%, or against water saturated with oxygen. Corrections are applied for barometric pressure and ambient temperature.

8.2.9 Immobilised Enzyme Electrodes

8.2.9.1 Construction and Theory

Enzymes are organic substances capable of catalysing specific chemical reactions, these reactions most often involving organic substances of a biological basis. The enzymes are, of themselves, of a biological basis of origin. Although largely applicable in clinical analysis and to an extent in pharmaceutical analysis, there are many possible analytical applications relative to foods. One of the factors mitigating against their use in this field, particularly in the form of immobilised-enzyme electrodes, is the high cost of the enzyme itself. This is based on the fact that, in almost all cases of analytical application, the enzyme

must be of high purity and, therefore, of high cost. An important point in favour of their use is the very high degree of specificity with respect to the reacting substance.

There are over 300 enzymes available commercially, and many of these can be used in one way or another for analytical purposes. One of methods of use involves the determination of an analyte or substrate by means of the enzyme which reacts specifically with that substrate. Examples are: 1. Glucose and glucose oxidase, O_2 released, measurement by O_2-ISE; 2. Urea and urease, NH_3 and CO_2 released, measurement by an NH_4^+- or CO_2-ISE; 3. Pectin and pectin-esterase, titration of H^+ released. In clinical work, the opposing approach is often used, and the amount of an enzyme determined by adding the proper substrate to a solution of the enzyme and measuring with an ion-selective electrode a product of the reaction. Early work in this area, and in that of immobilised enzyme electrodes, was carried out by Katz and Rechnitz [15,16], Guilbault and his co-workers [17] and Guilbault and Montalvo [18].

An enzyme-based technique which lends itself well to food analysis is that making use of an immobilised enzyme electrode. There are different ways of constructing such an electrode. One technique immobilises the enzyme in a gel, which is subsequently used to coat the surface of an appropriate ion-selective electrode. When the electrode is immersed in a substrate solution, diffusion of the reaction product to the surface of the ion-selective electrode takes place. When the electrode response stabilises a reading is taken. The response will be a linear function of the logarithm of the concentration of the substrate within a predetermined range. An example would be the use of a urease-coated cation-selective glass electrode in the determination of urea. The enzyme reaction produces $NH4^+$ which diffuses to the electrode face and provides a response. Enzymes may also be immobilised physically in semi-permeable membranes or attached covalently to a membrane. The aim in general is to attach the immobilised enzyme to the ion-selective electrode in a manner such that it can be removed and stored properly for further use. In this way, the ion-selective electrode can be used in connection with other compatible enzymes. The commonly used ion-selective electrodes are those selective to ammonium/ammonia, carbon dioxide, hydrogen peroxide and oxygen. The response system is often amperometric rather than potentiometric.

8.2.10 Applications of Direct Potentiometry

Examples of the recent application of such electrodes in food analysis are given by references [19 to 36]. Quite a few of these represent the application of immobilised enzyme electrodes, since much investigatory work is being done in this area.

The following provide actual preparatory and measuring details for two specific direct potentiometry analyses of food substances.

8.2.10.1 Chloride in Cheese and Meat Products

8.2.10.1.1 Calibration

The Cl-ISE is first calibrated using 5.00 mL of a standard solution of sodium chloride (*e.g.*, 5% w/v) with an addition of a volume of ion strength adjustment solution (ISA) (*e.g.*, 10.0 mL of 1.0M HNO_3). These solutions are added into a 100 mL volumetric flask, subsequently diluted to the mark with distilled water and mixed well. Prepare four (4) other diluted standard solutions for an appropriate range. Calibrate against these solutions, using the Cl-ISE (with an external 3M KNO_3 Ag/AgCl reference electrode if required, and produce a calibration curve of Cl^- concentration *versus* mV response. Using a single standard solution in *ca.* the midpoint of the range, check the calibration curve daily. When the response falls off, polish the electrode face with the polishing powder recommended by the manufacturer.

8.2.10.1.2 Sample analysis

Weigh out an appropriate weight of the well-homogenised sample into a 150 mL beaker and add 10.0 mL of ISE solution. Heat for 1/2 hour on a steam bath. Add 100 mL of water and cool to 5°C. Skim or filter and warm to room temperature. Place the electrodes in the solution, wait to stabilise (usually 1 minute) and read the mV value. Use the calibration chart to determine the Cl^- level and to calculate the chloride in the sample. Clean the electrode with a soft cloth or absorbent paper. The ISA solution also precipitates the interfering proteins (albuminoids). Manufacturers of some *p*H/potentiometers supply detachable scales which allow calibration and analysis to be reported in % NaCl.

8.2.10.2 Sodium in Vegetable Products

8.2.10.2.1 Calibration

The glass Na-ISE (with 3M KCl Ag/AgCl external reference system where required) is calibrated against standard NaCl solutions in a range appropriate to the determination of the cation in vegetables. In preparing the standard solutions, they should contain 20 mL of 2.5M triethanolamine (TEA)/100 mL of the prepared standard solution. Produce a calibration curve of Na *versus* response in mV. Check the calibration curve daily with an Na standard at the midpoint of the range.

8.2.10.2.2 Sample analysis

Weigh out an appropriate weight (*e.g.*, 5.00g) of the well-homogenised vegetable sample into a 150 mL beaker, add 20 mL of 2.5M TEA and 100 mL of distilled water. Heat on a steam bath for 1/2 hour. Cool to ambient temperature. Put

the electrodes in the solution, wait for stabilisation, read the sodium concentration from the calibration graph and calculate the sodium level in the sample. This may be calculated to any desirable reporting basis, such as mmol/kg, g/kg, %, *etc.* Clean the electrode with a soft cloth or absorbent paper. Hydrogen ions may interfere at low sodium values, and this interference is minimised by adding TEA to provide a solution *p*H of *ca.* 10. Ag^+ ions must be absent.

In most ISE methods such as these, a standard additions technique can be applied, particularly where the sample analyte concentration is reasonably well known (*e.g.*, control analyses in production). In this case, the ISE does not have to be calibrated, although its sensitivity (mV/concentration unit) in the concentration range to be used should be known and checked frequently. The addition technique minimises the effect of ionic strength and that of interferences. In application, the sample for the two methods already outlined is prepared in the same manner. The mV response is determined as mV_1. A known amount of the analyte is now added such that the solution concentration will be approximately doubled. The addition is made using a fairly high known-concentration solution of the analyte. Only a small volume of the solution will be required, thus preventing any significant volume addition effect. The mV response is again measured and recorded as mV_2. The value of the analyte in the sample is then given by:

$$(A \times mV_1 \times F)/((mV_2-mV_1).S) \quad \textbf{(14)}$$

where:

A	=	amount of analyte added
mV_1	=	response for sample solution
mV_2	=	response for sample solution + added analyte
F	=	units conversion factor, if required
S	=	weight of sample in solution under examination

Other practical applications can be obtained from the data of references [19-36].

8.3 INDIRECT POTENTIOMETRY - POTENTIOMETRIC TITRATIONS

8.3.1 Introduction[1]

One of the most fruitful uses of potentiometry in analytical chemistry is its application to titrimetry. Prior to this application, most titrations were carried

---

[1] Some text in this section is taken from "Analytical Chemistry", James G. Dick, McGraw-Hill, Inc., (1973), Chapter 12 (with permission).

out using colour change indicators to signal the titration endpoint. There are problems in the application of such indicators.

1. The indicator endpoint may or may not represent the equivalence point of the titration. Where it does not, indicator "blanks" are usually required. Depending on the nature of the indicator and the conditions of the titration reaction, these "blanks" can be quite substantial.

2. Titrations requiring the use of colour-change indicators often suffer from the lack of an indicator reacting in the equivalence point zone required. There is no lack of indicators to chose from for neutralisation titrations; there is often, however, a lack of indicator choices to meet the requirements of precipitation, complexation and oxidation-reduction titrations.

3. Another problem with colour-change indicators is the range over which the colour change takes place, and the decision on the part of the technician as to the endpoint volume may not always be identical or accurate for each titration. Such a problem can become increasingly serious, depending on the magnitude of the equilibrium constant for the titration reaction and with the strengths of both titrant and reactant. The use of photometric or spectrophotometric probes to detect the colour change minimises this problem. It does not always provide the required accuracy where the colour-change zone is extended, as it is in the case of titrations with poor equilibrium constants and/or low concentrations of titrant and/or reactant solutions.

4. The indicator colour change may be easily obscured where coloured solutions must be titrated, where the solution is turbid or where a coloured precipitate is the product of the titration reaction.

There are advantages to potentiometric titration over direct potentiometry, despite the fact that the two techniques very often use the same types of electrodes.

1. The technique is generally unaffected by the state (ionic, undissociated, sometimes complexed) of the analyte to be titrated. For example, the direct potentiometric determination of *p*H in a solution of a weak acid reports only the hydrogen ion concentration. Since the major portion of the acid is present in the undissociated form, direct potentiometry can not provide data yielding the total acid concentration. Potentiometric titration involves titrating the acid solution with a standard base, determining the equivalence point volume of standard base solution used, and calculating the total weak acid concentration from the stoichiometric data.

2. In direct potentiometry, an accurate and precise measurement of E_{cell} must be made in order to obtain, through the Nernst relationship, an accurate value of ion activity. For example, an absolute error of "1 mV in the measured value can lead to a "4% error in the activity for a single-charge analyte ion, with "8% and "12% errors for double- and triple-charge ions. The relationship between "$_{ion}$ and [ion] for the particular medium should be known in order to determine [ion] with accuracy. Even when the calibration method is applied, and much of the foregoing problems eliminated, the results may become doubtful where there is a significant difference between the ionic strength of the calibrating solution(s) and that of the unknown.

   In a potentiometric titration, only the changes in E_{cell} or *p*H (ΔE or ΔpH) with titrant addition are important. The position of the E_{cell}-*versus*-titrant-volume curve relative to the vertical axis (the E_{cell} axis) may vary with variations in $E_{junction}$, E_{ref}, nature of the solution, *etc.* For a particular titration, however, its position relative to the horizontal axis (the titrant volume axis) does not vary. The equivalence point for the particular titration is thus fixed relative to titrant-volume axis, regardless of its position with respect to the E_{cell} axis. In a simple *p*H potentiometric titration, where only the endpoint(s) may be required, it is not really necessary to calibrate the glass electrode unless there have been indications that its significant characteristics such as linearity and asymmetry have shown recent deterioration.

3. Again, since only the changes in electrode response are significant, the background ionic strength is relatively unimportant, providing interfering ions are held to within limiting concentrations with respect to electrode response factors.

4. Potentiometric titrations can be easily automated and controlled by microprocessors or computers. The extent of automation is such that, in the same vessel, multiple titrants may be used sequentially, providing for the determination of several analytes in one sample. Sample changers carrying up to and beyond 60 samples can be attached with ease, vastly decreasing the technician time to produce multiple sample results.

Potentiometric titrations can be applied with simple or advanced titrators, and the following gives the basic arrangements in this connection.

1. Simple manual systems involve a burette, an indicator and reference electrode couple, and a *p*H/potentiometer. The potential or pH values are logged against the titrant volume addition levels selected. The endpoint volume is then located by analysis and extrapolation of the $\Delta E/\Delta V$ *versus* V or $\Delta^2E/\Delta V^2$ *versus* V values.

2. Instrumental systems involving an automatic burette drive linked to a recorder to which is also linked the electrode couple potential output. A continuous rate of volume addition is selected, with a provision for slowdown near the titration equivalence point. The recorder plots the course of E *versus* V or *p*H *versus* V during the titration. For such plots, the equivalence point or endpoint is located manually with the use of various forms of curve-analysis plastic template overlays. Potentiographic titrators of this type often have a derivative circuit, so that the plot of $\Delta E/\Delta V$ *versus* V can also be drawn by the recorder. The peak of this curve provides a somewhat simpler means of locating the equivalence-point volume.

3. Titration systems similar to (2), but where the addition of titrant can be stopped automatically when a preset potential (or *p*H) representative of the equivalence point or endpoint is attained. The volume at this point is automatically read from a digital readout or from a printout. Most equipment of this type will allow the presetting of up to two endpoints. For such deadstop titrations, as they are called, the required equivalence point data is established by a normal potentiographic titration carried out under the same solution conditions. Type (2) and (3) are usually combined in one unit.

4. Microprocessor- or computer-controlled titration equipment where the parameters required for any specific titration can be logged into the memory system. These include, in part:

a. Volume addition of reagents before titration.
b. Preliminary volume of titrant added to shorten titration time.
c. As part of the titration "start", determination of the expected characteristic of E *versus* V change by input of the effect of small increments of titrant on the electrode potential.
d. Rate of titrant addition subsequent to any bulk addition.
e. Slowdown of titrant addition by a pulsing volume addition system around the neighbourhood of the equivalence point.
f. Automatic location of one or multiple equivalence points
g. Calculation, through specific logged-in formulas, of the analyte value expressed in the units preselected and for the significant figures preselected
h. Variation of the approach to endpoint location to cover the requirements of different titration characteristics.
i. With some units, real-time video screen representation of the entire titration.
j. Hardcopy printout of the titration curve in both E or *p*H *versus* V form, or first-derivative form, as well as the titration parameters and identification data.

k. Memory storage of complete programs for a significant number of methods (often 30 or more).
l. Selection of various methods of titration approach including straightforward titration with endpoint location, deadstop titration and monotonous titrant additions titration based on time spacing or potential drift.
m. Selection of method of endpoint location and variation of parameters for the method selected.

8.3.2 Development of the Potentiometric Titration Method

No effort will be made to provide a chronological history of the development of potentiometric titration equipment, and only representative highlights will be given. Not long after the appearance of *p*H/potentiometric equipment in the period around 1910, the use of the instrument as a means of carrying out potentiometric titrations was realised.

Potentiographic titrators and their requirements were outlined by Robinson [37] in 1947 and Lingane [38] in 1953, both authors specifying that they must satisfy two fundamental conditions. These were that the recorder chart length must be proportional to the volume of titrant delivered, and that the rate of titrant addition must be controlled in accordance with the changes in $\Delta E/\Delta V$ or $\Delta pH/\Delta V$), and in particular those associated with the area within the onset and offset of the equivalence point.

In titrators described by Irving [39] in 1959 and Glass [40] in 1961, the mechanisms for adding titrant and driving the recorder were operated from a single servomotor, a system which limits the choices for either parameter. That described by Kelly and Fisher [41] in 1960, however, covered the use of two servomotors. The syringe burette was introduced after 1950 as a means of avoiding drainage errors.

Miyake [42] in 1966 wrote about the use of a potentiographic titrator linked mechanically to a syringe burette, an improvement, but one which still did not solve the problem of time-lag resulting from mixing and reaction time. This was one of the problems eventually solved by improvements in electronics which permitted the titrant additions to be made either on a set time or a set drift basis. Modern titrators and their versatility, sensitivity and adaptability to advanced automation are largely the result of improvements in electronics and timing devices occurring over the last
30 years.

8.3.3 General Titration Theory[2]

It would be folly for this text to provide comprehensive titration theory coverage. Most of the details following are based on extracts from Dick [43]. These will yield at least a picture of the essentials. Further details can be obtained from Chapter 5 of the same reference.

Consider only the simple titration reaction:

$$R + T \leftrightarrow A + B \quad \textbf{(15)}$$

where:

R	=	(analyte) or reactant substance
T	=	titrant substance
A	=	reaction product
B	=	second reaction product if occurring

From the above we have, using molarities instead of activities:

$$[A][B]/[R][T] = K_{eq} \quad \text{(temperature constant)} \quad \textbf{(16)}$$

For any point in the titration between the start and the equivalence point we have, for a point of volume V_T:

$$[R](V_T) = (V_R M_R - V_T M_T)/(V_R + V_T) + ([A][B])/K_{eq}[R](V_T) \quad \textbf{(17)}$$

where:

$V_R M_R$	=	volume x molarity of R (at the start)
$V_T M_T$	=	volume x molarity of T (during titration)
$V_R + V_T$	=	total volume at any point V_T

The right member of the right-hand side represents $[R]_{br}$, or [R] from the back reaction. When K_{eq} is large (equilibrium for the reaction lies far to the right), and for titration points appreciably before the equivalence point, the contribution of $[R]_{br}$ may be ignored, and *Equation.*(17) reduces to:

$$[R](V_T) = (V_R M_R - V_T M_T)/(V_R + V_T) \quad \textbf{(18)}$$

For the exact equivalence point we have:

---

[2] Text, tables and illustrations in this section are taken from "Analytical Chemistry", James G. Dick, McGraw-Hill, Inc., (1973), Chapter 5 (with permission).

$$[R]_{ep} = [A][B]/K_{eq}[R]_{ep} = ([A][B]/K_{eq})^{1/2} \quad \textbf{(19)}$$

For any point V_T after the equivalence point, the substance T will be in the excess. The value of $[T](V_T)$ will be given by:

$$[T](V_T) = (V_TM_T - V_RM_R)/(V_T + V_R) + ([A][B]/K_{eq}[T](V_T) \quad \textbf{(20)}$$

Again, where K_{eq} is large and the titration points are well past the equivalence point, equation (20) reduces to:

$$[T](V_T) = (V_TM_T - V_RM_R)/(V_T + V_R) \quad \textbf{(21)}$$

For equations (20) and (21), the value of $[R](V_T)$ can be found by substituting the value of $[T](V_T)$ for each case into the modified Equation(16), whereupon we have:

$$[R](V_T) = [A][B]/K_{eq}[T](V_T) \quad \textbf{(22)}$$

Note, in all of the above, that the value of [R] during the titration decreases on the basis of both the reaction effect and the dilution effect of increasing V_T. The dilution effect can be ignored when $V_{T,ep} \leq V_R$ as it is for most common titrimetric situations. In some types of titrations, including amperometric, conductometric and spectrophotometric titrations, it is important to refer the changes in [R] to the reaction effect only. On this basis it is necessary to compensate for the dilution effect by referring the [R] concentration back to the original starting volume V_R. This is done by the multiplying the right-hand expression $(V_RM_R - V_TM_T)/(V_R + V_T)$ of equations (17) and (18) by $(V_R + V_T)/V_R$.

The development of similar expressions for the more general titration equation:

$$rR + tT \leftrightarrow aA + bB \quad \textbf{(23)}$$

are not, because of space requirements, shown here, but can be found on pages 215/218 of Dick [43].

The previous discussion establishes the basis for a brief explanation of the theory of titration curves. For this purpose, the simplest titration reaction will be used, with the understanding that the approach also applies to more complex titration reactions.

$$R + T \leftrightarrow A \quad \textbf{(24)}$$

This is a reaction typified by the titration forms:

Neutralisation	$H^+ + OH^- \leftrightarrow H_2O$
Precipitation	$Ag^+ + Cl^- \leftrightarrow AgCl(s)$
Complexation	$Cu^{2+} + \text{trien} \leftrightarrow Cu(\text{trien})^{2+}$

In this case, we have:

$$[R][T] = [A]/K_{eq} = K[A] \quad \textbf{(25)}$$

Here, the lower the value of K or K[A], the more complete the titration. Equation (17) is shown as:

$$[R](V_T) = (V_R M_R - V_T M_T)/(V_R + V_T) + [R]_{br} \quad \textbf{(26)}$$

$[R]_{br}$ being the [R] from the back-reaction. Taking logarithms on both sides, changing the signs and differentiating with respect to V_T, we have:

$$\frac{dpR(V_T)}{dV_T} = \frac{M_T - \{(d[R]_{br}/dV_T)(V_R + V_T) + [R]_{br}\}}{(V_R M_R - V_T M_T) + [R]_{br}(V_R + V_T)} + \frac{1}{V_R + V_T} \quad \textbf{(27)}$$

On the same basis, and for V_T points after the equivalence point, we have:

$$\frac{dpR(V_T)}{dV_T} = \frac{M_T + \{(d[T]_{br}/dV_T)(V_T + V_R) + [T]_{br}\}}{(V_T M_T - V_R M_R) + [T]_{br}(V_T + V_R)} + \frac{1}{V_T + V_R} \quad \textbf{(28)}$$

From equations 27 and 28 note that, if the titration were one where H^+ was the reactant (a neutralisation titration), the value of $dpR(V_T)/dV_T$ would represent dpH/dV_T. This is the rate of change of *p*H with V_T. Note the following:

1. The slope of the curve for the plot of $pR(V_T)$ *versus* V_T is represented by $dpR(V_T)/dV_T$.

2. Since the value of $(V_R M_R - V_T M_T)$ approaches zero at the equivalence point, the slope of the curve reaches a maximum at the equivalence point.

3. Because of the limitations imposed by the back reaction contribution of $[R]_{br}$, the slope attains a practical or finite maximum value at the equivalence point. The magnitude of this maximum value will be a function of the magnitude of the back-reaction contribution and will decrease with increasing value of this contribution. The back-reaction contribution increases, of course, with increasing values of K[A] or K.

4. The effect of dilution during titration is to decrease the slope for comparable points in the titration and to render less acute the rate of

change of $pR(V_T)$ relative to V_T, particularly in the zone close to the equivalence point. This effect is introduced in equations (27) and (28) by the terms in the right-hand member involving $(V_R + V_T)$.

5. Since the value of $(V_TM_T \pm V_RM_R)$ increases after the equivalence point, the slope of the curve decreases after this point.

6. Again, the limitations with respect to the back reaction contribution of $[T]_{br}$ and the dilution effect tend to render less acute the rate of change of $pR(V_T)$ relative to V_T

All of the foregoing will indicate to the reader that equations (27) and (28) demonstrate the origin of the S-shaped curves and reversed S-shaped curves typical of potentiometric titrations. The tables and figures to follow will illustrate the effects of various titration conditions on the shape of the titration curve.

Table 3 indicates the effect of titrant molarities and starting reactant molarities on the approach to the equivalence point for a strong acid/strong base titration, with figure 6 showing the situation from the graphic point of view.

In this titration the value of K will be $K_w = 10^{-14}$. Note the increasing restriction in the range of change of *p*H around the equivalence point, the range decreasing in extent with decreasing molarities of reactant and titrant. Some accuracy in locating the equivalence point would be lost when low molarity titrations are carried out with colour change indicators, although this situation affects potentiometric titrations to a vastly lesser degree.

Table 4 and figure 7 show similar situations with respect to the effect of increasing values of K on the approach to the equivalence point for titrations. Although left axis is logged as $pR(V_T)$ to generalise the situation, this could represent a weak acid/strong base titration with the values of K varying with the ratio K_w/K_a, K_a being the dissociation constant for the weak acid. Here the value of K increases as the value of K_a decreases. As the value of K increases, the range of change around the equivalence point decreases. For $K = 10^{-6}$, the range of change of $pR(V_T)$ is very small. If this was a precipitation titration, K would be given by the K_{sp} for the insoluble reaction product. The lower the value of K_{sp} the more extended the range of change of $pR(V_T)$ around the equivalence point.

Finally, table 5 and figure 8 show the effects of both decreasing values of molarities and increasing values of K. It is unlikely that the titration for the reaction conditions of Curve 2 for the $K = 10^{-8}$ solution would find an equivalence point consistently with most ordinary modern potentiometric titration equipment. Location of the equivalence point using colour-change indicators would be entirely impractical.

Table 3
Effect of various starting molarities on strong acid-strong base titrations*

	*p*H		
Titration	0.1M acid *versus* 0.1M base	0.01M acid *versus* 0.1M base	0.001M acid *versus* 0.001M base
0	1.0	2.0	3.0
10	1.1	2.1	3.1
25	1.2	2.2	3.2
50	1.5	2.4	3.5
75	1.9	2.6	3.9
90	2.3	3.0	4.3
95	2.6	3.3	4.6
99	3.3	4.0	5.3
101	10.7	10.0	8.7
110	11.7	11.0	9.7
120	12.0	11.3	10.0

* The titration data have been corrected, in each instance, for the back-reaction effect where required but not corrected for the titration-dilution effect. A volume of 100 mL of acid was used.

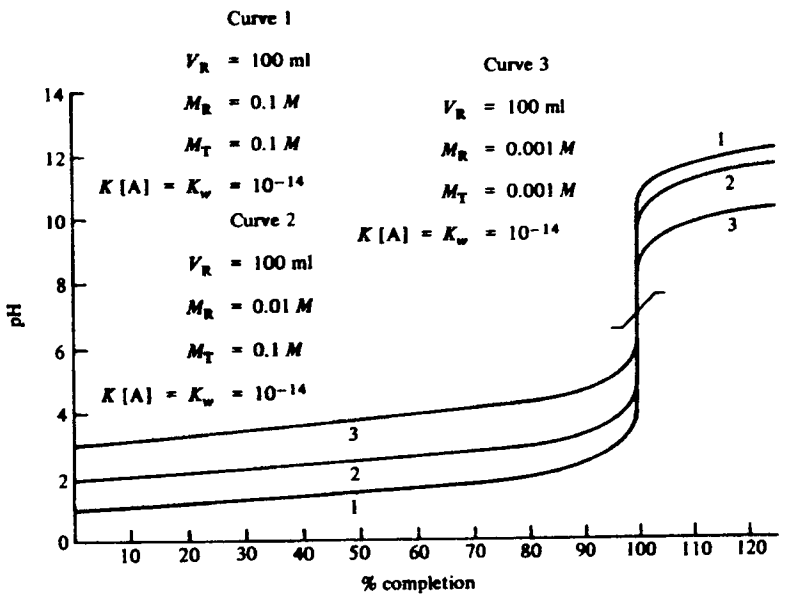

Figure 6: The effect of starting molarities on the range of change of *p*H around the equivalence point.

Table 4
The effect of the value of K on the range of change of pR(V_T) around the equivalence point*

Titration completion (%)	pR$_{VT}$ K = 10^{-10}	pR$_{VT}$ K = 10^{-8}	pR$_{VT}$ K = 10^{-6}
0	1.0	1.0	1.0
10	1.1	1.1	1.1
25	1.2	1.2	1.2
50	1.5	1.5	1.5
75	1.9	1.9	1.8
90	2.3	2.3	2.2
95	2.6	2.6	2.5
99	3.3	3.3	2.9
101	6.7	4.7	3.1
110	7.7	5.7	3.7
120	8.0	6.0	4.0

* The titration data have been corrected for the back-reaction effect where required but not corrected for the dilution effect during titration. All titrations are 100 mL of 0.1 M R *versus* 0.1 M T.

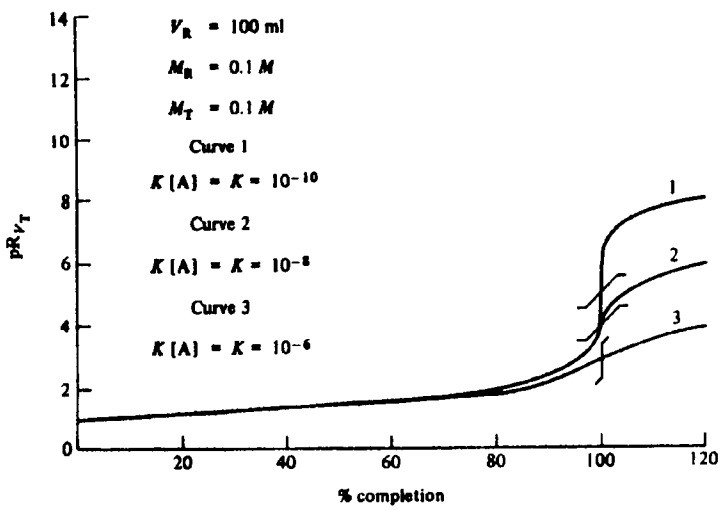

Figure 7: The effect of the magnitude of K on the range of change of pR(V_T) around the equivalence point.

Table 5
The effect of both K and the reactant and titrant molarities on the range of change of pR(V_T) around the equivalence point

Titration completion (%)	100 mL of 0.1 M R *versus* 0.1 M T	100 mL of 0.001M R *versus* 0.001M T
	$K = 10^{-14}$	
	pR_{VT}	pR_{VT}
0	1.0	3.0
10	1.1	3.1
25	1.2	3.2
50	1.5	3.5
75	1.9	3.9
90	2.3	4.3
95	2.6	4.6
99	3.3	5.3
101	10.7	8.7
110	11.7	9.7
120	12.0	10.0
	$K = 10^{-8}$	
0	1.0	3.0
10	1.1	3.1
25	1.2	3.2
50	1.5	3.5
75	1.9	3.7
90	2.3	3.9
95	2.6	3.9
99	3.3	3.9
101	4.7	4.0
110	5.7	4.1
120	6.0	4.2

* The titration data have been corrected for the back-reaction effect where required but not corrected for the dilution effect during titration.

In precipitation titrations, the value of K would be governed by the K_{sp} for the precipitated substance. In complexometric titrations K would be governed by the instability constant for the complex formed (this is the reciprocal of the stability constant). Where oxidation-reduction titrations are involved the value of K_{eq} for the titration reaction would govern the situation.

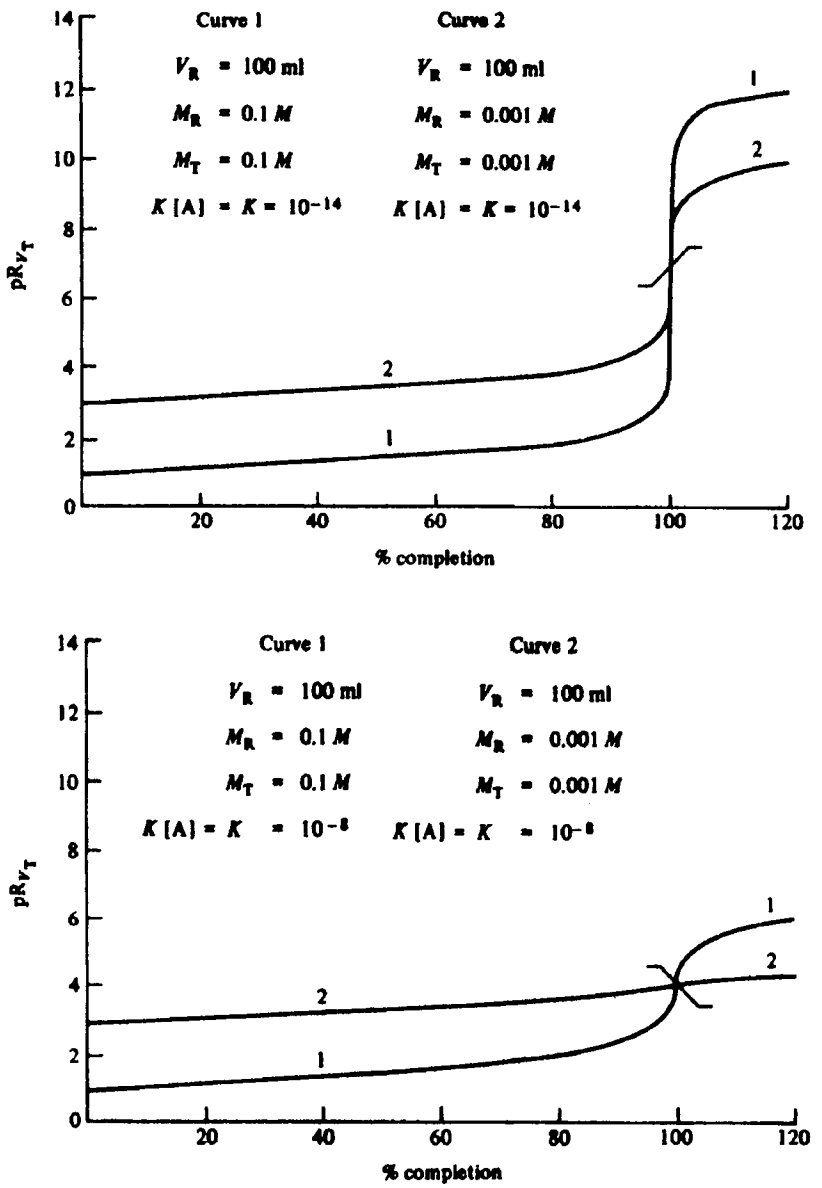

Figure 8: The effect of both K and the reactant and titrant molarities on the range of change of pR(V_T) around the equivalence point.

8.3.4 Equivalence Point (Endpoint) Location

This section will cover the location of the equivalence point or endpoint by modern microprocessor- or computer-controlled potentiometric titrators.

Equipment manufacturers may differ slightly as to the method of location. Only the most popular form will be covered here, and this involves endpoint location from first-derivative data.

Table 6 shows the data printed out on demand from the titration of a dibasic acid with a strong base using a Metrohm 636 Titroprocessor. The titration was carried out in the "drift" control mode, meaning that each titrant volume addition is controlled by a "drift" parameter (mV/min) limit dictated by the operator. The volume additions become smaller as the endpoints are approached and larger after they have been passed. The equipment calculates the change in *p*H for a set volume for each volume step near each equivalence point. This is the)*p*H/)V, and the set volume arbitrarily assigned here is 0.2 mL. From the Figure 9 titration curve there are two endpoints found, EP1 and EP2, at 9.748 mL and 10.045 mL respectively. The following shows the approximate method of endpoint location from data extracted from Table 6 for the points around the two endpoints.

	*p*H	V (mL)	Δ*p*H	ΔV	Δ*p*H/ΔV (0.2 mL)
For EP_1	4.262	9.708			
			0.241	0.023	2.096 (9.720)
	4.503	9.731			
			0.288	0.022	2.618 (9.742)
	4.791	9.753			
			0.295	0.021	2.809 (9.764)
	5.086	9.774			
			0.378	0.040	1.890 (9.794)
	5.464	9.814			
			0.128	0.021	1.219 (9.824)
	5.592	9.835			

EP_1 lies between 9.742 mL and 9.764 mL
EP_1 = 9.742+{(2.809-2.618)/(2.809+2.618)} x 0.2 = 9.749 mL
Actual EP_1 = 9.748 mL (see Figure 9)

For EP_2	5.948	9.900			
			0.502	0.069	1.455 (9.934)
	6.450	9.969			
			0.870	0.058	3.000 (9.998)
	7.320	10.027			
			0.631	0.021	6.000 (10.038)
	7.951	10.048			
			0.359	0.020	3.590 (10.058)
	8.310	10.068			
			0.220	0.020	2.200 (10.078)
	8.530	10.088			

EP_2 lies between 9.998 mL and 10.038 mL
EP_2 9.998+{(6.000-3.000)/(6.000+3.000)} x 0.2 = 10.064 mL
Actual EP_2 = 10.045 mL (see Figure 9)

Table 6
Hardcopy printout of titration data for the titration of a dibasic acid with a standard base. Metrohm 636 Titroprocessor

V/ML	0.000	0.020	0.040	0.060	0.678
*p*H	1.739	1.741	1.739	1.741	1.771
V/ML	1.263	2.000	2.721	3.432	4.132
*p*H	1.802	1.848	1.898	1.950	2.010
V/ML	4.813	5.485	6.138	6.768	7.358
*p*H	2.073	2.143	2.222	2.314	2.416
V/ML	7.917	8.398	8.823	9.129	9.336
*p*H	2.544	2.686	2.863	3.049	3.242
V/ML	9.455	9.537	9.598	9.642	9.677
*p*H	3.402	3.558	3.721	3.880	4.046
V/ML	9.708	9.731	9.753	9.774	9.814
*p*H	4.262	4.503	4.791	5.086	5.464
V/ML	9.835	9.900	9.969	10.027	10.048
*p*H	5.592	5.948	6.450	7.320	7.951
V/ML	10.068	10.088	10.108	10.160	10.229
*p*H	8.310	8.530	8.711	8.992	9.236
V/ML	10.324	10.441	10.584	10.753	10.952
*p*H	9.487	9.719	9.948	10.161	10.359
	V/ML	11.187	11.466	11.810	
	*p*H	10.538	10.690	10.831	

Calculations similar to these are carried out by the integral microprocessor or computer. The calculations for the monotonous titrations carried out with a constant volume addition made after a preselected time in seconds are not identical but very much the same. It should be pointed out for clarification, that the volumes to the right in the last column are the average values between the actual volumes recorded for each of the two points examined.

Where potentiometric titrations, other than those involving *p*H measurement are concerned, such as precipitation, complexation, oxidation-reduction, nonaqueous media, *etc.*, the data obtained will be in the form of E *versus* V. All of the titration theory, and that of titration curves, will apply to such titrations, as will the general methods of endpoint location.

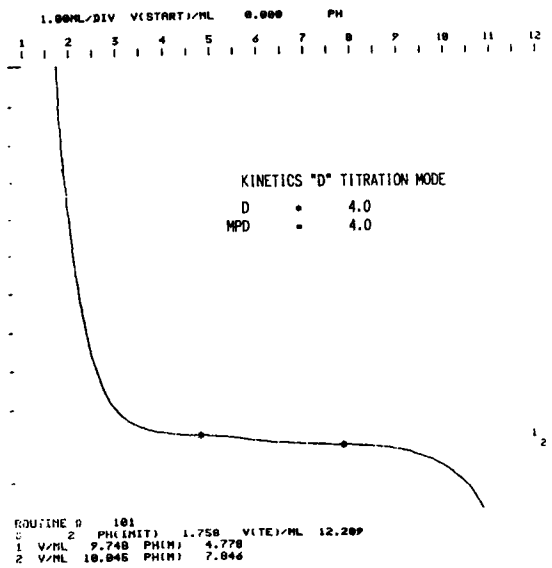

Figure 9: Hardcopy printout of the plot of *p*H *versus* V for the titration data of Table 6.

8.3.5 Applications - Potentiometric Titrations

The potentiometric technique involves the use of glass, ISE and platinum electrodes, the latter used in connection with nearly all oxidation-reduction titrations. These electrodes use external or internal reference electrodes. In the main, the reference is an Ag/AgCl (3M KCl) unit with an outer compartment capable of being filled with an electrolyte of choice and changeable. For chloride titrations, for example, the indicator electrode is often a silver billet coated with AgCl, with a Ag/AgCl reference 3M KNO_3 filled.

In many cases the application of a potentiometric titration to the analysis of a food sample is straight-forward. In determining the titratable acid in mustard the sample is taken up in distilled water, stirred for a set time period and then titrated directly with a standard NaOH solution. In other cases, such as solid or semi-solid foods, the sample must be homogenized in the uptake solution and treated to ensure solution of the analyte. It is necessary in some situations to separate the liquid sample portion by filtration, centrifuging, *etc.*, prior to titration with the standard solution involved.

The general conditions for the treatment of the electrodes of direct potentiometry apply when they are used in potentiometric titrations. They must be cleaned in a customary manner after use, and they must be checked

occasionally to determine that their physical condition has not deteriorated in a manner likely to cause decreased or inhibited response. The face of crystal membrane electrodes, for example, will occasionally require repolishing with a recommended polishing powder. Silver/silver halide electrodes will at times require renewal of the silver halide coating. Even platinum or gold electrodes will require periodic checking against special buffer solutions recommended by the manufacturer and polishing with a recommended powder.

The following gives a list of analytes often determined in foods by potentiometric titration. Only a few possibilities are listed. Specific applications are not cited, since these are too extensive.

acid value	acid, free mineral	acid, nonvolatile
acid number	acid, total titratable	acid, volatile
alkalinity	alkoxyl	allethrin
aluminum	alpha amylase	arsenic
ascorbic acid	benzoic acid	bicarbonate
boric acid	butyric acid	carbon dioxide
calcium	carbonate	catalase
chloride	citric acid	cholesterol
dyes	"decassage" (in wine)	esters
fat acidity	fatty acid, free	fatty acid, total
formol number	hydrocyanic acid	hydroxyl
hydroxyl number	iodide	iodine number
iron	isopropanol	lactose
lanolin	lipid phosphorous	magnesium
malic acid	monochloroacetic acid	methanol
nitrates	peroxidase	peroxide number
phosphorous	phosphate, o-, m-,poly	propylene glycol
reductones	reducing sugars	selenium
squalene	saponification no.	SO_2, total and free
sulphite	sodium chloride	starch
sugars	tannin	tin
urea	vitamin C	vitamin assays

The following gives the actual preparatory and measuring details for two potentiometric titrations, with a general discussion for a third.

8.3.5.1 Total Acidity of Mustard (Acetic Acid)

Weigh into a 250 mL beaker a sample close to but not less than 5.0 g. Record the weight to the third decimal place. Add 125 mL of distilled water and stir magnetically and briskly until the a smooth suspension is obtained (about 5 minutes). Immerse a calibrated (4.00 and 7.00 *p*H) combination glass electrode in the solution, making sure that, when stirring, the reference compartment frit

is well immersed. The titration is carried out on a Metrohm 682 Titroprocessor with 665 Dosimat and 20-mL burette unit.

The unit is operated in the GET *p*H mode, the mode which carries out a titration along drift control lines. The unit also carries out SET mode (deadstop endpoint) titrations. Both modes can be operated in *p*H or mV. Karl Fischer titrations can also be carried out.

For the titration reported here, the titrant was NaOH solution standardized at 0.16826 ± 0.00007 M.

The calibration record is shown on figure 10, as are the parameters set into the 682. Note that these include a start V of 8.00 mL, a titration rate of 4.00 mL/minute, an anticipation of 40, a stop after 1 endpoint and an EP crit. of 4. The anticipation value has a range of 0 to 100, and the higher the number the greater the slowdown. The EP crit. is the evaluation criterion, and ranges from 1 to 8. in two ranges, 1 to 4 and 5 to 8. The sensitivity decreases from 1 to 4. The settings of 5 to 8 duplicate those from 1 to 4 in sensitivity, but include a damping factor to smooth erratic curves.

Figure 10 also shows the hardcopy printouts of the duplicate titration data obtained. Note that this includes:- the endpoint volume EP1, the initial *p*H, the endpoint *p*H, the result R1, the calculation formula F1 with significant figure (3) and units (%) stipulations, the sample weight (C00) and the formula constants (C01 and C02). The hard copy also shows the curve of the titration from the 8.00 mL added titrant volume through to just after the endpoint, which is marked with a "1". The hardcopy could also supply the complete record of volume *versus* *p*H points if requested.

The calculation formula entered is derived from:

$$\begin{aligned} RS1 = F1 &= (EP1 \times NaOH\ M \times GMW\ Acetic\ acid \times 100)/(SW \times 1000) \\ &= (EP1 \times 0.16826 \times 60.05 \times 100)/(COO \times 1000) \\ &= (EP1 \times C01 \times C02)/COO \end{aligned} \quad \textbf{(29)}$$

where:

C01 = 0.16826
C02 = 6.005
C00 = sample weight.

Note that the duplicate results are 2.503% and 2.501% acetic acid. These are typical precisions for modern microprocessor-controlled potentiometric titrators.

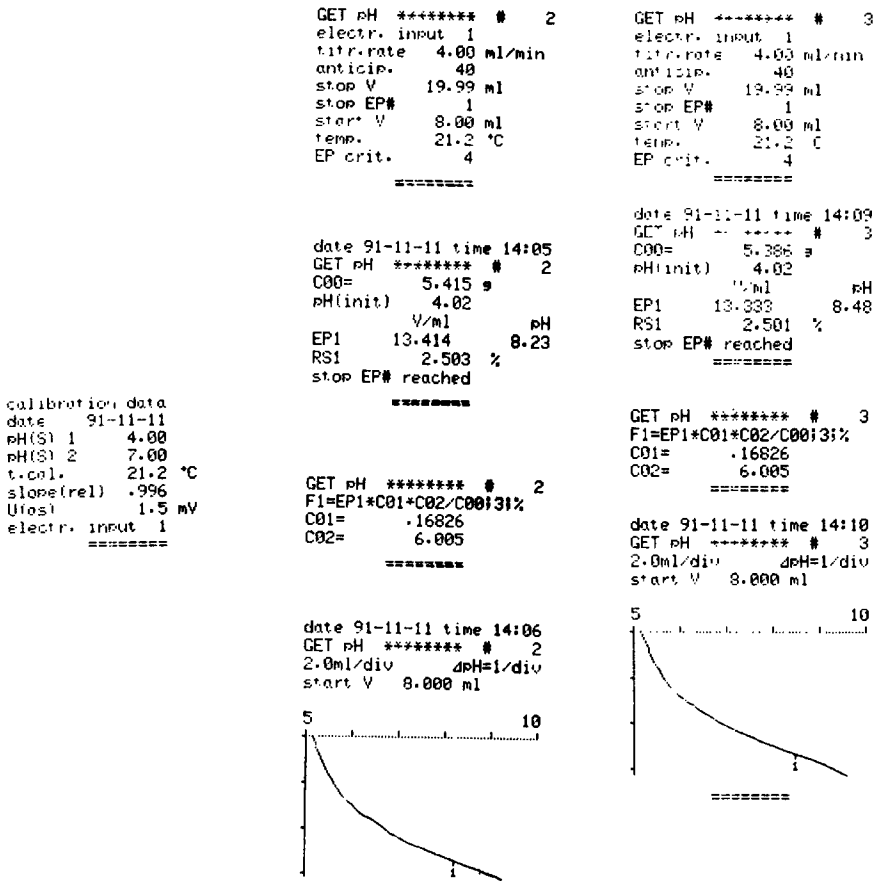

Figure 10: Calibration data and hardcopies for determination of acetic acid in mustard by potentiometric titration

8.3.5.2 Sulfate in Aspirin Tablets

The analytical approach to follow is a modification of the United States Pharmacopoeia method. The technique involves titrating a solution of aspirin with standard lead perchlorate solution in the presence of a Pb-ISE and reference electrode couple. Because of the $PbSO_4$ formed has a slight but significant solubility in water, the titration is carried out a solution of 37 mL acetone and 3 mL water. This solution lowers the solubility of $PbSO_4$ critically. The following solutions are required:

1. 0.02 M lead perchlorate prepared by dissolving 9.20 g of $Pb(ClO_4)_2.3H_2O$ dried over a powerful dessicant for 60 hours and kept over this dessicant.

2. A K_2SO_4 solution from the pure salt dried for 1 hour at 110°C prepared at exactly 1.00 mL = 2.000 mg K_2SO_4 = 1.102 mg $SO_4^=$.

3. Spectroscopic-grade acetone.

The $Pb(ClO_4)_2$ solution for the analyses reported here was standardized against the K_2SO_4 solution to yield a value of 0.0208 ± 0.0002M or 1.00 mL = 1.93 mg $SO_4^=$.

The sample is prepared by weighing out 6.00 g of aspirin powder into a 50 mL beaker and dissolving it in 37 mL of acetone. 3.0 mL of water is now added and the Pb-ISE and reference electrode lowered into the solution. The equipment used was a Metrohm 686 Titroprocessor with 665 Dosimat and a 5-mL burette. The 686 is put in the MEAS mV mode, and the E value observed until it becomes stable. The 686 is then switched to the MET mode for the titration.

The solution was stirred magnetically and titrated with the lead perchlorate solution. A "blank" titration was run and found to yield a value of 0.039 mL. Figure 11 shows the triplicate results and the parameters for the 686. These include a monotonous volume step of 0.05 mL each followed by a 5 second wait period before each successive addition. The parameters also call for a stop after a single EP, with an EP crit. of 30 mV. This latter is the evaluation parameter and is set, as it should be, higher than the actual ΔE around the endpoint of *ca.* 15 to 25 mV. The "blank" was set at 0.01 mL steps, with an EP crit. of 20 mV.

The hardcopy printouts also show the starting potential and the finishing potential as well as the volume at the endpoint. A calculation formula was not entered in the memory. The values $SO_4^=$ are calculated from:

$$\%SO_4^= = \{(EP1 - EP_{blank}) \times \text{titre of } Pb(ClO_4)_2 \times 100\}/\text{sple.wt. (mg)}$$

For the three samples titrated we have:

#7 (1.648 mL – 0.039 mL) x 1.93 mg/mL x 100/6000 mg = 0.052%
#8 (1.637 mL – 0.039 mL) x 1.93 mg/mL x 100/6000 mg = 0.051%
#9 (1.685 mL – 0.039 mL) x 1.93 mg/mL x 100/6000 mg = 0.053%

Note that, here again, the microprocessor-controlled potentiometric titration shows very good precision.

The next method involves the analysis of silage. While this has to do with cattle feed, the system represents very well the extent to which the potentiometric titration methods can be used to provide multiple data in a single titration. A discussion only is given.

8.3.5.3 Silage Assessment by Potentiometric Titration

The computer-controlled method of titration involved was developed by Moisio and Heikonen [44]. Its application to silage press-juice provides for the determination of lactic acid, acetic acid, reducing sugars, amino acid carboxyl groups and the protein degradation products -NH_2 and -NH- groups. The general method follows.

1. 5.00 mL of silage press-juice is pipetted to the titrator vessel and 10.0 mL of water added automatically.
2. The titrator first measures the *p*H of the sample, and then adds 1 M HCl until the *p*H falls below 2. 1 M NaOH is then added in monotonous 0.010 mL increments until the *p*H exceeds 11.9. The *p*H value and the volume after each addition is stored in the computer memory.
3. The time interval between additions is selective, but is usually 300 ms. All data is measured at the buffering capacity maximum, where the *p*H changes slowly and measurements are most accurate.

The following table shows the titration of the components in silage press-juice as to *p*H range.

Measuring range	Component	*p*H range	Consumed alkali (mmol)
I_1	Amino acid N	2.08 - 2.68	A_1
I_2	Lactic acid	3.45 - 3.95	A_2
I_3	Acetic acid	4.40 - 4.90	A_3
I_4	Total N	8.80 - 10.80	A_4
I_5	Reducing sugars	11.30 - 11.90	A_5

The table below shows the calculation formulas entered to the computer to determine the concentrations of each analyte in terms of g/liter.

Component	Concentration equations
Lactic acid	$76.86A_2 - 11.93A_1 - 5$
Acetic acid	$50.80A_3 - 2.83A_1 - 21.50A_2 - 1$
Amino acid N	$8.68A_1 - 1.90A_2 + 0.51A_3$
Total N	$4.13A_4$
Reducing sugars	$177A_5 - 10A_4 - 3$

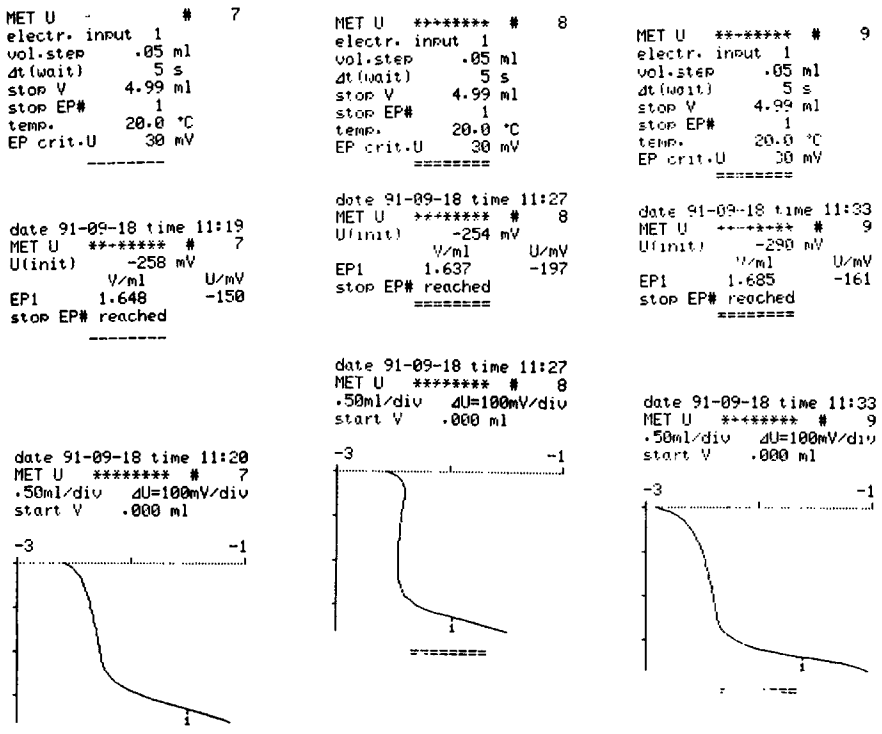

Figure 11: Hardcopies for the determination of sulfate in aspirin by potentiometric titration.

Although a computer was used to receive and store data for this titration, it was found by the writer that a microprocessor-controlled titrator could do equally as well, providing the measuring point list memory has sufficient storage to accept the large number of measuring points. These are large, since the monotonous addition is only 10 μL and the titration often exceeds 15 mL in total volume before 12 *p*H is reached. Most microprocessor-controlled titrators on the market do not have this capability as to measuring point list storage.

8.3.6 Potentiometric Titrations/Photometric EP Detection

It is possible to carry out a potentiometric titration where the endpoint is detected using a photometer, and a probe in the solution. Such titrations are carried out when problems with the potentiometric approach require the use of a colour-change indicator (*e.g.*, when no indicating electrode is available for the analyte to be determined). The probe is a fiber optics device. The source light passes from the entering optic path through the solution to a mirror at the base of the probe. It is then reflected through the return path, incorporating an

optical filter of the required wavelength, to the detector. The photometer is connected to the potentiometric titrator. In this way, the absorbance is recorded by the titrator as mV against the volume additions of titrant. Endpoint evaluation is carried out in the usual manner. In most cases, the titration is carried out in the monotonous additions mode with a "wait" time preselected. It can also be carried out in the deadstop endpoint mode. Additional methods [45-47] and texts for section 8.3 follow immediately after reference [44].

8.4 VOLTAMMETRIC AND POLAROGRAPHIC METHODS

8.4.1 Introduction[3]

Voltammetry is the study of the curves representing the plots of current *versus* applied potential for a working electrode of very small area, a reference electrode and an auxiliary electrode, both of relatively large area. In such a three-electrode system, the current is measured between the working electrode and the auxiliary, while the applied potential is measured between the working electrode and the reference electrode. The conditions of potential measurement involve a high impedance, so that practically no current flows in the working/reference circuit. Because of the small area of the working electrode, the currents in the working/auxiliary circuit are also very small. These may range, depending upon the concentration of the reducible or oxidizable analyte involved, from milliamps to picoamps (10^{-3} to 10^{-12} amps). The development relatively recently of electronic circuits capable of the measurement of extremely low currents accurately has greatly advanced the use of voltammetric equipment.

Voltammetry is usually concerned with the use of working electrodes that have fixed areas. These include all types of solid electrodes (gold, silver, glassy carbon, *etc.*) and liquid electrodes of fixed surface area, such as the hanging mercury drop electrode (HMDE) and solid electrodes with mercury coatings (*e.g.*, mercury on glassy carbon). Polarography, which is a division of voltammetry, refers to the use of mercury electrodes which have a constantly-renewed surface in application. This includes the dropping mercury electrode (DME) and the static mercury drop electrode (SMDE).

Since the area of the microelectrode is very small, and the associated current minute, the iR drop through the solution will also be very small. On this basis,

---

[3] Some text and illustrations in this section are taken from "Analytical Chemistry", James G. Dick, McGraw-Hill, Inc., (1973), Chapter 12, Section 12.5 (with permission).

any potential at the working electrode will be extremely close to the actual potential applied by the equipment.

In order for the current to be directly related to the concentration of the analyte of interest it must be a current that has no significant component other than that associated with the analyte. The sources of current which might contribute to the total current are the following:

1. The diffusion or mass-transfer current.

2. The current resulting from the attraction of the charge on the working electrode for the oppositely-charged analyte substance, sometimes called the electrostatic attraction current.

3. The current due to stirring, regardless of whether this arises out of mechanical stirring, that caused by convection due to heating effects of resistance to current passage, or that arising out of the liberation of gases due to electrode reactions (*e.g.*, the cathodic reaction $2H^+ + 2e \leftrightarrow H_2$).

4. The current required to sustain the charge on the working electrode against leakage losses. This is the charging or condenser current and forms part of the residual current.

5. The current due to trace substances in the "blank" yield solution such as traces of unremoved dissolved oxygen, impurities in the distilled or deionized water and traces of reducible or oxidizable impurities in the chemicals used to prepare the supporting electrolyte. These substances can be part of the faradaic current and provide the second component of the residual current.

The current which responds to the concentration of the analyte of interest is the diffusion or mass-transfer current, and the means of minimizing the other current sources will be discussed in the section following.

Voltammetry in its polarographic form was first discovered in the early 1920s by Heyrovsky [48]. Subsequently, in 1934, Ilkovi [49] provided a mathematical expression showing the manner in which the diffusion current or mass-transfer current varied directly as the analyte concentration. Although the Ilkovic equation was adequate to explaining the relationship between analyte concentration and diffusion current, others postulated refinements aimed at providing more comprehensive expressions. Lingane and Loveridge [50], Strehlow and von Stackelberg [51], Koutecky [53], Mhller [52] and Koutecky and von Stackelberg [54] and others were early contributors in this connection.

The period from 1940 to 1960 showed the development of alternate methods to straight-forward dc for relating the measured current to the analyte concentration. These included ac polarography investigations by Heyrovsky [55-57]; "tast" polarography, Wählin [58] and others [59-61]; pulse polarography, Barker and Gardner [15]; differential pulse polarography, Barker and Gardner [62]; square-wave polarography, Barker and Jenkins [62], and Barker [64]; stripping voltammetry, Zbinden [65] as an early starter and Wang [66] for a modern comprehensive discussion. The later development of these methods, particularly modes such as "tast", normal and differential pulse, square-wave, and anodic, cathodic and adsorptive stripping did not really attain the reliability and sensitivity they now possess until the relatively recent development of highly sophisticated electronic circuitry and timing devices.

To a considerable extent both voltammetry and polarography are concerned with analytes which can be reduced at the working electrode, although in many instances oxidation reactions may also be involved.

8.4.2 Theory of Polarography and Voltammetry [4]

The technique used by Heyrovsky in his originating paper was polarographic, with a dropping mercury electrode (DME). Since his basic principles do not differ greatly with respect to later developments, the DME and SMDE modes applied in ordinary dc polarography will be used to indicate the general theory involved.

8.4.3 DC Polarography with the DME and SMDE Modes

The various contributions to the limiting current were outlined in the previous section. All but the diffusion current are minimized by one means or another. The electrostatic current is minimized by adding one of the many available supporting electrolyte salt solutions to the solution under examination. This salt or salt mixture contains ions which are attracted to the charged mercury electrode but are not discharged. The salt KCl is an example of a supporting electrolyte used with negatively-charged working electrodes. The K^+ ions are attracted to the solution/electrode interface and have the effect of presenting to the solution a highly reduced apparent charge. The analyte ions are not attracted to the electrode electrostatically, but arrive there for discharge or reaction through a process of diffusion through the electrical double layer around the electrode. This is a mass transfer process and subject to Fick's laws. The mercury electrode is said then to be concentration polarized, and the current, beyond the applied potential specific for the analyte involved, will be

---

[4] Some text and illustrations in this section are taken from "Analytical Chemistry", James G. Dick, McGraw-Hill, Inc., (1973), Chapter 12, Section 12.5 (with permission).

controlled by the rate of diffusion. This rate will be a function of the difference in analyte concentration in the solution and that at the electrode surface. Since this latter is theoretically zero, the rate of diffusion is directly proportional to the analyte concentration in the solution, and not to any increase in the applied potential after the zone of the analyte-critical potential. As an example of the manner in which the supporting electrolyte salt can reduce the attraction current its effect on the transfer number of Cd^{2+} should be noted. The transfer number $t_{Cd^{2+}}$ is about 0.5 for 10^{-3} M $Cd(NO_3)_2$, decreasing to 0.009 in 0.1 M KNO_3 and to 0.0009 in 1 M KNO_3.

The current due to the various possible stirring sources is virtually eliminated by carrying the polarographic examination out under conditions of no mechanical stirring. Convection currents due to resistance heating do not exist because of the extremely small currents. Stirring by the evolution of gas bubbles is eliminated by the insignificant currents and the use of applied potentials normally less than that for the cathodic discharge of H^2 gas.

The condenser current can not be eliminated and, in point of fact, it is the factor that restricts the limit of detection of the DME in the straight-forward dc mode and "tast" dc mode to about 10^{-5} M. The minimization of this factor can be accomplished by the use, for example, of the differential pulse mode, and this will be discussed later.

The faradaic component of residual current due to impurities can be minimized by the thorough removal of dissolved oxygen by flushing the solution with an inert gas such as nitrogen or argon; by the use of double-distilled water or distilled deionized water, and by the use of high-purity chemicals.

The Ilkovic equation [31] relating diffusion current and analyte concentration has a component which refers to the fact that the surface area of each mercury drop grows before it falls off the capillary due to the effect of gravity. Under these conditions the time to fall-off is called the drop life. Selected drop times are obtained by tapping the capillary to induce earlier drop fall-off. This component is:

$$A = 4\pi.(3/4\pi d)^{2/3}.m^{2/3}.t^{2/3} \qquad \textbf{(30)}$$

where:

A = drop surface area in time t (cm^3)
d = density of mercury (g/cm^3)
m = rate of flow of mercury into the drop (g/s)
t = time during drop life (s)

The effect of the drop surface moving into the solution is compensated for by multiplication of the rate of diffusion by the factor $(7/3)^{1/2}$. A combination of these factors leads to the equation for an electrode reaction:

Ox – ne X Red

$$i_d = n.F.A.\ (7/3)^{1/2}.\{(D_o/\pi t)\}^{1/2}\ .\ C_o \qquad \textbf{(31)}$$

where:

i_d = diffusion current in μA when C_o is in mmol/L and m the mercury flow rate in mg/s
n = electron transfer for electrode reaction
F = the faraday
A = as above
D_o = the diffusion coefficient (cm^2/s)
C_o = analyte concentration (mmol/L)

Substitution of the value for the faraday and the density of mercury at 25°C yields the expression:

$$i_d = 708.n.m^{2/3}.t^{1/6}.D_o^{1/2}.C_o \qquad (25°C) \qquad \textbf{(32)}$$

Integration of both sides of the equation between 0 and τ (the drop life) yields the expression:

$$\bar{i}_d = 607.n.m^{2/3}.\tau^{1/6}.D_o^{1/2}.C_o \qquad (25°C) \qquad \textbf{(33)}$$

where $\bar{i}_d$ is the average current over the drop life τ. For a given situation, m will be constant as will be τ and D_o, so that the average diffusion current will be directly proportional to the concentration of the analyte. Since all of the components of the equation except n respond to temperature, particularly the value of D_o, the equation is temperature sensitive. This is relatively unimportant since readings for work in quantitative analysis are carried out over time intervals so short that significant temperature changes do not occur under normal conditions. In special instances, temperature can be controlled by the use of double-walled cells with circulating temperature-controlled water.

Figure 12 shows an idealised example of a polarogram for a dc DME scan of current *versus* applied potential. The $E_{1/2}$ value is the value at the point of inflection of the S-curve, and is characteristic for different analytes. Note the legends for residual and limiting currents. The line drawn perpendicular to the potential axis from the residual current line to a point well into the plateau of the curve represents $\bar{i}_d$. The length of this line will be proportional to the analyte concentration. Figure 13 shows the curve of a dc DME curve as it

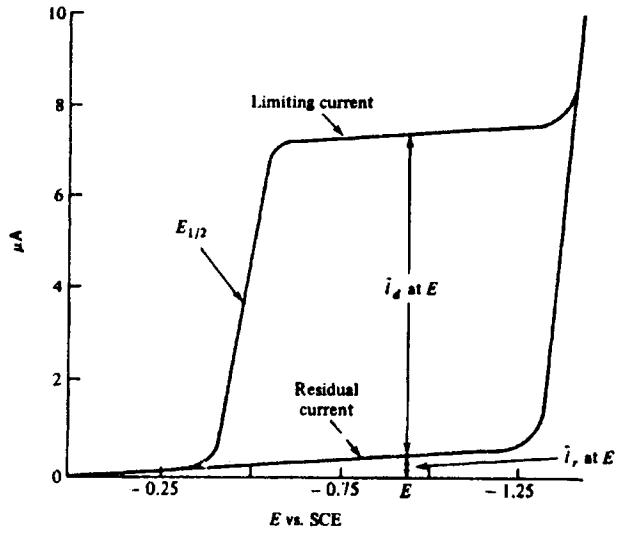

Figure 12: Idealized dc/DME polarographic curve.

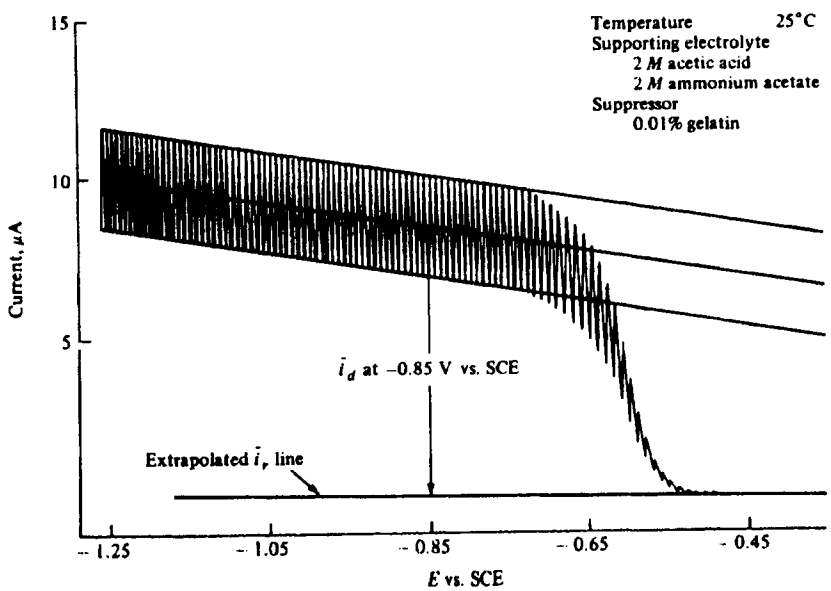

Figure 13: Actual dc/DME polarographic curve.

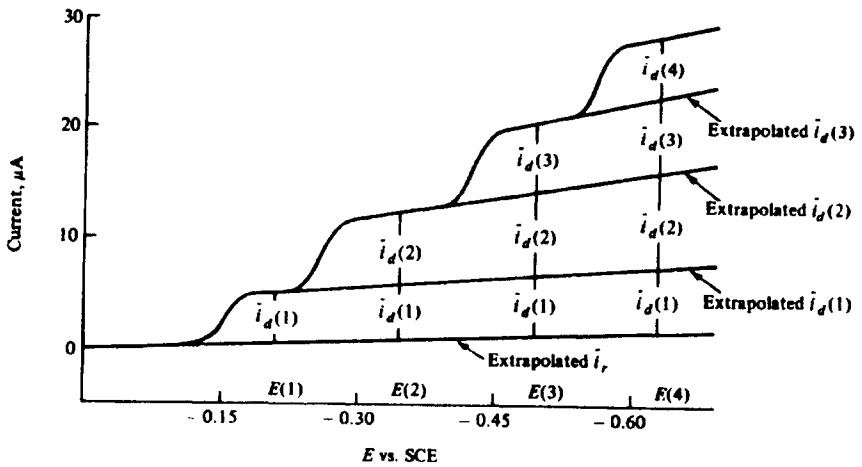

Figure 14: Idealized four-analyte dc/DME polarographic curves showing plateau heights for each analyte.

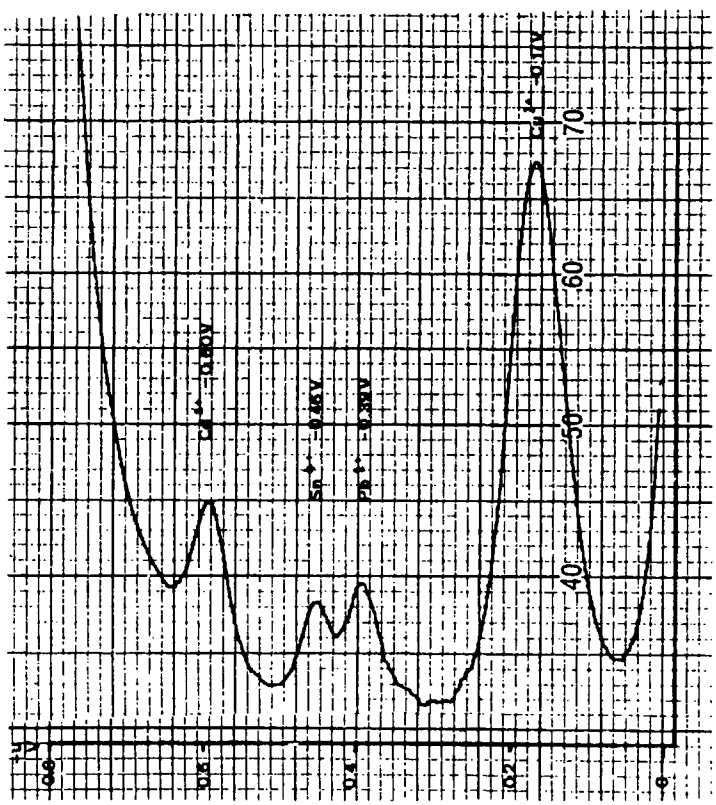

Figure 15: DP/DME polarographic curves for copper, tin, lead and cadmium in waste water.

actually looks. The oscillations are caused by the changing current over the life of each drop as it grows in surface area and falls off the capillary. Figure 14 shows the idealised outline for a multianalyte polarogram in the dc/DME mode. Notice the method for determining the plateau height for each analyte.

In the DME method, the current is integrated over the latter part of the drop life. Nevertheless, since the surface area is still growing over the measuring period, the current measured contains both components for the diffusion and for surface area growth. This is can be an undesirable situation where the analyte is present in relatively small quantities. The static mercury drop method (SMDE) endeavours to offset this situation by halting the flow of mercury near the end of the drop life for each drop, measuring the current for the static drop over a short period of time, and then knocking the capillary automatically to dislodge the drop.

8.4.4 Pulse and Differential Pulse Polarography

The limit of detection for the dc/DME method has already been mentioned. This does not permit the determination of analytes that are less than *ca.* 1 ppm in concentration. Today, the demand is for the determination of environmentally or health suspect analytes at the low parts per billion (ppb) level. This is three orders of magnitude better than the ordinary dc or dc "tast" technique can provide. The current signals at such levels are such that they are lower than the condenser current mentioned earlier. This current can not be eliminated, but its effect can be greatly minimised.

This requires the use of pulse and/or differential pulse polarography. In general, pulse polarography involves a single square-wave voltage impulse applied for a specific period at a pre-determined instant some time after the start of the drop. The amplitude of the pulses (the mV value) is increased linearly with time. The condenser current decays rapidly after the onset of the pulse, while the diffusion current decays much more slowly. The current measurement is made over a short interval at the end of each pulse, at a time when the influence of the condenser current is minimal. The drop is knocked off immediately after the final measurement of current. This situation provides polarographic waves of the regular S-shape, but the limit of detection is about 50 to 10 ppb depending on the characteristics of the analyte involved.

In differential pulse polarography, the situation is somewhat similar. In this case, the pulse amplitudes are constant for each drop. For a very brief period just before the application of the pulse, the current is measured. The pulse is then applied for a brief period. Near the end of this period, and just before the drop is knocked-off, the current is again measured. The same situation applies as was outlined before, the final measurement being made when there is relatively minimal interference by the condenser current with the diffusion current. In differential pulse polarography the difference between the current

measured before the pulse and that at measured at the end of the pulse is plotted against the applied potential. It follows that, since this is in effect a first-derivative plot of the regular S-shaped curve, the plot will have a peak which corresponds to the $E_{1/2}$ value for a regular pulse polarographic plot. The height of the peak above the baseline is directly proportional to the analyte concentration. This technique is capable of yielding detection limits of less than 1 ppb with some metals. It should be understood that, in both pulse methods, the duration of the pulse and that of the measuring intervals are in the 60 and 20 millisecond range. These intervals can be varied as required. Figure 15 shows typical differential pulse plots for copper, lead, tin and cadmium in the DP/DME mode.

8.4.5 Stripping Voltammetry

Although these pulse techniques would appear to provide excellent limits of detection, the determination of some analytes, highly dangerous in both the environmental sense and that of food intake, require methods capable of reaching consistently the 10 ppb level and substantially less. The stripping analysis techniques of the hanging mercury drop electrode, differential pulse stripping voltammetry (HMDE/DPSV) method satisfy this requirement. There are three main forms of stripping analysis, the anodic (HMDE/DPASV), the cathodic (HMDE/DPCSV) and the adsorptive (HMDE/DPAdSV).

In the first, the application is mainly to metallic substances which have (1) reduction reactions of good reversibility and (2) metals with good capabilities of forming an amalgam with mercury. The former is required in order that the metal reaction of Ox + ne = Red shall be sufficiently reversible so that the major portion of the metal plated into the drop will undergo the reaction Red – ne = Ox during stripping. This will provide a good response factor (high current per concentration unit). The second is required in order to ensure that the solubility of the analyte metal in the drop will be sufficient to permit a good degree of enrichment.

In this HMDE/DPASV technique a reproducible hanging mercury drop is created at the capillary tip in a solution of analyte concentration so low as to be at or lower than the limit of detection of either the pulse or the differential pulse techniques. The application of a negative charge of adequate potential to the drop, coupled with stirring of the solution, permits the deposition of one or more analyte metals on the drop, with subsequent amalgam formation and diffusion into the drop. The period of electrolysis and the magnitude of the potential will determine the degree of enrichment. After a selected period of deposition without stirring (to create the depleted or electrical double-layer zone around the drop), a differential pulse-modified potential is applied in the positive (decreasingly negative) direction. As decreasing potential passes at a selected rate through the E_{peak} for each metal, the usual differential curve is obtained where the peak heights are directly proportional to the associated

analyte concentrations. Because of the high analyte concentration in the drop and the low value in the solution (factors of 1000:1 are not at all unusual), excellent peak heights are obtained where the original solution would have shown no response at all. Typical HMDE/DPASV voltammograms shown in figure 24.

The HMDE/DPCSV method is applied where the deposition potential and period is followed by a scan in the increasingly negative potential direction. It is often applied to anions forming insoluble compounds with mercury. Figure 16 shows a typical HMDE/DPCSV scan in the determination of selenium at 1.5 ppb.

The HMDE/DPAdSV technique involves the formation of an organic chelate of the analyte, usually a metallic element, that has the ability to be adsorbed on the surface of the HMDE at a specific potential. Subsequently, during a scan in the potential direction dictated by the redox properties of the chelate, quantification of the metal and/or chelating substance is obtained. To a considerable degree, organic substances can be determined in this way also. A typical example of metal determination is the HMDE/DPAdSV determination of Ni as the Ni-dimethylglyoxime chelate. The sensitivity of HMDE/DPAsSV is often outstanding for many organic and metal chelates, frequently having the capability of attaining with ease the middle and low parts per trillion ranges for many analytes. Figure 17 shows a typical set of standard addition curves for the determination of nickel at low level in a treated waste water from an electroplating plant.

8.4.6 Mercury and Other Electrode Materials

There are advantages to the use of mercury for electrodes, whether in the form of drops or as coatings on, for example, glassy carbon electrodes. The main advantage is the high overvoltage of hydrogen on mercury, allowing the determination of metal analytes in acid solutions well into the negative zone. Depending on the *p*H of the solution, this could be as high as -1.5 V or higher under certain conditions. A second advantage is that, where drops are concerned, a new surface is available at each drop, so that no effect of previous treatment can obscure the examination, such as can occur with solid electrodes such as gold electrodes. This permits highly reproducible current-potential relationships. With mercury-coated electrodes, the coated surface can be reused or replaced with a new surface. This mercury electrode type often offers several advantages over the mercury drop. The worst feature of mercury as an electrode is the fact that, at potentials more positive than about +350 mV *versus* Ag/AgCl (3M KCl), mercury (I) is formed, with a current obscuring that for other species. It is in this zone of potential that solid electrodes such as gold, silver, and particularly glassy carbon find their application, much of this being involved in the determination of organics having their reactions well into the positive zone (*e.g.*, catecholamines at *ca.* 800 mV).

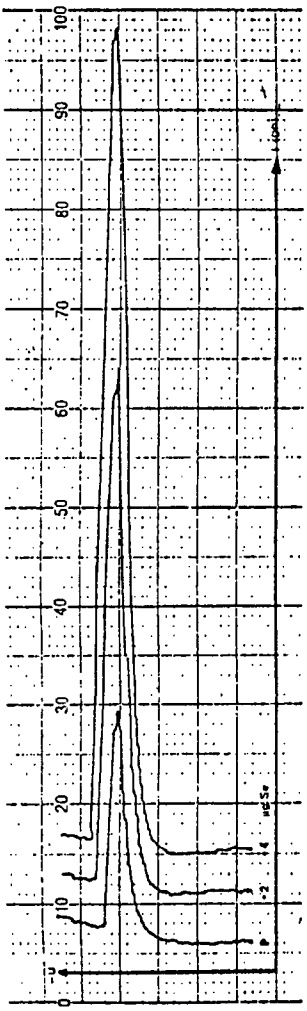

Figure 16: Typical HMDE/DPCSV scan for the determination of selenium.

8.4.7 Methods of Quantitative Determination

There are two main methods for quantifying polarographic and voltammetric data for analytical purposes. The first method involves a calibration technique. The DPP method is used here as the example of the technique. The solutions containing the analyte in at least five concentrations within the range of interest, as well as a "blank" solution, are polarographed at the appropriate parameters of scan range, pulse amplitude, scan rate, *etc.* The heights of all peaks obtained are measured. The "blank" peak value, if any, is deducted and the resulting corrected peaks are plotted against the analyte concentration.

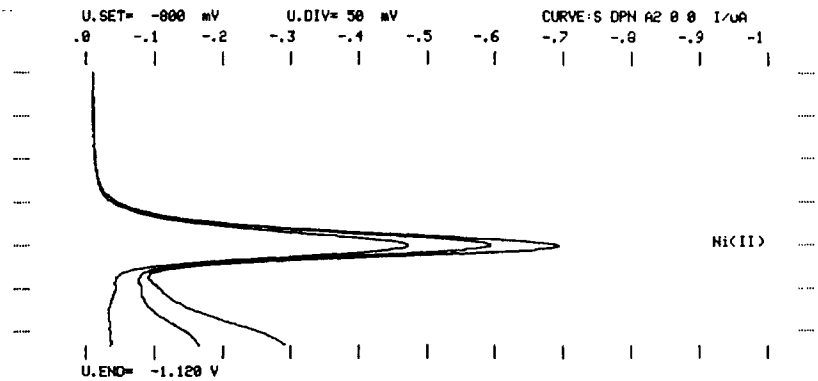

SMOOTHED CURVES FOR HMDE DPAdSV DETERMINATION OF Ni(II) IN SHIELD PLATING WASTE WATER AFTER DESTRUCTION OF ORGANICS

Treated Waste Water Survey

METROHM 646 VA-PROCESSOR (5.646.6041)
Detn. of Ni in Shields waste water-HMDE/DPCSV METHOD
MPL 1 EL.TYPE HME

SUPP.ELEC 500uL 0.1M NH4 OH/Cl
V.MEAS 20.500 mL
ALIQUOT 1.000

REMARK Ni(II) in waste water
Ag/AgCl (3M KCl) reference electrode
NAME Prof. J.G.Dick
RUN# 1

ANALYTE	L R S	U.SUBST	EV.VALUE	DELTA	m.ANALYTE
Ni(II)	A0 0 0	-1.000 V	376.0 nA		
	A1 0 0	-1.000 V	463.4 nA	87.34 nA	
	A2 0 0	-1.001 V	539.2 nA	75.80 nA	
	m.STD	100.0 ng	SLOPE	1.225 ug/uA	463.3 ng

rho(Ni) = 46.3 ug/L

SMPL.V.m 10.0000 mL IDENT Shield Plating Sple.
DATE 91-09-19 TIME 14:52

Figure 17: Typical set of standard addition curves for the determination of nickel at low level in a treated waste water from an electroplating plant.

This can provide a chart for future use. A better technique is to use the corrected peak height values and associated analyte concentrations to produce a linear equation. Any unknown has its corrected peak height inserted in the equation with subsequent solution for analyte concentration.

The above technique is satisfactory where the unknown substance contains no compounds or conditions of a variable nature such that they are capable of affecting the peak height for the analyte. One of the ideal situations for the application of the calibration technique is that involving pharmaceutical

preparations where, because of rigid quality control, the sample background is quite constant, and only the analyte may vary. Where situations are such that the sample background composition is unknown, such as it is with many sample types, the standard additions technique is best applied. In this technique a "blank" is run and determined. The sample solution is then run. After this initial run, the solution is "spiked" by the addition of an exact volume of a solution containing a known amount of the analyte. The solution is polarographed again, and this standard addition situation is repeated at least twice more, for a total of not less than three. The peak heights are measured and any "blank" peak height subtracted from each. The corrected peak heights and the increasing analyte standard addition values are subjected to linear regression analysis to provide the amount of analyte in the sample solution, which amount can be treated to obtain the analyte concentration in the original sample. Each standard addition should involve an amount of analyte giving a response *ca.* between 30 to 70% of that for the original sample solution. Figure 18 shows DP/DME curves for the determination of copper, lead and cadmium in a synthetic water sample. For all three metals, the standard additions were 5.000 μg each, and the automatic evaluation from the microprocessor-controlled VA Scanner is shown below the curves. Note that the linear regression is carried out, for copper as an example, by using the data shown for this element under EV.VALUE together with the accumulative amounts of the standard additions. With this instrument, any determined "blank" (in mass units) is automatically corrected for.

EV.VALUE (nA)	Cu added (μg)
27.87	0.0
39.50	5.0
51.25	10.0
62.66	15.0

8.4.8 Applications in Food Analysis

It should be pointed out at the outset of this section that, where previous oxidative treatment of the sample is not involved, it is possible to speciate with the polarographic/voltammetric techniques. Thus it is possible, for example, to determine separately Cr(III) and Cr(VI), Sn(II) and Sn(IV), Ti(III) and Ti(IV), Fe(II) and Fe(III), *etc.* This can be most important where one oxidative state of a substance is more toxic or more nutritionally valuable than an other.

One of the more important areas of application lies in the determination of metallic substances in liquid and solid foods, or the biological materials from which they originate. Because of the organic basis of these substances they very often contain compounds which can inhibit the responses of metallic

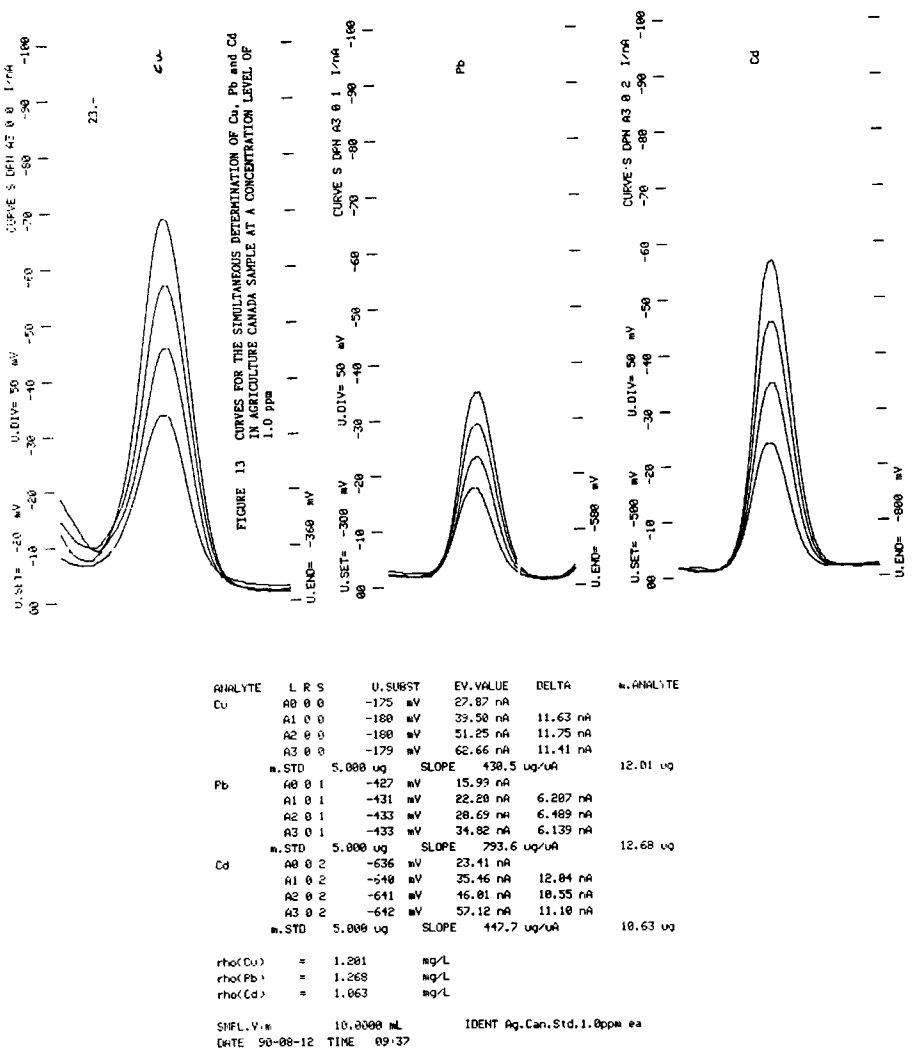

ANALYTE	L R S	U.SUBST	EV.VALUE	DELTA	m.ANALYTE
Cu	A0 0 0	-175 mV	27.87 nA		
	A1 0 0	-180 mV	39.50 nA	11.63 nA	
	A2 0 0	-180 mV	51.25 nA	11.75 nA	
	A3 0 0	-179 mV	62.66 nA	11.41 nA	
	m.STD 5.000 ug	SLOPE	430.5 ug/uA		12.01 ug
Pb	A0 0 1	-427 mV	15.99 nA		
	A1 0 1	-431 mV	22.20 nA	6.207 nA	
	A2 0 1	-433 mV	28.69 nA	6.489 nA	
	A3 0 1	-433 mV	34.82 nA	6.139 nA	
	m.STD 5.000 ug	SLOPE	793.6 ug/uA		12.68 ug
Cd	A0 0 2	-636 mV	23.41 nA		
	A1 0 2	-640 mV	35.46 nA	12.04 nA	
	A2 0 2	-641 mV	46.01 nA	10.55 nA	
	A3 0 2	-642 mV	57.12 nA	11.10 nA	
	m.STD 5.000 ug	SLOPE	447.7 ug/uA		10.63 ug

rho(Cu) = 1.201 mg/L
rho(Pb) = 1.268 mg/L
rho(Cd) = 1.063 mg/L

SMPL.V.m 10.0000 mL IDENT Ag.Can.Std.1.0ppm ea
DATE 90-08-12 TIME 09:37

Figure 18: DP/DME curves - Cu, Pb, and Cd in synthetic water sample.

analytes. It is necessary therefore in the majority of cases to subject the samples to wet-ashing, or microwave digestion under pressure, to destroy all organic matter. Such digestions are best carried out with HNO_3, $HNO_3 + H_2O_2$, HNO_3/H_2SO_4 or, preferably, with $HNO_3/HClO_4$ mixtures. There are many analytes where it is not necessary to digest the food sample.

For example vitamin C in jams, fruit and vegetable juices can be determined directly. In fact, a large number of the vitamins can be determined polarographically in pharmaceutical preparations without elaborate

predetermination treatment. The following gives a general list of a few of the applications of polarography and voltammetry to the analysis of foods.

aluminium	antimony	arsenic	barium
beryllium	bismuth	bromide	cadmium
calcium	cerium	caesium	chloride
chromium	cobalt	copper	gallium
germanium	gold	indium	iodide
iron	lead	magnesium	mercury
molybdenum	nickel	nitrate	nitrite
phosphorous	selenium	silver	strontium
sulphide	sulphate	sulphite	tellurium
thallium	tin	titanium	uranium
vanadium	zinc	zirconium	

Other metals such as the lanthanides and the platinum series can also be determined. Nearly all of the vitamins. A large number of organic substances, including substances active in pharmaceutical preparations. In many instances, the determination of organic substances is carried out using the glassy carbon electrodes at applied potentials in the positive zone relative to the Ag/AgCl reference electrode.

Several examples of analytical work based on voltammetric polarographic techniques follow. Additional techniques are provided in references [67-80], together with suggested texts. All of these cover section 8.4 material.

8.4.8.1 Selenium in Foods

Samples of this type require wet-ashing or microwave digestion carried out using minimal volumes of HNO_3/H_2SO_4 mixtures. For this sample, 10.00 g as-is is heated with 10 mL HNO_3/5 mL H_2SO_4, both acids being concentrated and of ULTREX or SUPRAPUR grade. When fumes of SO_3 appear, the solution is inspected. If it is still yellow or brown, it is cooled, 3 mL of HNO_3 added and re-evaporated to SO_3 fumes. The process is repeated as required until a clear solution is obtained. The cooled solution is then transferred to a polarographic vessel using 15.0 mL of distilled water. 6 M and 1 M NaOH solutions (from high-purity NaOH) are now used to adjust the *p*H to 2.2. 0.5 mL of Cu(II) solution (0.1 g/L prepared with $CuSO_4.5H_2O$) is added, followed by 2 mL of 0.1 M Na_2H_2EDTA and 7.8 g of ULTREX or SUPRAPUR $(NH_4)_2SO_4$. The solution is allowed to cool to ambient temperature if required and is dearated for 7 minutes by nitrogen passage. Voltammetry is carried out in the HMDE/DPCSV mode with an enrichment time of 60 s with stirring and 15 s without stirring. The enrichment potential is -200 mV with stirring and -400 mV without stirring, both *versus* Ag/AgCl (3M KCl). A Pt auxiliary electrode is used. The pulse amplitude for the DP mode is -30 mV, scan range -400 mV to -900 mV, drop time 600 ms and scan rate 4 mV/s. The E_{peak} value is *ca.* -670 mV.

Figure 19 shows the curves and the data for the original run and the runs for two standard additions each of 100 μL (2 μg Se(IV) of a solution 20 ppm to Se(IV). Since the equipment used in this case was not microprocessor-controlled, it was necessary to use the tangential baseline technique to measure the peak heights. These heights are shown on Figure 19, together with the result of linear regression to yield the Se(IV) content of the food sample. The "blank" sample did not show any measurable Se(IV) content when tested in exactly the same manner, including the preparatory digestion step. The result found for Se(IV) was 1.48 μg in 10.00 g of sample, or 148 ppb. Note: Other samples may require other weight and acid amounts.

8.4.8.2 Vitamin C in Orange Fruit Drinks

The supporting electrolyte here is 0.1M acetic acid/0.1M sodium acetate adjusted to *p*H 4.6 with either dilute acetic acid or dilute sodium hydroxide. 19.0 mL of the electrolyte is pipetted to a polarographic vessel, followed by 1.00 mL of the commercially-available fruit drink. The solution is dearated with nitrogen gas for 8 minutes and scanned in the DP/SMDE mode. The pulse amplitude is -50 mV; the starting and finishing potentials 150 and -150 mV respectively, the drop time 600 ms and the scan rate 4 mV/s. The E_{peak} is *ca.* 5 mV *versus* Ag/AgCl (3M KCl). No "blank" was required. The standard additions were 240 μL each (120 μg) of 500 ppm vitamin C (ascorbic acid) solution. Figure 20 shows the curves for the original and standard additions. This work was carried out on a Metrohm 646/647 microprocessor-controlled VA Scanner and Stand. The data are automatically linear regressed and the final result printed out. These data are also shown on Figure 20. Note that the sample analysed at 305 mg vitamin C/L or 30.5 mg/100 mL. The labelled value on the sample of fruit drink analysed was 30 mg of vitamin C/100 mL. Natural orange juice must be pretreated before the polarographic determination of vitamin C.

The following determinations are given without preparatory details in order to provide examples without excessive discussion. Figures 21 and 22 show the determination of total tin as Sn(IV) in a sample of tomatoes that had been homogenised using a Polytron. The method used was HMDE/DPASV. The curve to the right of the Sn(IV) curve is for lead. The value found was 708 ppb Sn(IV). Figure 23 shows the determination of total arsenic in the same sample. Prior to being polarographed, any As(V) was reduced to As(III), since the method used responds to the As(III) oxidation state only. The value obtained for total arsenic was 151 parts per trillion. Figures 24 and 25 show lead and cadmium as determined by the HMDE/DPASV technique in the same tomato sample. Finally, Figure 26 shows the HMDE/DPCSV determination of low total chromium in waste water.

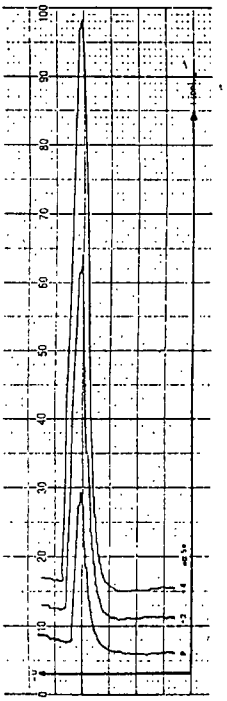

Original soln. 137.5 nA
1st addition 325 nA 187.5 nA
2nd addition 510 nA 185 nA

Linear regression

Coeff. of correlation 0.9999
Intercept (-) 1.48 ug
Slope 0.0107

Sample = 10 g
Se(IV) found = 1.48 ug
Se(IV) in sample = 0.148 ug/g
= 148 ppb

Figure 19: HMDE/DPCSV curve and calculation for Se(IV) in food sample.

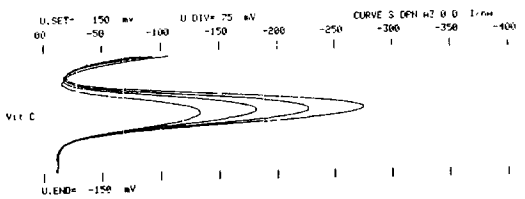

SERIES 3 - 646/647 VA Scanner Interpretation

METROHM 646 VA-PROCESSOR (5.646.6040)
Vitamin C ... TANG ORANGE METHOD 10
mPL 1 EL.TYPE MMF

SUPP.E.EC 0.1M NaOAc/HOAc
V.MEAS 20.000 mL
ALIQUOT 1.000

REMARK TANG ORANGE purchased Loblaw's 25/8/86
120 ug spikes
NAME Prof. J.G.Dick
RUN# 1

ANALYTE	L R S	U.SUBST	EV.VALUE	DELTA	m.ANALYTE
Vit C	A0 0 0	1.9 mV	119.0 nA		
	A1 0 0	6.6 mV	167.8 nA	48.82 nA	
	A2 0 0	9.0 mV	213.8 nA	46.09 nA	
	A3 0 0	11 mV	260.6 nA	46.79 nA	
	m.STD 120.0 ug	SLOPE	2.548 ng/uA		385.0 ug

rhx(VitC) = 385 mg/L

SMPL.V.m 1.00000 mL IDENT TANG ORANGE
DATE 86-08-31 TIME 13 48

Figure 20: DP/SMDE curves for the determination of vitamin C in an orange fruit drink.

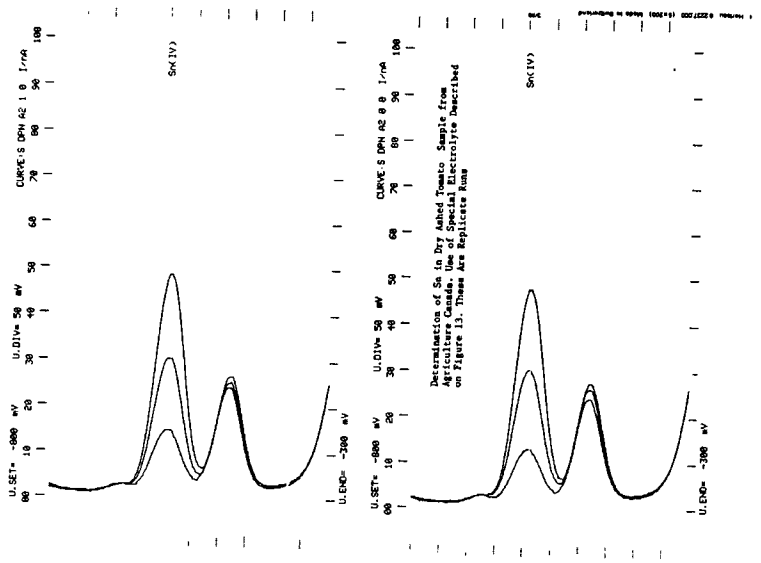

Figure 21: HMDE/DPCSV curves for the determination of Sn(IV) in dry ashed homogenised tomato sludge.

```
METROHM 646 VA-PROCESSOR  (5.646.6041)
Determination of Sn(IV) in Tomato Dry Ash.Aq.Can. METHOD   6
MPL  1          EL.TYPE   MME

SUPP.ELEC       Amm.ox/Amm.Cl/HCl
V.MEAS           20.000 mL
ALIQUOT          1.000

REMARK          Sn(IV) in Tomato Dry Ash - Agric. Canada)
                Ag/AgCl (3M KCl) reference electrode
NAME            Prof.J.G.Dick
RUN#             4

    ANALYTE    L R S       U.SUBST      EV.VALUE    DELTA        m.ANALYTE
    Sn(IV)     A0 0 0       -592  mV     11.19 nA
               A0 1 0       -592  mV     13.12 nA
               A1 0 0       -591  mV     29.26 nA
               A1 1 0       -591  mV     29.93 nA    17.44 nA
               A2 0 0       -590  mV     48.05 nA
               A2 1 0       -590  mV     49.24 nA    19.05 nA
            m.STD    1.000 ug      SLOPE    54.78 ug/uA          354.1 ug

    rho Sn(IV)  =    708.2         ug/L

    SMPL.V/m         500.000 uL          IDENT Ag.Can.dryash tomat.
    DATE  90-11-29  TIME   14:04
```

Figure 22: Automatic evaluation and determination of Sn(IV) from curves shown on figure 21.

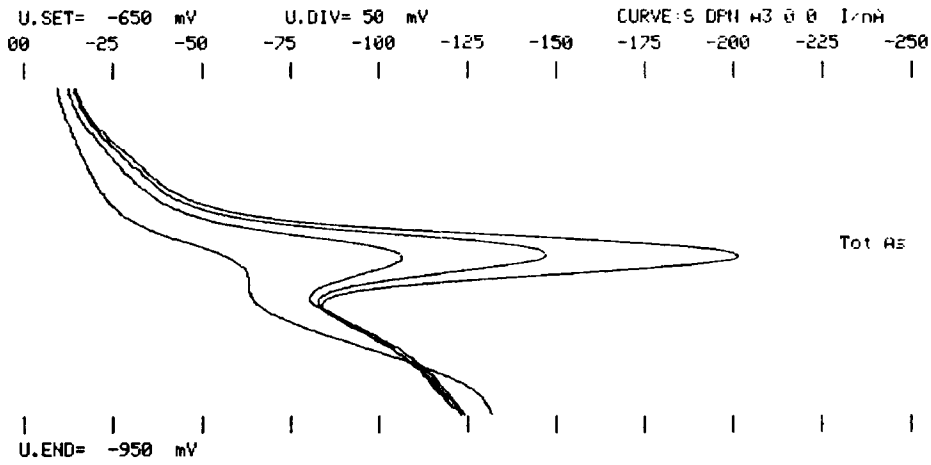

Determination of Total As in Tomatoe Sludge Sample Supplied by Mr. Michel Sigouin of Agriculture Canada. Test Run after Reduction of Any As(V) to As(III).

```
METROHM 646 VA-PROCESSOR (5.646.6041)
As(III) in Various Ag.Can.Stds. & Samples          METHOD  7
MPL  1        EL.TYPE   MME

SUPP.ELEC     0.75M HCl+100ug Cu
V.MEAS         20.000 mL
ALIQUOT        1.000

REMARK        As(III) in Ag.Can. Stds. & Tomato dry-ash smples.
              Ag/AgCl (3M KCl) reference electrode
NAME          Prof.J.G.Dick
RUN#           1

    ANALYTE    L R S       U.SUBST     EV.VALUE    DELTA        m.ANALYTE
    Tot As     A0 0 0      -808  mV    13.51 nA
               A1 0 0      -801  mV    47.68 nA    34.17 nA
               A2 0 0      -800  mV    90.81 nA    43.13 nA
               A3 0 0      -802  mV    143.6 nA    52.87 nA
             m.STD    1.000 ug     SLOPE    23.05 ug/uA          204.6 ng

    rho(tot as  =     .1509        ug/g

    SMPL.V/m          1.35580 g          IDENT Tot.As.Ag.Can.tomat
    DATE  90-12-03  TIME   11:48
```

Figure 23: HMDE/DPCSV curves and automatic evaluation and result for the determination of arsenic in wet ashed homogenised tomato.

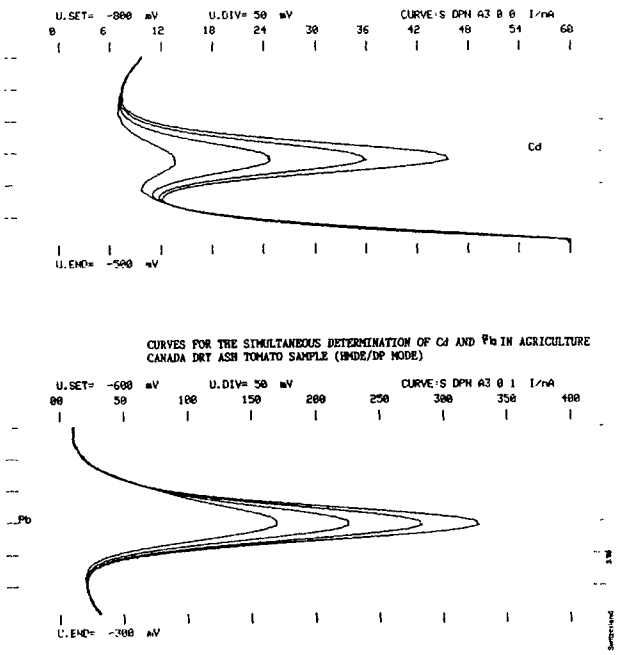

Figure 24: Replicated HMDE/DPASV curves for determination of cadmium and lead in dry ashed homogenised tomato.

```
METROHM 646 VA-PROCESSOR  (5.646.6041)
Cd,Pb in Ag. Can. Tomato Dry Ash Sample          METHOD   4
MPL  1        EL.TYPE   MME

SUPP.ELEC     adj. 2.5 pH NH3
V.MEAS         20.000 mL
ALIQUOT        1.000

REMARK        Adj. pH precaution against hydrogen inter.
              Reference electrode Ag/AgCl(3M KCl)
NAME          Prof.J.G.Dick
RUN#           1

    ANALYTE    L R S       U.SUBST     EV.VALUE    DELTA        m.ANALYTE
    Cd         A0 0 0      -639  mV    5.170 nA
               A1 0 0      -639  mV    15.77 nA    10.60 nA
               A2 0 0      -639  mV    26.20 nA    10.43 nA
               A3 0 0      -639  mV    35.62 nA    9.416 nA
             m.STD    200.0 ng     SLOPE    19.64 ug/uA          106.5 ng
    Pb         A0 0 1      -445  mV    130.1 nA
               A1 0 1      -444  mV    191.5 nA    61.40 nA
               A2 0 1      -444  mV    251.5 nA    59.97 nA
               A3 0 1      -444  mV    299.0 nA    47.57 nA
             m.STD    1.000 ug     SLOPE    17.64 ug/uA          2.346 ug

    rho(Cd)     =    10.6          ug/L
    rho(Pb)     =    234           ug/L

    SMPL.V.m          10.0000 mL          IDENT Tomato dry ash smple
    DATE  90-08-14  TIME   13:38
```

Figure 25: Evaluated data for determination of cadmium and lead from the curves shown on figure 24.

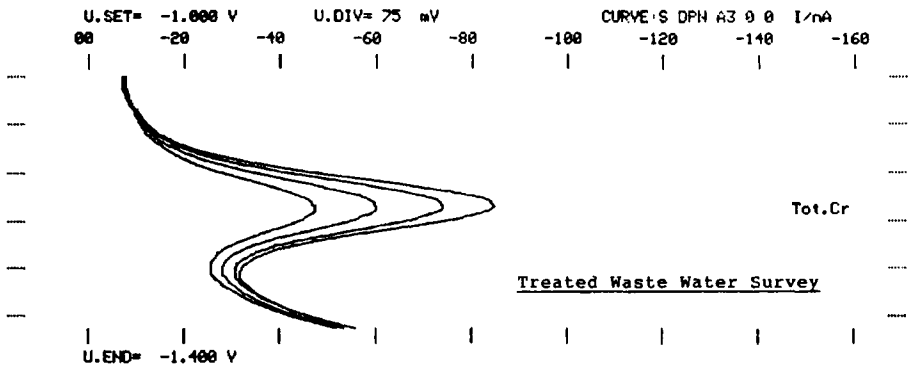

SMOOTHED CIRVES FOR THE HMDE DPCSV DETERMINATION
OF TOTAL CHROMIUM IN SHIELD PLATING WASTE WATER
AFTER DESTRUCTION OF ORGANICS. AUTOMATIC EVALUATION
OF CURVES AND CALCULATION OF RESULTS

METROHM 646 VA-PROCESSOR (5.646.6041)
Detn. Total Cr in Shields waste water-HMDE/DPCSV METHOD
MPL 1 EL.TYPE MME

SUPP.ELEC EDTA/NaNO3/NaAc/pH6
V.MEAS 20.000 mL
ALIQUOT 1.000

REMARK Total Cr in waste water
Ag/AgCl (3M KCl) reference electrode
NAME Prof. J.G.Dick
RUN# 1

ANALYTE	L R S	U.SUBST	EV.VALUE	DELTA	m.ANALYTE
Tot.Cr	A0 0 0	-1.204 V	28.77 nA		
	A1 0 0	-1.203 V	40.06 nA	11.28 nA	
	A2 0 0	-1.202 V	52.04 nA	11.97 nA	
	A3 0 0	-1.201 V	61.04 nA	9.002 nA	
	m.STD	1.250 ug	SLOPE	114.9 ug/uA	3.301 ug

rho(Cr) = 330 ug/L

SMPL.V.m 10.0000 mL
DATE 91-09-23 TIME 16:28

Figure 26: HMDE/DPCSV curves for the determination of trace total chromium in waste water.

8.5 POLARISATION TITRATIONS

8.5.1 Introduction and Theory

Polarisation titrations are often referred to as amperometric or biamperometric titrations. It is necessary that one of the substances involved in the titration reaction be oxidizable or reducible at the working electrode surface. These titrations are based on generally on the principles of polarography, voltammetry and potentiometry.

The general approach to biamperometric titration was suggested by Salomon [81-83] in 1897/98. It was not until some 30 years later that the technique was recognised as a useful analytical tool and described by Foulk and Bawden [84] in 1926 as a "dead-stop endpoint method". The single polarised electrode method of amperometry using a DME was explored by Heyrovsky and Berezicky [85] in 1929, while Laitinen and Kolthoff [86] in 1941 applied the same technique but with the use of a rotating platinum electrode. In general, the polarisation titration method is applicable to oxidation-reduction, precipitation and complexation titrations. Relatively few applications involving acid/base titration are found.

The principle of the method can best be explained by using an amperometric titration with a single polarised electrode (DME) as an example. Suppose a titration is carried out in a deaerated solution containing a supporting electrolyte, using a working microelectrode (*e.g.,* DME), and a relatively large-area Ag/AgCl (3M KCl) reference electrode and a burette. Suppose further that the analyte in this solution is Pb^{2+} as $Pb(NO_3)_2$ and the titrant is H_2SO_4. In this case the Pb^{2+} will act as the depolarizer. The reaction in titration will be:

$$Pb^{2+} + SO_4^{=} \text{ W } PbSO_4 \downarrow \qquad \textbf{(34)}$$

The fixed potential applied at the working electrode will be sufficient for the reduction of Pb^{2+} but for no other substance in the titration. Stirring is usually accomplished by passage of the deaerating gas (*e.g.,* nitrogen), sometimes aided by magnetic stirring. When the gas and stirring action are shut off after deaeration is finished, the potential at the working electrode (*e.g,* DME) will cause it to be polarised and a diffusion current will be noted, the magnitude of which will be established by the concentration of Pb^{2+}. When the titration starts, it is necessary to stir and deaerate by gas passage before measuring the current after each titrant addition has equilibrated. This procedure creates little hardship since the form of location of the endpoint, by extrapolation of the straight-line sections of the curve before and after the endpoint to intersection, requires that only a few points before and after the endpoint be located. The $[Pb^{2+}]$ decreases as the titration progresses with decreasing diffusion current. Since no other substance is active except Pb^{2+}, there is no change in the current after the equivalence point except for a slow decrease due to dilution by the

excess titrant volume. Figure 27A shows the typical L-shape of such a curve. The following important points should be noted: (1) The sections before the equivalence point zone are straight. This will only be the case where the dilution effect has been compensated for or where the titrant concentration is 20x or more than that of the analyte. This will be mentioned again later: (2) The slope of this section indicates the decay of the current with decreasing [Pb^{2+}]: (3) The rounded section at the junction of the arms of the L represents the effect of the equilibrium constant for the titration reaction. The lower the equilibrium constant the less complete the reaction and the more rounded this section: (4) The distance from the volume axis to the curve well after the equivalence point represents the approximate value of i_r, the residual current: (5) The extrapolated lines provide, at their intersection point, the equivalence point volume value.

Figure 27B shows the curve for an amperometric titration where the titrant is the active substance. This might exemplify the titration of Pb^{2+} with a solution of K_2CrO_4, yielding precipitated $PbCrO_4$. Here a DME could again be used, with a fixed constant potential applied capable of reducing the Cr^{6+} to Cr^{3+} and affecting no other substance in the analyte solution or titrant. In this case, Cr6+ will be the depolarizer. Note that this provides a titration curve of reversed L-shape. Little difference in diffusion current appears until after the equivalence point, when the excess of K_2CrO_4 results in an increasing current.

Figure 27C represents the case where a fixed potential to a DME is applied such that both the reactant (analyte) solution and the titrant supply active substances. An example would be the application of a fixed constant potential appropriate to the reduction of both Pb^{2+} and Cr^{6+} from the K_2CrO_4. In this case the curve will be V-shaped, the current first decreasing with decreasing [Pb^{2+}] and then increasing after the equivalence point with increasing titrant K_2CrO_4 excess.

Amperometric titrations may also be carried out with twin polarised electrodes. Commonly used are a pair of platinum wire microelectrodes. It is important to remember that, in such a situation, whatever charge is applied to one electrode will induce the opposite charge in the other. This may at times result in undesirable side reactions. Minimum effective potentials should always be used. In some cases, both the reactant (analyte) in the solution under analysis and the reactant in the titrant may behave reversibly at the electrodes. In some others, only the reactant (analyte) in the solution may act reversibly; in others again, only the titrant reactant may act.

Figure 28 shows amperometric titrations involving two polarised electrodes. Figure 28A represents the oxidation/reduction titration in an acid solution containing Fe^{2+}, and using a standard solution of Ce^{4+}. The titration uses twin Pt wire electrodes. This is a system where the reactants both have reversible

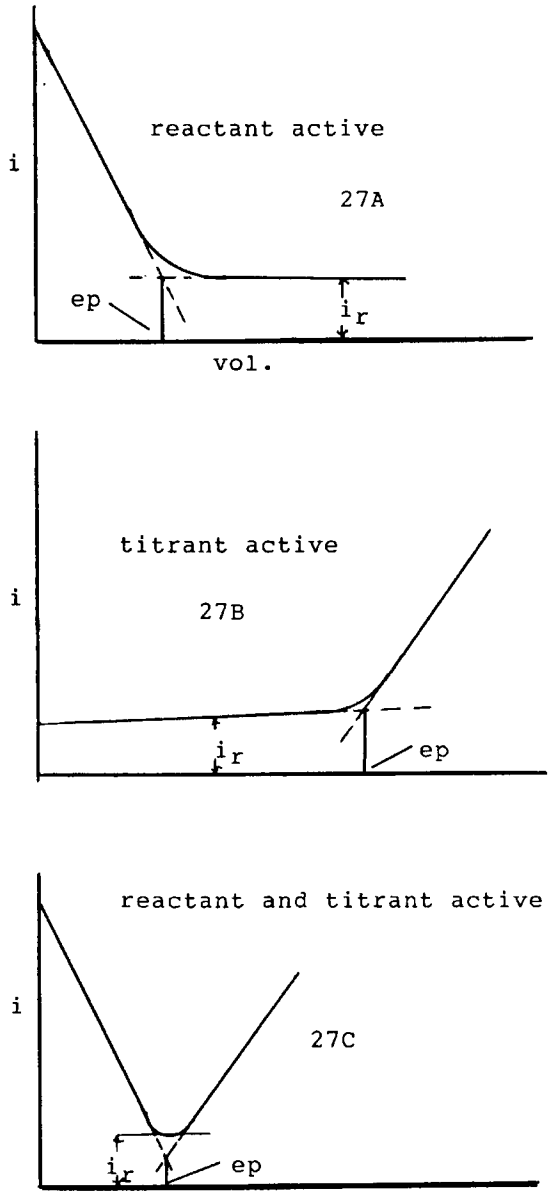

Figure 27: Amperometric titrations with one polarised electrode.

reactions. For example, in this biamperometric titration of Fe^{2+} (analyte) by a standard solution of $Ce(NO_3)_4$, the possible reactions are:

$Fe^{3+} + e \leftrightarrow Fe^{2+}$ **(35)**
$Ce^{4+} + e \leftrightarrow Ce^{3+}$ **(36)**

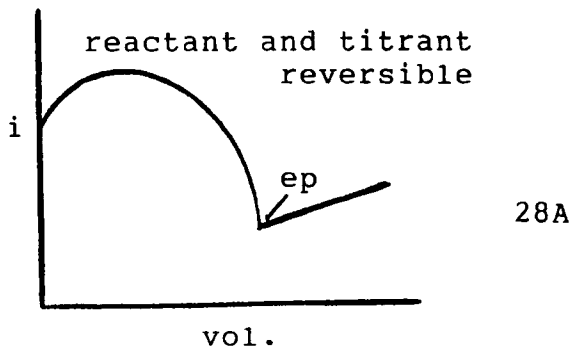

28A

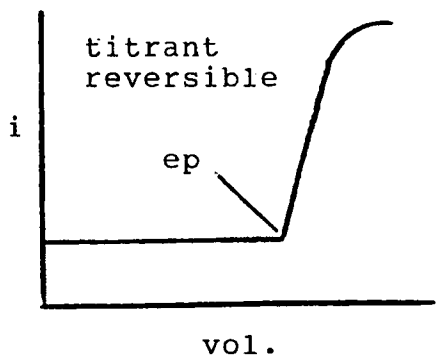

28B

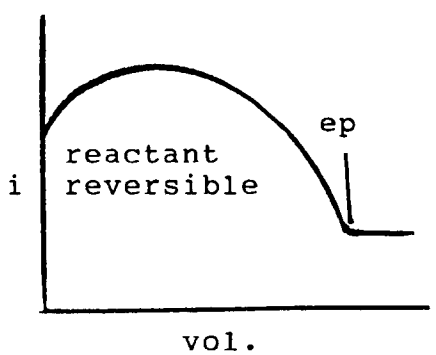

28C

Figure 28: Amperometric titrations with two polarised electrodes (biamperometric titrations).

The application of a fixed potential of 100 mV between the twin platinum microelectrodes in the solution before the start of the titration will result in a polarised electrode situation and only a minimal current will be observed, since

only Fe^{2+} is present. The magnitude of the current will always represent the rate at which the reactant of lower concentration is brought to the surface of the electrode. The reactions of the Fe species will be:

$$Fe^{3+} + e \leftrightarrow Fe^{2+} \quad \text{cathode} \qquad \textbf{(37)}$$

$$Fe^{2+} - e \leftrightarrow Fe^{3+} \quad \text{anode} \qquad \textbf{(38)}$$

Where the cerium species is concerned, the expected reactions will be:

$$Ce^{4+} + e \leftrightarrow Ce^{3+} \quad \text{cathode} \qquad \textbf{(39)}$$

$$Ce^{3+} - e \leftrightarrow Ce^{4+} \quad \text{anode} \qquad \textbf{(40)}$$

Again, the current can depend on the cerium species of lower concentration. At the start neither Ce species will exist, confirming a zero current. When the titration starts, the addition of Ce^{4+} results in the formation of Fe^{3+}, resulting in a current being obtained from the cathodic and anodic reactions (37) and (38). Until the midpoint of the titration, the current will be determined by the lesser but increasing concentration of Fe^{3+}; beyond the midpoint, the lesser and decreasing concentration will be that of Fe^{2+} and this will dictate the current. Note, on this basis, that current first rises and then falls. At the equivalence point, the titration system is completely polarised. After the equivalence point, the current will depend on the lesser concentration of the Ce species, namely that of Ce^{4+}. With increasing additions of the titrant beyond the equivalence point, the current will rise according to the increasing Ce^{4+}, the electrode processes being those for reactions (39) and (40).

Figure 28B represents a titration situation which has extended use in laboratories as the Karl Fischer titration for the determination of water. This titration will be covered in detail later. In the meantime the example used will be that of the titration of As^{3+} by I_2. This is a titration that can be carried in food analysis under the proper conditions. The arsenic reaction is

$$AsO_3^{3-} + H_2O \rightarrow AsO_4^{3-} + 2H^+ + 2e \qquad \textbf{(41)}$$

is slow and quite irreversible at the potential to be applied between the twin platinum wire electrodes. The reaction of iodine is reversible as

$$I_2 + 2e \leftrightarrow 2I^- \qquad \textbf{(42)}$$

so that the titrant alone will be active. At the start of the titration only As^{3+} will be present and no current will appear. After the start, As^{3+}, As^{5+} and I- will be present but, since no free I_2 will be present, the current situation remains unchanged until just after the equivalence point. The appearance of excess

iodine, the depolarizer, results in a current which increases with increasing excess iodine added.

Figure 28C represents a titration with two platinum wire electrodes and involving iodine in solution being titrated with sodium thiosulphate (I_2 by $S_2O_3^=$). Here the thiosulphate reaction

$$2S_2O_3^= - 2e \rightarrow S_4O_6^= \qquad \textbf{(43)}$$

is not reversible under the conditions of the technique, but the iodine/iodide reaction is (equation 42). At the start of the titration only I_2 exists in solution with no iodide, and minimal current will be noted. After the start, both I_2 and I^- will be present. Until the midpoint of the titration, I^- will be the lesser but increasing concentration, dictating the increasing current. After the midpoint the I_2 will be the lesser and decreasing concentration, dictating the decreasing current. After the equivalence point, since the thiosulphate species is not reactive, the current will remain essentially as it was at the equivalence point.

Biamperometric titrations carried out on modern equipment usually involve stirred solutions, with the current *versus* volume of titrant being recorded continuously. Such titrations usually provide a dead-stop endpoint location.

Amperometric titrations can be applied in the determination of analyte solutions as low as 10^{-5} M to 10^{-6} M in concentration.

There are several factors of general importance where amperometric titrations are concerned. Four of the most important of these are indicated by the following.

1. The prime advantage of polarisation titrations is the ability to handle reactions of poor equilibrium constant. This stems from the location of the endpoint by extrapolation to intersection from either side of the endpoint zone. This ability renders the method capable of carrying out titrations not easily possible by the potentiometric method. This characteristic is shared with other titration techniques (*e.g.*, conductometric, photometric).

2. Since the limiting current is a function of the rate of diffusion of the reactive species or depolarizer to the electrode surface, the rate of stirring in those titrations where stirring can be carried out on a continuous basis, must be held constant.

3. Since the curves obtained from the potentiograph or from manual tabulation can be seriously distorted by the degree of dilution of the solution by the titrant, endpoint location may be rendered difficult. This problem can be minimised. Where the titration data is obtained by

plotting the manually determined values of current and titrant volume for several points before and after the endpoint, each current value can be multiplied by the factor (V + v)/V, where V is the volume at the start and v the volume added to the point of titration of interest. These corrected current values are then plotted against the appropriate titrant volumes. Distortion can also be minimised by the use of a titrant much higher in concentration than that of the analyte. A factor of not less than 20x is common. This provides for titrant volumes very small in reference to the starting analyte solution volume. Although this leads to small titrant volumes at the endpoint, this is of little importance where modern piston microburettes record volume values to three decimal places accurately. This is the technique applied when carrying out biamperometric titrations with modern automatic equipment.

4. The rate of addition of titrant should never be excessive, and this of course applies to biamperometric titrations carried out under continuous current/titrant volume recording. For example, there are titrations where bromine is generated as the titrant to brominate an unsaturated organic as analyte. Too rapid a generation of the bromine depolarizer relative to the speed of bromination can prematurely trigger an endpoint indication where the titration has been set to dead-stop at a specific current value.

The electrodes used in amperometric work may be, as examples, the DME, gold, silver, tungsten, graphite, glassy carbon, twin platinum wire, twin platinum sheet, rotating platinum wire, rotating platinum disk, *etc.*

8.5.2 Polarisation Titration Equipment

Amperometric titrations can be carried out with relatively simple equipment. A manual polarograph suffices to apply the potentials required, while the current recording device can provide the current. The titrant can be added with the use of a microburette. The electrode can be a DME or, where applied potentials are too positive for mercury or where the reactant(s) may attack mercury, a rotating platinum wire may be used. The reference electrode can be double-compartmented, with the Ag/AgCl (3M KCl) reference in the inner compartment and an appropriate electrolyte solution in the outer, the outer being in contact with both the reference and the solution under investigation. The analyte should be held in a titration vessel of 50 to 100 mL capacity. Finally, a means of deaeration with nitrogen is required for pretitration deaeration and deaeration after titrant additions. Deaeration is not always required since, in some titrations, oxygen does not interfere at the potential applied. In most cases, the stirring action of deaeration suffices; where it is not felt sufficient, magnetic stirring can be used as an adjunct.

Today, with the availability of advanced electronic instrumentation, including microprocessor- or computer-controlled titrators with microburettes, amperometric titrations are carried out on a more or less automatic basis. This is particularly true of biamperometric titrations. The auxiliary equipment required to convert the usual modern potentiometric titrator into one capable of amperometric titration involves a unit called a "polarizer". This unit, linked to the potentiometric titration unit, provides the fixed applied potential required. It can also set the limit within which the current is expected to fall during the titration. The current changes are converted to mV values and the titrator plots these values against the titrant volume. The polarizer/titrator combination can also be used in dead-stop titrations to stop the titration at a current representative of the endpoint. Polarizers are also capable of carrying out titrations by fixing the current allowed to flow, and then plotting the potential changes required to sustain this current flow against titrant volume. Here again, this mode can be used to permit dead-stop titrations to be carried out.

8.5.3 Applications of Polarisation Titrations

The following are examples of analytes and analytical data, pertaining to foods or pharmaceuticals only, that are determinable by amperometric and biamperometric titrations.

aluminium	antimony	arsenic	barium
bismuth	bromide	cadmium	calcium
chloride	cobalt	copper	cyanide
disulphides	EDTA	fluoride	glucose
iodide	iodine no.	iron	isoniazide
magnesium	maleic acid	mercaptans	molybdate
nickel	nicotine	phenols	phosphate
sulphate	sulphide	sulphite	vitamins
water	many unsaturated organics		

Of these, water is perhaps by far the substance most determined in foods by biamperometric titration. The determination of water is perhaps worthy of a more complete coverage. The determination is based on the titrimetric procedure developed by Fischer [87] in 1935. His procedure involved the preparation of a titrating reagent consisting of a mixture of iodine, sulphur dioxide and pyridine in methanol. The titration reaction with water involves a two-stage reaction:

$$C_5H_5N.I_2 + C_5H_5N.SO_2 + C_5H_5N + H_2O \rightarrow 6\ 2C_5H_5N.HI + C_5H_5N.SO_3 \quad \textbf{(44)}$$

$$C_5H_5N.SO_3 + CH_3OH \rightarrow 6\ C_5H_5N(H)SO_4.CH_3 \quad \textbf{(45)}$$

At the time of its introduction, and for many years thereafter, the endpoint was detected as the first brown colour introduced by the iodine in the excess reagent. The odour of pyridine is obnoxious and the vapour is toxic to an extent. Although the reagent is still used, it has been largely superseded by newer pyridine-free reagents containing other amines and heterocyclic compounds. Methanol is not the only solvent for the titrant; others have been developed for special purposes. These reagents can be supplied as one- or two-component systems. Such reagents can be handled in the open air without serious contamination. They also provide for much faster reaction rates than the original reagent. The sample itself can be dissolved in a selection of solvents to suit its characteristics. A discussion will be given in the section on coulometry concerning the generation of iodine for the Karl Fischer titration by coulometric means.

The present day applications of the Fischer titration method for water determination involve titrators using the biamperometric approach to endpoint location. A fixed potential is applied across the two platinum wire microelectrodes that is capable of reducing iodine. As the titration progresses, and as long as excess water is present, the electrode system is concentration polarised and the current between the electrodes remains low. At the very first excess of iodine, the system becomes depolarized and the current increases sharply. There is also a bivoltammetric approach where a fixed current is set between the electrodes. In this case, the first excess of iodine causes a sharp drop in the monitored potential in order to sustain the preset current. Although the current *versus* titrant volume could be plotted, the normal technique is to set the unit to provide a dead-stop endpoint. In modern units, the endpoint volume is indicated by a digital readout on the microburette, but the best units provide a means of internally calculating the water content from the endpoint volume and input data involving the sample size. The following gives a very partial list of the Karl Fischer titration application to the determination of water in foods.

sugar	cheese	chocolate	cocoa
condensed milk	dried vegetables	edible oils	flour
bakery products	dried fruits	fatty acids	cereals
grains	gelatin	honey	maize
corn	malt	margarine	rice
marzipan	milk powder	syrup	jams
jellies	pasta products	vegetables	fruits
nuts	whole milk	yoghurt	coffee

The following are some categories of determinable substances: carbohydrates, fats, and high protein foods. The References section provides several additional applications (references 88-100) and suggested texts for use with section 8.5.

8.5.3.1 Determination of Water in Oils and Fats

The Karl Fischer reagent should be previously standardised against sodium tartarate dihydrate (standardisation grade - 1mg of the dihydrate = 0.1566 mg of H_2O). A "blank" determination should be run on the chloroform/methanol solvent.

Weigh to the nearest 0.01 g, 5 - 25 g of the sample containing not more than 100 mg of H_2O into the titration vessel of the Karl Fischer titrator. Dissolve in 50 mL of an anhydrous mixture of 1:4 chloroform and methanol. Titrate on a Karl Fischer titrator to a voltametric endpoint, using a Karl Fischer titrant (*e.g.*, Hydranal) of appropriate strength. Modern titrators such as those available from many manufacturers have facilities for entering the sample weight, performing the "blank" correction and calculating the sample water content in the units required (*e.g.*, %, ppm, *etc.*).

8.5.3.2 Isoniazide in Pharmaceutical Preparations

Weigh 20 tablets and reduce to a fine powder. Weigh into a 400 mL beaker a weight of powder capable of yielding about 400 mg of isoniazide. Record the weight to the nearest 0.0001 g. Add 150 mL of distilled water and stir until the sample is dissolved to the best possible extent. Dilute to about 200 mL and filter on a #40 Whatman paper or equivalent. Catch the filtrate in a 250 mL volumetric flask, and wash with distilled water until the volume is close to the mark. Dilute to the mark and mix well.

Pipette a 50.00 mL aliquot into a 200 mL titration vessel and add 50 mL of distilled water and 20.0 mL of concentrated HCl. Now add 0.2 g of KBr and a stirring bar. Use a recording potentiometric titrator, an interconnected automatic piston burette with a 50 mL capacity and an interconnected polarizer (this method was originally applied using a Metrohm 536 Potentiograph, a 535 Dosimat and a 585 Polarizer). Twin platinum sheet electrodes (0.5 cm^2) are connected to the polarizer. The polarizer is set to provide a value of E_{pol} equal to 100 mV, with the I_{pol} reading set at 5 μA/250 mV. This latter is the μA equivalent to the recorder setting at 250 mV, with an offset allowing the titration to start at about the centre of the scale. The titrant is a standard solution of 0.1N potassium bromate ($KBrO_3$) (actual value 0.0829N).

The rate of titrant delivery is set at 20 minutes/full burette volume of 50 mL. The speed of the magnetic stirrer is about medium rate and not changed for each titration. The titration is a bromination reaction, and is shown on Figure 29 as equation (46). Figure 29 also shows the titration curve and the location of the titration endpoint, as well as the calculation of the isoniazide per tablet based on a sample weight taken of 0.15626 mg and a weight/tablet of 0.5857 g. This sample weight was weighed to the 5th decimal place because the work was a preliminary experimental run to determine the method of approach. Note

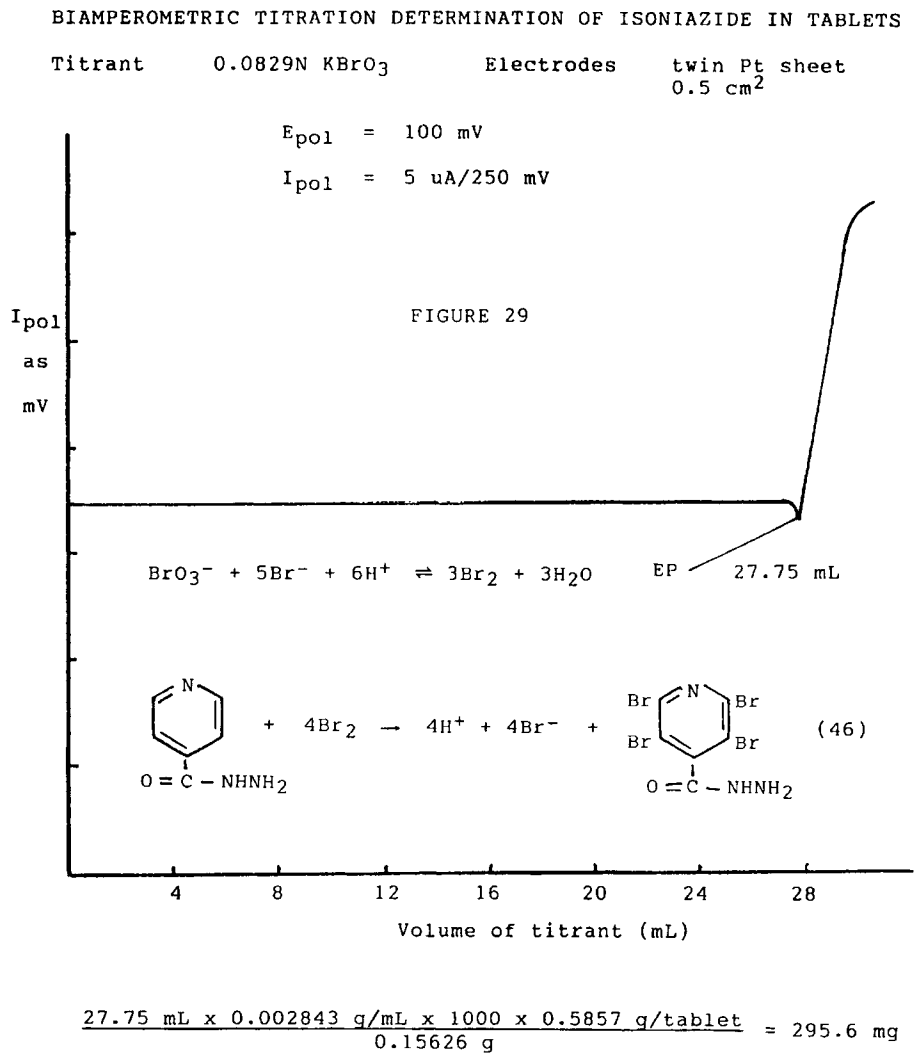

$$\frac{27.75 \text{ mL} \times 0.002843 \text{ g/mL} \times 1000 \times 0.5857 \text{ g/tablet}}{0.15626 \text{ g}} = 295.6 \text{ mg}$$

Figure 29: Biamperometric titration determination of isoniazide in tablets.

that the value obtained was 295.6 mg/tablet for a tablet with a labelled value of 300 mg isoniazide/tablet. Ten successive runs gave an rsd of 1%.

8.6 COULOMETRY AND CONDUCTOMETRY[5]

8.6.1 COULOMETRY

8.6.1.1 General Introduction

The methods of coulometry are based on the measurement of the quantity of electricity involved in an electrochemical electrolysis reaction. This quantity is expressed in coulombs and it represents the product of the current in amperes by the duration of the current flow in seconds. The quantity of electricity thus determined represents, through the laws of Faraday, the equivalents of reactant associated with the electrochemical reaction taking place at the electrode of significance. In the analytical chemistry sense, the process of coulometry, carried out to the quantitative reaction of the analyte in question, either directly or indirectly, will yield the number of analyte equivalents involved in the sample under test. This will lead to a quantitative determination of the analyte in the sample. Analytical coulometry can be carried out either directly or indirectly. In the former the analyte usually reacts directly at the surface of either the anode or cathode of the electrolysis cell. In the latter, the analyte reacts indirectly with a reactant produced by electrolytic action at one of the electrodes in the electrolysis cell. In either case, the determination will hinge on the number of coulombs consumed in the analytical process.

In general the relationship between the coulombs for an analytical process and the weight of analyte involved is given by:

$$W = (W_m Q/nF) \quad \textbf{(47)}$$

where: W = weight of analyte (reactant), g
W_m = gram-molecular weight of analyte (reactant)
n = electron transfer for analyte (reactant) in the electrode reaction involved
F = the faraday, (96,516 C/equiv)
Q = quantity of electricity consumed, C

8.6.1.2 Theory of Direct Coulometry

Direct coulometry is often referred to as coulometry at controlled potential. In the direct method, the electrode reaction nearly always involves the analyte

---

5 Text and illustrations in this section are taken from "Analytical Chemistry", James G. Dick, McGraw-Hill, Inc., (1973), Chapter 12, Sections 12.4 and 12.6 (with permission).

directly in one form or another, and less often a species directly related chemically to the analyte.

Although coulometric principles for analytical work were discussed by Szebeledy and Somogyi [101] in 1938, Hickling [102] wrote of determining copper by controlled potential coulometry in 1942. The current in direct coulometry decreases exponentially with time. The time to reach a quantitative completion, for most analytical applications, can be taken as that time when the current has decreased to a value indicative of analyte concentration in solution of 10^{-6} M or less. The final concentration will depend upon the requirement for analytical completion for the reaction involved. Alternatively, the critical time can be determined when some indicator system shows the required analyte or reactant concentration has been reached.

The current-time relationship can be evaluated for area within the limits of the initial time and the time to reach quantitative completion by an integrator. It is apparent that the result will be obtained from:

$$Q = \int i\,dt \qquad (48)$$

with

$$i = i^o e^{-kt} \qquad (49)$$

where:

i^o = current at the start of electrode reaction, A
k = constant specific for the electrode reaction
t = time to reach reaction completion level, s

and we have:

$$Q = \int_0^t i^o e^{-kt}\,dt \qquad (50)$$

In applying the integrator technique, the value of Q at any time t will be given by:

$$Q_t = \int_0^\infty i^o e^{-kt}\,dt = -(i^o/k).(e^{-kt} - 1) \qquad (51)$$

The value for Q_{max}, the quantity of electricity for the coulometric process to be carried to theoretical completion will be:

$$Q_{max} = \int i^o e^{-kt}\,dt \qquad (52)$$

$$= i^o/k \qquad (53)$$

From equations (51) and (53) we have the relative error in stopping the coulometric process at any time t as:

$$\text{Relative error in } Q_t = (Q_{max} - Q_t)/Q_{max} \quad \textbf{(54)}$$

$$= e^{-kt} \quad \textbf{(55)}$$

$$= 10^{-0.4343kt} \quad \textbf{(56)}$$

From this equation it is also possible to calculate the time at which the process should be stopped in order to obtain the desired level of accuracy in the final result.

There is a rather simple older method that can be applied for determining the value of Q where integrating equipment is not available. If logs are taken on both sides of equation (49) we have the relationship:

$$\log i = \log i^o - 0.4343\ kt \quad \textbf{(57)}$$

If i is determined for various values of t during the coulometric procedure, a plot of log i *versus* t will yield a straight line. The value of log io and i^o can be obtained from the intercept of the line with the log i axis at zero time, with the value of k being obtained from the line slope -0.4343 k. This determination of i^o and k now permits the estimation of Q_{max} from equation (53). The amount of the reacting species can then be estimated from equation (47) without the time necessary to carry out the electrochemical reaction to quantitative completion. The values of i determined for various t values can be corrected for the residual current, if this latter has been shown by previous tests to reach a level of significance.

The method is attractive, but requires multiple accurate determinations of i and t with expenditure of technician's time. The accuracy of the technique may be limited to *ca.* ±1 or ±2 percent (±10 to ±20 ppm), particularly where temperature variations may occur due to heating effects of current passage or where applied potential control is poor.

In coulometry at controlled potential, as in all coulometric methods applied in analytical chemistry, it is of prime importance that Q be related exclusively to the electrode reaction involving the analyte. The current, in other words, must be 100 percent efficient for the analyte reaction. Current expended on any other reaction will lead to error. For example, dissolved oxygen must be removed if there is a chance of this substance providing an electrode reaction. Since, in many cases, oxygen will be a substance generated at the anode from the reaction involving water, $2OH^- - 2e \leftrightarrow H_2O + 1/2O_2$, it is necessary in many cases to enclose the anode in a separate compartment where the electrode is in contact with the solution under analysis but where generated oxygen can not diffuse into this solution. Figure 30 shows such a controlled potential compartmented cell.

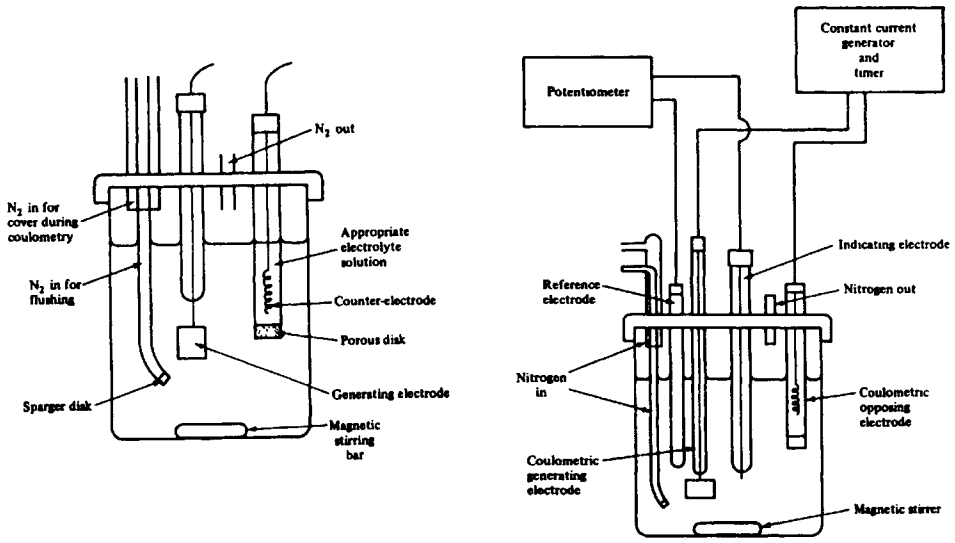

Figure 30: Left: Apparatus for controlled potential coulometry. Right: Apparatus for coulometric titration with potentiometric location of the endpoint.

8.6.1.3 Theory of Indirect Coulometry

Indirect coulometry is perhaps better known as "coulometric titration at constant current". The method requires the use of a very accurate means of controlling the current through the solution. In such titrations, a selected constant current is forced through the electrolyte. This current results in a reaction in the electrolyte where a substance is generated at one of the electrodes which is capable of reacting stoichiometrically with the analyte in the solution. The quantity of electricity required to bring the analyte reaction to some required point of quantitative completion is determined by multiplying the constant current by the time to reach this completion point. The relationship between the generating reaction and the reaction of the generated species with the analyte must be known. As usual in coulometric methods, the expectation is that the current will be 100 percent efficient in generation and that the reaction of the generated substance with the analyte will be rapid and stoichiometric.

In electrolytic processes involving constant current, the generating electrode will eventually become concentration polarised. This can result in a shift in the potential at the electrode and the possibility of a reaction occurring other than that intended. This will cause less than 100 percent current efficiency for the

primary species generated, except where the product of the second electrode reaction can react rapidly and stoichiometrically with the primary species generated. The following provides an example of this situation. Consider an attempt to determine cerium quantitatively by reacting Ce^{4+} at a platinum cathode according to:

$$Ce^{4+} + e \leftrightarrow Ce^{3+} \qquad \textbf{(58)}$$

under constant current coulometry using a compartmentized platinum anode as counterelectrode. Suppose the starting solution to be 0.001M to Ce^{4+} and 1 M to H^+ and the cathodic decomposition potentials to be 1.46 V for equation (58) and -0.50 V for the reaction $2H^+ + 2e \leftrightarrow H_2$. A well-stirred solution, properly deoxygenated at the start, would yield curve 1 of figure 31. Note that polarisation effects cause the current to level off at the value of i_1. This is the limiting current for 0.001 M Ce^{4+}. The current values i_2 and i_3 are the limiting currents when the solution starts off at one-half and one-quarter the value of the Ce^{4+} concentration (*e.g.*, 0.0005 M and 0.00025M) and are shown as curves 2 and 3. These current values will be respectively 0.5 and 0.25 of that for i_1, conditions being ideal.

For the 0.001 M Ce^{4+}, the application of a constant current at i_2 will cause Ce^{4+} to be reduced at the cathode to Ce^{3+} until the value of $[Ce^{4+}]$ reaches about 0.0005 M. At this point, because of concentration polarisation, Ce^{4+} ions can no longer reach the electrode surface fast enough to sustain the constant current demand of i_2. The cathode potential will therefore drift rapidly to more negative values until it reaches -0.50 V, at which point hydrogen ion is discharged and the current i_2 is sustained. The current efficiency for Equation (58) is no longer 100 percent, and the method can not provide a quantitative determination of Ce.

Suppose, however, that before the coulometric procedure, an amount of Fe^{3+} is introduced into the solution. The ion mobilities of Ce^{4+} and Fe^{3+} are, and must be, quite similar. Curve 4 of Figure 31 shows the limiting current i_4 for Fe^{3+} alone at 0.002M. The cathodic decomposition potential for Fe^{3+} in the reaction:

$$Fe^{3+} + e \leftrightarrow Fe^{2+} \qquad \textbf{(59)}$$

is 0.70 V. Now consider the solution of 0.002 M Fe^{3+} and 0.001M Ce^{4+} in 1 M H^+. The current efficiency will be 100 percent for reaction (58) until $[Ce^{4+}]$ reaches 0.0005 M. Polarisation will then cause the cathodic potential to drift negatively until it reaches 0.70 V at which point reaction (59) causes Fe^{2+} to be generated. The Fe^{2+} immediately reacts with Ce^{4+} to produce Ce^{3+} and Fe^{3+}:

$$Fe^{2+} + Ce^{4+} \leftrightarrow Fe^{3+} + Ce^{3+} \qquad \textbf{(60)}$$

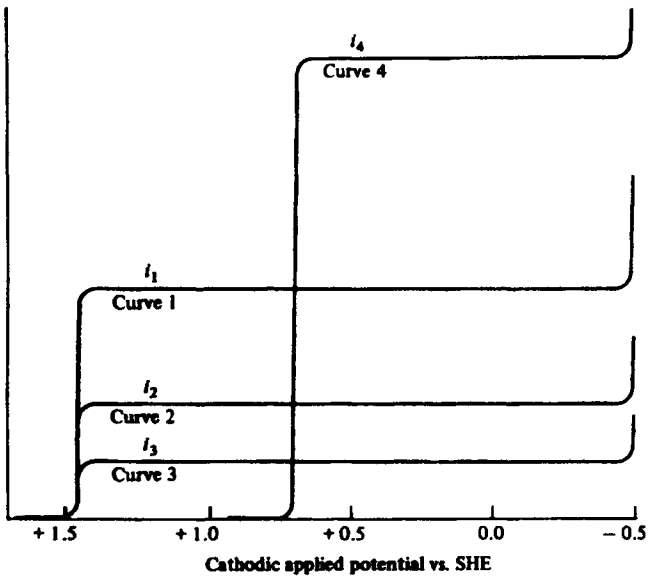

Figure 31: Limiting current curves for Ce^{4+} and Fe^{3+} in 1 M H^+.

The $[Fe^{3+}]$ remains constant and i_4 remains constant as long as the solution contains Ce^{4+}. The net reaction results in 100 percent efficiency for the reduction of Ce^{4+} under conditions of one equivalent of Ce^{4+} reduced for every faraday (96,516 C) passed through the solution.

This type of situation is applied on some occasions in coulometric titration, and the following points are important.

1. The constant current demanded should not exceed i_4 and should be appreciably less than this value.

2. The concentration of Fe^{3+} should be much higher than that for Ce^{4+}.

The above example was given to show the versatility of the coulometric titration method. A more typical example would be one where the constant current generates electrolytically, with 100 percent, a substance which reacts immediately with the analyte species in solution. A typical example is the generation of iodine between two platinum electrodes immersed in an oxygen-free solution of potassium iodide. The generating reaction at the anode is:

$$2I^- - 2e \leftrightarrow I_2 \quad \textbf{(61)}$$

with the cathodic being compartmentized (see figure 30 for compartmentization). The buffering of the iodide solution to a *p*H of 8 allows the titration of As^{3+} in the solution in the stoichiometric reaction:

$$H_3AsO_3 + I_2 + H_2O \leftrightarrow HAsO_4^{2-} + 2I^- + 4H^+ \quad \textbf{(62)}$$

Note that the iodide concentration and the limiting current remain constant throughout. The application of a constant current less than the limiting current for the iodine/iodide system permits 100 percent efficiency. The quantity of arsenic is calculated as Q from the constant current multiplied by the time to reach quantitative completion of reaction (62).

The generation of iodine coulometrically at the anode has an extensive application in the Karl Fischer technique of water determination. Instead of employing one of the modern Karl Fischer titrant reagents, the coulometric technique involves a cell with a compartmented cathode and an anodic compartment containing a prepared, often proprietary, potassium iodide solution. The generating platinum electrode pair is contained in the cathode and anode compartments, with the voltammetric or amperometric sensing electrodes in the anode compartment. Generation of iodine occurs at the anode under constant current, and the iodine reacts with water in the usual manner. The endpoint is located and the coulometer dead-stopped. The equipment involved is then capable of using the time and constant current to determine the water content of the sample under examination. The method has the advantage of not using a titrant with a limit to its shelf life, and also avoids the need for repeated titrant standardisation.

8.6.1.4 Indicator Techniques in Coulometric Titrations

Generally, the titration reactions of the coulometric titration method are identical to those of standard volumetric titrimetry, the basic difference being the electrical generation of the titrant substance. Also generally, the visual colour change indicators of standard titrimetry are often applied here where the analyte quantities involved are reasonable. For low and very low concentrations of analyte, instrumental methods of endpoint location are applied. These include potentiometric dead-stop, polarographic, conductometric and spectrophotometric (absorptiometric) techniques, and involve the normal measuring methods and equipment common to these approaches. In the case of potentiometric endpoint detection, the method can be applied to both low and high analyte concentration situations.

8.6.1.5 Applications

A great many methods involving the determination of metals and inorganic analytes exist. These can often be applied in food analysis, although the techniques of voltammetry/polarography, atomic absorption, ICP, *etc.*, have in

most cases supplanted the coulometric approach. In the last year, the CA Selects, Analytical Electrochemistry section, has only listed seven papers on coulometric methods, two of these being on the Karl Fischer coulometric approach and two being of pharmaceutical interest. Many organics are among the substances determinable, although many of these would be of minimal interest in food analysis. Some of these are listed below with the reference letters in brackets where applicable. These and other references [103-109] and suggested texts for section 8.6 can be found in the references.

aliphatic amines	[a]	vitamin C, ascorbic acid	[b]
acetic acid	[c]	adipic acid	[d]
benzoic acid	[d]	calcium	[e]
arsenic (see below)		cysteine	[f]
food dyes	[g]	hydrazine	[h]
mercaptans	[i]	phenols	[j]
fatty acids (unsat)		sodium carbonate	[k]
halides (Cl^-, Br^-, I^-	[l]	ammonia	[m]
iron [n]		lead	[o]
hydrogen peroxide	[p]	sulphite	[q]
zinc	[r]		

In many applications, particularly those involving the determination of metals in food substances, there is a necessity of wet- or dry-ashing the sample prior to analysis in order to remove possible interferences.

No practical applications are given in this area to cover food analysis, although the reader is referred to the References section, "additional recent references" portion, for some suggestions. The paper by Kalbus and Lieu represents, for example, a laboratory experiment in the coulometric titration determination of the iodine number of fats and oils. For a practical experiment the following determination of arsenic by coulometric titration is suggested. It is of interest since it presents to alternatives in the final estimation procedure.

8.6.1.5.1 Arsenic by Coulometric Titration

Prepare a solution 0.00200 M (0.00400M) to As_2O_3. Dissolve 0.1978 g of previously-dried As_2O_3 in 10 mL of 10% NaOH, dilute to 50 mL with distilled water (DW) and add 2 drops of 0.1% phenolphthalein in 80% ethanol. Add 1:1 HCl until the pink colour disappears and the solution is just acid. Transfer quantitatively to a 500 mL volumetric flask, dilute to the mark with DW and mix well. Keep stoppered in the flask. 1.00 mL = 0.3 mg As.

Place in the generating cell of a constant current coulometer 50 mL of DW, 2.0 g of KI and 2.0 g of Na_2CO_3. Add 5 mL of soluble starch solution (0.4%), insert the generating electrodes (twin platinum sheets 0.5 cm^2) and a stirring bar. Start stirring and apply a constant current of 10 mA. Stop the timer as soon as

the first blue colour appears. This should persist for 30 s, if it does not, start and stop the timer-generator until it does. Now pipette in 5.00 mL of the prepared As_2O_3 solution (1.50 mg As) and restart the timer-generator at a constant current of 10 mA. Titrate until a blue colour persisting for 30 s is obtained. Record the time interval. Multiply by the constant current to obtain the coulombs (Q) involved. Determine the weight of arsenic by substituting the Q value in equation (47).

8.6.2 Conductometry

8.6.2.1 Introduction and Theory

Because of the many complication which can arise out of the use of conductometry as applied to the complicated matrices of most food substances, the technique is not one that is at all extensively applied in the field. The theory will, nevertheless, be covered.

The determination of conductance is not carried out as a means of quantitative determination in food analysis. If applied at all, the conductometric approach is one of titration. In such titrations, the titrant substance and analyte react to alter the conductance of the solution during the titration, the conductance being plotted against the volume of titrant. Conductometric titrations were first investigated by Dutoit [110].

The conductance of a solution is a measure of all of the conducting ions in solution. Obviously, when the background conductivity is high, and where the analyte contributes only a small fraction to this total, the determination of the analyte will not be of great accuracy.

The smaller and more mobile an ion, the higher will be its conductivity. In addition, the more an ion hydrates in aqueous solution, the less mobile and less conductive it will be. Finally, the more polar the solvent, the higher the conductivity. Water is thus an ideal solvent, with methanol also being good.

The conductance of a solution is the reciprocal of its resistance. The resistance of a column of solution A cm^2 in cross-section between two electrodes separated by a distance of l cm is:

$$R = \rho(l/A) \text{ ohms} \qquad \textbf{(62)}$$

where ρ is the specific resistance in ohm/cm. The conductance is given by:

$$L = 1/R = \kappa(A/l) \qquad \textbf{(63)}$$

where κ is the specific conductance in $ohm^{-1}\ cm^{-1}$. The quantity A/l is called the cell constant and is specific for a given conductance cell. It is measured by determining the conductance for the cell when using solutions of known specific conductance.

The equivalent conductance, Λ, is defined as the conductance of a solution containing 1 g of solute between electrodes separated by 1 cm. Where the solution has a concentration of C gram equivalents per liter (close to 1000 cm^3), the value of A is given by:

$$\Lambda = 1000\kappa/C \qquad \textbf{(64)}$$

and with κ given by equation (63), we have:

$$\Lambda = 1000Ll/CA \qquad \textbf{(65)}$$

and

$$L = (A/1000l).\Lambda C \qquad \textbf{(66)}$$

In the final essence, the value of the conductance of a solution containing more than one conductive ion can be given as:

$$L = (A/1000\ l)\sum C_i\lambda_i \qquad \textbf{(67)}$$

where C_i and λ_i are the concentration and equivalent ionic conductance for each ion species in solution. For most conductometric titration purposes, λ_i^o can be used as a substitute for λ_i.

Although the Wheatstone bridge is not used now directly as a balancing instrument for the measure of resistance (conductance) in modern electronic instruments, the principle does not vary, nor does the use of ac current to avoid the compositional changes caused when dc is used. Figure 32 shows both a Wheatstone bridge and a conductometric conductance cell. As was the case with polarisation titrations, conductometric titration curves vary in shape. Figures 33/34 show the titration curves for seven types of conductometric acid-base titration. Note that, in all of these titrations, the endpoint is found by extrapolation to intersection of the straight line sections on either side of the curved zone in the endpoint neighbourhood. The straight line sections are obtained by having the titrant concentration not less than 20x that of the analyte in the solution under investigation. The curved section, as in polarisation titrations, represents the effect of the equilibrium constant for the titration reaction and, again as in polarisation titrations, indicates the ability of the method to handle titration reactions with poor equilibrium constants.

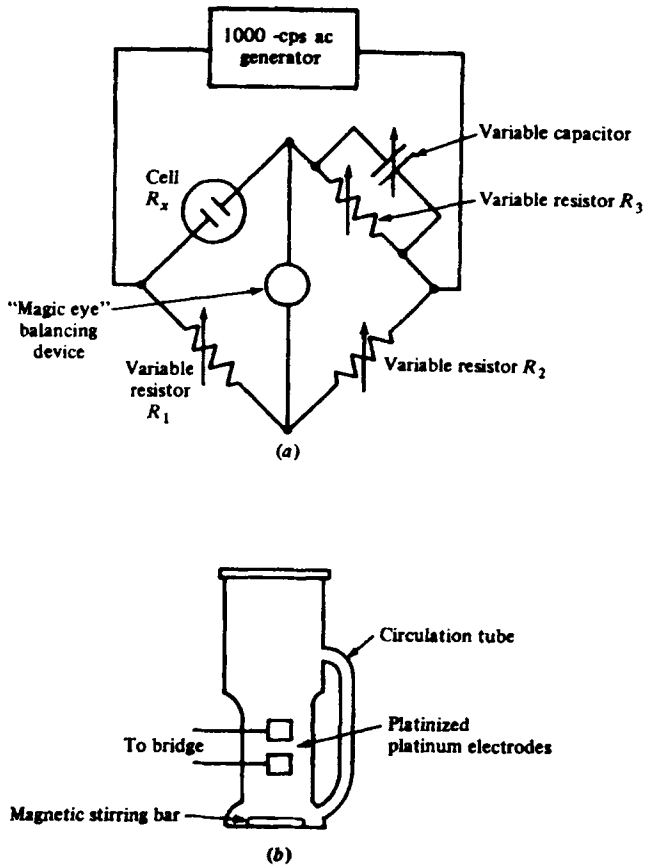

Figure 32: Top: Wheatstone bridge. Bottom: Conductometric titration cell.

8.6.2.2 Conductometric Titration Equipment

The commonest equipment used today to carry out conductometric titrations usually involves a conductometer, a conductometric titration vessel containing twin platinized platinum sheet electrodes with magnetic stirring and mixing arrangements, and a good potentiograph linked to a piston burette. As an alternative, a good recorder can be used linked in operation to an automatic piston burette. The active titrant reactant is usually *ca.* 20x the concentration of that of analyte in the solution to be titrated. The plot of conductance *versus* titrant volume is obtained from the recorder, and will show straight-line sections before and after the endpoint zone. The endpoint is found by the method of extrapolation outlined in the foregoing.

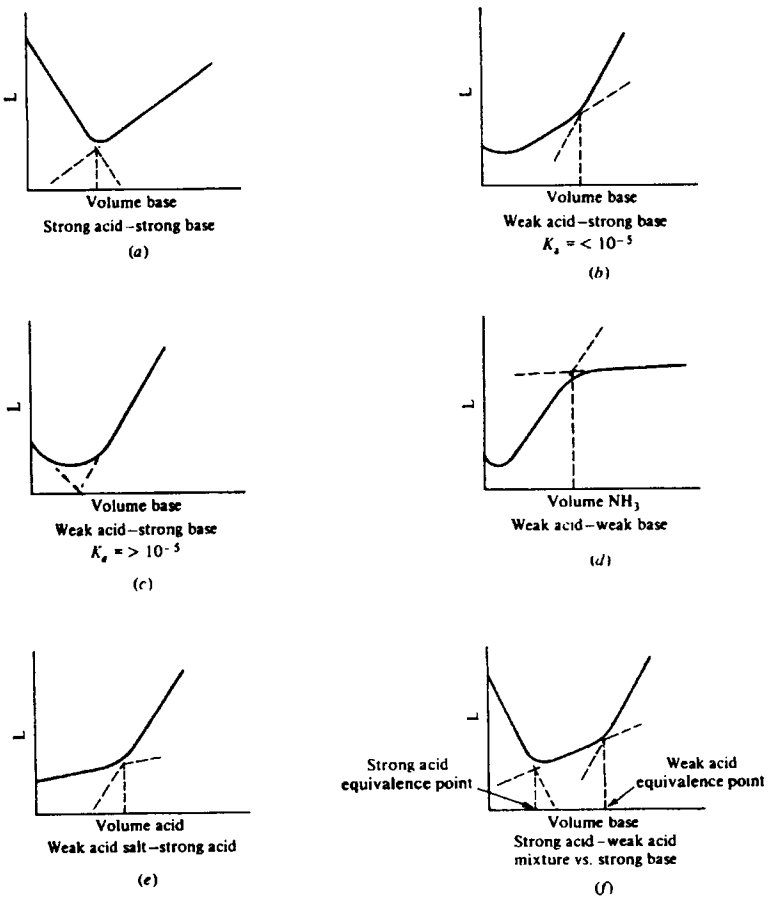

Figure 33: Conductometric titration plot forms.

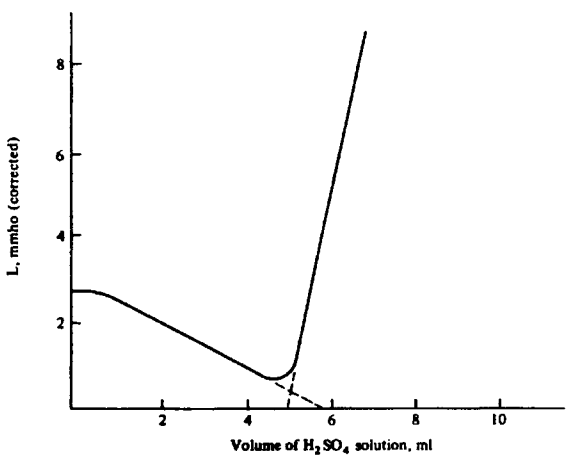

Figure 34: Titration of 0.05 M Pb acetate by H_2SO_4 corrected for dilution effect.

8.6.2.3 Applications

As mentioned previously, the conductometric method has few applications in food analysis. During the last year, CA Selects, Analytical Electrochemistry section, listed only three papers on conductometric titrations, one of them on a PC-controlled automatic operation. In most cases, the application involves the titration of acids or bases, although some application applies to the determination of the halides, sulphides and mercaptans.

8.6.2.3.1 Conductometric Titration of Lead Acetate

The following is intended only as a demonstration of the method of conductometric titration. Prepare a 0.05 M solution of lead acetate and a standardised 1.00 M solution of sulphuric acid. Pipette 50.0 mL of the acetate solution into a conductometric titration cell.

Depending on the conductometer used, set the μS range appropriately. Set the stirring action in the cell and use an automatic burette with a 5.0 mL capacity capable of reading to three decimal places. The equipment used in practice was a Metrohm 660 Conductometer, 6.0902.300 conductometric titration vessel, a 536 Potentiograph linked to the conductometer and to a 665 Dosimat with a 5.0 mL burette. The titration was started at a very slow delivery rate. The titration was stopped when two reasonable-length straight-line sections around the endpoint were obtained. The endpoint was found by extrapolation to intersection of the straight-line sections. The Pb value was calculated.

Some references [111-113] and suggested texts for section 8.6 can be found in the references.

8.7 ELECTROCHEMICAL DETECTORS

8.7.1 Introduction

The term "electrochemical detectors" can be a very general one. In point of fact, the following all qualify as detectors of chemical substances under the proper conditions.

1. Potentiometric electrodes of all types: In flow-injection analysis (FIA) glass, ion-selective, amperometric electrodes, *etc.*, can all theoretically be used in a detector cell to quantify some chemical substance.

2. The microelectrodes of voltammetry/polarography: Again in FIA and in high-performance liquid chromatography (HPLC) some of these electrodes may function as detectors.

3. Conductivity electrodes: These can serve as detectors in ion chromatography (IC).

4. Coulometric setups have also been used as detectors in some types of FIA work.

Insofar as this treatment is concerned, the focus will be on the use of electrochemical detectors in the HPLC, FIA and IC fields.

8.7.2 Electrochemical Detection in HPLC

The electrochemical detector (ELCD) used in HPLC applications consists of an amperometric microcell through which the eluent from the HPLC column is allowed to flow. The working electrode in the cell is usually a glassy carbon (GC) electrode, as is the auxiliary electrode. The reference is in nearly all instances an Ag/AgCl (3 M KCl) electrode. The cell working volume is extremely small and, in most equipment is in the low μL range. In the majority of instances the reaction at the working electrode surface is one of oxidation, and the applied potentials are in the positive range relative to the reference. The applied potentials and the limiting current measurements are provided by a voltammetric attachment. The limits of detection are in the pg range. The following indicates the importance of certain of the required characteristics of the HPLC/ELCD system (1).

1. The HPLC pump, the damping system, injector, column, capillaries, tube fittings, *etc.*, must be in perfect working order. The system is much more sensitive to column contamination and to pressure fluctuations due to pump operation or imperfect fittings than is, for example, that of UV detection.

2. All of the usual precautions for trace analysis must be taken. Corrosion of steel parts in contact with the eluent must be avoided, since the presence of Fe^{3+} can seriously interfere. The eluent substances, in addition, must not contain complex-forming substances.

3. Where a single-stage pump is used, it is common to find that pressure fluctuations occur in the cell, causing serious "noise" in the detector signal. An additional pulse damper working on the Bourdon tube principle can assist in minimising "noise" from this source.

4. Many of the solvents normal to HPLC use can be used for the eluent make-up. The additional conductivity required for electrochemical detection is provided by the addition of an electrolyte in the range of 1 to 10 g/L, yielding conductivities of 1 to 10 mS/cm. The eluent is degassed in the usual manner, using helium or a vacuum.

5. The eluent, wherever possible, should be used as the sample solvent in order to avoid disturbances caused by a change in the solvent front.

6. The mass of solute injected should not exceed 100 ng in order to avoid surface filming of the GC working electrode by reaction products.

The reactions at the electrode surface are no different from what they would be in a regular voltammetric measuring system. The virtue of the amperometric detector in HPLC work arises out of the following situation. It is possible, by applying standard voltammetry, to determine a catecholamine at a glassy carbon working electrode system. The applied potential is in the neighbourhood of 800 mV and, when a single catecholamine is present, the quantitative determination is very sensitive. In the presence of several catecholamines, however, a signal representing the accumulated total will be obtained, and separation as to type will be impossible. The ability of the HPLC method to elute the various catecholamines of a mixture at different times allows the electrochemical detection system to quantify each component separately.

The same detector system can be used in FIA work, although it is obvious that, without the use of an HPLC column, separation of compounds with similar electrode discharge potentials will not be possible. The FIA system does however have advantages over straight-forward voltammetry in that the volumes required for injection are of the same order as they are in HPLC work. The pump requirements are often simpler, and a motor-driven piston pump is very often adequate for precise and accurate work.

In the most accurate work, the elution peaks are assessed by integration to obtain the area under the each peak. The measurement of peak height may be adequate in many instances. Standards are used in order to provide a quantitative basis.

8.7.3 Electrochemical Detection in IC

One of the detectors used in ion chromatography (IC) work is an electrochemical conductivity cell, and this can be used in both cation and anion determinations. The eluted solvent material is first passed through the detector to establish a baseline conductance value. Subsequently, elution(s) resulting from a sample injection yield varying conductance values, the magnitude of the peaks for which are evaluated either by integration of the area or by peak height measurement. The integration method is by far the more accurate and precise.

There are many factors of importance in the use of conductivity cells in this manner. Foremost is the need to maintain a constant cell temperature, and this is obtained by close temperature control of the cell and the incoming

eluent. All IC equipment is equipped to maintain both cell and incoming eluent at a constant temperature high enough over room temperatures to eliminate interference. For the rest, the general precautions listed for the use of the amperometric detector in HPLC work apply here also.

A single general reference [114] and suggested texts for section 8.7 can be found in the references.

8.8 REFERENCES

1. Nicolsky, B.P., M.M. Shultz and E.A. Metrova, Vestm., Leningrad Univ., 4, 93, (1963).

2. Eisenmann, G., ed. Glass Electrodes for Hydrogen and Other Cations. Marcel Dekker Inc., New York, (1967).

3. Cremer, M., gber dreursache der elecktromotorischen Eigenschafter der Gewebe, Zugleichen Beitrag zur Lehre von den Polyphasischen elektrolytketten. Z.F.Biol., 47, 562-608, (1906).

4. Haber, F., and P. Klemenslewicz, gber elektrische phasengrenzkrafte. Z.F. physik.Chem., (Leipzig), 67, 385-431, (1909).

5. Eisenmann, G., D.O Rudin and J.U. Casby, Glass electrode for measuring sodium ion. Science, 126, 831-834, (1957).

6. Eisenmann, G. Cation selective glass electrodes and their mode of operation. Biophys. J., 2(Part 2), 259-323, (1962).

7. Eisenmann, G. Advances in Analytical Chemistry and Instrumentation, Vol. 4, Wiley, New York, (1965).

8. Dole, M., The Glass Electrode. Wiley, New York, (1941).

9. Ross Jr., J.W., Calcium ion-selective electrode with liquid ion exchanger. Science, 156, 1378-79, (1967).

10. Sandblom, J.P., G. Wisenman and J.L. Walker, J.Phys.Chem., 71, p.3862, (1967).

11. Durst, R.A., ed. Ion-Selective Electrodes. NBS Spec. Pub. 314, U.S. Govt. Prtg. Office, Washington D.C., 70-71, (1969).

12. Buck, R.P., J.Electroanal.Chem. Interfacial Electrochem., 18, p.381, (1968).

13. G. Eisenmann, Theory of Membrane Electrode Potentials. Chap. 1 in Ion-Selective Electrodes, R. A. Durst (ed.), NBS Spec. Pub. 314, U.S. Govt. Prtg. Office, Washington D.C. (1969).

14. J. W. Ross Jr., Solid State and Liquid Membrane Electrodes, Chap. 1 in Ion-Selective Electrodes, R. A. Durst (ed.), NBS Spec. Pub. 314, U. S. Govt. Prtg. Office, Washington D.C. (1969).

15. S. A. Katz and G. A. Rechnitz, *Z.Anal.Chem.* **196**, 248 (1963).

16. S. A. Katz, *Anal.Chem.* **36**, 2500 (1964).

17. G. G. Guilbault, R. K. Smith and J. G. Montalvo Jr., *Anal.Chem.* **41**, 600 (1969).

18. G. G. Guilbault and J. G. Montalvo Jr., *J. Am. Chem. Soc.* **91**, 2164 (1969).

19. T. Ikeda, F. Matushita and M. Senda, D-Fructose dehydrogenase-modified carbon paste electrode containing *p*-benzoquinone as a mediated amperometric fructose sensor, *Agric. Biol. Chem.* **54(11)**, 2919-24 (1990). (fructose in fruits).

20. M. B. Assoumani, *et. al.*, Use of a lysine oxidase electrode for lysine determination in soybean meal hydrolyzates, *Lebens.-Wiss.Technol.* **23 (4),** 322-27 (1990).

21. F. Schubert, *et. al.*, Enzyme electrode and method for fructose determination in the presence of glucose, Ak. Wiss. DDR, Ger. (East) DD 279505. Appl. 301809, 14 Apr. 1987, 3pp.

22. G. J. Kakabadse, *et. al.*, Direct potentiometry of ethanol in alcoholic beverages using ion-selective electrodes. *J. Am. Soc. Brew. Chem.* **49 (1),** 19-22 (1991).

23. Y. Yamamoto, *et. al.*, Potassium and sodium ion sensor based on amperometric ion-selective electrode, *Bunseki Kakagu*, **39 (11)**, 655-60 (1990). (simultaneous determination in foods)

24. F. Mizutani and M. Michihiko, Simultaneous determination of glucose and lactose in sour milk using an immobilized glucose oxidase electrode combined with β-galactosidase-attached measuring cell, Bunseki Kakagu, **39 (11)**, 729-34 (1990).

25. T. Katsu, *et. al.*, Amino acid analysis using amine-sensitive membrane electrodes, *Anal. Chim. Acta.* **239 (1)**, 23-7 (1990).

26. R. L. Villarta, *et.al.*, Amperometric enzyme electrodes for the determination of l-glutamate, *Talanta,* **38 (1)**, 49-55 (1991). (FIA system use on protein tablets and food products).

27. M. C. Martinez Rincon and L. M. Abuin Cabez, Fluorine content in Mentrida wines., *An. R. Acad. Farm.* **56 (2)**, 279-82 (1990).

28. A. Mulchandani, *et. al.*, Determination of sulphite in food products by an enzyme electrode, *J. Biotechnol.* **18 (1-2)**, 93-102 (1991). (sulphite oxidase enzyme).

29. J. L. Bernal, *et. al.*, Analytical application of ion-selective electrodes for the determination of nitrates in wine, *J. Environ. Sci. Health*, **A26 (3)**, 305-16 (1991).

30. H. Okuma, *et. al.*, Mediated amperometric biosensor for hypoxanthine based on a hydroxymethyl ferrocene-modified carbon paste electrode, *Anal. Chim. Acta.*, **244 (2)**, 161-4 (1991). (determination in tuna).

31. K. Hajisadeh, *et. al.*, Immobilization of lactate oxidase in a poly(vinyl alcohol) matrix on platinized graphite electrodes by chemical cross-linking with isocyanate, *Talanta*, **38 (1)**, 37-47 (1991). (lactic acid in dairy products).

32. K. Matsumoto, *et. al.*, Determination of glycerol in wine by amperometric flow injection analysis with an immobilized glycerol dehydrogenase reactor, *Agric. Biol. Chem.* **55 (4)**, 1055-9 (1991).

33. V. Laurinavicius, *et. al.*, Determination of lactose in milk with an enzyme electrode, *Zh. Anal. Khim.* **46 (4)**, 818-9 (1991).

34. M. A. Nabirahni and R. R. Vaid, Development and application of an immobilized enzyme electrode for the determination of sulphite in foods and feeds, *Anal. Lett.* **24 (4)**, 551-65 (1991).

35. M. G. Mitrakas, *et. al.*, Nitrate determination in sugar beet sap extracted with lead-acetate-lead monoxide using an ion-selective electrode, Commun. *Soil. Sci. Plant Anal.* **22 (5-6)**, 589-96 (1991).

36. E. Tamiya, and I. Karube, Micro-biosensors for clinical and foods analyses. *Trans. Mater. Res. Soc. Jpn.* **1**, 44-59 (1990). (monitoring fish freshness).

Reviews/Text

V. M. Maxwell, Ion-Selective Electrodes. Univ. Oxford, Oxford, UK. (1988) 376 pp. (general presentation).

J. D. R. Thomas, Enzyme electrodes for flow injection analysis, (REVIEW), *Port. Electrochim. Acta.* 457-70 (1989).

T. Gennett and W. C. Purdy, Electrochemical sensors, Part 1: A review of their theory, (REVIEW), Am. Lab (Fairfield, Conn.) **23 (3),** 60,62-4 (1991).

T. Gennett and W. C. Purdy, Electrochemical sensors, Part 2: Recent advances, (REVIEW) *Am. Lab* (Fairfield, Conn.) **23 (6)**, 60,62-6 (1991).

F. W. Scheller, *et.al.*, Second generation of biosensors, (REVIEW), *Biosens. Bioelectron.* **6 (3)**, 245-53 (1991).

G. K. McMillan, Understand some basic truths of *p*H measurement, *Chem. Eng. Prog.* **87 (10)**, 30-7 (1991). (Why actual accuracy of *p*H electrodes in most industrial applications falls far short of the level expected).

T. C. Tan and C. C. Liu, Principles and fabrication material of electrochemical sensors, (REVIEW), *Chem. Sens. Technol.* **3**, 105-16 (1991).

A. Lewenstam and A. Hulanicki, Selectivity coefficients of ion-sensing electrodes, (REVIEW), *Sel. Electrode Rev.* **13 (1)**, 129-31 (1991).

C. J. Coetzee, Inorganic ion exchangers for ion-selective electrodes, (REVIEW), *Inorg. Ion Exch. Chem. Anal.* 143-75, CRC Publishers, Boca Raton, Fla. (1991).

K. Tohda,. *Et. al.*, Ion sensors, (REVIEW), *Chem. Sens.*, 6 (4), 99-105, (1990).

Indirect Potentiometry - Potentiometric Titrations

37. H. A. Robinson, *Trans. Electrochem. Soc.* **92**, 445 (1947).

38. J. J. Lingane, Electroanalytical Chemistry, Chap. 8, Interscience, New York (1953).

39. H. Irving, *Analyst*, **84**, 641 (1959).

40. J. R. Glass, *Anal. Chem.* **33**, 494 (1961).

41. M. T. Kelley and D. J. Fisher, *Anal.Chem.* **32**, 61 (1960).

42. S. Miyake, *Talanta,* **13**, 1253 (1966).

43. J. G. Dick, Analytical Chemistry, McGraw-Hill, New York (1973).

44. T. Moisio and M. Heikenen, A titration method for silage assessment, *Animal Feed Sci. Tech.* **22**, 341-353 (1989), Elsevier Science Publishers B.V., Amsterdam.

45. J. O. Bosset, *et. al.*, Determination of free fatty acids in milk and cream, Parts I and II, Evaluation of a collaborative study employing visual and potentiometric titration methods, Mitt. Geb. Lebenmittelunters Hyg., 81 **(5)**, 510-20 (1990).

46. K. Nicolic and M. Medenica, Potentiometric determination of furosemide, *Acta. Pharm. Jogosl.*, **40 (4)**, 521-5 (1990).

47. N. E. de Sousa and O. E. S. Godinho, Simultaneous determination of tartaric, malic and succinic acids by potentiometric titrimetry and its application to wine analysis, *Arg. Biol.Tecnol.* **33 (4)**, 903-14 (1990).

Texts

J. G. Dick Analytical Chemistry, McGraw-Hill, New York (1973). Reprint: Robert E. Krieger Pub., Huntingdon, N.Y. (1978).

D. A. Skoog and D. M. West, Fundamentals of Analytical Chemistry, 3rd edition (or later), Chap.12, Holt, Rinehart and Winston (1976).

J. S. Fritz and G. H. Schenk, Quantitative Analytical Chemistry, 5th edition, Chaps. 8-12, Allyn and Bacon, Newton, Mass.

J. G. Dick Instrumental Methods of Chemical Analysis, CEGIR, Montreal, (1984).

D. A. Skoog and D. M. West, Principles of Instrumental Analysis, 2nd edition (or later), Saunders College/Holt, Rinehart and Winston (1980).

G. D. Christian, Analytical Chemistry, 4th edition, Wiley, New York (1986).

Voltammetric and Polarographic Methods

48. J. Heyrovsky, *Chem. Listy*, **16**, 256 (1922).

49. D. Ilkovic, Collect. Czechoslov. *Chem. Communs.* **6**, 498 (1934).

50. J. J. Lingane and B. A. Loveridge, *J. Am. Chem. Soc.* **72**, 438 (1950).

51. H. Strehlow and M. von Stackelberg, *Z. Electrochem.* **54**, 51 (1950).

52. O. H. MÜller, National Bureau of Standards Circular 524 (August 14, 1953).

53. J. Koutecky, *Czechoslov. Cas. Fys.* **2**, 50 (1953).

54. J. Koutecky and M. von Stackelberg, Progress in Polarography, Vol. I, p.21. P. Zuman and I. M. Kolthoff (eds.), Interscience, New York (1962).

55. J. Heyrovsky and J. Forejt, *Z. Physik. Chem.* 193, 77 (1943).

56. J. Heyrovsky, F. Sorm and J. Forejt, *Collection Czechoslov. Chem. Communs.* **12**, 11 (1947).

57. J. Heyrovsky, *Disc. Faraday. Soc.* **1**, 212 (1947).

58. E. Wählin, *Radiometer Polarogr.* **1**, 113 (1952).

59. E. Wählin and A. Bresle, *Acta. Chem. Scand.* **10**, 935 (1956).

60. A. Bresle, *Acta. Chem. Scand.* **10**, 943, 947, 952 (1956).

61. P. O. Kane, *J. Polarogr. Soc.* **8**, 10 (1962).

62. G. C. Barker and A. W. Gardner, *Z. Anal. Chem.* **173**, 79 (1960).

63. G. C. Barker and I. L. Jenkins, *Analyst*, **77**, 685 (1952).

64. G. C. Barker, *Anal. Chim. Acta.* **18**, 118 (1958).

65. C. Zbinden, *Bull. Soc. Chim. Biol.* **13**, 35 (1931).

66. J. Wang Stripping Analysis, VCH Publishers Inc., Deerfield Beach, Fla. (1985). (Comprehensive discussion; small section on food analysis).

67. L. A. Muratov and A. A. Murav'eva, Polarographic analysis of spasmolytin, *Farm. Zh. (Kiev)*, **4**, 65-66 (1990).

68. G. V. Prokhorova, *et. al.*, Polarographic determination of isoniazid in biological fluids, *Zh. Anal. Kkim.* **45 (11)**, 2246-50 (1990). (in urine, serum, *etc.*).

69. Z. Filipovic-Kovacevic, Voltammetric determination of nickel in margarine production. *Prehrambeno-Tehnol. Biotehnol. Rev.* **27 (4)**, 213-216 (1990).

70. F. Belal and M. S. El-Din, Polarographic behavior and determination of Flumequine, *Microchem. J.* 42 (3), 300-5 (1990).

71. T. J. Cardwell, *et. al.*, Determination of SO_2 in Red Wine by ac voltammetry, *Analyst*, **116 (3)**, 253-6 (1991).

72. M. Stoicheva, *et. al.*, Voltammetric methods for determination of iodides in mineral water and iodized salt, *Khranit.Prom-st.* **39 (5)**, 28-9 (1990).

73. G. Sadler, *et. al.*, Diacetyl measurement in orange juice using differential pulse polarography, *J. Food Sci.* **55 (4)**, 1164-5 (1990).

74. J. H. Luong, *et. al.*, Applications of polarography for assessment of fish freshness, *J. Food Sci.* **56 (2)**, 335-7, 340 (1991).

75. M. A. Jawad, *et. al.*, Electrochemical quantitative analysis of uric acid in milk, *J. Food Sci.* **56 (2)**, 594-5 (1991).

76. Y. Casrillejo, *et. al.*, Determination of food additive azo dyes at an HMDE with adsorptive stripping voltammetry, *Electroanalysis (N. Y.),* **2 (7)**, 553-8 (1990).

77. Z. Xi, *et. al.*, Determination of vitamin E by single-sweep oscillo-polarography with wax-impregnated graphite electrode, *Fenxi Huaxue,* **19 (4)**, 423-6 (1991). (in royal jelly and vegetable oil).

78. Z. Gao, *et. al.*, Determination of trace nitrite by single-sweep polarography, *Gaodeng XueXiao Huaxue Xuebao,* **12 (3)**, 329-31 (1991).

79. S. Yang and S. H. Wang, Determination of trace iodine in food and biological samples by cathodic stripping voltammetry, *Anal. Chem.* **63 (24)**, 2970-3 (1991). (table salt, laver and eggs).

80. R. Kalvoda, Adsorptive Stripping Voltammetry in Trace Aanalysis, (REVIEW), *Contemp. Electroanal. Chem.*, [Proc.Electro-Finn Analysis, Int. Conf. Electroanal. Chem.] (1988) (Pub. 1990), Plenum Press, New York, pp 403-5.

Texts

J. J. Lingane, Electroanalytical Chemistry, 2nd edition, Interscience Publishers, New York (1958).

I. M. Kolthoff and J. J. Lingane, Polarography, Vols. I and II, 2nd edition, Interscience Publishers, New York (1952).

Kh. Z. Brainina, Stripping Voltammetry in Chemical Analysis, Wiley, New York (1974).

C. L. Newbury and G. D. Christian, Anodic Stripping Voltammetry of Biological Samples, *J. Electroanal. Chem.* **9**, 468 (1965).

J. Wang, Stripping Analysis, VCH Publishers Inc., Deerfield Beach, Fla., (1985).

Polarisation Titrations

81. E. Salomon, *Z. Physik. Chem.* **25**, 55 (1897).

82. E. Salomon, *Z. Physik.Chem.* **25**, 366 (1898).

83. E. Salomon, *Z. Elektrochem.* **4**, 71 (1897).

84. C. W. Foulk and A. T. Bawden, *J. Am. Chem. Soc.* **48**, 2045 (1926).

85. J. Heyrovsky and S. Berezicky, *Collection Czechoslov. Chem. Commun.* **1**, 19 (1929).

86. H. A. Laitenen and I. M. Kolthoff, *J. Phys. Chem.* **45**, 1079 (1941).

87. K. Fischer, *Z. Angew. Chem.* **48**, 394 (1935).

88. F. Freede, Anodic amperometry as an indication method in complexometry, *Chem. Weekblad* **61**, 553-555 (1968).

89. F. Vydra, J. Vorlicek and K. Stulik, Biamperometrische indikation chelometrischer titrationen, *Chem. Listy*, **63**, 35-50 (1969). Also *Z. Anal. Chem.* **250**, 48 (1970).

90. G. D. Christian and P. H. Schur, Amperometric titration of disulfide bonds in γ-globulin, *Biochem. Biophys. Acta.* **97**, 358-361 (1965).

91. R. G. Bennett, *et. al.*, Determination of external water in white sugars by direct titration with Karl Fischer reagent, *Int. Sugar J.* **66**, 109-113 (1964).

92. E. A. Epps, The determination of water in molasses following the Karl Fischer method, *J. Assoc. Off. Anal. Chem.* **49**, 551-554 (1967).

93. D. G. Ammon, *et. al.*, Rapid and accurate chemical determination of the water content of plants containing volatile oils, *Analyst*, **110**, 917-920 (1985).

94. C. Moebroek and R. Muenger, Die Karl Fischer-Titration von wasser in lebensmittel, lebensmittel-Technologie, **19**, 135.137 (1986).

95. E. Schalch, P. A. Bruttel and G. Burton, Analysis of edible oils and fats, *Europ. Food and Drink Review*, 62-66 (1990).

96. A. Amine, *et. al.*, Amperometric determination of glucose in undiluted food samples, *Anal. Chim. Acta.* **242 (1)**, 91-8 (1991).

97. Z. El-Basyouni, *et. al.*, Biamperometric titration in the determination of pharmaceutical hydrazine derivatives, *Bull. Electrochem.* **6 (12)**, 943-6 (1990).

98. M. A. Baldo, *et. al.*, Amperometric monitoring of bacteria-induced milk acidity using a platinum disk microelectrode, *Analyst*, **116 (9)**, 933-6 (1991).

99. G. Wuensch and K. Schoeffski, Voltametric indication of the Karl Fischer titration, *Fresenius J. Anal. Chem.* **340 (11)**, 691-5 (1991).

100. L. F. Dryuk, *et. al.*, Amperometric determination of sugars, *Vopr. Khim. Khim. Tekhnol.* **92**, 23-7 (1991).

Texts

J. T. Stock Amperometric Titrations, Interscience, New York (1965).

J. J. Lingane Electroanalytical Chemistry, 2nd edition, Interscience, New York (1958) 267-295.

H. A. Strodel, Chemical Instrumentation, 2nd. edition, Addison-Wesley, Reading, Mass. (1973) 719-724.

101. L. Szebeledy and Z. Somogyi, *Z. Anal. Chem.* **112**, pp 313, 323, 332, 385, 391, 395, 400 (1938).

102. A. Hickling, *Trans. Faraday Soc.* **38**, 27 (1942).

The following references were obtained from Milner and Phillips (see text list below) and the papers involved examined.

a. C. A. Streuli, *Anal. Chem.* **28**, 130 (1956).

b. W. Jedrzejewski, *Chem. Anal. (Warsaw)*, **2**, 453 (1957).

c. W. N. Carson and R. Ko, *Anal. Chem.* **23**, 1019 (1951).

d. J. K. Taylor and J. W. Smith, *J. Nat. Bur. Stds.* **63A**, 153 (1954).

e. N. H. Furman and A. Fenton, *J. Anal. Chem.* **28**, 515 (1956).
f. E. P. Przybylowicz and L. B. Rogers, *Anal. Chim.Acta.* **18**, 596 (1958).

g. M. Munemori, *Talanta*, **1**, 110 (1958).

h. E. C. Olsen *Anal. Chem.* **32**, 1545 (1960).

i. F. A. Laisey, *Anal. Chem.* **26**, 1607 (1954).

j. C. N. Zyl and K. A. Murray, *South African Ind. Chemist*, 8, 243 (1954).

k. J. K. Taylor and J. W. Smith, *J. Nat. Bur. Stds.* **63A**, 153 (1954).

l. G. Marinenko and J. K. Taylor, *J. Nat. Bur. Stds.* **67A**, 31 (1963).

m. G. M. Arcand and E. H. Smith, *Anal. Chem.* **28**, 440 (1956).

n. A. J. Bard and J. J. Lingane, *Anal. Chim. Acta.* **20**, 463 (1959).

o. C. N. Reilley and W. D. Porterfield, *Anal. Chem.* **28**, 443 (1956).

p. T. Takahashi and H. Sakurai, *Talanta*, **9**, 189 (1962).

q. L. E. Hibbs and D. H. Wilkins, *Anal. Chim. Acta.* **20**, 344 (1959).

r. J. J. Lingane and A. M. Hartley, *Anal. Chim. Acta.* **11**, 475 (1954).

103. K. Nikolic and M. Medenica, Coulometric determination of levodopa, methyldopa and carbidopa, *Farmaco*, **45 (9)**, 1037-41 (1990).

104. G. E. Kalbus and Van T. Lieu, Dietery Fat and Health: An experiment on the determination of iodine number of fats and oils by coulometric titration, *J. Chem. Educ.* **68 (1),** 64-5 (1991).

105. K. Nikolic and M. Medenica, Coulometric determination of sulfisomidine, sulphamethoxy diazine and sulphamoxole, *Pharm. Biomed. Anal.* **9 (2)**, 199-201 (1991).

106. H. Katoh, *et. al.*, A study of the cathode reaction in Karl Fischer coulometric titration, *Anal. Sci.* **7 (2)**, 299-302 (1991).

107. W. Richter, and W. Huerlimann, A diaphragm-free measuring cell for Karl Fischer coulometric titration, Eur. Pat. Appl., EP390, 727 (Cl. GO1N31/16), 03 Oct (1990).

108. S. Uchiyama, *et. al.*, Selective biocoulometry of vitamin C using dithiothreitol, N-ethylmaleimide and ascorbate oxidase, *Anal. Chem.*, **63 (20)**, 2259-62 (1991) .

109. A. Cladera, A., *et. al.*, A fully-automated system for acid-base coulometric titrations, *J. Autom. Chem.* **12 (6),** 258-62 (1990).

Texts

J. J. Lingane, Electroanalytical Chemistry, 2nd. edition, Interscience, New York (1958) pp. 450-616.

J. W. C. Milner and G. Phillips, Coulometry in Analytical Chemistry, Pergammon Press, London (Eng.) (1967).

Conductometry and Conductometric Titrations

110. P. Dutoit, *J. Chim. Phys.* 8, 12 (1910).

111. H. Gerstenberg, Hop investigation within the frame of food monitoring, *Brauwelt*, **131 (1/2)**, 12-16, 25-6 (1991).

112. M. Tubino, *et. al.*, Conductometric and colorimetric determination of volatile acidity of vinegars by flow-injection analysis, *J. Assoc. Off. Anal. Chem.* **74 (2)**, 346-50 (1991).

113. M. Kolb, *et. al.*, PC-controlled conductivity titration, CLB, *Chem. Labor. Betr.* **42 (3)**, 140-2 (1991).

Texts

J. J. Lingane, Electroanalytical Chemistry, 2nd. edition, Interscience, New York (1958).

R. K. Freier, Wasseranalyse, Walter de Gruyter & Co., Berlin (1964).

M. Quintin, Electrochimie, Presses Univ. de France (Coll. Euclide) (1970).

Electrochemical Detectors

114. General HPLC Detection, Application Bulletin 128e, Metrohm AG, Herisau, Switzerland (1980).

Texts

D. T. Gjerde and J. S. Fritz, Ion Chromatography, 2nd. edition, Hhthig, Heidelberg (1986).

J. Ruzicka and E. H. Hansen, Flow Injection Analysis, John Wiley, New York (1981).

L. R. Snyder and J. J. Kirkland, Introduction to Modern Liquid Chromatography, 2nd edition, Wiley-Interscience (1979).

This Page Intentionally Left Blank

J.R.J. Paré and J.M.R. Bélanger (Editors)
Instrumental Methods in Food Analysis

Chapter 9

Capillary Electrophoresis: Principles and Applications

Sally Swedberg

Hewlett-Packard Laboratories, P. O. Box 10350, Palo Alto, CA 94303-0867, U. S. A.

9.1 INTRODUCTION

Though work in the 1970's is credited as being a harbinger of modern capillary electrophoresis (CE) [1,2], the inception of CE as it is currently known today, is generally traced to publications by Jogenson and Luckacs in 1981[3,4]. These publications reported the separations of molecules in small diameter fused silica capillary tubing (75 mm inner diameter) at high fields (*ca.* 300 V/cm).

Even though the separation technique gained steady recognition in the mid- to late-1980's, it is the ready availability of commercial instruments, making the technique widely available to a multitude of users, which has given CE the visibility it currently enjoys. The relative ease of use of the instrumentation, coupled with a technique which offers a multitude of separation formats, yields a separation method in CE which is often noted as easy to optimize in the process of methods development and validation.

It is the intention of this review to give the professional in the food industry an overview of the types of analyses currently possible using CE. While an overview of modes of separation will be introduced, it is not the intent of this review to go into the detail of theoretical considerations important to having a dynamic understanding of CE as a separation technique. Instead, the reader is referred to references which go into detail on these issues [5-8]. It is also not the intent of this review to give an exhaustive review of the literature for CE. For information on the use of CE in bioanalysis, the reader is referred to Landers, *et al.* [9] and Mazzio and Krull [10]. For a comprehensive review of CE, the reader is referred to the review by Kuhr and Monnig [11]. Finally, Zeece has reviewed CE as a tool specifically for food science [12].

This chapter is divided into two sections. The first section gives an overview of the instrument components and the modes of separation by CE. In order to demonstrate the scope of analyses possible by CE, separations from classes of solutes ranging from biopolymers, natural products, organic analysis in the pharmaceutical industry and inorganic ion analysis are provided. The second section gives a review of the literature where CE has been specifically used in food analysis.

9.2 OVERVIEW OF ANALYSES BY CE: A FLEXIBLE ANALYTICAL TOOL

9.2.1 Instrumentation and Components of CE

Figure 1 gives a schematic of CE instrumentation and components. A capillary, most commonly fused silica of dimensions 50-75 mm ID by 365 mm OD, and length to detection typically 25 to 80 cm, is positioned between two buffer reservoirs. Electrode connections between the reservoirs and a high voltage power supply are made. Generally, a bipolar power supply capable of delivering 30 kilovolts (KV) is used. These power supplies are current limited in the range of 0.400 mA, for safety reasons. Injection of the sample can usually be done from either end of the capillary, depending on the experimental conditions and desired results. A choice of injection by the adjustment of pressure or electromigration is desirable to provide a full range of mechanisms of injection. The most common type of detector used is UV-Vis. Detection *via* fluorescence, mass spectrometry, electrochemically based approaches and others have been described [11]. A recent report succinctly summarized range of commercially available instrumentation [13].

9.2.2 Clarification on Issues Regarding the Electroosmotic Flow

One term which is important to understand is the electroosmostic flow (EOF), which is the flow of water through the capillary (see Figure 2a). The EOF arises as a function of a double ion layer which accumulates at the interface between any solid-aqueous interface. In the case of fused silica, there will be an additional contribution due to deprotonated surface silanols, depending on the *p*H. Even the adsorbed ions in the compact layer are essentially immobile. The counter-ion layer, referred to as the diffuse layer, is mobile and will migrate to it's respective electrode in the presence of an applied field. In the example shown, which is the most common case, the ion-layer migrates to the cathode, and subsequently drags water molecules with it. Through capillarity, the rest of the water eventually moves at the same speed and direction as this layer just at the wall, producing a flat flow profile. It is this flow profile which gives rise to the high efficiency mass transport mechanism unique to capillary electrophoresis. This flat flow profile does not produce the significant axial band broadening, compared to the parabolic flow profile typical of liquid chromatography (Figure 2b).

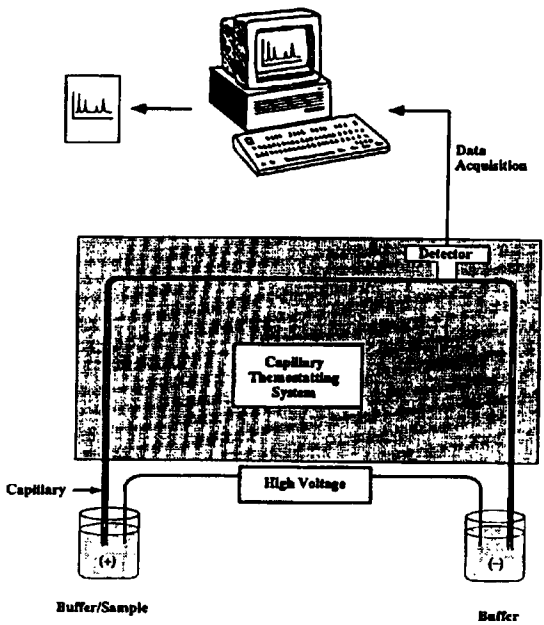

Figure 1: The schematic shown above demonstrates the basic simplicity of the CE apparatus -reference [9].

Though Hjerten suggested that the EOF would lead to significant band broadening and lack of reproducibility [14], in practice, the most serious problem is controlling the interactions of the solute species with the wall, so that this is small and reversible. Early work by Lauer and McManigill clearly showed that when the solute/wall interaction term is negligible, the efficiency in CE is relatively unaffected by the EOF [15,16]. The EOF then provides a very high efficiency mass transport mechanism so that complex mixtures of solutes of unlike charges may be transported past a single point of detection without requiring *p*H extremes. As will be demonstrated with the following examples, many additives can be successfully used to make the untoward solute/surface interactions minimal. Of particular interest are additives which reduce the interaction of basic solutes with the silica wall.

9.3 FLEXIBILITY IN MODE OF SEPARATION: THE FIVE MAJOR MODES OF CE

The five major formats of the CE experiment are capillary zone electrophoresis (CZE), micellar electrokinetic chromatography (MEKC), capillary gel electrophoresis (CGE), capillary isoelectric focusing (CIEF) and capillary isotachophoresis (CITP). The following gives a brief description of the mode of separation, and some examples of analyses which can be performed employing such separation strategies.

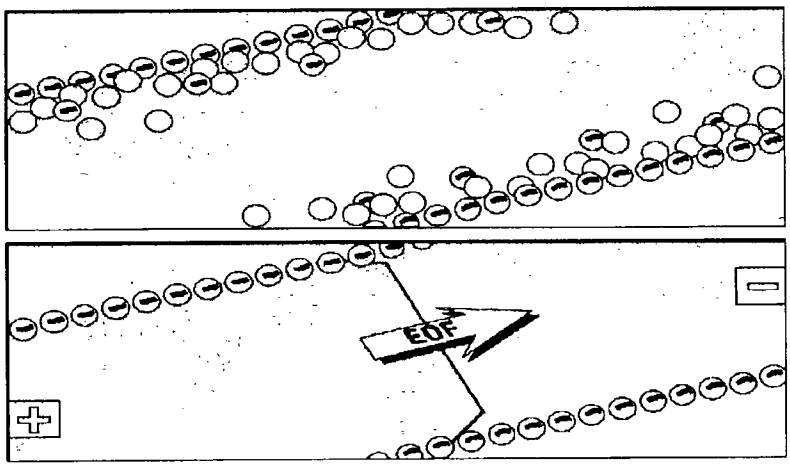

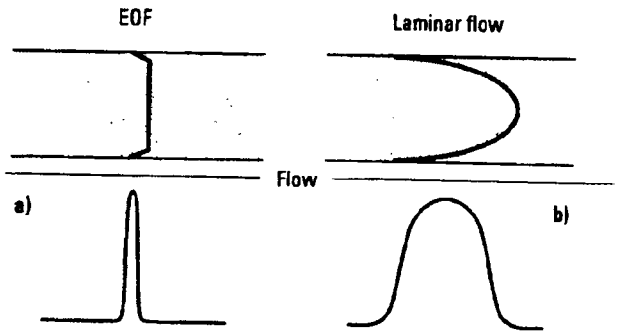

Figure 2: **A)** In 2A, the ion-double layer is shown (top), and the resultant flat profile that results from the electroosmotic flow (EOF) which results from the movement of the counter-ion layer in the presence of an applied field; **B)** In 2B, the result on band-width for the flat flow profile (CE) versus Laminar flow profile (LC) is shown.

9.3.1 Capillary Zone Electrophoresis (CZE)

CZE, also referred to as free solution capillary electrophoresis (FSCE), or open tubular capillary electrophoresis (OT CE), is the format originally described, in which the capillary is filled with an electrolyte buffer solution. In CZE, molecules are separated directly according to their charge, and inversely according to their solution drag force. Neutral molecules are moved through the capillary by the EOF. There are many additives which can be used to either dynamically deactivate the fused capillary wall, and prevent undesirable solute sticking, or to enhance solute selectivity, or both.

9.3.2 CZE in Biopolymer Analysis

After Lauer and McManigill first published the use of various biological buffers and organic ion additives to act as dynamic deactivants [17], there have been many successful demonstrations after this approach. Bullock and Yuan [18] demonstrated the separation of 6 basic proteins over a *p*H range of 3.5 to 9.0, by using different buffers in combination with 1,3 diaminopropane and alkali salts.

Several publications have demonstrated effective separations of proteins under high salt conditions [19-22]. McCormick first demonstrated that by using phosphate buffers, a phosphosilicate surface would form [19]. This biocompatible surface is produced through a simple preconditioning step of the silica capillary with phosphate buffer [22]. The conditioned capillary, in conjunction with various neutral salt additives can have an impact on selectivity and resolution for protein and peptide separations (Figure 3).

The possibility of separation and analysis of enzymes by CZE has been explored. Banke, *et al.* separated alkaline proteases from crude fermentation broth, and collected fractions from CZE for enzyme analysis. CZE was also used to monitor the progress of an enzyme reaction [23]. Konse, *et al.* reported modification of a microtitre plate assembly which was used to collect fractions on polyvinylidene difluoride (PVDF) membranes. Fractions blotted onto the PVDF membranes were then subsequently analyzed by a sequencer [24]. Emmer and Roeraade described an on-line micro-post column reactor which they used in conjunction with on-column detection. By using the two detector system, they were able to rapidly monitor enzyme activity in samples. Through careful optimization of conditions in the reactor, the loss of efficiency at the point of detection through the reactor capillary was minimal [25].

Peptide separations have been easier to optimize without severe problems of irreversible solute/surface interactions, demonstrating that in nature, the whole is not necessarily equivalent to the sum of its parts. An example of a peptide separation illustrating the selectivity which can be introduced into the CZE experiment by the judicious choice of organic modifiers was done by Oda *et al.* [26] (Figure 4a and 4b). Work demonstrating the reproducibility and μpreparative capabilities of CE was demonstrated by Herold and Wu [27]. In this investigation, the tryptic digest of human growth hormone was studied. The separation conditions were optimized to give excellent reproducibility in the analytical mode (Figure 5a) The separation was then scaled to μpreparative mode, and a specific peptide was collected (Figure 5b). This fraction was then analyzed by mass spectrometry off-line. Mass spectrometry appears to be a type of detection which will provide important capabilities for μcolumn separations in the future, since it provides information about molecular structure [28,29].

Carbohydrate analysis has been demonstrated in CZE using a variety of electrolyte conditions, and detection schemes. Lu and Cassidy obtained the

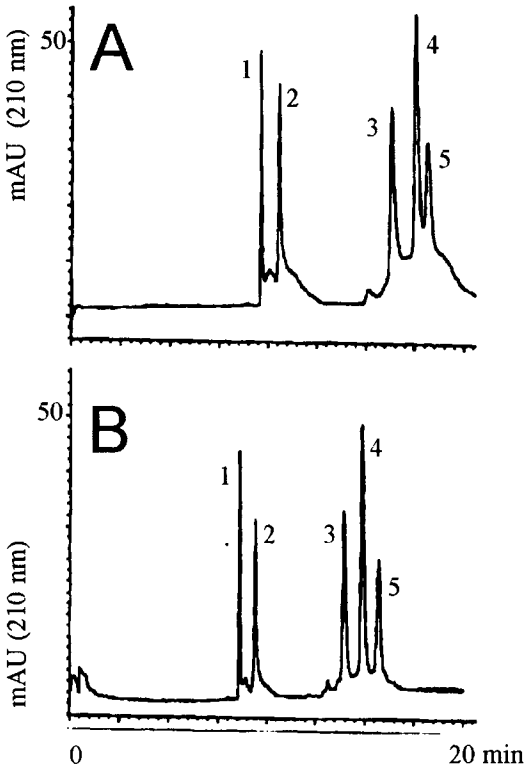

Figure 3: Variation in neutral salt additives may have an impact on separation selectivity by altering the cation from sodium (A) to ammonium (B). Peaks: (1) ribonuclease (2) myoglobin (3) ß-lactoglobulin (4) trypsin inhibitor, (5) ß-lactoglobulin B - reference [22].

separation of a mixture of mono- and di-saccharides by using 0.1M sodium hydroxide as the electrolyte solution. They were able to obtain low femtomole levels of detection of the saccharide mixture by using pulsed amperometric detection [30]. One successful approach to separation of cis-diol containing molecules by CZE has been the use of borate buffer to form the stable boronate complex at moderately alkaline *p*H. The formation of the stable charged complex changes the mobilities, and selectivities of closely related species, thereby effecting separation. Honda, *et al.* first demonstrated the usefulness of this approach for the separation of carbohydrates by CZE [31]. Hoffstetter-Kuhn, *et al.* used borate complexation and detection at 200 nm for the analysis of mono- and di- saccharides [32]. Stefansson and Novotny used covalent fluorescent tagging of branched and unbranched oligosaccharides [33]. They investigated the impact of borate buffer concentration and electric field strength on selectivity and resolution in the analysis of oligosaccharides.

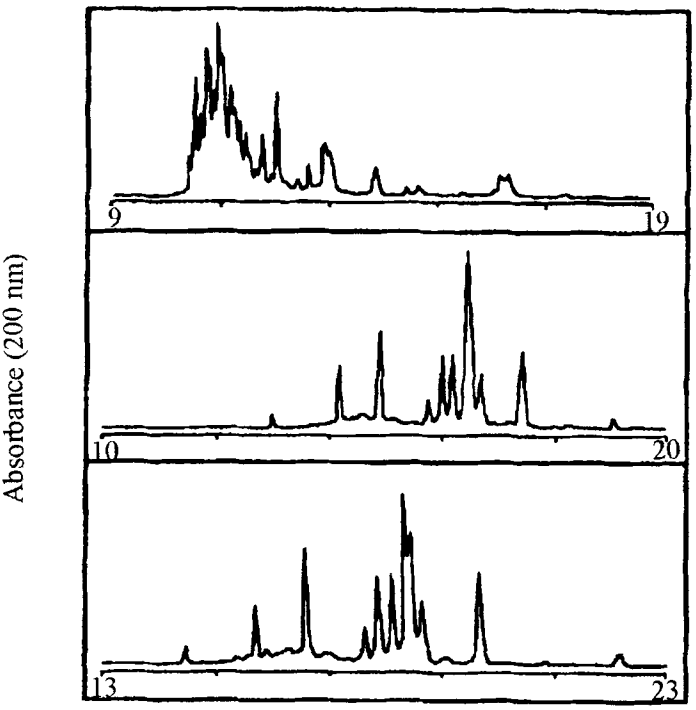

		101				105				110		112
1	Native	Lys	Thr	Asn	Tyr	Cys	Thr	Lys	Pro	Gln	Lys	Ser	Tyr
2	Ala	-	Ala	Ala	Ala	-	Ala	-	Ala	Ala	-	Ala	Ala
3	Ala	-	Ala	Ala	-	-	Ala	-	Ala	Ala	-	Ala	Ala
4	Reverse	Tyr	Ser	Lys	Gln	Pro	Lys	Thr	Cys	Tyr	Asn	Thr	Lys
5	Shuffle 1	Lys	Pro	Asn	Lys	Ser	Tyr	Cys	Tyr	Thr	Gln	Thr	Lys
6	Shuffle 2	Gln	Pro	Ser	Lys	Lys	Thr	Tyr	Cys	Lys	Thr	Tyr	Asn
7	Shuffle 3	Lys	Pro	Thr	Gln	Tyr	Asn	Lys	Ser	Thr	Tyr	Lys	Cys
8	Shuffle 4	Lys	Lys	Asn	Lys	Pro	Tyr	Cys	Thr	Gln	Thr	Ser	Tyr

Figure 4: In CE, the electrophoretic selectivity can be mitigated by judicious choice of organic additives. In the top, the mixture of eight synthetic 12mers (sequence shown bottom) is analyzed under different conditions: (top panel) 50 mM phosphate buffer, pH 2.0; (middle panel) 50 mM phosphate, pH 2.0 + 100 mM hexanesulfonic acid (HAS); (bottom panel) 50 mM phosphate, pH 2.0 + 100 mM HAS + 10% acetonitrile. Capillary: fused silica, 50 μm ID, 50 cm to detection; field: 260 V/cm (courtesy Dr. J. P. Landers, Mayo Clinic).

REPRODUCIBILITY RESULTS

	Peak 1	Peak 2	Peak3
Migration time	0.36%	0.6%	0.33%
Area	1.63%	1.89%	2.09%*

*Peak 3 not baseline separated

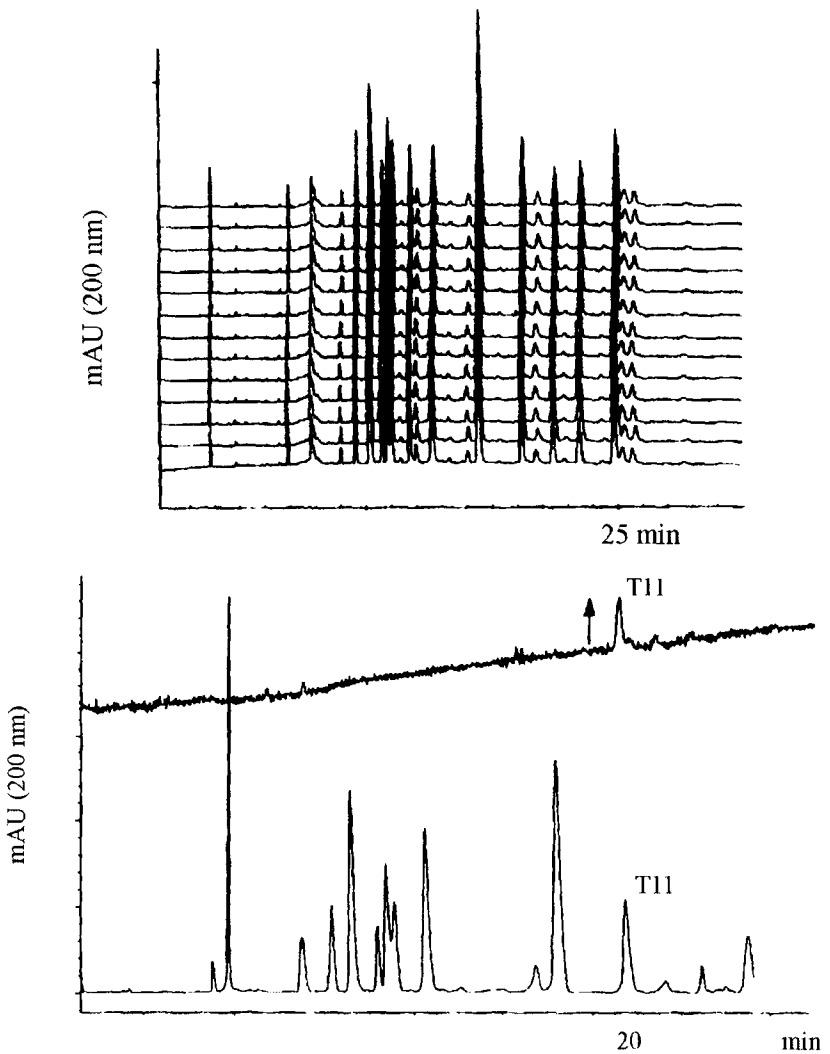

Figure 5: The good reproducibility of the CE peptide map in the analytical separation (50 μm ID capillary) demonstrates that automated fraction collection is possible (top panel). The separation is scaled to μprep (75 μm ID capillary), and four injections are collected (bottom pherogram). The collected sample is then reinjected to check for purity (bottom panel, top pherogram) - reference [27].

Finally, the cis-diol-borate complexation has also been a successful strategy for the analysis of glycoconjugates of macromolecules. Landers, *et al.* have used this approach successfully for the analysis of glycoforms of ovalbumin [34]. Morin, Villard and Dreux used this approach to demonstrate the CZE separation of mixtures of glycoconjugates of flavonoids [35].

9.3.3 Small Solute Analysis by CZE

Though originally conceived to be a method which would be well suited for bioploymers, CZE has proven to be very well suited for small solute analysis. Numerous examples of small solute analysis for CZE have been reported [11].

Using standard samples, Landers, *et al.* have shown the general utility of the cis-diol-borate complex approach for a variety of small bioactive compounds, such as hormone substances and nucleic acids [36]. Croft and Hinks did the analysis of a variety of classes of dyes by CZE [37].

Demonstrating the ability of CE to do analysis in complex matrices, Liu and Sheu [38] have reported the separation of 8 quaternary alkaloids from Coptidis rhizoma which are commonly found in Chinese herbal remedies (Figure 6). These investigators also determined ephedrine and pseudophedrine in Chinese herbal preparations [39]. Stuppner, *et al.* demonstrated the separation of 6 oxindole alkaloids from the root bark of Unicaria tomentosa [40].

Jegle [41] described the separation of water soluble vitamins by CZE, and gave an example of analysis from a commercial vitamin preparation (Figure 7). Lambert, *et al.* compared the analysis of B12 and analogues by HPLC and CZE. The CZE method was tested on multi-vitamin preparations [42]. Ma, *et al.*, used CZE and laser induced fluorescence for the fast microassay of vitamin A in serum samples [43].

Examples of using cyclodextrin modifiers for enhancement of separation has been shown by Baeyens, *et al.*[44] and Yeo, *et al.* [45]. The first group demonstrated the separation of pilocarpine and isopilocarpine in ophthalmic preparations, while the later demonstrated the separation of plant growth hormones.

Chiral separations of small solutes are gaining wide spread attention. Terabe, *et al.* first suggested that the cyclodextrans could act as a pseudophase, much in the same way that the micelle is a pseudophase for micellar electrokinetic chromatography (MEKC) [46]. Novotny, *et al.* have recently given an overview of CE and MEKC methods for chiral analysis [47].

Finally, inorganic ion analysis is easily adapted to the CZE format. Salomon and Romano [48] demonstrated the separation of 2 cations and 8 anions from the alkaline liquor taken from pulp processing in the paper industry (Figure 8). A comprehensive overview of ion analysis has been given by Jones [49].

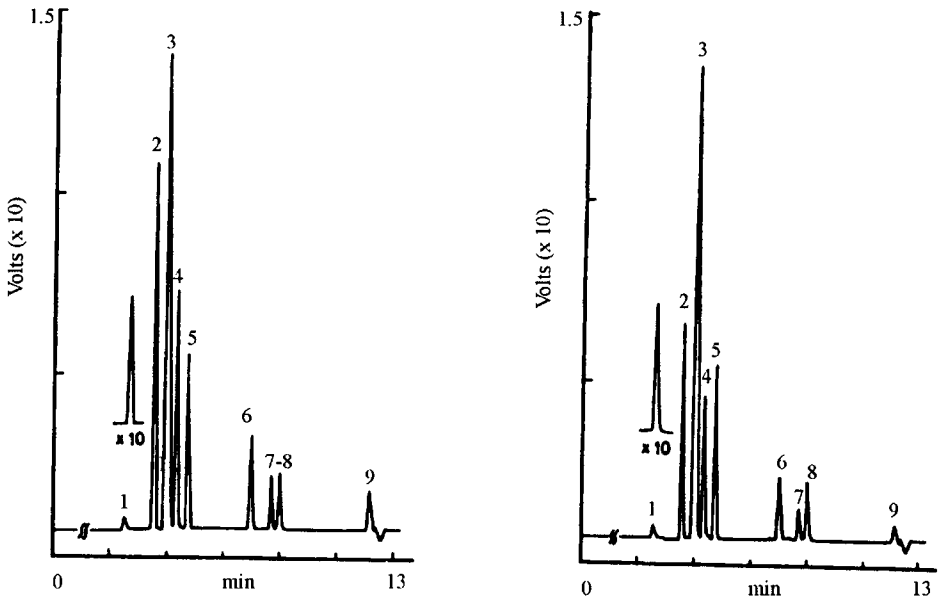

Figure 6: The CZE separation of quaternary alkaloid standards (right) compared to the alkaloids separated from a sample prepared from plant tissue (left). Peaks: (1) benzyltrimethylammonium chloride (internal standard); (2) coptisine; (3) berberine; (4) epiberberine; (5) palmatine; (6) columbamine; (7) berberastine; (8) jatrorrhizine; (9) magnoflorine - reference [39].

9.3.4 Micellar Electrokinetic Chromatography (MEKC)

MEKC, also referred to as electrokinetic capillary chromatography (EKCC), was first reported by Terabe [50]. In this format, surfactants at or above the critical micelle concentration (CMC) are used to create a pseudophase into which solute molecules may partition. The separation occurs due to the relative partitioning of the solutes into the pseudophase. The surfactant types may either be positively charged, as in the case of cetyltrimetylammonium bromide (CTAB), carry no net charge, such as the alkyl-glucoside surfactants, or carry a negative charge, such as sodium dodecyl sulfate (SDS). The EOF is generally faster than the velocity of the micelles, and under optimized separation conditions, will then act as the mass transport mechanism.

Based on the mechanism of separation by selective partitioning, even uncharged molecules may be separated using MEKC. This significantly extends the power of analysis by capillary electrophoresis. Though a number of surfactants can be used, the most popular so far has been SDS. Heiger has discussed approaches for methods development in the separation of active cold ingredients *via* MEKC with spectral identification of the eluting species using diode array detection [51].

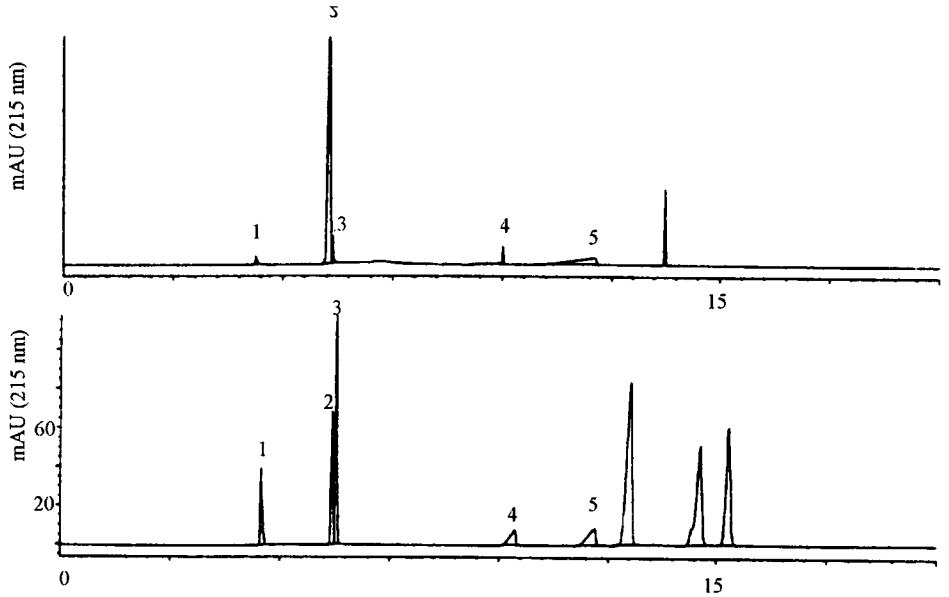

Figure 7: Comparison of the separation of vitamins from a standard sample (bottom) versus a commercial vitamin preparation (top) via CZE is shown. Peaks: (1) thiamine; (2) nicotinamide; (3) pyridoxide; (4) panthothenate; (5) ascorbic acid - reference [41].

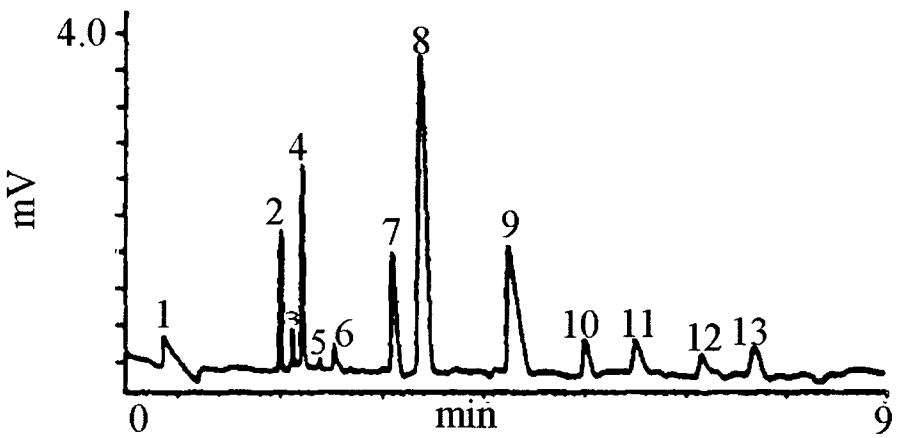

Figure 8: Separation of ions in kraft strong black liquor by CZE. Peaks: (1) hydroxide; (2) thiosulfate; (3) chloride; (4) sulfate; (5) oxalate; (6) sulfite; (7) formate; (8) carbonate; (9-13) sodium salts if organic acids - reference [48].

Other surfactants besides SDS have been used. By using the biologically compatible non-ionic surfactant, octyl glucoside, the separation of two bioactive peptides differing by one methyl group could be demonstrated [52]. Invardsen,

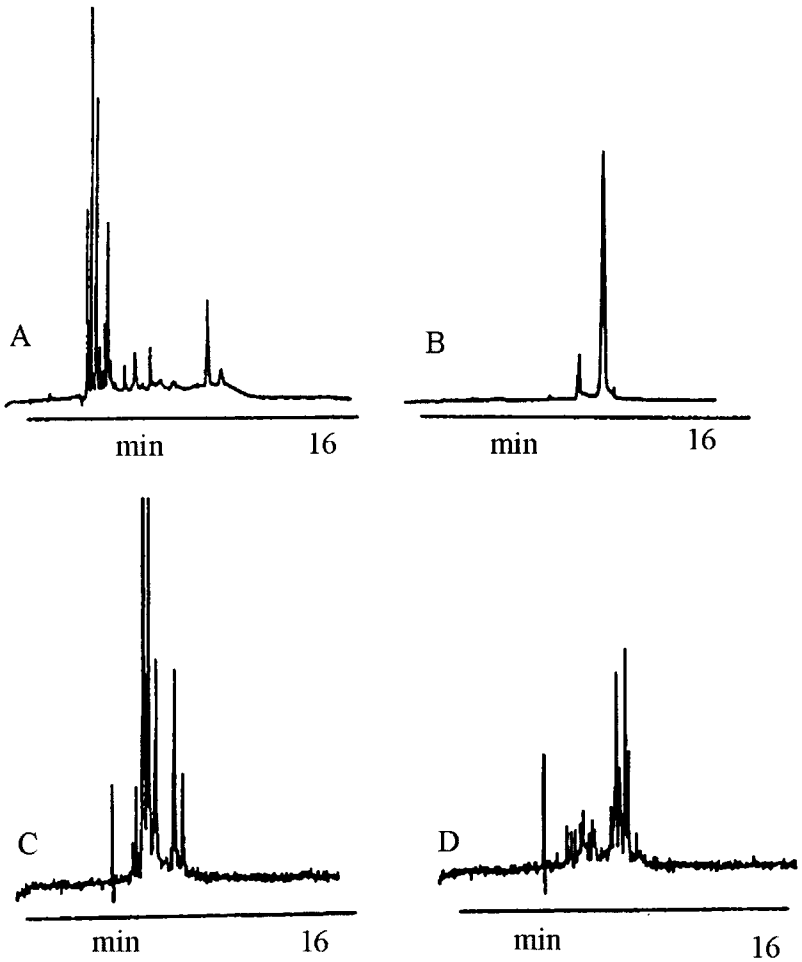

Figure 9: Separation of flavonoids from plant samples using two different micellar systems: CTAB (A, B) and cholate-taurine (C, D). Samples were taken from : (A, C) leaves of rapeseed; (B) vegetative parts of mustard; (D) vegetative parts of broccoli - reference [54].

Michaelsen and Sorensen used a cholate micellar system for the separation of phopholipids [53]. Bjergegaard, *et al.* compared the separation of 12 flavonoid standards using two surfactant systems; CTAB and cholate/taurine [54]. Examples of the separation of neutral flavonoid compounds isolated from rape seed leaves using the two surfactant systems were shown (Figure 9).

9.3.5 Capillary Gel Electrophoresis (CGE)

The separations which can be performed in the traditional slab format have also been adapted in the capillary format. Examples of separations of

oligonucleotides have been given in polyacylamide (PA) [55]. Molecular weight separation by SDS PA gel electrophoresis has also been demonstrated [56,57]. Finally, the separation of oligonucleotides and disaccharides (Figure 10) has been demonstrated in agarose [58].

Additionally, in the enclosed capillary format, unlike the traditional slab gel format, physically rigid gels are not required. Thus, separation of large molecules in solutions of entangled polymer networks is possible for some applications [59].

9.3.6 Capillary Isoelectric Focusing (CIEF)

Capillary isoelectric focusing, like CGE, is a direct adaptation of the traditional experiment to the capillary format. In isoelectric focusing (IEF), ampholytes are used to set up a *p*H gradient between the cathode and anode. Amphoteric species, generally proteins, migrate according to their net charge until reaching a *p*H region corresponding to their isoelectric point (pI). Since at this *p*H they have no net charge, they remain focused at this position. Separations of proteins differing by 0.01 *p*H unit or less have been reported. In CIEF, no gel support is required, and the gradient may be set in the ampholyte solution alone. Kilar and Hjerten [60] demonstrated the separation of the isoforms of transferrin from human serum (Figure 11).

9.3.7 Capillary Isotachophoresis (CITP)

Unlike the modes of separation described above, capillary isotachophoresis, CITP, is the only method which does not produce discrete zones, but rather continuous zones. The separation mechanism is based on a fast leading ion, and a slow terminating ion. In the separation, the leading ion must have the fastest mobility compared to the mobility of the solute ions of interest, and the terminating ion must have the slowest mobility. The solute zones then become separated according to their relative mobilities, and are sandwiched between the leading and terminating ion fronts. All species travel at the same velocity as determined by the leading ion.

Karovicova, *et al.* [61] demonstrated the separation of organic acids from two species of Sambucus (Figure 12). Seitz, *et al.* have utilized CITP for the analysis of flavonoids and phenolcarboxylic acids in plant extracts [62]. Krivankova, Foret and Bocek demonstrated the analysis of low concentrations (10^{-8} M) of the drug halofuginone in feedstuffs using CITP, with a relative standard deviation of about 1% [63].

Additionally, schemes employing isotachophoresis as a sample stacking technique at the beginning of the analysis have been reported. These techniques are used to concentrate the sample, and obtain greater sensitivity and resolution [64].

Table 1
Capillary Electrophoresis in Food Analysis (continues over 3*2pages)

Ref.	Title	Sample Description	Sample Preparation
Biopolymers in Food			
65	Determination of milk proteins by CE	Proteins (CN, α-Lg, β-La) in cow, goat and sheep milk (figure 13)	500 µL of skim milk in "reduction" buffer; incubate 1 h; used directly after incubation
66	Analysis of whey proteins by CE using buffer-containing polymeric additives	Proteins (β-Lg, A & B, α-La, BSA) in whey	Acidification to *p*H 4.6; filtered and used
67	Determination of milk proteins by CE	Proteins (CN, α-Lg, β-La) in fresh and powdered milk samples	Samples diluted 1:5 in PBS and spiked with DMF (0.01%) as a EOF marker
68	Application of CE to the qualitative analysis of sugars in sorghum hydrolysate	Xylose, arabinose, glucose and galactose in sorghum hydrolydate	Derivatization *via* reductive amination with 2-AP as the chromophore
69	Determination of carbohydrates by CZE with amperometric detection at a copper microelectrode	Glucose and fructose in cola drinks	Samples sonicated for 5 min., diluted with electrolyte solution
70	Determination of oligosaccharides by CZE	Raffinose, stachyose, verbascose and ajugose in legume seeds	Peas ground, then homogenized with MeOH/H_2O (7:3), supernatant recovered, dried dissolved in water; group separation done after Bjerg
Colour/Flavour Analysis in Food by CE			
71	Determination of synthetic colourants by CITP	Synthetic colorants from a variety of solid food samples (pudding, drink mix, candy)	Solids extracted with MeOH/ammonia (95:5) used directly ; preparation of liquids discussed

Table 1. Cont'd

Quantitative/Qualitative	Conditions
Qualitative migration time and peak area reproducibility reported	Capillary: 50 μm ID x 57 cm, hydrophilically coated (purchased); Buffer: 10 mM citrate + 6 M urea + 0.05% MHEC, *p*H 2.5; Field: 350-526 V/cm; Temp.: 45°C; Det.: 214 nm
Quantitative data compared to HPLC	Capillary: 25 μm ID x 27 cm, cross-linked PA (prepared); Buffer: 40 mM tris/borate + 0.01% SDS + 10% PEG, *p*H 8.6; Field: 593 V/cm; Temp.: 21°C; Det.: 214 nm
Qualitative peak area and peak height reproducibility reported	Capillary: 21 μm ID x 23-25 cm, silica Buffer: 500 mM phosphate + 4 M urea, *p*H 6-9 Field: 400-476 V/cm; Temp.: 23°C; Det.: 200 nm
Qualitative	Capillary: 50 μm ID x 44-70 cm, silica Buffer: 50 mM-250 mM borate, *p*H 10.5 Field: 286-454 V/cm; Temp.: 25-40°C; Det.: 195/240 nm
Qualitative calibration data for standards discussed	Capillary: 50 μm ID x 70 cm, silica and Teflon Buffer: 100 mM NaOH/LiOH; Field: 143 V/cm; Det.: amperometric at constant potential
Quantitative internal standard used, response factors for analytes reported	Capillary: 50 μm ID x 72 cm; Electrolyte: 100 mM borate, *p*H 9.9; Field: 139 V/cm; Temp.: 50°C Det.: 195 nm
Quantitative	Three different conditions for isotachophoretic separation of extracted dyes summarized

Table 1. Cont'd

72	Analysis of sugarcane flavonoids by CZE	Flavonoids from sugarcane	Rind removed from stalks, powdered in blender, extracted in 80% acetonitrile for 24 hrs, centrifuged
73	Hypoxanthine ratio determination in fish extract using CE and immobilized enzymes	IMP, HxR and Hx from cod, salmon and trout fillets	Fish sample homogenized with 10% TCA, supernatant centrifuged, neutralized, diluted and filtered
74	Lipid oxidation: effect on meat proteins	Aqueous extracts of beef	Centrifugation of aqueous extract
75	Separation of hop bitter acids by CZE and MEKC with UV-diode array detection	α-acid and β-acid fractions from commercial hop extract	Described by M. Verzele, *J. Inst. Brew.*, **92** (1986) 32

Organic Analysis in Food by CE

76	Det. of total vitamin C in fruits by CZE	AA, TAA and DAA analyzed in orange juice	AA- 12.5% TCA to juice (1:3 v/w), centrifuged, filtered, diluted; for TAA, reduced with D,L homocysteine
77	Measurement of vit. C by CE in biological fluids & fruit beverages using a stereoisomer as an I.S.	AA in biological fluids and a variety of fruit juices and wine	Sample diluted with MPA in a tube with internal standard, vortexed, filtered
78	Use of CE for monitoring citrus juice composition	Amines, flavonoids, polyphenols and AA in citrus juices- fig.14	Juices contrifuged, filtered, diluted
79	Quantitative det. of caffeine in beverages using CE	Caffeine in coffee, tea, cola & cocoa samples	Drinks made according to instructions, diluted, filtered
80	Quant. of organic acids in sugar refinery juices with CZE & ind. UV det.	Variety of organic acids in sugar beet and chicory root extract juices	Dilution of juices or syrups with DI water

Table 1. Cont'd

Qualitative reported as aspigenin equivalents	Capillary: 50 μm ID x 72 cm, silica; Buffer: 25 mM borate, *p*H 9.5 + 20% MeOH; Field:-417 V/cm; Temp.: 35°C; Det.: 395 nm
Quantitative compared to enzymatic method	Capillary: 50 μm ID x 72 cm, silica Buffer: 100 mM CAPS, *p*H 11 Field: 416 V/cm; Temp.: 30°C; Det.: 250 nm
Semi-quantitative used to assess shifts of beefy meaty peptide with time	Details not given; numerous methods for peptide analysis available in the literature [9, 11, 26, 27]
Qualitative diode array spectra used to identify acid types	Capillary: 100 μm ID x 100 cm; Buffer: 25 mM tris + 25 mM SDS, *p*H 9.0; Field: 100 V/cm; Det.: 219-400 nm
Quantitative compared to HPLC	Capillary: 100 μm ID x 40 cm, PA coated (prepared); Buffer: 20 mM phosphate, *p*H 7.0; Field: -150 V/cm; Det.: 254 nm
Quantitative	Capillary: 75 μm ID x 37 cm, silica; Buffer: 100 mM tricine, *p*H 8.8; Field: 297 V/cm; Det.: 254 nm
Qualitative data used to detect adulteration	Capillary: 50 μm ID x 70 cm, silica Buffer: 35 mM borate, *p*H 9.3 Field: 300 V/cm; Temp.: 25°C; Det.: 200/380 nm
Quantitative compared to HPLC	Capillary: 75 μm ID x 64 cm, silica Buffer: 50 mM borate, *p*H 9.6 Field: 344 V/cm; Det.: 280 nm
Quantitative	Capillary: 75 μm ID x 60 cm, silica; Buffer: 5 mM phthlate; *p*H 5.6; Field: 330 V/cm; Det.: 254 nm (indirect)

Table 1. Cont'd

81	Comparison of CZE with HPLC for the det. of additives in food stuffs	Caffeine, aspartame & benzoic acid in soft drinks & sweetening powders	Cola degassed, diluted; powders dissolved, filtered and diluted
82	Assessment of the capabilities of CZE for the det. of hippuric and orotic	Orotic and hippuric acid in rennet whey	Samples spiked with internal standard, diluted, filtered
83	Det. of propionate in bread using CZE	Propionate in lab. made & commercial bread	Water added to sample, sonicated, filtered, diluted
84	Det. of sulphon-amides in pork meat extracts by CZE	16 different sulphon-amides in pork meat	Meat samples homogenized; then extracted for 5 min., with acetonitrile
Inorganic Ion Analysis by CE			
85	Suppressed conductometric CE separation systems	Anion analysis in beer, soy sauce, tea and coffee (figure 15)	Filtration of sample through PTFE filter and dilution
86	Analysis of cationic nutrients from foods by ion chromatography	Cations from bread stuffs, cheese, parsley and peanut butter	Microwave digestion of sample in conc. nitric acid; peroxide added, digestion repeated, diluted and filtered
87	Effect of temperature on the salt balance of milk studied by capillary ion electrophoresis	Calcium, sodium, chloride, phosphate and citrate in milk samples	Sample filtered with cut-off at 10K, ultrafiltrate diluted, analyzed

Abbreviations: 2-AP = 2-aminopyridine; α-La = α-lactoalbumin; β-Lg = β-lactoglobulins; CAPS = 3-[cycloheylamino]-1-propane-sulfonic acid; CN = caseins; DMF = dimethylformamide; HIBA = α-hydroxyisobutyric acid; Hx = Hypoxanthine; HxR = inosine; ID = inner diameter; IMP = inosine 5'-monophosphate; MeOH = methanol; MHEC = methylhydroxycellulose; PA = polyacrylamide; PEG = polyethylene glycol; PBS = phosphate buffered saline; PTFE = polytetrafluoroethylene.

Table 1. Cont'd

Quantitative compared to HPLC	Capillary: 75 μm ID x 60 cm; silica: Buffer: 25 mM phosphate, *p*H11; Field: 250 V/cm; Det.: 214 nm
Quantitative compared to HPLC	Capillary: 75 μm ID x 57 cm, silica Buffer: AMPD/Bicine (40 mM AMPD), *p*H 8.8 Field: 439 V/cm; Temp.: 25°C; Det.: 254/280 nm
Quantitative	Capillary: 75 μm ID x 47 cm, silica Buffer: 5 mM tris/benzoate, *p*H 4.6 Field: 213 V/cm; Det.: 214 nm (indirect)
Quantitative	Capillary: 50 μm ID x 116.5 cm, silica; Buffer: 20 mM phosphate/borate, *p*H 7.0; Field: 258 V/cm; Det.: 254 nm
Qualitative	Capillary: 75 μm ID x 60 cm, silica Buffer: 2 mM borate; *p*H 10-10.5 Field: 333 V/cm Det.: suppressed conductometric (fabrication described)
Quantitative compared to atomic adsorption and ion chromatography	Capillary: 75 μm ID x 60 cm, silica Buffer: 1.2 mM UV-cat-2/3.0 mM tropolone Field: 333 V/cm; Det.: 185 nm (indirect)
Semi-Quantitative compared to atomic adsorption	Capillary: 75 μm ID x 60 cm, silica Buffer: (cation) 5 mM UV-cat-1/6 mM HIBA Buffer (anion) chromate + OFM anion-BT Field: 333 V/cm Det.: 214/254 nm (indirect)

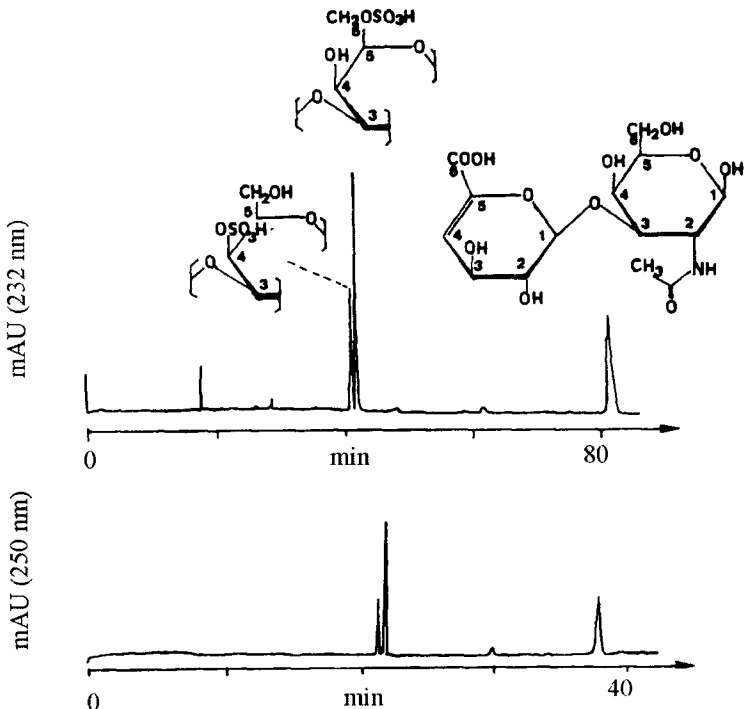

Figure 10: The separation of a mixture of three disaccharides using agarose (top) and linear polyacrylamide (bottom) gel electrophoresis is demonstrated [58].

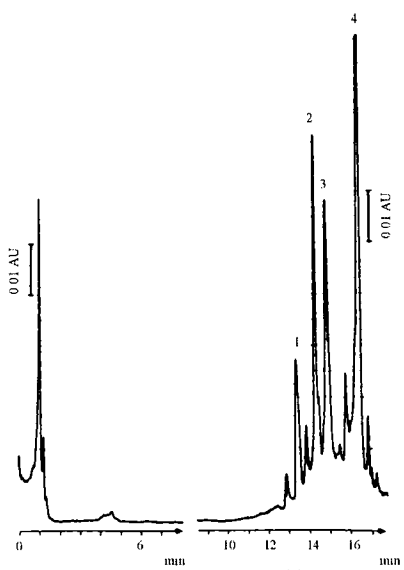

Figure 11: Isoelectrophoresis separations can be readily adapted to the capillary format. Peaks: (1) differic transferrin; (2, 3) monoferric transferrins; (4) transferrin [60].

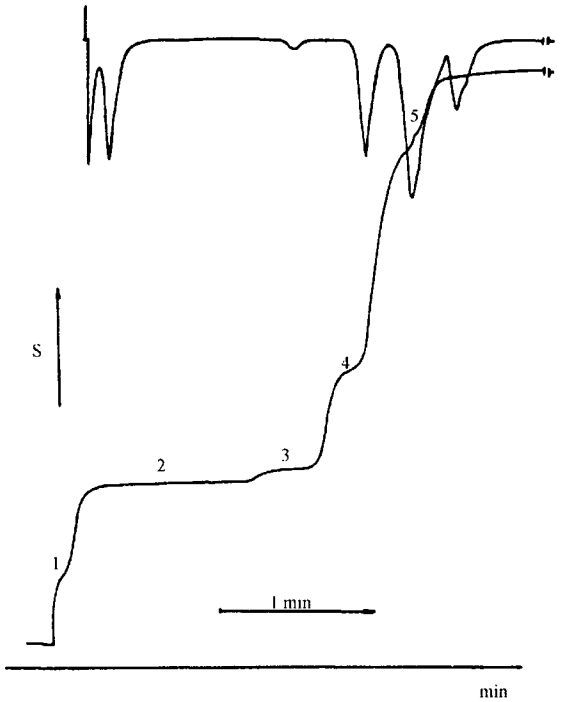

Figure 12: Separation of organic acids from Sambucus fruit *via* CITP. Peaks: (1) oxalic; (2) citric; (3) malic; (4) lactic; (5) ascorbic [71].

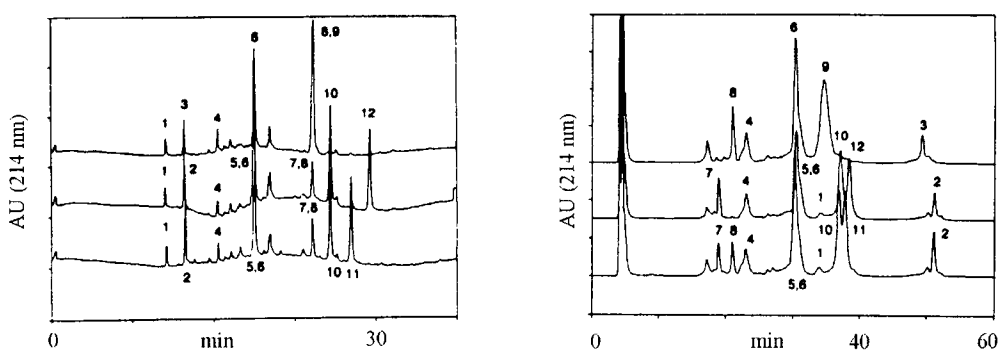

Figure 13: Separation of genetic variants of proteins from three milk samples by CZE (top) and RP-HPLC (bottom). Peaks: (1) αLa; (2) ß-Lg-A; (3) ß-Lg-B; (4) α_{S2} CN-A; (5) α-$_{S1}$ CN-C; (6) α_{S1} CN-B; (7) κCN-A; (8) κCN-B; (9) ßCN-B; (10) ßCN-Al; (11) ßCN-A2; (12) ßCN-A3 [65].

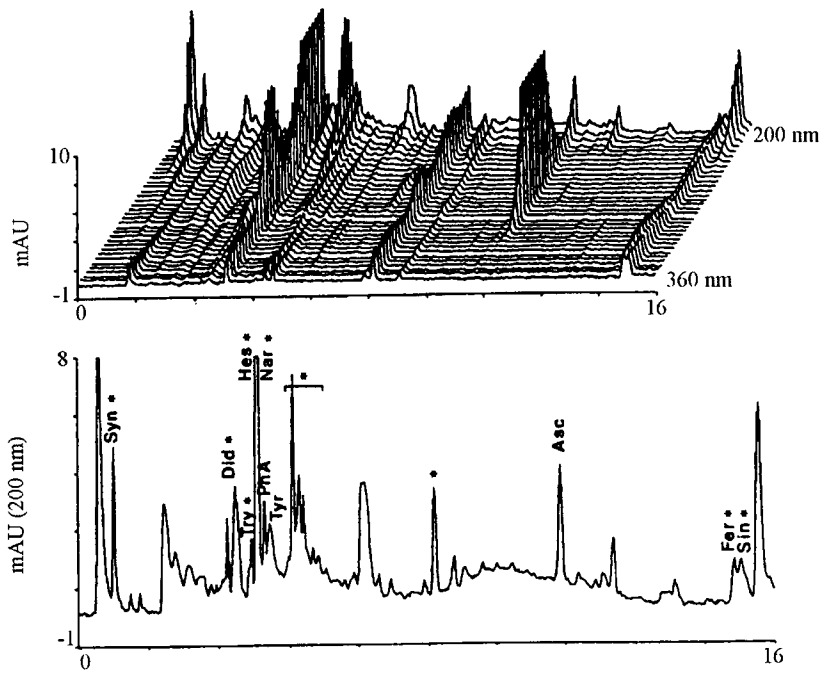

Figure 14: Multiple (top) *versus* single (bottom) wavelength pherograms of small solute analysis in an orange juice by CZE. Peaks: (1) synephrine; (2) didymin; (3) tryptophan; (4) hesperidin/narirutin; (5) phenylalanine; (6) tyrosine; (7) ascorbate; (8) feruloylglucose [78].

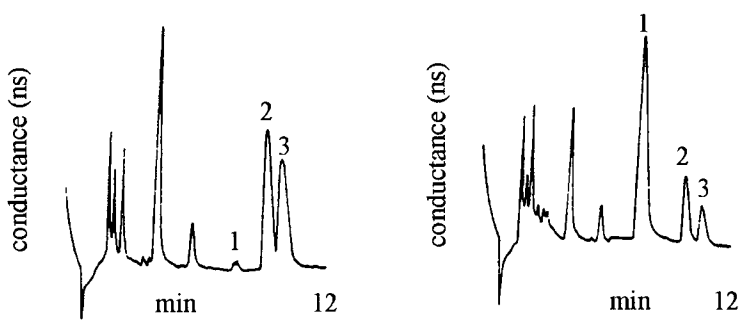

Figure 15: Analysis of ions in beer (left) and Chinese green tea (right) using CZE and suppressed conductometric detection. Peaks: (1) nitrate; (2) sulfate; (3) chloride [85].

9.4 APPLICATIONS OF CE IN ANALYSIS OF SUBSTANCES IN FOOD

The following tables are meant to be a concise summary of the conditions used to determine specific substances in food materials by CE. Most of the papers report considerably more details than shown. The information is meant as a guide to potential users as to the relevance and direct applicability of the methodology for a particular analytical problem. In all, 23 references were found in which direct analysis in food was reported.

9.5 CONCLUSION

It has been the goal of this chapter to quickly acquaint users unfamiliar with CE to the potentials it offers as an analytical technique in food analysis. The examples chosen in the first part represent only a small fraction of the current literature in analysis by CE, and were specifically picked for the possible relevance to professionals in the food industry.

The references in the second portion of the chapter bear direct relevance to analysis of substances in food. Remarks frequently made by investigators pertained to the ease of use of the method [65, 67, 70, 73, 76, 77, 79, 80, 87] and/or it's speed and efficiency [65-67, 72, 76, 77, 79, 80, 82, 87] compared to other analytical techniques [66, 73, 76, 79, 80, 81, 86, 87]. Many addressed aspects of CE which are still subject of analytical methods development; primarily matrix effects which cause shifts in elution times [67, 83, 84] and variation in peak area response [67, 70, 77, 81, 82].

While as a technique, CE is still in a state of evolution, it is clear from this literature that it has a future in analysis of substances from complex matrices, such as food. Part of adaptation to CE is a learning experience. Since CE is an electrophoretic technique, while elution times may vary more than that of HPLC, mobilities should be a constant under defined conditions. Reporting the effective sample mobility will give good reproducibility in a well optimized system [67, 83, 84]. The situation of area reproducibility was addressed by those who reported quantitative data by the use of an internal standard, in many cases [70, 77, 82].

It is apparent that the speed, efficiency, automation, reduced sample size, and flexibility in separation mechanism provided by the many modes of analysis are attributes of CE which are driving many analysts to further explore its unique capabilities.

9.6 REFERENCES

1. K. Virtanene, *Acta Polytech. Scand. Chem. Tech. Metal.* **Ser. 123**, 1 (1974).

2. F. E. P. Mikkers, F. M. Everaerts, and T. P. E. M. Verheggen, *J. Chromatogr.* **169**, 11 (1979).

3. J. W. Jorgenson and K. D. Lukacs, *Anal. Chem.* **53**, 1298 (1981).

4. J. W. Jorgenson and K. D. Lukacs, *J. Chromatogr.* **218**, 209 (1981).

5. S. F. Y. Li, Capillary Electrophoresis - Principles, Practice and Applications, Elsevier, Amsterdam, 1992.

6. Capillary Electrophoresis- Theory and Practice, P. D. Grossman and J. C. Colburn (eds), Academic Press, San Diego, 1992.

7. R. Weinberger, Practical Capillary Electrophoresis, Academic Press, San Diego, 1993.

8. Handbook of Capillary Electrophoresis, J. P. Landers (ed.), CRC Press, Boca Raton, 1993.

9. J. P. Landers, R. P. Oda, T. C. Spelsberg, J. A. Nolan, and K. J. Ulfelder, *BioTechniques*, **14**, 98 (1993).

10. J. R. Mazzeo and I. S. Krull, in Handbook of Capillary Electrophoresis, J.P. Landers (ed.), CRC Press, Boca Raton, 1993.

11. W. G. Kuhr and C. A. Monnig, *Anal. Chem.* **64**, 389R (1992).

12. M. Zeece, *Trends in Food Sci. and Tech.* **3**, 6 (1992).

13. R. P. Oda, T. C. Spelsberg, and J. P. Landers, *LC-GC*, **12**, 50 (1994).

14. S. Hjerten, *J Chromatogr.* **347**, 191 (1985).

15. D. McManigill and H. H. Lauer, 6th International Symposium on HPLC of Proteins, Peptides and Polynucleotides, Baden-Baden, Germany, Oct. 20-22, 1986.

16. S. A. Swedberg and D. McManigill, in Techniques in Protein Chemistry, T. Hugli (ed.), Academic Press, San Diego, 1989.

17. H. H. Lauer and D. McManigill, *Anal. Chem.* **58**, 166 (1986).

18. J. A. Bullock and L.-C. Yuan, *J. Microcol. Sep.* **3**, 241 (1991).

19. R. M. McCormick, *Anal. Chem.* **60**, 2322 (1988).

20. A. D. Tran, S. Park, P. J. Lisi, O. T. Huynh, R. R. Ryall, and P. A. Lane, *J Chromatogr.* **542**, 459 (1991).

21. F. A. Chen, L. Kelly, R. Palmieri, R. Biehler, and H. Schwartz, *J. Liq. Chromatogr.* **15**, 443 (1992).

22. S. A. Swedberg and C. A. Miller, Hewlett-Packard Application Note 12-5962-9965E, 1994.

23. N. Banke, K. Hansen and I. Diers, *J. Chromatogr.* **559**, 325 (1991).

24. T. Konse, T. Takahashi, H. Nagashima, and T. Iwaoka, *Anal. Biochem.* **214**, 179 (1993).

25. A. Emmer and J. Roeraade, *J. Chromatogr. A*, **662**, 375 (1994).

26. R. P. Oda , B. J. Madden, J. C. Morris, T. C. Spellsberg, and J. P. Landers, J. *Chromatogr.* **12**, 531 (1994).

27. M. Herold and S.-L. Wu, *LC-GC*, **12**, 531 (1994).

28. W. M. Mueck and J. D. Henion, *J. Chromatogr.* **495**, 41 (1989).

29. D. F. Hunt, J. Shabanowitz, M.A. Moseley, A. L. McCormack, H. Michel, P. A. Martino, K. B. Tomer, and J. W. Jorgenson, in Methods in Protein Sequence Analysis, H. Jornvall, J.-O. Hoog, and A.-M. Gustavsson (eds.), Birkhaüser Verlag, Basel, 1991.

30. W. Lu and R. M. Cassidy, *Anal. Chem.* **65**, 2878 (1993).

31. S. Honda, S. Iwase, A. Makino, and S. Fujiwara, *Anal. Biochem.* **176**, 72 (1989).

32. S. Hoffstetter-Kuhn, A. Paulus, E. Gassmann, and H. M. Widmer, *Anal. Chem.* **63**, 1541 (1991).

33. M. Stefansson and M. Novotny, *Anal. Chem.* **66**, 1134 (1994).

34. J. P. Landers, R. P. Oda, B. J. Madden, and T. C. Spelsberg, *Anal. Biochem.* **205**, 115 (1992).

35. P. Morin, F. Villard, M. Dreux, and P. Andre, *J Chromatogr.* **628**, 161 (1993).

36. J. P. Landers, R. P. Oda, and M. D. Schuchard, *Anal. Chem.* **64**, 2846 (1992).

37. S. N. Croft and D. Hinks, *Text. Chem. Color*, **25**, 47 (1993).

38. Y.-M. Yiu and S. J. Sheu, *J. Chromatogr.* **623**,196 (1992).

39. Y.-M. Liu and S. J. Sheu, *J. Chromatogr.* **637**, 219 (1993).

40. H. Stuppner and S. Sturm, *J. Chromatogr.* **609**,375 (1992).

41. U. Jegle, *J. Chromatogr.* A, **652**, 495 (1993).

42. D. Lambert, C. Adjalla, F. Felden, S. Benhayoun, J. P. Nicolas, and J. L. Gueant, *J. Chromatogr.* **608**, 311 (1992).

43. Y. Ma, Z. Wu, H. C. Furr, C. Lammi-Keefe, and N. E. Craft, *J. Chromatogr.* **616**, 31 (1993).

44. W. Baeyens, G. Weiss, G. Van Der Weken, and W. Van Den Bussche, *J. Chromatogr.* **638**, 319 (1993).

45. S. K. Yeo, H. K. Lee, and S. F. Y. Li, *J. Chromatogr.* **594**, 335 (1992).

46. S. Terabe, H. Ozaki, K. Otsuka, and T. Ando, *J. Chromatogr.* **332**, 211 (1985).

47. M. Novotny, H. Soini, and M. Stefansson, *Anal. Chem.* **66**, 646A (1994).

48. D. R. Salomon and J. Romano, *J. Chromatogr.* **602**, 219 (1992).

49. W. R. Jones, in Handbook of Capillary Electrophoresis, J.P. Landers (ed.), CRC Press, Boca Raton, 1993.

50. S. Terabe, K. Otsuka, K. Ichikawa, A. Tsuchiya, and T Ando, *Anal. Chem.* **56**,111 (1984).

51. D. N. Heiger, Hewlett-Packard Application Note 12-5091-9036E, 1993.

52. S. A. Swedberg, *J Chromatogr.* **503**,449 (1990).

53. L. Ingvardsen, S. Michaelsen, and H. Sorensen, *J. Am. Oil Chem. Soc.* **71**, 183 (1994).

54. C. Bjergegaard, S. Michaelsen, K. Mortensen, and H. Sorensen, *J. Chromatogr. A*, **652**,477 (1993).

55. D. Chen, H. R. Harke, and N. J. Dovichi, *Nucleic Acids Res.* **20**, 4873 (1992).

56. A. Widhalm, C. Schwer, D. Blaas, and E. Kenndler, *J. Chromatogr.* **549**, 446 (1991).

57. K. Tsuji, *J. Chromatogr.* **550**, 823(1991).

58. S. R. Motsch, M.-H. Kleemiss, and G. Schomburg, J. *High Res. Chromatogr.* **14**, 629 (1991).

59. P. D. Grossman and D. S. Soane, *Biopolymers*, **31**, 1221 (1991).

60. F. Kilar and S. Hjerten, *Electrophoresis*, **10**, 23 (1989).

61. J. Karovicova, J. Polonsky, and A. Probela, *Die Nahrung*, **34**,665(1990).

62. U. Seitz, G. Bonn, P. Oefner, and M. Popp, *J Chromatogr.* **545**,449 (1991).

63. L. Krivankova, F. Foret and P. Bocek, *J. Chromatogr.* **545**, 307 (1991).

64. B. J. Wanders and F. M. Everaerts, in Handbook of Capillary Electrophoresis, J.P. Landers (ed.), CRC Press, Boca Raton, 1993.

65. N. de Jong, S. Visser and C. Olieman, *J. Chromatogr.* A, **652**, 207 (1993).

66. A. Cifuentes, M. de Frutos, and J. C. Diez-Masa, *J. Dairy Science*, **76**, 1870 (1993).

67. F.-T. A. Chen and J.-H. Zang, *J. AOAC Int'l.* **75**, 905 (1992).

68. C. Delgado, T. Talon, and A. Gaset, *Analusis*, **21**, 281 (1993).

69. L. A. Colon, R. Dadoo, and R. Zare, *Anal. Chem.* **65**, 476 (1993).

70. A. M. Arenoft, S. Michaelsen, and H. Sorensen, *J. Chromatogr. A*, **652**, 517 (1993).

71. J. Karovicova and J. Polonsky, *Die Nahrung*, **35**, 403 (1991).

72. T. K. McGhie, *J. Chromatogr.* **634**, 107 (1993).

73. J. H. T. Luong, K. B. Male, C. Masson, and A.L. Nguyen, *J. Food Sci.* **57**, 77 (1992).

74. A. M. Spanier, J. A. Miller, and J. M. Bland, in Lipid Oxidation in Food, A. J. St. Angelo (ed.), American Chemical Society, Washington, DC, 1992.

75. J. Vindervogel, P. Sandra and L. C. Verhagen, *J. High Res. Chromatorgr.* **13**, 295 (1990).

76. M. Chiari, M. Nesi, G. Currea, and P. G. Righetti, *J. Chromatogr.* **645**, 197 (1993).

77. E. V. Koh, M. G. Bissell, and R. K. Ito, *J. Chromatogr.* **633**, 245 (1993).

78. P. F. Cancalon and C. R. Bryan, *J. Chromatogr. A*, **652**, 555 (1993).

79. W. J. Hurst and R. A. Martin, *Analusis*, **21**, 389 (1993).

80. S. P. D. Lalljie, J. Vindevogel, and P. Sandra, *J. Chromatogr.* **652**, 563 (1993).

81. M. Jimidar, T. P. Hamoir, A. Foriers, and D. L. Massat, *J. Chromatogr.* **636**, 179 (1993).

82. P. A. Tienstra, J. A. M. van Riel, M. D. Mingorance and C. Olieman, *J. Chromatogr.* **608**, 357 (1992).

83. M. T. Ackermans, J. C. J. M. Ackermans-Loonen, and J. L. Beckers, *J. Chromatogr.* **627**, 273 (1992).

84. M. T. Ackermans, J. L. Beckers, F. M. Everaerts, H. Hoogland and J. H. Tomassen, *J. Chromatogr.* **596**, 101 (1992).

85. P. K. Dasgupta and L. Bao, *Anal. Chem.* **65**, 1003 (1993).

86. J. Morawski, P. Alden, and A. Sims, *J. Chromatogr.* **640**, 359 (1993).

87. M. Schmitt, F. Saulnier, L. Malhautier, and G. Linden, *J. Chromatogr.* **640**, 419 (1993).

J.R.J. Paré and J.M.R. Bélanger (Editors)
Instrumental Methods in Food Analysis

Chapter 10

Microwave-Assisted Process (MAP™)[1]: Principles and Applications

J. R. Jocelyn Paré and Jacqueline M. R. Bélanger

Environment Canada, Microwave-Assisted Processes Division,
Environmental Technology Centre,
Ottawa, ON, Canada K1A 0H3.

10.1 INTRODUCTION[2]

The microwave-assisted process (MAP™)[1] is a relatively new series of technologies that relate to novel methods of enhancing chemistry using microwave energy. Of particular interest to this chapter is the work dealing with the extraction of soluble products into a specific fluid from a wide range of bio-materials of interest to food science. In these applications, generally speaking, MAP provides techniques whereby compounds can be extracted more selectively and more rapidly with similar or better recovery when compared to conventional extraction processes. Significant savings can also be made as a result of the reduced amount of solvent required to perform MAP extractions. Environment Canada (The Department of the Environment of Canada) holds some intellectual property rights to several microwave-assisted processes in numerous jurisdictions around the world. Because of the variety of these applications, that extend far beyond extraction, the general word "MAP" was

---

1 MAP is a Trademark of Her Majesty the Queen in Right of Canada as represented by the Minister of the Environment.

2 A portion of this chapter, such as the introduction and the descriptive text related to the physical phenomena surrounding MAP has been adapted from references [1-6].

used as a Trade-Mark (rather than a specific one based upon the word extraction) to encompass a "family" of techniques.

MAP applications extend from analytical-scale to industrial processing for commercial purposes. The pilot-scale and industrial-scale applications are well beyond the scope of this contribution. They are mentioned, however, because historically they were the first applications to be the subject of public disclosure and to be actively promoted in the industrial sector. The development of MAP was greatly accelerated because of its high potential for commercial success and the exceptionally high environmental gains that were anticipated from several "clean process technology" applications associated with it. In fact, MAP supports sustainable development as it offers one or more advantages over currently used technologies, such as reduced energy consumption, smaller volumes of chemical solvents, use of less toxic solvents, and smaller quantity of waste products. In some cases, it even allows for the further processing of waste products into useful products, such as recovery of biologically active compounds from biomass produced in fermentation processes [1-7].

The first applications of MAP that were disclosed publicly dealt with the extraction of essential oils from plant products [8], although the patented technology applies to the extraction of a variety of chemical substances from a wide range of matrices such as water, soils, animal and plant tissues, as well as a variety of man-made products [1-6]. The fields of application are also very diversified and include environmental, agricultural, food, biomedical, pharmaceutical, consumer products, and process monitoring and control.

In the analytical laboratory, MAP offers a radical change from conventional sample preparation work. This chapter will deal exclusively with areas of interest to the food analysis laboratory. The main emphasis will bear on "extraction" applications where a fluid, namely a liquid (*e.g.*, an organic solvent or a liquefied gas) or a gas (*e.g.*, surrounding air), acts as extractant. In all cases, MAP offers the potential for significant reductions in sample preparation time while providing enhanced analytical capabilities such as increased selectivity, higher sensitivity, while affording similar or better linearity and reproducibility factors. Furthermore, a given set of operating conditions is usually applicable to a broad range of matrices, thus simplifying method development work.

In view of the very broad range of applications of MAP, and as a result of the unusually high level of interest that has surrounded the process over the past few years, Environment Canada has put in place an extensive and far-reaching technology transfer and licensing activities program with the commercial and industrial sectors that is considered to be the most important program of that nature ever set forth by a Federal Department in Canada. By doing so, Environment Canada wanted to provide the end-users with easy and rapid

access to legitimate commercial instrumentation that would allow for a safe and efficient use this new technology.

10.2 SAFETY CONSIDERATIONS

The microwave-assisted process is a simple technology that can be readily understood in terms of the operating steps to be performed. Given the fact that the chemical and physical principles underlying the technology are deceptively simple, an extraordinary level of safety and attention to details when planning and performing experiments must be used by all personnel dealing with microwaves. The authors urge all readers and potential users to ensure that they seek proper information from knowledgeable sources and that they do not attempt to implement these techniques unless proper guidance is provided. The feeling of simplicity associated with MAP can enhance the level of hazard and exposure to accidents if procedures are not properly assessed and if due care and proper safety measures are not implemented prior to experimentation.

Only approved equipment and scientifically sound procedures should be used at all times. Despite the seemingly simple nature of the procedure described herein, workers should refrain from using domestic microwave ovens. The wide availability of such non-laboratory approved equipment combined to their relatively low cost make it tempting but at no time should the safety of operators be overlooked, and extreme care should be exercised as a result of the inherent danger of explosion. Furthermore, commercially available domestic ovens have so-called "duty cycles" (*i.e.*, the magnetron is not always ON), hence making it possible to give rise to hazardous conditions (such as increases in pressure and temperature) that enhance considerably the risk of explosion. This characteristic of domestic ovens also has for effect to reduce significantly the level of efficiency of the work to be carried out, especially with respect to reproducibility.

10.2.1 Liquid-Phase Extraction

The application of microwave energy to organic compounds, such as solvents, can pose serious hazards. The hazard is greater with flammable liquids. Two main types of apparatus are available commercially. They make use of single-mode or of multi-mode technology. The readers are invited to review commercial literature from CEM Corp. [9] and Prolabo [10], currently the only two manufacturers that offer legitimate MAP instrumentation.

10.2.2 Gas-Phase Extraction

Experiments and other empirical work discussed herein were carried out by highly-skilled personnel well abreast of risks and hazards associated with subjecting volatilised materials to microwave energy while within a confined volume. Special care should be exercised if and when attempting to

reproduce the present work. For example, using procedures described herein, the surface temperature of the headspace vial was measured to be above 110°C and the pressure up to above 12 psi. There should be no vigorous boiling or excessive distortion of the septum seal. The tab at the centre of the safety cap is designed to peel back by the bulging septum if the pressure limit is exceeded. During the microwave exposure period, interrupt the power application immediately upon hearing any noise (knocking, cracking, or bumping) which may be indicative of imminent release of excessive pressure. In handling the vial after irradiation, use adequate tools and always wear proper personal protection gear.

This hazard level will be reduced if not totally removed when commercial instrumentation is made available to the laboratory community in the near future. By the same token, when such instrumentation is available even better operating conditions will be available to users as the apparatus and peripherals used therefor will have been designed specifically for that purpose keeping the critical parameters in mind.

10.3 THE PROCESS

MAP methods in general, whether applied to liquid-phase extraction or to gas-phase extraction are based upon a basic physical principle, namely the fact that different chemical substances absorb microwave energy to different levels. The dielectric constant is generally used as the parameter to measure this physical property. In general terms we can say that the higher the absolute value of the dielectric constant, the higher the level of absorption of microwave energy. In reality, however, the situation is much more complicated than that because the ability demonstrated by a chemical substance to absorb microwave energy varies with the frequency applied as well as with the temperature of the substance when subjected to such microwaves [11-13]. This chapter deals exclusively with the food analysis applications of MAP. Consequently, the discussion will be limited to the use of only one frequency, 2450 MHz, the only frequency being currently used in MAP laboratory instrumentation.

The fact that different chemical species absorb microwave energy to a different extent implies that the thermal energy so-produced and imparted to the surrounding environment will also vary with the chemical species. Hence, for systems that possess inherent non-homogeneous structural characteristics, or that contain different chemical species with different dielectric properties dispersed into a homogeneous environment, it is possible to effect a selective heating of some areas, or components of the systems.

10.3.1 Liquid-Phase Extraction

Liquid-phase extraction using MAP is based upon the fact that it is possible to immerse the matrix to be extracted in a liquid that is characterised by a smaller

dielectric constant and is relatively transparent to microwaves. The greater the difference in dielectric properties, the better the efficiency of MAP and the greater the savings in terms of energy and in solvent used to extract. In open-vessel applications or in low-pressure applications the solvent can also be used as a "natural" coolant - in addition to its ability to solubilise the target material - because its temperature does not rise as rapidly as that of the matrix. For example, the temperature elevation observed in a solvent such as hexane results, for all practical purposes, only from the passive thermal energy diffusion from the matrix to the surrounding solvent. The latter is a relatively slow process compared to microwave energy excitation of the matrix.

One of the most important chemical species present in almost any food-related matrix to be extracted and analysed is water. This characteristic is especially suitable for MAP work. In fact, free water molecules possess a high dielectric constant and as such they exhibit a relatively high absorption of microwave energy (at 2450 MHz! - as opposed to bound water molecules which are characterised by a smaller dielectric constant and are virtually transparent to microwaves at that same frequency). To date, matrices involving plant tissues, animal tissues, soils, emulsions (gels, paste, creams, *etc.*), biomass (fermentation broth, micellar suspensions, *etc.*), even powders (as in pills and tablets) have been the subject of MAP activities, and it is only fair to say that the free water content of these matrices has been the single most important factor in the development of MAP analytical methods, irrespective of their nature. This, however, does not preclude the potential use of MAP for dry or dehydrated materials since most matrices can be re-hydrated, or impregnated with a substance that possesses a relatively high dielectric constant (compared to the extracting medium) in order to achieve the same result as would be obtained from fresh or moist samples.

The addition of a chemical species with a large dielectric constant to induce desired microwave effects in matrices devoid of such substances, or lacking substances with significantly different dielectric constants, can be compared, on a conceptual basis, to cross-polarisation experiments carried out in nuclear magnetic resonance spectroscopy (see Chapter 6). In that case, a nucleus that relaxes relatively rapidly is excited selectively and allowed to transfer that excitation energy to neighbouring nuclei with low or relatively lower relaxation rate (*e.g.*, ^{1}H nuclei being cross-polarised to ^{13}C nuclei).

The addition of such a substance prior to extraction is effected only when the added substance is a desirable component of the final product formulation where the extract will be used. Consequently, for liquid-phase extraction, this practice is more useful in industrial process applications such as, for example, the use of alcohol for the production of extracts to be used in the confection of liqueurs. In gas-phase extractions, however, this technique is very useful in enhancing the volatilisation of analytes. This has applications in the analytical

laboratory and as such it is described later in the corresponding gas-phase extraction section.

In liquid-phase extraction, provided that there is sufficient dispersed free water - or that an adequate amount of high dielectric constant material has been added to the matrix - it is possible to design a MAP extraction procedure with almost any of the organic solvents routinely used in chemical analysis, bearing in mind that the solvent must be selected for its ability to solubilise the desired product. Bear in mind that the selection of the "solvent" is not limited to substances that are liquid at ambient temperature and pressure. In fact, the use of liquefied gases, such as CO_2 or propane, are especially attractive to food science workers as a result of their low toxicity and the relative ease with which they can be virtually removed from the spent material. The latter comments also apply to gas-phase or "solvent-less" extraction made possible when using MAP.

The phenomena at play in MAP can be better understood and visualised when referring to our original investigations where we designed a series of liquid-phase extraction using various energy sources on a single source of plant material (mint leaves at the time). The effects of such extraction processes on the physical micro-structure of the material being extracted were closely monitored using scanning electron microscopy techniques. Selected extraction processes, representing various types and levels of energy, included: steam distillation, passive hot solvent extraction, Soxhlet extraction, mechanically agitated reflux extraction, supercritical fluid extraction, ultrasound-assisted extraction, and gamma ray-assisted extraction.

Scanning electron micrographs taken from control (non-treated) and leaves that were previously treated by the extraction processes mentioned above revealed significant differences between the microwave-assisted extracted leaves and all other mint leaves which had been extracted by means. This was true for dry, fresh, and re-hydrated leaves. In fact, it was clear that the process by which the extraction occurs when using microwaves was fundamentally different from any other extraction processes investigated at the time. Actually, to the best of our knowledge, this assertion still holds true. In summary, the conclusions drawn from the micrographs taken from mint leaves that were subjected to extraction in hexane were as follows [1-6]:

> "The microwave rays travel freely through the microwave-transparent solvent (relative to the leaves) and reach the leaves. The latter - like many other food-related materials - are made of a multitude of pocket-like cavities that are defined by the cells, glands, vascular vessels, and the like, all of which contain different chemical species and different levels of water. The microwaves interact selectively with the free water molecules and cause localised heating that give rise to a sudden non-uniform elevation in temperature with more pronounced effects where

the free water is in larger proportions. For mint leaves, the glandular and vascular systems are prime targets. The temperature increases rapidly to the boiling point of water and even above it. The result is a dramatic expansion in volume within the systems. The walls of these systems can not accommodate the high internal pressures that are created and rupture spontaneously, allowing the organic contents to flow freely toward the relatively cool surrounding solvent that solubilises them rapidly."

Figure 1 presents micrographs that offer a good visual insight in the processes that took place during the extraction treatment. All the non-MAP processes produced similar effects, hence for conciseness only micrographs of control, Soxhlet-extracted, and MAP-treated materials are reproduced here. Note that the degree of microstructure disruption produced by a microwave irradiation as short as 20 seconds (at 625 watts) proved to be more specific to the glandular systems, but was as widely spread in terms of extent, as the disruption resulting from a 6-hour (21600 seconds) extraction by Soxhlet. Furthermore, in this specific example, the specificity is clearly demonstrated in that the MAP-treated plants retained the structural characteristics of their leaf surfaces, while most of the morphological characteristics of the leaves were removed by the Soxhlet extraction.

Figure 1. Scanning electron micrographs of untreated (A), Soxhlet-extracted (B), and MAP-treated (C) fresh peppermint leaves (*Mentha piperita* L. Mitchum). The Soxhlet was carried out for 6 hours whereas the MAP treatment consisted of a single irradiation of 20 seconds. Hexane was used as solvent in both cases. Note the loss of structural characteristics of the surface of the Soxhlet-extracted specimen. The secretory gland is much reduced in size with the appearance of a deflated balloon as a result of the permeation and diffusion processes through its walls. Cavities created by the localised explosion of secretory glands characterise the MAP-treated sample (figure adapted from reference [6]).

This interpretation was further supported by the gas chromatography analysis of the extracts obtained by the various methods. In fact, the MAP-obtained extracts were superior in terms of yield. Furthermore, the relative selectivity of the MAP treatment was also evidenced by the gas chromatography analysis as these extracts contained almost no chlorophyll and less pulegone than the extract obtained by Soxhlet extraction for example.

The level of sophistication that can be implemented in applications of the process can be inferred by the degree of non-homogeneity that characterises the matrix. In the case of plant materials, it is possible to selectively rupture some systems over others (*e.g.*, glandular over vascular), provided that their respective ability to withstand internal pressure is sufficiently different to allow increasing levels of energy to be imparted to the materials by sequential irradiation. Thus, given this non-uniformity factor, it is theoretically possible to develop multiple extraction schemes that will effect the selective extraction of the contents of given systems. This laboratory has reported similar applications in its patents, such as the selective removal of undesirable "high notes" in *Thuja occidentalis* extracts [1-3] and the selective fractionation of fatty acids from micro-algae [7].

It is important to note that MAP is the only extraction process known to date that effects a direct migration of the desired components out of the matrix. This is the result of the selective application of energy right into the matrix. Each and every other extraction processes make use of a common action mechanism, namely the random transfer of energy to the container, the void spaces and, most importantly, to the surrounding extractant as well as to the matrix. The extractant, then, diffuses into the matrix and extracts the various constituents by solubilising them (*e.g.*, Soxhlet) or by entraining them (*e.g.*, steam distillation) out of the matrix. This sequence of phenomena, namely heat generation - permeation into - solubilisation or entrainment - permeation out, accounts for the fundamental importance of diffusivity and extraction time as parameters for all extraction processes. Furthermore, the very basic nature of such processes prevents to a large extent speciation, or selective extraction, from taking place because energy deposition and permeation are effected in a random fashion. In fact, limited selectivity can usually be obtained solely by varying the nature of the solvent - or solvents - used or the solvent contact time. The former is governed by the need for high solvent affinities with the substrate, while the latter implies reduced yields, two factors difficult to overcome. MAP, being less dependent upon high solvent affinity because of the free migration of the components toward the solvent, often affords a wider range of solvents that can be used readily.

From the above discussion, it is clear that MAP extraction can be performed under pressure, using appropriate containers. In fact, the claims associated with the patents rights to MAP cover this approach [1-3]. However, given the relative insensitivity of MAP to the diffusivity of solvents - or to diffusion

processes associated with analytes for that matter - it is generally not necessary to operate under high pressure conditions as it is relatively easy to design extraction protocols that provide appropriate cooling, when required. A point in case lies with samples where the matrix generates and transfers so much heat to the surrounding medium that the bulk temperature of the medium reaches the boiling point of the solvent. In these cases, it is possible to operate at ambient pressure by incorporating into the experimental set-up cooling features such as water-cooled condensers (outside of the microwave cavity!) or by adjoining dry ice jackets around the extraction flask. In fact, dry ice is transparent to microwaves, relative to most matrices and solvents used in organic extraction, hence it does not affect to any significant extent the overall load effectively felt by the microwave applicator. Techniques such as these offer the advantage of being able to further process the extract immediately after the completion of the work instead of requiring the depressurisation and cooling steps inherent to extractions performed under pressure. This is not to say that no application can benefit from high-pressure capability, it is simply not the most desirable operating conditions.

10.3.1.1 Liquefied gas extraction

Another area where MAP offers improved sample preparation methods for food analysis is in the use of liquefied gases as solvents. In fact, and as noted earlier, although the MAP concept was originally introduced as a liquid-phase extraction, it applies equally well to extraction in any type of fluid, liquid, liquefied gas, gas *per se*, or supercritical fluid. Work aiming at the hyphenation of MAP and liquefied gas extraction and supercritical fluid extraction (SFE - see Chapter 11) has already been undertaken in our laboratory. Conventional SFE is currently the subject of a relatively high level of development activity. Yet, it suffers from inherent technological drawbacks such as the requirements for relatively high pressures and temperatures, not to mention the relatively high costs associated with equipment meeting these requirements. The latter are resulting from the fact that the solubility of a given chemical species varies with its density, hence the temperature and the pressure at which the supercritical fluid is being used. Carbon dioxide *per se* is considered a desirable solvent in many extraction applications as it is relatively non-toxic and is easily separated and removed from the extract. Liquid carbon dioxide offers good solubility parameters but suffers from a poor diffusivity coefficient. The latter characteristics makes the use of liquid carbon dioxide as a solvent in current extraction processes virtually impossible within reasonable extraction time boundaries. However, as discussed above, diffusivity being a parameter of minor importance in MAP, it is possible to use liquid carbon dioxide when using MAP, instead of supercritical fluid carbon dioxide. This offers the advantage of eliminating, for some applications, the high pressure and temperature requirements for SFE operation, hence reducing significantly the costs associated with such work.

Other liquefied gases offering still better economic advantages while retaining highly desirable attributes such as low pressure and temperature, and relative ease of removal are under scrutiny. Liquefied propane shows high promise at this time. It is expected that commercial equipment designed to operate under such conditions will be made available soon after the first printing of this book.

10.3.2 Gas-Phase Extraction

As stated earlier, the principles behind all of the MAP extractions are fundamentally similar, that is, the use of microwaves to selectively apply energy to a matrix rather than to the environment surrounding it. Gas-phase extraction using MAP is based upon the fact that most gases absorb microwaves to a lesser extent than do liquid or solid materials [4-6, 14, 15]. Consequently, the microwave energy is imparted selectively to the sample because it possesses a larger dielectric constant than the surrounding gaseous medium. Sample preparation applications for volatile compounds (*e.g.,* flavours and aromas) analysis in the food science laboratory make extensive use of so-called static headspace analysis and, to a lesser extent, dynamic headspace sampling that is usually associated with some form of trapping (*e.g.,* purge and trap) or focusing techniques (*e.g.,* cryogenic focusing). The range of sample types is also very broad, and includes water, water-based solutions, gels, creams, sorbents, or other types of liquid or solid matrices.

To depict the phenomena occurring, we will use, as an example, a situation similar to that encountered a few years ago by a world leader in "mineral" water bottler. The sample consists of water as the matrix, benzene as the analyte of interest, and a gaseous headspace, air for the purpose of this example although other applications can be carried out under basically any gaseous atmosphere. The sample is contained in a closed vial that, preferably, should be made up of a microwave-transparent material. The current 20-mL septum-capped vials used in typical headspace analysis (mostly made up of borosilicates) are acceptable as they absorb microwaves only to a limited extent. When the microwaves are applied to the sample they reach freely the water matrix, because air is a poor absorber of microwaves. This results in a selective heating of the liquid phase rather than the gas phase in the container. Even within the liquid phase of the sample there is a difference in the rate at which the water matrix and the analyte, benzene which has a smaller dielectric constant, absorb microwave energy. However, water molecules can transfer some of their thermal energy to the benzene molecules that are in proximity and, in effect, contribute significantly to the enhanced volatilisation of the benzene. The volatilised benzene reaches the headspace of the container and can be sampled and analysed using conventional gas transfer apparatus and determined using an adequate analytical device such as a gas chromatograph for example. This specific set-up relates to conventional static headspace sampling and, as such, the handling of the resulting data can be performed as per conventional headspace analysis.

We reported on the use of MAP gas-phase extraction to monitor a broader range of contaminants in water [15]. Invariably, significant enhancement in response of the resulting headspace analysis was observed. By working within the pressure limit of commercially available headspace vials- which is far from being optimal - experimental conditions were established that allowed a relatively simple implementation of this novel method. In summary, the method consisted in a sequential application of two distinct 40-second periods of microwave energy that were separated by a 30-second quiescent period. The transfer of the headspace so-generated was performed by operating a conventional headspace sampler (HP19395A) under "passive" conditions, *i.e.*, with no incubation period. The set of model compounds used included aromatic hydrocarbons and normal alkanes. Enhancements in response for aromatic hydrocarbons by a factor of 5 and between 2 to 6 for alkanes were obtained. The precision of the method was comparable to automated headspace methods. For example, in the specific case of benzene present at a concentration of 58.5 ng/mL, and assuming a response factor of 1.0 for conventional headspace sampling, the equivalent MAP gas-phase extraction experiments yielded a response factor of 4.6!

Larger molecules, such as low molecular weight polycyclic aromatic hydrocarbons (PAHs - *e.g.*, naphthalene and the methylated analogues, which are normally not sampled by headspace techniques because of the low response that characterise them when subjected to conventional headspace sampling were also studied in the same report. The enhancement in response was even more significant, nominally by a factor of 20-30 more than headspace. The quantitation limit for these compounds in water was established to be at 1 ng/mL (ppb) level under such operating conditions. No attempt was made to further increase the level of enhancement because no commercial instrumentation was available and any further work must be governed by safety considerations associated with the pressure limit of currently available commercial headspace vials and sealing caps. When commercial laboratory equipment capable of safely generating higher pressures is made available, still much higher sensitivity will be achieved, thus making microwave-assisted headspace analysis similar to purge-and-trap analysis in terms of sensitivity while offering much faster turnaround times and lower operating costs.

Another configuration of MAP gas-phase extraction relates to dynamic headspace sampling, often referred to as purge and trap sampling. The container can be fitted with an aperture enclosing a trap, or a sorbent, cooled by some common means. This allows the application of a prolonged, low-power irradiation, or of a multi-pulse irradiation of the sample, thus providing a means to extract all of the volatile analytes from the matrix. The contents of the trap can then be transferred (by elution for a chemical or sorbent trap, or by thermal desorption for a cold trap) to an analytical instrument, such as a

chromatographic apparatus for example, for subsequent analysis. We reported, earlier, on such a method applied to the monitoring of volatiles from lemon [16].

The advantages of the process are evident. Again, however, MAP is deceptively simple. In fact, although the foregoing description is simple to understand and seemingly easy to implement, the phenomena involved are complex and interconnected. This makes a large number of experimental parameters available to the user. For example, as the amount of energy being applied increases, so does the temperature of the matrix. In the example described above involving the closed container, if enough energy is applied, the temperature of the liquid phase will eventually reach the boiling point of the benzene, at which point volatilisation of benzene will be greatly favoured over that of water. It must be borne in mind that volatilisation of a substance is dependent upon its partial vapour pressure and its heat of vaporisation, whereas its ability to absorb thermal energy is dependent upon its heat capacity. All three factors favour the volatilisation of benzene (see Table 1), hence under thermal considerations only, benzene volatilises more readily than water at a given temperature and pressure.

In MAP however, there is another important factor to take into account, namely the capacity to convert the microwave energy into thermal energy. This physical parameter is the loss factor. The loss factor of water is much larger than that of benzene, thus water is able to release its energy to benzene at a much greater rate than benzene can do the reverse (actually, benzene having a low dielectric constant, it basically does not absorb energy). Hence for a given rate or quantity of microwave energy applied, the vaporisation of benzene will be greatly favoured over that of water. The optimal quantity of microwave energy is dependent upon the analyte. In general, however, it lies between the amount of energy necessary to bring the matrix to a temperature that exceeds its boiling point at the operating pressure, and the energy required to volatilise the matrix, a condition known as the superheating effect. The latter phenomenon is seen as the key factor in obtaining increased levels of sensitivity.

TABLE 1
Selected Physical Characteristics of Benzene and Water

Substance	b.pt. (°C)	Cp(l) @ 25°C (J/g °C)	ΔH_{vap} ($J.g^{-1}$) @ 25°C	ΔH_{vap} ($J.g^{-1}$) @ b. pt.	Vapour Pressure (KPa) @ 25°C	Vapour Pressure (KPa) @ 100°C	Dielectric constant @ 20°C
Benzene	80.1	1.57	393.2	433.1	12.7	180	2.284
Water	100.0	4.18	2441	2256	3.54	90.5	80.2

* Taken from CRC Handbook of Chemistry and Physics, 75th Edition (1995).

It must be noted that the number of molecules vaporising into the gas phase increases with the temperature, thus giving rise to an increase in pressure inside the vial. This is another operating phenomenon that can be controlled in a unique fashion when using MAP and that no other technology known to date can match. The dielectric constant of water varies with temperature and drops off dramatically when it passes from the liquid phase to the gas phase (*ca.* 80 at 20°C to *ca.* 55 at 100°C in liquid phase and to *ca.* 1 at 373°C in gas phase). Hence, here again MAP actually effects a selective heating of the liquid phase relative to the gas phase above it. This characteristic property allows the user to favour the vaporisation process and to create reproducible non-equilibrium conditions where the respective concentrations of substances found in the gas phase are closer to those originally present in the liquid phase.

There are limitations to this advantage, however, such as:

- the extent at which the so-created pressure can be handled safely by the extraction containers;

- the very short periods of time involved for the diffusion of the gaseous molecules out of the liquid phase and for the subsequent - or simultaneous - removal and sampling of the resulting non-equilibrium headspace;

- the need for accurate energy deposition for reproducible results.

Each and all of these limitations, however, is well within the scope of today's technological advancements and they can be easily overcome. For example, the incorporation of a proper trap system - as described earlier [4, 5, 16] - can alleviate all three factors at once. Another approach aims at optimising the concentrations of the analytes obtained in the gas phase with the closed container approach and at effecting a more selective transfer of the gaseous materials. For example, we have described earlier a novel device that allows the instantaneous transfer of all the gases generated during the irradiation period [4-6]. It is based upon the use of a specially-designed container that encloses a retractable hydrophobic semi-permeable membrane. The membrane provides for selective (thus higher!) recoveries while minimising the interferences brought about by the water vapours. The implementation of such a device provides a technology that can be used for applications requiring high sensitivity without involving any intermediate trapping steps.

Finally, it must be emphasised that, as for liquid-phase extraction, it is possible to enhance thermal energy transfers, if desired, by simply impregnating matrices that are not good microwave absorbers, or by dispersing within them, some strongly microwave-absorbing species. The selection of such a substance will be made according to the level of microwave absorption and heat dissipation exhibited by that substance. Furthermore, the added substance

must not interfere with the subsequent analytical scheme used. The first such examples were conducted in our laboratories and dealt with MAP gas-phase extraction of water where an ionic species was added prior to irradiation and with volatile compounds determination in dried spices where water (or an aqueous saline solution) was added prior to microwave irradiation. Again, by no means do these results correspond to the best achievable since no real optimisation was attempted as we are still awaiting commercial instrumentation.

10.4 EXAMPLES OF APPLICATIONS OF MAP IN FOOD SCIENCE

10.4.1 Extraction of Fat in Meat, Dairy, and Egg Products

A wide range of methods for the estimation of the fat content of foods has been developed and modified over the years. These methods are primarily based on the extraction of fats in non-polar organic solvents such as petroleum ether, diethyl ether, chloroform and dichloromethane. Meat, meat products, dairy products, and egg products are all of prime importance to the food analyst.

The current methods used for the determination of fat in meat and meat products include tedious Soxhlet and Soxtec extractions (AOAC method 991.36) - which suffer from being time, energy and solvent consuming techniques - and an automated method that uses microwaves to dry the sample before extracting the dried sample with solvent while agitating it mechanically [17, 18]. All these methods have in common the requirement that the sample must be dry because efficient permeation of the solvent is hindered by residual moisture, hence decreasing the ability to dissolve the fat.

Dairy products represent a different challenge as the extraction of fat is characterised by the formation of fat-protein emulsion and, in the case of cheese samples for example, is plagued by severe interference from casein. Conventional chemistry would prescribe the concurrent use of heat and aqueous alkali solutions (*e.g.*, KOH or NH_4OH) to dissolve the protein and to free the fat which can then be separated, collected, washed and dried. Not surprisingly current AOAC methods are based upon such principles. Generally, the samples are heated in presence of alkali solution in solvents such as diethyl ether and petroleum ether. Ethanol is also used to minimise the formation of emulsion, to further assist in breaking up fat-protein interactions, and to precipitate the proteins.

Finally, egg products present a similar problem with respect to the difficulty in achieving a complete dissolution of the sample. Here, an overall treatment

protocol similar to that of dairy products can be used but substituting the alkali treatment by an aqueous acidic solution (*e.g.*, HCl) one.

We have reported on atmospheric pressure MAP methods, using focused microwave irradiation for the extraction of fat from meat, dairy and egg products [19, 20]. These methods are characterised by efficiency, ease of use, and speed, in addition to offer significant economic and environmental advantages (*e.g.*, disposal of solvents). In these methods, we adhered to "conventional" chemistry principles applied in current methods but simply substituted the usual "heating and extraction" steps by a microwave treatment one while the materials are immersed into solvents that are transparent to microwaves relative to the sample in order to impart most, if not all, of the microwave energy to the sample.

The protocol used is summarised below and the readers can refer to the methods published earlier for the complete and detailed experimental section [19, 20].

10.4.1.1 Meat samples

The meat products are treated in a commercial food processor until a homogeneous paste is obtained. Accurately weighed homogenised meat samples are placed onto a filter paper that is then folded to contain all the meat sample and placed in a quartz extraction vessel. An open-vessel focused microwave-assisted extraction system is used (in the original work, a Soxwave 100, Prolabo, was used). Petroleum ether (boiling point range of 60-80°C) - or hexane - is then added. The vessel is inserted inside the extraction cavity and fitted with a condenser. The irradiation is carried out at full power (300 W - sequence of 60s ON - 30s OFF - 90s ON). The temperature of the extractant is monitored using an appropriate temperature probe (*e.g.*, Megal 500, Prolabo). Upon the completion of the irradiation, all the glassware is washed with acetone and the washings collected in the extraction vessel. The extract is then filtered under vacuum. The residue left over in the extraction vessel is washed with petroleum ether - or hexane - and the washings are filtered and added to the extract. The combined extracts are evaporated *in vacuo*. Upon completion of the evaporation, the flask is heated to dry for 30 minutes. The flask is then cooled and weighed. The fat content in the sample is determined by weight difference.

In the original work, triplicate determinations of the fat content of each sample were performed and the standard deviations (SD) were calculated. The empirical values obtained by MAP proved to be statistically equivalent to values obtained by the official agency that provided the meat standards. The method used to "certify" the samples were AOAC methods 24.005 and 7.056 (13th edition, 1980) which are based upon a four-hour extraction of the dried sample with petroleum ether using a Goldfisch or a Soxhlet extractor.

10.4.1.2 Dairy products (cheese and milk powder)

Samples of milk powder are weighed accurately. Samples of cheese are cut into pea size pieces and weighed accurately. Each sample is deposited individually in a quartz extraction vessel of the microwave-assisted extraction system (original work carried out using a Soxwave 100, Prolabo). An aliquot of diluted aqueous ammonium hydroxide is added and the resulting mixture is mixed on a vortex for a few seconds. The vessel is then inserted inside the extraction cavity of the extractor, fitted with a condenser, and irradiated for one minute at 60 watts (corresponding to 20% of the power for the instrument used originally). The sample is cooled and ethanol is added. The resulting mixture is mixed on a vortex for a few seconds and subsequently extracted with ethyl ether first, then with petroleum ether. This extraction step is repeated twice. The organic phase is separated and the two extracts are combined and concentrated *in vacuo*. The flask is heated gently to dry for 30 minutes, then cooled and weighed. The fat content of the samples is determined by differences in weight.

As for the meat samples described previously, in the original work, triplicate determinations of the fat content of each sample were performed and the standard deviations (SD) were calculated. Again, the empirical values obtained by this novel MAP method proved to be statistically equivalent to values obtained by Agriculture and Agri-Food Canada (Canada's official agency for food safety and quality) [21] which is using a method that is closely related to other widely used procedures [22, 23].

10.4.1.3 Egg products

Samples of egg powder are weighed and placed in a quartz extraction vessel used in the microwave-assisted extraction system (original work carried out with a Soxwave 100, Prolabo). An aliquot of diluted HCl (50%) is added and the resulting mixture is mixed on a vortex for few seconds. The vessel was then inserted inside the extraction cavity, fitted with a condenser, and irradiated for 4 minutes at 30 watts (10 % power for the equipment used originally). The mixture is cooled and an aliquot of ethanol is added prior to mixing it on the vortex again for a few seconds. The mixture is then extracted sequentially with ethyl ether and petroleum ether, the latter extraction being performed by means of mixing for a few seconds on the vortex. The latter step is repeated a second time. The organic phase is separated and the two extracts are combined and concentrated *in vacuo*. The mixture is further heated to dry for 30 minutes, subsequently cooled and weighed. The fat content is determined by differences in weight.

Again, as for the meat and dairy products cases, the original work reported triplicate determinations of the fat content and corresponding standard deviations (SD) for each sample. Once again, the empirical values obtained

by this novel MAP method proved to be statistically equivalent to values obtained when using a modified Rose-Gottlieb or Mojonnier procedure [24-26].

10.4.1.4 Validation of these methods

The validation of the microwave-assisted extraction technique was performed by comparing the values obtained to that of the standard samples and by performing conventional prescribed official methods associated with each products under study. Table 2 presents a summary of data presented in references [19] and [20]. The results demonstrate that, in all cases, the microwave-assisted extraction procedures yielded data that were, for all practical purposes, similar to the accreditation values of fat content obtained for the same samples using conventional official methods. These results support the current trend whereby several microwave-assisted extraction methods are being evaluated for accreditation purposes. This trend is not exclusive to food analysis [27].

TABLE 2
Fat content (%) of various food products obtained by MAP compared to other conventional methods of determining fat

Sample	Solvent	Fat content by MAP™ (%)	RSD[a] (%)	Target fat content (%)
Kam lunch meat	Pet. ether	15.6 ± 0.1	0.52	16.3 ± 0.4[b]
Picnic Ham	Pet. ether	7.5 ± 0.3	4.35	7.5 ± 0.2[b]
Salami	Pet. ether	22.0 ± 0.4	1.83	23.0 ± 1.6[b]
Chicken wieners	Pet. ether	12.9 ± 0.6	4.9	14.0 ± 1.6[b]
Sausages	Pet. ether	30.46 ± 0.15	0.51	30.35[c]
	Hexane	31.06 ± 0.06	0.20	30.35[c]
Bacon	Pet. Ether	54.23 ± 0.28	0.51	49.00[d]
	Hexane	54.51 ± 0.82	1.52	49.00[d]
Cheddar Cheese	Pet. ether	35.361	0.822	33[c]
Milk Powder	Pet. ether	25.359	2.772	26.765[b]
Egg Powder	Pet. ether	47.007	2.429	45.45[d]

Notes: a) % RSD = % Relative standard deviation = standard deviation / mean (triplicate) x 100; b) Fat content (%) as obtained from Agriculture and Agri-Food Canada (corresponds to the accreditation values); c) Labelled value; and d) Value obtained by conventional method.

10.4.1.5 Further observations on these methods

Whenever possible, users should select solvents for their ability to dissolve the target compound and for their relative transparency to the microwaves. This will result in the most energy-efficient applications possible, while maintaining relatively mild conditions, thus minimising the possibility of

thermal degradation resulting from heat dissipation. It is worth noting that the performance of MAP protocols such as those presented in these example should help the readers to better "visualise" the true power and characteristics of MAP. The moisture content of the material to be extracted is a critical factor related with MAP™ efficiency. In fact, irradiation times vary with the residual moisture content of the sample since water is very efficient at absorbing microwave radiation (water molecules behave as a dipole and bind strongly to surfaces by a number of non-covalent forces [28]). The moisture content inside the tissues creates localised superheating, therefore causing a rapid expulsion of fat from fat cells. In turn, the microwave energy generates a sudden temperature increase in the biological material (differential heating between the biological material and the non-aqueous extractant) which causes a disruption of the microstructure and thereby migration of the fat into the extractant whose temperature is below the temperature at which the fat is extracted from the biological material.

For example, in the examples provided here, the temperature of the extractant at the end of the irradiation was measured to be *ca.* 60°C, slightly below the boiling points of the solvents used while the temperature was of the order of 20 to 25°C before irradiation. This temperature differential, clearly demonstrate that the localised heating of the water contained in the samples caused the migration of the water outbound, toward the surrounding, relatively cold, extractant medium thus increasing the bulk temperature of the "mixture". The excellent recoveries obtained using this approach also support the fact that the solubility is not the predominant factor and that the process of disrupting the physical micro-structure of the sample is efficient enough to allow for the complete release of the fat. The use of appropriate peripheral equipment, such as a condenser, ensures that no solvent losses occur during the irradiation.

10.4.1.6 Microwave-assisted extraction - advantages

Finally, the protocols described here are representative of the characteristics of MAP methods in general. They are rugged, as evidenced by the small variations in procedures required to obtain excellent recoveries and precision from a wide range of products (in the examples described herein, meat, meat products, fresh milk products, dry milk products, and egg products). Furthermore, the fact that the method requires smaller volumes of solvents is another advantage of potential significance in the current trend of minimising operating costs while attempting to "green" the laboratory operations. For example, in the specific methods described above, the substitution of hexane for petroleum ether, brought about a more desirable solvent (less hazardous and better solubility characteristics for fat) in addition to require a much reduced volume. Overall, these methods also represent significant reduction in energy consumption.

In general, the use of the open-vessel focused methods described above leads to the successful atmospheric pressure extraction (minimising risks) of fat from a variety of sources, without incurring any solvent loss. The extraction time is shortened considerably while maintaining excellent precision and reproducibility, and respecting or exceeding all the specifications of conventional Soxhlet extraction. The integrity of all the extracted molecules is maintained. Temperature control is also possible during the extraction using appropriate commercially available instrumentation. The advantages associated with these applications of the MAP™ technology can be summarised as follows:

i) large tolerance to sample size (from sub-gram to multiple-gram possible);

ii) low consumption of solvent, therefore reduced solvent costs and reduced waste management costs compared to conventional Soxhlet and automated Soxhlet methods [17, 18];

iii) reduced processing time and reduced energy consumption: total extraction can be completed in a few minutes compared to several hours with conventional Soxhlet and automated Soxhlet [17, 18];

iv) no drying of the sample is necessary as it is for current methods; and

v) limited pre-processing is required (*e.g.* only homogenisation - which in some cases proved to be critical as per other conventional methods) while the conventional methods [18] are often associated with the need to spread the sample (*e.g.*, using sand).

10.4.1.7 Novelty of the approach

The examples described in this section 10.6.1 constituted the first report ever of *in situ* reaction-extraction work involving foodstuffs. We had reported earlier on a related approach in a different field, namely a derivatisation-extraction procedure whereby phenols and methylated phenols were acetylated-extracted from environmental matrices in a one-step MAP procedure (15). The latter procedure, however, was performed under much harsher conditions that could not be used with foodstuffs where the potential of creating artefacts is a prime concern. This approach of one-pot, multiple-step procedures opens the avenue to numerous applications of direct interest to the food analysts and are especially versatile and valuable when using microwave-assisted extraction performed in open-vessel systems. This, along with solvent-less extraction (such as MAP gas-phase applications!) is believed

by some - including these authors - to be the route of the future in terms of extraction technology.

10.4.2 Paprika Extracts by MAP

Paprika (*Capsicum annuum* Linné, or *Capsicum longum* D.C.) belongs to the Solanaceae family. It is a spice highly praised by the food industry that uses it for its colouring properties as well as for its characteristic "hot" taste. Various carotenoids-type pigments such as capsanthin, zeaxanthin, and β-cryptoxanthin account for the rich purplish red hues that range from deep purple to orange-yellow and that are found in paprika extracts. Several genetic engineering projects have been carried out with the purpose to create clones that would be characterised by improved organoleptic properties and would offer extended fruit shelf-life. Two reviews provide extensive background on *Capsicum* [29, 30].

We reported earlier [31] on the extraction of paprika by MAP and by conventional processes. We summarise here these findings as they represent a good example of the potential benefits to be derived from the use of MAP.

The official ASTA method 20.1 provides the methodology used to extract paprika and to determine the colour characteristics of the resulting extract. The extracts are evaluated for their colour and the term "international unit of colour", uic, is used to set a basic scale to which we refer to assess the colouring power of the extract. For the purpose of our experiment we purchased a commercially available standard paprika extract and arranged to procure a crude, dried sample of paprika (from Morocco) along with a commercial sample of the extract obtained from this same material (*i.e.* the same lot of plant material that was used to produce the commercial extract was sent to us along with the extract sample).

We performed a very basic MAP extraction procedure, namely subjecting 30 g of paprika to microwaves at 625 watts for 30 seconds while immersed in 200 mL of hexane. The resulting solution was filtered over anhydrous sodium sulphate, rinsed with two aliquots of 30 mL of hexane. All filtrates were combined and the solvent was removed *in vacuo*. The resulting sample, labelled "MAP" throughout the text below, was used in subsequent analytical work and compared to the commercial standard which was rated as 100,000 uic (labelled as "standard"), the commercial product provided by the manufacturer (labelled "commercial"), and to an extract made in our laboratory the same day we performed the MAP extraction experiment using the same material and applying the ASTA method 20.1 (labelled ASTA).

The basic colour determination results were astounding. In fact, while the standard was characterised by colour properties of 108,684 uic which were in close agreement with the value found on the label of this product, significant

differences were found between the other three extracts which were prepared from the same plant material. The commercial extract exhibited 30,595 uic while the MAP extract exhibited a remarkably high value of 140,740 uic. More surprising was the fact that the ASTA extract exhibited only 7,640 uic! Hence compared to this conventional ASTA extract, MAP produced an extract which was characterised by a colouring power of over 2000% superior. Figure 2 presents, in black and white, a thin layer chromatography plate that illustrates very well (despite the loss in resolution resulting from the digitalisation procedure) this colour comparison between the standard and the MAP extract.

The difference obtained from our performance of ASTA 20.1 and that exhibited by the commercial sample can come from at least two sources, namely that we did not perform the ASTA 20.1 up to expectations, and that the product, as received, was deteriorated since, as we stated earlier, paprika does not age, nor travel well.

Clearly, before reporting such remarkable data, we repeated the experiments and proceeded to a further comparison of the standard, commercial, and MAP extracts to determine whether other characteristics of the extracts differed significantly. Hence a series of sensory analytical experiments were carried out to determine the appearance, the viscosity, and the aroma of the extracts. In summary, the standard was a viscous liquid characterised by capsicum and mouldy aromas while exhibiting a deep orange-brown colour; the MAP extract was less viscous, possessed the same aromas and exhibited a red hue brown colour; the commercial extract was slightly viscous, possesses similar aromas

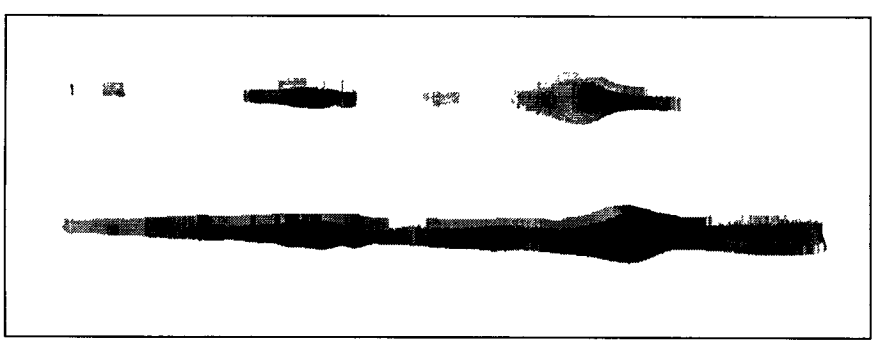

Figure 2: Thin layer chromatography plate (K6F - Whatman) traces of the standard extract labelled at 100,000 uic (top) and the MAP extract (bottom). The plate was eluted in a hexane:propanol mixture (92:8) and did not require any developing agent given the deep coloration of the extracts. For the purpose of reproduction we have digitised the plate at 16,000,000 colours and converted the digital file into a 256-tone gray-scale one. Note that despite this dramatic graphical loss in resolution the differences between the two products are readily observed.

but exhibited only a brownish orange colour. This combination of reduced viscosity and enhanced hue of red clearly made the MAP extract even more interesting.

Further analytical work was carried out aimed at the physical characteristics of the extracts. Salt plates were prepared as follows: 0.5% extract, 1.5% Polysorbate-80, and 98% sodium chloride. Here the standard extract exhibited a light brownish orange colour and a fine granular oily aspect. The MAP extract exhibited a deeper hue of the same colour and similar oily aspect. The commercial product, in turn, was very light orange but exhibited the same fine granular oily aspect.

These same products as per above were further diluted as a 2% solution in 98% of water and the colour characteristics were recorded. The standard was medium orange with yellow hues presenting a clear solution without insoluble particles. The MAP extract was a lighter orange with similar yellow hues and also exhibited the same clear solution without insoluble particles. The commercial extract yielded a clear solution, without insoluble particles, that was yellow with a very faint hue of orange.

For a more direct comparison, the extracts were diluted to a similar level of colour power, namely of 609 to 619 uic, using a salad-quality vegetal oil. The resulting mixtures were then applied onto salt plates as follows: 2% diluted extract (*i.e.* 0.56% standard + 1.44% oil for standard; 0.44% MAP extract + 1,56% oil for MAP); as is for the commercial extract), 2% Polysorbate-80, and 96% sodium chloride. Under these conditions the standard exhibited a brownish orange colour with fine oily granules, the MAP extract exhibited more intense orange hues with similar oily granules, while the commercial extract, used as is, was for all practical purposes similar to the diluted MAP extract.

Furthermore, these same plates were then left to stand in open air and daylight for a period of three days to evaluate their relative stability. At the end of that period, the standard extract exhibited only 20% residual colour power, the MAP extract 35%, and the commercial extract only 5-10%. These data suggest a better stability of the MAP extract. This characteristic, along with the higher colour power could be the result of a cleaner extract. In fact, the presence of fatty acids, for example, tends to mask the colour while accelerating the degradation rate of the extract. Thus one could assume that if MAP produces extract with a lower contents in fatty acids, then it would follow that the viscosity of the extract would be different (which was the case), the colour power would appear higher, although the concentration of the components responsible for the colour may well be similar to that found in other extracts where there are less fatty acids to mask the colour, and these extracts would "age" relatively better as a result of the reduction in the oxidation level in fatty acids. Although this hypothesis is sound, it remains to be proven. In fact, work is still underway and only once the extract will be characterised more fully, by

separating, isolating, and determining the structure of various components of the extract (*i.e.* making use of the techniques discussed in this book!) will we be able to confirm its accuracy.

As a final set of data, the relative solubility of the extracts in oil and in water was evaluated. In oil, the standard extract is soluble; a droplet deposited at the oil surface spreads in part and the rest precipitates at the bottom of the container, the extract is easily dispersed by gentle agitation. The MAP extract and the commercial extract exhibited similar solubility characteristics in oil. They were soluble; the droplet disperses rapidly at the oil surface, it floats at the surface of the oil but is easily dispersed with moderate to rapid agitation. In water, the standard extract was insoluble; it readily dispersed at the water surface with the droplet at the centre with fine particulates spreading along the sides of the container, upon agitation the droplet converts into insoluble oleoresin aggregates at the surface of the water. The MAP and the commercial extracts, in turn, exhibited similar properties. They spread at the surface of the water as only one oil entity. Upon agitation they divided into insoluble oleoresin droplets at the surface of the water.

10.5 CONCLUSION

In all cases, MAP makes use of physical phenomena that are fundamentally different compared to those applied in current sample preparation techniques. It provides for dramatic reduction in the preparation time required per sample. The analytical methods developed to date indicate that MAP also offers, in most cases, net advantages in terms of sensitivity and selectivity, with similar, or better, linearity and reproducibility parameters. The significant reduction in sample preparation time, on a per sample basis, along with the relative ease of rapidly implementing widely varying operating parameters are attributes of choice for methods to be used during field analytical activities. More specifically, Environment Canada, along with laboratories from its American counterpart, the United States Environmental Protection Agency, and some academic laboratories have undertaken joint projects aiming at the evaluation and validation of MAP field screening methods to be used during analytical operations associated with emergency response (*e.g.* during chemical spills), or more simply during site assessment work.

In summary, MAP is a process making use of the ability that microwaves have to selectively heat some chemical species over others. The fact that most materials, whether from plant, animal, soil or man-made origins are made up of non-homogeneous structures allows for the direct heating of selected portions or areas of such materials. Most organic solvents absorb microwave energy to a lesser degree than free water and, consequently, can be used effectively in solubilising and cooling the desired components of the materials being subjected to MAP for their extraction. Moreover, MAP gas-phase extractions take advantage of selective heating of some chemical species over others and

selective heating of the liquid - or solid - phase over the gas phase for a given sample matrix. Hence MAP provides a valuable, often improved, alternative to conventional liquid- and gas-phase extractions.

10.6 REFERENCES

1. J. R. J. Paré, M. Sigouin, and J. Lapointe, *U.S. Patent* 5,002,784, March 1991 (various international counterparts).

2. J. R. J. Paré, *U. S. Patent* 5,338,557, August 1994 (various international counterparts).

3. J. R. J. Paré, *U. S. Patent* 5,458,897, October 1995 (various international counterparts).

4. J. R. J. Paré, *U.S. Patent* 5,377,426, January 1995 (various international counterparts).

5. J. R. J. Paré, *U. S. Patent* 5,519,947, May 1996 (various international counterparts).

6. J. R. J. Paré, J. M. R. Bélanger, and S. S. Stafford, *Trends Anal. Chem.* **13** (1994) 176.

7. J. R. J. Paré and J. M. R. Bélanger, "Procédé Assisté par Micro-Ondes (MAP™): Application aux micro-algues", *C.-R. XIIèmes Journées Internationales sur la Valorisation des Produits de la Mer*, Nantes, pp.19-25 (1993).

8. J. R. J. Paré and J. M. R. Bélanger, "Microwave-Assisted Process (MAP™): Applications to the Extraction of Natural Products", *Proc. 28th Microwave Power Symposium*, IMPI, pp. 62-67 (1993).

9. CEM Corp, P. O. Box 200, Matthews, NC28106, USA - Telephone No. 1-704-821-7015; Fax No. 1-704-821-5185.

10. Prolabo, 94126 Fontenay-sous-Bois, France, Tel. No. 33-1-45-14-85-00; Fax No. 33-1-45-14-86-16

11. P. Debye, *Polar Molecules*, Chemical Catalog Co., New York, 1929.

12. P. Debye, *Polar Molecules*, Dover Publications, New York, 1945.

13. J. Thuéry, in E. H. Grant (ed.), *Microwaves: Industrial, Scientific, and Medical Applications*, Artech House, London, Part I, Ch. 3, 1992.

14. J. R. J. Paré, J. M. R. Bélanger, K. Li, and S. S. Stafford, *J. Microcolumn Sep.***7, 37** (1995).

15. J. R. J. Paré, J. M. R. Bélanger, D. E. Thornton, K. Li, M. Llompart, M. Fingas, and S. A. Blenkinsopp, *Spectrosc. Int. J.* **13,** 23 (1996).

16. J. R. J. Paré, J. M. R. Bélanger, A. Bélanger, and N. Ramarathnam, *in* G. Charalambous (ed.), *Food Science and Human Nutrition*, Development in Food Science Vol. 29, Elsevier, Amsterdam, pp. 141-144, 1992.

17. S. C. James, in *Analytical Chemistry of Foods*, Chapman & Hall (Eds), London, pp. 46-51, 91-105, 1995.

18. *Official Methods of Analysis*, 16th Ed. AOAC, Arlington, VA, vol. 2, Chapter 39, sec. 985.15, 1995.

19. J. R. J. Paré, G. Matni, V. Yaylayan, J. M. R. Bélanger, K. Li, C. Rule, B. Thibert, D. Mathé, and P. Jacquault, "*Novel Approaches in the Use of the Microwave-Assisted Process (MAP™) Part I: Extraction of Fat from Meat and Meat Products Under Atmospheric Pressure Conditions*", submitted for publication.

20. J. R. J. Paré, G. Matni, V. Yaylayan, J. M. R. Bélanger, and Z. Liu, "*Novel Approaches in the Use of the Microwave-Assisted Process (MAP™) Part II: Extraction of Fat from Dairy Products Under Atmospheric Pressure Conditions*", submitted for publication.

21. Agriculture and Agri-Food Canada, *personal communications.*

22. G. H. Richardson, in *Standard Methods for the examination of Dairy Products* - 15th Edition, pp. 358-362, 1985.

23. *Official Methods of Analysis*, 16th Ed. AOAC, Arlington, VA, Method 933.05, p.63, 1995.

24. *Official Methods of Analysis*, 16th Ed. AOAC, Arlington, VA, Method 920.15, p. 63, 1995.

25. American Dry Milk Institute Inc., "*Standard for Grades of Milk including Methods of Analysis*", Bulletin 916, pp. 24-25, 1971.

26. *Official Methods of Analysis*, 16th Ed. AOAC, Arlington, VA, Methods 17.012 (b) and 17.013, 1995.

27. K. Li, J. M. R. Bélanger, M. Llompart, R. D. Turpin, R. Singhvi, and J. R. J. Paré, *Spectros. Int. J.* **13,** 1 (1996).

28. A. H. Varnam and J. P. Sutherland, in *Meat and Meat Products, Technology, Chemistry and Microbiology,* Chapman and Hall, London, Vol. 3, Food Products Series, 1995.

29. V. S. Govindarajan, *CRC Crti. Rev. Food Sci. Nutr.* **22**, 109 (1986).

30. V. S. Govindarajan, *CRC Crti. Rev. Food Sci. Nutr.* **22**, 245 (1986).

31. J. M. R. Bélanger and J. R. J. Paré, *Riv. Ital. EPPOS* **5**, 127 (1994).

J.R.J. Paré and J.M.R. Bélanger (Editors)
Instrumental Methods in Food Analysis

Chapter 11

Supercritical Fluid Extraction: Principles and Applications

Dennis R. Gere (1), Lenore G. Randall (1),
and Daniel Callahan (2)

1) Hewlett-Packard Company, Little Falls Site, 2850 Centerville Road, Wilmington, Delaware, 19808, USA; and 2) Dean Foods Company, 1126 Kilburn Avenue, Rockford, Illinois, 61101, USA.

11.1 INTRODUCTION

Analytical laboratories are under ever-increasing pressure to improve productivity while cutting costs and meeting more and more regulations. With respect to the regulatory issues, there are two recent actions that have an impact on laboratories performing food assays.

The first of these is the Montreal Treaty Protocol concerning Chemicals which may affect Ozone in the Atmosphere, an agreement to reduce the use of substances that affect the amount of ozone in the atmosphere [1-4]. This international treaty addresses the reduction of the use of halogen-containing chemicals such as chlorofluorohydrocarbons and other halocarbons. Many of these solvents are commonly used in extractions during the sample preparation part of a food assay.

The second recent regulatory issue is the Nutritional Labelling and Education Act in the United States [5]. With this legislation, food companies must provide more information on labels so they are faced with a surge of work in the short-term to do assays to provide information for new labels. Over the long-term after the initial efforts to update labels, it is anticipated that more analytical work will be necessary on an on-going basis compared to pre-NLEA laboratory workloads.

The technique of supercritical fluid extraction (SFE) can be an aid in addressing the laboratory management problems imposed by the Montreal Protocol (solvent reduction) and the NLEA (improved productivity with more detailed information) while contributing to lowered cost per analysis and maintaining/improving the quality of analytical results (precision, accuracy). Moreover, many sample preparation processes (extraction, fractionation, concentration, solvent exchange, reconstitution) can be reproducibly controlled in an automated fashion by using SFE as a core technology; such automation allows the potential gains in productivity to be realised with workforces that are increasingly less-skilled.

11.1.1 What is SFE?

In SFE, a supercritical fluid is used as the extraction solvent instead of the typical liquids encountered in the laboratory today -- *e.g.*, methylene chloride, hexane, methanol. Just as in conventional extraction, the sample to be extracted is exposed to the supercritical solvent which dissolves and removes some subset of extractables from a raw sample. Supercritical fluids have received intense interest as solvents since they are an interesting hybrid of gases and liquids: liquid-like, but adjustable densities; gas-like viscosities; and diffusivities that are intermediate between those of gases and liquids. In the following section, supercritical fluids will be more rigorously positioned relative to the gases and liquids that we normally encounter in the laboratory. However, by means of introduction, it should be pointed out that this "hybrid" nature results in the overall simplification that supercritical fluids *"dissolve like liquids and behave/handle like gases."* In an extraction process, the liquid-like density enables the fluid to dissolve components from a matrix; subsequently, the gas-like behaviour allows easy separation of the solvent fluid from the resultant extracted material and sample matrix -- often at mild thermal conditions! The thermal operation range is largely determined by the selection (identity) of the supercritical fluid: usually operation is above the critical temperature of the bulk substance. Critical temperatures of fluids like ethylene, ethane, and carbon dioxide are mild (all under 45°C); critical temperatures of ammonia, pentane, acetone, and water are much higher and require lowest operating temperatures from 132°C for ammonia to 374°C for water.

At this time the most widespread supercritical fluid solvent is carbon dioxide. This enables practitioners to operate at mild conditions (typically 40 to 150°C) with an innocuous solvent that is readily abundant at reasonable costs.

11.1.2 What Samples are Possible Candidates for SFE?

The analysis of foods and food products is a complicated technology. There is a tremendous variety in the possible samples -- analytes as well as sample matrix. As a result, the analyst is faced with selecting the most appropriate

analytical techniques and processes from a wide array of possibilities. At the same time the analyst selects the proper and expedient analytical technique, the appropriate sample preparation and/or clean-up steps must also be considered.

As a first step in designing the assay, the analyst often considers polarity. Foods and food products are made up of mixtures of components that range from non-polar species to very polar species. Examples of non-polar species include volatile flavour compounds such as limonene as well as thermally labile (thus not considered to be volatile compounds) such as the fat-soluble vitamins. Examples of polar compounds present in foods are amino acids, carbohydrates, starches, and water soluble vitamins. In general, in this chapter, we will be addressing food constituents ranging from the non-polar to moderately polar compounds. The more extreme end of polar compounds (those soluble only in water, for instance) will not be addressed in this chapter. The primary reason for this is that supercritical fluid extraction (SFE), as it is practised on an analytical scale today, uses supercritical carbon dioxide and supercritical carbon dioxide "modified" with small percentages of organic solvents. These extracting fluids tend to be non-polar to moderately polar with regard to dissolving power. The age-old adage of "like dissolves like" applies to the technology of SFE just as it does to dissolving the same analytes in typical liquids and solvents encountered in traditional sample preparation techniques.

In addition to having a wide range of analytes in food products, the food matrix is also quite complicated and varied. Food products range from liquids (oils, beverages) to solids (baked goods, meats, vegetables), and many times the food matrix is an almost undefined matrix known as semi-solids (ice cream, milk, eggs, vitamin gels). SFE is best used when dealing with solids and semi-solids. Liquids can be handled with SFE as the sample preparation technique if some simple pre-treatment is done to stabilise the sample in the extraction vessel during the time that the extraction fluid is flowing through the sample (dynamic extraction step).

11.1.3 A Unique Property of Supercritical Fluids

SFE has a good potential for selective extractions. With typical liquid solvents, the extraction solvent parameters that can be adjusted by the chemist are the chemical composition (polarity, composition of mixtures) and temperature. These parameters are adjustable with supercritical fluids as well. However, with SFE a third parameter, fluid density, can have a significant impact on the extraction process. In fact, with SFE, temperature takes on an even more important role since the fluid density is a strong function of temperature in the supercritical fluid region. The other parameter impacting density is the pressure. Supercritical fluids are highly compressible; significant pressure (tens to hundreds of bar) must be applied to them to achieve liquid-like densities. (Why this is so will be discussed in detail below.) The high degree of

compressibility leads to variable densities -- with the density directly dependent upon both temperature and pressure.

What is unique to supercritical fluids compared to typical liquids at ambient conditions is that the variable density allows the same fluid to have a variable solvent power -- *i.e.*, the degree of solubility of a particular component depends upon the density of the supercritical fluid solvent. Now the chemist has three parameters to exploit: density (pressure), temperature, and composition. With supercritical fluids it is common to exploit the variable solvent power afforded by adjusting the density first. This allows the same fluid to be used to dissolve families of components selectively just by changing a physical parameter (pressure at a given temperature). At the highest densities, the solvent power of the supercritical fluid is very nearly that of the same fluid as a liquid. At that point, it is common to exploit mixtures of typical solvents in the bulk supercritical fluid to achieve more selectivity for an additional range of solutes/analytes.

What is gained by the chemist is the capability to replace conventional sample preparation processes of extraction and fractionation (*via* column chromatography or back extractions) with the processes of step-wise extracting fractions with concurrent concentration. There are many examples of fractionation using supercritical fluids.

In a later section, we will describe examples where selective extraction has been used to advantage. In one case [6,7], lipid-free-fractions of polychlorinated biphenyls (PCBs) were extracted by SFE from sea gull eggs. An independent liquid-solvent extraction and analysis of the lipid fraction of the eggs indicated a 35 % by weight fat content, while after the selective extraction (judicious choice of density/temperature conditions at each selective fractionation step) the fat or lipid content was less than 0.1% in the PCB-containing fraction. In a similar experiment, cholesterol has been selectively extracted from cod liver oil samples (an oil-free extract from a sample which contains 99 % lipid or oil). This is shown in Figure 1. The details of this experiment will be discussed in a later section.

In another similar example [8] France *et al.* used a bed of activated alumina in the extraction vessel downstream of the sample itself to "scrub-out" (retain) the lipids while allowing lipophilic pesticides extracted from a grain sample to pass on to the collection/reconstitution device to produce a lipid-free fraction to pass on to a GC/ECD for analysis of the pesticides. This is particularly important since lipids must normally be removed from pesticide-containing extracts by long and tedious manual-column methods, evaporation and solvent exchange.

The bitter acids of hops [9] have been selectively extracted in a three-step method away from the essential oil fraction (fraction 1) and a lipid fraction (fraction 3). All of the bitter acids were contained in the middle fraction

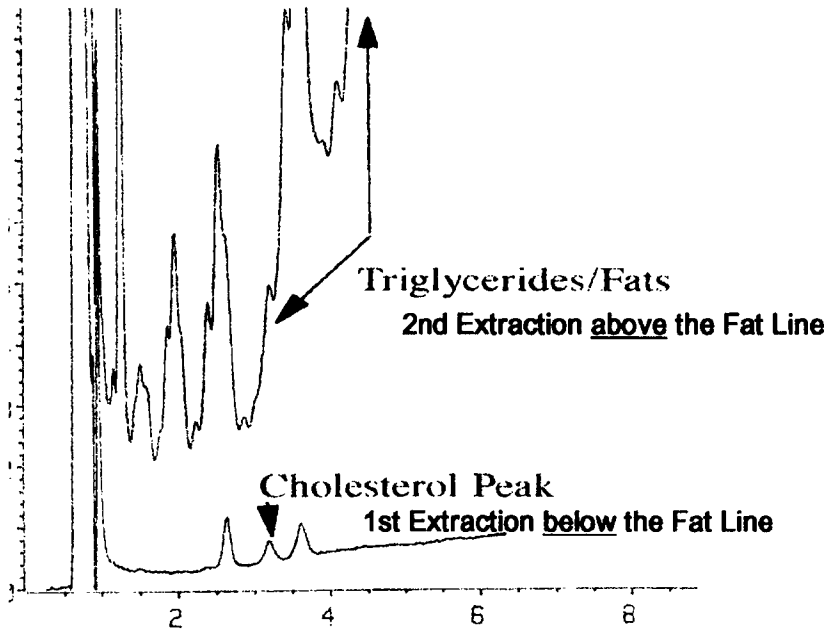

Figure 1: Selective fractionation of cholesterol from total fats in cod liver oil sample.

(fraction 2) -- free of interferences from the other two classes of compounds. Also, the other fractions were available for analysis as the need arose. This fractionation was carried out by judicious choice of temperature/ density combinations.

11.1.4 The Contribution of Supercritical Fluids to Laboratory Automation

Extreme cases of "non-selectivity" are encountered at the maximum and minimum densities. At maximum densities, the supercritical fluid has maximum solvent power so usually everything that is soluble at the various discrete lower densities is soluble at the maximum density -- *i.e.*, there is no selectivity if just the highest density is used in the extraction scheme. At that point, a different selectivity can be superimposed on the highest-density supercritical fluid by adding additional components, called modifiers, to the bulk fluid to form solvent mixtures. Typical modifiers are methanol, ethanol, methoxy ethanol, and methylene chloride. With carbon dioxide, the onset of noticeable solvent power occurs at about 0.1 g/mL; this is the point at which the carbon dioxide makes a transition from ideal-gas behaviour (PVT equations) to critical-region behaviour where the density is an even more sensitive function of pressure (compared to ideal-gas behaviour). The result is that liquid-like, but selective, solvation occurs for carbon dioxide over the density range of about 0.1

g/mL to 1 g/mL. We noted what happens at the high values of density. At densities below 0.1 g/mL (40-50 bar, 40°C), the density of the fluid does not support liquid-like solvation. If the supercritical fluid dissolves an analyte to saturation at higher densities (*e.g.*, 0.5 g/mL) and then the pressure imposed on the solution is lowered so that a lower density occurs, some or all of the analyte will precipitate out. This loss of solvent power by decreasing the density is used to good advantage in removing dissolved components from a mixture with a supercritical fluid.

In analytical-scale SFE, the usual approach has been to expand the compressed mixture to nearly ambient pressure: the supercritical fluid expands to ideal-gas conditions and the solutes precipitate in a collection region. This makes an SFE instrument conceptually quite simple. Contact a sample with a supercritical fluid at the designated temperature, density (controlled by pressure), and chemical composition to dissolve the analytes of choice; impose a flow through the sample to remove the dissolved analytes from the sample region; and expand the resultant mixture of extraction solvent plus extracted components to ambient pressure to get rid of the solvent and collect the concentrated extracts. At that point, what is left is a reconstitution step to get the extract into a solvent compatible with the target analytical instrument.

All the parameters in such an instrument are easily controlled by appropriate engineering. This is what makes SFE such an attractive technique to use for automating sample preparation. In one instrument, there can be extraction, fractionation, concentration, solvent exchange and reconstitution. Engineering technologies borrowed from both HPLC and GC facilitate the engineering of an SFE. With SFE, the user can input the sample and receive multiple fractions with no manual intervention. The hands-on labour associated with sample preparation decreases from tens-to-hundreds of steps and manipulations to less than ten. Since there is automated control of timed sequences (valving, static/dynamic contact of the fluid with the sample, injection of modifier) and the operating parameters (pressure, zone temperatures, fluid composition, and flow rates), the sample preparation methods are made far more independent of manual technique. Once a method is developed, less-skilled labour can run methods by inputting samples and receiving fractions. Exposure to harmful organic solvents is minimised.

Not only are four important sample preparation processes automated by an SFE instrument, but furthermore, with a modular design approach, the SFE instrument can become a component in an automated system. One example is the direct coupling of SFE and analytical instruments. One such system is referred to as a "bridge" configuration between the SFE and GC (or GC/MS, HPLC, SFC) [10]. In such a system the operator inputs a queue of samples to the SFE and receives the analytical report -- with no manual intervention. Operation of the SFE and the analytical instrument can be overlapped to maximise through-put. Sample tracking capabilities are strengthened. This

configuration can be expanded by adding other sample preparation instruments to facilitate automating other preparative steps that may intervene between the SFE and the analytical instrument -- *e.g.*, solvent exchange, internal standard addition, serial dilutions for calibration curve generation, solid phase extraction (SPE) for further clean-up of the extract output by the SFE, derivatisation of components within the SFE extract, and many other (currently) manual-human intervention techniques.

The capacity for lab automation that SFE brings to sample preparation is analogous to the analytical instrument automation that has been developing for the last twenty years. Such tools as automatic injectors and integrators for gas and liquid chromatographs are examples. The shift from manual technique towards instrument control helps to improve the robustness and repeatability of laboratory methods.

11.1.5 The Rest of the Chapter

In this introduction, we have presented an overview of the benefits of applying the technique of SFE to the area of food analysis. There are substantially reduced costs derived from use of SFE *versus* traditional extraction in the areas of solvent purchase costs, solvent disposal costs, reduced labour charges, and even less need to repeat experiments due to reduced human errors in the overall analytical scheme. Moreover, productivity can be improved and the use of environmentally-unfriendly solvents is greatly reduced. In the rest of this chapter we will explore the fundamental principles of SFE in more detail, discuss some of the aspects of current SFE instrumentation, present a number of examples of applying SFE to food samples, and briefly summarise some hints for methods development.

11.2 PRINCIPLES OF SUPERCRITICAL FLUIDS

11.2.1 An Overview of the Relationship of Phases: A Refresher on Phase Diagrams

Common definitions of the supercritical fluid state are varied; the technically rigorous definition is somewhat complicated since it is expressed as an equation. It is easier to gain an appreciation of the physicochemical significance of supercritical fluids through consideration of the basic physical chemistry of phase equilibria. This sort of a discussion is made somewhat easier by considering some of the more common diagrams that represent states of matter (phase diagrams). Figure 2 is a phase diagram in which pressure is plotted against temperature for the chemical "water." The actual form of the diagram roughly looks like a forked branch of a tree. For the sake of qualitative discussion, the axes are not rigorously displayed.

For the moment, the axes of Figure 2 allow a mapping of the regions of interest. There are depicted the three physical states of matter (zones from left to right): solid, liquid, and gas. A fourth zone, at the far right is called the supercritical fluid region (not a fourth state of matter). The solid lines dividing the individual zones are the boundaries between solid-liquid, solid-gas, and liquid-gas. The dotted line that sets off the supercritical fluid zone separates both liquids and gases from supercritical fluids. This suggests that a supercritical fluid is neither a gas nor a liquid, but, in fact, supercritical fluids possess some characteristics of both gases and liquids. There are also three "points" in this diagram that merit some discussion.

The first point which we will discuss is the juncture of the solid-gas line, the solid-liquid line and the liquid-gas line. This is known as the triple point, and it is the one set of invariant conditions in which solid, liquid and gaseous states can coexist in equilibrium. For the pure compound water, this point is at 0°C temperature and 0.06 bar pressure. It is also commonly known as one of the freezing-melting points of water that form the solid-liquid line; note that as more pressure is imposed on the system, only the solid and liquid phases can coexist along the solid-liquid line. Another invariant point on the diagram is the critical temperature. For water, this is at 374°C and 220 bar. A third point is commonly known as the boiling point -- the temperature at which the liquid state changes to the gas state. In this diagram a boiling point is shown at 100°C and 1.0 bar. However, there is not a single boiling point since the boiling point is a "dependent-variable"; there is a transition line dividing liquid and gas phases comprised of all boiling points for the various combinations of temperature and pressure. By contrast, the triple point and the critical point are true constants, being a unique combination of conditions for a particular coexistence of phases.

11.2.2 The Supercritical Fluid Region

Let us now focus upon the critical temperature and consider a few of the definitions that can describe this invariant point. It is important to note that the critical point is defined by the temperature only; the value of the critical pressure appears to have a lesser or secondary significance. The critical (or supercritical) fluid region exists at all pressures at or above the critical temperature for a pure substance. Above this critical temperature, there exists only one phase, completely independent of the pressure. That is, no matter how high (or how low) you cause the pressure to be, the one phase will not condense to a liquid.

The supercritical phase is a phase distinct from other fluid phases by virtue of the Gibbs energy. As noted by Moore [11], phase changes are "characterised by discontinuous changes in certain properties at some definite temperature and pressure." Gases and liquids, the fluid phases with which we are most familiar, differ from each other by the degree of condensation and order (the balance of

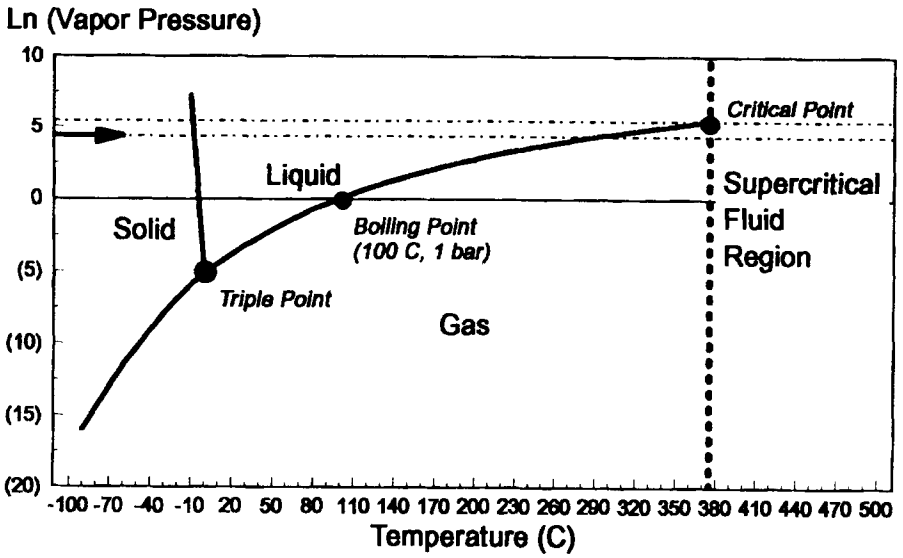

Figure 2: A schematic of a phase diagram for water showing solid, liquid and gas phases relative to the supercritical fluid region.

potential and kinetic energy content). Furthermore, depending upon the choice of temperature and pressure, there can be transitions between the two phases and, depending on the temperature, there can be transitions between the liquid and gas phases to the supercritical phase. The properties of a gas (such as low density, high compressibility, and positive temperature coefficient of viscosity) are very different from those of a liquid at temperatures well below the critical temperature (high density, low compressibility, and negative temperature coefficient of viscosity).

Next let us consider Figure 3 which is a plot of the logarithm of the vapour pressure *versus* the reciprocal of the temperature (in degrees Kelvin). If this were a straight line, the slope of the line would be the enthalpy of vaporisation, or the energy necessary to convert one mole (18 grams of water) from the liquid state to the vapour state. This is never a true straight line, but is a continuous concave curve. If one wishes to know the value of the enthalpy of vaporisation at any given temperature, one then simply converts the temperature to reciprocal temperature (1/degrees Kelvin) and measures the slope tangent to the curve at that point. For instance, at 100°C (0.00268 = 1/K) the enthalpy of vaporisation is -9.73 kcal/mole. If one continues to measure the tangent to the curve for higher temperatures (*i.e.*, smaller values of reciprocal temperature), the slope tangent to the curve becomes smaller in value (negative sign) -- simply saying that it is necessary to inject less additional heat/energy to vaporise the liquid as the temperature of the liquid increases.

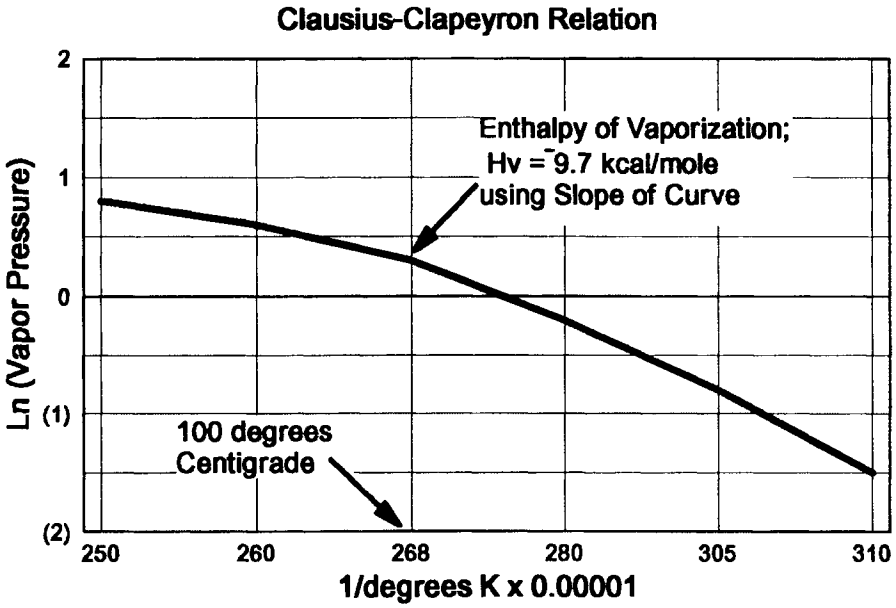

Figure 3: The vapour pressure as a reciprocal function of temperature for water. The slopes of the tangents to the curve are the enthalpies of vaporisation.

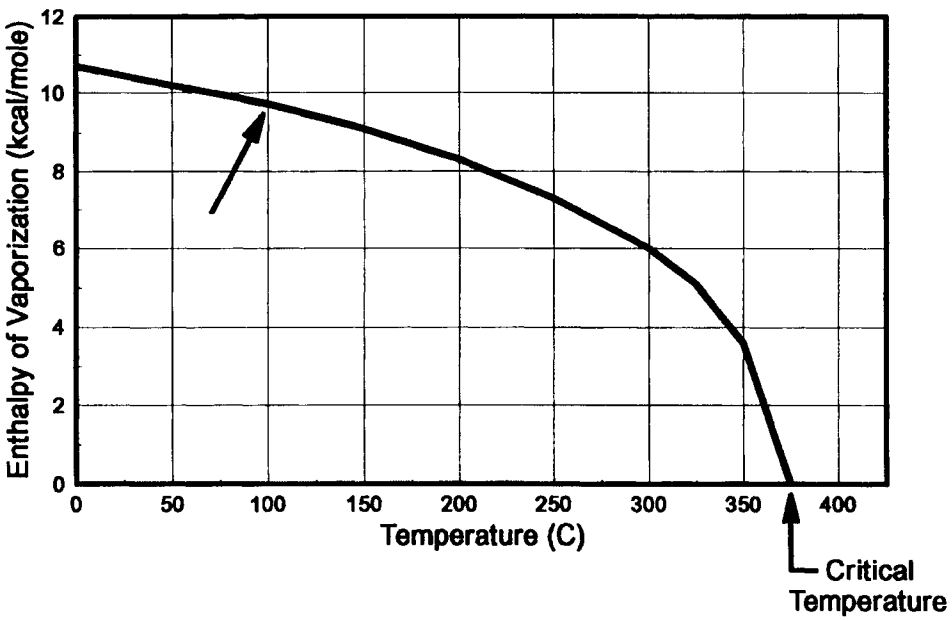

Figure 4: Determination of critical temperature from the relationship of the enthalpy of vaporisation as a function of temperature.

Figure 4 shows a plot of the enthalpy of vaporisation *versus* the temperature (C). The arrow denotes the value of the enthalpy of vaporisation at 100°C (-9.73 kcal/mole). This is an interesting curve considering that the value for the enthalpy of vaporisation decreases at an accelerated rate until it reaches a value of 0.00 kcal/mole at 374°C. This happens to be the critical temperature of water and can help to explain the nature of the critical temperature. Recall that the enthalpy of vaporisation is the energy (or heat) required to convert one mole of liquid from the liquid state to the vapour state. If one finds that no energy is required to transfer between the physical states, it implies that only one phase now exists. Figures 2, 3 and 4 represent experimental values for water; however, the same behaviour with different values of pressure, temperature, and enthalpy exists for all pure compounds.

Another way of defining a critical (or supercritical) fluid is the consideration of kinetic energy and the potential energy of a simple closed system. The kinetic energy is a measure of the molecular motion -- *i.e.*, a manifestation of the degree of "heat" -- within a system. A higher kinetic energy implies a higher temperature and thus more motion of a given set of molecules within this closed system. Visualise a small cube in space containing one mole of a pure substance (*e.g.*, 18 grams of water or 44 grams of carbon dioxide) with the molecules vibrating, rolling, and moving in three dimensions. The potential energy is the "intermolecular-glue" holding similar molecules of a pure substance together in a "condensed-phase" such as a liquid. Refer to Figure 2 and visualise a spot or point on the graph positioned on the Y axis at 100 bar [ln (100 bar) = 4.6] and the lowest value on the X axis. On the graph, move from this point, left to right, in a line parallel to the X axis (temperature). As one moves from left to right towards the line dividing the solid phase from the liquid phase, the kinetic energy (the temperature) increases. The potential energy is a constant value, intrinsic to the type and degree of atoms making up the molecules while the kinetic energy is increasing.

Approaching the solid-liquid line in Figure 2, the increase in kinetic energy now exceeds the lattice potential energy. This represents enough energy to exceed the bonding strength of the three dimensional physical "connections" (the transition from a solid to the less condensed liquid state). The kinetic energy continues to increase as our imaginary progression across Figure 2 moves over the liquid-gas line boundary. At that junction or line, sufficient kinetic energy is available in the system to allow molecules free, three-dimensional travel over significantly longer distances (compared to liquids, the increased mean free path is often 100 to 1000 times the molecular diameter). This higher content of kinetic energy *versus* potential energy allows gases (compared to liquids at a significantly improved transport properties such as lower viscosities and higher diffusivities).

At the gas-liquid transition (along the boiling point line) there is a distinct break in viscosity and diffusivity curves between gases and liquids. Super-

critical fluids "tie the two levels together" -- displaying a continuous transition between the extreme values displayed by the other two distinct phases. This is shown for viscosity in Figure 5. Below the critical temperature, there is a discontinuous change in viscosity for gases and liquids in equilibrium for all temperatures and pressures at which the two phases coexist. However, above the critical temperature, the viscosity is a continuous function of temperature for a given pressure. In the gas region at sufficiently high pressures, but at temperatures less than the critical temperature, if two gas molecules of the same type collide, the collision can be somewhat inelastic. Under these conditions, when gas molecules of the same kind collide, the probability is that the molecules will "stick-together" for a short, but finite period of time. This has an impact upon the transport properties of viscosity and diffusivity (restricting the limiting values).

One of the assumptions of our travel across the phase diagram on our route parallel to the X-axis is that the temperature is changing, but the pressure is constant. One consequence of this is that the density will decrease continuously. If we changed our assumption to focus on a constant density instead, then the transport properties would not change compared to the constant pressure scenario described above [12]. This is noted by the constant density lines drawn in Figure 5.

Continuing the imaginary trip from left to right, we next encounter the gas-supercritical region border. This transition is much more subtle than the previous transitions as denoted by a dotted line in Figure 2, rather than a solid line. For gases, when we are considering behaviour along the isotherm of the critical temperature, ideal-gas behaviour (linear PVT equations) ceases at values of pressure above about 0.6 time the critical pressure (for water the critical pressure is 220 bar so the deviation from ideality occurs at about 132 bar). For liquids, the transition to a supercritical fluid is somewhat more tangible. If we cross the phase diagram again but this time at a pressure of 220 bar (the critical pressure) or higher by increasing the temperature, we encounter the border of the liquid-supercritical regions. It is instructive to remember that this line between the liquid and supercritical phases is comprised of points (conditions) at which the enthalpy of vaporisation goes to a zero value or disappears from consideration. Thus, right at, and beyond the dotted line transition line, there is no further energy needed to take a mole of pure compound from the liquid "state" to the next "region" (supercritical fluid). For gases making the gas-supercritical fluid transition, the heat of vaporisation has already been input into the liquid to vaporise it to a gas state; as gases are heated and pressure is applied to move to conditions near the critical point, a more complex equation of state is necessary to describe the PVT behaviour -- note that for low pressures, well away from the critical pressure, at temperatures at and above the critical temperature, ideal-gas behaviour is still observed..

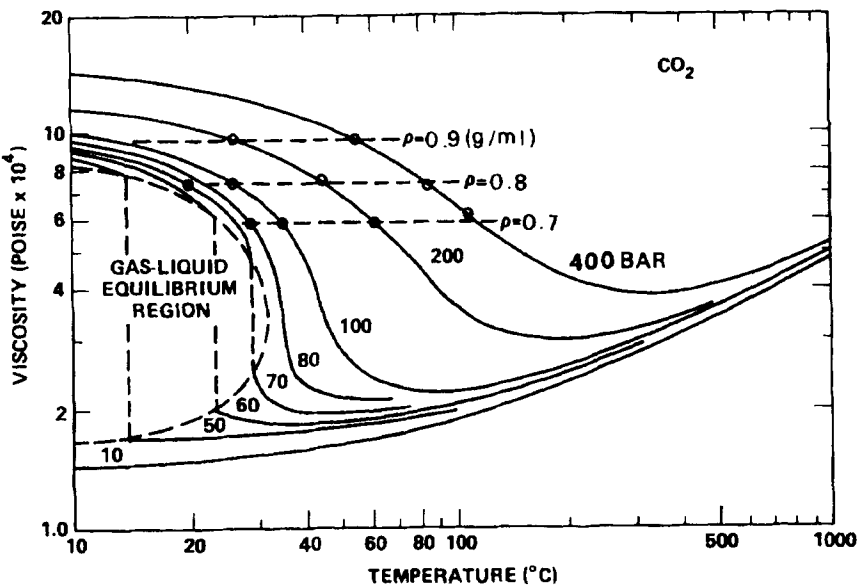

Figure 5: The viscosity of carbon dioxide as a function of temperature and pressure. Broken lines indicate constant density conditions. Reprinted with permission from Reference 12; copyright 1983, American Chemical Society.

What then is the difference? The difference is that, in the supercritical region, molecules have long mean free paths comparable to those in a gas phase; now when one molecule collides with another similar molecule, the collision is more elastic, whatever the applied pressure. The molecules collide, and then they bounce-off each other without a finite "sticking-together." This is another way of saying that at the critical temperature, the kinetic energy is equal and equivalent to the potential energy. Because this is independent of the pressure, the supercritical region goes from the "bottom" of the graph (the X axis) all the way to an infinitely high pressure with no distinction at the critical pressure (that pressure corresponding to the Y axis position of the critical temperature). The only thing that happens as we move "up" in this diagram (*i.e.*, increasing pressure) in the supercritical region is that the density increases with pressure.

11.2.3 The Practical Ramifications of Operating in the Supercritical Fluid Region

Let us pause here for a moment and consider what we have gained in the supercritical region. The density of the supercritical fluid varies in a continuous manner. The variable density results in a variable solvent power, thereby supporting selective solvation with a single fluid: the solvent power can be selected and controlled by controlling physical parameters (temperature,

pressure). At the transition between gases and liquids (along the boiling point line), there is a discontinuous change in density. With a supercritical fluid, liquid-like densities are encountered near the critical point (starting at pressures of about 0.6 times the critical point pressure).

As noted above, even for supercritical fluids at liquid-like densities, there is no heat of vaporisation to move the fluid to gas-like densities -- just lower the pressure at a given temperature. With typical liquids, heat must be supplied to evaporate them. That means that when a chemist wants to remove the solvent from a solution of liquid solvent-plus-extract, heat is usually applied and the temperature of the solution is elevated to the boiling point of the liquid solvent. If the raffinate (what is left after extraction) is the desired product, usually there is some liquid solvent left in it as well, so heat is often used again to elevate the temperature. This can be a problem when working with thermally labile components and matrices. With a supercritical fluid, when pressure is lowered sufficiently, the supercritical solvent is effectively removed from both the extract and the raffinate. Usually heat is only input to offset the cooling due to the expansion process so very mild temperatures can be used during supercritical solvent removal.

In the supercritical fluid region, the transport properties of viscosity and diffusivity have become "more-favourable" in the sense that the individual molecules (of the same kind) have less "drag" or retarding of their velocity as they pass close to each other or actually collide. These two properties have very positive effects upon the use of supercritical fluids as solvents in both chromatography and extraction. In chromatography, more favourable diffusion implies more narrow peaks (with regard to time) and therefore more resolution per time -- *i.e.*, more peaks can be base-line separated in a unit period of time. Lower or more favourable viscosity implies the capability of operating at higher volumetric flow rates (faster linear velocity) with less penalty for pressure drop across the column.

In extraction, a more favourable diffusivity implies a more efficient penetration of matrices with the supercritical fluid and thus a more favourable mass transfer with shorter extraction times (compared, for example, with liquid-solid Soxhlet-type extraction). As in the chromatographic application, a more favourable viscosity compared to liquid viscosities imparts the ability to use relatively high flow rates with lower pressure drops -- useful for employing small-volume capillary tubing throughout the extraction system. For example, the fluid dynamics will not contribute significantly to the overall pressure gradient between the pump (the fluid compressor) and the front end of the sample. The impact is even more important in the region containing the sample to be extracted. In analytical-scale SFE, samples are placed in flow-through extraction vessels (very much resembling liquid chromatographic columns). Hence, it is advantageous that the pressure drop across the sample, produced as the extraction fluid flows through the sample, is similarly attenuated for

higher flow rates compared to using liquid solvents for this purpose. This allows a well-controlled set of parameters for the extraction: flow rate of the fluid, density, pressure, diffusion and repeatability of the method.

In the next section, we will give an overview of the instrumentation generally used to carry out analytical-scale supercritical fluid extraction.

11.3 AN OVERVIEW OF ANALYTICAL-SCALE SFE INSTRUMENTATION

SFE has been used as a technique by chemical engineers for at least the past 25 years. Compared to the practice at the laboratory scale (*i.e.*, the analytical-scale SFE we are currently discussing), chemical engineers are far advanced both in understanding the principles and in carrying out the practice in very large scale processes as well as bench scale experimentation. Chemical engineering literature is filled with excellent background material, including theoretical equations and the fit of these equations to actual experimentation. The SFE instrumentation that is used today in analytical laboratories, whether it is home-built or one of the currently available commercial systems, is virtually all derived from drawings and descriptions of chemical engineering equipment. The analytical equipment is usually just scaled down. In some cases the scaling-down is more difficult than it might appear at first consideration. This is particularly true in the design and fabrication of the expansion nozzle (restrictor) -- a key component in analytical-scale instruments. On an engineering scale, the approach to creating and controlling pressure drops (how, when in the process, by how much) to separate the supercritical solvent from both the extracted components and the raffinate is typically different from that of analytical-scale SFE.

A simple diagram outlining key elements in the process of analytical-scale supercritical fluid extraction is shown in Figure 6. As noted earlier, the process is straightforward:

- bring a fluid to the appropriate operating conditions;

- introduce the fluid into a region containing a (finely divided or well-distributed) sample at precisely controlled conditions of temperature, density, and composition for some repeatable time of static extraction followed by a timed dynamic extraction (having a controlled flow rate) to dissolve and remove components from the sample;

- remove the dissolved components from the supercritical (or near critical) solvent by drastically lowering the pressure of the solution; and

collect the precipitated or condensed extracted components.

Finally, although it is not rigorously part of supercritical fluid extraction, a last step generally afforded by analytical-scale supercritical fluid extractors is reconstitution of the extracted components in a solution that is appropriate for the subsequent analytical instrument. In the case of gravimetric assays, the net loss of sample weight or the net weight of extract components can be measured and reconstitution of extracted components is not necessarily employed.

In general, the above process is carried out by using both a liquid pump and a flow restrictor to pressurise liquid carbon dioxide withdrawn from gas cylinders to the operating pressures appropriate for the selected density. Physically, the two components are at opposite ends of the flow path -- the pump is one of the first components encountered by the fluid and the flow restrictor is encountered at the end. However, the integrated control of both components is crucial to the proper control of the extraction process. Once pressurised, the liquid is preheated to form a supercritical fluid solvent and then directed into (and ultimately through) a region containing the sample; the pressurised conditions are maintained along the entire flow path until the expansion device (flow restrictor or nozzle) is encountered where the pressurised fluid is exposed to near-ambient pressure in a very short distance.

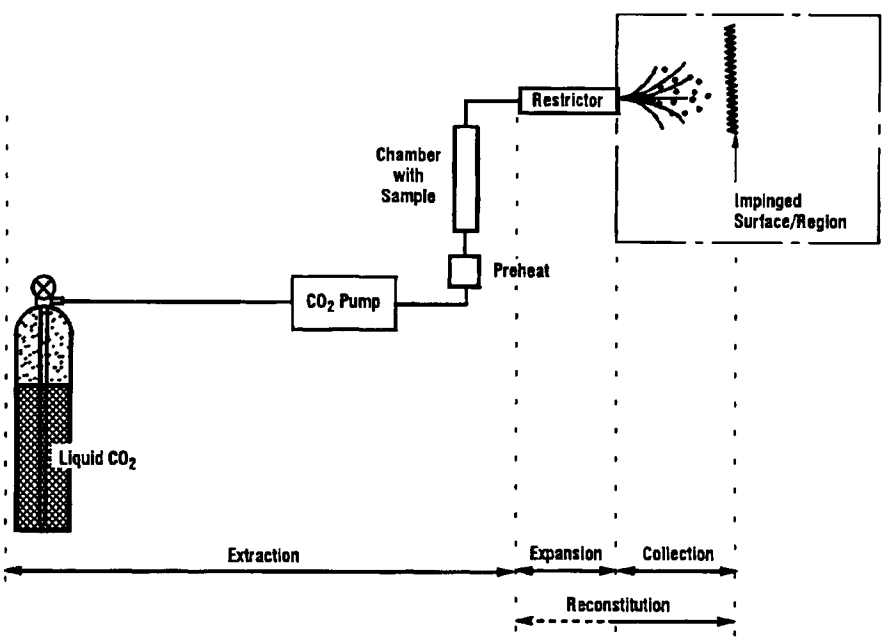

Figure 6: A block diagram of a generic SFE. Reprinted with permission from Reference 13; copyright 1993, Hewlett-Packard Company.

The rest of this section will present details about various aspects of the process: getting the extraction solvent from a gas cylinder to the extraction chamber, controlling the extraction conditions, separating the extracted components from the supercritical extraction fluid, and collecting and reconstituting extracted components. Note that the discussion will focus on using carbon dioxide as the primary, bulk extraction fluid since this is the most widespread fluid in use for analytical-scale SFE at this time.

11.3.1 The Source of the Supercritical Fluid: How to get the Extraction Solvent from the Gas Cylinder to the Extraction Chamber

11.3.1.1 The Source of the Carbon Dioxide

The equipment or hardware begins with the source of carbon dioxide. Although the carbon dioxide used for SFE comes in metal cylinders that are most familiar as "gas-cylinders" or "gas-tanks," it sometimes is a surprise to the neophyte SFE experimenter to find that it is really the liquid carbon dioxide contained in the cylinders that is being used as the supply fluid for the SFE instrument. Carbon dioxide does not have a boiling point at ambient laboratory conditions (20-30°C and 1 bar); at those conditions, it is in the middle of the gas-phase region. In the laboratory, we chemists are most familiar with defining a boiling point as the temperature of a liquid at which the vapour pressure equals the surrounding pressure (normally defined at 1 bar). It is also usually assumed that this temperature is at or above ambient temperature -- *i.e.*, we think of a liquid with a conventional boiling point as something that we could pour into a beaker in the laboratory and have it stay there. Carbon dioxide has a vapour pressure of approximately 58 bar at 21°C (70°F). The triple point is low in temperature, but high in pressure (-57°C, 5.1 bar). At the triple point, the vapour pressure is five times normal atmospheric pressure. If a person somehow tried to pour a volume of liquid carbon dioxide into an open beaker in the laboratory, it would rapidly expand to a gas and disappear from sight. However, if enough pressure is exerted upon carbon dioxide at room temperature, then both the liquid and gaseous phases can co-exist. This is what happens in a gas cylinder.

When contained in a metal cylinder, liquid carbon dioxide is quite stable. A typical cylinder will contain perhaps 60 pounds (27 kilograms) of carbon dioxide. Initially, this will be distributed approximately 1/3 in the gas phase and 2/3 in the liquid phase. The exact distribution between the phases and the pressure within the cylinder is a function of ambient temperature. For example, cylinder pressures range from 57 bar (830 psi) to 72 bar (1045 psi) for room temperatures of 20°C to 30°C. Within the cylinder, since the liquid phase is the more dense phase, then the upper 1/3 of the cylinder volume is occupied by gas and the lower 2/3 of the cylinder volume is occupied by liquid. This phase ratio changes continually as the liquid is drawn out from the bottom of

the cylinder. When the cylinder contents are withdrawn until the cylinder is almost empty, the gas will occupy 9/10 of the volume and the remaining liquid occupies only 1/10 of the volume.

The liquid is conducted out of the cylinder by a "dip-tube" (siphon-tube or eductor tube) which comes down from the top open-shut valve and extends down into the liquid layer well below the original liquid-gas interface. The dip-tube usually stops short of the bottom of the cylinder in order to avoid drawing-up into the tubing any particulate matter that may be at the bottom of the cylinder. The pressure within the cylinder (exerted by the gas phase), pushes the liquid phase up through the eductor tube and to the hydraulic system of the receiving instrument. When the liquid level drops below the open bottom end of the dip-tube, then liquid can no longer be forced up through the inner diameter of the tube and out through the valve and on to the SFE apparatus; pressurised gaseous carbon dioxide will fill those lines. The combination of remaining gaseous carbon dioxide and small pool of liquid carbon dioxide below the bottom of the dip-tube usually makes up about 10 pounds (4.6 kg) of carbon dioxide that is left in the tank at the end of use. To the neophyte who has not realised the make-up inside the cylinder, this can initially be distressing. You think you purchased 60 pounds of usable carbon dioxide but you can use only 50 pounds.

11.3.1.2 Compressing and Heating the Liquid to reach Supercritical Operating Conditions

The fluid coming from the cylinders is pressurised liquid carbon dioxide at ambient temperatures. As noted above, the density of this fluid is a function of room temperature; however, the density is quite high[1] compared to the working range for a supercritical fluid. In order to exploit the adjustable density of a supercritical fluid and to achieve optimal diffusivities and viscosities, the compressed liquid carbon dioxide must be turned into supercritical fluid by adjusting both the temperature and the pressure of the fluid before it contacts the sample to be extracted. This is commonly done in SFE instruments by first compressing the liquid carbon dioxide to reach the higher operating pressures for the system and then heating the carbon dioxide to temperatures above the critical point of carbon dioxide.

---

1 Liquid carbon dioxide at liquid-like densities can be used as an effective extraction solvent. In fact, the viscosities and diffusivities of a near-critical liquid (*i.e.*, one that is within 30-40°C of the critical temperature) are nearly as advantageous as those of the fluid in the supercritical region. What is lost with a compressible near-critical liquid is the adjustable solvent power. Furthermore, as temperature is increased in order to support increased solvation of compounds with higher melting points and/or molecular weights, the user moves into the supercritical region anyway.

The mechanics of increasing the pressure on the fluid can be done in a couple of ways. One would be to increase the temperature surrounding the liquid carbon dioxide [14]. As noted above, the pressure exerted on the liquid carbon dioxide in the cylinder is a function of its ambient temperature. Only at higher ambient temperatures would the resultant system pressures be enough to reach the nearly liquid-like densities of 0.1 to 1.0 g/mL that are required to use supercritical fluid carbon dioxide as an extraction solvent for extraction temperatures ranging from 40°C to 150°C. This approach is not widely used at this time. Liquid pumps (such as those used in liquid chromatographs) are more commonly used.

While liquid pumps are used to compress liquid carbon dioxide, their implementation for doing so differs from pumping typical liquids in that the carbon dioxide is both highly compressible and pressurised so it has been necessary to adapt liquid pumps and their controlling systems for this new application. Note that liquid carbon dioxide flowing from a pressurised cylinder at ambient conditions is dense enough to support a normal reciprocating liquid pump. However, gaseous carbon dioxide flowing from a gas cylinder at the same cylinder pressure simply does not provide enough material -- not dense enough -- to pump with a liquid pump; a gas compressor would be necessary.

Part of the adaptation of reciprocating pumps has been to accommodate the high compressibility of the liquid carbon dioxide. In some implementations, the liquid carbon dioxide is cooled to sub-ambient temperatures to lower the compressibility, thereby making the liquid "stiffer." Additionally, pump control algorithms can be superimposed to adjust the speed of the pump during each stroke so that pressure variation during pumping (often called pressure ripple) is minimised. In other implementations, an additional pressure charge to as much as 170 bar (usually with helium) is added to the cylinder of carbon dioxide to artificially increase the density in the pump to help minimise the compressibility. Although use of an additional pressure charge works in principle, a major drawback is an inability of the SFE system to provide low density extractions which favour selective extraction of volatile fractions (aroma constituents).

Still other implementations have employed syringe pumps. This type of pump is advantageous in that pressure ripple is avoided so syringe pumps are good constant pressure sources. However, these pumps have often required an additional pressure charge to the tank (usually with helium) as discussed above to facilitate the compression within the syringe region. A drawback to syringe pumps is that they cannot provide a continuous supply of solvent for hours at a time; once the syringe is exhausted, it must be refilled -- interrupting the extraction cycle. Moreover, the supply of modifier/carbon dioxide mixtures from the same syringe pump that dispenses carbon dioxide requires long switch-over times between solvent compositions. Using multiple syringe pumps -- one for the carbon dioxide and one for a modifier -- addresses the changeover time

issue. In general, single syringe pumps are no longer incorporated in the construction of new equipment.

Pumping systems include pressure measuring transducers that provide an indication of the actual supply pressure or, in more sophisticated equipment, provide a feedback signal for pressure (density) control. After the pump, the carbon dioxide (still in the liquid phase) passes through small diameter tubing until it approaches the extraction region where the sample is contained. Before the carbon dioxide passes into the extraction region to contact the sample, the temperature around the stream of extraction solvent is adjusted to the choice desired for the supercritical extraction -- *i.e.*, the carbon dioxide finally becomes a supercritical fluid as defined by the choice of temperature and density (pressure). In Figure 6, this is indicated as a "preheat zone." Note that the design of the preheat zone must accommodate transferring enough heat to the flowing stream of solvent at all possible operating values of pressure and flow rate so that the carbon dioxide is at the correct temperature as it first contacts the sample.

11.3.2 Control of the Extraction Conditions

Density is such a sensitive function of temperature and pressure in the supercritical region that good thermal and pressure controls are absolutely necessary for reproducibility -- particularly, when fractionation will be exploited. In the extraction region, the flow rate of the carbon dioxide does not affect the nature of the supercritical phase but rather has secondary effects upon the mass transport. The capability of a variable flow rate allows the user to choose the flow rate that is best for the application at hand. Higher flow rates can be used to dissolve and remove solutes that are both highly soluble in carbon dioxide and quite accessible (on the surface of a matrix) so that the extractions are done in a timely manner. In contrast, lower flow rates might be employed to remove highly encapsulated or bound components while minimising the consumption of the carbon dioxide. The extreme of low flow rate is no flow rate; this is known as "static extraction" or "equilibration." Often a combination of static and dynamic extraction steps is used in a single extraction method.

11.3.3 Separating the Extracted Components from the Supercritical Extraction Fluid

After passing through the necessary capillary tubing (usually stainless steel), the moving phase of carbon dioxide (now containing analytes/solutes that were extracted from the sample in the extraction region) is directed on to the "flow restrictor." Mechanically this is perhaps the most crucial part of the equipment both from the design and the operation of apparatus. In principle, this restrictor (nozzle) serves one important function and several secondary functions. The restrictor is the throttle point or the narrowing of the passage ways. It is the

most restrictive flow region between the pump and ambient pressure conditions. This is the point at which the major pressure drop occurs, *i.e.*, where the density of the extraction fluid changes from liquid-like to gas-like.

In a system like a gas chromatograph that operates with a fluid having gaseous densities and high compressibilities, there are restrictions in the flow paths to contain the fluid in order to achieve operating pressures. Every pressure drop is an opportunity for the gas to expand to lower pressures (and lower densities). Sometimes the restrictive regions are quite short with narrow diameters -- such as a gas flow controller on the source end. Other times, the chromatographic columns act as long distributed restrictors. In a system like a liquid chromatograph that operates with a fluid having liquid densities and low compressibilities, there is no need to contain the fluid to achieve operating pressures. The expansion of typical liquids upon encountering a pressure drop is minimal (compared to gases and supercritical fluids): the density of a liquid is essentially the same from one side of a pressure drop to the other. With a supercritical fluid, pressure is necessary to maintain liquid-like densities; *each time a pressure drop is encountered, the density decreases and the ability to maintain solvation decreases.*

With fluids, we think of the pump as the source of pressure as well as the flow rate determining device. However, with supercritical fluids (in contrast to typical liquids), a pump needs a control point downstream to limit the passage of molecules per unit time. This restriction then "holds-back" the previously unlimited flow of molecules to a definite, but not always pre-determined level. Ideally then, the restrictor serves to restrict the flow until the density of molecules distributed from the pump through the extraction region right up to the final restriction point in space is such that the operating density desired in the extraction zone is achieved. This is much easier to state in words than it is to achieve in actual experimental practice. This is especially true if you wish to achieve an experimental set of parameters and hold those values over a finite period of time (ranging from minutes to hours) and do it with the statistical precision and accuracy that are necessary to attain the final quantitative analytical results.

11.3.3.1 Distributed Fixed Restrictors

In a simple apparatus, such as home-built SFEs, the restrictor often is a length of small-diameter capillary tubing. For instance, a restrictor can be fashioned from a 15-cm length of 10 micrometer internal diameter tubing placed at the end of the apparatus with the exit end of the capillary tubing exhausting into a sample collection tube. This is one example of a so-called "fixed-restrictor." A fixed restrictor has fixed (invariable) dimensions for its length and diameter. With a fixed restrictor, the system pressure is determined by the combination of the flow-rate delivered by the pump and the physical dimensions of the

restrictor. Higher pressures require higher flow rates. With fixed restrictors, the flow rate and pressure cannot be independently selected and controlled.

If the flow-rate varies by itself or is deliberately varied by the experimenter, the pressure adjusts proportionately, as the restriction itself is fixed and constant. It may be even more perplexing, that although the flow would not be varied at the pump, the restriction can increase within a fixed piece of tubing. This is a very plausible and likely result. The finite length of tubing has a distributed resistance, meaning the resistance is additive from the front of the 15-cm length (as mentioned above) to the end of the 15 cm. That means that the pressure drops continuously (but not necessarily linearly) from the operating extraction pressure of perhaps several hundred bar at the beginning of the 15-cm down to one bar at the end of the 15-cm length (ambient pressure). This decrease in pressure yields a decrease in density that always leads to diminished solubility of analytes.

At the terminal end of the restrictor, the goal is the complete removal of the solvating power of the flowing carbon dioxide to precipitate the solutes. However, in the case of such a fixed restrictor with distributed resistance, the loss of solvating power will be gradual and continuous throughout the length of capillary tubing. Thus, it is likely that precipitation will begin "prematurely" within the restrictor itself. If the concentration is small and the resulting precipitate is formed under conditions of very small particle size, it may simply be physically blown through the open space in the tube and on into the collection zone. More likely, however, it will adhere to the inner walls of the tubing and further restrict flow (now increasing the pressure locally) until, in the worst case, the tubing closes itself completely to further flow (minimally, a cessation of extraction; in the extreme, possibly, catastrophic over-pressure where the capillary tubing breaks or the pressure is relieved in some other way).

This situation is further compounded by the fact that during the significant expansion of the carbon dioxide from a highly dense fluid (perhaps at several hundred bar pressure) down to a low-density gas at ambient pressure, there is an accompanying " Joule-Thomson " cooling effect. This cooling can produce a temperature gradient over a very short distance of several hundred degrees. The cooling of the narrow opening of the tubing encourages "freezing" of high-concentration bulk solutes such as water or triglycerides, for example. Localised heating of the capillary tube can help minimise this effect, but the actual temperature setting is problematic. If the tubing is fused silica, it often breaks under these conditions of stress. Stainless steel capillary is somewhat more tolerant, but most people choose to dry their sample to avoid this. That drying helps avoid the problem if precipitated water is the cause of the plugging. If lipids or oils are causing restrictor plugging, resolution of the problem can be even more difficult.

11.3.3.2 Minimal-Length Fixed Restrictors

The problems with distributed fixed restrictors have led to the development of a variety of minimal-length fixed restrictors. Conceptually, such a restrictor is easy to visualise and make. For example, one simply takes a small piece of capillary fused silica tubing, and with a small flame, the end of the tubing is drawn down to a very small diameter. In practice, this fabrication process can be difficult to control. The first question might be, "what diameter is appropriate?" The second question might be, "how can the specified size of the opening at the terminus of the tubing be obtained?" If the first two questions could be answered, a third question might be, "how can the process be repeated precisely and accurately whenever needed?"

The answers to all of these three questions are difficult, if not impossible, for the average practitioner to obtain. The first question brings up the observation that a fixed restrictor couples the flow rate and pressure: pressure is a variable dependent upon flow rate and vice versa. As flow rate increases, the system pressure increases; similarly, a decrease in flow yields a decrease in pressure. If this is combined in an environment where the resistance changes as a solute flux passes, then the flow rate-pressure domain is uncontrolled, unpredictable and very difficult to reproduce between any two fixed restrictors. Flow rate, pressure (density), temperature, and time must be controlled precisely in order to deliver the same quantity of supercritical fluid needed to partition a given amount of analyte from a unit amount of matrix. Quoting extraction efficiency or percent recovery under such uncontrolled parameters is thus an empirical matter where coincidence is random or indiscriminate.

There are many variations on fixed restrictors including a carefully defined fritted zone at the end of a capillary tube. Most of these have led to a un-ending number of comments at supercritical fluid extraction conferences such as "the biggest hurdle in SFE is limited restrictor availability and technology." Greibrokk [15, 16] has summed up general experience and feeling about fixed restrictors, especially for SFC.

11.3.3.3 Variable Restrictors

Gere *et al.* [17] described a variable back-pressure regulator as a post-column restrictor for SFC in 1982, although this was by no means the first of such devices to be made from off-the-shelf apparatus. For at least 20 years, SFE and supercritical fluid chromatography (SFC) have been practised successfully (under certain favourable combinations of experimental parameters) with "back-pressure regulators" at the terminus of the apparatus. These favourable circumstances usually involve larger-scale equipment than is compatible for the analytical-scale supercritical fluid extractors that address the needs of analytical laboratories. Larger-scale work with larger flow pumps, flow rates and appropriately-sized ancillary hardware can tolerate rather large labyrinth

void volumes in the expansion zone where fluids at high pressures are expanded to ambient gas[2]. If such large, poorly-swept volumes can be tolerated, back pressure regulators have a fine characteristic in that they can decouple flow and pressure. Thus, one gains independent control over two very important parameters involved in the integrity of SFE.

These large-scale devices are mismatched with the need for small-scale volumes in analytical-scale SFE instruments, which are applied to recovering trace concentrations of analytes in minimal volumes of reconstitution solvents. Thus, it has taken some additional years of development before miniaturised, automated back-pressure regulating restrictors, known as variable restrictors, have become commercially available. Variable restrictors are designed to have a very short length in the expansion region in order to minimise problems with distributed pressure drops; however, the cross-sectional area of the region is variable so that wide ranges in mass flow rates can be accommodated for a given pressure. The overall expansion volume is kept quite small. The dynamic range of possible flow rates over the pressure range necessary for carbon dioxide (70 bar to about 400 bar) is similar to what the user could have by going from a static restrictor made of a 5 μm diameter pinhole to another static restrictor made from a 25 μm pinhole; in the case of a variable restrictor, one restrictor covers the full range. In fact, in one implementation, the orifice can be opened wide enough to allow passage of liquid solvents with source pressures of less than 7-8 bar; this is not possible with a static orifice. What is attractive about this capability is the fact that a liquid solvent can be used to clean the expansion region.

Such devices can be implemented within an analytical-scale SFE to control either pressure (need a pressure transducer) or flow rate (need a flow transducer); the fluid pump control system would be used to control the complementary parameter. The two control systems allow the decoupling of flow rate and pressure. The Hewlett-Packard model 7680 T contains just such a device, and similar devices are becoming available through other commercial sources. With properly implemented devices, the restrictor can become transparent to the user -- providing settable control of parameters and operation that is highly reproducible and more robust to wider ranges of extractable components.

---

2 In SFC, in early years of experimentation [17, 18], often the on-line detectors were UV/Visible (spectroscopy) types where it was useful, and even necessary, to maintain supercritical or at least high density conditions through and beyond the detector. Expansion into a large unswept zone was not a parameter that needed to be considered or controlled

11.3.4 Collection and Reconstitution of the Extracted Components

Finally, in Figure 6, we shall focus our attention on the zone just beyond the restrictor where the expanding carbon dioxide and precipitating analytes impinge upon a solid surface or a retaining liquid. The zone which we discussed above in detail can be defined as the expansion zone, whereas the zone we will now discuss is defined as the collection zone. Collectively (as seen in Figure 6) these two zones make up the reconstitution zone.

Simplistically, the collection zone can be made up of an empty container such as a test tube or small vial with the restrictor exit placed right at or within this zone, perhaps vertically with the restrictor exit close to but not touching the bottom or the walls of the vessel. (Usually in a simple home-built apparatus, the vessel is glass.) Thus, the bottom or the walls of the vessel are surfaces to be impinged by the expanding mixture of supercritical solvent plus extracted components. To a first approximation, extracted solutes would be expected merely to precipitate out of solution as the expanding carbon dioxide changes to a low-density gas, dropping to the bottom of the collection vessel and providing a clean gas-solid phase separation.

Reality is often quite different. When a supercritical fluid mixture expands into pressures as high as ambient conditions, the resultant expansion plume can be a complex mixture: it is a high velocity gas stream that entrains precipitated particles of extracted materials and often frozen carbon dioxide. Much adjustment needs to take place in the collection zone in order to achieve something close to 100 % recoveries of solutes with concentration ranges from parts per billion (PCBs) up to 50 % (total fat in a chocolate candy). Besides the flow dynamics of the expansion, several physicochemical parameters cause the deviation from the initial simple model. They include, but are not limited to, volatility of the solute, degree of co-precipitation of solid carbon dioxide (followed almost immediately with uncontrolled sublimation of the solid), aerosol formation, surface tension, occlusion in solid carbon dioxide, rebound from impinging surface, and many other interacting phenomena.

Beyond simple empty vessels, a time-honoured approach has been to bubble the expanding carbon dioxide into another liquid. Although an improvement, this approach still suffers from many of the other above complications and a few new ones such as solute volatility and aerosol formation between the solutes and the chosen trapping liquid.

Most recently, some of the commercial SFEs have used a thermally controlled solid trap as a collection zone; such a trap is comprised of a porous packing material that can have some chemical affinity for analytes. In effect, the trap acts as a mechanical, thermal, and chemical filter to separate the extracted components from the expanding gas. Since the extracted components are

retained on the packing material of the trap, the SFE also includes a means to reconstitute the concentrated extracts in liquid solvents. Such a scheme appears to have the maximum flexibility for full recovery over the widest range of analytes. For example, the use of a non-polar packing material (PoraPak Q or DIOL-bonded silica) at low temperatures (perhaps -10°C) can trap volatile compounds quantitatively (*e.g.*, pentane, BHA, and volatile constituents of perfume). Although it may be possible to accomplish the same collection-reconstitution with a liquid trapping approach, it is more problematic to choose optimal liquids. For instance, an alcohol may indeed provide near optimal trapping but may be very inappropriate for introduction into a GC capillary column. This then would lead to an evaporation followed by solvent exchange to obtain the proper solvent for the GC; however, the evaporation step introduces several new difficulties.

What the user must do in order to reconstitute the extracted components into a fraction that is ready for hand-off to a subsequent analytical instrument, by using a compatible solvent, an appropriately small fraction volume, and an internal standard, depends greatly on the particular SFE design of the collection and reconstitution zones. SFE instrumentation ranges from designs that require much manual intervention between the SFE and the analytical instrument to those that promote easy integration into automatic systems with the analytical instruments. The manner in which the collection and reconstitution steps are implemented has a direct impact on the degree to which the full potential of SFE for automating sample preparation is realised.

The preceding sections have outlined the theoretical basis of supercritical fluids as solvents and some engineering considerations for designing an analytical-scale instrument. In the next section we will present details of specific examples of applying SFE to samples of interest in the food industry and a summary of other examples.

11.4 EXAMPLES OF SFE METHODS IN FOODS AND FOOD PRODUCTS

The most common method for the quantitative analysis of total fats in foods has been gravimetric, where the components of the sample are extracted into a suitable solvent (*e.g.*, methylene chloride), the solvent is then removed by evaporation, and the residue is weighed. When using such a classic traditional technique, the final liquid extraction volume (liquid organic solvent) required may exceed 100 mL.

This approach is rapidly changing in North America, if not around the world. As noted in the introduction to this chapter, two economic-political factors are motivating profound changes in such traditional procedures: the "Montreal Treaty Protocol concerning Chemicals which may affect Ozone in the Atmosphere" [2-4] and the USA's "Nutritional Labelling and Education Act" [5].

The "Montreal Protocol" suggests that halogenated solvents either be significantly reduced or eliminated in laboratories and industrial applications.

The NLEA may prove to have an equally dramatic effect on the extraction and analysis of fat. Officially, the NLEA takes effect in May of 1994, but changes are already underway and will continue for some years to come. A recent book, Methods of Analysis for Nutritional Labelling [19] published by the Association of Official Analytical Chemists (AOAC, the organisation that co-ordinates the compilation of food methods and protocols for FDA-regulated food products), has definitions and suggestions for future methods. This book states, "Final nutritional labelling regulations published in the Federal Register on January 6, 1993, defined total fat as the sum of all lipid fatty acids expressed as triglycerides, *i.e.*, the fatty acids from mono-, di-, and triglycerides, fatty acids, phospholipids and sterol esters." The book goes on to discuss the impact in detail, describing current methods in fat methodology and outlining serious shortcomings of several of the current methods. Mention is made of the environmental concerns with halogenated solvents, noting that studies are underway to develop more environmentally-friendly procedures without compromising recovery efficiency.

Chapter 5 in reference [19] concludes with a paragraph concerning future methods for fats in foods and food products [20]. It begins by saying, "The current fat methodologies should at least be used until new validated procedures are in place to meet the NLEA definition of fat. ... A total lipid extract is crucial to accurate total fat analysis." The section concludes with the following sentences: "Supercritical fluid extraction is an emerging technology that shows promise as a fat extractant. This technique offers the luxury of "solvent-less" extraction by using liquid carbon dioxide as an extractant. This is an active area of study, and more work needs to be done to demonstrate recovery and reliability for a wide range of food matrixes. Instrumentation is expensive but can be automated to reduce operating costs."

The potential impact of the Montreal Protocol can be seen by perusing the rest of the AOAC manual: 21 of 28 current methods for fats in the AOAC manual use chlorinated solvents. Even those methods that do not include chlorinated solvents suggest such solvents as petroleum ether or diethyl ether. One of these methods uses 3,000 mL of ether for each food sample extracted. Extraction is an area where considerations about safety in the workplace are being focused so SFE with carbon dioxide addresses the area of safety as well as the concerns outlined above. After being used to extract components, carbon dioxide, the most widely used supercritical fluid, can be evaporated as an innocuous gas that can be safely vented upon depressurisation; moreover, carbon dioxide is much more environmentally friendly than chlorinated organic solvents. Current SFE instruments do not use carbon dioxide alone but the quantities of organic solvents that are used -- both as modifiers and as

reconstitution solvents -- are minimal compared to the consumption imposed by traditional techniques.

It is not surprising then, that SFE is very attractive as an alternative to conventional liquid extraction. Note, however, that SFE should not be construed as a panacea that is applicable to all samples. There are a number of applications for which the technique has been successfully used. Detailed examples (protocols) that have been developed and used in the collective labs of the three co-authors of this manuscript as well as many other labs around the world will be described in this section.

11.4.1 Examples of Protocols for SFE of Foods

In the following examples, HP7680 SFE instruments (Hewlett-Packard) were used. With these instruments, samples are input to the instrument *via* containers referred to as "extraction thimbles." Extracted components are collected and concentrated on solid traps. The temperature of the solid trap can be independently set for extraction and reconstitution steps in a method. The chemical functionality (none to quite polar) of the trap is selected by the choice of the packing material. A reconstitution solvent is used to move extracted components from the solid trap to automatic liquid sampler vials (or to waste). Depending upon the application, the vials are presented to a subsequent analytical instrument or possibly manipulated for a gravimetric assay. With this instrument implementation, samples are input and fractions of extracted components in liquid solvents in 2-mL vials are output with no manual intervention between input and output steps.

11.4.1.1 Total Fat Extraction from Olives

The extraction of fat from olives proved to be a relatively straightforward method to develop. The analysis is a gravimetric determination of the weight of fat extracted and collected from the sample. In this example, the two key considerations that had the most impact were:

- reducing the size of the food material to small particles, and

- dealing with the water content.

Initially, the sample was prepared by grinding a composite sample in a food processor. However, this preparation was not sufficient alone. In order to speed extractions, the *particle size was reduced by adding water* to the composite sample during pre-SFE sample manipulation. The particle size was reduced by adding a known amount of water to the sample while in the food processor; the result is a "puree" with a particle diameter of the solid material much smaller than it would have been if the water had not been added. The added water content must be taken into account when doing quantitative

extractions: thus, the comment " --adding a known amount (weight) of water--." It is also important not to add too much water so that the sample may be as homogenous as possible. Typically, a 100-gram sample of olives was taken as the gross sample to be reduced in particle size, and 20-30 grams of water was added *before the chopping*. A ratio of 10:2 weight: weight was found to give acceptable results.

TABLE 1
SFE Recovery of Total Fats from Olives: Experimental Development Sets

Experimental Treatment Set	% SFE Recovery *versus* Conventional Liquid Extraction
Set 1: High Chopping (3 minutes)	67
Set 2: High Chopping (3 minutes) + Drying	92
Set 3: High Chopping (3 minutes) with Additional Water (10:2, w:w)	93
Set 4: High Chopping (3 minutes) with Additional Water (10:2, w:w) + Drying	99

TABLE 2
SFE Conditions for Total Fats from Olives

Parameter	Values
Sample Size	500 mg
Solid Trap Material	DIOL SPE packing
Extraction Conditions	
Density	0.91 g/mL
Pressure	352 bar (5100 psi)
Temperature	50°C
Static Time	2 minutes
Dynamic Extraction Time	35 minutes
Flow Rate (Liquid CO_2)	4.0 mL/min
Solid Trap Temperature	30°C
Reconstitution Conditions	
Reconstitution Solvent	Methylene chloride
Solid Trap Temperature	38°C
Reconstitution Volume	1.00 mL

Once the proper particle size was achieved, the water was removed from the sample prior to subjecting it to SFE. In the usual, preferred approach the analytical-size sample was taken from the water-blended composite sample, placed/weighed on filter paper, and dried in an oven (110°C) for one hour. A mortar and pestle should be used to mix the dehydrated sample with the diatomaceous earth, to further dry and disperse the sample.

An alternate sample pre-extraction preparation was to blend the composite sample without the addition of water. Then, the *analytical sample* was weighed, ethyl alcohol was added, the sample was homogenised again, diatomaceous earth was added, and finally the pre-treated, chopped sample was placed in the thimble. At this point, the sample should not be dried in an oven due to the fire hazard with ethyl alcohol. The ethyl alcohol will be extracted away in the first few minutes of the dynamic extraction. It may be preferable to carry out the alcohol drying step of the SFE at a low density (lower than 0.40 g/mL) and a temperature of perhaps 80°C. The pre-treated sample -- enveloped in the filter paper -- was input to the SFE where extraction and reconstitution proceeded.

At the end of the extraction, the extracted fat was reconstituted in a previously tared automatic sampler vial using methylene chloride. The methylene chloride was evaporated to leave a dry fat extract which was then weighed. For the development of this method, the appropriate combination of chopping and drying procedures was explored in a series of experiments. These are outlined in Table 1.

In experiment Set 1 (Table 1) the gross sample with no additional water was chopped for a short period of time (3 minutes at a high chopping setting) and no subsequent drying step was included. In experiment Set 2, the same "water-less" chopping step was combined with the oven drying step. In experiment Set 3, the chopping process was applied to the composite gross sample to which water had been added (10:2, w:w) but no subsequent drying step was included. Chopping with water produced a puree-like semi-solid. In experiment Set 4 , chopping with water was followed by a drying step.

The SFE conditions are shown in Table 2. In Table 2 note that the temperature of the solid trap is changed between the extraction and reconstitution steps. During the optimisation of the SFE method, it was observed that a higher temperature in the trap during reconstitution greatly improved the efficiency of that step and the overall sample preparation process -- *i.e.*, the solubility of the fat in the solvent was increased so that less reconstitution solvent was necessary, resulting in smaller fraction output volumes (one vial) and less time spent in reconstitution and subsequent blow-down for the gravimetric measurement. The final method incorporated all of the conditions of Table 2 and experiment Set 4 from Table 1. The combined pre-SFE sample manipulation process then yielded a 99 % recovery of a

composite sample known from previous traditional methods to have an 11.4 % fat content by weight. Compared to a number of traditional methods that were studied, the results afforded by SFE were superior. First, the accuracy was comparable to the best manual method and 5% higher than the next competing manual method. The precision achieved with the SFE-based method was improved by an order of magnitude compared to the manual methods. Finally, once the samples are ready for extraction, the extraction process with SFE is half the time required by some of the faster manual methods. Therefore, while the pre-SFE sample manipulation and post-SFE blow-down involve hands-on labour by the chemist, using SFE-based method for this application became the preferred sample preparation approach compared to methods based on fully manual sample preparation processes.

11.4.1.2 Total Fat Extraction from Fried Snack Foods

The following summarises some of the more relevant considerations and results from SFE of a few food products such as fried snack foods, baked products, breakfast cereal and chocolate bars.

11.4.1.2.1 The constraints imposed by the chosen assay

For this study, we chose gravimetric measurement as the quantitative step. When extracting total fats from samples that have some water content, it would appear to be a more rigorous approach to ensure that the quantitation of water is separate from the quantitation of the fat. Therefore, whether the weight loss of the sample (original sample weight less raffinate weight) or weight of the resultant extract is used, the chemist may choose to dry the sample (*e.g.*, at 115°C for 1 hour) prior to performing the extraction. When the weight of the resultant extract is the approach to be followed, the method will require the chemist to obtain the tare weight of each of the vessels (*e.g.*, automatic sampler vials) used for collection of the output fractions. After a fraction is output from the SFE, the reconstitution solvent is evaporated to dryness. Although this may be accomplished with an inert gas such as nitrogen or helium, a vacuum oven is preferable. The solution of extract in a reconstitution solvent is placed in a vacuum oven at 115°C and left there for 5 minutes under a simple vacuum, thereby removing solvent and any carbon dioxide gas dissolved in the fat extract. This is a somewhat labour-intensive and time-consuming step, but extract solutions can be handled in batches. A relatively volatile solvent aids this step.

More fully automated approaches can be tried. For example, one of the authors [21] has incorporated a preliminary drying step as part of the SFE method. Water, cholesterol, and fat were step-wise extracted from cookies: Step 1 at 0.15 g/mL and 80°C to remove the water, Step 2 at 0.4 g/mL and 60°C to remove cholesterol, and Step 3 at 0.80 g/mL and 80°C to remove the fat. The trade-off was dealing with a longer sample throughput time in order

to minimise hands-on labour in that work. Yet another approach might be to superimpose adsorption on the extraction process. This could be done by placing an adsorbent that retains water but passes fat at the exit end of the extraction thimble; alternatively, it could be done by using an adsorptive-type trapping material in the solid trap so that fats, but not water, are reconstituted in the resultant output fraction. In fact, another of the authors [22] has had success in recovering water-free fat extracts by placing an adsorbent (magnesium sulphate, sodium sulphate) in the thimble downstream of samples of milk distributed on an inert particulate material (sea sand, diatomaceous earth). The approach of using a water-retaining adsorbent as the packing material in the solid trap has not been explored by the authors for total fat assays.

If one is willing to accept the limitations of simultaneous extraction of the water during the extraction and residual carbon dioxide (at ambient conditions) surrounding the raffinate (instead of air) after the extraction, it is faster to simply weigh the sample in the extraction thimble before (*i.e.*, with no pre-SFE drying step) and after the SFE process. The analyst must make this decision based upon the needs and goals of the specific analytical situation.

So far this discussion has focused on just gravimetric assays. For the work described in this example, we attained rapid results that were appropriate for our goals by using gravimetric measurements. There are many alternatives to gravimetric analysis for the total fat content, including the hydrolysis of the mono-, di- and triglycerides, followed by derivatisation of the fatty acids and analysis of the derivatives on a GC. Future work would be aided by the GC analysis, if, for instance, the speciation of unsaturated and saturated fatty acids were relevant and useful. As another possibility, the sample may be injected directly into either a liquid chromatograph (HPLC) or a supercritical fluid chromatograph (SFC). Both of these analytical instruments have the advantage of being able to separate and detect free acids, monoglycerides, diglycerides, and triglycerides without prior saponification and derivatisation.

11.4.1.2.2 The experimental approach

In this example, a series of cumulative extractions at increasing density (at a constant temperature) was carried out initially. Then when the optimum density (0.81 g/mL) was selected -- with optimum determined by the fastest time to constant weight loss, the temperature was systematically varied. This yielded the information that a temperature of 80°C and a density of 0.81 g/mL would provide an initial optimal set of conditions; again the criterion for "optimal" was the fastest time to constant weight loss from the sample. Then an extensive set of statistically chosen parameters was selected to further

refine the method regarding the temperature, density, carbon dioxide flow rate, sample size and extraction time.

11.4.1.2.3 The results of the optimisation experiments

Figure 7 represents the plot of cumulative % recovery of total fats as a function of net volume of extraction fluid at supercritical conditions in the extraction region. The 100% value for these experiments was based upon Soxhlet extraction of the fried snack foods in independent studies. Each data point in Figure 7 is the mean of at least three replicates. Several things are apparent upon studying the results presented in the graph of Figure 7. Three different temperatures were chosen at the same pressure (380 bar). Thus the density decreased as the temperature was increased. The curve representing "80°C" yielded the optimum results.

The shape of the curves indicate that the initial stage of the extraction is limited by solubility. Note the initial rise was greatest at 40°C (0.95 g/mL); at those conditions the recovery reached 82 % when only 60 mL of supercritical carbon dioxide had passed through the extraction thimble. For the same volume of the supercritical fluid (60 mL), the recovery was only 78 % for 80°C(0.81 g/mL), and 58 % for 120°C (0.67 g/mL). However, as the analyte flux begins to diminish (the easy-to-extract solutes are removed, and the more difficult solutes deeper within the matrix are now being removed), the extraction mechanism is no longer limited by saturation solubility. Rather, the extraction mechanism in the later stages of SFE is diffusion limited for

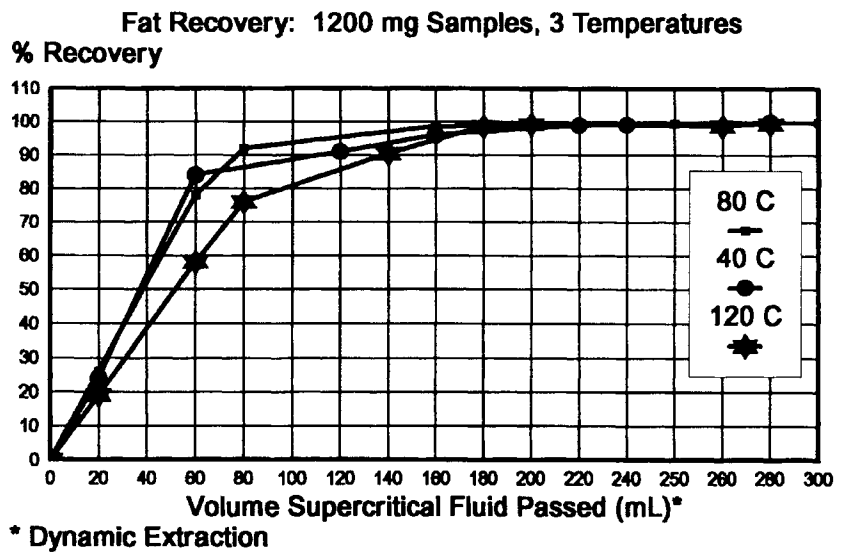

Figure 7: Recovery of total fats in snack foods as a function of volume of supercritical extraction fluid passed through the sample held at the noted extraction conditions.

transfer of the analyte mass from the three-dimensional matrix. This diffusion limiting step is aided by higher temperature. Thus, the 80°C curve shows an enhanced asymptotic approach to the expected 100 % value.

The net effect of the two contributing mechanisms is problematic depending upon many variables. In this case, the solubility at 80°C was only slightly less than that at 40°C; thus, the advantage of much greater diffusion at 80°C compared to the diffusion at 40°C leads to the overall faster 100 % recovery for 180 mL of carbon dioxide compared to 190 mL of carbon dioxide at 40°C. At 120°C, where the density is only 0.67 g/mL, the solubility is so much less than at the corresponding densities at 40°C (0.95 g/mL) and 80°C (0.81 g/mL) that the early rising part of the graph has a significantly smaller initial slope, and even a very favourable diffusion contribution cannot compensate. Empirically, it appears that a favourable asymptotic approach to the final value of recovery is only helpful in the last 20 % of an extraction. This is an example where the empirical experiments yielded information that could not be predicted theoretically. Just as in the case of solubility of solutes in condensed liquids, the solubility of solutes in supercritical fluids cannot be predicted *a priori*. There simply are no models that predict solubility at this time.

Figure 8 shows the same recovery data, but plotted as a function of the dynamic extraction time. This is referenced to the flow rate of the liquid carbon dioxide at 4°C (*i.e.*, constant pumping conditions of the supply fluid), while in Figure 7 the recovery is plotted as a function of the total volume of supercritical carbon dioxide contacting the sample for each extraction temperature and density. Figure 8 illustrates useful information for practical routine analysis (how long does the method take?). For method development, on the other hand, the information in Figure 7 is useful as a means of separating the optimum variables relative to the fluid dynamics and physical chemistry in the extraction thimble [23].

11.4.1.2.4 The final results

During the methods optimisation work, approximately 1100 samples were run on three instruments in 21 working days. During that time, no problems with plugging of the variable restrictors were encountered. The summary of the recoveries and precisions is presented in Table 3; the recommended SFE conditions are summarised in Table 4.

11.4.1.2.5 Sample size considerations – putting this work in context of other work

The nature of the SFE extraction may reduce the amount of sample required for analysis. With fried snack foods extracted for total fat content, the sample size was varied from 0.4 to 5.0 grams and the precisions of the replicate

TABLE 3
Results for Total Fat from Snack Foods for 15 Samples of 9 Products

Set	Sample Size (g)	% Weight Target	N	% Weight Mean *via* SFE	% Recovery SFE *versus* manual	% RSD
1	1.200	34.6	3	34.1	98.6	0.3
2	1.200	36.0	3	37.3	103.6	3.3
3	1.200	23.9	5	23.3	97.5	3.6
4	1.200	36.0	3	34.8	96.7	1.3
5	0.800	34.6	3	35.4	102.3	2.2
6	1.200	34.6	3	34.1	98.6	0.3
7	1.200	36.8	4	35.8	97.3	6.8
8	1.200	23.0	6	22.8	99.1	3.2
9	1.200	24.9	6	23.7	95.2	2.0
10	1.200	38.1	5	37.1	97.4	1.3
11	1.200	38.1	4	37.5	98.4	1.8
12	1.200	23.9	4	24.6	102.9	3.2
13	1.000	45.0	6	43.4	96.4	1.7
14	0.700	36.4	5	38.2	104.9	5.9
15	1.200	29.9	4	31.1	104.0	4.5
Grand Mean					**99.5**	**2.8**

TABLE 4
Final SFE Conditions for Total Fats from Snack Foods

Parameter	Values
Sample Size	0.7-1.2 g
Solid Trap Material	DIOL SPE packing
Extraction Conditions	
Density	0.81 g/mL
Pressure	379 bar (5500 psi)
Temperature	80°C
Static Time	1 minute
Dynamic Extraction Time	45 minutes
Flow Rate (Liquid CO_2)	4.0 mL/min
Solid Trap Temperature	40°C
Reconstitution Conditions	
Reconstitution Solvent	Ethyl acetate
Solid Trap Temperature	40°C
Reconstitution Volume	1.5 mL, Rinse to waste

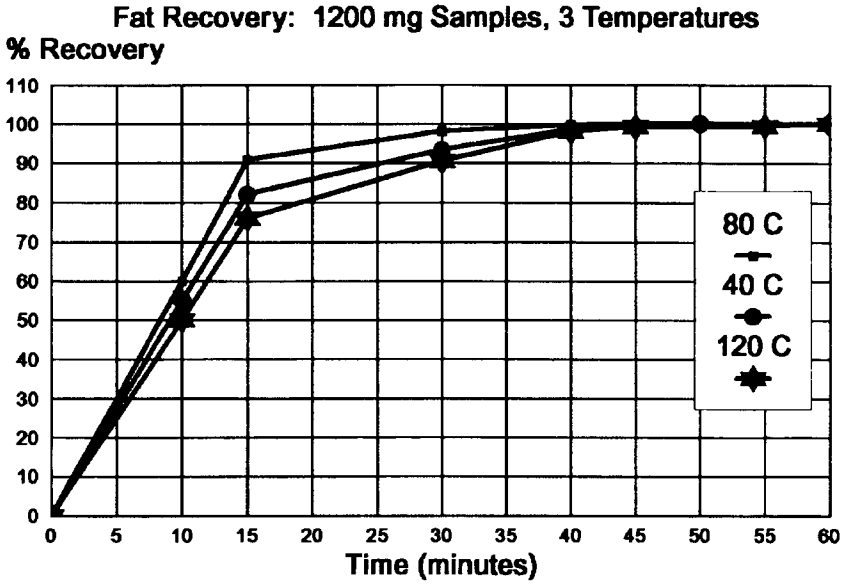

Figure 8: Recovery of total fats in snack foods as a function of time.

experiments were compared. With samples larger than 1 gram, the precision (percent relative standard deviation-% rsd) was about 1.5%. Traditional Soxhlet extractions require sample sizes significantly larger (as much as 30-50 grams) to achieve the same degree of precision. Of course, the smaller sample size requires serious consideration of time-honoured statistical sampling protocols. According to Diehl [24], "If the material to be analysed is homogenous, that is, has the same composition throughout the mass, sampling is no problem. Any portion of the mass may be taken as the sample for the analysis. If the sample is non-homogeneous, however, the problem is not so simple, for a small portion taken at one point may not at all represent the composition of the total mass. Obviously, the problem is more difficult if the particles are large, and if they vary greatly in composition from piece to piece. Under such conditions, the sample first taken, the so-called gross sample, is quite large and this large preliminary sample is subjected to a careful process of alternate crushing and dividing until a suitable amount of material of much smaller particle size remains. In actual practice in industrial and clinical laboratories consideration must always be given to the origin of the sample and the manner in which it was taken and subsequently handled. Often the best analysis is one that is not made at all because the sample was faulty and the labour of any analysis would only have been wasted."

In Figure 9 we see an illustration of the compromise between sample size and replicate precision. The data in Figure 9 are taken from experiments with extraction of total fats from fried snack foods, cookies, cake mix, and chocolate

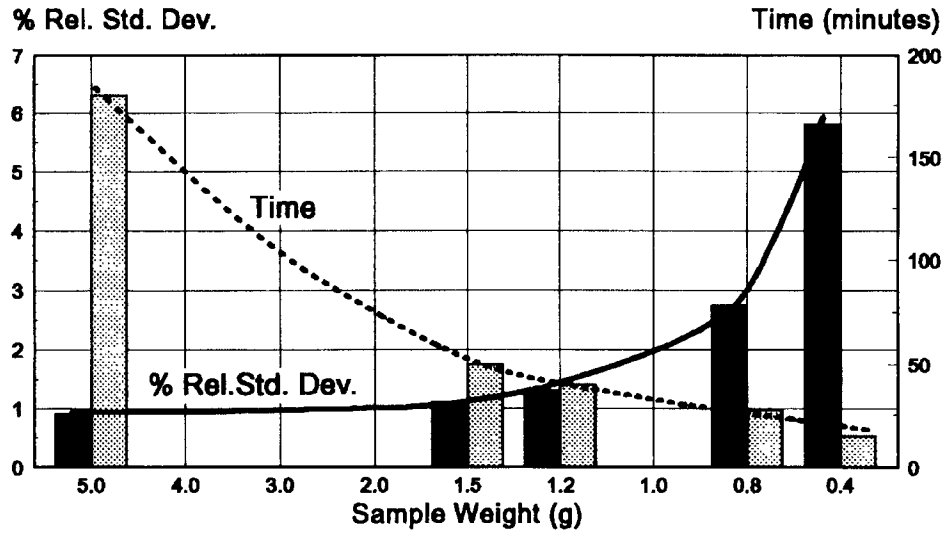

Figure 9: A schematic showing the trade-off between sample size, extraction time, and precision by presenting experimental precision (% RSD) and time-to-extract as functions of sample size.

candy. The bar graph depicts the traditional statistical measurement of % relative standard deviation for a series of replicate extraction recoveries (the left hand Y-axis) plotted against the mass of sample placed in the extraction thimble (the X-axis). The right hand Y-axis parameter is the total dynamic extraction time required to yield the precision shown on the left hand axis plotted against the mass of sample. The resultant of the two dependent variables provides a very practical way to determine the optimum trade-off of sample size and precision. In Figure 9, curved lines have been added to join the top values of the respective bars. The solid line represents the % rsd as a function of sample size. This precision is less than 1% rsd at the 5 gram sample size, and then increases (*i.e.*, degrades) exponentially as the sample size is 1 gram or less. This increase suggests inhomogeneity which leads to "sub-sampling" errors becoming substantial with small sample sizes. This observation is a general one that has been observed in most SFE methods.

Verschuere *et al.* [25] observed a similar trend in the extraction of essential oils and bitter acids of hops when using samples as small as 0.25 grams. They observed, "Compared to conventional methods for extraction of alpha-acids and beta-acids, % rsd's are higher with SFE. Typical values are in the order of 10 % for 6 replicates on the same hop sample. This is due to the small sample size requirements if contamination problems have to be avoided. With the extractor used and taken into consideration that the concentration of the bitter acids in hops range as high as 10 %, 250 milligram sample size is the maximum which can be extracted without breakthrough or contamination (of the lipid-free

essential oils) of the trap. Such small samples may not be representative of the overall sample, biasing the analytical result. According to the Official Methods of Analysis 1990 [26] at least 5 grams should be extracted to compensate for inhomogeneities in the sample. This is also the main reason why, for samples in which the compounds are present in high concentration, off-line SFE is preferred over on-line SFE."

Just as in the case of the hops acids and essential oil extractions where the sample size was optimised for the selective fractionation of acid-free essential oils, in the case of the total fats in foods, we optimised the sample size by considering the time of the dynamic extraction. In Figure 9, the dotted-line curve depicts the time of extraction as a function of the sample size. Ordinarily, this would be a linear function. In the case of Figure 9, we have chosen a non-linear X-axis (sample size) for the sake of clarity of the bar graphs, making it appear that the sample time decreases non-linearly with size. Despite the axis, it is obvious from the overlapping curves that an optimum compromise of time and precision may be reached in the range 1.0 to 1.5 grams of sample. This data, of course, may reflect some other considerations during sampling that exaggerate the sub-sampling errors. For instance, the fried snack foods were not reduced in size to the very small slurry or puree that is usually necessary for efficient extraction. It is estimated that an average particle diameter in the sample in the order of 10-20 microns would be ideal for fast, efficient mass transfer and optimal diffusion. If samples were routinely reduced to this size prior to SFE, it would probably have a very beneficial secondary effect of homogenising the sample and thus reducing sub-sampling errors.

King *et al.* [27] demonstrated the impact of finely subdividing a sample very effectively in the extraction of total fats from meat products by SFE. Figure 10 shows a replot of some of their data. In this illustration, the relative recovery of fat from meat is plotted as a function of the relative amount of supercritical fluid extractant carbon dioxide passed per sample (partition ratio, similar to thimble volume concept outlined in Reference [13]. The two comparative experiments were carried out on samples of link sausage. In the lower curve, the link sausage sample was not finely ground prior to SFE. The upper curve shows the relative recovery of a similar replicate sample, but in this case the link sausage sample was finely ground in an electric grinder prior to SFE. The comparative results are what has been observed in many other extractions. In any SFE experiment, the early part of such a curve rises rapidly on the Y-axis in the beginning where the rate-limiting step is analyte solubility. The limit of the sample flux is the saturation solubility of the analytes under the conditions of the extraction (in this case, 80°C, 0.95 g/mL) where the analyte within the matrix is easily accessible to the supercritical carbon dioxide. As the analytes on the outer periphery of the matrix are removed, the less accessible analytes deeper within the three-dimensional matrix are extracted at a slower rate. This rate is diffusion-limited. There are several variables that can aid this diffusion, and average particle diameter of the sample matrix is one of the very

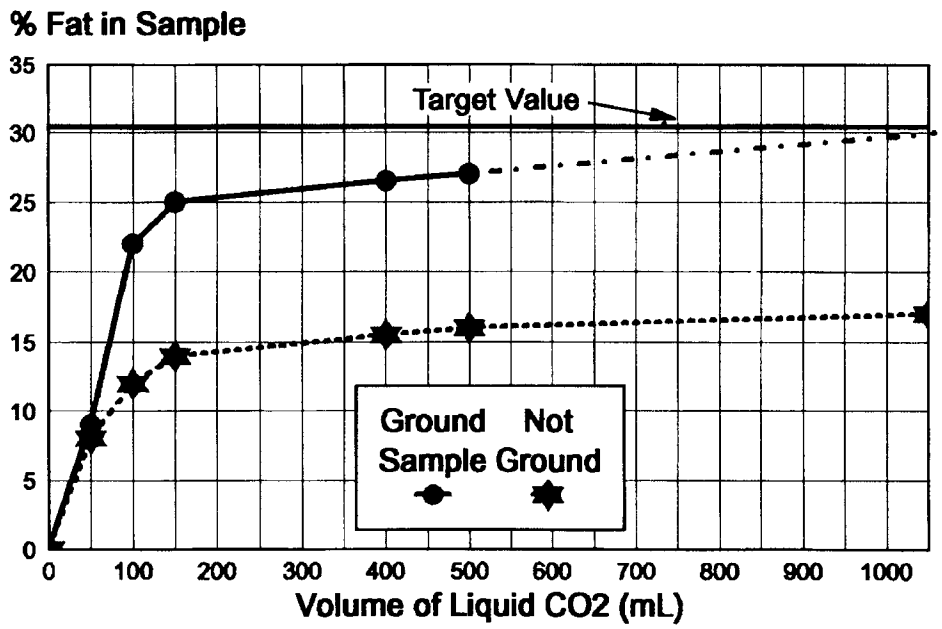

Figure 10: Comparison of recoveries of total fats from meat with and without reducing particle diameter by grinding the sample before extraction. Data courtesy of J. King [27].

significant parameters to be adjusted. Thus, we see in both curves in Figure 10 the last fraction of the analyte is removed at a slower rate (sample flux). However, the fluid diffusion rate is more favourably matched to the smaller particle diameters in the ground sample so the extraction is finished more quickly -- *i.e.*, the analyte is fully recovered from the matrix in a much shorter period of time. The net extraction curve (in both cases) is a compromise of the early solubility-limit and the later diffusion-limit.

11.4.1.3 Selective Fractionation of Cholesterol from Fat Containing Samples via *SFE*

Cholesterol [28] has been selectively extracted from cod liver oil samples (an oil-free extract from a sample that is more than 99 % lipid). This is shown in Figure 1. The selective fractionation was carried out quite simply by starting at a mild set of extraction conditions: 60°C and 0.40 g/mL (115 bar). The cholesterol was extracted from a sample of 1.0 g of cod liver oil that had been mixed with diatomaceous earth and then placed in the extraction thimble. A ten-minute extraction at a flow rate of 2.0 mL/ minute was sufficient to remove all of the cholesterol. After this analyte was reconstituted in a rinse solvent of 1:1 methylene chloride: acetonitrile, the resultant solution was injected into an

HPLC. Cholesterol and other similar sterols were eluted and quantitated in a 6 minute chromatogram. Meanwhile, the remaining cod liver oil sample was further extracted with more aggressive conditions: 40°C and 0.93 g/mL (310 bar). A 20-minute extraction at a flow rate of 2.0 mL/minute extracted all of the oil/lipids from the extraction thimble. This extract was reconstituted with the same solvent, but in a different collection vial. An aliquot of this solution was injected into the same HPLC under the same chromatographic conditions and the lipids were eluted over a period of 12 minutes and quantitated. The HPLC had a diode array detector set at wavelengths of 200-226 nm and the entire unresolved mono-, di- and triglyceride peak envelope was integrated as a total sum. In the previous HPLC chromatogram, the cholesterol and sterols were individually separated and quantitated at the same low wavelength settings. This experiment has been repeated on a variety of baked food products and yields the same two-step fractionation of cholesterol and total lipids. In the case of baked goods, a longer extraction time as well as a higher flow rate were used in both extraction sub-steps. In the first step, a 20-minute extraction at 2 mL/minute was used for the cholesterol. In the second step, a 30-minute extraction at 4 mL/minute was used.

TABLE 5
Conditions for SFE of Cholesterol and Other Sterols from Cod Liver Oil – Step 1

Parameter	Values
Sample Size	1.0 gram
Solid Trap Material	DIOL SPE packing
Extraction Conditions	
Density	0.40 g/mL
Pressure	115 bar (1670 psi)
Temperature	60°C
Static Time	1 minutes
Dynamic Extraction Time	10 minutes
Flow Rate Liquid CO_2	2.0 mL/min
Solid Trap Temperature	20°C
Reconstitution Conditions	
Reconstitution Solvent	1:1 Methylene Chloride:Acetonitrile
Solid Trap Temperature	20°C
Reconstitution Volume	1.00 mL

TABLE 6
Conditions for SFE of Neutral Lipids from Cod Liver Oil – Step 2

Parameter	Values
Sample Size	1.0 gram
Solid Trap Material	DIOL SPE packing
Extraction Conditions	
Density	0.93 g/mL
Pressure	310 bar (3830 psi)
Temperature	40°C
Static Time	0.5 minutes
Dynamic Extraction Time	20 minutes
Flow Rate Liquid CO_2	2.0 mL/min
Solid Trap Temperature	20°C
Reconstitution Conditions	
Reconstitution Solvent	1:1 Methylene Chloride:Acetonitrile
Solid Trap Temperature	20°C
Reconstitution Volume	1.80 mL

For larger samples with high fat contents extracted with an SFE with a solid trap as the collection device, it is helpful to stop every 10 minutes in the second extraction sub-step to rinse a 600-μL reconstitution volume into the collection vial. This aids in full recovery of the fats, since a solid trap has a limited mass capacity that is defined by the open volume between and within the packing particles (typically, 0.5-0.7 mL). The total 1.80 mL (sum of the three sub-rinses) is vortexed prior to injecting an aliquot into the HPLC. There are many alternate means of the quantitation in addition to the HPLC assay [16]. The analyst should choose the appropriate one for the equipment available in the laboratory. Tables 5 and 6 provide the conditions for the cholesterol-lipid fractionation from cod-liver oil.

King [29] has repeatedly carried out SFC separations of similar samples where the cholesterol and lipids were not pre-fractionated by SFE. In these cases, he used a density program for the separation of the classes. Several interesting observations were made by King, and it was because of his observations and at his suggestion that the current authors carried out the SFE fractionation. One observation was that, during an SFC density program, cholesterol and compounds such as alpha-tocopherol (and associated esters) eluted around the density of 0.40 g/mL (the SFC experiments were at 120°C), whereas the lipids did not begin to elute until the SFC column was at a density of approximately 0.50 g/mL. The broad unresolved (individual peak resolution may be obtained *via* high performance packed column SFC, if

desired) lipid fraction eluted until approximately a density of 0.60 g/mL was reached. This observation was also made with samples of lanolin from sheep wool. In that case, cholesteryl acetate eluted in the region of a density of about 0.4 g/mL and a similar envelope of lipid peaks eluted between the densities of 0.50-0.60 g/mL. This is another example of the synergistic effect of using data from SFC to anticipate conditions for SFE; of course, the opposite is also true. In subsequent SFE experiments, we have found that at the lower temperatures (40-60°C *versus* 120°C), the cholesterol and similar plant sterols/sterol esters extract at the same low density of approximately 0.40 g/mL. Interestingly, at the lower temperatures, the lipid fraction is extracted at a higher density range (0.60-0.70 g/mL). This provides even more selective fractionation possibilities with temperature as an influential parameter.

These experiments and observations have led to the description of a zone in a table or graph of density-temperature-pressure values for SFE called the "fat band." This is seen in Figure 11, where density is plotted as a function of temperature at constant pressure, resulting in the curved isobaric lines. Note the curves are following the phase diagram and we are seeing segments of sigma-shaped lines. The "fat band" is labelled. The utility of this diagram is that any SFE conditions below the bottom boundary of the fat band are conditions in which no fats or lipids (mono-, di- and triglycerides) will extract. Thus, if lipid-free fractions are desired, any sets of conditions of temperature-pressure-density below the boundary will be sufficient. Above the upper boundary of the fat band, any sets of conditions are almost assured to extract the lipids. Within the band itself, the results are unpredictable, and may depend upon the actual sample matrix as well as the extraction parameters of flow rate and length of dynamic extraction time as to whether any lipids will extract.

11.4.1.4 SFE of beta-Carotene in Fruits and Vegetables

Vitamin A[3] activity in foods and food products serves as an example where typical problems arise with traditional liquid solvent extraction and then where SFE has been used to address these concerns [30]. In addition to the routine assay of food products, there is a considerable amount of research being conducted on the role of carotenoids and xanthans as antioxidants in the human body. This antioxidant-role may address many health concerns such as aging and various diseases. The "friendly-extracting-environment" of SFE has some merit of consideration for such studies, particularly with regard to the lesser possibility of oxidation of the analytes during the sample preparation step.

---

[3] Its precursor, beta-carotene, is often the component that is added or analyzed.

Two fundamental building-blocks of natural product chemicals are isopentyl pyrophosphate and isoprene [31, 32]. Isoprene is incorporated in compounds known as isoprenoids. The function and occurrence of isoprenoids cover a very broad range in nature; according to Stryer [31], "-isoprenoids can bring delight by their colour as well as their fragrance. Indeed, isoprenoids can be regarded as the sensual molecules! The colour of tomatoes and carrots comes from carotenoids, specifically lycopene and beta-carotene, respectively."

Carotenoids[4] are 40-carbon compounds made up of eight isoprene units. Carotenoids serve as light absorbing molecules in photosynthesis and also protect certain tissues from the deleterious effects of light. Beta-carotene is the precursor of vitamin A (which does not occur in plants). Beta-carotene occurs abundantly in the liver oils of fish and is extracted from that matrix commercially. Nutritionists recommend tomatoes, carrots, and green vegetables in daily quantities in order that carotenoids can be converted into vitamin A, a compound necessary for vision and other vital functions.

Carotenes are relatively non-polar compounds which are soluble in lipophilic solvents. Most of the known natural carotenoids are oxygenated compounds, often termed xanthophylls, and may be classified as derivatives of the hydrocarbons lycopene or alpha-, or beta-carotene. Although alpha, beta, and gamma all have vitamin A activity in food products, only beta-carotene is used for calculating the vitamin A in vegetables. Carotenes are readily oxidised by light, air and many of the typical extraction solvents (or solvent impurities) including tetrahydrofuran (THF), chloroform, methylene chloride and hexane.

Traditional official methods, such as the AOAC method for pre-analytical extraction of vitamin A-active compounds, call for 300 mL of extraction solvent. The traditional method includes significant evaporation of a chlorinated solvent to concentrate the large volume, followed by centrifugation of the extract. These steps are very labour intensive operations. In addition, these operations are carried out in the open laboratory, necessitating protective lighting.

When SFE is used for sample preparation, the sample is weighed, manipulated, and then placed in the sample extraction thimble. After those initial steps, the sample is no longer in contact with air, oxygen, light or significant amounts of organic solvent until just before introduction ("just-in-time" concept) into the analytical measuring device. The amount of organic

---

[4] Carotenoids have been the subject of scientific research for the past 160 years. A compound named carotene was isolated from carrots by Wackenroder [33] in 1831. In 1906, Tswett [34] investigated the colored components of leaves and thus invented chromatography. In 1941, Kuhn [35] successfully separated carotene into three separate isomers by liquid adsorption chromatography.

solvent used for the sample reconstitution is one or two orders of magnitude less than conventional methods (about 1.5 mL); thus very high purity (high cost) solvent[5] can be used to preclude decomposition from impurities as found in lesser quality solvents. Moreover, no centrifugation is required, nor is there a need for protective lighting since the sample and the sensitive extracted components are confined within the extraction thimble and closed tubing of the instrument until the extract is output in the receiving fraction vial. In this last process, the extracted vitamin A-active compounds are reconstituted in a 1.5-mL solution of an appropriate organic solvent. The resulting solution is dispensed from the closed tubing environment (absence of light, air, and oxygen) directly into an amber-coloured, capped automatic sampler vial. In a fully automated system of the SFE-plus-analytical instrument, the resulting solution is injected into an HPLC (for example) for the analytical measurement less than 2 minutes after reconstitution.

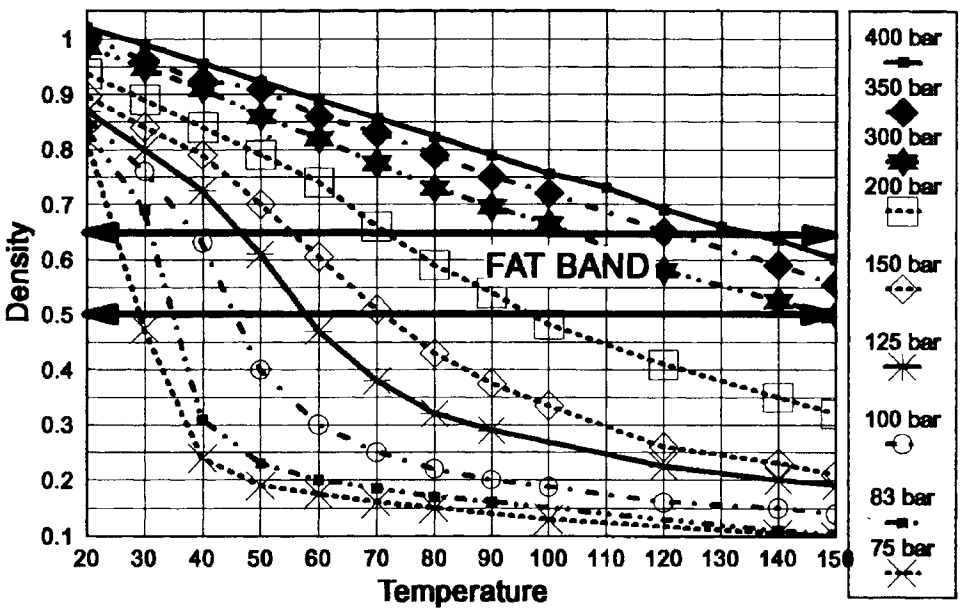

Figure 11: Illustration of "Fat Band" in plot of density as a function of temperature at constant pressure.

---

5 The disposal of organochlorine solvents costs as much or more than the purchase price of the solvent. Thus, a 100-fold decrease in solvent use can reflect a 200-fold decrease in solvent costs. Further, workplace environment regulations are becoming increasingly more stringent and increased emphasis on health considerations of laboratory workers suggests that SFE may provide improvement in several areas of current concern.

In the situation where vitamin A-active compounds are being extracted from fruits and vegetables, the carotenes are mostly in plant cell chloroplasts. This environment does not permit easy access by low-diffusivity organic liquids which are not soluble in water (*i.e.*, methylene chloride or hexane). Supercritical carbon dioxide (higher diffusivity than conventional liquids, by 2 orders of magnitude) handles problems associated with the water-containing chloroplasts in an easy manner. The mechanism that is responsible for SFE's advantage has not been clearly elucidated; in fact, there is some indirect evidence that this advantage is most likely due to the pre-treatment of the sample -- specifically, the homogenisation with ethyl alcohol. Tonucci and Beecher [36, 37] have reported recoveries of carotenoids from food products such as tomato paste, canned pumpkin, fresh spinach, red palm oil, butter and cheese by using SFE as part of the sample preparation. They noted that the recoveries varied depending upon the type of sample. Among the many parameters that they varied to account for this was the addition of alcohols to the sample thimble along with the sample. They observed (although not quantitatively) that isopropanol added in an experiment using only static extractions greatly enhanced recovery; in fact, in a similar experiment with no addition of any alcohol, little recovery was achieved. Another very valuable observation was that if only dynamic extraction mode were used (no static extraction time), they also saw very little recovery. Marsili and Callahan [30] extended this work to other foods and examined the static time quantitatively. This data is seen in Figure 12 where the % recoveries for alpha- and beta-carotenes are plotted as a function of the static extraction time (a subsequent dynamic time of 10 minutes was constant for all experiments). A static time of 20 minutes was needed for

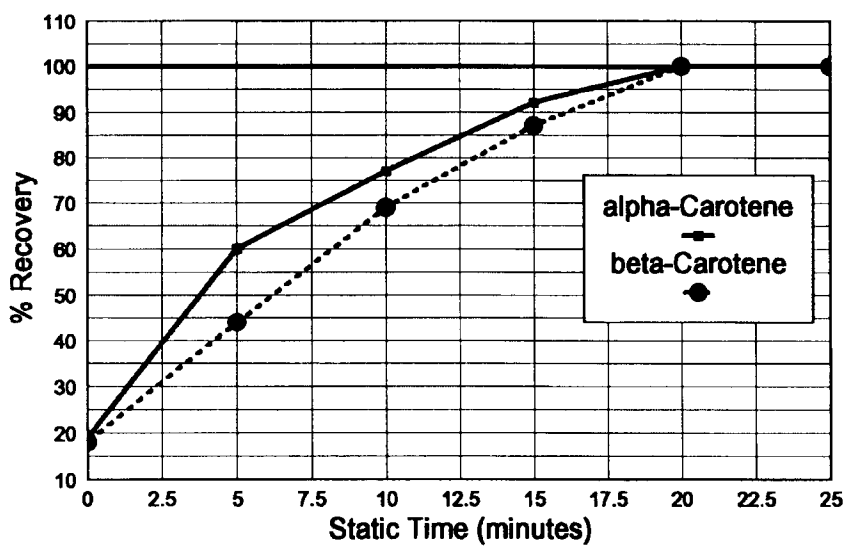

Figure 12: Recoveries of α-and β-carotenes as functions of static extraction time with a constant dynamic extraction time of 10 minutes.

both analytes in order to achieve 100 % recovery. The plot of the recovery of alpha-carotene *versus* time had a slightly steeper initial slope to the curve than did recovery data for beta-carotene. Although this was not significant for the development of this method, it is suggestive that the alpha-carotene is more soluble in supercritical fluid carbon dioxide than the beta-carotene.

This is consistent with the observation by Giddings *et al.* [38] that the order of elution of the compounds in SFC was alpha-carotene followed by beta-carotene. They easily separated the two compounds using only carbon dioxide (no modifier) in 26 minutes at chromatographic conditions of 40°C and 0.82 g/mL (170 bar). Gere [39] extended the SFC separation to include lycopene and added ethyl alcohol as a continuous modifier to the supercritical fluid carbon dioxide. Again, the order of elution was lycopene, alpha-carotene, and beta-carotene. The order of elution in SFC is usually in the same rank order as the intrinsic solubility[6]. In that regard, Tonucci and Beecher [37 reported difficulty in achieving greater than 60 % recovery of lycopene from tomato paste using only static extraction with no appreciable dynamic step. This suggests that the problems are in the removal from the matrix rather than intrinsic solubility limitations. Also, their static extraction was carried out without on-line modifier addition, that is, the modifier was only added to the extraction thimble in the beginning of the SFE. It would be expected that use of a continuous on-line addition of modifier along with a combination of static and dynamic steps may significantly enhance the recovery of lycopene.

The total elapsed time is substantially less with SFE extraction than with conventional liquid-solid extractions. Moreover, the hands-on time required of the operator for the pre-extraction steps prior to SFE (5-10 minutes) would be only a fraction of the total hands-on sample preparation time required by employing tradition preparation processes (30 minutes) -- an advantage over traditional methods. In the case of the vitamin-A active compounds, the extraction and analysis for four samples with two replicates each (a total of 8 extractions and 8 analyses) using the conventional manual method requires 4 hours. For the combined SFE and analyses for the 8 extractions and 8 analyses, the total elapsed time is 3 hours. However, until an operator has worked with both SFE and traditional liquid-solid sample preparation, it is not obvious that the operator intervention (or hands-on) time is much different. It is estimated that this may be as much as 70 % of the 4 hours in the traditional method and as little as 10 % in the 3 hours of the SFE method.

---

[6] Both of the SFC publications point out the value of searching prior litera-ture to find both SFE and SFC papers to aid in methods development. Furthermore, with packed-column SFC (used in both studies), the solid packing in the SFC column can be analogous to solid matrices in SFE.

Thus, sample throughput of the laboratory was increased *while* the hands-on labour was substantially reduced.

Callahan and Marsili [30] published an SFE method for the extraction of alpha- and beta-carotene from carrots, broccoli, yellow squash, zucchini, collard greens, kale, mustard greens, corn, and turnip greens. In their method, they first combined 1 gram of sample with 2 grams of ethyl alcohol and thoroughly blended it in a Biohomogenizer (Biospec Products, Bartlesville, Oklahoma) for 3 minutes. In order to absorb any moisture, a clean, inert material, such as diatomaceous earth was added. For a mixture as described above (1 g sample + 2 g ethanol) approximately 2 gram of inert material would be adequate. This resulting mixture would be transferred into the SFE extraction thimble and extracted by the conditions listed in Table 7.

Several valuable observations were made in this study concerning various choices of materials and details of individual sub-steps of the SFE process. First of all, the extracted analytes are deposited onto solid trapping material at the exit of the flow restrictor (or nozzle) as the supercritical carbon dioxide is decompressed to a gas (losing its solvating power). The trap could have been packed with any number of materials, and two were studied here: stainless steel beads and octadecylsilane (ODS), a common packing for HPLC and SPE. In this case, the SPE grade ODS packing was used. Although stainless steel beads are capable of trapping the carotenes when no ethanol

TABLE 7
Conditions for SFE of Carotenes from Fruits and Vegetables

Parameter	Set points
Sample Size	1 g
Solid Trap Material	Octadecylsilane
Extraction Conditions	
Density	0.93 g/mL
Pressure	338 bar (4900 psi)
Temperature	40°C
Static Time	20 minutes
Dynamic Extraction Time	10 minutes
Flow Rate Liquid CO_2	1.5 mL/min
Solid Trap Temperature	10°C
Reconstitution Conditions	
Reconstitution Solvent	Isooctane
Solid Trap Temperature	40°C
Reconstitution Volume	1.00 mL (20 :L injected in HPLC)

modifier was used, with the stainless steel beads, a significant portion of the carotenes passed on through the trap and was found in the waste line when as little as 200 μL of ethanol modifier was mixed with the sample in the extraction thimble. The ODS material was capable of retaining all of the carotenes when large amounts of ethanol were used, provided the trap temperature was maintained no higher than 10°C. It was also noted that the ODS trap needed to be "primed" at the beginning of each day with a rinse of 2.0-5.0 mL of ethanol, followed by at least as much iso-octane. This step assured an efficient reconstitution step for the remainder of the working day. Several rinse or reconstitution solvents were considered. Because the ODS material has a high retentivity for carotenes, the solid trapping material must be rinsed (during the reconstitution step) with a solvent that readily dissolves these compounds. Methylene chloride and chloroform both have the solvent power to rinse the carotenes easily from the ODS. However, frequently, significant decomposition, perhaps as much as 50 % of the original beta-carotene, was observed. Both of these solvents also presented injection band-broadening in the HPLC method that was unacceptable. Hexane has much less solvent power for dissolving the carotenes, but it was sufficient to displace all of the precipitated carotenes from the solid trap with as little as 1.0 mL of solvent. Again, some problems developed depending upon the purity (grade) and age of the hexane. Degradation and isomerisation of beta-carotene was seen when the trap was rinsed with hexane that had been in the rinse solvent reservoir for more than 24 hours. This problem was alleviated by changing the hexane in the rinse reservoir daily, purging with helium at regular intervals and covering the exterior of the glass rinse bottle with aluminium foil to prevent exposure to light. While the decomposition was more prevalent with lower quality solvent grades, it was present even in top quality hexane. The problem can be completely eliminated by replacement of the hexane with isooctane. This problem has been seen in other SFE experiments with other compounds that are susceptible to oxidation. It is speculated that hexane typically will have low levels of unsaturated (double bond) compounds. When exposed to air and light, these compounds easily react with oxygen to form peroxides and peroxyacids. These secondary compounds then react with carotenes to form decomposition products [27].

Figure 13 shows a comparison of results obtained by Callahan and Marsili [30] with SFE and liquid-solid solvent extraction for the recovery of 10 vegetables. The carrot samples were fresh. Collard greens, turnip greens, diced turnips with greens, kale mustard greens, and diced yellow squash were wet-pack frozen. Broccoli, corn and zucchini were individually quick-frozen. For these vegetables, SFE extracted an average of 23 % more beta-carotene than solvent extraction. (Typical levels of beta-carotene in these vegetables are on the order of 0.5 to 100 ppm.) The tendency for SFE to provide higher recovery of beta-carotene may be caused by more favourable diffusivity of supercritical fluid carbon dioxide compared to liquid solvents as

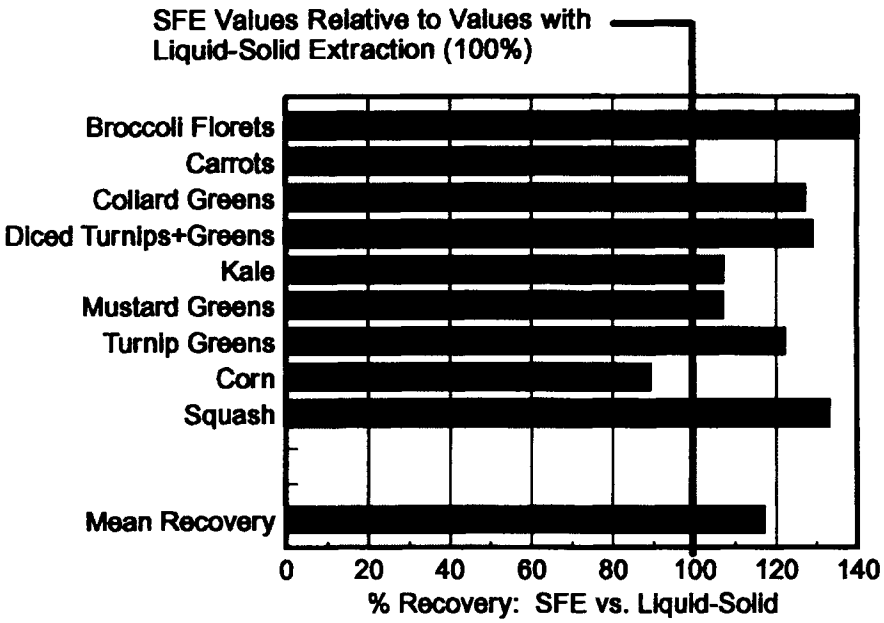

Figure 13: Recoveries of β-carotene from fruits and vegetables by SFE relative to liquid-solid extraction.

well as a better understanding of the impact of solvent decomposition products on the labile analytes.

Of the ten vegetables extracted, only corn yielded lower extraction recovery with SFE compared to liquid solvent extraction. Corn posed a difficult problem for SFE, presumably due to its high solids and starch content. When the corn sample was extracted by SFE using the method described in Table 7, a second extraction -- if performed with addition of another increment of ethyl alcohol -- would be sufficient to recover the remaining beta-carotene. This suggests that a continuous on-line addition of ethyl alcohol would have accomplished full recovery in the first step. With simple addition of modifier to the extraction thimble before the onset of the SFE extraction step, the ethyl alcohol is usually removed in the first minute of the 10-minute dynamic step. Perhaps continuously refreshing this with an on-line modifier pump would be advantageous.

11.4.1.5 SFE of Vanilla Flavour Constituents from Baked Cookies

Anklam and Mueller [40] successfully extracted vanillin and ethylvanillin from vanilla-flavoured sugar cookies with SFE. They used mild conditions of 45°C and 0.80 g/mL (189 bar). With a flow rate of 2.0 mL/minute of carbon dioxide and a dynamic extraction time of 10 minutes, they achieved good results in recovery, efficiency, and precision. The average recovery for 14

samples, from various European countries, ranged from 98-104% of the declared values on the commercial packages. The concentration range was typically 10 to 60 mg per gram of sample. The coefficient of variation (% relative standard deviation) ranged between 1.3-4.0 %. They stated, "This SFE method is both convenient and reliable for HPLC analysis for said flavouring compounds. Since this method does not involve the extraction of sugar but only vanillin and ethyl vanillin, no overloading of the HPLC column will take place. Comparing the SFE method to the classical method (Soxhlet) a shorter extraction time (10 minutes compared to 3-4 hours) is needed and the use of solvent is minimised. On determination of concentrations of the said flavour compounds in the various sugar cookies, a good correlation was found with the declared values on the package (when given). Vanillin is the flavour compound used in the majority of investigated commercial vanilla sugars."

11.4.1.6 SFE of Capsaicin from Peppers

It is interesting to discuss the SFE of capsaicin next, directly after the discussion of the SFE of vanillin. Capsaicin is an amide (containing isoprene units) derivative of vanillin. Ten parts per million can be detected by tasting. Capsaicin is the compound responsible for the pungency (heat) of Jalapena and other peppers. It is the pungent principle in fruit of various species of *Capsicum Solanaceae.*

TABLE 8
Conditions for SFE of Vanillin and Ethyl Vanillin in Sugar Cookies

Parameter	Values
Sample Size	1 g
Solid Trap Material	Diol
Extraction Conditions	
Density	0.80 g/mL
Pressure	189 bar (2740 psi)
Temperature	45°C
Static Time	0 minutes
Dynamic Extraction Time	10 minutes
Flow Rate Liquid CO_2	2.0 mL/min
Solid Trap Temperature	20°C
Reconstitution Conditions	
Reconstitution Solvent	Methyl Alcohol
Solid Trap Temperature	20°C
Reconstitution Volume	1.00 mL (10 µL injected in HPLC)

The "heat" of a food product may be adjusted by adding capsicum oleoresin. This oleoresin (oil) is derived [41] from various fruits such as cayenne pepper. Capsicum is the dried ripe fruit of *Capsicum frutescens L., Capsicum Solanaceae* (known in commerce as African chillies), or *Capsicum annuum L.* (known in commerce as tabasco pepper) or of other hybrid species of peppers. The oleoresin makes up approximately 0.1-1.0 % of the weight of the dried fruit. Considering the previous suggestion that 10 ppm can be detected by tasting, the term "hot peppers" (which could contain as much as 10,000 ppm) is meaningful to those who may not have acquired a taste for such food products.

The official method of the American Spice Trade Association (ASTA) requires extraction with 50 mL of ethyl alcohol saturated with sodium acetate at 60°C for 2 hours. An SFE method developed by Callahan and Marsili [42] allows the extraction in less than 25 minutes. As with most of the previously discussed food-related SFE sample preparations, capsaicin extractions require some specific pre-extraction treatments in order to achieve full efficiency. It should be noted here, that the SFE method offers a significant advantage over the traditional method in that the SFE approach will provide a lower temperature, non-oxidising atmosphere. The 60°C, two-hour conventional extraction provides an oxidising, higher temperature atmosphere which is conducive to oxidation and variation of the sample integrity. It is generally accepted that cooked foods containing peppers taste less "hot" because the capsaicin content has diminished.

The sample pre-extraction begins with taking a representative sample from the produce to be analysed: 100-gram samples are considered to be the minimum to take at the outset. Homogenise this gross sample in a blender or food processor for two minutes. Then, take a representative 500-milligram sample of the homogeneous gross sample and blend it with 0.5-1.0 grams of ethyl alcohol for 2-3 minutes. As discussed previously, this will result in a semi-solid puree or slurry with small particle diameter solids. Mix this resulting puree with a sufficient amount (perhaps 3 grams) of an inert dispersant solid such as diatomaceous earth to absorb the liquid. Transfer all of this mixture to the extraction vessel (thimble) and proceed with the SFE steps. Table 9 gives the conditions for the SFE.

While the description seems similar to other samples, the pre-SFE sample manipulation for this application is somewhat different than that for two other examples given previously. For capsaicin from peppers, the sample can be blended with either water or ethanol to produce the puree. For the example of beta-carotene from fruits and vegetables, *it was found to be necessary to use just ethanol* in the size-reducing blending step. Also note that in this application, the analytical sample of 500 milligrams of homogenised pepper was the sample subjected to further blending with water. For the example of fat from olives, *the water-assisted chopping to*

produce smaller particle sizes must be done with the gross chopped sample. This is because the fat globules from the olives tend to stick to the blades of the rotor during the size reduction chopping; with an analytical-size sample, the error introduced by this loss of fat can be significant.

Because capsaicin is soluble in ethyl alcohol, the modifier requires some special consideration during the extraction step and the reconstitution step. There are several ways to do this. If solid trapping is used, it is helpful to think of the solid trapping material as a small GC-like column during the extraction sub-step. Any mobile phase (the expanding carbon dioxide) must remain as a gas during this operation so that the precipitating analytes stay in the collection zone. This is normally not a problem as the supercritical fluid has expanded to gaseous carbon dioxide. However, when a modifier is added to the thimble, or if liquid modifier is continuously added (via either a pre-mixed tank or injection into the carbon dioxide stream by a separate pump), care must be taken to assure that the liquid modifier does not condense to a liquid in the solid trap and thereby rinse some of the analytes on through to the waste container. This condensation (with subsequent trap flooding) can be avoided by raising the temperature of the solid trap during the extraction to above the boiling point of the modifier liquid. In the case of ethyl alcohol this is 78°C. This disturbs chemists sometimes as there is a fear of thermally decomposing or oxidising the compounds at such a temperature.

TABLE 9
Conditions for SFE of Capsaicin from Peppers

Parameter	Values
Sample Size	0.5 g
Solid Trap Material	ODS
Extraction Conditions	
Density	0.70 g/mL
Pressure	115 bar (1670 psi)
Temperature	40°C
Extraction Fluid	CO_2, 100-200 µL EtOH dispersed on sample
Static Time	15 minutes
Dynamic Extraction Time	10 minutes
Flow Rate Liquid CO_2	2.5 mL/min
Solid Trap Temperature	5-10°C
Reconstitution Conditions	
Reconstitution Solvent	LC mobile phase
Solid Trap Temperature	30°C
Reconstitution Volume	1.00 mL (10 µL injected in HPLC)

TABLE 10
Comparison of SFE of Capsaicin to Traditional Liquid Extraction

Sample	Recovery (ASTA Heat Units)		Precision (Standard Deviations)	
	Liquid Extraction	*SFE*	*Liquid Extraction*	*SFE*
1	28.1	32.6	± 1.2	± 2.1
2	24.7	27.6	± 0.8	± 1.7
3	37.2	35.4	± 0.7	± 3.2
4	47.0	40.3	± 2.7	± 1.1

Furthermore, one of the advantages of carbon dioxide-based SFE is that normally extractions are carried out at low temperatures. The resolution of this dilemma can be as simple as adding a short sub-step in the beginning to remove the ethyl alcohol in the extraction thimble. Recall that the capsaicin extraction is carried out at 40°C and a density of 0.70 g/mL. The ethyl alcohol can be readily removed at a density of 0.25 g/mL at 40°C in a short three-minute dynamic extraction step. This is well below the "threshold-density" at which the capsaicin would extract or be soluble in supercritical carbon dioxide. The mechanism of using the carbon dioxide to remove ethyl alcohol from the extraction thimble under supercritical conditions is quite different than the evaporation mechanism that would be taking place in the solid trap after expansion of the carbon dioxide plus ethyl alcohol to a mixture of gas plus condensing liquid. *Note that the fact that ethanol can be pre-extracted ahead of the analyte of interest demonstrates that the role of the modifier in this application is mainly matrix modification; had a more polar solvent (like that afforded by a mixture of ethanol in carbon dioxide) been necessary to solvate the capsaicin, the pre-extraction step to remove the ethanol would have been detrimental to the extraction of the capsaicin.*

A different approach to collecting analyte while dealing with quantities of modifier condensing in a cold collection trap is to place the capillary line exiting the trap directly into a 5-mL volumetric flask. Then, any analyte that inadvertently passes through the trap will be deposited in the volumetric flask. At the end of the extraction, the remaining analyte on the solid trap would normally be rinsed off into a small auto-sampler vial. This solution in the vial may be added to any residual in the volumetric flask. This resultant solution mixture is then brought to the volumetric mark on the flask, shaken for homogeneity and an aliquot (*i.e.*, 10-20 µL) is injected into the HPLC. This application also represents a case where sub-ambient solid trapping is unnecessary and the solid trap could be replaced with liquid trapping in a vessel containing an appropriate trapping solvent (because the capsaicin exhibits little or no significant vapour pressure at room temperature).

Table 10 shows the results obtained by Callahan using the SFE method outlined in Table 9 and compares the results to those typically obtained using the standard ASTA liquid-solid method. As can be seen in Table 10, the results of the SFE extraction and the standard ASTA liquid method give similar results in terms of sample recovery. The precision appears to be somewhat better for the classic technique, although the SFE precision is deemed adequate. The difference may be due to the fact that the sample weights used for liquid extraction were 5-10 times larger than for SFE. If the same size sample were used in SFE as in the liquid extraction, the SFE time with all of the other conditions being the same will necessarily increase by the same factor of 5-10 times (from 25 minutes up to 250 minutes), taking away any time advantage of SFE over the traditional method. There are many permutations in between those extremes; however, it is important to note that the reduction in precision is only a factor of 1.5 times -- a reasonable compromise with the reduced time and operator effort. Callahan and Marsili specifically chose these conditions and found the compromise acceptable.

11.4.2 Summary of other Food Applications employing SFE as Part of the Sample Preparation Process

Several detailed examples have been presented to show how SFE can be applied to a wide range of samples. The following table summarises other work of interest to those involved in the analysis of food products, as well as highlighting some of the results discussed in detail in this chapter.

11.4.3 Basic Method Development

There are several approaches to method development in SFE. They range from an exhaustive study of the effects and interactions of as many as 10 parameters, to a simple heuristic, empirical approach. Experienced SFE experimenters already have their own preferred approach to SFE method development and do not need yet another opinion in this area. However, those new to the technique may appreciate some guidance in the first tentative steps to be taken. One approach to an SFE methods development strategy has been outlined in reference [13]. Essentially, the idea is to start looking at the quantitative feasibility of applying SFE to a particular sample by starting with the simplest sample systems and then moving to increasingly more complex sample systems:

- Standard solutions of analytes
- Simulated samples
- Real samples.

As described in Reference [13], a phased approach to varying SFE and sample parameters is superimposed on the progression of sample complexity. This is outlined in Figure 14. The approach shown in Figure 14 can be turned into an

experimental template as shown in Figure 15. Once the methods development work has evolved into work with the real (complex) samples, Knipe *et al.* [13] note that more rigorous experimental designs as outlined by Otero-Keil [66] or textbooks on appropriate statistical design of experiments [67, 68].

11.5 SUMMARY AND CONCLUSIONS

In this chapter, we have discussed some of the basic principles underlying SFE as well as general approaches to the instrumentation used for optimal application of supercritical fluids to the area of analytical-scale SFE. The latter part of this chapter dealt with the application of SFE to specific, representative food product sample preparation. It is expected that these and other new applications will support some needed challenges in food analysis.

The advantages of applying SFE to foods and food products should include a significant enhancement in laboratory productivity. The illustrations of selective SFE fractionation provide a previously unattainable result from traditional single-solvent extractions, thereby allowing a simpler, and thus faster, analysis of complex food products. Current traditional sample preparation techniques require multiple separate and labour-intensive sample manipulation steps (tens to hundreds). An example of achieving gains in productivity (less hands-on labour) with accompanying faster turn-around-times per sample by using SFE compared to traditional extraction and fractionation processes has been outlined by Knipe *et al.* [13]. The model application was the selective extraction of lipids, monogalactosyldiglycerides, and digalactosyl-diglycerides from wheat flour [69]. In the glycolipid assay, with the SFE-based approach, there were a total of four steps leading to the analysis. The four steps were weighing, recording the sample data, labelling the input and output vials, and extracting the flour *via* SFE. Tweeten, Wetzel and Chung [70] had previously worked out the traditional extraction of the same classes of compounds from wheat flour; this method, although very practical and robust, required 29 separate manipulations leading to the analysis. This comparison is discussed and described in detail in reference [13]. The key point here is that an SFE instrument can be designed as a single "standalone" instrument that can be used to replace a range of manual processes: extraction, fractionation, concentration, solvent exchange, and reconstitution. Moreover, with the proper attention to detail, an SFE instrument can be designed to function as either a standalone instrument *(samples in, fractionated extracts out)* or as a module in integrated systems that automate sample preparation and analysis *(samples in, reports out).*

TABLE 11
Analyte-Matrix SFE Conditions for Selected Food Applications

Ref.	Analyte	Matrix	T (°C)	Density (g/mL)	Pressure (bar)
[30]	α-,β-Carotenes	Fruits, vegetables	40	0.93	338
[9, 25]	Humulene, Myrcene, β-Caryophyllene	Hops	50	0.20	92
[9, 25]	n-Humulone, n-Lupulone	Hops	50	0.40-0.70	101-151
[9, 25]	Waxes, Lipids	Hops	50	0.90	350
[7]	PCBs	Sea gull eggs	60	0.40	115
[40]	Vanilla Flavour	Baked cookies	45	0.80	190
[43]	Pesticides	Fruit juices	60	0.75	218
[43]	PAHs	Roasted meat	60	0.80	264
[44]	*Camphene, α- & β-Pinene, Cineole, Camphor, Borneol, Bornyl Acetate, Humulene	*Rosemary plant, and spruce needles	45	0.90	300
	*Cinnamaldehyde, Coumarin, $C_{15}H_{24}$ Isomers	*Cinnamon;			
	*Limonene, α- & β-Pinene, $C_{15}H_{24}$	*Orange peel;			
	*Limonene, Menthol, Isomenthone, Carvone, Menthone, $C_{15}H_{24}$	*Chewing gum			
[44]	Borneol, Thymol, Carvacrol	Thyme	45	0.25	80
[45]	Essential Oils	Aromatic plants	70	0.83	390
	*α- & β-Pinene, ρ-Cymene, γ-Terpinene Carvacrol	*Savory			
	*α- & β-Pinene *cis*-Sabinenehydrate, Menthone, Menthol, Menthylacetate, β-Carophyllene	*Peppermint			
	*Neral, Geraniol, Thymol, Geranial, Carvacrol, Neryl Acetate, Geranyl acetate	*Dragonhead			
[46]	α-Pinene	Plant material	--	--	250
[47]	Caffeine	Roasted coffee beans	48	0.80	200
[48]	* Vitamin K1	*Infant formula powders: milk- and soy-based	60	0.95	552
	* Menadione	* Animal feed			
[49]	Natural Products (Carvone, Terpene)	Plant material (caraway seed, valerian root)	40	0.80	165
[50]	Cholesterol	Egg yolk, blood serum	45	0.79	177
[51, 52]	Fatty Acids, Ketones	Food products (butter, beef fat, cheese, rapeseed oil, coffee, tobacco)	40	0.62	100
[53]	Chlorpyrifos, Malathion, Aldrin, Diuron,	Oranges, strawberries	50	0.75	175
[53]	Diazinon, Chlorpyrifos, Malathion	Lettuce	50	0.90	350

Table 11 Continued

[53]	Diazinon, Chlorpyrifos, Malathion, Aldrin, Diuron	Green onions	40	0.25	77
[53]	DDD, DDE, DDT	Freeze-dried fish tissue	70	0.30-0.84	111-371
[54]	PCBs	Fish tissue	100	0.71	350
[55]	Essential Oil	Plant material	40	0.95	383
[56]	Organophosphorous- & Organochloro-pesticides	Spinach powder	40	0.75	134
[56]	Organochloro-pesticides	Fresh strawberries	40	0.85	211
[56]	Organochloro- pesticides	Human milk	60	0.85	329
[57]	Polar Drug	Rat feed	50	0.90	350
[58]	Free Fatty Acids, Esters	Mushrooms	50	0.90	350
[59]	Fluvalinate Residues	Honey	70	0.45	138
[60, 61]	Ergosterol	Fungi (mouldy bread flour, mushrooms, soil)	40	0.70	281
[62]	Veterinary Drugs, Pesticides	Food products	--	--	--
[63]	Vitamin D3	Skim milk	40	0.55	93
[63]	Carbamate pesticides	Potatoes	40	0.55	93
[64]	Valepotriates, Valerenic Acid Derivatives	Plant roots	40	0.78	150
[65]	Pyrrolizidine Alkaloids	Plant material	55	0.65	150
This paper: Total Fats		Snack foods, cake, chocolate	80	0.81	382
This paper: Capsaicin		Peppers	40	0.70	115

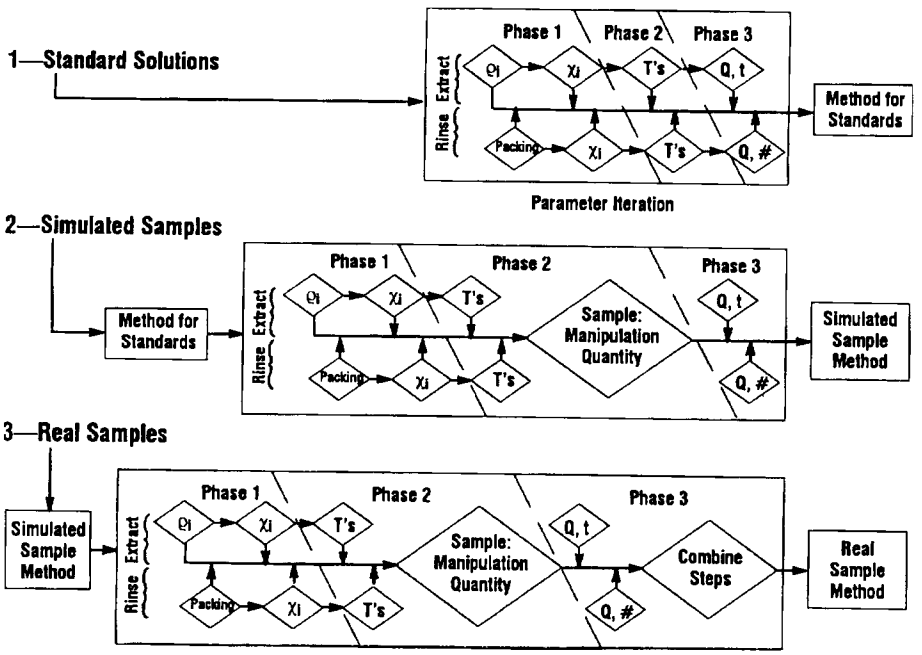

Figure 14: Caption on top of next page.

Figure 14: (On previous page) An approach to SFE method development. In "Phase 1" the density and composition of the extraction fluid are varied for the extraction step while the packing composition (of a solid trap having a porous packing material) and the reconstitution solvent composition are varied for the reconstitution part of the process. In "Phase 2" the extraction and reconstitution temperatures are explored. In "Phase 3" the extraction fluid flow rate and dynamic and static extraction times are optimised for the extraction step; the reconstitution solvent flow rate and number of reconstitution fractions (or rinses of the solid trap) are adjusted to minimise reconstitution time. Reprinted with permission from Reference [13]; copyright 1993, Hewlett-Packard Company.

Phase 1. Exploring Primary Parameters

Starting Point for Method Design → **Density**
- Use three to four steps at 40°C, pure CO_2 (0.25 g/mL, 0.40, 0.65, 0.90)

Starting Point for Sample Contact with Extraction Fluid → **Three to Five Thimble-Volumes-Swept, Intermediate Flow Rates**
As sample fills more of the thimble, remember to incorporate that in considering thimble-volumes-swept.

Starting Point for Sample → **Sample Quantity**
- Begin with quantities less than 1 gram

Starting Point Rules See Setpoint Tables for Extraction Steps and Rinse Substeps → **Collection/Concentration**
- Minimum temperatures, pure CO_2
- Maximum temperatures, long-term CO_2/modifier mixtures
- ODS, intermediate volatiles; stainless steel, involatiles

- **Modifiers**
  - Explore selectivities
    - basic—methanol, ethanol
    - acidic—chloroform
    - dipolar—methylene chloride, acetone
  - Explore exposures
    a. Short-term: Add up to 200 µL to sample (initial solubility enhancement, matrix modification)
    b. Long-term: 2 molar %, 40°C; 10 molar %, 80°C

Phase 2. Exploring Secondary Parameters and Sample Impact

- **Increase the Extraction Temperature**
  - Exploit analyte volatility or match crystal lattice energy
  - Increased diffusivity (minimum density; maximum temperature)
  - Sample matrix modification
- **Manipulate the Sample**
  - Chop, grind, dry, etc
- **Scale Sample Quantity**

Phase 3. Minimizing the Method Time

- **Adjust Extraction Fluid Flow Rate, Extraction Time**
  - To give complete extraction in the least time
- **Adjust Number of Rinses, Rinse Solvent Flow Rates**
  - To minimize output fractions and prep time
- **Adjust Number of Extraction Steps**
  - To minimize total number of steps while achieving cleanest analyte fractions

Figure 15: A template for SFE method development. Reprinted with permission from Reference 13; copyright 1993, Hewlett-Packard Company.

A second major advantage of SFE discussed in this chapter is the significant reduction in the use of liquid solvents (and their disposal). This results in lower laboratory operating costs, contributes to enhanced worker safety, and facilitates adjusting to new, world-wide environmental regulations.

From a chemical environment perspective, SFE has an advantage over traditional techniques in that the closed system instrumentation significantly reduces exposure of light-sensitive and oxidation-prone analytes to oxygen and UV radiation. This was discussed in detail relative to fat-soluble vitamins and flavour/fragrance chemicals.

Finally, we discussed the ability with SFE to handle smaller quantities of food samples with recoveries and precisions similar to those obtained with traditional methods. This smaller amount of sample allows economies of scale in the food laboratory as long as care is taken with regard to gross sampling, homogeneity and the statistical requirements of sampling/sample preparation/analysis.

11.6 BIBLIOGRAPHY

1. H-B. Lee, T. E. Peart, R. L. Hong-You, and D. R. Gere, *J. Chromatogr.* **653**, 83 (1993).

2. "Looming Ban on Production of CFCs, Halons Spurs Switch to Substitutes," *Chemical & Engineering News* **71**, 12 (November 15, 1993).

3. "*Partially Halogenated Chlorofluorocarbons (Methane Derivatives)*," Environmental Health Criteria 126, World Health Organisation, Geneva (1991).

4. "Concerns Broaden over Chlorine and Chlorinated Hydrocarbons," *Chemical & Engineering News* **71**, 11 (April 19, 1993).

5. "Nutritional Labeling and Education Act of 1990," Federal Register **58**, 2079, USA Government Printing Office (1993).

6. F. David, A. Kot, E. Vanluchene, E. Sippola, and P. Sandra, "Optimizing Selectivity in SFE and Chromatography for the Analysis of Pollutants in Different Matrices," Proc. 2nd European Symposium on Analytical Supercritical Fluid Chromatography and Extraction, Riva del Garda, Italy, May 1993.

7. F. David, M. Verschuere, and P. Sandra, *Fresenius J. Anal. Chem.* **344**, 479 (1992).

8. J. E. France, J. W. King, and J. M. Snyder, *J. Ag. Food Chem.* **39**, 1871 (1991).

9. F. David, P. Sandra, W. S. Pipkin, and J. Smith, "*Supercritical Fluid Extraction of Hops*, Application Note 228-115, Hewlett-Packard Company Publication No. (43)5952-2342 (1990).

10. D. R. Gere, C. R. Knipe, P. Castelli, J. Hedrick, L. G. Randall Frank, J. Orolin, H. Schulenberg-Schell, R. Schuster, H.B. Lee, and L. Doherty, *J. Chromatogr. Sci.* **31,** 246 (1993).

11. W. J. Moore, *Physical Chemistry, Fourth Edition*, Prentice-Hall, Inc., Englewood Cliffs, New Jersey, p. 202 (1972).

12. H. H. Lauer, D. McManigill, and R. D. Board, *Anal. Chem.* **55**, 1370-1375 (1983).

13. C. R. Knipe, W. S. Miles, F. Rowland, and L. G. Randall, *Designing a Sample Preparation Method That Employs Supercritical Fluid Extraction*, Hewlett-Packard Company, Part No. 07680-90400, (1993).

14. N. Alexandrou and J. Pawliszyn, "*Supercritical Fluid Extraction for the Rapid Determination of Polychlorinated Dibenzo-p-Dioxins and Dibenzofurans in Municipal Incinerator Fly Ash*," Paper No. 548, The Pittsburgh Conference and Exposition on Analytical Chemistry and Applied Spectroscopy, New York, New York, March 1990.

15. B. E. Berg, E. M. Hansen, S. Gjorven, and T. Greibrokk, *J. High Res. Chromatogr.* **16**, 358 (1993).

16. T. Greibrokk, B. E. Berg, A. L. Blilie, J. Doehl, A. Farbrot, and E. Lundanes, *J. Chromatogr.* **394**, 429 (1987).

17. D. R. Gere, R. Board, and D. McManigill, *Anal. Chem.* **54**, 736 (1982).

18. R. E. Jentoft and T. H. Gouw, *Anal. Chem.* **44**, 681 (1972).

19. D. M. Sullivan and D. E. Carpenter (eds), *Methods for Analysis for Nutritional Labeling* , AOAC International, Arlington, VA (1993).

20. D. E. Carpenter, J. Ngeh-Ngwainbi, and S. Lee, "Lipid Analysis," in *Methods for Analysis for Nutritional Labeling*, D. M. Sullivan and D. E. Carpenter (eds), AOAC International, Arlington, VA , Chapter 5 (1993).

21. D. R. Gere, Hewlett-Packard, Little Falls Site, Wilmington, Delaware, USA, unpublished results.

22. D. Callahan, Dean Foods Co., Rockford, Illinois, USA, unpublished results.

23. D. R. Gere, C. R. Knipe, D. C. Messer, and L. T. Taylor, "*Fundamental Supercritical Parameters Used in Extraction and Chromatography*," Proc. of the 5th International Symposium on Supercritical Fluid Chromatography and Extraction, Baltimore, Maryland, Paper No. A-16, January 1994,

24. H. Diehl, *Quantitative Analysis, Elementary Principles and Practice, 2nd Edition*, Oakland Street Science Press, Ames, Iowa, p. 71 (1974).

25. M. Verschuere, P. Sandra, and F. David, *J. Chromatogr. Sci.* **30**, 388 (1992).

26. K. Helrich (ed), *Official Method of Analysis, Acids (Alpha and Beta) in Hops, 15th Edition*, AOAC, Arlington, VA, USA, p. 732 (1990).

27. J. W. King, J. H. Johnson, and J. P. Friedrich, *J. Agric. Food Chem.* **37,** 951 (1989).

28. D. R. Gere, L. G. Randall, C. R. Knipe, W. Pipkin, and L. C. Doherty, "*The Extraction and Analysis of Polychlorinated Biphenyls (PCBs) by SFE and GC/MS. Improvement of Net Detection Limits*," Paper No 53, Proc. 9th Annual Waste Testing & Quality Assurance Symposium, Arlington, VA, pp. 397-405, July 1993.

29. J. W. King, National Center for Agricultural Utilization Research, ARS/ USDA, Peoria, Illinois, personal communication.

30. R. Marsili and D. Callahan, *J. Chromatogr. Sci.* **31**, 422 (1993).

31. L. Stryer, *Biochemistry, 2nd Edition*, W.H. Freeman and Company, New York City, NY USA, Chapter 20 (1981).

32. L. F Fieser and M. Fieser, *Organic Chemistry*, DC Heath and Company, Boston, MA, USA, pp. 951-960 (1957).

33. H. Wackenroder, *Geigers Mag. Ph.* **33,** 144 (1831).

34. M. S. Twsett, *Ber. Dtsch. Bot. Ges.* **24,** 316 (1906); *ibid.*, p. 384.

35. R. Kuhn, A. Winterstein, and E. Lederer. *Z. Physiol. Chem.* **197,** 141 (1941).

36. L. H. Tonucci, G. R. Beecher, A.. P. Emery, and S. N. Chesler, "*Supercritical Fluid Extraction of Carotenoids from Foods*," *Proc. 4th International Symposium on Supercritical Fluid Chromatography and Extraction*, Cincinnati, Ohio, USA, pp. 119-120, May 1992.

37. L. H. Tonucci and G. R. Beecher, *"Supercritical Fluid Extraction of Carotenoids From Tomato Paste," Proc. International Symposium on Supercritical Fluid Chromatography and Extraction*, Baltimore, Maryland, USA, Paper Number F-4, January 1994.

38. J. C. Giddings, L. McLaren, and M. N. Myers, *Science* **159**, 197 (1968).

39. D. R. Gere, *"Separation of Paprika Oleoresins and Associated Carotenoids by Supercritical Fluid Chromatography,"* Hewlett-Packard Application Note AN 800-5, Avondale, Pennsylvania, USA, (1983).

40. E. Anklam and A. Mueller, *Deutsche Lebensmittel-Rundschau* **89**, 344 (1993).

41. M. Windholz, S. Budavari, R. F. Blumetti, and E. S. Otterbein (eds), *The Merck Index, An Enclycopedia of Chemicals, Drugs, and Biologicals, Tenth Edition*, Merck & Co., Inc., Rahway, New Jersey, USA, p. 243 (1983).

42. D. J. Callahan and R. Marsili, Dean Foods Co., Rockford, Illinois, USA, unpublished results.

43. F. David, A. Kot, E. Sippola, and P. Sandra, submitted for publication.

44. S. B. Hawthorne, M. S. Krieger, and D. J. Miller, *Anal. Chem.* **60**, 472 (1988).

45. S. B. Hawthorne, M. L Riekkola, K. Serenius, Y. Holm, R. Hiltunen, and K. Hartonen, *J. Chromatogr.* **634**, 297 (1993).

46. M. Lohleit and K. Bachmann, *Fresenius Z. Anal. Chem.* **332**, 718 (1989).

47. K. Sugiyama, M. Saito, T. Hondo, and M. Senda, *J. Chromatogr.* **332**, 107 (1985).

48. M. A. Schneiderman, A. K. Sharma, K. R. R. Mahanama, and D. C. Locke, *J. Assoc. Off. Anal. Chem.* **71**, 815 (1988).

49. H. Engelhardt and A. Gross, *J. HRC & CC* **11**, 38 (1988).

50. C. P. Ong, H. M. Ong, S. F. Y. Li, and H. K. Lee, *J. Microcol. Sep.* **2**, 69 (1990).

51. W. Gmuer, J. O. Bosset and E. Plattner, *J. Chromatogr.* **388**, 143 (1987).

52. W. Gmuer, J. O. Bosset and E. Plattner, *J. Chromatogr.* **388**, 335 (1987).

53. W. S. Miles and L. G. Randall, *ACS Symposium Series 488*, F. V. Bright and M. E. P. McNally (eds), American Chemical Society, Washington, DC, Chapter 19 (1992).

54. H-B. Lee, T. E. Peart, A. J. Niimi, and C. R. Knipe, "*A Rapid Supercritical Carbon Dioxide Extraction Method for the Determination of Polychlorinated Biphenyls in Fish*," Environment Canada, NWRI Contribution No. 94-53, Burlington, Ontario, Canada (1994).

55. G. P. Blanch, E. Ibanez, M. Herralz, and G. Reglero, *Anal. Chem.* **66**, 888 (1994).

56. H. Schulenberg-Schell, E. Klein, and J. Hahn, "*SFE Applikationen in der Lebensmittelanalytik*," Poster No. LM33, Gesellschaft Deutscher Chemiker, Hauptversammlung, Kurzreferate und Teilnehmerverzeichnis, Hamburg, September 1993.

57. D. C. Messer and L. T. Taylor, *J. High Res. Chromatogr.* **15**, 239 (1992).

58. M. I. Abdullah, J. C. Young, and D. E. Games, *J. Ag. Food Chem.* **42**, 718 (1994).

59. J. Atienza, I. Negro, J. J. Jimenez, J. L. Bernal, and M. T. Martin, *J. Chromatogr.* **655**, 95 (1993).

60. J. C. Young and D. E. Games, *J. Ag. Food Chem.* **41**, 577 (1993).

61. D. E. Games, M. P. L. Games, H. Hernandez, P. J. Jackson, D. Thomas, and J. C. Young, "*The Potential of Supercritical Fluid Extraction (SFE) for the Analysis of Drugs and other Contaminants in Food. In Vitro Toxicological Studies and Real Time Analysis of Residues in Food*", Proc. Workshops of Ghent, Belgium, May 1992 and Thessaloniki, Greece, October 1992, H. A. Kuiper and L. A. P. Hoogenboom (eds), RIKILT, Wageningen, The Netherlands, p. 149 (1993).

62. D. E. Games, H. Hernandez, J. R. Perkins, E. D. Ramsey, and D. Thomas, *Acta Veterinaria Scandinavica* **87**, 471 (1991).

63. D. Thomas, *Ph.D. Thesis*, University of Wales, 1992.

64. M. Morvai-Vitanyi and D. E. Games, *Acta Horticulture* **344**, 386 (1993).

65. C. Bicchi, P. Rubiolo, C. Frattini, P. Sandra, and F. David, *J. Nat. Prod.* **54**, 941 (1991).

66. Z. Otero-Keil, "*Optimisation of SFE by Statistical Methods*," Paper No. 677, The Pittsburgh Conference and Exposition on Analytical Chemistry and Applied Spectroscopy, New Orleans, March 1992.

67. G.E.P. Box, W.G. Hunter, and J.S. Hunter, Statistics for Experimenters, An Introduction to Design, Data Analysis, and Model Building, John Wiley & Sons, New York (1978).

68. H. M. Wadsworth, Jr., K. S. Stephens, and A. B. Godfrey, *Modern Methods for Quality Control and Improvement*, John Wiley & Sons, New York (1986).

69. L. G. Randall, Hewlett-Packard, Little Falls Site, Wilmington, Delaware, USA, unpublished data.

70. T. N. Tweeten, D. L. Wetzel and O. K. Chung, *J. Am. Oil Chem. Soc.* **58**, 664 (1981).

Subject Index

Erratum

Typesetting problems associated with a virus infection have led to the introduction of errors at final printing time, prior to press. The Editors assume responsibility for these errors. The editors wish to stress that all authors have done an excellent job of proof reading and that although their suggested changes were implemented, they did not approve the final copy that was sent to the printers. The nature of the virus itself made for different versions arising every time a chapter was printed.

As authors ourselves we, the Editors, are unhappy with this situation but we are confident that these minor errors will not detract from or alter the overall value of the book for those involved in the field.

The following examples of errors are drawn from Chapter 8, the chapter with the most chemical and mathematical symbols:

- the symbol for pH varies between pH and *p*H (should be pH throughout);
- the signs, especially the sub/subscripts as well as some superscripts used to denote the oxidation number are not all of the proper size/alignment;
- some symbols did not convert properly (*e.g.*, some ± and α appears as ", in References 3 and 4 "gber" should read "Über", *etc.*);
- Equations and Tables are not aligned properly; *etc.*

Consequently, special care must be exercised in reading the equations or symbols to ensure that one understands the intention of the author. The correct versions of the equations are given below.

Equation (7): $Ksp,Ag_2S = (\alpha_{Ag}+)^2 . \alpha_S^=$

Equation (8): $\alpha_{Ag}+ = (Ksp,Ag_2S/\alpha_S^=)^{1/2}$

Equation (9): $Ksp,CdS = \alpha_{Cd}^{2+} . \alpha_S^=$

Equation (10): $\alpha_S^{=} = Ksp,CdS/\alpha_{Cd}^{2+}$

Equation (11): $Ksp,Ag_2S = (\alpha_{Ag}+)^2 . \alpha_S^{=}$

Equation (12): $\alpha_{Ag}+ = (Ksp,Ag_2S/\alpha_S^{=})^{1/2}$

Equation (13): $E = \text{constant} + 0.059/2 \log \alpha_{Cd}^{2+}$

Equation (27): $$\frac{dpR(V_T)}{dV_T} = \frac{M_T - \{(d[R]br/dV_T)(V_R + V_T) + [R]br\}}{(V_R M_R - V_T M_T) + [R]br(V_R + V_T)} + \frac{1}{V_R + V_T}$$

Equation (28): $$\frac{dpR(V_T)}{dV_T} = \frac{M_T + \{(d[T]br/dV_T)(V_T + V_R) + [T]br\}}{(V_T M_T - V_R M_R) + [T]br(V_T + V_R)} - \frac{1}{V_T + V_R}$$

Equation (34): $Pb^{2+} + SO_4^{=} \rightarrow PbSO_4 \downarrow$

Equation (44): $C_5H_5N.I_2 + C_5H_5N.SO_2 + C_5H_5N + H_2O \rightarrow 2C_5H_5N.H^+I^- + C_5H_5N.SO_3$

Equation (45): $C_5H_5N.SO_3 + CH_3OH \rightarrow C_5H_5N.H^+CH_3SO_4^-$

Equation (49): $i = i_o e^{-kt}$

Equation (50): $Q = \int i_o e^{-kt} dt$

Equation (51): $Q_t = \int_0^t i_o e^{-kt} dt = -(i_o/k).(e^{-kt} - 1)$

Equation (52): $Q_{max} = \int_0^\infty i_o e^{-kt} dt$

Equation (53): $= i_o/k$

Equation (57): $\log i = \log i_o - 0.4343kt$

Page 311, 4th line should read: $Ox + ne \leftrightarrow Red$

Page 316: 1.5 ppb should read 1.5 µg

Page 322: 151 parts per trillion should read 151 ppb

This Page Intentionally Left Blank